EURASIAN JOURNAL
OF SCIENTIFIC AND MULTIDISCIPLINARY RESEARCH (EJSMR)

EURASIAN JOURNAL OF SCIENTIFIC AND MULTIDISCIPLINARY RESEARCH

JALAL-ABAD INTERNATIONAL UNIVERSITY

RESEARCH JOURNAL

JALAL-ABAD INTERNATIONAL UNIVERSITY - JAIU.KG

Foreword

Narbaev Mirsadyk Rakhimberdievich

Rector , Jalal-Abad International University

Candidate of Physical and Mathematical Sciences, Associate Professor

It is with great pleasure and pride that I introduce Jalal-Abad International University Research Journal.The Research presented here embodies our institution's commitment to excellence, innovation , and the pursuit of knowledge. I extend my sincerest appreciation to excellence, innovation, and the pursuit of knowledge. We are committed to shaping the future by equipping our students with the knowledge and skills necessary to become leaders in medicine, business, and IT. Our mission is to foster a generation of professionals who are not only adept in their fields but also capable of addressing the global challenges of sustainable development. We strive to create an academic environment that nurtures innovation, critical thinking, and ethical responsibility, ensuring that our graduates are well-prepared to meet the evolving demands of the modern labor market. Welcome to JAIU, where education meets excellence and opportunity.

Publications of Session 2024 - 2025

Jalal-Abad International University

ADVANCES IN MENINGIOMA DIAGNOSIS AND TREATMENT: A COMPREHENSIVE REVIEW

Dipak Chaulagain[1, 2]
[1]Jalal-Abad International University, Jalal-Abad, Kyrgyzstan
[2]Uzhhorod National University, Uzhhorod, Ukraine

Abstract
Meningiomas, the most prevalent primary intracranial tumors, account for over one-third of brain neoplasms. Though often benign, their diagnosis and treatment are complex due to variability in clinical presentation, anatomical location, and biological behavior. This review examines cutting-edge diagnostic tools, including MRI, PET, and molecular profiling, alongside treatment modalities such as surgery, radiotherapy, and emerging targeted therapies. We address challenges in managing atypical and malignant meningiomas, emphasizing recurrence and resistance to conventional approaches. The integration of multidisciplinary strategies and future research directions, including immunotherapy and precision medicine, are highlighted as critical for improving patient outcomes.

Keywords: Meningioma, diagnosis, treatment, surgery, radiotherapy

ДОСТИЖЕНИЯ В ДИАГНОСТИКЕ И ЛЕЧЕНИИ МЕНИНГИОМ: ВСЕСТОРОННИЙ ОБЗОР

Дипак Чаулагаин [1, 2]
[1]Джалал-Абадский Международный Университет, Джалал-Абад, Кыргызстан
[2]Ужгородский Национальный Университет, Ужгород, Украина

Аннотация
Менингиомы, наиболее распространенные первичные внутричерепные опухоли, составляют более трети новообразований мозга. Хотя они часто доброкачественные, их диагностика и лечение сложны из-за вариабельности клинической картины, анатомического расположения и биологического поведения. В этом обзоре рассматриваются передовые диагностические инструменты, включая МРТ, ПЭТ и молекулярное профилирование, наряду с такими методами лечения, как хирургия, лучевая терапия и новые таргетные методы лечения. Мы рассматриваем проблемы в лечении атипичных и злокачественных менингиом, подчеркивая рецидивы и устойчивость к традиционным подходам. Интеграция междисциплинарных стратегий и будущих направлений исследований, включая иммунотерапию и прецизионную медицину, подчеркивается как критически важная для улучшения результатов лечения пациентов.

Ключевые слова: Менингиома, диагностика, лечение, хирургия, лучевая терапия.

Correspondence: Dipak Chaulagain, Associate Professor, Jalal-Abad International University, Jalal-Abad, Kyrgyzstan, Email: neurodipak@gmail.com

Introduction

Meningiomas arise from arachnoid cap cells in the meninges and constitute approximately 36% of primary intracranial tumors [1]. The World Health Organization (WHO) classifies them into Grade I (benign), Grade II (atypical), and Grade III (malignant) based on histopathological and molecular features, with recurrence risk escalating across grades [2]. Often asymptomatic and detected incidentally via imaging, meningiomas can also present with seizures, focal deficits, or intracranial hypertension, necessitating intervention. Advances in diagnostic imaging and molecular understanding have refined detection and prognosis, while treatment options—ranging from observation to surgery and novel therapies—continue to evolve. This review comprehensively explores these advancements, focusing on diagnostic precision and therapeutic innovation.

Comprehensive Review

Literature Review

Epidemiology and Risk Factors

Meningiomas predominantly affect adults, with incidence peaking between 60 and 70 years and a notable female predominance (2:1), potentially linked to hormonal influences like progesterone receptor expression [3]. Ionizing radiation, a well-established risk factor, increases incidence decades after exposure, as seen in atomic bomb survivors and patients treated with cranial irradiation [4]. Neurofibromatosis type 2 (NF2), caused by mutations in the NF2 gene on chromosome 22, predisposes individuals to multiple meningiomas, often presenting in younger patients [5]. Emerging research also explores obesity, diabetes, and head trauma as potential contributors, though causality remains debated [1]. Environmental and genetic interactions likely underpin meningioma etiology, warranting further longitudinal studies.

Diagnostic Advances

Neuroimaging drives meningioma diagnosis, with MRI as the cornerstone due to its ability to delineate tumor margins, dural attachment, and edema. Typical features include a homogeneous, contrast-enhancing mass, often with a "dural tail" sign [6]. Advanced MRI techniques—diffusion-weighted imaging (DWI), perfusion imaging, and magnetic resonance spectroscopy—enhance differentiation of tumor grade by assessing cellularity, vascularity, and metabolic profiles [5]. For example, lower apparent diffusion coefficient (ADC) values on DWI correlate with higher-grade meningiomas due to increased cellular density [6].

Positron emission tomography (PET) with somatostatin receptor ligands (e.g., 68Ga-DOTATATE) has emerged as a powerful adjunct, particularly for skull base meningiomas or post-treatment evaluation, distinguishing tumor from scar tissue with high specificity [7]. Histopathology, guided by the 2021 WHO classification, remains definitive, incorporating molecular markers like TERT promoter mutations, CDKN2A/B deletions, and SMARCE1 alterations to predict aggressive behavior [2]. Liquid biopsies detecting circulating tumor DNA are under investigation, offering a non-invasive diagnostic frontier [8].

Treatment Modalities

Management hinges on tumor characteristics and patient health. Asymptomatic Grade I meningiomas, often incidental, may be monitored with serial imaging, as growth rates are typically slow (0.5–2 mm/year) [4]. Symptomatic or enlarging tumors usually require surgery, aiming for Simpson Grade I resection (complete tumor and dural removal), which minimizes recurrence to less than 10% at 10 years [5]. However, locations near critical structures—e.g.,

cavernous sinus or optic chiasm—often preclude total resection, necessitating subtotal approaches (Simpson Grade III–IV) with higher recurrence rates [9].

Radiotherapy complements surgery, particularly for Grade II/III or inoperable tumors. Stereotactic radiosurgery (SRS) delivers precise, high-dose radiation, achieving 90–95% control for small Grade I meningiomas, while fractionated radiotherapy suits larger lesions near eloquent areas [9]. Adjuvant radiotherapy post-resection reduces recurrence in atypical meningiomas, though survival benefits in malignant cases remain modest [10].

Systemic therapies have historically lagged, with chemotherapy (e.g., hydroxyurea, temozolomide) yielding limited responses [11]. However, molecular advances are reshaping this landscape. Somatostatin receptor expression has spurred trials of analogs like octreotide, with variable efficacy [12]. Angiogenesis inhibitors (e.g., bevacizumab) target VEGF in recurrent meningiomas, stabilizing disease in small cohorts [13]. Immunotherapy, including PD-1/PD-L1 inhibitors, is being explored for high-mutation-burden tumors, with early-phase trials showing promise [8] mTOR inhibitors like everolimus also target the PI3K/AKT pathway, offering a precision medicine approach [11].

Discussion

The evolution of meningioma diagnosis reflects a synergy of imaging and molecular science. MRI's precision, augmented by DWI and PET, allows earlier detection and grade prediction, yet challenges persist in distinguishing benign from malignant tumors preoperatively. Molecular profiling, integrating TERT mutations and other markers, enhances prognostic accuracy but requires broader clinical adoption and cost reduction [2]. Disparities in access to advanced diagnostics, especially in resource-limited regions, further complicate equitable care [7].

Surgery remains the gold standard for symptomatic meningiomas, yet recurrence—30–40% for Grade II and 50–80% for Grade III—underscores its limitations [5]. Intraoperative technologies like fluorescence-guided resection (e.g., 5-ALA) and neuronavigation improve extent of resection, particularly in eloquent areas, but their availability is not universal [6]. Radiotherapy's role has solidified, with SRS offering excellent control for small tumors, though long-term risks like secondary malignancies or neurocognitive decline warrant caution, especially in younger patients [10].

Systemic therapy's slow progress reflects meningiomas' molecular heterogeneity. While bevacizumab and mTOR inhibitors show potential, their efficacy is confined to subsets of patients, highlighting the need for biomarker-driven trials [11,13]. Immunotherapy's success in other cancers fuels optimism, but meningiomas' low mutational burden may limit checkpoint inhibitor efficacy, necessitating combination strategies [8]. Skull base meningiomas exemplify treatment dilemmas, balancing tumor control with cranial nerve preservation—often best achieved via subtotal resection plus SRS [9].

Patient-specific factors, including age, comorbidities, and tumor biology, increasingly guide management. Elderly patients with incidental meningiomas may benefit more from observation than aggressive intervention, while younger patients with NF2-associated tumors require lifelong surveillance [4]. Psychosocial support and shared decision-making are vital, particularly for asymptomatic cases where "watchful waiting" may provoke anxiety [1].

Future advances hinge on integrating diagnostics and therapeutics. Artificial intelligence (AI) could refine imaging interpretation, predicting tumor behavior from radiographic features, while gene-editing technologies like CRISPR may target NF2 mutations [6]. Collaborative

registries and international trials will accelerate these innovations, addressing gaps in rare Grade III meningioma management.

Conclusion

Meningiomas exemplify the intersection of diagnostic sophistication and therapeutic challenge. Advances in MRI, PET, and molecular profiling have sharpened diagnostic precision, while surgery and radiotherapy remain foundational treatments. Emerging therapies—targeting somatostatin receptors, angiogenesis, and immune checkpoints—signal a shift toward personalized care, though their full potential awaits rigorous validation. Multidisciplinary collaboration is essential to navigate meningiomas' complexity, particularly for recurrent or malignant subtypes. Future research must prioritize accessible diagnostics, novel therapeutics, and patient-centered outcomes to transform meningioma management in the coming decades.

References

1. Ostrom, Q. T., Price, M., & Neff, C. (2023). CBTRUS statistical report: Primary brain and other central nervous system tumors diagnosed in the United States in 2015–2019. Neuro-Oncology, 25(Supplement_4), iv1–iv99. https://doi.org/10.1093/neuonc/noad149
2. Louis, D. N., Perry, A., & Wesseling, P. (2021). The 2021 WHO classification of tumors of the central nervous system: A summary. Neuro-Oncology, 23(8), 1231–1251. https://doi.org/10.1093/neuonc/noab106
3. Wiemels, J., Wrensch, M., & Claus, E. B. (2010). Epidemiology and etiology of meningioma. Journal of Neuro-Oncology, 99(3), 307–314. https://doi.org/10.1007/s11060-010-0386-3
4. Goldbrunner, R., Minniti, G., & Preusser, M. (2020). EANO guidelines for the diagnosis and treatment of meningiomas. Lancet Oncology, 21(9), e416–e425. https://doi.org/10.1016/S1470-2045(20)30396-5
5. Rogers, L., Barani, I., & Chamberlain, M. (2021). Meningiomas: Knowledge base, treatment outcomes, and future directions. Neuro-Oncology, 23(Supplement_1), i1–i12. https://doi.org/10.1093/neuonc/noab028
6. Nabavizadeh, S. A., Akbari, H., & Davatzikos, C. (2019). Advanced imaging techniques in meningioma: Beyond conventional MRI. American Journal of Neuroradiology, 40(8), 1298–1305. https://doi.org/10.3174/ajnr.A6123
7. Galldiks, N., Albert, N.L., & Langen, K.J. (2022). Role of PET imaging in meningioma diagnosis and management. Current Opinion in Neurology, 35(6), 765–772. https://doi.org/10.1097/WCO.0000000000001103
8. Bi, W. L., Zhang, M., & Wu, W. W. (2021). Emerging molecular therapies for meningiomas: Current perspectives and future directions. Neurosurgery Clinics of North America, 32(2), 241–251. https://doi.org/10.1016/j.nec.2020.11.006
9. Sheehan, J. P., Starke, R. M., & Kano, H. (2015). Stereotactic radiosurgery for meningiomas: A review of outcomes and complications. Journal of Neurosurgery, 122(5), 1018–1027. https://doi.org/10.3171/2014.10.JNS141428
10. Aizer, A. A., Arvold, N. D., & Catalano, P. J. (2019). Adjuvant radiotherapy for atypical and malignant meningiomas: A systematic review. Neuro-Oncology, 21(5), 628–636. https://doi.org/10.1093/neuonc/noz014
11. Kaley, T., Barone, D., & McDermott, M. (2018). Management of recurrent meningiomas: Systemic therapies and future directions. Neuro-Oncology Practice, 5(3), 141–150. https://doi.org/10.1093/nop/npy013
12. Graillon, T., Romano, D., & Dufour, H. (2020). Somatostatin analogs in the management of meningiomas: A systematic review. Journal of Neuro-Oncology, 149(1), 1–10. https://doi.org/10.1007/s11060-020-03562-8
13. Shih, K. C., Chowdhary, S., & Rosenblatt, P. (2016). Bevacizumab in recurrent meningiomas: A retrospective study. Journal of Neuro-Oncology, 130(1), 133–140. https://doi.org/10.1007/s11060-016-2238-8

Received / Получено 12.01.2025
Revised / Пересмотрено 20.02.2025
Accepted / Принято 20.03.2025

УДК 616-007.7-053.2/7-036.22

ОСОБЕННОСТИ ФИЗИЧЕСКОГО РАЗВИТИЯ ТУБИНФИЦИРОВАННЫХ ДЕТЕЙ И ПОДРОСТКОВ В ВОЗРАСТЕ 6-15 ЛЕТ (ЖАЛАЛ-АБАДСКАЯ ОБЛАСТЬ)

Садырова Нургуль Адылгазиевна[1]
[1]к.м.н. Жалал-Абадского международного университета, г. Жалал-Абад Кыргызстан

Аннотация
Оценка показателей физического развития детей и подростков, является основным критерием оценки здоровья. Важнейшим элементом мониторинга состояния здоровья подрастающего поколения является наблюдение за ростом и развитием подростков, стоящих на пороге взрослой жизни. В Центральной Азии у Кыргызстана очень высокие показатели заболеваемости туберкулезом на 100 тыс. населения. Страна на 50% обгоняет Таджикистан и на 76% — Казахстан. По данным Национального центра фтизиатрии, в 2023 году в Кыргызстане наблюдалось снижение заболеваемости туберкулезом по сравнению с предыдущими годами. В 2023 году снизилась заболеваемость туберкулезом среди детей, составив 11,9 на 100 тыс. населения (в 2022 году – 14,5 на 100 тыс. населения). Уровень заболеваемости туберкулезом среди подростков за прошлый год немного повысился и составил 41,2 на 100 тыс. населения (в 2022 году – 29,8 на 100 тыс. населения).

Ключевые слова: физическое развитие, тубинфицированные дети, туберкулез, здоровье, дети

FEATURES OF PHYSICAL DEVELOPMENT OF TUBERCULOSIS-INFECTED CHILDREN AND ADOLESCENTS AGED 6-15 YEARS (JALAL-ABAD REGION)

Sadyrova Nurgul Adylgazievna[1]
[1]Ph.D. Jalal-Abad International University Kyrgyzstan, Jalal-Abad

Abstract
Evaluation of physical development indicators of children and adolescents is the main criterion for assessing health. The most important element of monitoring the health of the younger generation is monitoring the growth and development of adolescents who are on the threshold of adulthood. In Central Asia, Kyrgyzstan has very high rates of tuberculosis per 100,000 population. The country is 50% higher than Tajikistan and 76% higher than Kazakhstan. According to the National Center for Pathobiology, in 2023, Kyrgyzstan saw a decrease in tuberculosis incidence compared to previous years. In 2023, the incidence of tuberculosis among children decreased, amounting to 11.9 per 100 thousand population (in 2022 - 14.5 per 100 thousand population). The incidence rate of tuberculosis among adolescents increased slightly last year and amounted to 41.2 per 100 thousand population (in 2022 - 29.8 per 100 thousand population).

Keywords: physical development, tuberculosis infected children, tuberculosis, health, children

Correspondence: Sadyrova Nurgul Adylgazievna, Associate Professor, Jalal-Abad International University, Jalal-Abad, Kyrgyzstan, Email: sadyrova.n73@mail.ru

Цель
Сравнительная оценка и анализ влияния инфицированности туберкулезом на особенности физического развития детей и подростков.

С целью изучения особенностей морфофункционального развития детей, проведено сравнительное исследование антропометрических показателей у 322 детей и подростков в возрасте от 6 до 15 лет, состоящих на диспансерном учете, и 261 здоровых детей (контрольная группа). Проведён сбор первичного материала, формирование аналитических таблиц, статистическая обработка данных и анализ результатов.

Введение
Дети и подростки - это основная индикаторная группа населения, остро реагирующая на неблагоприятные факторы окружающей среды [О.А. Бутова и соавт., 1998; А.А. Баранов, 1998; 1999; С.Г. Кривощеков и соавт., 2000; Э.М. Казин и соавт., 2006], в том числе на распространение инфекции.

Особенностью современной санитарно-эпидемиологической ситуации, является повышение уровня заболеваемости на фоне роста инфицированности, выявляемой уже в младшем дошкольном и школьном возрастах [И.А. Сиренко и соавт., 2004; А.Ф. Стукалов и соавт., 2007; Х.Н. Халафли, 2013].

Физическое развитие (ФР) детей и подростков –это уникальный критерий здоровья, который позволяет оценить, как глобальные изменения биологической природы развития человека, так и быстротечные изменения в популяции [1].

Методы изучения физического развития у детей включают: измерение размеров и массы тела (антропометрия или педометрия), осмотр и описание признаков телосложения и внешнего облика (соматоскопия), динамометрию, исследование физической работоспособности с помощью степ-теста или велоэргометрии.

Длину тела, массу тела, окружность грудной клетки (тотальные размеры) считаются наиболее существенными медико-социальными и санитарно-гигиеническими показателями, по которым в определенной мере можно судить как о положительном, так и об отрицательном влиянии заболеваемости, условий жизни, и факторов окружающей среды на организм растущего и развивающегося человека [2, 3].

Туберкулез у детей, протекает, как хроническое инфекционное заболевание, течение и исход, которого в большой степени зависит от сопротивляемости детского организма [4].

В работах Е.А.Аркин [5] указывал, что туберкулезная интоксикация представляет собой частую форму заболевания. У детей с туберкулезом этот вид интоксикации характеризуется целым рядом проявлений, которые в дошкольные годы складываются в определенную клиническую картину. Основные черты этой картины составляют: отставание в росте и особенно в весе; потеря аппетита; длинная, узкая, плоская грудь; увеличение и уплотнение лимфатических желез; нервная возбудимость, чувствительность, быстрая утомляемость, головные боли; повышение температуры до 37-37,4 градусов; положительные туберкулиновые реакции; уменьшенное количество гемоглобина и красных кровяных шариков [6].

Проведено сравнительное исследование антропометрических показателей тубинфицированных 322 детей и подростков (54,7% от общего числа детей), состоящих на диспансерном учете в Жалал-Абадском областном центре борьбы с туберкулезом имени Р.Г. Бауэра".

По мере взросления инфицированность туберкулезом детей снижается. Наибольшая инфицированность отмечается среди детей 6-8 лет. Удельный вес инфицированных детей этого возраста варьирует от 13,7±2,1% (8 лет) до 19,9±2,2% у детей 6 и 7 лет. Начиная с 11-летнего возраста, инфицированность подростков снижается и находится примерно на одинаковом уровне.

• *Таблица 1 – Половозрастное распределение детей, состоящих на диспансерном учете в Жалал-Абадском областном центре борьбы с туберкулезом имени Р.Г. Бауэра*

№	Возраст	Мальчики	Девочки	Всего			
		абс. число	удельный вес (%)	абс. число	удельный вес (%)	абс. число	удельный вес (%)
1.	6 лет	29	19,1	35	20,6	64	19,9
2.	7 лет	32	21,1	32	18,8	64	19,9
3.	8 лет	20	13,2	24	14,1	44	13,7
4.	9 лет	9	5,9	13	7,6	22	6,8
5.	10 лет	15	9,9	18	10,6	33	10,2
6.	11 лет	9	5,9	8	4,7	17	5,3
7.	12 лет	11	7,2	9	5,3	20	6,2
8.	13 лет	9	5,9	14	8,2	23	7,1
9.	14 лет	10	6,5	9	5,3	19	5,9
10.	15 лет	8	5,2	8	4,7	19	5,9
11.	Итого	152	100,0	170	100,0	322	100,0

Для удобства анализа инфицированных туберкулезом дети разделены на возрастные группы (рис1).

От общего числа обследованных детей и подростков 47,2±2,8% составляют мальчики и 52,8±2,8% девочки. Все обследованные дети были подразделены на 4 руппы.

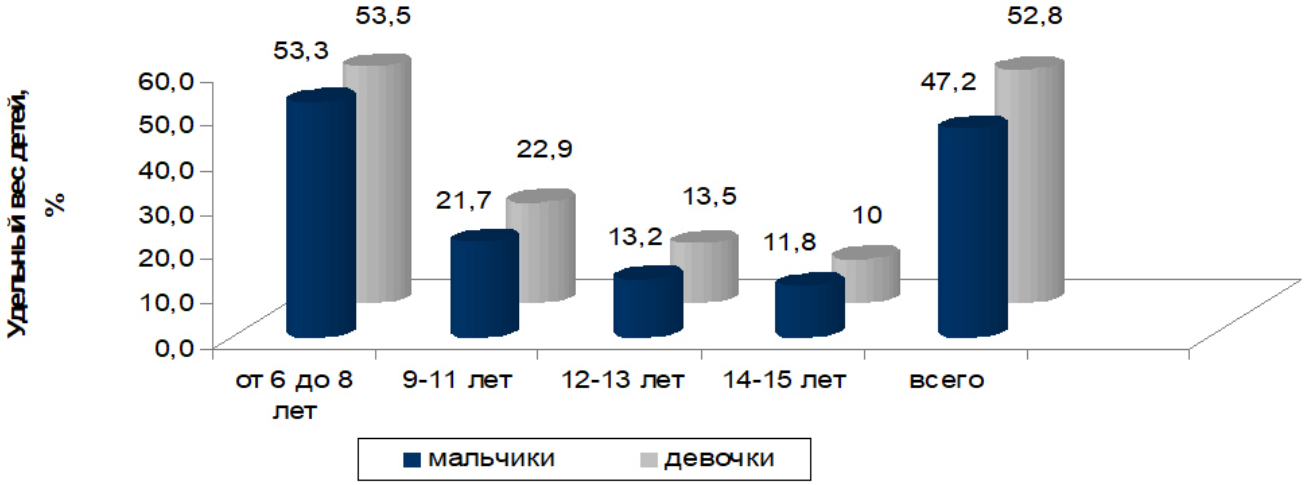

Рис. 1. Половозрастные группы инфицированных туберкулезом детей Жалал-Абадского областного центра борьбы с туберкулезом.

Первая возрастная группа – тубинфицированные дети 6-8 лет (мальчики – 53,3±2,8% и девочки – 53,5±2,8%). Вторая возрастная группа - 9-11 лет (мальчики – 21,7±2,3%, девочки – 22,9±2,3%). Третья возрастная группа - 12-13 лет (мальчики – 13,2±1,8%, девочки – 13,5±1,9%). Четвертая возрастная группа - 14-15 лет (мальчики – 11,8±1,8%, девочки – 10,0±1,7%).

Анализ гармоничности физического развития проводился по результатам оценки методом сигмальных отклонений. Масса тела у 6-8-летних тубинфицированных мальчиков (табл. 2) колеблется от 17 до 30 кг, средний вес равен 22,0±3,8 кг. Величина фактического отклонения от -5 до +8 кг, сигмальных отклонений от -1,7 до +2,8.

• Таблица 2 - Сравнительный анализ гармоничности развития тубинфицированных мальчиков 6-8 лет

№	Показатель		Мальчики «Д» Жалал-Абадский ОЦБсТ		
			Масса тела	Длина тела	ОГК
1.	Индивидуальный показатель		от 17 до 30 кг	от 115 до 136 см	от 52 до 63 см
2.	Станд. показатель	M	22,0±3,8	118,4±3,6	55,9±2,2
		σ	2,9	4,4	4,8
3.	Величина фактического отклонения		от - 5 кг до +8 кг	от – 3,4 см до +12,6 см	от – 3 см до +5,0 см
4.	Величина сигмального отклонения		от -1,7 до +2,8	от -1,0 до +4	от -1,3 до +1,5

Величина сигмальных отклонений от -1,0 до +1,5.

Из рис. 2 видно, что 40,7% мальчиков 6-8 лет имели среднюю массу тела. Низкую массу, очень низкую массу тела имели 40,7% мальчиков. Избыточную массу тела имели 9,9% детей.

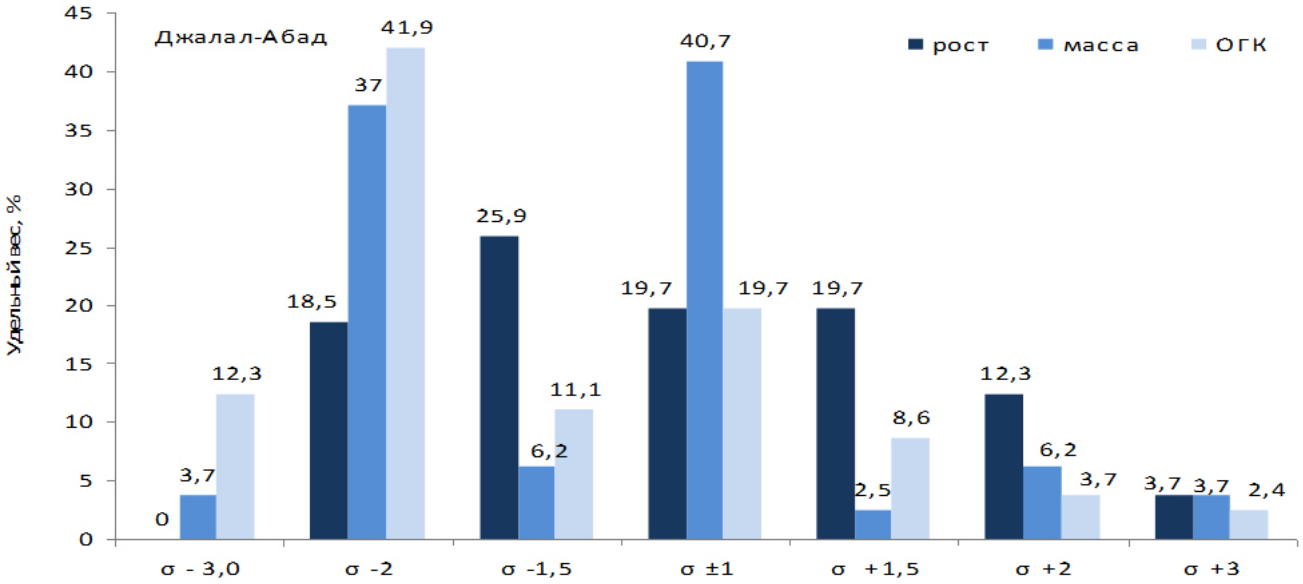

Рис. 2. Удельный вес (%) анализа гармоничности тубинфицированных 6-8-летних мальчиков

• *Таблица 3 - Анализ гармоничности развития девочек 6-8 лет*

№ пп	Показатель		Жалал-Абадский ОЦБсТ		
			Масса тела	Длина тела	ОГК
1.	Индивидуальный показатель		от 18 до 30 кг	от 110 до 133 см	от 45 до 65 см
2.	Станд. показатель	M	20,3±3,9	117,3±6,8	51,3±3,9
		σ	3,8	5,3	4,4
3.	Величина фактического отклонения		от – 2,3 кг до +9,7 кг	от – 7,3 см до +15,7 см	от – 6,3 см до +13,7 см
4.	Величина сигмального отклонения		от -3,8 до +2,5	от -5,2 до +2,9	от - 3,9 до +3,1

** Примечание – M – средняя величина, σ – среднеквадратическое отклонение.*

По ОГК, 54,2% детей, имели узкогрудость и выраженную узкогрудость, у 30,8% детей ОГК была средней либо ниже средней. Имели широкогрудость 6,1% детей.

Результаты свидетельствуют о дисгармоничности физического развития тубинфицированных детей в Жалал-Абадской области и разнятся по сравнению с данными центильных шкал В. О. Быкова (2004) [7]

Средний показатель ОГК для девочек - 51,3±3,9 и 61,0±1,4 с достоверностью t=2,3 Фактическим отклонением – 2,3 см и +9,7 см. Величина сигмальных отклонений от -3,9σ до +3,1σ. Из числа обследованных тубинфицированных девочек 6-8 лет по массе тела, 49,4% имели M ± 1σ, 6,6% M ±-1,3σ (ниже средней), 30,7% - 2,8σ (дефицит массы тела) и 6,6% -3,8σ (выраженный дефицит массы тела). 2,2% +1,2σ и 4,4% +2,8σ выше средней и избыточную массу тела.

По росту, 50,5% обследованных девочек данного возраста – имели M ± 1σ (среднее развитие роста),8,7% - 1,2σ (ниже среднего), 4,4% - 1,5σ (низкий), 2,2% - до 5,2σ (очень низкий рост) и 13,2% +1,2σ (выше среднего), 11,0% +2,3σ (высокий рост) и около 10% (9 девочек) +2,9σ (очень высокий рост).

Для оценки физического развития тубинфицированных детей, проведено сравнительное исследование антропометрических показателей (табл. 4).

• *Таблица 4 - Сравнительная оценка физического развития возрастных групп здоровых и тубинфицированных детей*

№ пп	Возраст, годы	Гр.	Число детей		Масса тела, кг		Длина тела, см		ОГК, см	
			М	Д	М	Д	М	Д	М	Д
1.	6-8	К	44	16	24,0±3,8 Δ	24,2±4,2 Δ	131,9±2,2 ΔΔ	131,5±2,3 ΔΔ	62,3±3,1 Δ	61,7±3,3 ΔΔ
		О	81	91	22,0±3,8	20,3±3,9	118,4±3,6	117,3±6,8	55,9±2,2	51,3±3,9
2.	9-11	К	43	46	32,4±3,0	32,0±2,9	137±2,2 Δ	138,7±2,2 Δ	67±3,0 Δ	71,7±2,8 Δ; ▲
		О	33	39	30,9±3,6	33,0±2,9▲	132,4±2,9	134,4±2,5▲	62,6±2,2	63,8±3,2

3.	12-13	К	51	26	36,8±3,0 Δ	38,9±3,2	146,5±2,2 Δ	148,5±2,3 ΔΔ	71,0±2,8 ΔΔ	70,0±3,0 ΔΔ
		О	20	23	32,0±2,5	31,4±2,9	143,5±2,5	141,5±2,9	62,3±2,5	63,5±1,6
4.	14- 15	К	23	12	50,8±3,5 ΔΔ	49,1±3,4	165,0±4,2 ΔΔ	160,6±2,5	77,8±2,9	78,1±2,8Δ
		О	18	17	42,8±2,2	50,9±1,9▲	153,6±2,0	154,2±1,9	75,7±1,9	72,6±1,4

Примечание - Δ - p<0,05; ΔΔ- p<0,01; ΔΔΔ -p<0,001 сравн-е К с О группой по поло- возрасту среди одного региона.▲ - p<0,05; ▲▲ - p<0,01; ▲▲▲ - p<0,001 сравне К с О группой по полу и возрасту между 2-мя региона, К – контрольная группа (здоровые дети); О - опытная группа (тубинфицированные дети).

В I группе - (6-8-летних) детей по половой принадлежности имеются ниже следующие достоверные различия: среди детей при сравнении контрольной с опытной группой, как у мальчиков, так и у девочек имеется достоверные различия: МТ контрольной группы детей от 2 до 4 кг (p<0,05), ДТ у мальчиков (М) - на 13,5 см и у девочек (Д) – на 14,2 см (p<0,01), ОГК у М – на 6,4 см и Д – на 10,4 см (p<0,05; p<0,01) больше, чем в опытной группе.

Во II группе (9-11 лет) имелись достоверные различия при сравнении с контрольной группой, в контрольной группе по ДТ и ОКГ, как у мальчиков, так и у девочек имеют достоверные различия (ДТ - на 4,6 см и 4,3 см; ОКГ – на - 4,4 см и 7,9 см у мальчиков и девочек, соответственно больше, чем в опытной группе (p<0,05).

В III группе детей (12-13 лет при анализе показателей в контрольной и опытной группах у мальчиков МТ на 4,8 кг (p<0,05), ДТ на 3 см (p<0,05) и ОГК на 8,7 см (p<0,01), у девочек в ДТ на 7 см и ОГК на 6,5 см (p<0,01) больше, чем в опытной группе.

Заключение

Физическое развитие тубинфицированных детей и подростков в сравнении со здоровыми выявили достоверные различия по морфофункциональным показателям. У них отмечаются задержка физического развития, о чем свидетельствуют основные антропометрические параметры (длина и масса тела), а также преобладает дисгармоничный и резко дисгармоничный варианты развития независимо от пола и место проживания.

У тубинфицированных детей и подростков выявлено снижение основных параметров физического развития по сравнению с контролем – длины и массы тела, окружности грудной клетки. у 6-8-летних тубинфицированных детей независимо от пола по ОГК имеются достоверные различия (p<0,05). В большинстве изученный детский контингент относится к мезоморфному типу телосложения (нормостеники), а по анатомическим особенностям приближаются к усредненным параметрам нормы (с учетом возраста, пола), за исключением 6-8-летних девочек - долихоморфный (длинные конечности и узкие туловище)

Литература

1. Антропова, М.В. Морфофункциональное созревание основных физиологических систем организма детей дошкольного возраста / М.В. Антропова, М.М. Кольцова. - М.: Педагогика, 1983. - 160 с.
2. Баранов, А.А. Физиология роста и развития детей и подростков (теоретические и кинические вопросы) / А.А. Баранов, Л.А. Щеплягина. - М.: ГЭОТАР-Медиа, 2006. - Т.1. - С. 430-432.
3. Трубня, Н.П. Атмосферное загрязнение как фактор риска для здоровья детского и подросткового населения / Н.П. Трубня, О.К. Федоренко // Гигиена и санитария. - 2002. - № 2. - С. 21-23.

4. 27. Богданова, Е.В. Туберкулез у детей раннего и дошкольного возраста из семейного контакта: автореф. дис. … канд. мед. наук: 14.00.26 / Е.В. Богданова. - М., 1998. - 27 с.
5. Аркин, Е.А. Ребенок в дошкольные годы / Е.А. Аркин. - М., 1968. - 445 с.
6. Апанасенко, Г.Л. Физическое развитие детей и подростков / Г.Л. Апанасенко. - Киев: Здоровье, 1985. - 282 с.
7. Баранов, А.А. Основные закономерности морфофункционального развития детей и подростков в современных условиях / А.А. Баранов, В.Р. Кучма, Н.А. Скоблина // Вестник РАМН (Актуальные вопросы педиатрии). - 2012. - № 12. - С. 35-40.8.

Received / Получено 02.01.2025
Revised / Пересмотрено 22.02.2025
Accepted / Принято 20.03.2025

УДК:613.96(576.2)

ОТНОШЕНИЕ ПОДРОСТКОВ К ЗДОРОВЬЮ И УРОВЕНЬ САНИТАРНО-ГИГИЕНИЧЕСКИХ ЗНАНИЙ

Орозбекова Бубусайра Толобаевна[1], Абдраева Феруза Асылбековна[2]
[1]Кыргызско-Российский Славянский Университет, Бишкек, Кыргызстан
[2]Ошский Государственный Университет, Ош, Кыргызстан

Аннотация
Результаты анкетирования по самооценке состояния здоровья 2280 подростков разной национальностей 15-17 лет в двух крупных городах КР (г. Бишкек и г. Ош). Учащиеся СОШ КРСУ составляли контрольную группу в количестве 232 подростков того же возраста. А также, дана оценка уровня санитарно-гигиенической состоянии в семье и гигиенические навыки подростков. По данным анкетирования из анализа: как у подростков, так и у родителей почти сходный уровень оценки санитарного состояние жилищно-бытовых условий. В связи с этим опрошенные подростки (41,7%) у себя отмечали наличие частого насморка, острого бронхита, пневмонии, а 9,1% подростков отметили наличие хронического сердечно-сосудистого заболевания, 4,8% опрошенные указали на частые головные боли и гипертонии, хронический бронхит - 37,2%, кожные заболевания - 1,2%, беспокойство и депрессии - 2,8%, артрозы - 0,5%, бронхиальную и аллергические астмы 2,7%. Из всех обследованных 69,3% выходцы из неполных семей, это на 100 обследованных от 38 до 50 случаев в группе юношей и от 20 до 30 случаев в группе девушек.

Ключевые слова: самооценка, здоровья, подростки 15-17 лет, санитарно-гигиенические состояние, гигиенические навыки

THE LEVEL OF SANITARY AND HYGIENIC KNOWLEDGE AND SELF-ASSESSMENT OF ADOLESCENT HEALTH IN THE KYRGYZ REPUBLIC

Orozbekova Bubusaira Tolobaevna[1], Abdraeva Feruza Asylbekovna[2]
[1]Kyrgyz-Russian Slavic University, Bishkek, Kyrgyzstan
[2]Osh State University, Osh, Kyrgyzstan

Annotation
The results of a self-assessment survey of the health status of 2280 adolescents of different nationalities aged 15-17 in two major cities of the Kyrgyz Republic (Bishkek and Osh). Students of the KRSU Secondary School made up a control group of 232 teenagers of the same age. The assessment of the level of sanitary and hygienic situation in the family and hygiene skills of adolescents is given. According to the survey data from the analysis: Both adolescents and parents have an almost similar level of assessment of the sanitary condition of housing and living conditions. 41,7% of adolescents reported frequent colds (runny nose, acute bronchitis, pneumonia) and associated them with the sanitary and hygienic condition of their homes, 9,1% of adolescents noted the presence of chronic cardiovascular diseases, 4,8% of frequent headaches and hypertension, 37,2% of chronic bronchitis, 1,2% of skin diseases, anxiety depression 2,8 %, osteoarthritis 0,5%, bronchial and allergic asthma 2,7%. In 69,3%, the rate of single-parent families ranges from 38 to 50 cases per 100 persons.

Key words: self-esteem, health, adolescents 15-17 years old, sanitary and hygienic condition, hygienic skills

Correspondence: Orozbekova Bubusaira Tolobaevna, Professor, Kyrgyz-Russian Slavic University, Bishkek, Kyrgyzstan, Email: oosp@rambler.ru

Актуальность

Одним из важных проблем которая характеризует здоровья подростков обусловлена сменой факторов патологии, как преобладанием неинфекционных эндогенных факторов заболеваемости и смертности [1] и относительно низкий уровень культуры здоровья и культуры поведения в сфере здоровья [2]. А также, преобладание частных медицинских услуг (платных), которые привели изменению функционированию государственной гарантированной системы здравоохранения. Однако, здоровья поведение человека определяется их уровнем осведомленности об образе жизни и здоровье окружающей среды, для которых самооценка образа жизни имеет большое значение и способствует созданию положительной мотивации к саморегуляции [3-6]. Ухудшение показателей здоровья подростков в стране, имеет научную и социальную значимость данной проблемы.

Цель

Целью является на примере в двух крупных городах Кыргызстана (г. Бишкек и г. Ош). оценить уровень санитарно-гигиенической знании и состоянии в семьи, самооценка уровня здоровья.

Методика

Анонимное анкетирование 2280 подростков различных национальностей в возрасте 15-17 лет в двух городах КР (г. Бишкек и г. Ош). В анкете отражены вопросы как самооценка здоровья, факторы риска негативно влияющих на здоровье, оценка образа жизни, уровня санитарно-гигиенической состоянии в семье, гигиенические навыки и др. (всего 25 вопроса). Учащиеся СОШ КРСУ составляли контрольную группу в количестве 232 подростков того же возраста.

С помощью программы Statistic 7,0 (StatSoft, 2009), проведена статистическая обработка материала. набранный материал результатов проводилась Excel 10.0 с использованием набора непараметрических параметров. Принимали различия достоверны на 5%-ом уровне значимости (уровень значимости $p < 0,05$).

Результаты исследования

С каждым из подростков и их родителями составлена анкета согласования, в которой он предварительно был ознакомлен с предстоящими исследованиями и было получено его согласие на обследование. Сведения обследуемых вошедший в обработку 2280 подростков различных национальностей в двух городах КР (15-17-лет по г. Ош, и г. Бишкек), и в том числе учащиеся СОШ КРСУ составляющие контрольную группу в количестве 232 старших классов.

• Таблица 1. Сведения об обследуемых подростках г. Ош и г. Бишкек, возраст 15-17 лет (по национальности)

Школа	Кыргызы		Узбеки		Др. национальности		Всего	
г.Ош, школьники	432	39,8 ± 1,5	439	40,5 ± 1,5	214	19,7 ± 1,2	1085	100
Учащиеся СОШ КРСУ	109	46,9 ± 3,2	41	17,6 ± 2,5	82	35,3 ± 3,1	232	100
г. Бишкек, школьники	496	51,5 ± 1,6	96	9,9 ± 0,96	371	38,5 ± 1,56	963	100
Итого Бишкек	605	50,6 ± 1,44	137	11,5 ± 0,9	453	37,9 ± 1,4	1195	100
Всего:	1037	45,5± 1,0	576	25,3± 0,9	667	29,3± 0,95	2280	100

Как видно из табл. 1. по удельному весу респонденты составили г. Ош 47,58±1,0%, а г. Бишкек - 52,41±1,44%. По национальному составу: кыргызы – 39,8±1,5% и 50,6±1,4%; узбеки - 40,5±1,5% и 11,5±0,9%; другие национальности 19,7±1,2% и 37,9±1,4% соответственно из всех обследованных. Тогда, учащихся СОШ КРСУ (контрольная группа) составили кыргызы 46,9±3,2%, узбеки – 17,6±2,5% и другие национальности – 35,3±3,1%.

• Таблица 2. Возрастная структура учащихся 15-17 лет

Школа	15		16		17		Всего	
г. Ош, школьники:	397	36,6±1,5	345	31,8±1,4	343	31,6±1,4	1085	100
Учащиеся СОШ КРСУ	97	41,8±3,2	83	35,8±3,1	52	22,4±2,7	232	100
г. Бишкек, школьники	516	53,6±1,6	338	35,1±1,5	109	11,3±1,0	963	100
Итого Бишкек	613	51,3±1,4	421	35,2±1,4	161	13,5±1,0	1195	100
Всего:	1010	44,3 ± 1,0	431	33,6 ± 1,0	240	11,8 ± 0,7	2280	100

По данным нашего анализа (табл. 2.) возрастная структура исследованных составляли по г. Бишкек: всего 15 - летние 51,3±1,4%; 16 лет – 35,2±1,4%; 17 лет – 13,5±1,0%, а по г. Ош 15 - летние 36,6±1,5%; 16 лет - 31,8±1,4%; 17 лет - 31,6±1,4%. По г. Бишкек школьники и в СОШ КРСУ (как контрольная группа) 15 - летние 53,6±1,6% и 41,8±3,2%; 16 лет - 35,1±1,5% и 35,8±3,1%; 17 лет - 11,3±1,0% и 22,4±2,7% соответственно.

Параллельно было проведено анкетирование подростков и семей по их самооценке уровня санитарной и гигиенической состоянии в семье.

Наука доказывает, опрятный ребенок чувствует себя увереннее, легче адаптируется в социуме. Через гигиеническое воспитание он привыкает заботиться о своем теле и здоровье в целом, и эти устойчивые привычки личной гигиены прививаются (помыть руки перед едой, почистить зубы перед сном и умыться утром) с малых лет в семье.

• *Таблица 3. Самооценка уровня санитарной и гигиенической состоянии в семье*

Показатели	Оценка	Подростки	Родители
Общая оценка санитарной состоянии жилищно-бытовых условий	хороший	28,6 ± 0,1	26,3 ± 2,3
	удовлетворительный	53,4 ± 1,1	51,3 ± 0,3
	неудовлетворительный	18,0 ± 0,7	22,4 ± 1,8
Общая оценка гигиенических навык	хороший	10,2 ± 0,6	16,4 ± 2,0
	удовлетворительный	62,8 ± 1,1	58,8 ± 2,4
	неудовлетворительный	27,0 ± 1,1	24,8 ± 1,8

Как видно, в табл. 3. подростки и родители имеют почти сходный уровень оценки санитарной состоянии жилищно-бытовых условий: 28,6±0,1% и 26,3±2,3% оценено на «хорошо», 53,4±1,1% и 51,3±0,3% на «удовлетворительно» соответственно.

«Неудовлетворительно» оценено у подростков и родителей 18±0,7% и 22,4 ± 1,8% соотв., отметив причину на «нет собственного жилья». В то время гигиенические навыки на «хорошо» подростки оценили значительно ниже 10,2±0,6%, чем их родители 16,4±2,0%. На «удовлетворительно» оценено подростками - 62,8±1,1% и родителями - 58,8±2,4%. Гигиенические навыки признали «неудовлетворительными» 27,0±1,1% подростки, а родители 24,8±1,8%.

В рис. 1. и 2. отражены результаты анкетирования по самооценке состояния здоровья юношей подростков.

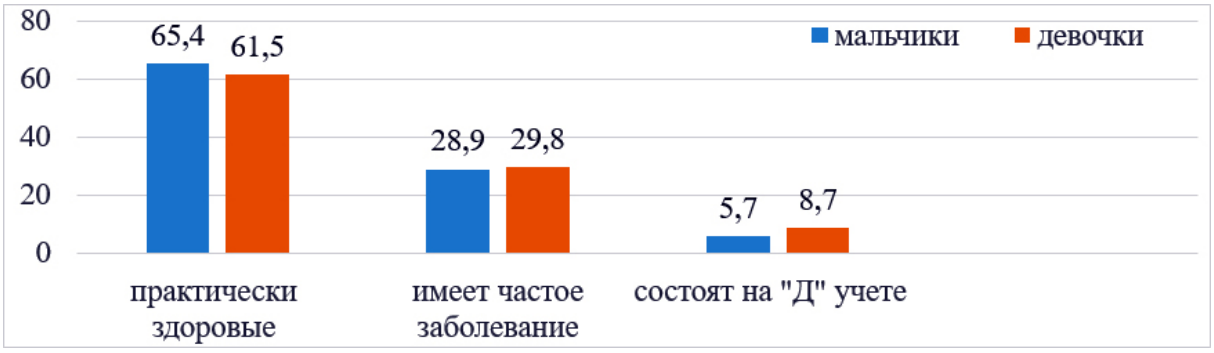

Рис. 1. Самооценка состояния здоровья подростков г. Ош

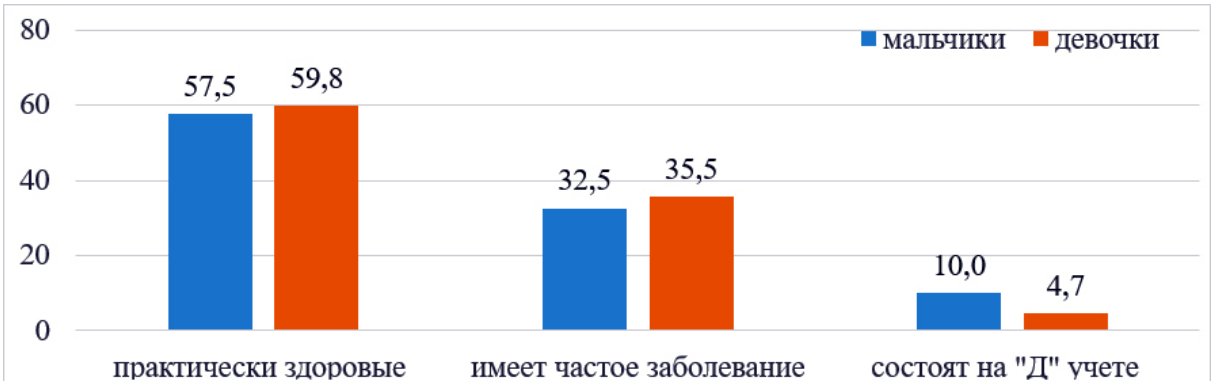

Рис.2. Самооценка состояния здоровья подростков г. Бишкек

По данным анкетирование лица как мужского, так и женского пола г. Ош указали на наличие хронических заболеваний, которые состоят на «Д» учете (5,7% и 8,7% соотв.) и жалобы на проявление частных простудных заболеваний как: ОРВИ, ОРЗ, ангина, ларингит, насморк, частые кашли и др., считали чаще себя здоровыми подростки мужского пола (65,4%), чем лица женской группы (61,5%). Когда, жители г. Бишкек указали на более низкий уровень здоровья, подростки мужского пола признали себя здоровыми 57,5%, а в числе женского пола – 59,8%. На наличие хронических заболеваний (на «Д» учете) в группе женского пола указали 4,7%, и 10,0% мужской пол.

Практически 41,7% подростки отмечали частые простудные заболевания как: насморк, острый бронхит, пневмонии и связывали их с санитарно-гигиеническим условиям жилища. Около 9,1% опрошенных подростков отметили наличие у них хронических сердечно-сосудистых заболеваний, на частые головные боли и гипертонии 4,8%, хронический бронхит 37,2%, кожные заболевания 1,2%, беспокойство и депрессии 2,8%, артрозы 0,5%, бронхиальную и аллергические астмы 2,7%.

Причины санитарных условий связывали на показатель неполной семьи (69,3%) и неудовлетворительные взаимоотношения в семье. Данные показатели на 100 обследованных в группе у юношей и у девушек колеблется в пределах: от 38 до 50 и от 20 до 30 случаев лученные соответственно.

Поведение подростков, направленное на сохранение и укрепление своего физического состояния, зависит во многом от образа и стиля жизни (санитарно-гигиенические нормы, рациональное питание, отказ от вредных привычек как, табакокурения и употребления алкогольных напитков, физическая активность) Исследование показало, что подростки увлекаются курением электронных сигарет: «несколько раз в день» выбрали 12%, «нет» 73%, «пробовали курить» 9,4%, не дали ответ 5,6%. Практически 84% подростки информацию о электронных сигаретах получили от интернета и друзей. Но, по результатам анкетирования процент недостоверности данных анкетированных составляет 31,8%. Это означает, что каждый третьей из опрошенных намеренно солгал о себе; или свершил случайную ошибку, бегло заполнял анкету, не обращая внимания на поставленные вопросы. Как показывает рис. 3. у всех подростков (15-17 лет) почти одинаковый уровень знания. Данную проблему обсуждают между собой, но не с родителями.

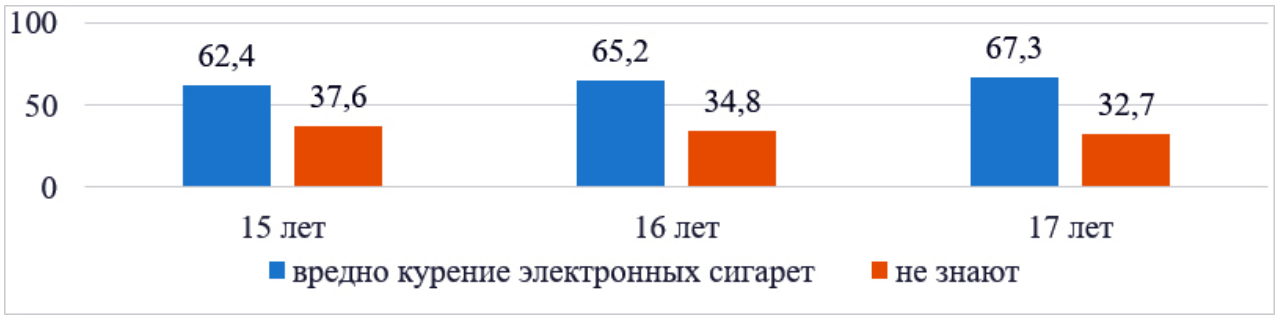

Рис.3. Уровень осведомленности о вреде электронного сигарета.

Выводы

1. По данным анализа анкетирования: у подростков, и родителей имеют почти сходный уровень оценки санитарного состояние жилищно-бытовых условий, который у 28,6±0,1% и 26,3±2,3% оценено на «хорошо», 53,4±1,1% и 51,3±0,3% на «удовлетворительно» соотв., и не имея собственного жилья 18±0,7% и 22,4±1,8% отметили «неудовлетворительно» соотв. В то время гигиенические навыки на «хорошо» подростки оценили значительно ниже 10,2±0,6%, чем их родители 16,4±2,0%. На «удовлетворительно» оценено подростками - 62,8±1,1% и родителями - 58,8±2,4%. Гигиенические навыки признали «неудовлетворительными» 27,0±1,1% подростки, а у родителей 24,8±1,8%.

2. 41,7% подростки отмечали частые простудные заболевания как: насморк, острый бронхит, пневмонии и связывали их с санитарно-гигиеническим условиям жилища. Около 9,1% опрошенных подростков отметили наличие у них хронических сердечно-сосудистых заболеваний, на частые головные боли и гипертонии 4,8%, хронический бронхит 37,2%, кожные заболевания 1,2%, беспокойство и депрессии 2,8%, артрозы 0,5%, бронхиальную и аллергические астмы 2,7%. У 69,3% показатель неполных семей колеблется в пределах от 38 до 50 случаев на 100 обследованных в группе юношей и от 20 до 30 случаев в группе девушек.

3. Отношение подростков к здоровью является недостаточно изученным в КР, необходимо исследований по выявлению и уточнению факторов, способствующих формированию у подростков позитивного отношения к своему здоровью не смотря на условия жизни. Настораживает тот факт, что 5,6% не дали ответ, и «пробовали курить» 9,4%, это от 5 до 15 случаев на 100 обследованных низкое информированность ценностные установки в отношении здоровья, деятельность по его сохранению.

Литература

1. Журавлева И. В. Здоровье подростков: социологический анализ. – М.: Изд-во. Ин-та социологии. РАН, 2002. – 240 с.
2. Журавлева И. В. Отношение к здоровью индивида и общества. – М.: Наука, 2006. – 238 с.
3. Юрьев В. К., Жирков П. Г. Распространённость некоторых факторов риска образа жизни, негативно влияющих на здоровье старшеклассников // Педиатр. - 2018. - Т.9. - №2. - С. 4954.
4. Gender and Health in Adolescence / Editors P. Kolip, B. Schmidth. - Copenhagen: World Health Organization Regional Office for Europe, 1999. - 38 p.
5. Health and Health Behaviour among Young People. WHO Policy Series: Health policy for children and adolescents Issue 1. International Report / Editors C. Currie, K. Hurrelmann, W. Settertobulte, R. Smith, J. Todd. - Copenhagen: World Health Organization Regional Office for Europe, 2000. - 132 p.
6. Young people's health in context. Health Behaviour in School-aged Children (HBSC) study: international report from the 2001/2002 survey / Editors C. Currie, C. Roberts, A. Morgan, R. Smith, W. Settertobulte, O. Samdal, V. Rasmussen. - Copenhagen: World Health Organization Regional Office for Europe, 2004. - 248 p.

Received / Получено 12.01.2025
Revised / Пересмотрено 20.02.2025
Accepted / Принято 20.03.2025

УДК: 613.96 (576.2)

ОСНОВНЫЕ ТЕНДЕНЦИИ ЗАБОЛЕВАЕМОСТИ ПОДРОСТКОВ НА ФОНЕ РОСТА ХРОНИЧЕСКОЙ ПАТОЛОГИИ

Орозбекова Бубусайра Толобаевна[1], Абдраева Феруза Асылбековна[2]
[1]Кыргызско-Российский Славянский Университет, Бишкек, Кыргызстан
[2]Ошский Государственный Университет, Ош, Кыргызстан

Аннотация
В статье изучено и проанализировано социально значимые болезни подростков и структура общей заболеваемости подростков 15-17 лет на 1000 детей соответствующего возраста по классам болезни за 15-летний период (2009-2023 гг.). К сожалению, несмотря на утверждения постановлением Правительства КР СаН ПиН пункт 11/184, которые не применяются на практике в соответствующих учреждениях, растет показателей таких заболеваний и обращаемость врачам как: H00-H59 - болезни глаза и его придаточного аппарата 6,3%; H60-H95 – болезни уха и сосцевидного отростка 4,7% в структуре общей заболеваемости. Из анализа на 2022г. увеличилась посещаемость врачу невропатологу 3,5 (1873,3), офтальмологу и отоларинголог 3,4 и 3,2 раза (1762,6 и 1980,4 соответственно число случаев на 1000 детей) больше составляют по сравнению с 2005 годом. А также, настораживает учет E00-E90 - болезни эндокринной системы, расстройства питания и нарушения обмена веществ как распространенности и заболеваемости составив 4,6‰ и 3,1‰ соответственно. Актуальность научной проблемы однозначны, определяющиеся гендерными особенностями подростков и свидетельствующих о необходимости проведения дальнейших исследований в этой направлении.

Ключевые слова: здоровье, здоровый образ жизни, поведенческие факторы здоровья подростков

THE MAIN TRENDS IN ADOLESCENT MORBIDITY AGAINST THE BACKGROUND OF AN INCREASE IN CHRONIC PATHOLOGY

Orozbekova Bubusaira Tolobaevna[1], Abdraeva Feruza Asylbekovna[2]
[1]Kyrgyz-Russian Slavic University, Bishkek, Kyrgyzstan
[2]Osh State University, Osh, Kyrgyzstan

Abstract
The article examines and analyzes socially significant diseases of adolescents and the structure of the overall incidence of adolescents aged 15-17 years per 1,000 children of the appropriate age by disease class over a 15-year period (2009-2023). Unfortunately, despite the approval of the decree of the Government of the Kyrgyz Republic SaN PiN paragraph 11/184, which are not applied in practice in the relevant institutions, the rates of such diseases and medical treatment are growing as: H00-H59 - diseases of the eye and its appendage 6,3%; H60-H95 – diseases of the ear and mastoid process 4,7% in the structure of the overall incidence. From the analysis for 2022, the number of visits to neurologists increased 3,5 (1873.3), ophthalmologists and otolaryngologists 3,4 and 3,2 times (1762.6 and 1980.4, respectively, the number of cases per 1000 children) more than in 2005. It is also alarming to consider E00-E90 - diseases of the endocrine system, eating disorders and metabolic disorders as the prevalence and incidence

of 4,6% and 3,1%, respectively. The relevance of the scientific problem is unambiguous, determined by the gender characteristics of adolescents and indicating the need for further research in this area.

Keywords: health, healthy lifestyle, behavioral determinants of health of children and adolescents

Correspondence: Orozbekova Bubusaira Tolobaevna, Professor, Kyrgyz-Russian Slavic University, Bishkek, Kyrgyzstan, Email: oosp@rambler.ru

Актуальность

Нормы поведения подростка в обществе определяет его состояние здоровья [1-4]. Актуальность проблемы охраны репродуктивного здоровья подростков определяется снижением репродуктивного потенциала подростков, низкими репродуктивными установками и неадекватным репродуктивным поведением, наличием неблагоприятного медико-биологического фона: высокого уровня первичной заболеваемости и хронической патологии, увеличением частоты нарушений функции репродуктивной системы.

Цель исследования

Оценка здоровья подростков 15-17 лет, проживающих в Кыргызской Республики.

Предмет исследования – ретроспективный анализ заболеваемости с 2009-2023 гг.

По данным ретроспективного анализа оценена уровень, структура, тенденция и значимые особенности распространения заболеваемости среди подростков 15-17 лет в КР на 1000 детей по классам болезни принятым МКБ-10, за 15-летний период.

Ниже из таблицы 1., видно, что у подростков регистрируются все заболевания из 18 групп классов болезней МКБ-10 (из 22-х). При этом, необходимо отметить, что в динамике отмечается периодический рост как показатель распространённости и инцидентности совокупной заболеваемости детей. Усредненные интенсивные показатели данных показателей равны 530,6‰ и 362,1‰, минимальный 270,4‰ и 203,1‰ (2020г) и максимальный 658,3‰ и 440,6‰ (2012г.) соответственно на 1000 детей соответствующего возраста.

А также, из табл. 1. и рис.1. видно, что удельный вес заболеваний верхних дыхательных путей (J00-J99) в общей структуре совокупной заболеваемости составляет 34,4%, как по распространенности, так и показателю заболеваемости занимая ведущее место.

В динамике за анализируемый период показатели распространенности и заболеваемости имели стабильно высокие уровни. Средний интенсивный показатель распространенности и заболеваемости составил 182,3‰ и 109,8‰, минимальный 132,0‰ и 107,4‰ (2012г.), максимальный 380,1‰ и 192,2‰ (2023г.) соотв. как по распространенности, так и показателю заболеваемости (на 1000) детей соответствующего возраста.

• *Таблица 1. - Заболеваемость подростков по основным классам и группам болезней, Кыргызская Республика на 1000 детей соответствующего возраста*

(1- зарегистрировано больных подростков; 2 - т. ч. с д/з, установлен впервые в жизни.)

Класс и группы болезней		2009	2010	2011	2012	2013	2014	2015	2016	2017	2018	2019	2020	2021	2022	2023	Усред.	Уд. вес (%)	Ранг
Все	1	597,7	577,7	566,5	658,3	642,8	611	637,4	565,4	510,8	476,6	467,9	270,4	375,9	416,5	584,2	530,6		
бол-ни	2	395,9	379,1	381,7	440,6	405,1	407,6	417,8	352,02	335,9	335,2	339,7	203,1	285,8	310,8	441,2	362,1		
A00-B99	1	24,6	25,1	24,6	27	29,2	24,6	26,9	15,6	16,2	15,6	14,7	7,8	11,6	13,8	18,5	19,7	3,7	11
	2	19,9	20,3	18,8	20,2	19,7	19	19,6	10,1	11,1	11,3	10,7	5,2	9,7	10,6	15	14,7	4,1	11
C00-D48	1	0,5	0,8	0,7	1,1	1,1	1	1,1	1,42	1,8	1,4	1,5	0,7	0,8	1,3	1,45	1,1	0,2	17
	2	0,3	0,4	0,3	0,7	0,5	0,6	0,6	0,7	0,95	1	1,2	0,6	0,5	1	1	0,7	0,2	17
D50-D89	1	37,8	39,9	34,6	35,1	34,3	33,6	34,3	24,8	20,8	17,1	13,7	7,2	9,8	12,5	16,05	24,8	4,7	9
	2	22,2	26,4	21	22,2	18,5	22,2	21	12,6	10,04	9,1	8,1	3,7	5,3	7,9	9,25	14,6	4,0	9
E00-E90	1	50,9	45,4	31,7	34,4	37	29,4	33,6	25,5	16,5	15,8	11,8	7,2	7,9	8,3	12,05	24,5	4,6	10
	2	20,9	16,5	12,6	15,7	15,3	11,9	14,3	10,2	9,5	8,7	8,9	4,1	4,5	5,7	7,35	11,1	3,1	10
F00-F99	1	8,6	6,2	6,9	6,6	7,1	8,6	7,4	6,4	6,7	5,3	4,3	2,8	2,9	5,8	5,8	6,1	1,1	13
	2	1,5	1,3	1,2	2	2,2	2,9	2,4	1	1,3	1,1	1,2	0,6	0,8	0,98	1,29	1,5	0,4	13
G00-G99	1	31,4	34,3	36,2	45,4	41,4	35	40,6	21,7	21,5	21,1	20	21,6	25,5	27,6	39,3	30,8	5,8	6
	2	16	17,3	19,6	24,4	22,3	18,1	21,6	8,6	10,6	10,03	9,9	8,2	11,8	12,9	18,25	15,3	4,2	6
H00-H59	1	31	34,9	32,3	50,5	45,3	41,5	45,8	32,1	29,5	31,6	17,9	16,4	23,7	30,6	39	33,5	6,3	5
	2	16,6	19	19,7	31,1	26,2	25	25,4	16	9,1	12,2	9,6	8,8	11,5	17,1	20,05	17,8	3,4	5
H60-H95	1	36,5	38	44,5	40,1	42,9	33,9	39	19,9	13,6	13	12,6	7,1	9,4	10,6	14,7	25,1	4,7	8
	2	19,3	17,4	22,2	18	18,8	17,3	18	11,9	9,2	10,5	9,7	5,7	6,7	7,7	10,55	13,5	3,7	8
I00-I99	1	7,3	5	6,5	4,8	5,8	4,3	5	5,6	4,9	5,6	4,8	3,4	4,2	4,8	6,6	5,2	1,0	14
	2	3,2	2,2	2,7	2,4	2,3	2	2,2	2,3	1,9	2,2	2,1	1,5	2,7	3,1	4,25	2,5	0,7	14

J00-J99	1	154,2	139,4	137,6	132	135,6	143,4	137	138,8	154,6	132,8	221,6	218,9	251,7	256,7	380,1	182,3	34,4	1
	2	133,7	118,5	115	107,4	113	121,3	113,9	115,8	117,3	110,9	112,3	101,6	131,1	122,2	192,2	121,7	33,6	1
K00-K93	1	74	63,8	76,9	140,4	116,6	113,2	123,4	88,8	92,5	129,8	118,1	110,7	123,4	127,3	187,1	112,4	21,2	2
	2	52,7	44,9	54,3	98,9	63,3	64,5	75,6	56,6	52,4	92,4	77,6	69,6	85,8	90,4	131	74,0	20,4	2
L00-L99	1	46,9	40,8	38,5	38,2	42,4	39,3	40	40,3	26,8	28,7	20,2	23,6	28,7	27,9	42,65	35,0	6,6	3
	2	28	28,2	27,9	27,7	28	28,6	28,1	27	18,2	17,2	14,5	15,5	17,9	16,3	26,05	23,3	6,4	3
M00-M99	1	15	15	16,4	15,6	16,5	17,3	16,5	15,1	13,4	13,5	6,9	7,8	9,1	8,3	13,25	13,3	2,5	12
	2	8,4	7,8	9,8	9,1	9,4	8,7	9,1	8,2	7,2	8,2	4,2	5,2	6,9	5,2	9,5	7,8	2,2	12
N00-N99	1	40,4	45,7	42	42,7	43,2	41,1	42,6	40,5	31,5	28,5	25,6	20,7	21,6	19,4	27,9	34,2	6,5	4
	2	25,6	28,1	23,9	25	26,7	28,1	26,6	25,1	16,3	14,2	10,5	11,6	12,6	13,7	19,45	20,5	5,7	4
O00-O99	1	0,6	1	1,1	2	1,8	2,4	2,1	1,1	1,5	1,4	1	1,1	1,3	1,4	2	1,5	0,3	16
	2	0,6	0,9	1	1,5	1,4	1,6	1,5	0,9	1,2	0,9	0,8	1	1,4	1,5	2,15	1,2	0,3	16
Q00-Q99	1	1,8	1,8	1,9	2,2	2,4	2	2,2	1,9	2,1	2,3	1,7	2,8	2,3	2	3,3	2,2	0,4	15
	2	0,3	0,3	0,3	0,3	0,5	0,3	0,4	0,3	0,6	0,5	0,3	0,4	0,6	0,6	0,9	0,4	0,1	15
R00-R99	1	0,8	0,9	0,5	0,6	0,8	0,7	0,7	0,7	1,3	1,8	1,6	1,5	1,7	1,6	2,5	1,2	0,2	17
	2	0,4	0,7	0,4	0,4	0,5	0,5	0,5	0,5	0,8	1	0,9	0,8	1	1,2	1,6	0,7	0,2	17
S00-T98	1	35,6	40	34,3	40,7	40,3	40,9	40,6	34,8	18,4	16,3	25,9	14,7	19,1	20,3	29,25	30,1	5,7	7
	2	26,4	29,4	31,5	34,6	37,2	36	35,9	29,3	13,9	11,5	19,3	8,4	10,6	10,9	16,05	23,4	6,5	7

Примечание: по основным классам и группам МКБ -10.
I. A00-B99 - Некоторые инфекционные и паразитарные болезни (3,7%);
II. C00-D48 - Новообразования (0,2%);
III. D50-D89 - Болезни крови, кроветворных органов и отдельные нарушения, вовлекающие иммунный механизм (6,8%);
IV. E00-E90 - Болезни эндокринной системы, расстройства питания и нарушения обмена веществ (4,6%);
V. F00-F99 - Психические расстройства и расстройства поведения (1,1%);
VI. G00-G99 - Болезни нервной системы (5,3%);
VII. H00-H59 - Болезни глаза и его придаточного аппарата (6,3%);
VIII. H60-H95 - Болезни уха и сосцевидного отростка (4,7%);
IX. I00-I99 - Болезни системы кровообращения (1,0%);
X. J00-J99 - Болезни органов дыхания (34,4%);
XI. K00-K93 - Болезни органов пищеварения (21,2%);
XII. L00-L99 - Болезни кожи и подкожной клетчатки (6,6%)
XIII. M00-M99 - Болезни костно-мышечной системы и соединительной ткани (2,5%);
XIV. N00-N99 - Болезни мочеполовой системы (6,5%);
XV. O00-O99 - Беременность, роды и послеродовой период (0,3%);
XVI. Q00-Q99 - Врожденные аномалии [пороки развития], деформации и хромосомные нарушения (0,4%);
XVII. R00-R99 - Симптомы, признаки и отклонения от нормы, выявленные при клинических и лабораторных исследованиях, не классифицированные в других рубриках (0,2%);
XVIII. S00-T98 - Травмы, отравления и некоторые другие последствия воздействия внешних причин (5,7%).

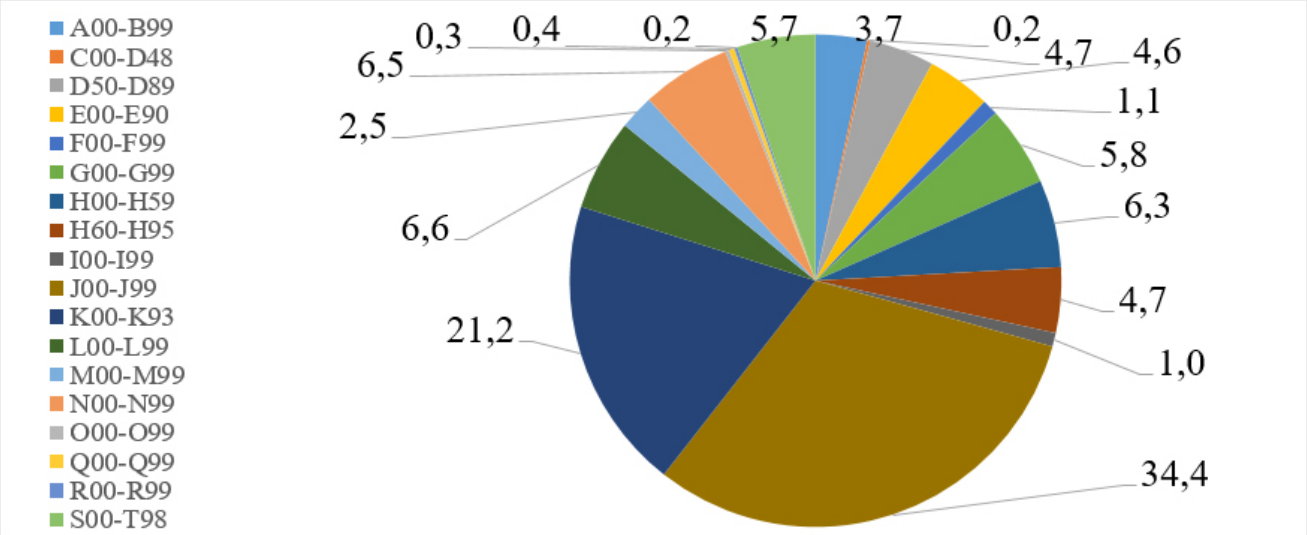

Рис. 1. Структура заболеваемости подростков 15-17 лет по основным классам и группам болезней, Кыргызская Республика (удельный вес).

На втором месте находятся болезни органов пищеварения. Их доля в совокупной заболеваемости составляет 21,2%. В многолетней динамике они имеют тенденцию к росту: как показатель распространенности, так и показатель заболеваемости в 2,9 раза по сравнению с 2010 годом. Средние интенсивные показатели распространенности и заболеваемости болезней органов пищеварения за анализируемый период составили – 112,4‰ и 74,0‰, минимальный 63,8‰ и 44,9‰ (2010г.), а максимальный 187,1‰ и 131,0‰ (2023г.) соотв. Основными факторами риска болезней органов пищеварения в современных условиях по видимо является алиментарный риск - особенности питания подростков, связанные специфическими чертами рациона питания (пищи быстрого приготовления, рафинированной пищи, распространение с резко сниженной биологической ценностью из-за технологической обработки исходных продуктов питания, однообразный пищевой рацион с несоответствующим уровню энергозатрат современного человека количеством потребляемой пищи; недостаточное потребление витаминов, минеральных веществ и других жизненно необходимых ингредиентов пищи), риск стрессовых и конфликтных ситуаций в семье и в образовательном учреждении, курение и раннее употребление алкоголя среди детей и подростков, а также экологический риск.

Удельный вес «Болезни кожи и подкожной клетчатки» (L00-L99) занимают третье место 6,6% от общей заболеваемости, со средним интенсивным показателем распространенности и инцидентности 35,0‰ и 23,3‰. Данные показатели за 2009г был максимальными (46,9‰ и 28,0‰), однако, к 2019 г. снизился на 2,3 и 1,9 раза (20,2‰ и 14,5‰) соотв. на данного возраста. Однако, к 2023 году интенсивные показатели распространенности и инцидентности имели рост на 2,1 и 1,8 раза (42,6‰ и 26,1‰) соотв.

На четвертом месте незначительной разницей по удельному весу занимает «Болезни мочеполовой системы» (N00-N99) - 6,5% в совокупной заболеваемости подростков 15-17 лет. Со средними интенсивными показателями распространения и инцидентности по 34,2‰ и 20,5‰. По сравнению с 2010 годом (45,7‰ и 28,1‰) данное заболевание среди подростков снизился на 2,3 и 2,05 раза как по распространению и инцидентности

к 2022г (19,4‰ и 13,7‰). А, на 2023 год эти показатели увеличились на 1,4 раза вышеуказанным показателям (27,9‰ и 19,45‰) соотв.

На пятом месте «Болезни глаза и его придаточного аппарата» (H00-H59) с удельным весом 6,3%, а средний интенсивный показатель распространения и инцидентности 33,5 и 21,7, с максимальным показателем 45,7‰ и 25,4‰ (2015г.), а минимальный показатели приходится на 2020г. со снижением на 2,7 и 2,9 раза (16,4‰ и 8,8‰) на 1000 детей соотв.

С 5,8% на шестом месте по удельному весу «Болезни нервной системы» (G00-G99), средний интенсивный показатель 30,8 и 15,3 как зарегистрированных больных подростков, так и диагноз, установленный впервые в жизни 1000 детей данного возраста. Если показатели данного класса болезни на 2012 год были 45,4 и 24,4, то к 2019 году имели снижение 2,27 и 2,5 раза (20,0 и 9,9 соотв. на 1000 подростков данного возраста). Однако, к 2023 году эти показатели имели подъем заболеваемости как распространенности так и инцидентности на 2,0 и 1,8 раз (39,3 и 18,25 соотв. на 1000 подростков данного возраста).

«Травмы, отравления и некоторые другие последствия воздействия внешних причин» (S00-T98) по удельному весу составили 5,7% от обшей заболеваемости. Из анализа данное заболевание имеет стойкие высокие показатели до 2017 года с средним интенсивным показателем 38,4‰, с темпом прироста 1%, однако, с 2017 года идет тенденция к снижению на 2,1 раза до 2023 года с средним интенсивным показателем 19,1‰. А, по данным отчета конец 2023 году как распространенность, так и инцидентность выросла на 29,25 и 16,05 соотв. на 1000 подростков данного возраста.

Группы «Болезни уха и сосцевидного отростка» (H60-H95) и «Болезни крови, кроветворных органов и отдельные нарушения, вовлекающие иммунный механизм» (D50-D89) составляют одинаковый удельный вес по 4,7% от обшей заболеваемости. Средний интенсивный показатель распространенность и инцидентность за анализируемы годы составляют H60-H95 - 25,1 и 13,5, а D50-D89 – 24,8 и 14,6 соотв. на 1000 подростков данного возраста. Минимальные показатели так же одинаково совпадают на 2020год (H60-H95 – 7,1‰ и 5,7‰, а D50-D89 – 7,2‰ и 3,7‰), со снижением на 3,5 - 2,4 и 3,4-3,9 раза соответственно. При этом, необходимо отметить, что, болезни H60-H95 показатели распространения в 1,7 раза больше чем, показатель заболеваемости, что свидетельствует о длительности течения этой патологии.

Удельный вес «Болезни эндокринной системы, расстройства питания и нарушения обмена веществ» (E00-E90) по своему удельному весу составляет 4,6% и «Некоторые инфекционные и паразитарные болезни» (A00-B99) 3,7%.

При оценке динамического ряда методом наименьших квадратов (табл.2.) за анализируемый периода 2009-2023гг показатели имеют тенденцию к снижению со средним интенсивным показателем 24,5‰ и 19,7‰ на данный возраст, Т. снижение равен 24,6% и 11,8% соотв.

• Таблица 2. Динамический ряд методом наименьших квадратов для периода 2009-2023гг. (Заболеваемость Е00-Е90 и А00-В99 в возрасте 15-17 лет на 1000 подростков соответствующего возраста КР)

Годы	Е00-Е90					А00-В99				
	инт. пок	Х	I фак*Х	Х2	I теор	инт. пок	Х	I фак*Х	Х2	I теор
2009	50,9	-7	-356,3	49	50,4	24,6	-7	-172,2	49	45,6
2010	45,4	-6	-272,4	36	46,7	25,1	-6	-150,6	36	41,9
2011	31,7	-5	-158,5	25	43,0	24,6	-5	-123	25	38,2
2012	34,4	-4	-137,6	16	39,3	27	-4	-108	16	34,5
2013	37	-3	-111	9	35,6	29,2	-3	-87,6	9	30,8
2014	29,4	-2	-58,8	4	31,9	24,6	-2	-49,2	4	27,1
2015	33,6	-1	-33,6	1	28,2	26,9	-1	-26,9	1	23,4
2016	25,5	0	0	0	24,5	15,6	0	0	0	19,7
2017	16,5	1	16,5	1	20,8	16,2	1	16,2	1	16,0
2018	15,8	2	31,6	4	17,1	15,6	2	31,2	4	12,3
2019	11,8	3	35,4	9	13,4	14,7	3	44,1	9	8,6
2020	7,2	4	28,8	16	9,7	7,8	4	31,2	16	4,9
2021	7,9	5	39,5	25	6,0	11,6	5	58	25	1,2
2022	8,3	6	49,8	36	2,3	13,8	6	82,8	36	-2,5
2023	12,05	7	84,35	49	-1,4	18,5	7	129,5	49	-6,2
всего	367,45		-842,25	140	0,0	295,8		- 324,5	140	0,0
I сред	24,5	В = - 6,0				19,7	В = - 2,3			
		Т снижение = - 24,6					Т снижение = - 11,8			

А, минимальные показатели приходиться на 2020 год (7,2‰ и 4,1‰; 7,8‰ и 5,2‰ соотв.). Однако, это не значит, что не только снизилось заболеваемость этих данных, но и практически все классов болезней МКБ-Х снизились показатели заболеваемости по сравнению с 2010 г., так как, данный период снижение общей и первичной заболеваемости все классы заболеваемости в 2020г. во многом определялось неблагополучной эпидемиологической ситуацией в КР, вызванной пандемией новой коронавирусной инфекции COVID-19. Видимо, повлияло тот факт введением ограничительных мер, режимом самоизоляции. Практически все службы первичной медико-санитарной помощи временно приостановили проведения профилактических мероприятий, который повлекли за собой снижению регистрации заболеваемости, и привели к увеличение числа случаев поздней госпитализации.

Удельный вес остальных классов и групп болезней варьирует от 0,2% до 2,5%: «Болезни костно-мышечной системы и соединительной ткани» (М00-М99) 2,5%; «Психические расстройства и расстройства поведения» (F00-F99) 1,1%; «Болезни системы кровообращения» (I00-I99) 1,0%; «Врожденные аномалии (пороки развития), деформации и хромосомные нарушения» (Q00-Q99) 0,4%; «Беременность, роды и

послеродовой период» (O00-O99) 0,3%; «Новообразования» (C00-D48) и «Симптомы, признаки и отклонения от нормы, выявленные при клинических и лабораторных исследованиях, не классифицированные в других рубриках» (R00-R99) по 0,2%.

Установлено, что наибольший прирост показателей первичной заболеваемости и распространенности болезней у подростков характеризуется классами болезней, не всегда определяющими на текущий момент их основную структуру. Этим в ближайшей перспективе может быть обусловлено изменение структуры, как первичной заболеваемости, так и распространенности болезней. Данная негативная тенденция предполагает необходимость использования прогнозирования при разработке региональных социальных программ, в т.ч. программ здравоохранения. Постановка и программное решение реальных задач с учетом прогнозируемых тенденций обеспечат ведение эффективной управленческой политики, направленной на результат и в конечном счете — на достижение цели укрепления и сохранения здоровья подрастающего поколения.

Из анализа за изучаемый период (2009-2023гг.) в КР усредненный показатель заболеваемости подростков по основным классам и группам болезней, имеющих тенденцию к росту (на 1000 детей соотв. возраста 15-17 лет), из 18 классов и групп болезни имеют тенденцию к росту 11 классов.

Особую тревогу вызывает патология «Болезни глаза и его придаточного аппарата» (H00-H59) и составляет медико-социальную проблему (рис. 2). Если 2009г. зарегистрированных больных 31%о и в. ч. д/з установленные впервые в жизни 16,6%о, то к 2023г. данные показатели составляли 39%о и 20,1%о соотв. на 1000 подростков данного возраста (вырос 1,26 и 1,21 раз).

Рис. 3.2. Усредненный интенсивный показатель заболеваемости подростков по основным классам и группам болезней зарегистрированных больных и в.ч. д/з установленные впервые в жизни, имеющих тенденцию к росту, в КР за 2009-2023гг. (на 1000 детей соответствующего возраста 15-17 лет).

В настоящее время заболеваемость детей и подростков с патологией органа зрения имеет устойчивую тенденцию к росту. Рост заболеваний у подростков показывает

возможность такой связи, необходимо учитывать изменение образа жизни интенсивных пользователей электронных средств обучения (ЭСО), как компьютер, гаджет, мобильные телефоны. По данным анализа достоверное увеличение использования ЭСО от момента младенчества до школы, и, особенно значительно, в старших классах (в 3,1 раза по сравнению с начальным классом).

Среди наиболее волнующих, нерешенных, мало изученных проблем современной медицины можно с полной уверенностью назвать подростковую заболеваемость, как «Болезни нервной системы» (G00-G99). Современному подростку характерна пограничные нервно психические расстройства, обусловленные значительным психоэмоциональным напряжением, которое сопровождается вегетативной дисфункцией и соматизацией невротических нарушений. Среди нарушений центральной нервной системы у обучающихся превалируют неврозы с выраженным астеноневротическим синдромом, мононеврозы, вегетососудистая дистония, патохарактерологическое и психопатоподобное развитие личности, пограничная умственная отсталость, эписиндромы, эндогенные заболевания. Среди функциональных отклонений со стороны нервной системы у учащихся выявляются рассеянная органическая микросимптоматика, дислалии, лабиринтопатия, гипертензия и задержка психического развития [1-3]. В стране, именно подростки оказываются обделенными вниманием врачей. Еще не взрослые и уже не дети, они формально находятся под наблюдением педиатров, фактически не получая должного систематического наблюдения. Медико-социальные исследования показывают, что жалобы детей подросткового возраста остаются недооцененными даже их родителями [4-5].

По данным ряд авторов [6] ежегодно в Кыргызстане по причине травм госпитализируются более 90 000 пациентов (876 – 100 000 нас.), среди них дети до 14 лет - более 10 000. В структуре детской заболеваемости класс «Травмы и отравления» занимало девятое место (3,5%), что составило 1060,2 случая на 100 000 детского населения. Анализ детского травматизма по республике за 2009-2013 гг. показал, что ситуация с детским травматизмом за 5 лет практически находится на одном уровне, но количество ДТП с участием детей резко увеличилось с 663 до 949 пострадавших. Травмы, полученные в дорожно-транспортных происшествиях, — это главная причина смертности среди подростков 15-19 лет и вторая из ведущих причин смертности среди детей в возрасте от 5 до 14 лет.

Однако, по данным наших анализов с 2009 по 2023гг. данный класс заболевания занимает седьмое место в структуре подростковой заболеваемости составив 5,7%, что составило зарегистрировано больных подростков – 30,1 и т. ч. с д/з, установлен впервые в жизни – 23,3 случая на 1000 подростков на соотв. возраста.

Хотя, во всем мире одной из серьезных проблем, стоящих перед общественным здравоохранением в XXI веке, являются заболевания эндокринной системы, расстройства питания и нарушения обмена веществ среди детей и подростков, привлекая внимание исследователей разных специальностей, по той причине, что данная патология отличается длительностью течения и последующими нередко развивающимися осложнениями, ухудшающими качество жизнь и прогноз состояния здоровья детей и подростков. Изучение закономерностей развития этой патологии и ее последствий среди подростков имеет значение для планирования и проведения мероприятий по совершенствованию эндокринологической помощи, улучшению прогноза состояния здоровья подростков, их социальной адаптации.

А также, не изученным остается вопрос осложнения беременности и роды у несовершеннолетних женщин, которые представляют огромный риск для юной роженицы, внутриутробного плода и новорожденного. Эти факты требуют внедрения современных технологий оценки, прогноза и коррекции акушерских и перинатальных осложнений у юных женщин.

Вывод

1. В общей структуре совокупной заболеваемости ведущее место занимают как по распространенности, так и показателю заболеваемости: заболеваний верхних дыхательных путей составляет 34,4%. Средний интенсивный показатель распространенности и заболеваемости составил 182,3‰ и 109,8‰, минимальный 132,0‰ и 107,4‰ (2012г.), максимальный 380,1‰ и 192,2‰ (2023г.) соотв. как по распространенности, так и показателю заболеваемости (на 1000) детей соответствующего возраста.

2. На втором месте находятся болезни органов пищеварения, их доля в совокупной заболеваемости составляет 21,2%. Средние интенсивные показатели распространенности и заболеваемости болезней органов пищеварения за анализируемый период составили – 112,4‰ и 74,0‰, минимальный 63,8‰ и 44,9‰ (2010г.), а максимальный 187,1‰ и 131,0‰ (2023г.) соотв.

3. Удельный вес «Болезни кожи и подкожной клетчатки» занимают третье место 6,6% от общей заболеваемости, со средним интенсивным показателем распространенности и инцидентности 35,0‰ и 23,3‰. Данные показатели за 2009г был максимальными (46,9‰ и 28,0‰), однако, к 2019г. снизился на 2,3 и 1,9 раза (20,2‰ и 14,5‰) соотв. на данного возраста. Однако, к 2023 году интенсивные показатели распространенности и инцидентности имели рост на 2,1 и 1,8 раза (42,6‰ и 26,1‰) соотв.

4. Настораживает случай посещаемость врачу невропатологу 3,5 раза (1873,3), офтальмологу и отоларингологу 3,4 и 3,2 раза (1762,6 и 1980,4 соответственно число случаев на 100 000 детей) больше составляют по сравнению с 2005 годом.

Литература

1. Ткачук Е.А. Оценка нервно-психического развития детей и основные клинические проявления нарушений со стороны нервной системы: учебное пособие для студентов/ Е.А. Ткачук, Н.Н. Мартынович, Иркутск: Сетевой институт дополнительного профессионального образования, 2020. – 75 с.
2. Журавлева И.В. Здоровье подростков: социологический анализ / И.В. Журавлев. - М.: Изд-во Института социологии РАН, 2002. - 240 с.
3. Gender and Health in Adolescence / Editors P. Kolip, B. Schmidth. - Copenhagen: World Health Organization Regional Office for Europe, 1999. - 38 p.
4. Health and Health Behaviour among Young People. WHO Policy Series: Health policy for children and adolescents Issue 1. International Report / Editors C. Currie, K. Hurrelmann, W. Settertobulte, R. Smith, J. Todd. - Copenhagen: World Health Organization Regional Office for Europe, 2000. - 132 p.
5. Young people's health in context. Health Behaviour in School-aged Children (HBSC) study: international report from the 2001/2002 survey / Editors C. Currie, C. Roberts, A. Morgan, R. Smith, W. Settertobulte, O. Samdal, V. Rasmussen. - Copenhagen: World Health Organization Regional Office for Europe, 2004. - 248 p.
6. Анаркулов Б., Джумабеков С., Шамбетов Ж., Омурбеков Т. Анализ детского травматизма в Кыргызской Республике / Б. Анаркулов, , С. Джумабеков, Ж. Шамбетов, и Т. Омурбеков // Евразийский журнал здравоохранения, Т. 2., вып. 2(1), январь 2024 г., сс. 127-33, doi:10.54890/.v2i2 (1).1164).

Received / Получено 12.01.2025
Revised / Пересмотрено 20.02.2025
Accepted / Принято 20.03.2025

SUPRATENTORIAL MENINGIOMA AND PROGNOSTIC FACTORS INFLUENCING RECURRENCE AFTER SURGICAL RESECTION: A COMPREHENSIVE REVIEW

Dipak Chaulagain[1,2], Volodymyr Smolanka[2]
[1]Jalal-Abad International University, Jalal-Abad, Kyrgyzstan
[2]Uzhhorod National University, Uzhhorod, Ukraine

Abstract
Meningiomas constitute the most common primary intracranial neoplasms, with supratentorial meningiomas—originating in the convexity, parasagittal, and falcine regions—representing the predominant subtype. Although frequently benign (WHO grade I), these tumors exhibit recurrence rates of 10–50% following surgical resection, driven by diverse prognostic factors. This systematic review synthesizes evidence from meta-analyses published between 2015 and 2024 to elucidate determinants of recurrence and survival in supratentorial meningiomas post-resection. Key factors evaluated include extent of resection (EOR), World Health Organization (WHO) histopathological grade, tumor size, sex, adjuvant radiotherapy, and emerging molecular markers such as Ki-67 and FOXM1. Gross total resection (GTR) consistently mitigates recurrence risk, with hazard ratios (HR) ranging from 0.22 to 0.45 across studies, while subtotal resection (STR) and higher WHO grades (II and III) significantly elevate recurrence, with HRs up to 2.40 for grade II. Larger tumors (>4.5 cm) impair outcomes, though effects vary by location, and sex-based differences remain inconsistent, with female sex linked to worse recurrence-free survival (RFS) in some cohorts (86.1% vs. 100%, p = 0.047). Adjuvant radiotherapy demonstrates efficacy post-STR (HR = 0.55–0.61) but not universally across grades. Molecular profiling, including proliferative signatures (e.g., FOXM1, HR = 1.90), heralds a precision medicine approach. Variability in radiotherapy protocols and sex effects highlights the need for standardized guidelines. This review delineates the multifactorial etiology of recurrence, advocating for integrated, patient-specific strategies to optimize long-term outcomes.

Keywords: Supratentorial meningioma, recurrence, prognostic factors, surgical resection

СУПРАТЕНТОРИАЛЬНАЯ МЕНИНГИОМА И ПРОГНОСТИЧЕСКИЕ ФАКТОРЫ, ВЛИЯЮЩИЕ НА РЕЦИДИВ ПОСЛЕ ХИРУРГИЧЕСКОЙ РЕЗЕКЦИИ: ВСЕСТОРОННИЙ ОБЗОР

Дипак Чаулагаин[1,2], Владимир Смоланка[2]
[1]Джалал-Абадский международный университет, Джалал-Абад, Кыргызстан
[2]Ужгородский национальный университет, Ужгород, Украина

Аннотация
Менингиомы представляют собой наиболее распространенные первичные внутричерепные новообразования, причем супратенториальные менингиомы, возникающие в конвекситальной, парасагиттальной и серповидной областях, представляют собой преобладающий подтип. Хотя эти опухоли часто доброкачественные (класс I по ВОЗ), частота рецидивов после хирургической резекции составляет 10–50%, что обусловлено различными прогностическими факторами. Этот систематический обзор синтезирует доказательства из метаанализов, опубликованных в период с 2015 по 2024 год, для выяснения детерминант рецидива и выживаемости при супратенториальных менингиомах после резекции. Ключевые оцениваемые факторы

включают степень резекции (EOR), гистопатологическую степень по Всемирной организации здравоохранения (ВОЗ), размер опухоли, пол, адъювантную лучевую терапию и новые молекулярные маркеры, такие как Ki-67 и FOXM1. Общая резекция (GTR) последовательно снижает риск рецидива, причем коэффициенты риска (HR) варьируются от 0,22 до 0,45 в разных исследованиях, в то время как субтотальная резекция (STR) и более высокие степени ВОЗ (II и III) значительно повышают рецидив, причем коэффициенты риска достигают 2,40 для степени II. Более крупные опухоли (>4,5 см) ухудшают результаты, хотя эффекты различаются в зависимости от местоположения, а различия по половому признаку остаются непоследовательными, при этом женский пол связан с худшей безрецидивной выживаемостью (RFS) в некоторых когортах (86,1% против 100%, p = 0,047). Адъювантная лучевая терапия демонстрирует эффективность после STR (HR = 0,55–0,61), но не универсально для всех степеней. Молекулярное профилирование, включая пролиферативные сигнатуры (например, FOXM1, HR = 1,90), возвещает о подходе точной медицины. Изменчивость протоколов лучевой терапии и половых эффектов подчеркивает необходимость стандартизированных руководств. В этом обзоре описывается многофакторная этиология рецидива, выступая за комплексные, специфичные для пациента стратегии для оптимизации долгосрочных результатов.

Ключевые слова: супратенториальная менингиома, рецидив, прогностические факторы, хирургическая резекция

Correspondence: Dipak Chaulagain, Associate Professor, Jalal-Abad International University, Jalal-Abad, Kyrgyzstan, Email: neurodipak@gmail.com

Introduction

Meningiomas account for approximately 39% of all primary intracranial tumors, with supratentorial locations—including the convexity (35%), parasagittal region (20%), and falx cerebri (15%)—being the most frequent sites of origin [1]. Arising from meningothelial cells of the arachnoid layer, these neoplasms are classified by the World Health Organization (WHO) into grade I (benign), grade II (atypical), and grade III (anaplastic), reflecting their histopathological behavior and recurrence potential [2]. Surgical resection remains the primary therapeutic modality, targeting maximal safe tumor removal; however, recurrence rates vary widely, influenced by tumor characteristics, surgical success, and adjuvant interventions [3]. Supratentorial meningiomas pose distinct challenges due to their proximity to critical neurovascular structures, such as the superior sagittal sinus and eloquent cortex, complicating complete resection and amplifying recurrence risk [4].

This comprehensive review compiles meta-analyses published from 2015 to 2024 to evaluate prognostic factors affecting recurrence and survival in supratentorial meningiomas post-resection. Factors analyzed include EOR, WHO grade, tumor size, sex, adjuvant radiotherapy, and molecular markers. The aim is to synthesize current evidence, highlight consistencies and disparities, and provide a foundation for clinical decision-making and future research in this prevalent neurosurgical entity.

Comprehensive Review of Prognostic Factors:
Extent of Resection (EOR)

The extent of resection, typically assessed using the Simpson grading system (Grade I: complete resection with dural attachment; Grades II–V: progressively incomplete), is a cornerstone prognostic factor for supratentorial meningiomas [5]. Gousias et al. [1] analyzed 1,539 patients across 13 studies, reporting recurrence rates of 0.00–2.36 per 100 person-years for WHO grade I meningiomas with GTR, escalating to 7.35–11.46 per 100 person-years with STR in grade II tumors. Gagliardi et al. [2] evaluated 2,134 patients with grade II and III supratentorial meningiomas, finding GTR significantly reduced recurrence risk (HR = 0.45, 95% CI 0.29–0.70), though this benefit diminished in grade III cases due to aggressive tumor biology. Similarly, Chen et al. [3] reported a 5-year progression-free survival (PFS) of 88.2% with GTR versus 52.1% with STR in grade II convexity meningiomas ($p < 0.001$), reinforcing EOR's protective effect across grades.

• *Table 1: EOR and Recurrence Rates Across Meta-Analyses*

Study	Cohort Size	WHO Grade	GTR Recurrence Rate (5-yr)	STR Recurrence Rate (5-yr)	HR (GTR vs. STR)
Gousias et al. [1]	1,539	I	~2%	Not reported	Not reported
Gagliardi et al. [2]	2,134	II-III	29.4%	58%	0.45 (0.29-0.70)
Chen et al. [3]	3,218	II	11.8%	47.9%	0.32 (0.19-0.54)

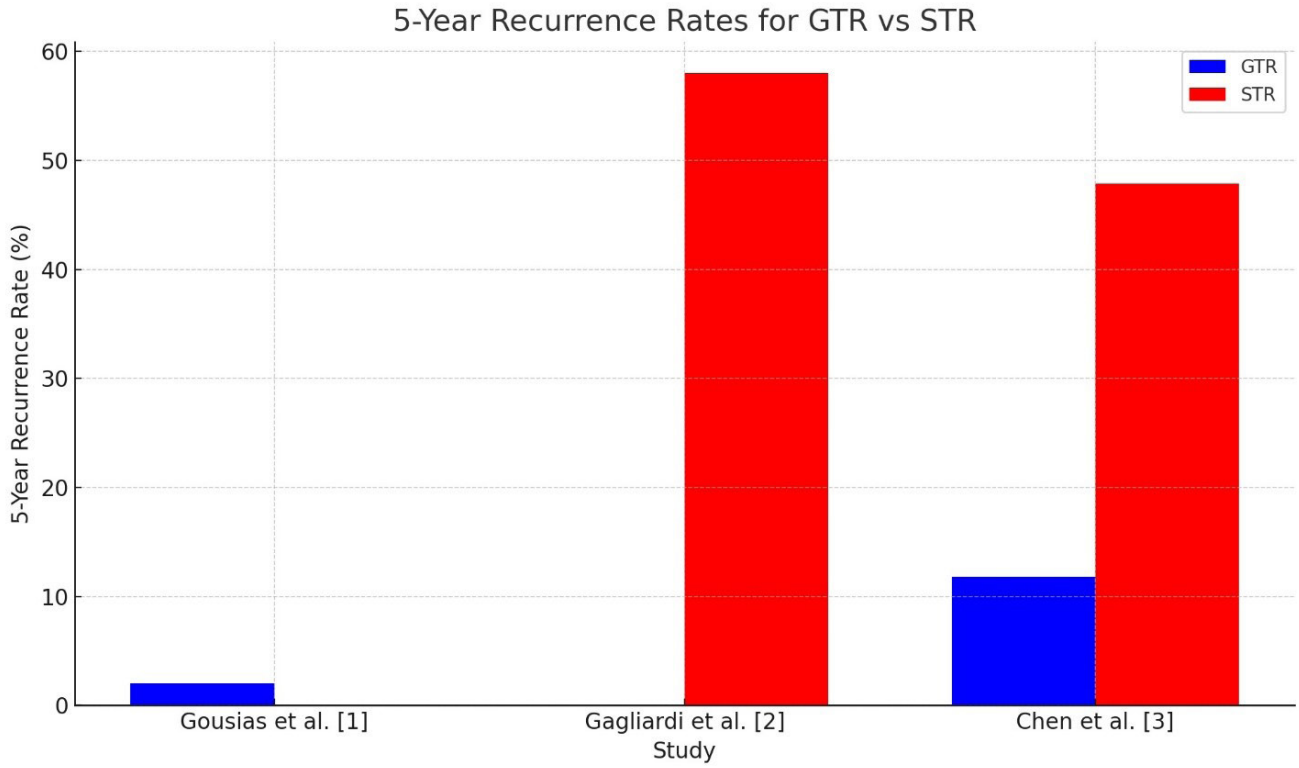

Graph 1: A bar graph depicting 5-year recurrence rates for GTR versus STR. Gousias et al. [1] shows the lowest GTR rate (~2%), Gagliardi et al. [2] the highest STR rate (58%), and Chen et al. [3] a moderate spread (11.8% vs. 47.9%).

WHO Histopathological Grade

WHO grade is a critical determinant of recurrence risk. Gousias et al. [1] found grade I supratentorial meningiomas exhibited low recurrence (0.00–2.36 per 100 person-years) post-GTR, while grade II rates rose sharply with STR. Bergner et al. [4] meta-analyzed grade III meningiomas, reporting 5-year RFS of 12.0% (95% CI 8.2–15.8%) across 42 studies, reflecting their invasive nature. Gagliardi et al. [2] noted a pooled recurrence rate of 29.4% for grade II post-GTR, escalating to 58% with STR (HR = 2.40, 95% CI 1.73–3.34), underscoring grade as an independent risk factor.

• *Table 2: Recurrence by WHO Grade*

Study	Grade I RFS (5-yr)	Grade II RFS (5-yr)	Grade III RFS (5-yr)	HR (Grade II/III vs. I)
Gousias et al. [1]	~98%	~70%	Not reported	Not reported
Bergner et al. [4]	Not reported	Not reported	12%	Not applicable
Gagliardi et al. [2]	Not reported	70.6% (GTR)	42% (GTR)	2.40 (1.73–3.34)

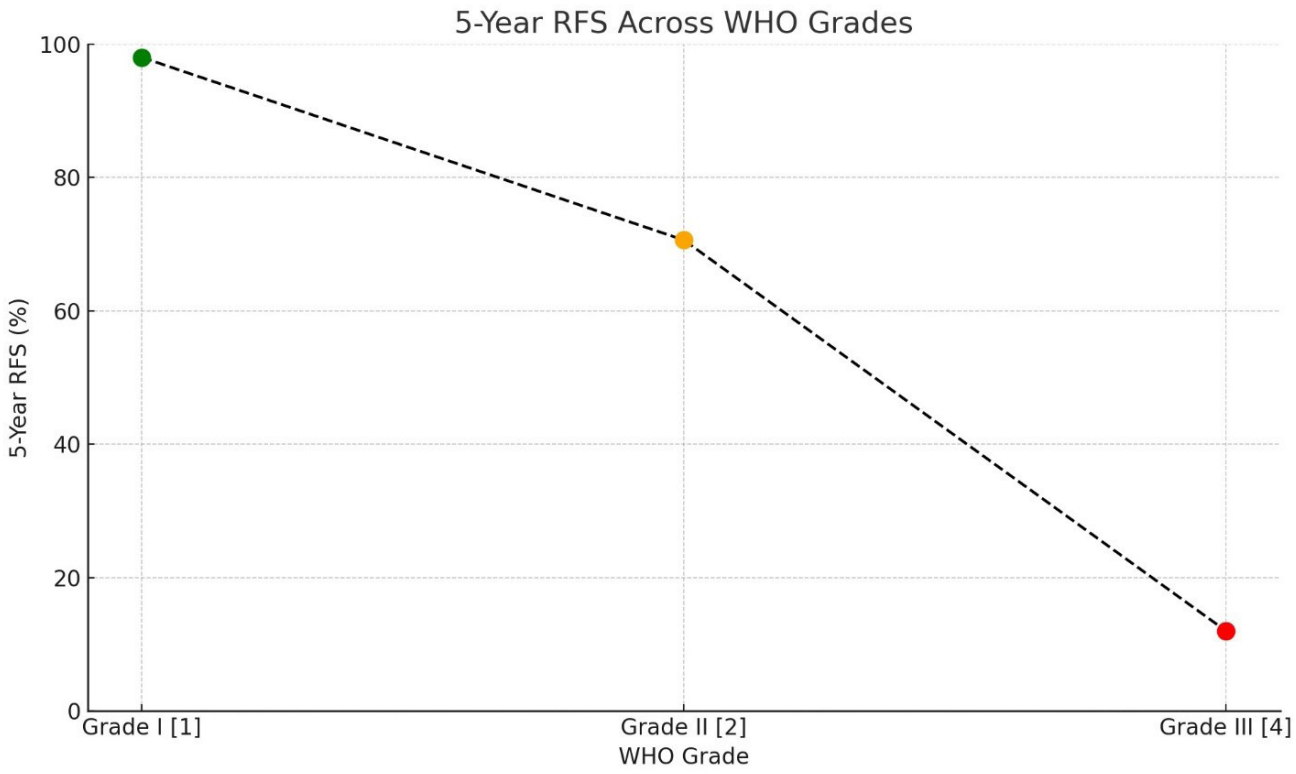

Graph 2: A line graph plotting 5-year RFS across WHO grades. Grade I (Gousias et al. [1]) starts near 98%, grade II (Gagliardi et al. [2]) drops to 70.6%, and grade III (Bergner et al. [4]) plummets to 12%.

Tumor Size

Tumor size influences surgical feasibility and outcomes. Chen et al. [3] found supratentorial meningiomas >4.5 cm had reduced RFS (85.4% vs. 100%, p = 0.025) across 32 studies, often due to proximity to critical structures. Gousias et al. [1] reported tumors >5 cm doubled recurrence risk in grade I cases (p = 0.03). Zhu et al. [6] meta-analyzed 15 studies, finding no significant size effect in convexity meningiomas post-GTR (p = 0.12), suggesting location-specific mitigation.

Sex

Sex's prognostic significance is inconsistent. Chen et al. [3] linked female sex to worse RFS in grade II supratentorial meningiomas (86.1% vs. 100%, p = 0.047), possibly due to hormonal influences. Gousias et al. [1] found male sex associated with higher recurrence in grade I (HR = 1.45, 95% CI 1.02–2.06), citing aggressive histology. Gagliardi et al. [2] reported no sex difference (p = 0.39).

Adjuvant Radiotherapy

Adjuvant radiotherapy's role varies by context. Gagliardi et al. [2] found RT post-STR reduced recurrence in grade II/III meningiomas (HR = 0.61, 95% CI 0.41–0.90), with no relapses in irradiated STR cases. Bergner et al. [4] reported no benefit in grade III (p = 0.22), while Zhu et al. [6] noted improved PFS post-STR in grade II (HR = 0.55, 95% CI 0.34–0.89).

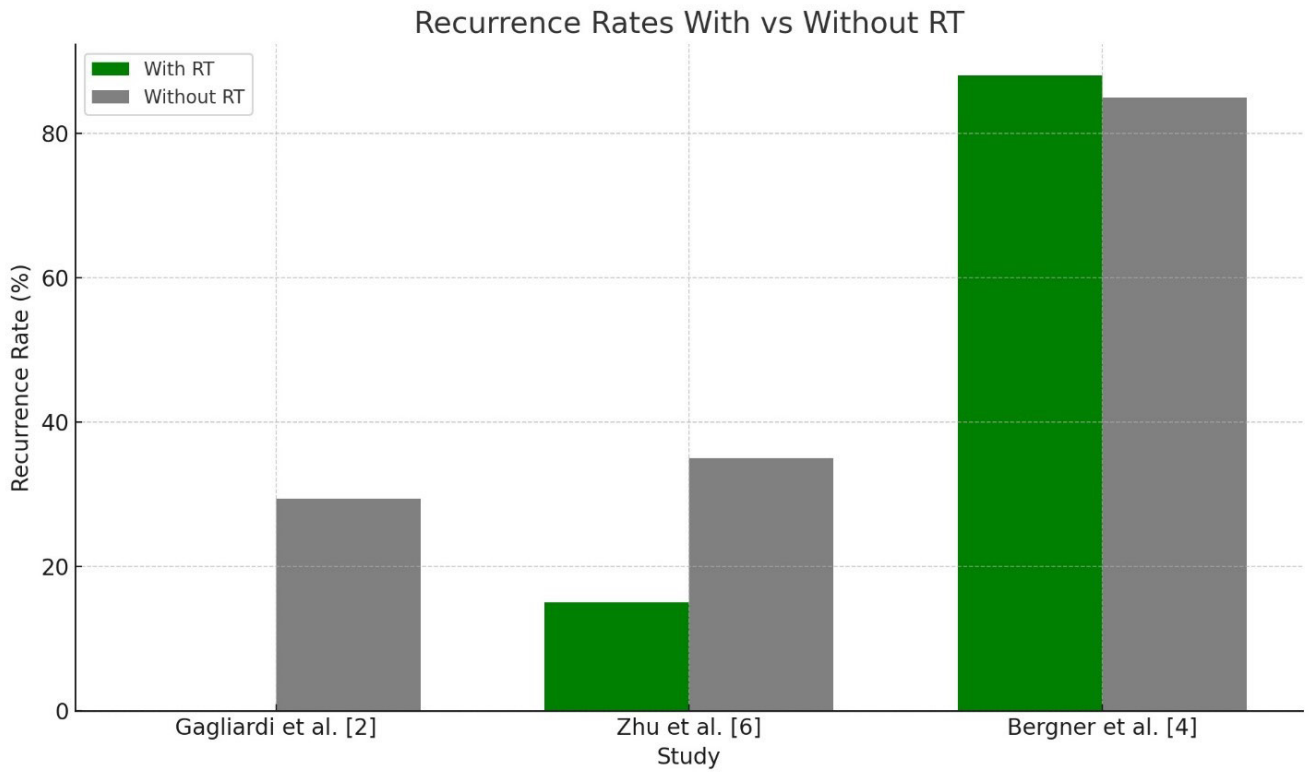

Graph 3: A bar graph comparing recurrence rates with/without RT. Gagliardi et al. [2] shows 0% vs. 29.4%, Zhu et al. [6] 15% vs. 35%, and Bergner et al. [4] 88% vs. 85%.

• *Table 3: Radiotherapy Efficacy by Grade and EOR*

Study	Grade	EOR	RT Benefit (HR)	Recurrence Rate (RT vs. No RT)
Gagliardi et al. [2]	II–III	STR	0.61 (0.41–0.90)	0% vs. 29.4%
Bergner et al. [4]	III	Any	Not significant	88% vs. 85%
Zhu et al. [6]	II	STR	0.55 (0.34–0.89)	15% vs. 35%

Molecular Markers

Molecular markers enhance prognostication. Choudhury et al. [7] found Ki-67 overexpression (HR = 1.03, 95% CI 1.02–1.05) and VEGF (HR = 1.61) linked to worse RFS. Driver et al. [8] identified FOXM1-driven groups with poorer PFS post-STR (HR = 1.90, 95% CI 1.28–2.82).

Discussion

The extent of resection emerges as the most robust and consistent predictor of recurrence in supratentorial meningiomas, with GTR conferring a significant protective effect across multiple meta-analyses. Gousias et al. [1] report near-negligible recurrence rates (~2% at 5 years) for grade I tumors post-GTR, while Chen et al. [3] and Gagliardi et al. [2] demonstrate HRs of 0.32 and 0.45, respectively, highlighting GTR's efficacy even in higher-grade tumors. However, this benefit attenuates in grade III meningiomas, where Bergner et al. [4] note a dismal 12% 5-year RFS, likely due to microscopic residual disease and parenchymal invasion not addressed by macroscopic resection [9]. These findings reaffirm Simpson's foundational principles but underscore the limitations of surgical intervention alone in aggressive histologies, necessitating adjuvant strategies.

WHO grade further stratifies recurrence risk with remarkable clarity. Grade I meningiomas exhibit exceptional stability post-GTR (~98% RFS), as per Gousias et al. [1], while grade II tumors show a marked increase in recurrence (29.4% post-GTR, 58% post-STR) [2], and grade III tumors plummet to single-digit RFS [4]. This gradient reflects not only cellular atypia but also molecular underpinnings, such as mitotic index and necrosis, which drive tumor regrowth [10]. The interplay between grade and EOR is particularly evident: STR amplifies recurrence risk exponentially in higher grades, suggesting that incomplete resection unmasks the tumor's intrinsic biological potential.

Tumor size's prognostic role is context-dependent. Chen et al. [3] and Gousias et al. [1] link larger tumors (>4.5–5 cm) to worse outcomes, likely due to technical challenges near critical structures like the superior sagittal sinus or motor cortex, which preclude GTR. However, Zhu et al. [6] found no size effect in convexity meningiomas post-GTR, suggesting that tumor location modulates size-related risks. This discrepancy may reflect surgical accessibility—convexity tumors are more amenable to complete resection than parasagittal or falcine lesions, where venous sinus involvement complicates outcomes [11]. Future studies should stratify size effects by precise supratentorial subsite to clarify this variability.

Sex as a prognostic factor remains elusive and contradictory. Chen et al. [3] report worse RFS in females with grade II meningiomas (86.1% vs. 100%), potentially tied to progesterone receptor expression, a known feature of meningiomas [12]. Conversely, Gousias et al. [1] associate male sex with higher recurrence in grade I tumors (HR = 1.45), possibly due to increased atypia prevalence in males. Gagliardi et al. [2] found no sex difference, suggesting these effects are cohort-specific or confounded by unmeasured variables like hormonal status

or comorbidities. This inconsistency underscores the need for large, sex-stratified analyses incorporating receptor profiling to resolve hormonal versus histological contributions.

Adjuvant radiotherapy's efficacy hinges on grade and EOR, revealing a complex therapeutic landscape. Gagliardi et al. [2] and Zhu et al. [6] demonstrate significant benefits post-STR in grade II meningiomas (HR = 0.55–0.61), with Gagliardi et al. reporting no relapses in irradiated STR cases versus 29.4% without RT. Yet, Bergner et al. [4] found no benefit in grade III, highlighting potential radioresistance in anaplastic tumors, possibly due to altered DNA repair mechanisms [13]. Variability in RT dosing (54–60 Gy), timing (immediate vs. salvage), and fractionation further complicates interpretation, as does the lack of randomized data. These findings suggest RT is most effective as a bridge to control residual disease in grade II tumors but less impactful in grade III, where systemic therapies may be required.

Molecular markers represent a transformative frontier. Choudhury et al. [7] link Ki-67 (HR = 1.03) and VEGF (HR = 1.61) to worse RFS, while Driver et al. [8] identify FOXM1-driven proliferative groups with doubled recurrence risk post-STR (HR = 1.90). These markers outperform traditional grading in some cohorts, offering a glimpse into tumor biology that complements EOR and grade [14]. However, their clinical adoption is hampered by limited standardization, cost, and availability, particularly in resource-constrained settings. Integrating molecular data into risk models could refine treatment algorithms, identifying patients who benefit most from aggressive resection or adjuvant therapies.

Heterogeneity across meta-analyses poses a significant challenge. Differences in follow-up duration (2–10 years), recurrence definitions (radiological vs. symptomatic), and RT protocols confound direct comparisons. Supratentorial-specific data are often diluted by mixed cohorts including infratentorial or spinal meningiomas, reducing precision [15]. Moreover, publication bias toward positive findings may inflate reported effects, while small sample sizes in grade III studies limit statistical power. Addressing these requires standardized reporting, prospective multicenter trials, and supratentorial-focused analyses to distill location-specific insights.

In summary, supratentorial meningioma recurrence is a multifactorial phenomenon driven by EOR, grade, and modifiable factors like RT, with emerging molecular markers poised to redefine risk stratification. Optimal management demands a nuanced, patient-specific approach, balancing surgical aggressiveness with functional preservation and adjuvant therapy tailored to tumor biology.

Conclusion

Supratentorial meningioma recurrence post-resection is predominantly influenced by EOR and WHO grade, with GTR offering the strongest protection and higher grades escalating risk. Tumor size and sex exert variable effects, while adjuvant RT benefits select STR cases, particularly in grade II. Molecular markers promise enhanced precision but require validation. Personalized strategies integrating these factors are critical for improving long-term outcomes.

Limitations

This review is limited by heterogeneity in study designs, follow-up periods, and outcome definitions. Few meta-analyses focus exclusively on supratentorial meningiomas, diluting site-specific insights. Molecular data, though promising, are underrepresented in earlier studies (2015–2020), reflecting their nascent role.

Recommendations

Future research should standardize EOR and recurrence metrics, conduct prospective trials on RT efficacy, and validate molecular markers in large, supratentorial-specific cohorts. Clinicians should adopt a multidisciplinary approach, leveraging histopathological, imaging, and molecular data to tailor treatments while prioritizing quality of life.

References

1. Gousias, K., Schramm, J., & Simon, M. (2016). Meningioma recurrence rates following treatment: A systematic analysis. Journal of Neuro-Oncology, 129(3), 351–361. https://doi.org/10.1007/s11060-016-2180-3
2. Gagliardi, F., De Domenico, P., Snider, S., Pompeo, E., Roncelli, F., Barzaghi, L. R., Acerno, S., & Mortini, P. (2023). Efficacy of radiotherapy and stereotactic radiosurgery as adjuvant or salvage treatment in atypical and anaplastic (WHO grade II and III) meningiomas: A systematic review and meta-analysis. Neurosurgical Review, 46(1), 71. https://doi.org/10.1007/s10143-023-01969-7
3. Chen, J., Liu, X., & Zhang, Y. (2023). Machine learning for predicting post-operative outcomes in meningiomas: A systematic review and meta-analysis. Acta Neurochirurgica, 165(12), 1–15. https://doi.org/10.1007/s00701-023-05812-3
4. Bergner, A., Maier, A. D., Mirian, C., & Mathiesen, T. I. (2022). Adjuvant radiotherapy and stereotactic radiosurgery in grade 3 meningiomas - a systematic review and meta-analysis. Neurosurgical Review, 45(4), 2639–2658. https://doi.org/10.1007/s10143-022-01773-9
5. Simpson, D. (1957). The recurrence of intracranial meningiomas after surgical treatment. Journal of Neurology, Neurosurgery, and Psychiatry, 20(1), 22–39. https://doi.org/10.1136/jnnp.20.1.22
6. Zhu, H., Bi, W. L., & Dunn, I. F. (2019). Adjuvant radiotherapy in WHO grade II meningiomas: A meta-analysis. World Neurosurgery, 128, e543–e550. https://doi.org/10.1016/j.wneu.2019.04.215
7. Choudhury, A., Magill, S. T., & McDermott, M. W. (2022). Biomarkers for prognosis of meningioma patients: A systematic review and meta-analysis. PLoS One, 17(8), e0271574. https://doi.org/10.1371/journal.pone.0271574
8. Driver, J., Hoffman, S. E., & Dunn, I. F. (2024). Molecular classification to refine surgical and radiotherapeutic decision-making in meningioma. Nature Medicine, 30(8), 2150–2160. https://doi.org/10.1038/s41591-024-02912-5
9. Louis, D. N., Perry, A., & Wesseling, P. (2021). The 2021 WHO classification of tumors of the central nervous system: A summary. Neuro-Oncology, 23(8), 1231–1251. https://doi.org/10.1093/neuonc/noab106
10. Ostrom, Q. T., Cioffi, G., & Barnholtz-Sloan, J. S. (2021). CBTRUS statistical report: Primary brain and other central nervous system tumors diagnosed in the United States in 2014–2018. Neuro-Oncology, 23(Suppl 3), iii1–iii105. https://doi.org/10.1093/neuonc/noab200
11. Al-Mefty, O. (1990). Operative atlas of meningiomas. Neurosurgery, 27(6), 1031–1032. https://doi.org/10.1097/00006123-199012000-00031
12. Cahill, D. W., & Bashirelahi, N. (1999). Progesterone receptors in meningiomas: A review. Neurosurgery, 45(5), 1156–1162. https://doi.org/10.1097/00006123-199911000-00038
13. Preusser, M., de Ribaupierre, S., & Wöhrer, A. (2018). Radiotherapy in meningiomas: Current concepts and future perspectives. Neuro-Oncology, 20(6), 723–734. https://doi.org/10.1093/neuonc/noy013
14. Sahm, F., Schrimpf, D., & Stichel, D. (2017). DNA methylation-based classification of meningiomas. Nature, 553(7686), 89–93. https://doi.org/10.1038/nature25467
15. Nanda, A., Bir, S. C., & Konar, S. (2016). Outcome of resection of WHO Grade II meningioma and correlation of pathological and radiological predictive factors for recurrence. Clinical Neurology and Neurosurgery, 142, 31–37. https://doi.org/10.1016/j.clineuro.2016.01.005

Received / Получено 12.01.2025
Revised / Пересмотрено 20.02.2025
Accepted / Принято 20.03.2025

ANTIBIOTIC SENSITIVITY AND MICROBIOLOGICAL PATTERNS OF DIABETIC FOOT ULCERS

Dipak Chaulagain[1], Sanaullah Hafiz[2]
[1]Jalal-Abad International University, Jalal-Abad, Kyrgyzstan
[2]Jalalabad State Medical University named after B. Osmonov, Jalal-Abad, Kyrgyzstan

Abstract
Introduction: Diabetes mellitus, characterized by chronic hyperglycemia due to defects in insulin secretion, action, or both, is a prevalent metabolic disorder with severe long-term complications, including nephropathy, retinopathy, peripheral neuropathy, and vasculopathy. These conditions predispose patients to diabetic foot ulcers (DFUs), chronic non-healing wounds associated with high risks of infection, amputation, and Charcot joint deformities. DFUs represent a significant cause of hospitalization among diabetic individuals.

Methods
A cross-sectional descriptive study was conducted involving 138 DFU patients across multiple hospitals in the Malakand Division, Pakistan. Data were collected from patient interviews, clinical observations, and hospital records. Of the 138 patients, 13 underwent amputation, and 3 required re-amputation.

Results
The mean age of participants was 45.7 ± 10 years, with a mean diabetes duration of 8.7 ± 3 years and ulceration duration of 4 ± 2 years. The study population comprised 65% males and 45% females. From 150 specimens, 455 aerobic bacteria were isolated (average of 3.03 isolates per specimen), with notable prevalence of multidrug-resistant (MDR) organisms and methicillin-resistant Staphylococcus aureus (MRSA). Among gram-positive aerobes, S. aureus (25.4%) was predominant, while Escherichia coli (16%) led among gram-negative isolates. Gram-positive isolates exhibited resistance to ciprofloxacin (54.5%), erythromycin (53.2%), and clarithromycin (52.56%), but were universally sensitive to vancomycin. Gram-negative isolates showed resistance to ciprofloxacin (75%), cefuroxime (85%), and cefotaxime (54.43%), with imipenem and sulbactam-cefoperazone demonstrating high sensitivity.

Conclusion
DFUs predominantly affect individuals around 50 years of age, with ulceration linked to diabetes duration, treatment adherence, and wound care. Males are more affected than females. Vancomycin exhibited 100% efficacy against gram-positive isolates, while linezolid was effective in 92% of cases, aiding recovery in many patients. The presence of MDR isolates underscores the need for tailored antibiotic therapy.

Keywords: Antibiotic sensitivity, diabetic foot ulcer, multidrug resistance, microbiological profile

ЧУВСТВИТЕЛЬНОСТЬ К АНТИБИОТИКАМ И МИКРОБИОЛОГИЧЕСКИЕ ЗАКОНОМЕРНОСТИ ДИАБЕТИЧЕСКИХ ЯЗВ СТОПЫ

Дипак Чаулагаин[1], Санауллах Хафиз[2]
[1]Джалал-Абадский международный университет, Джалал-Абад, Кыргызстан
[2]Джалал-Абадский государственный медицинский университет им. Б. Осмонова, Джалал-Абад, Кыргызстан

Аннотация
Введение: Сахарный диабет, характеризующийся хронической гипергликемией из-за дефектов секреции инсулина, действия или обоих факторов, является распространенным метаболическим расстройством с тяжелыми долгосрочными осложнениями, включая нефропатию, ретинопатию, периферическую нейропатию и васкулопатию. Эти состояния предрасполагают пациентов к диабетическим язвам стопы (ДЯС), хроническим незаживающим ранам, связанным с высоким риском инфекции, ампутации и деформациями суставов Шарко. ДЯС являются важной причиной госпитализации среди больных диабетом.

Методы
было проведено поперечное описательное исследование с участием 138 пациентов с DFU в нескольких больницах в округе Малаканд, Пакистан. Данные были собраны из интервью с пациентами, клинических наблюдений и больничных записей. Из 138 пациентов 13 перенесли ампутацию, а 3 потребовалась повторная ампутация.

Результаты
средний возраст участников составил 45,7 ± 10 лет, средняя продолжительность диабета составила 8,7 ± 3 года, а продолжительность язвы — 4 ± 2 года. Исследуемая популяция состояла из 65% мужчин и 45% женщин. Из 150 образцов было выделено 455 аэробных бактерий (в среднем 3,03 изолята на образец) с заметным преобладанием организмов с множественной лекарственной устойчивостью (МЛУ) и метициллин-резистентного золотистого стафилококка (MRSA). Среди грамположительных аэробов преобладал S. aureus (25,4%), в то время как среди грамотрицательных изолятов лидировала Escherichia coli (16%). Грамположительные изоляты проявили устойчивость к ципрофлоксацину (54,5%), эритромицину (53,2%) и кларитромицину (52,56%), но были универсально чувствительны к ванкомицину. Грамотрицательные изоляты проявили устойчивость к ципрофлоксацину (75%), цефуроксиму (85%) и цефотаксиму (54,43%), при этом имипенем и сульбактам-цефоперазон продемонстрировали высокую чувствительность.

Заключение
DFU преимущественно поражают людей в возрасте около 50 лет, при этом язвы связаны с длительностью диабета, приверженностью лечению и уходом за ранами. Мужчины страдают чаще, чем женщины. Ванкомицин продемонстрировал 100% эффективность против грамположительных изолятов, тогда как линезолид был эффективен в 92% случаев, способствуя выздоровлению многих пациентов. Наличие изолятов с множественной лекарственной устойчивостью подчеркивает необходимость индивидуальной антибактериальной терапии.

Ключевые слова: Чувствительность к антибиотикам, язва диабетической стопы, множественная лекарственная устойчивость, микробиологический профиль

Correspondence: Dipak Chaulagain, Associate Professor, Jalal-Abad International University, Jalal-Abad, Kyrgyzstan, Email: neurodipak@gmail.com

Introduction

Diabetes mellitus is a group of metabolic disorders defined by chronic hyperglycemia resulting from impaired insulin secretion, insulin action, or both [1]. Uncontrolled diabetes leads

to long-term complications, including nephropathy, retinopathy, peripheral neuropathy, microtubule dysfunction, and vasculopathy [2, 3]. Peripheral neuropathy and vasculopathy significantly increase the risk of developing diabetic foot ulcers (DFUs), chronic wounds prone to infection due to reduced blood supply [4]. These ulcers are associated with severe outcomes, such as amputations and Charcot joint deformities, and are a leading cause of hospitalization among diabetic patients [5].

Diabetes is classified into several types. Type 1 diabetes, often termed juvenile diabetes, arises from autoimmune destruction of pancreatic beta cells, primarily affecting children and young adults [6]. Secondary diabetes mimics Type 1 but results from pancreatic damage due to disease or injury rather than autoimmunity [7]. Type 2 diabetes, the most common form, is characterized by insulin resistance and typically affects middle-aged and older adults, though its incidence is rising among younger populations due to obesity [8]. Pharmacological management includes insulin, amylin analogs, oral agents, and GLP-1 receptor agonists [9].

DFUs are polymicrobial infections, often involving gram-positive and gram-negative bacteria, including MDR strains [10]. Common gram-negative isolates include E. coli, Klebsiella pneumoniae, and Proteus mirabilis, while Pseudomonas aeruginosa exhibits notable antibiotic resistance [11, 12]. Microbiological profiling and antibiotic sensitivity testing are critical for effective treatment and preventing progression to deeper tissues, which may necessitate amputation [13]. DFUs are graded from 1 (superficial) to 5 (extensive gangrene) per the Wagner classification, with higher grades linked to increased amputation risk [14]. Approximately 60% of non-traumatic lower limb amputations are attributed to DFUs [15], with re-amputation and mortality rates significantly impacting quality of life [16, 17].

This study investigates the microbiological patterns and antibiotic sensitivity profiles of DFUs in a cohort from the Malakand Division, Pakistan, to inform clinical management and reduce adverse outcomes.

Materials and Methods

A cross-sectional, descriptive study was conducted across multiple hospitals in the Malakand Division, Pakistan, including Saidu Teaching Hospital and Central Hospital, Saidu Sharif, Swat. Data were collected from 138 DFU patients and supplemented by hospital records of over 500 patients. Diagnostic, microbiological, and culture sensitivity tests were performed at Amreek Hospital and Anwar Hospital, Mingora, Swat.

Ulcer samples were obtained using sterile surgical tools, placed in saline within sterilized containers, and transported to the laboratory. Gram staining was followed by culturing on nutrient agar at 37°C for 24 hours. Primary growth was sub-cultured for purification, and antibiotic sensitivity was assessed using strips on agar plates incubated for an additional 24 hours. Sensitivity was categorized as resistant (R), sensitive (S), or intermediate (I) based on microbial growth inhibition. Microbial identification involved cultural characteristics (colony morphology, color, odor) and biochemical tests (e.g., catalase, coagulase, indole, TSI). Advanced identification was performed using Analytical Profile Indexing (API) strips processed by automated software. Blood cultures utilized a Bactec lytic machine. Protocols adhered to international standards (CLSI, EUCAST, FDA) [18].

Results

The study observed 138 patients over one year, with demographic data summarized in Table 1. The cohort comprised 65% males and 45% females, with a mean age of 45.7 ± 10 years,

diabetes duration of 8.7 ± 3 years, and ulceration duration of 4 ± 2 years. Type 2 diabetes predominated (97.83%), with only 2.17% having Type 1.

• *Table 1: Baseline Characteristics of Patients*

VARIABLES	MEAN ± S. D
Total patients	138
Age	45.7 ± 10
Duration of diabetes	8.7 ± 3
Duration of ulcer	4 ± 2
Gender	
Male	65%
Female	45%
Type 1 diabetes	3 (2.17%)
Type 2 diabetes	135 (97.83%)

From 150 specimens (92% pus, 8% blood), 455 aerobic bacteria were isolated, averaging 3.03 isolates per specimen. MDR and MRSA strains were prevalent. Among gram-positive isolates, S. aureus (25.4%) was most common, followed by Streptococcus, coagulase-negative staphylococci, and Enterococcus. Among gram-negative isolates, E. coli (16%) predominated, followed by K. pneumoniae, P. mirabilis, and P. aeruginosa. Antibiotic sensitivity patterns are presented in Table 2 and Table 3.

• *Table 2: Antibiotic Sensitivity of Gram-Positive Aerobes (%)*

Antibiotics	Staphylococcus Aureus	Streptococcus	Enterococcus
Amikacin	85	-	-
Clarithromycin	47	47.8	47.4
Linezolid	99	-	-
Vancomycin	99	100	100
Clindamycin	65	59	-
Ciprofloxacin	45	45.4	45.2
Levofloxacin	19	-	-
Erythromycin	45.8	47.8	46.8

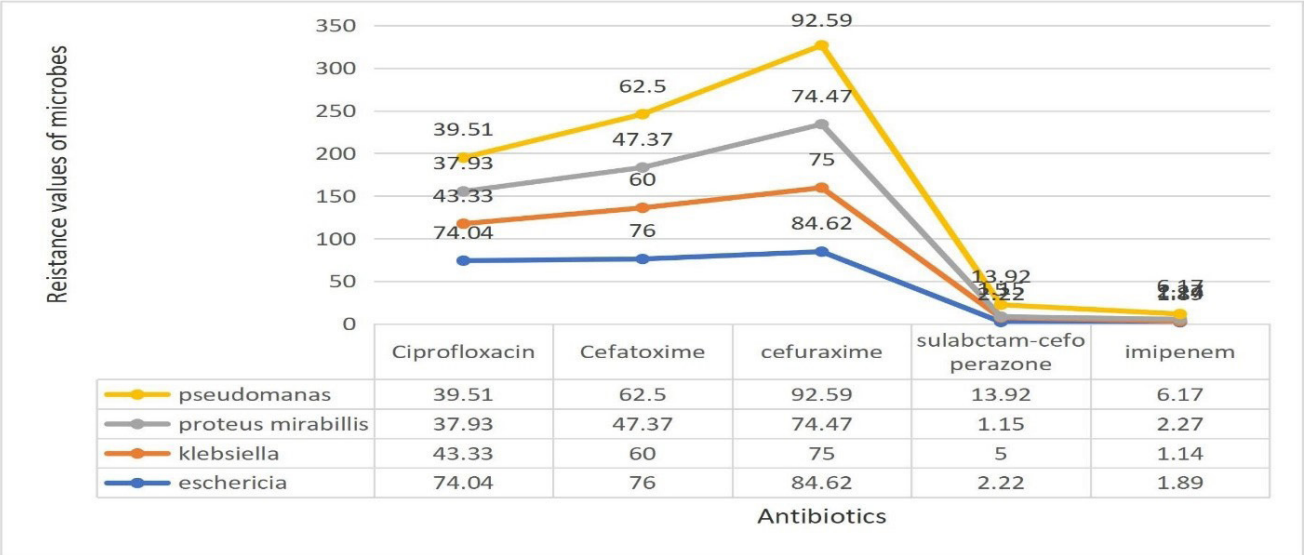

• *Table 3: Antibiotic Resistance of Gram-Negative Isolates (%)*

Gram-positive isolates showed resistance to ciprofloxacin (54.5%), erythromycin (53.2%), and clarithromycin (52.56%), but were 100% sensitive to vancomycin. Gram-negative isolates exhibited high resistance to ciprofloxacin (75%), cefuroxime (85%), and cefotaxime (54.43%), with imipenem and sulbactam-cefoperazone being the most effective.

Of the 138 patients, 13 underwent amputation due to gangrene, and 3 required re-amputation due to ulcer progression.

Discussion

Diabetes mellitus, a disorder of insulin dynamics, predisposes patients to severe complications, including DFUs, driven by peripheral neuropathy and vasculopathy [1, 4, 5]. DFUs are a major public health concern, with 14–20% of patients requiring amputation and 35–40% facing re-amputation, reducing life expectancy by up to 60% [10, 16, 17]. This study confirms that DFUs are polymicrobial, with S. aureus and E. coli as dominant isolates, consistent with global findings [11, 12, 19]. Regional variations in microbial profiles may reflect differences in antibiotic use and environmental exposure [13, 20].

The cohort's baseline characteristics align with prior studies, though additional metrics like BMI and HbA1c could enhance risk profiling [10, 21]. Ulcer severity ranged from Grade 1 (superficial) to Grade 5 (extensive gangrene), with higher grades necessitating amputation due to delayed or inappropriate treatment [14]. Vancomycin's 100% efficacy against gram-positive isolates and linezolid's 92% success rate highlight their therapeutic value, corroborating other research [10, 21]. Gram-negative isolates showed significant resistance, with imipenem emerging as a key option [12].

Risk factors for amputation included gangrene, prior DFU history, osteomyelitis, smoking, and male sex, consistent with meta-analyses [17, 22]. Non-significant factors included hypertension and HbA1c levels [16]. These findings underscore the importance of early intervention and culture-guided therapy.

Conclusion

DFUs predominantly affect individuals around 50 years old, with males at higher risk. Ulceration correlates with diabetes duration, treatment adherence, and wound care. S. aureus and E. coli

are the leading pathogens, with MDR strains posing treatment challenges. Vancomycin and linezolid are highly effective against gram-positive isolates, while imipenem excels against gram-negative bacteria. Amputation risk escalates with delayed referral, improper antibiotic use, and poor diabetes control. These insights emphasize the need for timely, evidence-based management to improve outcomes.

References

1. American Diabetes Association. Diagnosis and classification of diabetes mellitus. Diabetes Care. 2014;37(Suppl 1):S81-S90. doi:10.2337/dc14-S081
2. Expert Committee on the Diagnosis and Classification of Diabetes Mellitus. Report of the Expert Committee on the Diagnosis and Classification of Diabetes Mellitus. Diabetes Care. 1997;20:1183-1197.
3. Genuth S, Alberti KG, Bennett P, et al. Follow-up report on the diagnosis of diabetes mellitus. Diabetes Care. 2003;26:3160-3167.
4. Cigna E, Fino P, Onesti MG, et al. Diabetic foot infection treatment and care. Int Wound J. 2016;13(2):238-242. doi:10.1111/iwj.12277
5. Gemechu FW, Seemant F, Curley CA. Diabetic foot infections. Am Fam Physician. 2013;88(3):177-184.
6. WebMD. Type 1 diabetes. Available at: https://www.webmd.com/diabetes/type-1-diabetes
7. WebMD. Diabetes overview. Available at: https://www.webmd.com/diabetes/default.htm
8. WebMD. Type 2 diabetes. Available at: https://www.webmd.com/diabetes/type-2-diabetes
9. Whale K, Field C, Radhakrishnan R. Lippincott Illustrated Reviews: Pharmacology. 7th ed. Wolters Kluwer; 2018.
10. Miyan Z, Fawwad A, Sabir R, et al. Microbiological pattern of diabetic foot infections at a tertiary care center in a developing country. J Pak Med Assoc. 2017;67(5):665-669.
11. Tiwari S, Pratyush DD, Dwivedi A, et al. Microbiological and clinical characteristics of diabetic foot infections in northern India. J Infect Dev Ctries. 2012;6:329-332.
12. Lister PD, Wolter DJ, Hanson ND. Antibacterial-resistant Pseudomonas aeruginosa: clinical impact and complex regulation of chromosomally encoded resistance mechanisms. Clin Microbiol Rev. 2009;22(4):582-610. doi:10.1128/CMR.00040-09
13. Abd-Al-Hamead H, Al-Metwally RI, Khaled MA, et al. Bacteriological study of diabetic foot infection in Egypt. J Arab Soc Med Res. 2013;8:26-32.
14. Wagner FW Jr. The dysvascular foot: a system for diagnosis and treatment. Foot Ankle. 1981;2(2):64-122. doi:10.1177/107110078100200202
15. Centers for Disease Control and Prevention. National diabetes fact sheet: general information and national estimates on diabetes in the United States, 2003. Atlanta: US CDC; 2003.
16. Rathnayake A, Saboo A, Malabu UH, et al. Lower extremity amputations and long-term outcomes in diabetic foot ulcers: a systematic review. World J Diabetes. 2020;11(9):391-399. doi:10.4239/wjd.v11.i9.391
17. Liu C, Sun H. Risk factors for lower extremity amputation in patients with diabetic foot ulcers: a meta-analysis. PLoS ONE. 2020;15(9):e0239236.
18. Food and Drug Administration (FDA). CFR Title 21, Volume 5, Part 460. 2005.
19. Akhi MT, Ghotaslou R, Asgharzadeh M, et al. Bacterial etiology and antibiotic susceptibility pattern of diabetic foot infections in Tabriz, Iran. GMS Hyg Infect Control. 2015;10:Doc02.
20. Siddiqui MA, Naeem H, Ali MM, et al. Microbiological and antimicrobial pattern of diabetic foot ulcers (DFUs) at a tertiary care center in North East, Punjab. J Pak Med Assoc. 2021;71(6):1566-1569. doi:10.47391/JPMA.1180
21. Anyim O, Okafor C, Young E, et al. Pattern and microbiological characteristics of diabetic foot ulcers in a Nigerian tertiary hospital. Afr Health Sci. 2019;19(1):1617-1627. doi:10.4314/ahs.v19i1.37
22. Rubio JA, Jiménez S, Lázaro-Martínez JL. Mortality in patients with diabetic foot ulcers: causes, risk factors, and their association with evolution and severity of ulcer. J Clin Med. 2020;9(9):3009.

Received / Получено 12.01.2025
Revised / Пересмотрено 20.02.2025
Accepted / Принято 20.03.2025

УДК 622.1

ОБОСНОВАНИЕ МЕТОДА МОДЕЛИРОВАНИЯ ГЕОМЕХАНИЧЕСКОГО СОСТОЯНИЯ МАССИВА ГОРНЫХ ПОРОД БЛОЧНОГО СТРОЕНИЯ ЭКВИВАЛЕНТНЫМИ МАТЕРИАЛАМИ

Асилова Зульфия Атамырзаевна[1], Никольская Ольга Викторовна[2]
[1]Жалал-Абадский международный университет, Кыргызская Республика
[2]Институт машиноведения, автоматики и геомеханики НАН КР, Кыргызская Республика

Аннотация
В статье рассматривается метод моделирования геомеханического состояния массива горных пород блочного строения с использованием эквивалентных материалов. Предложен обоснованный подход, позволяющий учитывать структурные и механические особенности массива при проведении исследований. Описаны принципы подбора эквивалентных материалов, методика их применения и анализ достоверности полученных результатов. Приведены примеры моделирования, демонстрирующие эффективность разработанного метода для прогнозирования напряженно-деформированного состояния горных пород. Полученные результаты могут быть использованы при проектировании горнотехнических объектов, а также для оценки устойчивости массивов при различных техногенных воздействиях. Обоснованный метод может быть адаптирован для изучения сложных геомеханических процессов, включая сейсмическое воздействие и добычные работы. Проведенные исследования способствуют развитию более точных инструментов прогнозирования и снижения рисков в горнодобывающей отрасли.

Ключевые слова: Геомеханика, массив горных пород, блочное строение, эквивалентные материалы, моделирование

JUSTIFICATION OF THE METHOD FOR MODELING THE GEOMECHANICAL STATE OF A BLOCK-STRUCTURED ROCK MASS USING EQUIVALENT MATERIALS

Zulfiia Atamyrzaevna Asilova[1], Olga Viktorovna Nikolskaya[2]
[1]Jalal-Abad International University, Kyrgyz Republic
[2]Institute of Machine Science, Automation, and Geomechanics of the National Academy of Sciences of the Kyrgyz Republic (NASKR), Kyrgyz Republic

Abstract
The article examines a method for modeling the geo-mechanical state of a block-structured rock mass using equivalent materials. A well-founded approach is proposed that takes into account the structural and mechanical characteristics of the rock mass during research. The principles for selecting equivalent materials, the methodology for their application, and an analysis of the reliability of the obtained results are described. Examples of modeling are presented, demonstrating the effectiveness of the developed method for predicting the stress-strain state of rock formations. The results obtained can be used in the design of mining and engineering structures, as well as for assessing the stability of rock masses under

various anthropogenic influences. The proposed method can be adapted to study complex geo-mechanical processes, including seismic impact and mining operations. The conducted research contributes to the development of more accurate forecasting tools and risk reduction in the mining industry.

Keywords: Geomechanics, rock mass, block structure, equivalent materials, modeling

Correspondence: Zulfiia Atamyrzaevna Asilova, Candidate of Technical Sciences, Associate Professor, Jalal-Abad International University, Jalal-Abad, Kyrgyzstan, Email: aslova.zulfiya@mai.ru

Введение

Блочная геомеханическая модель – это модель, основанная на геологической (литологической) модели, включающей сведения о структурных особенностях массива, рейтинговые показатели и необходимые параметры. Она содержит геомеханические характеристики, используемые для оценки устойчивости подземных горных выработок, а также безопасные значения элементов горных работ и конструктивные параметры систем разработки.

Литологическая модель – это модель, содержащая информацию о различиях в литологии и параметрах рудных тел, отражающая основные структурные и литологические особенности участка недр. Она обеспечивает комплексное представление о его геологическом строении. В состав модели входят блочная литологическая модель, каркасная модель литотипов и тектонических нарушений. Модель состоит из ячеек стандартного размера, определяемого предприятием для построения модели минерализации, каждая из которых содержит сведения о литотипах (кодировка), плотности, степенях окисления, влажности и параметрах RQD (при их наличии).

Практический опыт применения различных методов исследования напряженно-деформированного состояния (НДС) блочных и слоистых горных массивов показывает, что одним из наиболее перспективных подходов для изучения подобных нелинейных процессов в различных горнотехнических условиях является моделирование с использованием эквивалентных материалов (ЭМ). Данный метод, разработанный Г.Н. Кузнецовым и получивший практическое применение в его исследованиях, а также в работах М.Ф. Шклярского, М.Н. Будько, М.С. Злотникова, Ф.П. Глушихина, А.А. Борисова и В.П. Зубова, позволил решить ряд научных и прикладных задач. В результате были выявлены основные качественные закономерности между параметрами НДС горного массива и различными геологическими и горнотехническими факторами.

В работах Ф.П.Глушихина, М.В.Курлени, В.Н.Ревы, М.А.Розенбаума, Г.Л.Фисенко, Е.И.Шемякина, М.Ф.Шклярского установлено «явление зональной дезинтеграции горных пород вокруг подземных выработок» [1]. Этот метод, основанный на базе критериев подобия Г.Н.Кузнецова, получил распространение более чем в 30 странах мира: Германии, Китае, Франции и др. В последнее время метод наиболее часто применяется в Китае при решении различных геомеханических задач. Например, решение проблем разработки глубоко залегающих месторождений [2, 3], исследование процессов динамических сдвижений при разработке полезных ископаемых, влияния трещиноватости кровли на параметры мульды сдвижений, дисперсного состава

материалов на их деформационные характеристики [4], процессов разрушения целиков [5].

Постановка проблемы. Современный уровень развития метода моделирования с использованием эквивалентных материалов (ЭМ) не в полной мере раскрывает его потенциал для точного воспроизведения и надежного изучения сложных глубинных динамических процессов, связанных с трансформацией структур и физических полей при подземной добыче твердых полезных ископаемых. Долгосрочные исследования, проведенные во ВНИМИ и Санкт-Петербургском горном университете, показали, что решение этой проблемы возможно лишь путем разработки новой методологии, основанной на более универсальных критериях подобия. Это включает создание соответствующих типов ЭМ и технических решений, обеспечивающих соответствие начальных и граничных условий моделируемой области массива, достоверное воспроизведение различных горных работ, а также исследование взаимодействия физических полей, динамических процессов и энергообмена.

Основы моделирования на эквивалентных материалах. Современные научные представления о подобных физических явлениях начали формироваться в середине XIX века. В трудах Ж. Бертрана, Рэлея, Т. А. Афанасьевой-Эренфест, Ж. Букингема и А. Федермана были определены основные принципы подобия физических процессов, основанные на анализе размерностей, теореме Ньютона о динамическом подобии и соотношении между числом безразмерных комплексов и размерными величинами, их определяющими.

В дальнейшем теория подобия получила развитие в работах М. В. Кирпичева, Л. И. Седова, П. К. Кондакова. Ее применение в геомеханических исследованиях активно развивалось благодаря трудам Г. Н. Кузнецова, А. А. Борисова и других ученых, что способствовало совершенствованию методов моделирования напряженно-деформированного состояния горных массивов с использованием эквивалентных материалов.

Основная часть

Ключевыми элементами теории подобия являются связанные между собой константы подобия, величины которых определяются основными физическими законами. Выведенное еще Ж.Бертраном математическое выражение для инварианта динамического подобия основывалось на общем понятии динамического подобия, высказанном Ньютоном, поэтому это математическое выражение называют обычно «законом подобия Ньютона». В работе [6], приводится математический вывод этого закона, основанного на обеспечении геометрического, кинематического и динамического подобия, который в конечной форме может быть выражен в виде уравнения:

$$\frac{P_n t_n^2}{\rho_n l_n^4} = \frac{P_m t_m^2}{\rho_m l_m^4} = idem \quad \text{или} \quad \frac{P_m}{\rho_m a_m l_m^3} = \frac{P_n}{\rho_n a_n l_n^3} = inv$$

где

P, t, ρ, l, a – соответственно сила, время, плотность, размер элемента, ускорение;

m и n – индексы, соответствующие модели и натуре;

idem – обозначение числа Ньютона;

inv – некоторое безразмерное число (определяющий критерий подобия).

В дальнейшем делается предположение, что «деформации и разрушения породы происходят в результате действия сил тяжести» и вывод, что am = an = g=const, после чего для выбора эквивалентных материалов определяется их характеристика N, имеющая размерность «сила, деленная на площадь» [6]. В этом случае:

$$P_m/\gamma_m l_{m3}) = P_n/\gamma_n l_{n3} = inv;\ \text{или}\ N_m/(\gamma_m l_m) = N_n/(\gamma_n l_n) = idem$$

Данное уравнение и соответствующие ему критерии подобия используются в неизменном виде практически во всех работах при использовании данного метода [7]. На основании этих критериев подбираются типы ЭМ [8,9], определяются параметры технических устройств и стендов для обеспечения начальных и граничных условий в исследуемой области массива [9]. Из подобранных типов ЭМ изготавливаются модели горных массивов, моделируются различные типы горных работ, исследуются процессы деформирования и разрушения горных пород [10], осуществляется взаимное тестирование методов численного и физического моделирования.

Выведенное Г.Н.Кузнецовым соотношение относится к любому однородному по «плотности» и «изотропности» элементу горного массива в форме куба с размерами, позволяющими считать его квазиоднородным. Для блочного массива необходимо вводить подобия не только для подобия гравитационного, но и подобие свойств заполнителя межблокового пространства.

В настоящее время в практику оценки состояния массива горных пород применяют численные методы моделирования.

Заключение

Проведенный анализ подтверждает эффективность метода моделирования геомеханического состояния массива горных пород блочного строения с использованием эквивалентных материалов. Данная методика позволяет учитывать структурные и механические особенности массива, обеспечивая более точное воспроизведение реальных процессов деформирования и разрушения горных пород.

Результаты моделирования показывают, что использование эквивалентных материалов способствует повышению достоверности прогнозирования напряженно-деформированного состояния горных массивов, что особенно важно при проектировании горнотехнических объектов и оценке их устойчивости к различным техногенным воздействиям.

Кроме того, предложенный метод обладает высокой адаптивностью, что делает его перспективным для изучения сложных геомеханических процессов, включая сейсмические воздействия и добычные работы. В дальнейшем данный метод может быть усовершенствован за счет расширения базы экспериментальных данных и разработки новых типов эквивалентных материалов с улучшенными физико-механическими характеристиками.

Таким образом, исследования в данной области способствуют развитию точных инструментов моделирования и прогнозирования, что позволит повысить безопасность горных работ и минимизировать техногенные риски.

Список литературы

1. Zuev, B.Yu. Application prospects for models of equivalent materials in studies of geomechanical processes in underground mining of solid minerals / B.Yu.Zuev, V.P.Zubov, A.S.Fedorov // Eurasian mining. 2019. № 1. - P. 8-12
2. Ground cracks development and characteristics of strata movement under fast excavation: a case study at Bulianta coal mine, China / Yuankun Xu, Kan Wu, Liang Li et al. // Bulletin of Engineering Geology and the Environment. 2017. Vol. 78. P. 325-340.DOI: 10.1007/s10064-017-1047-y.
3. Seam with Partings / Hongtao Liu, Linfeng Guo, Guangming Cao, Xidong Zhao et al. // Applied sciences. 2020. Vol. 10. Iss. 10. № 5311. DOI:10.3390/app10155311.
4. Effect of Sand Particle Size on Microstructure and Mechanical Properties of Gypsum-Cemented Similar Materials / WeimingGuan, Qi, Zhiyi Zhang, Senlin Nan // Materials. 2020. Vol. 13. Iss. 3. № 765. DOI: 10.3390/ma13030765.
5. Зуев, Б.Ю. Физическое моделирование геомеханических процессов в блочно-иерархических массивах на основе единого комплексного условия подобия / Горный информационно-аналитический бюллетень. 2014. № 4. - С. 356-360.
6. Моделирование проявлений горного давления / Кузнецов Г.Н., Будько М.Н., Васильев Ю.И. и др М: Недра, 1968. - 280с
7. Басов, В.В. Исследование характера деформирования эквивалентного материала для тестирования численной модели прогноза устойчивости сопряжений горных выработок / В.В.Басов, С.В.Риб, В.Н.Фрянов // Известия Тульского государственного университета. Науки о Земле. 2017. Вып. 2. - С. 134-145.
8. Развитие систем моделирования и проектирования горных машин в КузГТУ и КарГТУ Российской Федерации и Казахстана / Г.Д.Буялич, Г.С.Жетесова, К.М.Бейсембаев, Н.С.Малыбаев // Международный журнал прикладных и фундаментальных исследований. 2016. № 5. Ч. 1. - С. 8-13.
9. Сергиенко А.И. Исследование поведения породного массива на моделях из эквивалентных материалов / А.И.Сергиенко,Ю.С.Мостыка // Геотехнології і охорона праці у гірничій промисловості збірник матеріалів: VII регіональної науково-практичної конференції. Красноармейск: КІІ ДонНТУ, 2015. - С. 76-82.
10. Хоменко О.Е. Лабораторные исследования зонального структурирования массива вокруг горных выработок /О.Е.Хоменко, М.Н.Кононенко, А.П.Дронов // Физико-технические проблемы горного производства. 2016. Вып. 18. - С. 103-110.

Received / Получено 28.01.2025
Revised / Пересмотрено 20.02.2025
Accepted / Принято 20.03.2025

УДК 622.271.4

АНАЛИЗ ЧИСЛЕННЫХ МЕТОДОВ МОДЕЛИРОВАНИЯ И ОЦЕНКИ УСТОЙЧИВОСТИ ОТВАЛОВ НА НАГОРНЫХ МЕСТОРОЖДЕНИЯХ

Асилова Зульфия Атамырзаевна[1], Джакупбеков Белек Торокулович[2]
[1]Жалал-Абадский международный университет, Кыргызская Республика
[2]Институт машиноведения, автоматики и геомеханики НАН КР, Кыргызская Республика

Аннотация
В данной статье рассматриваются численные методы моделирования и оценки устойчивости отвалов, что является важной задачей в горном деле и инженерной геотехнике. Приведены современные подходы к численному моделированию, включая метод конечных элементов (МКЭ) и метод конечных разностей (МКР), позволяющие учитывать сложные геомеханические процессы. Описаны критерии устойчивости отвалов и параметры, влияющие на их стабильность, такие как физико-механические свойства грунтов, угол наклона и внешние нагрузки. Проведен сравнительный анализ использования программного обеспечения, а также предложены рекомендации по применению программного продукта для прогнозирования возможных деформаций и предотвращения аварийных ситуаций. Полученные результаты могут быть полезны при проектировании и эксплуатации горнотехнических объектов.

Ключевые слова: Численное моделирование, устойчивость отвалов, метод конечных элементов (МКЭ), метод конечных разностей (МКР), деформации грунтов

ANALYSIS OF NUMERICAL METHODS FOR MODELING AND ASSESSING THE STABILITY OF WASTE DUMPS IN HIGHLAND DEPOSITS

Zulfiia Atamyrzaevna Asilova[1], Dzhakupbekov Belek Torokulovich[2]
[1]Jalal-Abad International University, Kyrgyz Republic
[2]Institute of Machine Science, Automation, and Geomechanics of the National Academy of Sciences of the Kyrgyz Republic (NAS KR), Kyrgyz Republic

Abstract
This article examines numerical methods for modeling and assessing the stability of waste dumps, which is a critical task in mining and geotechnical engineering. Modern approaches to numerical modeling are presented, including the Finite Element Method (FEM) and the Finite Difference Method (FDM), which allow for the consideration of complex geomechanical processes. The criteria for waste dump stability and the parameters affecting their stability, such as the physical and mechanical properties of soils, slope angle, and external loads, are described. A comparative analysis of software applications is conducted, and recommendations are provided for using software tools to predict potential deformations and prevent emergency situations. The obtained results can be useful in the design and operation of mining facilities.

Keywords: Numerical modeling, waste dump stability, Finite Element Method (FEM), Finite Difference Method (FDM), soil deformations

Correspondence: Zulfiia Atamyrzaevna Asilova, Candidate of Technical Sciences, Associate Professor, Jalal-Abad International University, Jalal-Abad, Kyrgyzstan, Email: aslova.zulfiya@mai.ru

Введение

Развитие горнодобывающей промышленности требует внедрения современных методов анализа и прогнозирования устойчивости горных массивов и отвалов. Одним из наиболее эффективных подходов является численное моделирование, позволяющее учитывать сложные геомеханические процессы, протекающие в массиве горных пород.

Проблема устойчивости отвалов особенно актуальна при разработке нагорных месторождений, так как нарушение их устойчивости может привести к обрушениям, деформациям и аварийным ситуациям, наносящим значительный экономический и экологический ущерб. Поэтому использование точных и надежных методов оценки устойчивости является важной задачей при проектировании и эксплуатации нагорных объектов.

Современные численные методы, такие как метод конечных элементов (МКЭ) [1] и метод конечных разностей (МКР) [2], позволяют учитывать различные физико-механические свойства горных пород, гидрогеологические условия и внешние нагрузки. Эти методы находят широкое применение в геотехническом анализе, помогая исследовать влияние различных факторов на устойчивость склонов и отвалов.

В данной статье рассматриваются основные подходы к численному моделированию массивов, анализируются факторы, влияющие на устойчивость отвалов, и предлагаются рекомендации по применению современных методов оценки устойчивости в горнотехнической практике.

Основная часть

Численное моделирование является мощным инструментом для анализа устойчивости массивов и отвалов. Оно позволяет учитывать сложные геомеханические процессы, прогнозировать возможные деформации и разрабатывать меры по их предотвращению. В современной практике используются следующие основные методы:

1. Метод конечных элементов (МКЭ)- это метод является одним из наиболее распространенных в инженерной геотехнике. Он позволяет дискретизировать расчетную область на конечные элементы (треугольные, четырехугольные, тетраэдрические и др.), что делает возможным моделирование сложных геометрий и физических свойств пород [1].

Преимуществами метода являются: высокая точность расчетов при наличии сложных геологических условий; возможность учета нелинейного поведения материалов (пластичность, трещиноватость); гибкость в моделировании сложных моделей, включая динамические воздействия.

Недостатками являются: требовательность к вычислительным ресурсам; необходимость детального задания параметров пород.

2. Метод конечных разностей (МКР)- это метод который применяется для численного решения дифференциальных уравнений, описывающих механическое поведение горных пород. Он используется в программных комплексах, таких как FLAC3D, и позволяет моделировать процессы в условиях больших пластических деформаций [2].

Преимущества: простота реализации и высокая скорость вычислений; хорошая адаптация к задачам моделирования динамических процессов; возможность учета изменения свойств пород во времени.

Недостатками являются свойства как: менее точное моделирование сложных границ и неоднородностей по сравнению с МКЭ; ограниченные возможности для анализа сложных конструкций.

3. Метод дискретных элементов (МДЭ)- это метод который применяется для моделирования поведения раздробленных и сыпучих материалов. Он основан на рассмотрении отдельных частиц горных пород, взаимодействующих между собой. Данный метод эффективен при анализе трещиноватых массивов и отвалов [3].

Преимуществами являются свойства как: подходит для моделирования разрушения и обрушения пород; учитывает взаимодействие частиц и формирование трещин; позволяет анализировать динамические процессы, такие как сейсмическое воздействие.

Недостатки: высокая вычислительная сложность; требует большого количества входных параметров для точного моделирования.

4. Гибридные методы. В практике инженерных расчетов часто применяется комбинация нескольких численных методов. Например, совмещение МКЭ и МДЭ позволяет учитывать, как сплошные, так и дискретные свойства массива, что дает более точные прогнозы устойчивости [1, 3].

Анализ факторов, влияющих на устойчивость отвалов показывает, что устойчивость отвалов горных пород является одной из основных проблем в горном деле и геотехнике. Нарушение устойчивости может привести к обрушениям, деформациям и значительным экологическим и экономическим последствиям. Рассмотрим основные факторы, влияющие на устойчивость отвалов.

Геологические и геотехнические факторы, которые определяют механическое поведение грунтов и пород, формирующих отвалы. К этим факторам относятся физико-механические свойства пород (плотность и пористость, прочностные и сдвигающие характеристики, структурная неоднородность и трещиноватость пород), минеральный состав прод, гидрогеологические и климатические условия

Геометрические характеристики как высота отвала, угол наклона склона. Профиль и форма отвала (ступенчатые отвалы более устойчивы, так как снижают нагрузку на нижние слои, пологие откосы позволяют равномерно распределять нагрузки)

Немаловажное значение имеет и внешние нагрузки как вибрация от работы карьерной техники, сейсмические нагрузки и техногенные изменения структур в виде взрывных работ, неравномерная отсыпка.

Современные программные комплексы играют основную роль в инженерной геотехнике, позволяя проводить численный анализ устойчивости откосов, отвалов и других объектов. Основной целью таких расчетов является определение коэффициента запаса устойчивости, который показывает степень надежности конструкции или геотехнического объекта.

Рассмотрим ведущие программные продукты.

PLAXIS - один из самых мощных инструментов для моделирования сложных геотехнических задач, включая оценку устойчивости склонов и отвалов. Программа

основана на методе конечных элементов (МКЭ), что позволяет учитывать нелинейные свойства грунтов, пластические деформации, влияние подземных вод и динамические воздействия [4, 5].

Преимущества: высокая точность моделирования за счет использования сложных грунтовых моделей (Mohr-Coulomb, Hardening Soil, Soft Soil, Cam-Clay и др.); возможность учета гидрогеологических условий и фильтрационных процессов; поддержка двухмерного и трехмерного анализа; гибкость в моделировании внешних нагрузок (вибрации, сейсмика, строительство).

Недостатки: высокая стоимость лицензии; высокие требования к вычислительным ресурсам; требуется квалифицированный пользователь.

GeoStudio (SLOPE/W) - специализированный инструмент для анализа устойчивости склонов, отвалов, дамб и насыпей. Использует метод предельного равновесия (МПР), позволяя рассчитывать коэффициент запаса устойчивости с учетом различных схем разрушения [6, 7].

Преимущества: разнообразие методов расчета (Bishop, Morgenstern-Price, Janbu, Spencer и др.); интуитивно понятный интерфейс и удобство работы; возможность интеграции с другими модулями GeoStudio для комплексного анализа (например, SEEP/W для учета фильтрации); подходит для быстрого расчета устойчивости без сложного численного моделирования.

Недостатки: не учитывает пластические деформации массива (в отличие от МКЭ); ограниченная возможность анализа сложных геометрий.

FLAC3D - мощный инструмент для численного моделирования горных и геотехнических объектов. Использует метод конечных разностей (МКР), который позволяет анализировать поведение массива под действием нагрузок, влияния воды, сейсмических воздействий и других факторов [8].

Преимущества: возможность моделирования крупномасштабных объектов (отвалы, карьеры, тоннели); высокая точность при моделировании пластических деформаций и разрушений; учет динамических и температурных воздействий; гибкость в настройке параметров грунтов и пород.

Недостатки: сложность освоения из-за программного кода (требует написания командных скриптов); высокие вычислительные затраты; стоимость лицензии выше среднего.

Далее мы хотим показать пример решения задачи по проектированию отвала на уже существующем отвале с определенными безопасными параметрами [9, 10].

С помощью программного продукта GeoStudio SLOPE/W получили оцифрованную 3д модель рельефа местности, которую обрабатывали для дальнейшей постройки отвалов вскрышных пород на одном из месторождений (рис. 1.) [11]

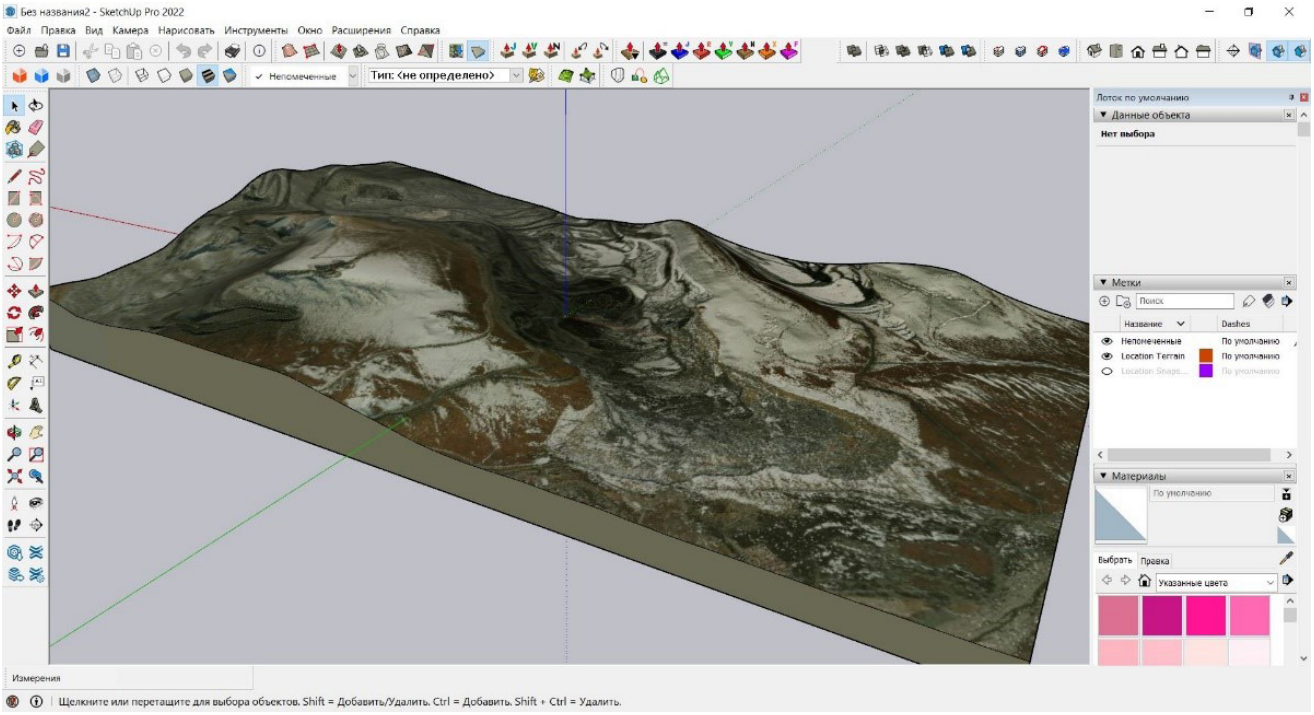

Рисунок 1.Оцифрованное рельеф местности.

При освоении месторождения отвалообразование производится на отведенной площади. Как правило, отгрузка пород каждый год производится на тело уже существующего отвала. При проектировании нового отвала вскрышных пород следует в качестве основания, принять поверхность и свойства уже существующего отвала. На рисунке 2 показана 3Д-модель существующего и проектируемого отвала.

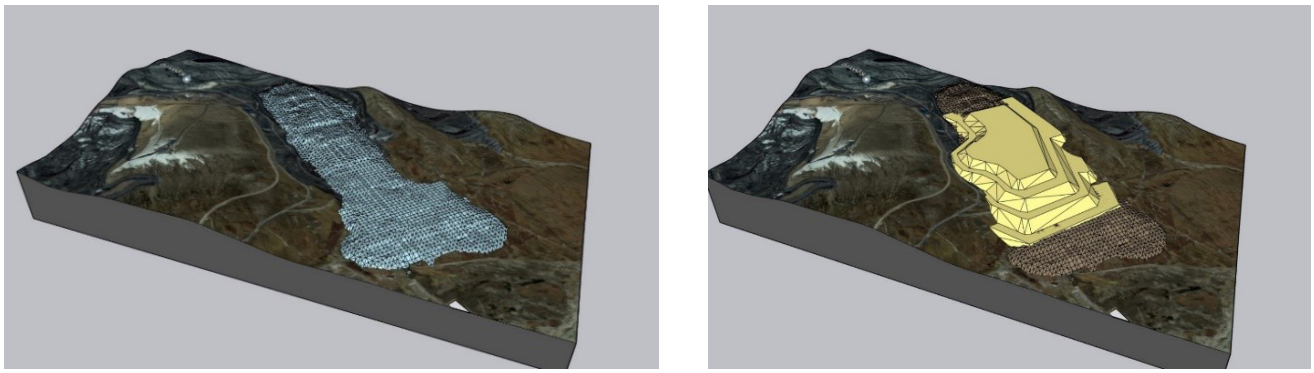

а) б)

Рисунок 2. Модель существующего (а) и проектируемого (б) отвала.

На существующий отвал был наложен новый отвал с учетом геометрических параметров и несущей способности основания.

Процесс работы с разрезом в масштабе 1:1.

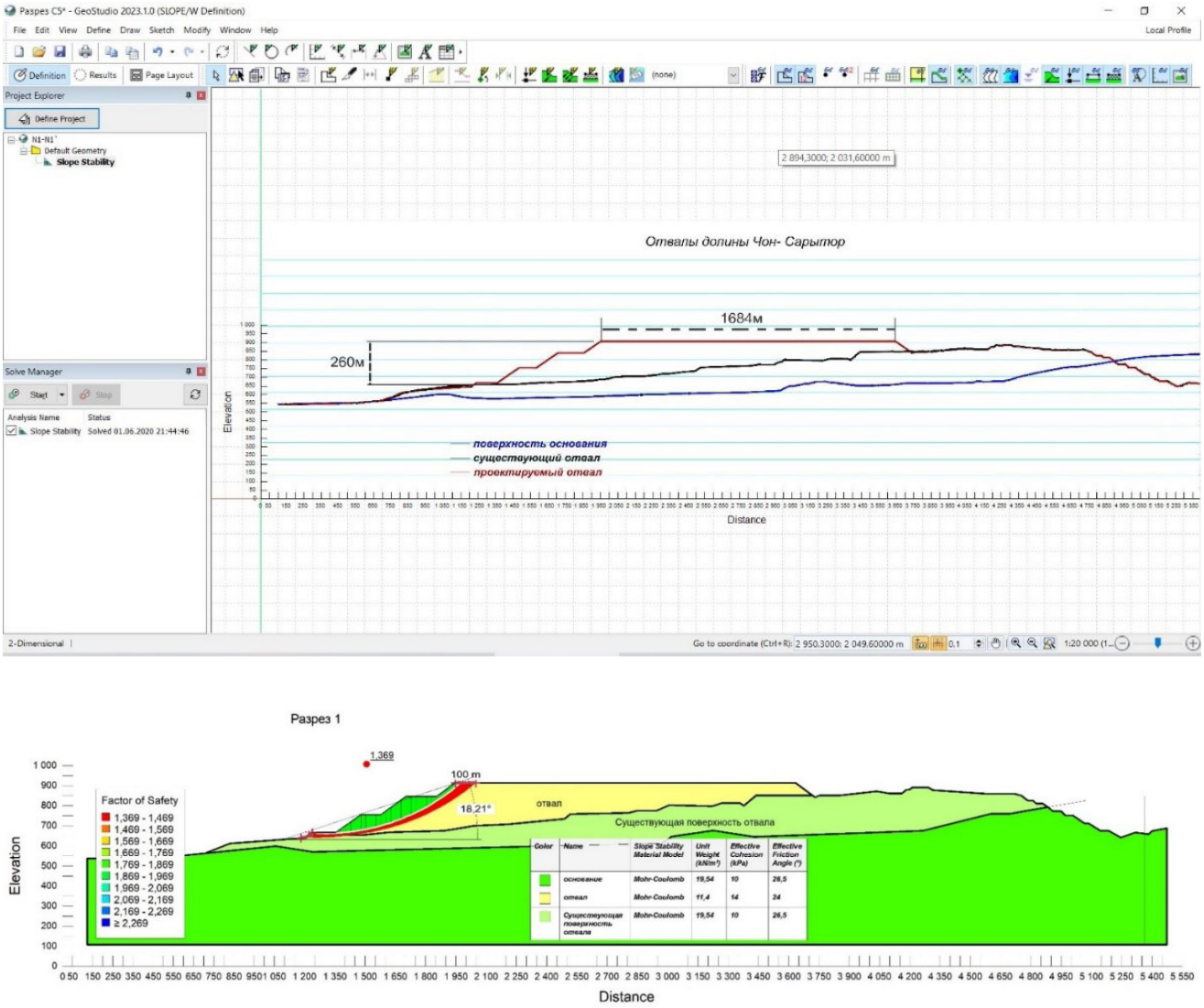

Рисунок 1. 10 Порядок расчета коэффициента устойчивости отвала на склоне. а-разрез отвала; б-результат расчета коэффициента устойчивости с выделением потенциальной поверхности скольжения

Выводы

Выбор метода численного моделирования зависит от конкретных условий задачи: характеристик массива, геологических условий, наличия трещиноватости и динамических воздействий. Метод конечных элементов подходит для детального анализа устойчивости массива, метод конечных разностей – для быстрого анализа динамических процессов, а метод дискретных элементов – для моделирования разрушений. Совмещение нескольких методов позволяет получить более точные результаты и снизить риски при проектировании горнотехнических объектов.

Устойчивость отвалов зависит от множества взаимосвязанных факторов, таких как свойства грунтов, геометрия склона и откосов, наличие внешних нагрузок и климатических условий. Для предотвращения аварийных ситуаций необходимо комплексное моделирование и мониторинг состояния отвалов, использование оптимальных конструктивных решений и применение мер инженерной защиты.

Из анализа использования ведущих программных продуктов по определению коэффициента запаса устойчивости сделаны следующие выводы и рекомендации

- Для быстрого расчета коэффициента устойчивости методом предельного равновесия рекомендуется использовать программу SLOPE/W.
- Для сложных нелинейных расчетов с учетом пластичности и больших деформаций - PLAXIS, FLAC3D
- Для анализа динамических и сейсмических воздействий - FLAC3D
- Для гидрогеологических расчетов в сочетании с устойчивостью склонов - PLAXIS, SLOPE/W.

Выбор программного обеспечения зависит от задач, стоящих перед проектировщиком. В большинстве случаев комбинирование методов (например, МПР и МКЭ) позволяет получить наиболее надежные результаты при анализе устойчивости отвалов и склонов.

Список литературы

1. Зенкевич, О. Метод конечных элементов в технике / О Зенкевич. – М:. Мир, 1975. – 542 с.
2. Тихонов, А.Н. Уравнения математической физики / А.Н. Тихонов. - М.: Наука, 1981. -512 с.
3. Чепеленкова, В. Д. Применение метода дискретных элементов для оценки прочностных свойств упругих сред / В. Д. Чепеленкова, В. В. Лисица [Электронный ресурс] DOI 10.33764/2618-981X-2022-2-2-209-214. Режим доступа: file:///C:/Users/User /Downloads/primenenie-metoda-diskretnyh-elementov-dlya-otsenki-prochnostnyh-svoystv-uprugih-sred.pdf
4. Официальный сайт PLAXIS [Электронный ресурс]. Режим доступа: https://www.plaxis.com
5. Качурин, Н. М. Численное геомеханическое моделирование параметров отвала в карьерной выемке с применением драглайна / Н.М. Качурин, Е. В. Курехин // Известия ТулГУ. Науки о Земле. - 2022. - Вып. 4. - С. 367–379.
6. Беляев, Е. Н. Прогнозирование и оценка устойчивости бортов, уступов разрезов и откосов отвалов на каменноугольном месторождении с использованием программных комплексов geostudio и plaxis 3D / Е. Н. Беляев, А. Е. Бурдонов, Н. В. Мурзин // Известия ТулГУ. Науки о Земле. - 2023. - Вып. 1. - С. 138–158.
7. Официальный сайт GeoStudio [Электронный ресурс]. Режим доступа: https://www.geoslope.com
8. Официальный сайт FLAC3D [Электронный ресурс]. Режим доступа: https://www.itascacg.com/software/flac3d
9. Джакупбеков, Б. Т. Определение параметров отвалов на горных склонах с применением программного приложения Google Sketchup/ Б. Т. Джакупбеков // Современные проблемы механики. 2016, № 26 (4). – С. 58-64.
10. Asilova, Z.A. Determination of safe parameters of storage overburden dumps on slopes during the development of upland deposits/ Asilova,Z.A. Kokumbaeva.K.A., Ocmonova N.T., Ysenov K.J. // IOP Conference Series: Earth and Environmental Science., 2024, 1374(1), 012030. - С. 1-6.
11. Джакупбеков, Б. Т. Численное моделирование устойчивости отвалов вскрышных пород при освоении нагорных месторождений / Джакупбеков Б.Т., Асилова З. А., Никольская О. В. // Фундаментальные и прикладные вопросы горных наук. Новосибирск. 2023. - Том10, № 1. - С. 30-37.

Received / Получено 08.01.2025
Revised / Пересмотрено 22.02.2025
Accepted / Принято 20.03.2025

УДК 332.05

ВЛИЯНИЕ ЦИФРОВИЗАЦИИ НА УПРАВЛЕНИЕ ПРЕДПРИЯТИЕМ В УСЛОВИЯХ ПЕРЕХОДНОЙ ЭКОНОМИКИ: ОПЫТ КЫРГЫЗСТАНА

Бекташев Мухаммадсодик Сирожидинович[1]
[1]Жалал-Абадский международный университет, Жалал-Абад Кыргызская Республика

Аннотация
В статье исследуется влияние цифровизации на управление предприятиями в Кыргызстане, где переход к цифровой экономике осложняется географическими, культурными и экономическими особенностями. На основе анализа 50 предприятий различных отраслей выявлены ключевые барьеры цифровизации, такие как низкая доступность интернета в сельских районах (только 23% охвата 4G), недостаток квалифицированных кадров и высокая стоимость внедрения технологий. Предложены адаптивные стратегии для SME, включая гибридные модели автоматизации и использование open-source решений. Приведены кейсы успешной цифровой трансформации, такие как внедрение блокчейна на текстильной фабрике «Ак Жол» и разработка AI-алгоритма для прогнозирования цен стартапом «НуриАй».

Ключевые слова: цифровизация, управление предприятием, Кыргызстан, гибридные модели, SME

THE IMPACT OF DIGITALIZATION ON ENTERPRISE MANAGEMENT IN A TRANSITION ECONOMY: KYRGYZSTAN'S EXPERIENCE

Bektashev Mukhammadsodik Sirozhiddinovich[1]
[1] Jalal-Abad International University, Jalal-Abad Kyrgyz Republic

Abstract
The article examines the impact of digitalization on enterprise management in Kyrgyzstan, where the transition to a digital economy is complicated by geographical, cultural and economic features. Based on an analysis of 50 enterprises in various industries, key barriers to digitalization have been identified, such as low Internet availability in rural areas (only 23% of 4G coverage), a lack of qualified personnel and the high cost of technology implementation. Adaptive strategies for SME are proposed, including hybrid automation models and the use of open-source solutions. The cases of successful digital transformation are presented, such as the introduction of blockchain at the Ak Zhol textile factory and the development of an AI algorithm for price forecasting by the NuriAi startup.

Keywords: digitalization, enterprise management, Kyrgyzstan, hybrid models, SME

Correspondence: Бекташев Мухаммадсодик Сирожидинович, Jalal-Abad International University, Jalal-Abad, Kyrgyzstan, Email: msodik98@gmail.com

Введение

Цифровизация стала неотъемлемой частью глобальной экономики, трансформируя подходы к управлению предприятиями и создавая новые возможности для роста. Однако в странах с переходной экономикой, таких как Кыргызстан, этот процесс сталкивается с уникальными вызовами, которые требуют адаптивных решений. Согласно данным Национального статистического комитета Кыргызской Республики (2024), только 34% предприятий активно используют цифровые технологии, что значительно ниже среднемирового показателя (70%) [1].

Основными барьерами для цифровизации в Кыргызстане являются:

Географическая изолированность: 73% территории страны занимают горные районы, где доступ к высокоскоростному интернету ограничен [2].

Культурные особенности: 54% сотрудников старше 45 лет не готовы к изменениям из-за страха перед новыми технологиями [3,4].

Экономические ограничения: 87% предприятий — это микробизнесы с ограниченным бюджетом на IT [5].

Цель данной статьи — предложить элементы к стратегии цифровой трансформации страны, которые учитывают специфику Кыргызстана и помогают преодолеть существующие барьеры.

Материалы и методы исследования

Для достижения цели исследования использовались следующие методы:

1. Сравнительный анализ:

• Сравнение уровня цифровизации предприятий Кыргызстана с аналогичными показателями в других странах с переходной экономикой (Казахстан, Узбекистан).

• Анализ успешных кейсов цифровой трансформации в регионе.

2. Статистический анализ:

• Обработка данных Национального статистического комитета Кыргызской Республики за 2023–2024 годы [6].

• Использование методов корреляционного и регрессионного анализа для оценки влияния цифровизации на ключевые экономические показатели предприятий.

3. Кейс-стади:

• Изучение опыта 50 предприятий различных отраслей (сельское хозяйство, текстильная промышленность, банковский сектор, логистика).

• Глубинные интервью с руководителями и IT-специалистами.[7]

4. Опросы и анкетирование:

• Проведение опроса среди 100 сотрудников предприятий для оценки уровня цифровой грамотности и готовности к изменениям.

• Анкетирование 50 руководителей SME для выявления барьеров и потребностей в цифровизации.

5. Контент-анализ:

• Анализ отчётов и публикаций по цифровой трансформации в Кыргызстане.

• Изучение государственных программ, таких как «Цифровой Кыргызстан», и их влияния на бизнес.

Выборка исследования

• 50 предприятий из различных регионов Кыргызстана.

• Отраслевой охват: сельское хозяйство (30%), текстильная промышленность (20%), банковский сектор (20%), логистика (15%), другие (15%).

• Размер предприятий: микробизнес (50%), малый бизнес (30%), средний бизнес (20%) [8].

Уникальные вызовы цифровизации в Кыргызстане

1. Географические барьеры:

• В горных районах доступ к интернету ограничен, что делает невозможным использование облачных технологий в реальном времени.

• Решение: внедрение гибридных моделей, где данные собираются офлайн, а затем синхронизируются через мобильные хабы. Например, агрохолдинг «Таза Шаар» успешно использует IoT-датчики для мониторинга урожая, которые работают в автономном режиме и передают данные раз в сутки.

2. Культурные особенности:

• Многие сотрудники старшего возраста воспринимают цифровизацию как угрозу своей занятости.

• Решение: программы «Цифровой наставник», где молодые сотрудники обучают старшее поколение. Например, в компании «МегаКом» такая программа помогла повысить уровень цифровой грамотности на 40% за год.

3. Экономические ограничения:

• Большинство предприятий не могут позволить себе дорогостоящие IT-решения.

• Решение: использование open-source решений и облачных сервисов с минимальными затратами. Например, стартап «НуриАй» разработал AI-алгоритм для прогнозирования цен на рынке Дордой, используя бесплатные библиотеки Python.

4. Кибербезопасность:

• С ростом цифровизации увеличивается риск кибератак.

• Решение: внедрение базовых мер кибербезопасности, таких как двухфакторная аутентификация и регулярное обучение сотрудников [9].

Кейсы успешной цифровой трансформации

1. Текстильная фабрика «Ак Жол» (Бишкек):

- Проблема: высокие логистические издержки из-за отсутствия прозрачности в цепочке поставок.

- Решение: внедрение блокчейна для отслеживания поставок хлопка.

- Результат: сокращение логистических издержек на $15 тыс./мес.

- Проблема: сопротивление профсоюзов из-за автоматизации учёта.
- Решение: переговоры с включением 10% экономии в премии сотрудников.

2. Стартап «НуриАй» (Ош):

- Проблема: нестабильность цен на рынке Дордой.
- Решение: разработка AI-алгоритма для прогнозирования цен.
- Результат: точность прогнозов — 89%, увеличение прибыли на 25%.
- Уникальность: адаптация под «челночную» торговлю с учётом неформальных сделок.

3. Банк «Mbank»:

- Проблема: низкий уровень цифровизации клиентов.
- Решение: внедрение мобильного приложения с функцией управления финансами.
- Результат: увеличение количества клиентов на 25% за два года.

4. Агрохолдинг «Таза Шаар»:

- Проблема: низкая эффективность мониторинга урожая.
- Решение: использование IoT-датчиков с офлайн-синхронизацией данных.
- Результат: повышение урожайности на 18%.

Заключение

Цифровизация открывает новые возможности для повышения эффективности управления предприятиями, однако в условиях Кыргызстана требуется адаптивный подход, учитывающий географические, культурные и экономические особенности.

Основные выводы

1. Гибридные модели цифровизации, такие как офлайн-синхронизация данных, являются оптимальным решением для горных регионов.

2. Программы обучения, такие как «Цифровой наставник», помогают преодолеть культурные барьеры.

3. Использование open-source решений и облачных сервисов позволяет снизить затраты на IT.

Рекомендации

1. Для государства:

• Создание региональных IT-хабов с обучением на кыргызском языке.

• Льготы для SME, внедряющих open-source решения (например, налоговая скидка 5%).

2. Для бизнеса:

• Внедрение гибридных CRM, таких как интеграция мессенджеров (WhatsApp Business) с ERP.

• Создание «цифровых бригад» — мобильных IT-специалистов для работы в отдалённых регионах.

Цифровая трансформация — это не только внедрение технологий, но и изменение культуры управления. Успешные кейсы, такие как «Ак Жол» и «НуриАй», показывают, что даже в условиях ограниченных ресурсов можно достичь значительных результатов.

Литература

1. Ассоциация IT-компаний Кыргызстана. Цифровизация SME: барьеры и решения. 2023.
2. Digital Chui Valley. Сборник локальных кейсов. Фонд «Сорос-Кыргызстан»; 2024.
3. Национальный статистический комитет Кыргызской Республики. 2024.
4. McKinsey & Company. Цифровая трансформация в развивающихся странах. 2023.
5. Deloitte. Экономический эффект цифровизации, 2023.
6. Хаммер М., Чампи Дж. Реинжиниринг корпорации: Манифест революции в бизнесе. Harvard Business Review Press; 1993.
7. Дэвенпорт Т. Big Data at Work: Dispelling the Myths, Uncovering the Opportunities. Harvard Business Review Press; 2014.
8. Schwab K. The Fourth Industrial Revolution. Crown Business; 2016.
9. Tapscott D. Blockchain Revolution: How the Technology Behind Bitcoin is Changing Money, Business, and the World. Penguin Random House; 2016.

Received / Получено 04.01.2025
Revised / Пересмотрено 08.02.2025
Accepted / Принято 20.03.2025

IOP Conference Series:
Earth and
Environmental Science

PAPER • **OPEN ACCESS**

Determination of safe parameters of storage overburden dumps on slopes during the development of upland deposits

To cite this article: Asilova Zulfiia Atamyrzaevna *et al* 2024 *IOP Conf. Ser.: Earth Environ. Sci.* **1374** 012030

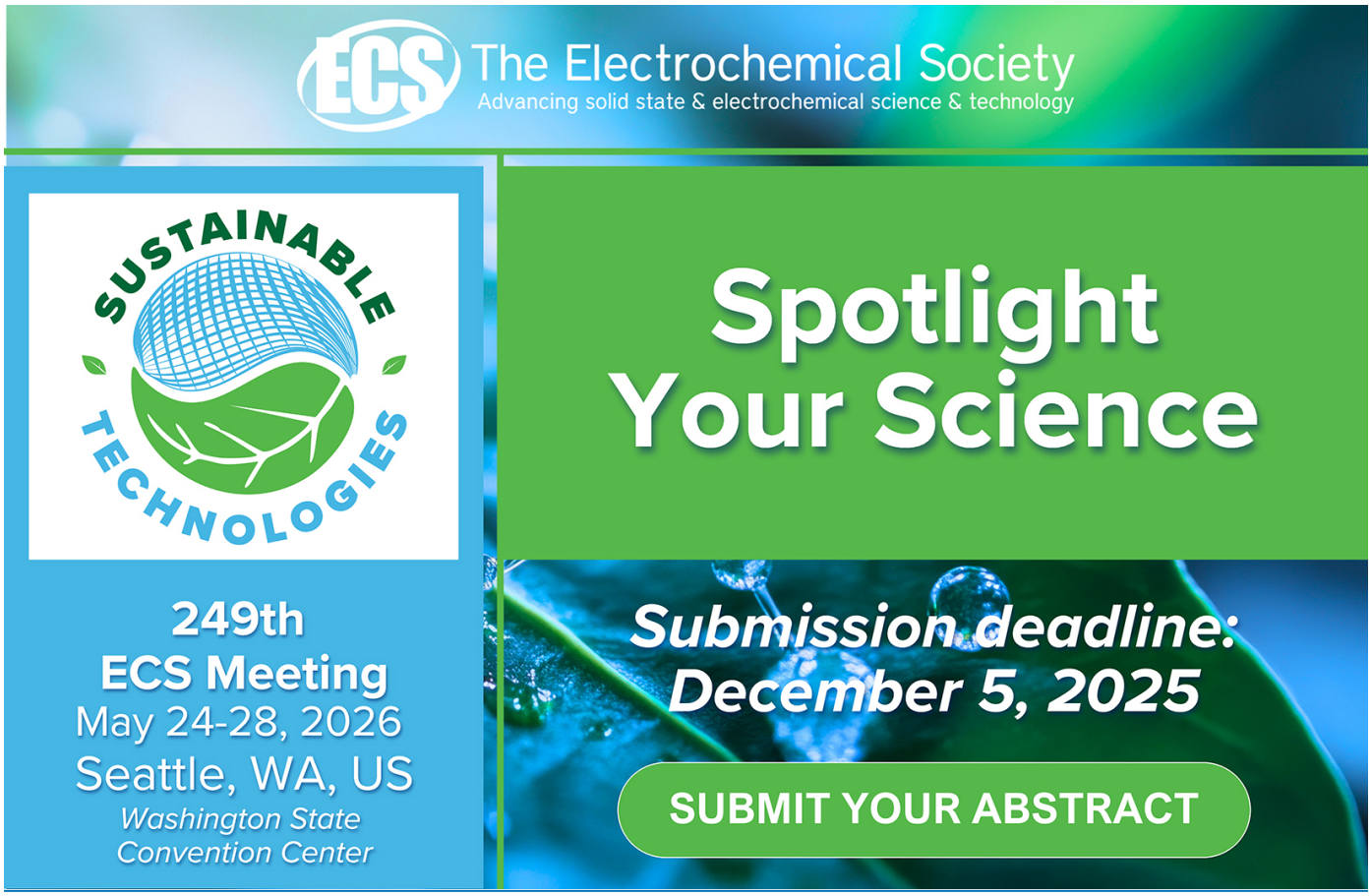

Determination of safe parameters of storage overburden dumps on slopes during the development of upland deposits

Asilova Zulfiia Atamyrzaevna[1,a *], Kokumbaeva Kulumkan Asanovna[2,b], Osmonova Nurgul Tashtanovna[3,c], Usenov Keneshbek Zhumabekovich[3,d]

[1]Department of Information Technology and Mathematics, International University named after K.Sh.Toktomamatov, Jalal-Abad, Kyrgyzstan.

[2]Department of Electric Power Engineering and Mechanics, Jalal-Abad State University named after Bekmamat Osmonov, Jalal-Abad, Kyrgyzstan.

[3]Department of Physics and Computer Science, Jalal-Abad State University named after Bekmamat Osmonov, Jalal-Abad, Kyrgyzstan.

[a]asilova.zulfiya@mail.ru, [b]ms.kulumkan@mail.ru, [c]n_osmonova@mail.ru, [d]usenov@rambler.ru

*Corresponding author

Abstract. Dumping during open-pit mining of upland deposits is one of the most difficult problems when storing overburden dumps on mountain slopes. Dump formation is accompanied by deformations of the dumps, which depend on the properties of the overburden rocks, in particular lumpiness, humidity. In order to ensure the safety of work on the dump, dump operations can be conditionally divided into dump formation with ensuring the stability of the dump tiers at all stages of the formation of the array and dump formation under controlled deformation conditions. In this article, the authors present the results of calculations of the stability of the overburden dump formed over mountainous terrain in the gold deposit of Kyrgyzstan.

Keywords: Overburden dumps, geotechnical object, dump on the slope, stability of dump, mining operations

1. INTRODUCTION

Dump formation during the development of upland deposits is one of the most difficult problems when storing overburden dumps on mountain slopes. A prerequisite for dumping is to ensure industrial and environmental safety.

The works of [1-6] are devoted to the issues of safe storage of dumps. Most of which consider dumps placed on a horizontal surface.

Deformations in the dump depend on the engineering and geological features of the dump rocks and their bases, such as:

- The degree of crushing of rocks;
- Natural separation of rocks into fractions and self-rejuvenation of dump slopes;
- Changes in the strength characteristics of rocks in the dump over time (shear resistance increases due to compaction or decreases when the rocks of the embankment and base are moistened);
- The occurrence of pore pressure in water-saturated rocks and their bases, which is an essential factor in the development of landslides of various types [7].

An important factor determining the parameters of the dumps is the relief of the base and the type of rock lying in the bottom of the dump. The stability of dumps placed on a solid foundation is determined, first of all, by the shear resistance of the rocks composing them. Precipitation and fluctuations in air temperature have the greatest influence on the stability of dumps. Of the technological factors affecting the stability of dumps, the most important are the height and configuration of the dump slopes, the length and speed of the slide front, and the rate of dumping of the dump. The schemes of dumping (frontal or block) determine the nature of the processes of compaction of rock masses of dumps and their strength properties. And also, the stability of the blade is influenced by [8,9]:

- The relief of the surface on which overburden rocks are deposited
- Precipitation and snow cover height
- Seasonal temperature fluctuations
- Physical and mechanical properties of the rocks of the base of the dumps
- Composition and properties, including humidity, of the rocks stored in the dump;
- Geometric parameters of the blade.

As an example of choosing and justifying a place-to-place overburden dumps on a slope, consider the «Chaarat» deposit in Kyrgyzstan. Kyrgyzstan is a mountainous country, more than 90% of which are occupied by mountains above 1000 m above sea level. Mineral deposits are located in high-altitude conditions at an altitude of over 1500-2000 m above sea level. In this regard, the formation of overburden dumps occurs on a

slope and stability calculations in such cases require a special approach, i.e., calculations are required not only of the dump, but also of the slope.

2. METHODOLOGY

Numerical modeling using the SLOPE/W program was used to calculate slope stability. And for the condition of stability of a layer of bulk material with a capacity h for the case i>φ, it was determined as follows [10-15]. The resistance forces at the interface of the bulk material are sufficient to neutralize the shear forces:

$$\tau_n = \tau_o + P_n tg\varphi \quad (1)$$

where τ_o - the effective adhesion force, φ - the angle of internal friction, P_n - the effective normal pressure

In an elementary volume, the planes of action of vertical stresses and stresses acting on these planes are parallel to each other and are conjugate. I.e., others have a deflection angle equal to angle i, as well as an angle between the plane of action of vertical stresses and the blade plane equal to 90^0 (Figure 1).

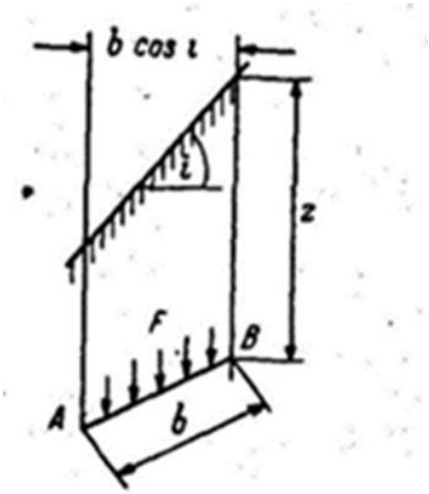

Figure 1: Schemes for calculating the maximum width of the dump. Vertical stress distributions.

The pressure per unit area at depth z is:

$$F = \gamma z \cos i \quad (2)$$

The components of this pressure at depth h:

$$P\_n = \gamma h \; 〚\cos〛 \; ^2 i \quad (3)$$

$$\tau_n = \gamma h \sin i \cos i \quad (4)$$

Substituting (3) and (4) into (1), it is possible to express the permissible thickness of the bulk material layer:

$$h = (\tau\_0 \cos\varphi)/\gamma \cos i \sin(i - \varphi) \quad (5)$$

The maximum width of a stable dump is a new criterion that is more convenient for operational monitoring of the condition of dumps on mountain slopes. The previously existing criterion (the height of a stable blade) is convenient only if the blade is located on a horizontal base. During stripping operations during the development of the «Chaarat» deposit within the Tulkubash ore zone, the total volume of overburden is planned to exceed 20.0 million m^3. The dump is planned to be placed on the slope in the immediate vicinity of the quarry in the dry river within the elevation of the slope 3050-2505 m above sea level. The slope surface has a slope of 17^0 in the upper part and 14^0 in the lower part. The length of the river is 450 m. The angle of inclination of the surface is $25\text{-}31^0$. The general view of the slope on which the dump is planned to be placed is shown in Figure 2 and 3 [16-18].

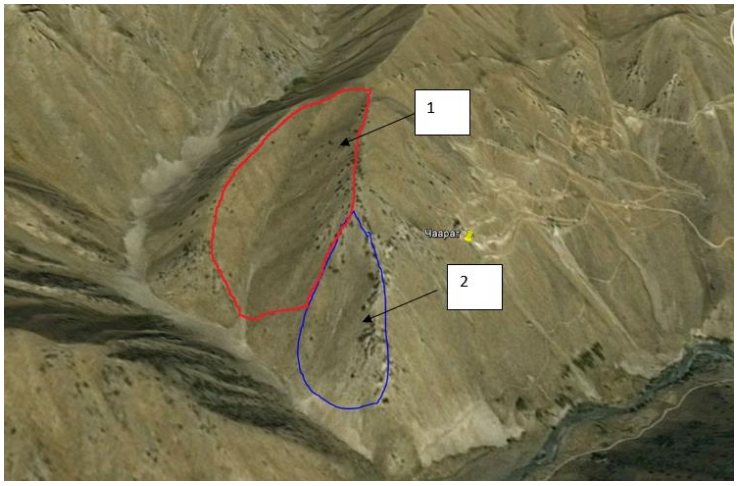

Figure 2: Location of overburden dump: 1) main dump; 2) additional dump.

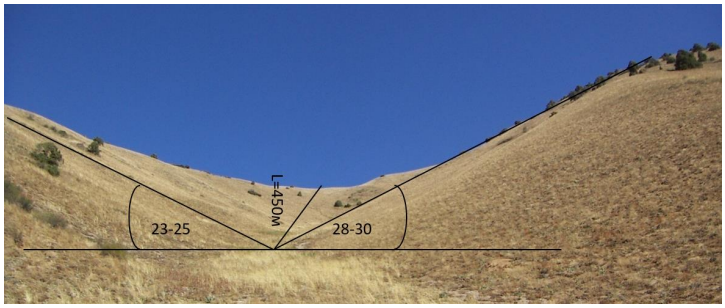

Figure 3: General view of the base of the main dump for overburden placement.

The average monthly air temperature in the area is shown in the diagram (Figure 4). The absolute maximum of negative temperatures is registered -38˚C, the absolute maximum of positive temperatures is +38˚C. The snow cover is formed in the first days of December, the snow lies almost until April. The weight of the snow cover per 1 m^2 is 22.6 MPa. The zero isotherm was recorded at a depth of 1.60-1.80 m from the surface.

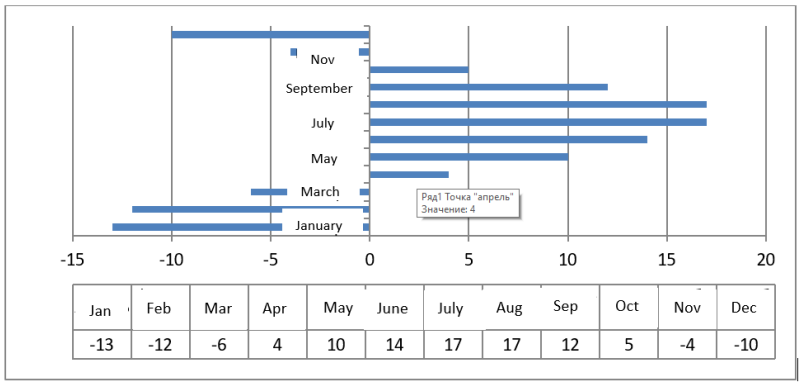

Jan	Feb	Mar	Apr	May	June	July	Aug	Sep	Oct	Nov	Dec
-13	-12	-6	4	10	14	17	17	12	5	-4	-10

Figure 4: Average monthly air temperature values in one of the fields of Kyrgyzstan.

An important parameter of the dump, which ensures the safety of dumping, is its height. The reliability of calculating the height of the dump on the slope is determined by such parameters as the volume weight of rocks in the dump, the angle of internal friction of these rocks, the angle of slope of the dump. Since the storage of rocks is planned to be carried out not on a horizontal site, but on a slope, parameters such as the angle of

inclination of the base are included in the calculation. To determine the height of the dump, the following most unfavorable initial parameters of the dump rocks were taken (Table 1).

3. MATERIALS USED IN THE STUDY

Table 1: Calculated data for determining the geometric parameters of the main dump.

Calculated data	Values
Volume weight of rocks, kg/m^3	2100
Bulk weight, kg/m^3	1170.00
Density, kg/m^3	2140
Cohesion, MPa	0.04
The angle of internal friction, degree	38
Coefficient of friction	0.78

The parameters of the dump were determined within the selected territory by 6 calculated sections: horizontal A-A, B-B, C-C, D-D, E-E and one section F-F selected directly along the river bottom (as shown Figure 5). The initial geometric parameters for calculating the volume of the dump are shown in Table 2.

Table 2: Initial data for calculating the parameters of the main dump.

Initial parameters	Values	
Volume of overburden, m^3	40000000	
Loosening coefficient	1,8	
Planned weight of overburden, t	775000000	
The length of the drop section, m	442.5	
	The steepness of the slope along the stretch	The length of the section along the stretch
section A-A	24	87,5709
section B-B	31	93,33067
section C-C	23	76,04523
section Д-Д	28	101,9313
section E-E	28	54,36336

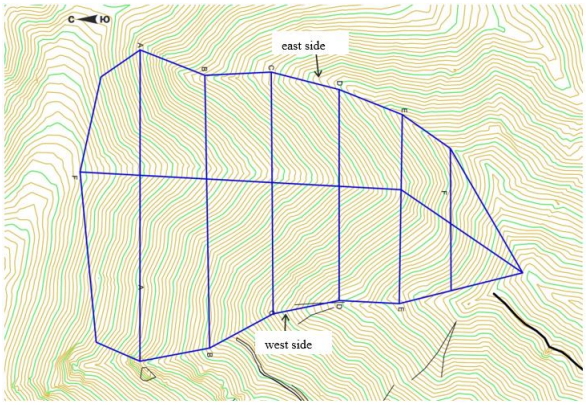

Figure 5: The surface of the base of the main dump (topological alignment with the applied boundaries of the dump).

Considering that at least 20 million cubic meters of overburden must be placed on the allocated area, simple experiments were carried out to seal the fragmented rocks. As a result, it was found that the volume of the dump after compaction can be increased to 40% and up to 5 million m^3 can be placed. The total volume of the dump will increase to 17.4 million cubic meters. in addition, after compaction of rocks, their shear resistance increases (Figure 6). The calculated stability coefficient of the blade must be at least 1.5. Such a coefficient of stability of the dump is necessary to prevent accidents or create a threat to the personnel servicing the dumps. Given the terrain, it is possible to start dumping from the lower point of the eastern slope of the dry river. The width of the approach will be determined after the accepted dimensions of dump trucks. After the first tier is fully filled, it is recommended to seal it in order to create a natural dam to prevent displacement of the rocks of the upper tiers of the dumps. It should be borne in mind that during thawing, the rocks turn into a fluid state

and the dump rocks turn into an unstable state. Based on the results of calculating the stability of the slope on which the dump will be formed and calculating the stability of the dump itself, it is recommended to store as follows (Figure 7).

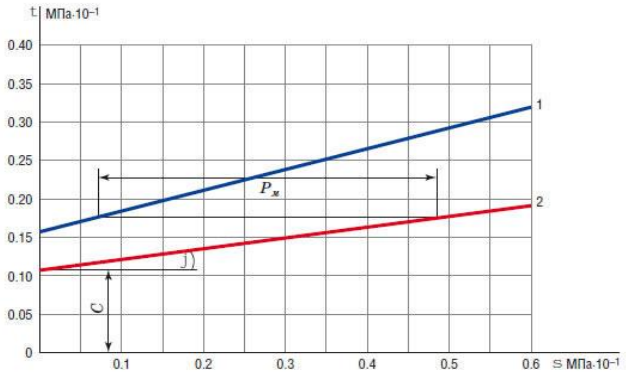

Figure 6: Graph of the shear resistance of the dump rocks at various degrees of compaction: 1) Degree of sealing 0.4; 2) without sealing.

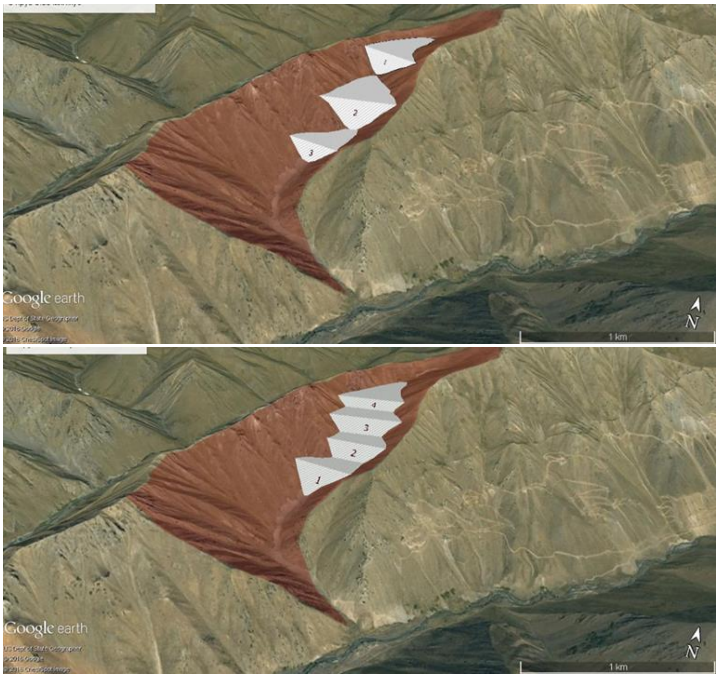

Placement of the blade in 3 tiers

Placement of the blade in 4 tiers

Figure 7: Options for the placement of the dump according to the calculations of numerical modeling of the slope and the overburden dump.

As a general criterion for dangerous deformations within the prism of a possible collapse, it is proposed to consider the rate of deformations exceeding 50 cm/day.

4. CONCLUSIONS

Based on the results of studying the formation of overburden dumps on the slope, the following general conclusions were obtained:

- The safe parameters of dumps depend on many factors, the dominant of which is the terrain.

- To increase the reliability of determining the stability of dumps, additional study of the physical and mechanical properties of the dump mass and rheological changes is necessary, as well as the organization of a system for monitoring the stability of dumps.
- The main factors influencing the stability of dumps on slopes and the development of deformations have been identified.
- In accordance with the Uniform Safety Rules for Open-pit Mining and mining and transport equipment on dumps must be placed outside the possible sliding prism.

Based on the results of calculating the stability of the «Chaarat» deposit dump, the following conclusions and recommendations were obtained.

- The stability assessment was carried out and the general angle of inclination of the «Chaarat» mining quarry was determined, taking into account the quality index of the massif.
- The height of the tiers should not exceed the height of the sides of the river in which the dump is located.
- For long-term safety of the dump, the dump should be divided and stored in several tiers, at least 3 or 4 tiers.

REFERENCES

[1] Eremina G.M., Smolin A.Yu. Numerical study of the mechanical behavior of the hip joint under therapeutic acoustic influence. Russian Journal of Biomechanics, 2023, No. 1, pp. 40-54. DOI: 10.15593/RZhBiomeh/2023.1.04
[2] Kuzmin E.V., Uzbekova A.R. Rating classifications of rock formations: prerequisites for creation, development and scope. GIAB, No.4, pp.201-202, 2004.
[3] Terzaghi K. (1965). Sources of error in joint surveys. Geotechnique. (15). publ. The Institution of Civil Engineers, London. pp. 287–304.
[4] 6. N Bar, J Semi, M Koek, G Owusu-Bempah, A Day, S Nicoll, J Bu. Practical waste rock dump and stockpile management in high rainfall and seismic regions of Papua New Guinea. Slope Stability 2020 - PM Dight (ed.), © Australian Centre for Geomechanics, Perth,
[5] S. K. Gara, N. N. Singh, R. Singh, and K. S. Rao. Slope stability analysis for optimisation of overburden dump capacity in opencast coal mines. R. E. Hammah et al. (Eds.): RIC 2023, AHE 19, pp. 109–118, 2023. (https://doi.org/10.2991/978-94-6463-258-3_11).
[6] Kirichenko Yu.V. Engineering and geological features of the formation of dump arrays. Mining industry No.3. 2002.
[7] BeniawskiZ.T. Engineering rock mass classification. Wiley, New York, 251 p., 1989.
[8] Kadyralieva G.A. Kozhogulov, K.C., Aitkuliev, N.A. Deformation properties and mechanism of destruction of a block structure rock mass. Smart Geotechnics for Smart Societies, Astana. 2023, p.896–900
[9] Asilova Z.A., Dzhakupbekov B.T. Distinctive signs of the stability of dumps, ensuring the safe storage of overburden rocks on the slope. News of universities of Kyrgyzstan. 2023. №. 3. C. 12-15.
[10] Krahn J. Stability Modeling with SLOPE/W: An Engineering Methodology. The 3rd Edt. – Canada, 2007. – 355p. 10.3 Pseudostatic analysis.
[11] Dzhakupbekov B.T., Asilova Z.A., Nikolskaya O.V. Numerical modeling of stability of overburden dumps during the development of upland deposits. Fundamental and applied issues of mining sciences. 2023. Vol. 10. No. 1. pp. 30-36.
[12] Dzhakupbekov B.T., Asilova Z.A. Three-dimensional modeling of overburden dumps during the development of upland deposits. News of universities of Kyrgyzstan. 2023. №. 3. C. 16-20
[13] Bouali MF, Karkush MO, Bouassida M. Impact of wall movements on the location of passive Earth thrust. Open Geosciences. 2021 May 19;13(1):570-81.
[14] Karkush MO, Aljorany AN. Analytical and numerical analysis of piled-raft foundation of storage tank. In Construction in Geotechnical Engineering: Proceedings of IGC 2018 2020 (pp. 373-384). Springer Singapore.
[15] Karkush MO. Impacts of soil contamination on the response of piles foundation under a combination of loading. Engineering, Technology & Applied Science Research. 2016 Feb 5;6(1):917-22.
[16] K. Ch. Kozhogulov, O.V.Nikolskaya, G.A.Kadyralieva. Features of physic-mechanical properties metamorphic breeds at an estimation of stability of slopes. //Disaster mitigation in special geoenvironmental conditions/ 6th International geotechnical symposium/. Madras, Chennai, India. 2015
[17] L. Borrelli, R. Greco, G. Gullà. Weathering grade of rock masses as a predisposing factor to slope instabilities: Reconnaissance and control procedures. Geomorphology Volume 87, Issue 3, 15 June 2007, Pages 158-175.
[18] Z. Yang, X. Ding, X. Liu, A. Wahab, Z. Ao, Y. Tian, V.S. Bang, Z. Long, G. Li, P. Ma. Slope Deformation Mechanisms and Stability Assessment under Varied Conditions in an Iron Mine Waste Dump. Water 2024, 16, 846. pp.1-26.

IOP Conference Series:
Earth and
Environmental Science

PAPER • **OPEN ACCESS**

Features of assessing the stability of the open pit - overburden dump geotechnical system during the development of upland deposits in an open-pit manner

To cite this article: Asilova Zulfiia Atamyrzaevna *et al* 2024 *IOP Conf. Ser.: Earth Environ. Sci.* **1374** 012031

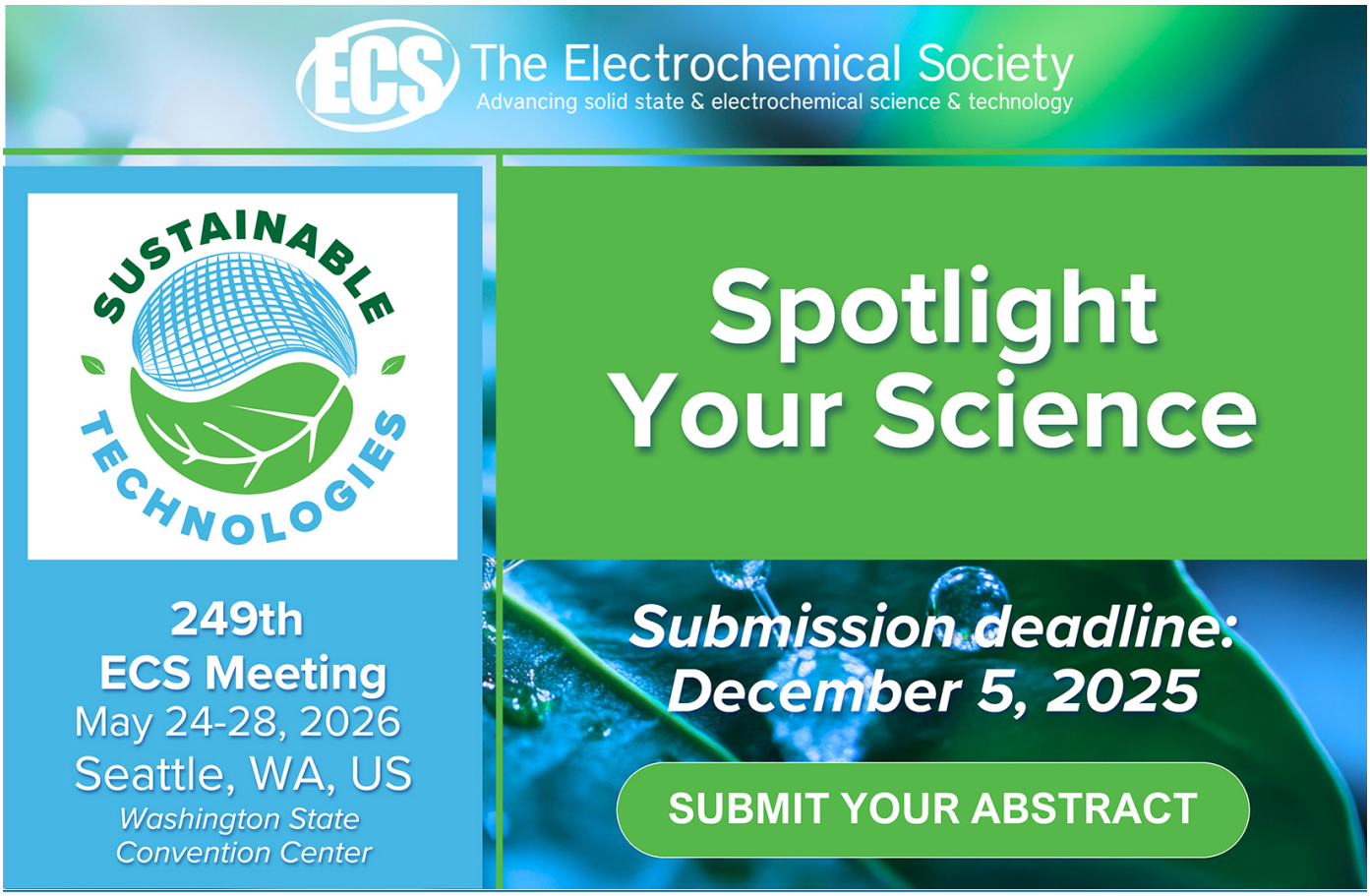

Features of assessing the stability of the open pit - overburden dump geotechnical system during the development of upland deposits in an open-pit manner

Asilova Zulfiia Atamyrzaevna[1,a *], Mamatova Gulshair Tynybekovna [2,b], Kokumbaeva Kulumkan Asanovna[3,c] , Shamiev Zhakyp Bakirovich [4,d]

[1] Department of Information Technology and Mathematics, International University named after K.Sh.Toktomamatov, Jalal-Abad, Kyrgyzstan.

[2] Department of Physics and Computer Science, Jalal-Abad State University named after Bekmamat Osmonov, Jalal-Abad, Kyrgyzstan

[3] Department of Electric Power Engineering and Mechanics, Jalal-Abad State University named after Bekmamat Osmonov, Jalal-Abad, Kyrgyzstan.

[4] Department of Electric Power Engineering and Mechanics, Jalal-Abad State University named after Bekmamat Osmonov, Jalal-Abad, Kyrgyzstan.

[a]asilova.zulfiya@mail.ru, [b]gulshair_mam@mail.ru, [c]ms.kulumkan@mail.ru, [d]jakypshamiev@mail.ru.

Abstract. The main criterion for mining operations in the development of upland deposits by open-pit mining is the safety of their operation, and therefore the assessment of the stability of the geotechnical system is always relevant and requires a special approach and study. The article reveals the features of the assessment of the geotechnical system of the open pit - overburden dump of the a mountainous, consisting in studying the interaction of the geological and geomechanical environment. The factors of both the geological and geomechanical environment affecting the change in the natural stress state of the studied object are described. A scheme for evaluating a geotechnical system has been constructed, the essence of which is to study the elements of both the geological and geomechanical environment.

Keywords: Slope, quarry, dump, geological environment, geomechanical environment, deformation, stability, landslide.

Introduction

Safe storage of overburden rocks on mountain slopes during the development of upland deposits is one of the difficult and main tasks that must be solved during the operation of the mine [1]. In Kyrgyzstan, overburden dumps during the development of high-altitude deposits are placed on slopes in the immediate vicinity of a quarry in nearby rivers on slopes whose steepness varies from 100 to 200 at an altitude of 3,500 to 4,000 m above sea level. In addition to the parameters of the dump itself (height and width), the amount of precipitation, seasonal and daily fluctuations in air temperature, the stability of such dumps is also influenced by the parameters of the quarry [1,2].

To date, studies of the deformed state of the rock mass have been carried out in connection with the appearance of a problem, i.e., the influence of either a quarry or a dump has been determined, while considering the phenomenon of a change in the stress state or a consequence – a violation of the stability of the side of the open pit or overburden dump.

The development of upland deposits by the open method is complicated by the limited territory on which the upland quarry, dump, gold extraction factory, tailings storage, administrative and economic facilities should be located.

One of the main tasks in the development of mineral deposits by the open method is to ensure the stability of geotechnical facilities (quarries, dumps). However, even before the start of work, it is necessary to assess not only the natural conditions (rock properties, slope stability), but also the area of interaction between a geotechnical object and a rock mass, within which significant changes occur.

A complex object of nature that objectively exists independently of man and his activities is called a "geological environment" [3,4]. The geological environment includes such elements as terrain, rock mass and their properties, groundwater, permafrost, natural gravitational processes.

The geological environment, being exposed to man-made effects, changes its state depending on the relief, tectonics, structure and properties of the massif, as well as on the quality of the massif.

The geomechanical processes occurring in the rock mass during mining operations depend on the properties of the geological environment and the parameters of man-made impact.

The parameters of the quarry and the dump have the greatest influence on the change in the natural stress state. To date, the geotechnical system "slope - open pit - overburden dump" has practically not been considered and, as a result, the influence of this system on the change in the natural stress state of the rock mass, the main causes of instability of both the sides of the quarry and the dump have not been identified.

Methodology

The main geomechanical processes in the instrument array of upland quarries that affect the stability and safety of mining operations are deformation processes that lead to additional stresses on the contour of the quarry, the development of the process of shifting not only the side of the quarry, but also the slope on which it is built [5].

The methodology of our research is based on the identification of the causes, the essence of the formation of separation cracks in the sides of upland quarries and the development of landslide processes in the dump on the slopes. That is, a comprehensive study of changes in the natural stress state and an assessment of the stability of the "slope - open pit - overburden dump" geotechnical system under the influence of the parameters of both the quarry and the dump.

The stages of object cognition are aimed at identifying the features of the study of geomechanical processes in the instrument array of the slope, establishing qualitative and quantitative interactions of the geological and geomechanical environment, depending on:

- properties of the geological environment, those of its physical parameters that are responsible for the formation of individual elements and which can be considered relatively static in real time;
- parameters of man-made impact, which are extreme values of forces, the degree of change in the forces of impacts under the influence of processes of damage and degradation of objects.

The geological environment is a natural multicomponent dynamic subsystem with all its inherent internal interactions, a structure in which, under the influence of human activity, new technogenic and geological processes [5-8].

The study includes the following construction of object cognition (Figure 1.):

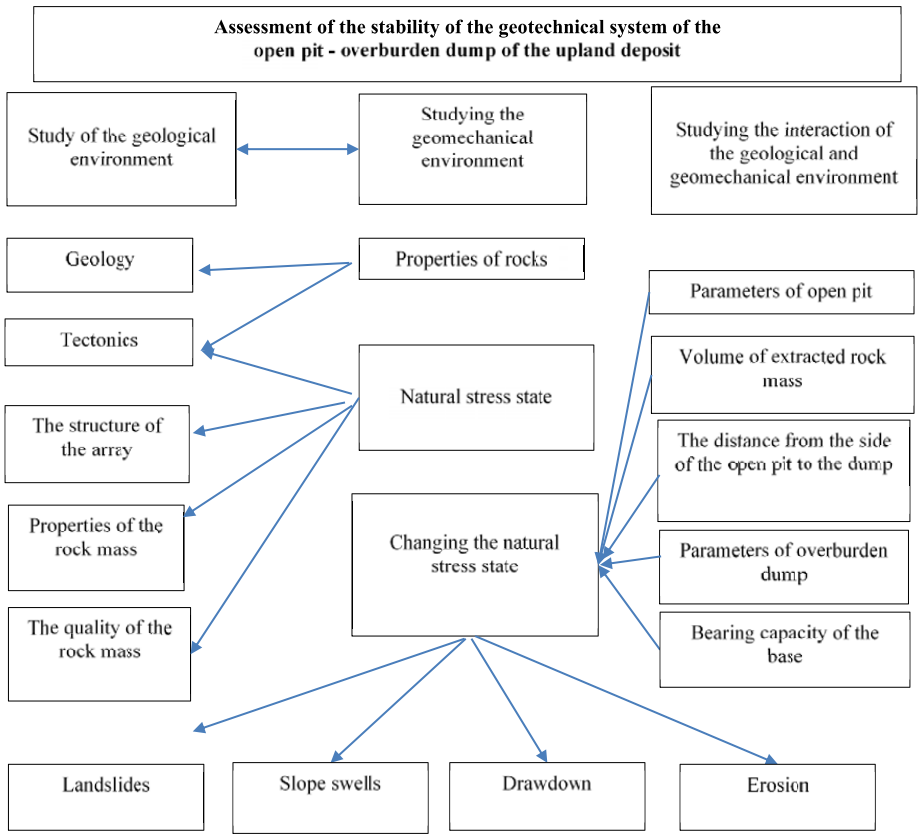

Figure 1: Geotechnical system assessment scheme.

Factors and causes of its development are necessary for the formation of landslide processes and deformations in the quarry and when dumping dumps on the slope. In this case, the reason is the geomechanical environment, in which the following groups of parameters can be distinguished:

1) Geometric parameters of the dump and the quarry, such as the angle of the underlying slope, the angle of the slope of the dump and the quarry, the height and width of both the dump and the quarry, the distance from the side of the quarry to the dump;

2) Changes in the structure and properties of the dump mass, especially waterlogging;

3) Additional load, which includes seismic, hydrodynamic effects;

4) Methods of storing dumps.

Based on this, deformations in the quarry and during dumping of dumps on mountain slopes depend on the parameters of the quarry and the dump, the volume of rock being extracted, the distance from the side of the quarry to the dump, as well as on the bearing capacity of the base of the dump.

The stability of the overburden dump is determined by forces in the direction of the 00' line. The material within the triangle AOO' will be in equilibrium (at rest) if the resistance forces at the interface of the bulk material are sufficient to neutralize the shear forces: (Figure 2, a) [8]

$$\tau_n = \tau_o + P_n tg\varphi \quad (1)$$

where τ_o - the effective adhesion force, φ - the angle of internal friction, P_n - the effective normal pressure

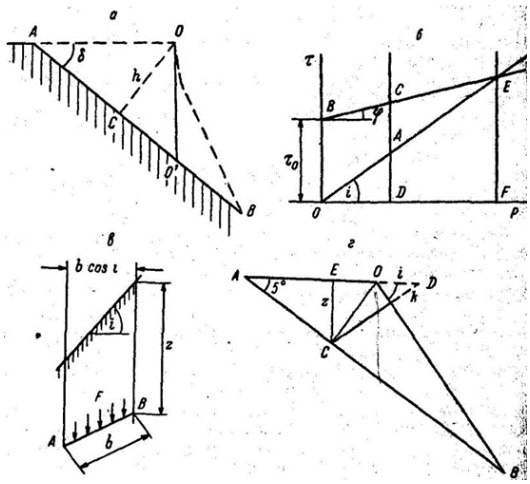

Figure 2: Schemes for calculating the maximum width of the blade.

a — the longitudinal section of the blade; b — the ratio of vertical and tangential stresses in the bulk medium; c — the distribution of vertical stresses; d — the conclusion of the calculation formula.

Of the physical properties of bulk materials, shear resistance is the most complex and depends on many factors. Formula (1) is approximate, but for practical purposes there is a sufficient degree of accuracy. The values of τ_o and φ in the case under consideration depend on the density, snow cover and moisture content of the bulk material and can vary very widely.

The ultimate shear resistance can be expressed in analytical and graphical forms (BC in Figure 2, b). At normal pressure OD, the shear resistance value is determined by the DC segment. If i<φ, then the BC and OA lines will not intersect, and, therefore, there will be no shift in the plane parallel to the dump surface. If i<φ, then the shear stresses in the plane parallel to the dump surface are less than the shear resistance at some depth, where the normal pressure is characterized by a segment exceeding OF.

The pressure per unit area at depth z is:

$$F = \gamma z cosi \quad (2)$$

The components of this pressure at depth h:

$$P_n = \gamma h cos^2 i \quad (3)$$

$$\tau_n = \gamma h sinicosi \quad (4)$$

Substituting (3) and (4) into (1), it is possible to express the permissible thickness of the bulk material layer:

$$h = \frac{\tau_0 cos\varphi}{\gamma cosisin(i-\varphi)} \quad (5)$$

From the formulas (3) and (4) it can be seen that

$$z = hcosi \tag{6}$$

where h is represented by the segment CD in Figure 2, d).
To find the maximum width of the dump r = AO, it is necessary to replace h with h1 = OC, then

$$r = \frac{h}{sin\delta} \tag{7}$$

Knowing that $OC \perp AB$ and $CD \perp OB$ (Figure 2, d), we find

$$h = h_1 \frac{cos\delta}{cosi} \tag{8}$$

And after simple transformations, we get

$$r = \frac{2\tau_0 cos\varphi}{\gamma sin2\delta \sin(i-\varphi)} \tag{9}$$

Thus, the maximum width of a stable blade r is directly proportional to the adhesion forces in the dump mass, inversely proportional to its volumetric weight and depends on the angles of internal friction, the underlying slope and the slope of the blade. These values are determined as a result of laboratory tests and field observations. The maximum width of a stable dump is a new criterion that is more convenient for operational monitoring of the condition of dumps on mountain slopes. [9,10]

In the process of pouring loose rocks onto a base with a close location of groundwater, the dump body is waterlogged due to capillary rise of water, which also leads to a decrease in the strength of the dump masses and the formation of subsidence and landslides.

According to various data, up to 15% of landslides on dumps are caused by the occurrence of pore pressure at the base of the man-made massif.

We have proposed a scheme for water saturation of dump rocks with groundwater due to capillary uplift (Figure 3). This scheme is conditional and requires clarification after carrying out appropriate work on engineering and hydrogeological surveys. To exclude capillary uplift in the body of the dump, it is necessary to isolate the contact of the watered base with the rocks being laid in the dump.

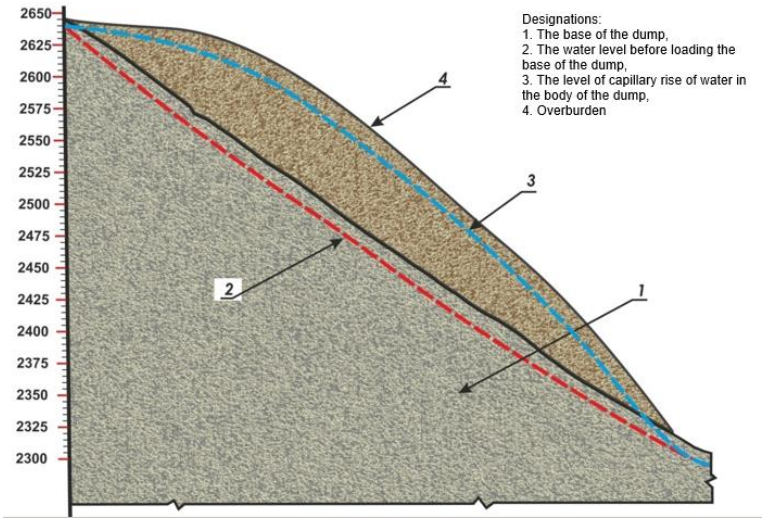

Figure 3: A conditional diagram of the possible groundwater level.

In accordance with the Uniform Safety Rules for Open-pit Mining, mining equipment on dumps must be placed outside the possible sliding prism. The width of this prism should be set depending on the physical and mechanical properties of the rocks of the dump and its base and the additional load created by the equipment. The width of the prism of possible sliding of deformable dumps is at the same time the width of the safety berm, within which the presence of people and equipment is not allowed. The width of the safety prism will be determined according to a special graph of the relationship between the height of the blade and the width of the collapse prism. According to the accepted physical and mechanical properties of rocks in the dump, the

width of the collapse prism is also determined for the case when the angle of internal friction is 32^0 and 38^0. Instead of the bulk weight of rocks in the dump, we calculate the bulk weight, i.e., un = 2.18 t/m3. The width of the prism of a possible collapse is determined taking into account the loads from working equipment (the weight of the loaded BelAZ dump truck is assumed to be 75 tons.) [11-13]

The shear forces in the dump on the mountain slope and the movement of the dump mass are caused by gravity, the pressure of water filtering through the dump, as well as periodic concussions during blasting operations in the quarry, when resistance to shear in any plane of the dump is sufficient to neutralize these forces. In the conditions of the Arctic, the magnitude of shear resistance experiences significant seasonal fluctuations throughout the year. Thawing and moistening of bulk material in the spring and summer period significantly reduce the amount of shear resistance, the study of seasonal fluctuations of which in the body of the dump is very difficult, but it is extremely necessary to solve the problem of stability. Obviously, the calculations should use the maximum value of shear resistance, which corresponds to the lowest strength of the dump mass that occurs in the spring and summer period.

Prevention of landslides and collapses, as well as the development of measures to reduce the harmful effects of deformations of dumps and territories adjacent to the quarry, is a prerequisite for the smooth operation of a mining enterprise. The purpose of the complex of works on the monitoring of deformations of dumps and the development of measures to ensure their stability is:

1. study of deformations of the sides of quarries, ledges and dumps and identify the causes of their occurrence;
2. establishment of optimal parameters of slopes of mining sites;
3. prevention of landslides and slope collapses in quarries, development and application of measures that exclude the manifestation of deformations that are dangerous to human life and entail a decrease in the economic efficiency of mining.

To develop measures to prevent the dangerous manifestation of deformations of dumps, it is necessary to perform the following types of work:

- conducting systematic visual observations of the condition of the slopes on the dumps;
- identification of zones and areas of possible manifestation of destructive deformations of dumps and the organization of stationary instrumental observations in these areas.

The purpose of observations (monitoring) is:

- to establish the boundaries of the distribution and type of deformations in overburden dumps;
- determination of the rate and magnitude of deformations;
- determination of the critical value of the displacements preceding the beginning of the active stage;
- prediction of the development of deformations over time during the formation of the dump.

Conclusions

Based on the analysis of scientific and technical literature and calculations of the stability of dumps in mountainous areas, the following conclusions and recommendations were obtained:

- The peculiarity of assessing the stability of the open pit – overburden dump geotechnical system during the development of upland deposits is the comprehensive study of the stability of the geotechnical system through the study of the interaction of the geological and geomechanical environment, taking into account both the parameters of the open pit and the dump.
- The dependence of the strength characteristics of rocks on the type of metamorphism is revealed.
- When carrying out work on these dumps, surveys should be carried out to identify and develop displacement and subsidence cracks along the entire work front.
- To develop and install a system for monitoring the displacement of dumps, the base of dumps, humidity and temperature of dumps and the base.
- It is necessary to determine the specific volume of overburden placed in each dump, for which it is necessary to establish the coefficient of loosening of overburden and the area allocated for the dump. To assess the stability of each dump, information is needed on the speed of advance of the front of work on the dumps.

References

[1] All—Union norms of technological design of enterprises of non-metallic building materials: Ministry of Industry of building materials of the USSR 20.12.85]. - L.: Stroyizdat. - 1988. — 78 p.

[2] Kozhogulov K.Ch., Nikolskaya O.V., Dzhakupbekov B.T. Stability of overburden dumps in the development of upland deposits // Fundamental and applied issues of mining sciences. – T. 8. - №1, - 2021. - Pp.93-96.

[3] Lomtadze.D.V. Engineering geology. Engineering geodynamics. L. Nedra. 1977.479 p

[4] Asilova Z.A., Dzhakupbekov B.T. Distinctive signs of the stability of dumps, ensuring the safe storage of overburden rocks on the slope. News of universities of Kyrgyzstan. 2023. №. 3. C. 12-15
[5] Reimers N.F. Nature management: Dictionary-reference. M. Mysl, 1990, 637c.
[6] Z. Yang, X. Ding, X. Liu, A. Wahab, Z. Ao, Y. Tian, V.S. Bang, Z. Long, G. Li, P. Ma. Slope Deformation Mechanisms and Stability Assessment under Varied Conditions in an Iron Mine Waste Dump. Water 2024, 16, 846. pp.1-26.
[7] Sergeev E.M. Engineering geology. Moscow: Publishing House of Moscow State University. 1982, 248 p.
[8] Sergeev E.M. Problems of engineering geology in connection with the protection and rational use of the geological environment. Vestn. MSU. Ser. 4. Geology. 1987. No.5. pp.77-86
[9] L. Borrelli, R. Greco, G. Gullà. Weathering grade of rock masses as a predisposing factor to slope instabilities: Reconnaissance and control procedures. Geomorphology Volume 87, Issue 3, 15 June 2007, Pages 158-175.
[10] Kozhogulov K.Ch., Nikolskaya O. V. Features of geomechanical processes in the development of gold deposits in Kyrgyzstan// Fundamental and applied issues of mining sciences. – Vol. 6. - №1, - 2019. - Pp.135-138.
[11] Kadyralieva G.A., Dzhakupbekov B.T., Forecasting the stability of dumps during the development of high-altitude mineral deposits. Proceedings of materials of the scientific and technical conference of young scientists of Kyrgyzstan "Start in big science". Publishing house. "Ilim" of the National Academy of Sciences of the Kyrgyz Republic, Bishkek 2013 (pp. 3-6)
[12] Krahn J. Stability Modeling with SLOPE/W: An Engineering Methodology. The 3rd Edt. – Canada, 2007. – 355p. 10.3 Pseudostatic analysis.
[13] Dzhakupbekov B.T., Asilova Z.A. Three-dimensional modeling of overburden dumps during the development of upland deposits. News of universities of Kyrgyzstan. 2023. №. 3. C. 16-20

Discover Applied Sciences

Research

Impacts of climate change on hydrological patterns and implications for hydroelectric power generation in Khimti River Basin, Nepal

Deepak Chaulagain[1,2] · Ram Lakhan Ray[3] · Abdulfatai Olatunji Yakub[1,2] · Noel Ngando Same[1,2] · Jaebum Park Jong[1,2] · Wook Roh[4] · Dongjun Suh[1] · Jeong-Ok Lim[2] · Jeung-Soo Huh[1,2]

Received: 4 February 2025 / Accepted: 6 June 2025
Published online: 01 July 2025

Abstract
Climate change has considerable influence on mountain environments and the related hydrological processes, in turn affecting hydropower. Climatic unpredictability and rising temperatures cause soil water depletion, leading to unpredictable downstream runoff. This study examines the consequences of climate change on hydrological regimes and their effect on hydropower production in Khimti River basin of Nepal. This study used the soil and water assessment tool (SWAT) in the shared socioeconomic pathway (SSP2 4.5 and SSP5 8.5) emission scenarios of three climate models (CanESM5, MIROC6, and MRI-ESM2-0) from the Coupled Model Intercomparison Project Phase 6 (CMIP6). The study encompassed recorded temperature and rainfall data to correct errors. River discharge data were utilized for calibration and validation the SWAT model, leveraging 21 hydrological parameters. The result revealed that the projected stream flow is higher than the observed flow in all seasons except CanESM5 for the monsoon season from 2023 to 2074. Results showed the average annual flow increased by 0.2–54% in all time intervals for both scenarios. The excess energy power generation and economic benefits increase extensively in the future, with the greatest contribution during the spring season followed by the winter season. The information obtained from this study can be useful for policymakers, planners, and investors for hydropower generation in Nepal.

Article Highlights

- Annual future water balance in Khimti river basin will rise in the current century.
- Annual power generation will increase under the influence of climate change.
- Spring and winter seasons are the major contributors to excess energy generation.

Keywords Climate models · Precipitation · Projected stream flow · Power generation · River basin · Temperature

Abbreviations

CUP	Calibration and uncertainty procedures
CV	Coefficient of variation

✉ Jeung-Soo Huh, jshuh@knu.ac.kr | [1]Department of Convergence and Fusion System Engineering, Graduate School, Kyungpook National University, Sangju 37224, Republic of Korea. [2]Institute for Global Climate Change and Energy, Kyungpook National University, Daegu 41566, Republic of Korea. [3]Cooperative Agricultural Research Center, College of Agriculture, Food, and Natural Resources, Prairie View A&M University, Prairie View, TX 77446, USA. [4]Department of Nano and Advanced Materials Science and Engineering, Kyungpook National University, Sangju 37224, Republic of Korea.

DEM	Digital elevation model
ESGF	Earth system grid federation
GCM	General circulation models
HKH	Hindu Kush Himalayas
HRU	Hydrological response unit
KETEP	Korean Institute of Energy Technology Evaluation and Planning
KRB	Kabompo River Basin
MoTIE	Ministry of Trade, Industry & Energy
RCP	Representative concentration pathway
RoR	Run-of-river
ST	Storage-type
SWAT	Soil and water assessment tool

1 Introduction

Human activities have accelerated climate change, leading to disruptions in the hydrological cycle and affecting water resource management globally. This changes have led to fluctuation in water availability, driven by shift in meteorological parameters such as precipitation and temperature, as well as accelerated glacier melting [34, 62]. Consequently, extreme and frequent water-related incidents occur, and these events cause variations in the seasonal flow of rivers and affect hydropower generation [39, 41]. Furthermore, changes in precipitation patterns alter the water availability in terms of its spatial and temporal distributions, causing difficulties in managing reservoir operations because of the need to balance conflicting goals [34].

Adapting to hydrological changes is a global challenge, particularly in the Himalayan region of Asia, where the complex interplay between climate change, glaciers, and water resources creates significant uncertainty. The Hindu Kush Himalayas (HKH), spanning Afghanistan, Bangladesh, Bhutan, China, India, Myanmar, Nepal, and Pakistan, is among the most climate-sensitive regions due to its high-altitude environment and extensive glacial coverage. While these countries share similar geographic features, Nepal uniquely embodies the full range of HKH characteristics, including diverse topography and climate. The southern regions of Nepal have a subtropical monsoon climate, while the higher northern areas have an alpine climate. The country has abundant freshwater reserves, with perennial rivers flowing across a wide range of altitudes, making Nepal one of the most suitable and favorable region for hydropower generation [1, 39]. However, hydropower generation here is vulnerable to climate change, which can impact both storage-type (ST) and run-of-river (RoR)-type hydropower plants [5]. Although ST hydropower plants are more flexible because of their storage capacity, RoR-type plants are sensitive to any changes in flow availability. Despite this susceptibility, hydropower continues to be one of the most important source of environment-friendly renewable energy for Nepal.

The majority of Nepal's hydropower plants are of the RoR types. The output of these plants reduces drastically during the dry season [27]. It is anticipated that the net worldwide hydropower generation and operation will experience a substantial reduction by the close of the century under the Representative Concentration Pathway RCP 2.6 and RCP 8.5 [9, 12]. The future forecasts indicate an increase in hydroelectricity production in certain regions such as India, Northeast China, Canada, Central Africa, and Northern Europe [71]. In contrast, studies conducted in the European Alps and the Western United States suggest that hydropower output will decline because of climate change. Reduced water availability is projected to cause critical issues and problems in some nations that rely greatly on river water for electricity generation, water distribution, and agricultural production [12]. Therefore, efficient and sustainable water utilization is crucial.

Shrestha et al. [60, 61] studied adaptation alternatives to optimize hydropower output in Nepal's Kulekhani Hydropower Project considering climate change impacts. Future changes in rainfall and temperature were predicted by using three regional climate models. The study concluded that while average and extreme temperatures will rise, precipitation will become unpredictable, showing no clear pattern other than a shift in peak timing. Future discharge and hydropower outputs were predicted using hydrological models and were projected to decline by 0.5% to 13%.

Furthermore, the effects of global warming on electricity generation at Nepal's Upper Tamakoshi Hydropower Project were studied by Shrestha et al. [62]. Based on projections from three GCMs, their anticipated streamflow range was + 37.83% to + 47%. The three GCMs were used to quantify the risk for energy production relative to baseline production levels, and the results showed risks spanning from mild to moderate, i.e., 0.69% to 13.24%. The effects of climate change on the hydrological regime in the HKH were examined by Bajracharya et al. [5]. In the RCP 8.5 setup, they

estimated a 4 °C increase in temperature, including a 26% increment in rainfall by 2100, by applying a soil and water assessment tool (SWAT) and downscaled GCM results. The simulations showed that by 2090, both the water flow at the outlet of the basin and the contribution from snowmelt would have increased by 50%. Similarly, Budhathoki et al. [10] also applied a SWAT model to simulate hydrologic responses and studied the effects of climate change on water balance. Their findings indicated that the Middle Mountain area is the most likely to see an increase in precipitation and water supply.

The new climate model based on the latest CMIP6 is widely accessible and will be incorporated in the sixth assessment report (AR6) of IPCC https://esgf-node.llnl.gov/search/cmip6/ and Lu et al. [35]). Future possibilities have become more plausible because SSPs are combined with RCPs. Researchers examined how well the CMIP6 models capture past climate variability, extremes, and the interplay between the ocean and atmosphere. Compared to the CMIP5 models, the CMIP6 models have less bias in the distribution of sea surface temperatures [30, 35, 66]. The Phase Six of Coupled Model Intercomparison Project (CMIP6) data, particularly under the Scenario Model Intercomparison Project (ScenarioMIP) introduces five alternative narratives, known as Shared Socioeconomic Pathways (SSPs) [11, 47], depicting different global societal developments by the end of the twenty-first century. SSP1 and SSP5 envision an optimistic future with robust institutions, economic growth, and investments in health and education. However, SSP1 leans towards sustainable energy, while SSP5 leans towards fossil-based energy. In contrast, SSP3 and SSP4 depict a more pessimistic future with limited investment in education and health, rising inequalities, and increased vulnerability to climate change. SSP3 prioritizes regional security, while SSP4 highlights large international and intra-national inequalities. SSP2 represents a central pathway, assuming historical trends continue without significant deviations [11, 24, 47]. These scenarios are crucial for projecting climate change using global climate models.

The study has mainly aimed to predict future river flow at hydropower dams and estimate energy generation using CMIP6 GCM models for moderate-to-high emission set-ups where most affected hydrological parameters for river flow are: precipitation, runoff, infiltration, evaporation, transpiration, snowmelt, base flow, ground water inflow, ground water outflow and channel storage. The models adopted in this study include recently organized global climate modeling experiments to understand various climate responses and mechanisms [16] and have higher spatial resolution compared to previous models to simulate climate more practically and capture interaction between the land surface, atmosphere, ocean, and cryosphere more accurately than in the previous models. Furthermore, improved data management and sharing practices make data analysis easier. Nonetheless, using CMIP6 GCM models for future river flow and hydro energy generation projection is limited in Nepal. Zhao et al. [76] used a CMIP6 coupled model for future river flow and energy projection in the Yangtze River in Tibet plateau using downscaled GCM data in the Variable Infiltration Capacity model, which is a large-scale gridded hydrological model mostly suitable for large river basins [72].

Different methods and models have been developed to assess rainfall-runoff processes. Shahid et al. [56] categorized these methods into the paired catchment method, statistical method, and hydrological modeling method. The paired catchment method faces challenges in identifying hydrologically identical catchments, while statistical methods have limited physical interpretability and struggle to directly assess the effects of land use changes on runoff and infiltration [56, 75]. Among hydrological models, commonly used approaches include the Variable Infiltration Capacity (VIC) model, distributed hydrological models, lumped hydrological models, and the Soil and Water Assessment Tool (SWAT). The VIC model, though suitable for large river basins, but it demands extensive computational resources. Distributed and lumped models require a large set of parameters for calibration and validation, making them less practical for data-scarce regions [56].

In contrast, SWAT was selected for this study due to its versatility in simulating river discharge across both large and small river basins, its ability to integrate land use, soil, and climate data at a watershed scale, and its proven effectiveness in long-term hydrological simulations [21]. Unlike lumped models, which treat entire basins as a single unit, SWAT's semi-distributed structure allows spatially explicit representation of hydrological processes, capturing the impact of land use and climate variability with greater accuracy. Furthermore, SWAT effectively balances computational efficiency with physical process representation, making it superior to complex distributed models that require extensive calibration.

Recent studies on climate change impacts on river flow in the Himalayan region using CMIP6 coupled models have provided valuable insights into hydroenergy generation but remain limited as compare to the geographic and climatic diversity of the Nepalese Himalayas, as well as unable to assess the economic implications of fluctuating river flows and seasonal variability [6, 28, 32, 49, 59, 67]. Addressing this gap, the research introduces a novel climate model by integrating CMIP6 (CanESM5, MIROC6, MRI-ESM2-0) climate projections with economic valuation techniques to assess the projected economic impacts of hydro energy generation in Nepal's Himalayas. This research considers the limitation in time interval of observed precipitation, temperature, and river flow data collected from authorized source (DHM Nepal), inconsistent spatial resolution of used map and the assumption of constant land use change over time. By evaluating

the economic performance of one of the first foreign-invested hydropower plants built two decades ago, this study provides a comparative analysis of past and projected economic outcomes, offering critical insights into the long-term sustainability of hydropower investments which can be extended to other river basins globally. This study informs to planners, policymakers, and investors about potential policy amendments and future investment strategies, highlighting both economic losses and benefits to support resilient and adaptive energy planning in the face of climate change.

2 Materials and method

2.1 Study area

The research was conducted on the Khimti River (Fig. 1), which flows along the boundary of two of Nepal's most climate-vulnerable districts, Dolakha and Ramechhap. The Khimti River originates from the Himalayas and merges with the Tamakoshi River at Khimtibeshi. The area along the riverbank has a warm, subtropical climate, with temperatures in the range of 22–27 °C during the summer and 10–15 °C during the winter. In the monsoon season, which lasts from June to September, the average monthly rainfall is 250–450 mm [42]. As reported by the closest station (Jiri), temperatures in the catchment, range from 25 to − 2 °C [62].

The Khimti hydropower project is designed as a RoR-type hydropower plant to produce 60 MW of electricity and around 350 GWh/yr. The total catchment area at the river intake is 358 km^2. The water flow at the intake is 31.5 m^3/s, with a minimum daily discharge of 3.5 m^3/s (https://hpl.com.np/projects/). The reason behind the study area selection is that the river basin is most vulnerable to climate change because its origination and ending point is within the most vulnerable district.

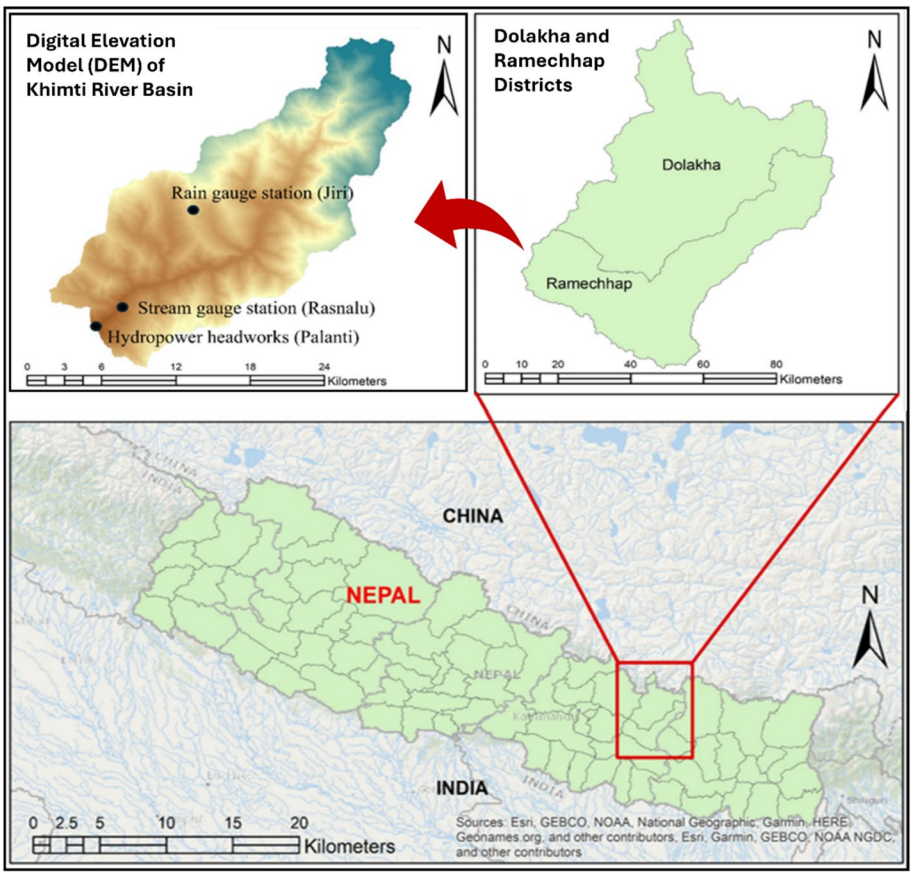

Fig. 1 Map of the study area

2.2 Data

2.2.1 Climate and hydrological data collection and processing

The Department of Hydrology and Meteorology of the Government of Nepal provided data of the nearest station covering more than 30 years (1965–2016 for temperature, 1961–2016 for precipitation, and 1964–2009 river flow) of measurement. Jiri is the weather station closest to the hydropower intake, while Rasnalu is the closest river flow station located about 3 km upstream (Table 1). For comparison and analysis of data deviation generated by climate models, missing data which were less than 5% were substituted by considering the average of historical data from the same dates in previous and subsequent years after the missing value [14]. The period 1994–2003 was selected to calibrate and validate the SWAT model because consistent and uninterrupted datasets were available for this timeframe. These datasets had a higher degree of correlation with the simulated flow, thereby justifying their selection for calibration and validation purposes. Although shorter calibration and validation periods can introduce uncertainties into model parameter estimation, the SWAT model was chosen based on its demonstrated effectiveness and reliable performance in similar mountainous river basins within the Himalayan region [10, 60, 61]. Furthermore, calibration employed the SUFI-2 algorithm (in SWAT-CUP software), providing comprehensive uncertainty assessment through parameter sensitivity analyses and uncertainty bounds (95% prediction uncertainty intervals).

The Earth System Grid Federation (ESGF) (https://esgf-node.llnl.gov/search/cmip6/), which is hosted by the Department of Energy, Lawrence Livermore National Laboratory of the United States, provided the CMIP6 data for three climate models CanESM5, MRI-ESM2-0, and MIROC6. Using Arc GIS, the downloaded meteorological data for the Shared Socioeconomic Pathway SSP2 4.5 and SSP5 8.5 scenarios from the ESGF were extracted in the form of a NetCDF file to determine the precise location of the observed data and bias-corrected from CMhyd software [38, 57]. The climate models used in this study were selected based on their historical accuracy in simulating precipitation, temperature patterns, and their capability to capture extreme climatic events. Previous studies have indicated that several CMIP models can exhibit significant biases and inconsistencies when representing regional hydrological processes, potentially increasing uncertainty in river flow projections [53]. Therefore, the model selection from the CMIP6 involved, identifying suitable models from existing literature based on proven performance in Nepal and HKH region [7, 15, 18, 29, 31, 37, 48, 49, 58, 64, 70] and subsequently evaluating their historical precipitation and temperature outputs against locally observed datasets using statistical metrics (mean bias, RMSE, and R^2). Through this precise approach, the three best-performing climate models for the Khimti River basin were determined.

2.2.2 Geophysical data collection and processing

In addition to meteorological data, the SWAT model also requires geophysical data, such as the Digital Elevation Model (DEM), land cover, and soil. The watershed of the hydropower intake and stream flow patterns were defined using an ASTER DEM with a 30 m resolution. This study utilized a soil map digitized by FAO-UNESCO at a 1:5,000,000 scale and a map of land use/land cover developed by the International Centre for Integrated Mountain Development in 2021.

2.2.3 Bias correction of climate models data

The statistical characteristics of practical observations may not be fully represented by the meteorological variables such as temperature and precipitation generated by different climate models mainly because of the great impact of local terrain and variations in altitude [17, 54]. Therefore, bias correction was performed using variance scaling and power transformation tools of CMhyd software for temperature and precipitation, respectively, to reduce the discrepancy between the simulated and observed data. These two tools (one pair) were chosen out of a total of eight tools (four pairs) within the CMhyd program because they were more effective than the others for analyzing data based on frequencies [23, 68]. The CMhyd software used in this study is a python based model which is able to use for global and regional climate model data in hydrological modeling. It performs both temporal and spatial bias

Table 1 Geographic location of hydrological and meteorological station

Station name	Type of station	Latitude	Longitude	Elevation (m)
Jiri	Meteorology	27° 38′	86° 14′	2003
Rasnalu	Hydrology	27° 34′	86° 11′	1520

correction on climate model data, ensuring that the data accurately reflects the observations from gauges used as inputs for hydrological models [51].

In the power transformation procedure, the rainfall data generated by the models were rectified by fitting them with observed data. The coefficient of variation (CV) was calculated using a power transformation tool. To correct the rainfall amounts for each day "P," Eq. (1) was used to transform them into corrected values denoted as P^*.

$$P^* = aP^b \tag{1}$$

The coefficient "b" was derived by comparing the CV of observed rainfall data with the rainfall data obtained from GCMs, and its average value was obtained. Similarly, the coefficient "a" was calculated by comparing the average value of observed rainfall data with the simulated value during the assessment period.

Similarly, the process of correcting temperature errors also included scaling and shifting to align the average and variance of the observed and GCM data with the observed data and its standard deviation. By fitting the GCM data with the observed data, the corrected daily temperature values, represented as "T," were obtained usi ng Eq. 2.

$$T = \overline{T}_{obs} + \frac{\sigma\left(T_{obs}\right)}{\sigma\left(T_{gcm}\right)}\left(T_{gcm} - \overline{T}_{gcm}\right) \tag{2}$$

In the equation, T represents the daily temperature after correction; T_{gcm}, the GCM temperature without bias correction; T_{obs}, the recorded temperatures for each day. The overbar represents the average value of the variable, while σ represents the standard deviation.

2.3 Method

Figure 2 provides a diagrammatic representation of the methodology used in this study. The geophysical data and observed meteorological data (temperature and precipitation) were used to set up the SWAT model.

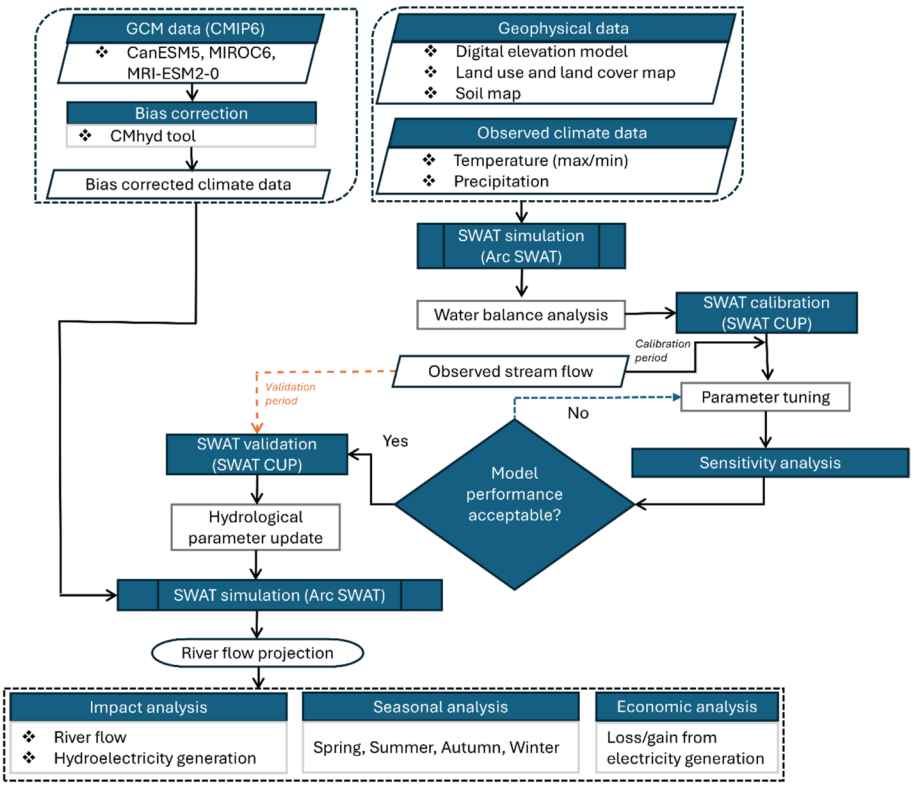

Fig. 2 Methodological framework

2.3.1 SWAT model setup and simulation

SWAT is a computational software designed to simulate the movement and characteristics of surface water, groundwater, and sediment in river basins of varying sizes, encompassing both small and large river systems [14]. The simulation and projection process in ArcSWAT 2012 model consisted of six steps, namely, watershed delineation, defining the hydrological response unit (HRU), formatting climate and weather data, performing SWAT model simulation, performing model calibration, and performing validation based on SWAT Calibration and Uncertainty Procedures (CUP). In the SWAT model, an HRU represents a component consisting of land areas sharing similar attributes related to land use, soil type, and slope characteristics [50]. Aster DEM with 30 × 30 km resolution was used for the watershed delineation. Five outlets were selected, and five sub-basins were generated, the study area automatically generated 25 outlets. The sub-basins were subsequently categorized into HRUs based on the distribution of land use, soil properties, and slope characteristics. The surface runoff within each sub-basin and the total runoff from the final outlet of the sub-basin with the lowest elevation were calculated by using the Eqs. (3), (4), (5), (6) [45]. The SWAT model was calibrated and validated using observed streamflow data from gauging stations within the study area. The calibration process was conducted using SWAT-CUP with the SUFI-2 algorithm to optimize key hydrological parameters. Model performance was evaluated using statistical metrics, including the Nash–Sutcliffe Efficiency (NSE), coefficient of determination (R^2), and Percent Bias (PBIAS), Standard Deviation Ratio (RSR) ensuring an accurate representation of the hydrological processes.

$$SW_t = SW_0 + \sum_{i=1}^{t} (R_{day} - Q_{surf} - E_a - W_{sweep} - Q_{gw})_i \tag{3}$$

This equation computes the final water content (SW_t) in millimeters by considering several factors, including the initial soil water content (SW_0) on the day *i*, passage of time (*t*) in days, amount of precipitation (R_{day}) on day *i* in millimeters, the water infiltrating into the vadose zone (W_{seep}) from the soil profile on day *i*, and groundwater flow (Q_{gw}) on day *i* in millimeters. The equation given below is used to determine the surface runoff.

$$Q_{surf} = \left(\frac{R_{day} - I_a}{R_{day} - I_a + S} \right)^2 \tag{4}$$

Equation (4) calculates the accumulated runoff or rainfall excess (Q_{surf}) in millimeters. It considers the daily rainfall amount (R_{day}) in millimeters, the initial abstractions (I_a) that include canopy interception, surface storage, and infiltration before runoff in millimeters, and the retention parameter (S). The retention parameter (S) is determined using the following equation.

$$S = 25.4 \left(\frac{1000}{CN} - 10 \right) \tag{5}$$

Equation (5) includes the curve number for the specific day, where the initial abstractions (I_a) are often estimated as 0.2 times the retention parameter (S). The accumulated runoff or rainfall excess (Q_{surf}) is expressed as follows.

$$Q_{surf} = \left(\frac{R_{day} - 0.2S}{R_{day} + 0.8S} \right)^2 \tag{6}$$

Water discharge occurs when the daily rainfall amount (R_{day}) surpasses the initial abstractions (I_a).

Figure 3 illustrates the hydrological system and its key water balance components affecting river flow in the Khimti River Basin. Precipitation serves as the primary water input, with monsoon rains increasing surface runoff and the risk of flash floods, while part of the water infiltrates into the soil, contributing to groundwater recharge. Baseflow from shallow and deep aquifers sustains river discharge during dry seasons, ensuring hydropower availability in the Khimti River Basin. Lateral flow, tile flow, and percolation regulate water movement, while bank storage and return flow help manage floods and maintain baseflow. Evaporation and outflow beyond the watershed represent water losses from the river system.

2.3.2 Power generation computation

Hydroelectricity generation computation is the multiplication of river flow, water density, head distance, gravitational force, and turbine efficiency. The gross hydroelectricity generation in watts is calculated using the following equation [25].

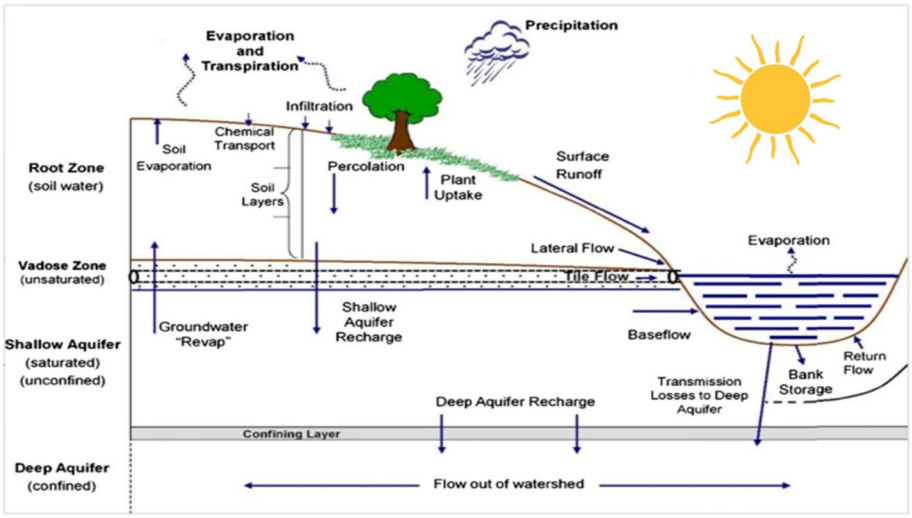

Fig. 3 Conceptual diagrams of hydrological cycle with SWAT simulation processes [44]

$$E = \rho g Q \Delta h \eta \tag{7}$$

where E represents energy generation; ρ is the density of water, with $\rho = 10^3$ kg/m^3; g represents the gravitational force (g = 9.81 m/s^2); Q is the river flow (m^3/s); Δh represents net head height, which is 660 m in Khimti hydropower plant; and η is the turbine efficiency (η = 80%).

2.3.3 Calculation of surplus hydro energy generation and economic analysis

The surplus hydro energy generation values presented in this study were directly derived from the simulated river discharge outputs generated by the calibrated SWAT hydrological model, driven by future climate scenarios obtained from the CMIP6 climate models (CanESM5, MIROC6, MRI-ESM2-0). Surplus energy generation was calculated based on modeled river flows exceeding baseline hydropower generation capacities, ensuring consistency with hydrological simulations. Additionally, to confirm accuracy and enhance reliability, the estimated surplus energy was cross-verified against historical energy generation data and observed streamflow records from the Khimti Hydropower Project. After determining the annual energy production, an economic analysis was conducted by multiplying the prevailing per-unit average energy price in Nepal.

3 Results

This section presents the findings of detailed hydrological modeling, various climate scenarios, future hydrological projections, future hydropower generation, seasonal variation, economic risk, and benefit analyses for the future.

3.1 SWAT model calibration and validation using SUFI-2 algorithm

To achieve the optimal alignment between the simulated and observed daily river flows, the SWAT model should be calibrated as it comprises default parameter values without calibration, and these values cannot simulate the surface runoff at the gauge station properly. The default parameter in the model underestimates the base flow and peak discharge in the snow-feeding river. Still, it overestimates the peak flow and underestimates the base flow for the seasonal river. Twenty one hydrological characteristics were selected for SWAT model calibration, as summarized in Table 2. The calibration and validation were performed at the Khimti hydropower dam site using SUFI-2 algorithm in SWAT-CUP software. The calibration phase involved using a seven-year dataset of stream flow for 1994–2000, while model validation was performed using a three-year dataset for 2001–2003 (Fig. 4). A warm-up period of five years was incorporated to establish favorable groundwater table conditions. The warm-up period 1989–1993 was adopted for calibration and 1996–2000, for model validation.

Table 2 Hydrological parameters used for calibration and validation

S.N	Parameter	Description	Rank	Min-value	Max-value	Fitted value
1	V_CH_N2.rte	Manning's 'n' value for the main channel	1	0.06	0.21	0.081
2	V_CH_K2.rte	Effective hydraulic conductivity in main channel alluvium	2	162.1	486.39	286.95
3	V_SMFMN.bsn	Minimum melt rate for snow during the year (winter solstice)	3	0	5.64	1.68
4	V_DEEPST.gw	Initial depth of water in the deep aquifer (mm)	4	11,710.7	37,239.2	21,628.51
5	V_PLAPS.sub	Precipitation lapse rate	5	− 139.77	580.78	307.32
6	R_SOL_K(..).sol	Saturated hydraulic conductivity	6	763.42	2000	1799.05
7	V_GW_DELAY.gw	Groundwater delay (Days)	7	230.35	500	427.05
8	R_SOL_AWC(..).sol	Available water capacity of the soil layer	8	0	0.56	0.05
9	V_ESCO.bsn	Soil evaporation compensation factor	9	0	0.57	0.29
10	V_GWHT.gw	Initial groundwater height (m)	10	6.51	19.54	14.09
11	V_CN2.mgt	SCS runoff curve number	11	35	98	79.32
12	V_SHALLST.gw	Initial depth of water in the shallow aquifer (mm)	12	0	31,689.23	522.87
13	V_REVAPMN.gw	Threshold depth of water in the shallow aquifer for 'revap' to occur (mm)	13	181.1	500	330.18
14	V_GWQMN.gw	Threshold depth of water in the shallow aquifer required for return flow to occur (mm)	14	2321.07	5000	2461.71
15	V_SMTMP.bsn	Snow melt base temperature	15	− 1.63	4.96	0.99
16	V_SMFMX.bsn	Maximum melt rate for snow during year (summer solstice)	16	0	6.07	5.04
17	V_ALPHA_BF.gw	Baseflow alpha factor (days)	17	0	0.54	0.06
18	V_CH_K1.sub	Effective hydraulic conductivity in tributary channel alluvium	18	95.91	287.77	187.7
19	V_RCHRG_DP.gw	Deep aquifer percolation fraction	19	0.02	0.67	0.34
20	V_TLAPS.sub	Temperature lapse rate	20	− 10	10	− 2.29
21	V_GW_SPYLD.gw	Specific yield of the shallow aquifer (m3/m3)	21	0.05	0.28	0.16

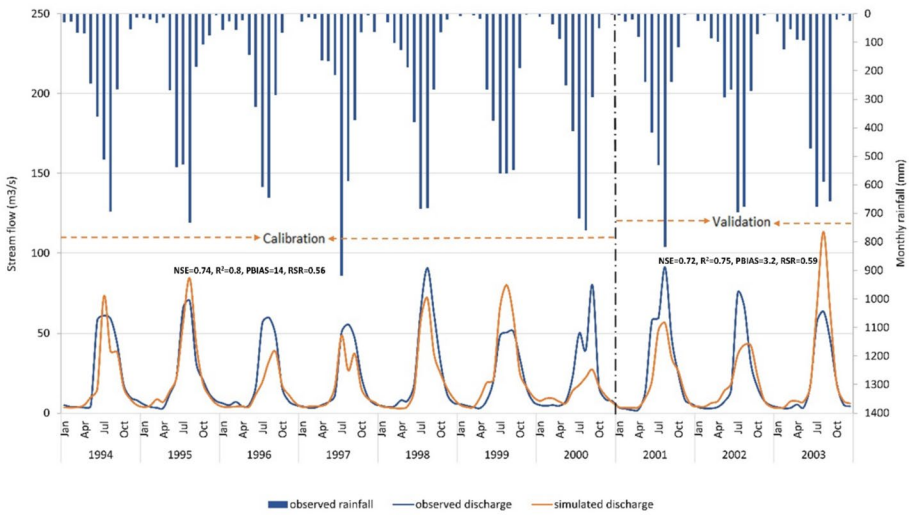

Fig. 4 Calibration and validation of the soil and water assessment tool (SWAT) model

Table 3 Calibration and validated results of the SWAT model

Statistics	Rasnalu Station	
	Calibration	Validation
NSE	0.74	0.72
R^2	0.8	0.75
PBIAS	14	3.2
RSR	0.56	0.59
WBE	13	15.1

The SWAT model parameters were selected for the calibration and validation based on previous studies in Nepal [22, 40, 46, 63, 69, 73]. The sensitivity analysis of the SWAT model in Khimti river basin, based on SUFI-2 t-statistics and *p*-values [55], revealed that channel hydraulics parameters were the most influential during calibration. Specifically, Manning's "n" value for the main channel (CH_N2) and effective hydraulic conductivity in main channel alluvium (CH_K2) ranked highest in sensitivity, indicating their strong control on flow velocity and in-stream water movement. Similarly, minimum melt rate of snow during the year (SMFMN), initial depth of water in the deep aquifer (DEEPST) and precipitation lapse rate (PLAPS) ranked in 3, 4, and 5 respectively, shown in Table 2 revealed that strongly influence hydrological parameters. Although the curve number (CN2), commonly associated with surface runoff generation, was identified in the narrative as the most sensitive parameter, it ranked 11th in the statistical analysis, suggesting moderate influence during this calibration [2, 20, 26, 33, 36, 52, 65]. Other important parameters included saturated hydraulic conductivity (SOL_K), available water capacity (SOL_AWC), soil evaporation compensation factor (ESCO), and groundwater delay (GW_DELAY), all of which shape surface and subsurface flow dynamics. Parameters like baseflow alpha factor (ALPHA_BF) and threshold depth for return flow (GWQMN) also showed relevance but with lower sensitivity rankings. Overall, while traditional runoff-related parameters remain significant, the analysis highlights the dominant role of channel and subsurface flow characteristics in governing streamflow response in the Khimti river basin.

Model performance evaluation involved assessing four statistical parameters: the Nash–Sutcliffe coefficient (NSE), coefficient of determination (R^2), root mean square error (RMSE)-observations standard deviation ratio (RSR), percent bias (PBIAS), and water balance error (WBE). The data in Table 3 indicate a strong agreement between the simulated and recorded flows, indicating a good fit for the model [43].

3.2 Climate model results for future projection

3.2.1 Effect of climate change on the average seasonal stream flow

The impacts of climate change on the water balance of the river were measured at the Khimti hydropower dam site at Palanti for three scenarios—one GCM and two SSPs for forthcoming periods 2023–2049 (called the 2040s),

2050–2074 (called the 2060s), and 2075–2099 (called the 2090s). Figure 5 shows the change in stream flow at different time intervals for SSP2 4.5 and SSP5 8.5 climate settings for CanESM5, MRI-ESM2-0, and MIROC6 models and compares the results with the observed baseline flow. All three GCMs show a decrease as well as an increase in average monthly flow.

During the dry seasons from January to April, MRI-ESM2-0 has the highest stream flow, followed by CanESM5 and MIROC6 for SSP2 4.5 in all time intervals and for the 2040s in SSP5 8.5. However, CanESM5 has the highest stream flow for the same dry season in SSP5 8.5 for the 2060s and 2090s, followed by MRI ESM2-0 and MIROC6. Compared to the results with the observed baseline, all three models have a nearly average flow for January and February. In contrast, the least flow is observed in March and April in the dry season in all time intervals. The stream flow in the river increases rapidly from May for all three models, similar to the observed flow, and reaches its peak flow in August. In August, MIROC6 showed the maximum peak flow, followed by MRI-ESM2-0 in both climate scenarios for all time intervals, though the difference in peak flow was not significant in the 2040s for both scenarios. The peak flow of CanESM5 is less than the observed baseline flow for SSP2 4.5 and 2040s and 2060s for SSP5 8.5. However, the highest water flow was greater than the recorded baseline water flow for the 2090s on SSP5 8.5. The stream flow rapidly decreased for all models as well as the baseline and reached its minimum value in December. Figure 5 shows that the post-monsoon flow (November–December) is greater than the pre-monsoon flow (January–March). Although the MRI-ESM2-0 has the highest flow in pre-monsoon period, it has the lowest flow in post-monsoon period in all time intervals for both scenarios. MIROC6 shows the highest flow for the post-monsoon periods for all time intervals of SSP2 4.5 and for the 2040s and 2060s of SSP5 8.5, while CanESM5 shows the maximum flow for the 2090s of SSP5 8.5 scenario. The baseline flow is almost average for all three models in both scenarios. The average flow of the three models for the pre-monsoon and post-monsoon periods will be 6.5 and 8 m^3/s, respectively. Similarly, the highest peak flow for MIROC6 model fluctuates between 110 and 120 m^3/s in all time intervals for both scenarios, whereas the least peak discharge for CanESM5 is 56 m^3/s for SSP2 4.5 scenario in the 2040s.

3.2.2 Projected impacts of climate change on future average annual streamflow

The percentage change of the annual average stream flow from the recorded reference point of water flow is shown in Fig. 6 for SSP2 4.5 and SSP5 8.5. In the SSP5 8.5 scenario, the CanESM5 model predicts a 41.9% rise by the 2060s and a 54% increase in river flow by the 2090s. In contrast, the SSP2 4.5 scenario projects the lowest growth rate of 0.2% in the 2040s. Similarly, according to MRI-ESM2-0 model in SSP2 4.5 scenario, stream flow will fall by 0.2% in the 2060s. For all three models and both scenarios, the stream flow increased by 15.8%–25.7%, during the remaining time intervals. Overall, the figure demonstrates significant variability with the increased range 0.2%–54% among different climate models, time intervals, and emission scenarios.

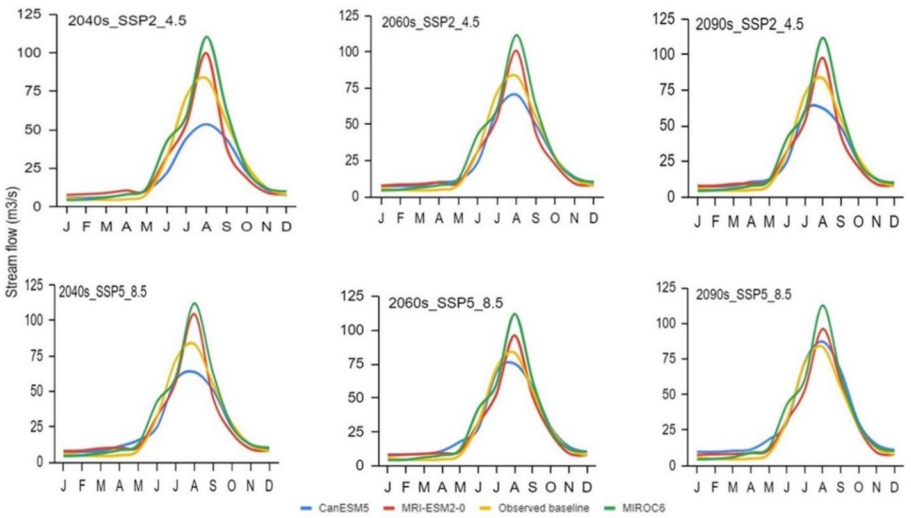

Fig. 5 Seasonal average stream flow in different time intervals

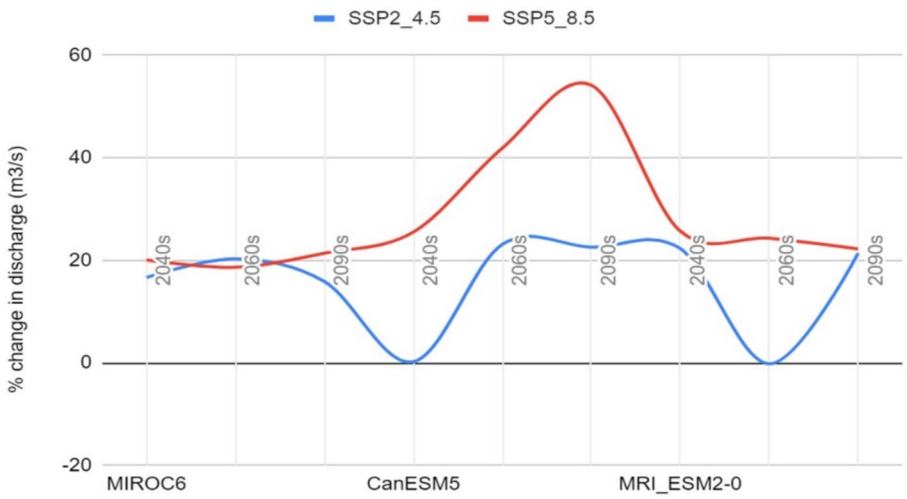

Fig. 6 Change in the average predicted stream flow compared with the observed flow

3.2.3 Seasonal stream flow in different time intervals

Table 4 compares projected seasonal streamflow across various climate scenarios (SSP2-4.5 and SSP5-8.5), future time periods (2040s, 2060s, and 2090s), and climate models (CanESM5, MRI-ESM2-0, and MIROC6) against historical observations. Notably, summer consistently records the highest streamflow across all scenarios and time periods, while winter demonstrates the lowest values, highlighting clear seasonal variability. Streamflow generally increases progressively over time, particularly under the more severe SSP5-8.5 scenario, with MIROC6 typically projecting higher values compared to CanESM5 and MRI-ESM2-0. Compared to historical data, future scenarios illustrate considerable increases in streamflow, especially in summer and autumn, highlights the potential climate-induced intensification of seasonal hydrological patterns.

3.2.4 Energy generation

Increasing greenhouse gas (GHG) emissions in the atmosphere causes changes in temperature and precipitation, which, over time, directly affect river discharge and, ultimately, hydroelectricity production. Although the average flow at intake is 31.5 m^3/s, the minimum flow at intake is only 3.5 m^3/s. The goal of the hydropower project was to generate a total of 62.5 MW at an intake flow of 11.65 m^3/s. Following auxiliary use, the hydropower produces approximately 350 GWh per year, as mentioned in the salient features in the project documents.

Nevertheless, the stream flow data at the intake were acquired from the Department of Hydrology and Meteorology of the Ministry of Energy, Water Resources and Irrigation of the Government of Nepal, and data for the period 1989–2008 were computed. After considering auxiliary uses, the calculated baseline resulted in an annual net energy generation of 382 GWh. This study eliminated the auxiliary uses from the net energy generation in each model for all scenarios. The resulting values were then compared to both the energy projected for the baseline and the energy calculated based on the observed stream flow data, as illustrated in Table 5.

Both the scenarios SSP2 4.5 and SSP5 8.5 clearly result in higher energy generation compared to the baseline mentioned in Table 5 for all time periods across the three GCMs. The CanESM5 model predicts that energy generation will increase slightly in the 2040s under the SSP2 4.5 scenario, which is only 14.8% and 5.2% higher than the project and calculated baselines, respectively.

The energy generation is expected to reach its highest point in the SSP5 8.5 scenario during the 2090s. This peak is projected to be 37% higher than the project baseline and 25.5% higher than the calculated baseline. In both scenarios, SSP2 4.5 and SSP5 8.5, the MIROC6 model predicts an increase in energy generation compared to the baseline. This increase is in the range of 17.4–19.4% compared to the project baseline and 7.6–9.4% compared to the calculated baseline. Similarly, the MRI-ESM2-0 model predicts an increase of 21.6–25% compared to the project baseline and an increase of 11.5–14.6% compared to the calculated baseline over the given time period.

Table 4 Historical and projected future stream flow (m^3/s)

Season	2040s_SSP2_4.5			2060s_SSP2_4.5			2090s_SSP2_4.5			2040s_SSP5_8.5			2060s_SSP5_8.5			2090s_SSP5_8.5			Historical observed
	CanESM5	MRI-ESM2-0	MIROC6	CanESM5	MRI-ESM2-0	MIROC6	CanESM5	MRI-ESM2-0	MIROC6	CanESM5	MRI-ESM2-0	MIROC6	CanESM5	MRI-ESM2-0	MIROC6	CanESM5	MRI-ESM2-0	MIROC6	
Spring	23.3	26.3	30.0	25.3	28.7	33.7	28.0	31.0	36.0	24.3	27.7	32.3	26.3	29.7	34.7	29.7	32.7	38.0	5.9
Summer	86.7	91.7	96.7	90.7	96.0	101.7	95.0	100.0	106.0	89.0	93.7	99.7	93.0	98.3	104.0	97.7	102.7	110.0	66.6
Autumn	50.0	55.0	60.0	55.0	58.0	65.0	60.0	62.0	68.0	53.0	57.0	63.0	58.0	60.0	66.0	63.0	65.0	70.0	30.4
Winter	7.0	8.3	10.0	8.3	9.7	11.7	10.0	11.0	13.0	8.0	9.3	11.3	9.3	10.7	12.7	10.7	12.0	14.3	6.1

Table 5 Projection of future energy generation and comparison with the baseline

GCMs	Scenario	Project baseline energy	Calculated baseline energy	Energy generated (GWh/yr)			% Difference as compared to project baseline			% Difference as compared calculated baseline		
				2040s	2060s	2090s	2040s	2060s	2090s	2040s	206 s	2090s
CanESM5	4.5	350 GWh/yr	382 GWh/yr	401.9	437.9	440.8	14.8	25.1	25.9	5.2	14.6	15.3
	8.5			441.3	460.8	479.6	26.1	31.7	37	15.2	20.6	25.5
MIROC6	4.5			412.5	417.6	411.1	17.8	19.3	17.4	7.9	9.3	7.6
	8.5			418	415.1	417.7	19.4	18.6	19.3	9.4	8.6	9.3
MRI-ESM2-0	4.5			433	431.7	430.4	23.7	23.3	22.9	13.4	13	12.6
	8.5			437.8	432.4	425.9	25	23.5	21.6	14.6	13.2	11.5

3.2.5 Surplus energy and economic benefits

Figure 7 illustrates the surplus hydropower generation and its corresponding economic benefits in US dollars (USD) for all time intervals, scenarios, and models examined in this work. First, with regard to the surplus energy compared to the project baseline and the related economic benefits, CanESM5 estimates the lowest surplus energy and economic gains in the 2040s for SSP2 4.5 and the highest for SSP5 8.5 in the 2090s, at around 2.9 million and 7.4 million USD, respectively, or 51.9 and 129.6 GWh/yr, respectively. According to MIROC6, the benefits to the economy are nearly constant at 3.8 million USD during the 2040s and 2090s under SSP5 8.5 and under SSP2 4.5 in the 2060s; however, the economic benefit fluctuates between 3.4 and 3.7 million USD in the other scenarios. Similarly, according to MRI-ESM2-0, there is a moderate decline in economic benefits from 5 million to 4.3 million USD for the SSP5 8.5 scenario and from 4.7 million to 4.5 million USD for the SSP2 4.5 scenario on increasing the time interval because of the surplus energy generation. Second, the surplus energy compared to the calculated baseline and its economic benefits is 32 units lesser than the result of project baseline energy generation and 1.8 units lesser than the results of economic benefits by project baseline on the same increasing trend.

3.2.6 Seasonal energy generation analysis

Figure 8 reflects the percentage change in energy generation for four seasons: spring (March–May), summer (June–August), autumn (September–November), and winter (December–February) within the time interval of 2023–2099. This analysis was conducted by comparing the projected energy generation with the historical stream flow data of 1989–2008. The horizontal axis of the figure indicates the seasons and time intervals of the three GCM models, namely, the 2040s, 2060s, and 2090s.

The results indicate that in the spring and winter seasons, the projected energy generation in the CanESM5, MIROC6, and MRI-ESM2-0 models for both scenarios SSP2 4.5 and SSP5 8.5 surpasses the energy obtained from observed river flow. Specifically, the CanESM5 model predicts a substantial 92% increase in energy generation, particularly notable during the winter season, in the 2090s. Furthermore, this model forecasts a 66% increase in energy generation for the SSP2 4.5 scenario during the spring of the 2090s but only a 35% increase during the winter. According to the MIROC6 model, during the winter of the 2060s, the SSP2 4.5 scenario exhibits an 8% higher energy generation than the SSP5 8.5 scenario; both scenarios perform similarly during the spring season. Additionally, the MRI-ESM2-0 model predicts higher energy generation in the spring of the 2040s under the SSP2 4.5 scenario. Both scenarios exhibit a similar percentage increase in energy generation during the 2060s; however, the energy generation is higher in the spring season in both scenarios SSP2 4.5 and SSP5 8.5, with increases of 66% and 58%, respectively, compared to the baseline. For the MRI-ESM2-0 model, the energy generation during winter is relatively similar between the two scenarios.

During the summer season, the three models exhibit almost indistinguishable performance in terms of electricity production across the three time intervals. However, in the autumn season, the projected energy levels are consistently lower than the energy obtained from the observed flow. Specifically, the CanESM5 model predicts a slightly lower energy

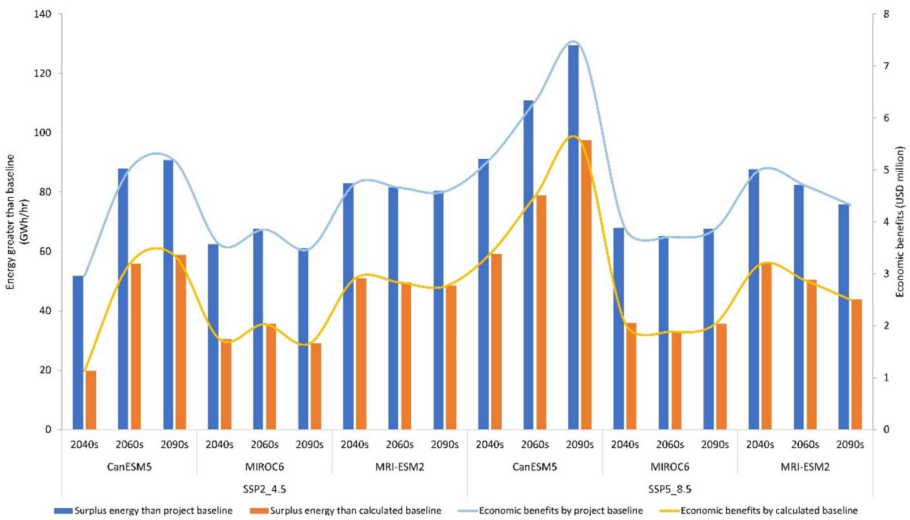

Fig. 7 Excess energy generation and economic benefits compared to baseline production

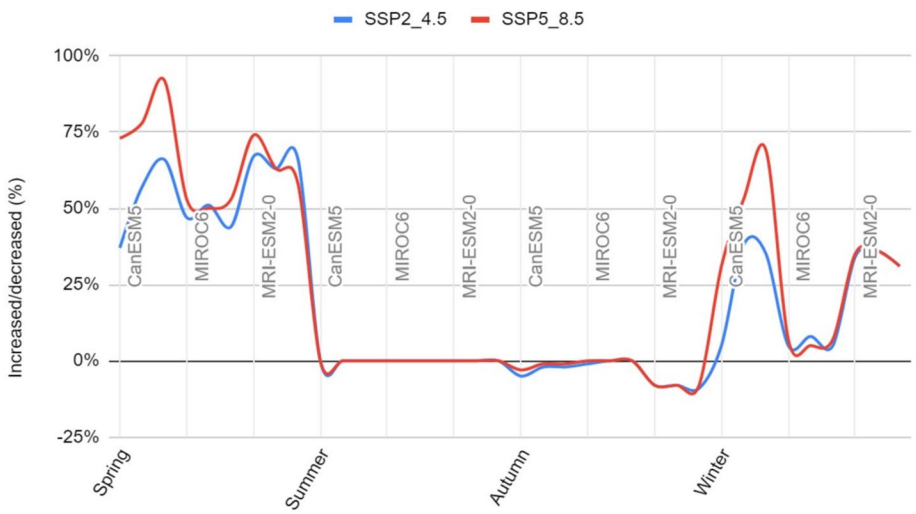

Fig. 8 Percentage differences in seasonal energy generation compared to the project baseline

generation by 5%–1% throughout all time intervals. Similarly, the MIROC6 model indicates a lower energy generation by 1% in the 2040s under the SSP2 4.5 scenario; otherwise, the generation remains consistent with the energy generated by observed flow. The MRI-ESM2-0 model predicts a more remarkable drop of 8%–9% in energy generation across the projected time intervals.

4 Discussion

Our study specifically investigated the implications of climate change on the water balance of the Khimti River basin, focusing on the Khimti hydropower dam site. We projected the future annual and seasonal energy generation, as well as the associated economic benefits, using three GCMs. The main objective was to assess how climate change affects the water balance at the hydropower intake and its influence on hydroelectricity generation. The novel aspect of this study is seasonal analysis of river flow and analyze the loss and gain from the hydropower in different climate scenarios which has not explored by previous studies in Nepal [6, 28, 32, 49, 59, 67].

We used the SWAT with GCM data of three models, namely, CanESM5, MIROC6, and MRI-ESM2-0, under the SSP2 4.5 and SSP5 8.5 climate scenarios of CMIP6. The temperature and precipitation data generated from these models were subjected to error correction by CMhyd software. Several studies employed SWAT models and different versions of the aforementioned climate models to project future water balance in different time periods [3–5, 19]. Bias correction of GCM data is important to adjust the output and improve its accuracy and reliability for use on a local scale. Various approaches for bias correction, encompassing statistical and dynamical methods, are available. Each method has its own advantages and limitations. The selection of a particular method depends on the specific application requirements and data availability. Marahatta et al. [39] adopted the quantile mapping method to correct the bias in GCM data. This bias correction technique was implemented to evaluate the impacts of climate change on the interconnected dynamics of water, energy, and economics, with a specific focus on the water storage type of the hydropower project.

Similarly, Adhikari et al. [1] employed the statistical downscaling model (SDSM, version 4.2.9) to assess the influence of climate change on the water conditions within a mountain river basin, considering various climate scenarios represented by RCPs. Chaemiso et al. [13] applied nonlinear correction for precipitation and linear correction for temperature to transform unbiased variables into corrected precipitation data. The objective of employing this approach was to evaluate the consequences of climate change on the hydrological processes occurring in Omo–Gibe Rivers in Ethiopia. Furthermore, Chakilu et al. [14] conducted a study in the upper Blue Nile river basin to evaluate stream flow response to climate change. They used variance scaling and power transformation methods for temperature and rainfall, respectively, in the CMhyd program because it is more effective than other methods. Their approach is aligned with the bias correction methodology adopted in our study.

The calibration and validation of the model involved comparing simulated annual and seasonal streamflow against observed historical discharge records at the Khimti hydropower intake using robust statistical indicators, including Nash–Sutcliffe Efficiency (NSE), coefficient of determination (R^2), percent bias (PBIAS), and the RMSE-observations

standard deviation ratio (RSR). Additionally, surplus energy projections derived from simulated seasonal flows were cross validated with historical energy production data from the Khimti hydropower project. We used the sequential uncertainty fitting (SUFI-2) algorithm from the SWAT-CUP along with seven years of observed river flow data to calibrate 21 hydrological parameters. A similar investigation was conducted by Bhatta et al. [8] in the West Seti River basin, Nepal, using datasets from a comparable time interval for calibrating 39 hydrological parameters. Short period data similar to [74] for the calibration and validation, results showed that the SWAT model performed well, with an NSE of 0.74, 0.72, and R^2 of 0.8, 0.75, indicating a strong correlation between observed and simulated streamflow. However, slight overestimations were noted during peak flow periods, likely due to the model's sensitivity to precipitation variability. These calibrated results were reasonably consistent with the study conducted by Bhatta et al. [8]. To quantify uncertainties in hydrological projections, a sensitivity analysis was conducted to identify key parameters affecting runoff. The SUFI-2 algorithm in SWAT-CUP provided 95% prediction uncertainty (95PPU), ensuring robust confidence intervals for the simulations. Additionally, multiple CMIP6 climate models (CanESM5, MIROC6, MRI-ESM2-0) were incorporated to assess variability in future runoff projections, reducing uncertainties in climate-driven hydrological impacts.

The three climate models show slightly higher projected stream flow than the observed flow in all time intervals in pre- and post-monsoon seasons: for MIROC6 and MRI-ESM2-0, higher flow is predicted in the monsoon season, whereas for CanESM5, the flow is lower in both climate scenarios except for the 2090s. The average annual flow projected by the three models varied significantly, with increases ranging from 0.2 to 54%. CanESM5 predicts a higher increase in the 2090s for the SSP5 8.5 scenario. A comparison of our results with those of similar previous studies shows that the river discharge in Tamakoshi River will be changed by – 37.83% to + 47%, indicating a mild risk of 0.69% to 6.63% for electricity generation at the Tamakoshi hydropower project [62]. Furthermore, according to a study on Kaligandaki River basin in Nepal, the river flow is expected to increase by 50% in RCP 4.5, and 8.5 scenarios [5], and a study on the West Seti River basin assumed a higher flow increase of 10.7% [10]. In this study, we found that surplus energy generation and economic benefits increased significantly across all three models compared to the project and calculated baselines. The most important contributions to the benefits were noted in spring followed by winter. During the summer and autumn seasons, there was no significant disparity between the recorded and predicted energy generation, possibly because the hydropower facility operated at near-full capacity for both recorded and predicted flows. This observation partially agrees with the results of a study conducted by Chilkoti et al. [17] in the C.H Corn Hydro project on the Ochlockonee River in the US; which demonstrated that there was less uncertainty in the spring and summer seasons.

The results of this study not only validate the theoretical expectation that increased temperature leads to increased streamflow due to enhanced precipitation and snowmelt but also extend existing hydrological theories by explicitly incorporating economic valuation of hydro-energy generation. Contrary to earlier theories that generalized runoff increase uniformly across seasons, this study highlights significant seasonal variations, particularly emphasizing economic benefits in the spring and winter seasons. Thus, this research advances the theoretical understanding by demonstrating that a nuanced seasonal analysis combined with economic evaluation is essential for sustainable hydropower planning under climate change scenarios. The Khimti River Basin provides a representative case study for understanding the impact of climate change on hydropower generation in Himalayan basins. However, to enhance the broader applicability of our findings, we compare our results with studies conducted in similar glacial-fed river systems, such as the Tamakoshi, Kaligandaki, and Upper Indus basins. These studies have reported both positive and negative trends in hydropower availability, depending on glacier melt dynamics and seasonal flow variations. The methodological approach used in this study including SWAT model calibration and CMIP6 climate projections can be replicated in other high-altitude, snow-fed basins with comparable topography and climatic conditions. While our conclusions are particularly relevant to Nepal, the framework can inform hydropower adaptation strategies across the broader Hindu Kush Himalayan region and other mountainous hydropower-reliant regions worldwide.

4.1 Policy recommendations

The river flow projection in the Khimti River basin for different time intervals suggests that there will be an increase in river flow under climate change, which directly influences hydroelectricity generation. Especially during the pre- and post-monsoon seasons. Water scarcity problems for hydropower operation will slightly decrease in the future, which will push to generate more hydroelectricity in the Himalayas region of Nepal. For the capturing of these opportunities with more beneficial approaches, implementation of multipurpose reservoirs upstream to store the surplus water during monsoon periods can consistently stabilize energy supply in drier seasons. Since the energy consumption rate of Nepal is comparatively low as per energy generation capacity, the establishment of long-term energy trade agreements with

nearby countries such as India, Bangladesh, Bhutan, and China help to increase the consumption of surplus electricity and enhance the country's economy.

Furthermore, authorities should offer targeted financial incentives, including tax reductions and direct subsidies, to attract private investment in reservoir-based hydropower projects. Allocating a portion of hydropower revenues to local forest user groups can fund initiatives aimed at forest conservation, runoff reduction, reservoir sedimentation control, and improved groundwater recharge, thus maintaining consistent river flows throughout the year. Lastly, directing increased hydropower-generated revenues towards rural electrification infrastructure can significantly improve rural communities by promoting small-scale industries, creating employment opportunities, and fostering broader socioeconomic development, which will accelerate consumption of electricity inside the country.

5 Conclusion

This study examined the impact of climate change on streamflow and its implications for hydro-energy generation in the Khimti River Basin, Nepal. Using the SWAT model calibrated with observed river flow data to ensure the reliability of the results, this research projected future discharge under SSP2-4.5 and SSP5-8.5 climate scenarios. The findings indicate a significant increase in annual river flow, ranging from 0.2 to 54% across all time intervals, with the highest increase of 54% projected for the 2090s followed by 41.9% for 2060s. Seasonal variations suggest higher monsoon flows for MIROC6 and MRI-ESM2-0, whereas CanESM5 predicts comparatively lower flow except in the late century. The projected increase in streamflow presents a positive opportunity for hydropower generation and economic benefits, particularly in the spring and winter seasons, when additional energy production can enhance grid stability. These findings provide valuable insights for policymakers, planners, and investors to optimize hydropower potential through strategic infrastructure development, climate-adaptive policies, and foreign investment in energy projects.

Future work should focus on integrating reservoir management strategies and adaptive energy storage solutions to enhance hydropower sustainability. Additionally, real-time hydrological forecasting could improve the reliability of energy generation estimates, ensuring efficient hydropower operation under changing climatic conditions. Similarly, this research also recommended to explore nature-based solutions for managing excessive rainwater and identifying suitable upstream sites for reservoir construction to optimize seasonal energy production in Himalaya region.

Author contribution D. C; conceptualization, methodology, software, analysis, and writing—original draft. R. L. R; Critical revision, Write up. Y. A. O; Draft preparation. S. N. N; data analyst, J. P; Data analysis, J. W. R; Software, D. S; software, validation, J. L; review, J. H; supervision, funding acquisition.

Funding This work was supported by the National Research Foundation of Korea (NRF) grant funded by the Korean government (MIST) [No. RS-2021-NR060108]; the Korean Institute of Energy Technology Evaluation and Planning (KETEP); and the Ministry of Trade, Industry & Energy (MoTIE) of the Republic of Korea [No. RS-2022-KP002719].

Data availability No, I do not have any research data outside the submitted manuscript file.

Declarations

Ethics approval and consent to participate Not applicable.

Consent for publication Not applicable.

Competing interests No, I declare that the authors have no competing interests as defined by Discover, or other interests that might be perceived to influence the results and/or discussion reported in this paper.

References

1. Adhikari TR, Talchabhadel R, Shrestha S, Sharma S, Aryal D, Pradhanang SM. The evaluation of climate change impact on hydrologic processes of a mountain river basin. Theoret Appl Climatol. 2022;150(1–2):749–62. https://doi.org/10.1007/s00704-022-04204-3.
2. Ahn SR, Kim SJ. Analysis of water balance by surface–groundwater interaction using the SWAT model for the Han River basin, South Korea. Paddy Water Environ. 2018;16(3):543–60. https://doi.org/10.1007/S10333-018-0647-X/FIGURES/10.
3. Aizawa T, Ishii M, Oshima N, Yukimoto S, Hasumi H. Arctic warming and associated sea ice reduction in the early 20th century induced by natural forcings in MRI-ESM2.0 climate simulations and multimodel analyses. Geophys Res Lett. 2021. https://doi.org/10.1029/2020GL092336.
4. Azizi AH, Asaoka Y. Assessment of the impact of climate change on snow distribution and river flows in a snow-dominated mountainous watershed in the western hindukush–himalaya, afghanistan. Hydrology. 2020;7(4):1–24. https://doi.org/10.3390/hydrology7040074.
5. Bajracharya AR, Bajracharya SR, Shrestha AB, Maharjan SB. Climate change impact assessment on the hydrological regime of the Kaligandaki Basin, Nepal. Sci Total Environ. 2018;625:837–48. https://doi.org/10.1016/j.scitotenv.2017.12.332.
6. Baniya R, Regmi RK, Talchabhadel R, Sharma S, Panthi J, Ghimire GR, Bista S, Thapa BR, Pradhan AMS, Tamrakar J. Integrated modeling for assessing climate change impacts on water resources and hydropower potential in the Himalayas. Theoret Appl Climatol. 2024;155(5):3993–4008. https://doi.org/10.1007/S00704-024-04863-4/METRICS.
7. Bhardwaj SS, Jha MK, Uniyal B. Impact of climate change on hydrological fluxes in the Upper Bhagirathi River Basin, Uttarakhand. Environ Monit Assess. 2025. https://doi.org/10.1007/s10661-025-13676-5.
8. Bhatta B, Shrestha S, Shrestha PK, Talchabhadel R. Modelling the impact of past and future climate scenarios on streamflow in a highly mountainous watershed: a case study in the West Seti River Basin, Nepal. Sci Total Environ. 2020. https://doi.org/10.1016/j.scitotenv.2020.140156.
9. Bhattarai U, Devkota LP, Marahatta S, Shrestha D, Maraseni T. How will hydro-energy generation of the Nepalese Himalaya vary in the future? A climate change perspective. Environ Res. 2022. https://doi.org/10.1016/j.envres.2022.113746.
10. Budhathoki A, Babel MS, Shrestha S, Meon G, Kamalamma AG. Climate change impact on water balance and hydrological extremes in different physiographic regions of the West Seti River Basin, Nepal. Ecohydrol Hydrobiol. 2021;21(1):79–95. https://doi.org/10.1016/j.ecohyd.2020.07.001.
11. Buhay Bucton BG, Shrestha S, Kc S, Mohanasundaram S, Virdis SGP, Chaowiwat W. Impacts of climate and land use change on groundwater recharge under shared socioeconomic pathways: a case of Siem Reap, Cambodia. Environ Res. 2022. https://doi.org/10.1016/j.envres.2022.113070.
12. Carvajal PE, Li FGN, Soria R, Cronin J, Anandarajah G, Mulugetta Y. Large hydropower, decarbonisation and climate change uncertainty: Modelling power sector pathways for Ecuador. Energ Strat Rev. 2019;23:86–99. https://doi.org/10.1016/j.esr.2018.12.008.
13. Chaemiso SE, Abebe A, Pingale SM. Assessment of the impact of climate change on surface hydrological processes using SWAT: a case study of Omo-Gibe river basin, Ethiopia. Model Earth Syst Environ. 2016;2(4):1–15. https://doi.org/10.1007/s40808-016-0257-9.
14. Chakilu GG, Sándor S, Zoltán T, Phinzi K. Climate change and the response of streamflow of watersheds under the high emission scenario in Lake Tana sub-basin, upper Blue Nile basin, Ethiopia. J Hydrol Region Stud. 2022. https://doi.org/10.1016/j.ejrh.2022.101175.
15. Chanda N, Chintalacheruvu MR, Choudhary AK. Hydrological modelling of a mountainous watershed: simulating streamflows under present and projected climate conditions. Theor Appl Climatol. 2025. https://doi.org/10.1007/s00704-024-05250-9.
16. Chen H, Sun J, Lin W, Xu H. Comparison of CMIP6 and CMIP5 models in simulating climate extremes. In *Science bulletin*, vol. 65, Issue 17. Elsevier B.V. 2020. pp. 1415–1418. https://doi.org/10.1016/j.scib.2020.05.015.
17. Chilkoti V, Bolisetti T, Balachandar R. Climate change impact assessment on hydropower generation using multi-model climate ensemble. Renew Energy. 2017;109:510–7. https://doi.org/10.1016/j.renene.2017.02.041.
18. David Raj A, Kumar S, Sooryamol KR. Downscaling future precipitation with shared socioeconomic pathway (SSP) scenarios using machine learning models in the North-Western Himalayan region. Model Earth Syst Environ. 2024. https://doi.org/10.1007/s40808-024-02113-0.
19. de Oliveira VA, de Mello CR, Viola MR, Srinivasan R. Assessment of climate change impacts on streamflow and hydropower potential in the headwater region of the Grande river basin, Southeastern Brazil. Int J Climatol. 2017;37(15):5005–23. https://doi.org/10.1002/joc.5138.
20. Desai S, Singh DK, Islam A, Sarangi A. Multi-site calibration of hydrological model and assessment of water balance in a semi-arid river basin of India. Quatern Int. 2021;571:136–49. https://doi.org/10.1016/J.QUAINT.2020.11.032.
21. Devia GK, Ganasri BP, Dwarakish GS. A review on hydrological models. Aquatic Procedia. 2015;4:1001–7. https://doi.org/10.1016/j.aqpro.2015.02.126.
22. Devkota N, Lamichhane S, Bhattarai PK. Multi-site calibration of the SWAT hydrological model and study of spatio-temporal variation of water balance components in the Narayani River Basin, central part of Nepal. H2Open J. 2024;7(1):114–29. https://doi.org/10.2166/H2OJ.2024.084.
23. Fang GH, Yang J, Chen YN, Zammit C. Comparing bias correction methods in downscaling meteorological variables for a hydrologic impact study in an arid area in China. Hydrol Earth Syst Sci. 2015;19(6):2547–59. https://doi.org/10.5194/hess-19-2547-2015.
24. Fricko O, Havlik P, Rogelj J, Klimont Z, Gusti M, Johnson N, Kolp P, Strubegger M, Valin H, Amann M, Ermolieva T, Forsell N, Herrero M, Heyes C, Kindermann G, Krey V, McCollum DL, Obersteiner M, Pachauri S, Riahi K. The marker quantification of the Shared Socioeconomic Pathway 2: a middle-of-the-road scenario for the 21st century. Global Environ Change. 2017;42:251–67. https://doi.org/10.1016/j.gloenvcha.2016.06.004.
25. Hasan MM, Wyseure G. Impact of climate change on hydropower generation in Rio Jubones Basin. Ecuador Water Sci Eng. 2018;11(2):157–66. https://doi.org/10.1016/j.wse.2018.07.002.
26. Himanshu SK, Pandey A, Shrestha P. Application of SWAT in an Indian river basin for modeling runoff, sediment and water balance. Environ Earth Sci. 2017;76(1):1–18. https://doi.org/10.1007/S12665-016-6316-8/TABLES/7.
27. Hurford AP, Harou JJ, Bonzanigo L, Ray PA, Karki P, Bharati L, Chinnasamy P. Efficient and robust hydropower system design under uncertainty—a demonstration in Nepal. Renew Sustain Energy Rev. 2020. https://doi.org/10.1016/j.rser.2020.109910.

28. Khatri D, Pandey VP, Lamsal GR, Baniya R. Climate change impact on hydropower generation and adaptation through reservoir operation in a Himalayan river, Tamor. J Water Clim Change. 2024;15(9):4631–46. https://doi.org/10.2166/WCC.2024.246.
29. Konda G, Chowdary JS, Gnanaseelan C, Parekh A. Improvement in the skill of CMIP6 decadal hindcasts for extreme rainfall events over the Indian summer monsoon region. Sci Rep. 2023. https://doi.org/10.1038/s41598-023-48268-1.
30. Konda G, Vissa NK. Evaluation of CMIP6 models for simulations of surplus/deficit summer monsoon conditions over India. Clim Dyn. 2022. https://doi.org/10.1007/s00382-022-06367-1.
31. Kumar N, Singh SK, Dubey AK, Ray RL, Mustak S, Rawat KS. Prediction of soil erosion risk using earth observation data under recent emission scenarios of CMIP6. Geocarto Int. 2022;37(24):7041–64. https://doi.org/10.1080/10106049.2021.1973116.
32. Lamichhane M, Phuyal S, Mahato R, Shrestha A, Pudasaini U, Lama SD, Chapagain AR, Mehan S, Neupane D. Assessing climate change impacts on streamflow and baseflow in the Karnali River Basin, Nepal: a CMIP6 multi-model ensemble approach using SWAT and web-based hydrograph analysis tool. Sustainability. 2024;16(8):3262. https://doi.org/10.3390/SU16083262.
33. Larbi I, Obuobie E, Verhoef A, Julich S, Feger KH, Bossa AY, Macdonald D. Water balance components estimation under scenarios of land cover change in the Vea catchment, West Africa. Hydrol Sci J. 2020;65(13):2196–209. https://doi.org/10.1080/02626667.2020.1802467.
34. Liu J, Long A, Deng X, Yin Z, Deng M, An Q, Gu X, Li S, Liu G. The impact of climate change on hydrological processes of the glacierized watershed and projections. Remote Sens. 2022. https://doi.org/10.3390/rs14061314.
35. Lu Z, Zhao T, Zhou W. Evaluation of the antarctic circumpolar wave simulated by CMIP5 and CMIP6 models. Atmosphere. 2020. https://doi.org/10.3390/atmos11090931.
36. Lu Z, Zou S, Xiao H, Zheng C, Yin Z, Wang W. Comprehensive hydrologic calibration of SWAT and water balance analysis in mountainous watersheds in northwest China. Phys Chem Earth Parts A/B/C. 2015;79–82:76–85. https://doi.org/10.1016/J.PCE.2014.11.003.
37. Maharjan KR, Bhattarai U, Bhattarai PK, Devkota LP. Climate change impacts on flood dynamics and seasonal flow variability in central Nepal: the Kaligandaki River Basin case. Theor Appl Climatol. 2025. https://doi.org/10.1007/s00704-025-05378-2.
38. Malik MA, Dar AQ, Jain MK. Modelling the influence of changing climate on the hydrology of high elevation catchments in NW Himalaya's. Model Earth Syst Environ. 2022;8(4):4487–96. https://doi.org/10.1007/s40808-022-01407-5.
39. Marahatta S, Bhattarai U, Devkota LP, Aryal D. Unravelling the water-energy-economics-continuum of hydroelectricity in the face of climate change. Int J Energy Water Resour. 2022;6(3):323–35. https://doi.org/10.1007/s42108-021-00174-w.
40. Marahatta S, Devkota LP, Aryal D. Application of SWAT in hydrological simulation of complex mountainous River Basin (Part I: model development). Water. 2021;13(11):1546. https://doi.org/10.3390/W13111546.
41. Meema T, Tachikawa Y, Ichikawa Y, Yorozu K. Uncertainty assessment of water resources and long-term hydropower generation using a large ensemble of future climate projections for the Nam Ngum River in the Mekong Basin. J Hydrol Region Stud. 2021. https://doi.org/10.1016/j.ejrh.2021.100856.
42. Michelle. Climate risk case study Khimti 1 hydropower scheme Himal Power Limited-NEPAL; 2011.
43. Moriasi DN, Arnold JG, Liew MW, Van Bingner RL, Harmel RD, Veith TL. Model evaluation guidelines for systematic quantification of accuracy in watershed simulations. Trans ASABE. 2007;50(3):885–900. https://doi.org/10.13031/2013.23153.
44. Nasiri S, Ansari H, Ziaei AN. Simulation of water balance equation components using SWAT model in Samalqan Watershed (Iran). Arab J Geosci. 2020;13(11):1–15. https://doi.org/10.1007/S12517-020-05366-Y/FIGURES/10.
45. Neitsch SL, Arnold JG, Kiniry JR, Williams JR. College of Agriculture and life Sciences Soil and Water Assessment Tool Theoretical Documentation Version 2009; 2011.
46. Nepal J, Pant RR, Shrestha S, Paudel S, Bishwakarma K, Awasthi MP, Dhital YP. Water balance estimation and runoff simulation of Chameliya Watershed. Nepal Environ Earth Sci. 2024;83(3):1–15. https://doi.org/10.1007/S12665-024-11430-7/TABLES/6.
47. O'Neill BC, Tebaldi C, Van Vuuren DP, Eyring V, Friedlingstein P, Hurtt G, Knutti R, Kriegler E, Lamarque JF, Lowe J, Meehl GA, Moss R, Riahi K, Sanderson BM. The scenario model intercomparison project (ScenarioMIP) for CMIP6. Geosci Model Dev. 2016;9(9):3461–82. https://doi.org/10.5194/gmd-9-3461-2016.
48. Pandey S, Mishra BK. Spatial and temporal analysis of extreme precipitation under climate change over Gandaki Province, Nepal. Architecture. 2022;2(4):724–59. https://doi.org/10.3390/architecture2040039.
49. Pradhan AMS, Silwal G, Shrestha S, Huynh TC, Dawadi S. Can a spatially distributed hydrological model effectively analyze hydrological processes in the Nepal Himalaya River Basin? Environ Model Assess. 2024;29(6):1037–58. https://doi.org/10.1007/S10666-024-09975-9/FIGURES/13.
50. Rahman K, da Silva AG, Tejeda EM, Gobiet A, Beniston M, Lehmann A. An independent and combined effect analysis of land use and climate change in the upper Rhone River watershed, Switzerland. Appl Geogr. 2015;63:264–72. https://doi.org/10.1016/j.apgeog.2015.06.021.
51. Rathjens H, Bieger K, Srinivasan R, Chaubey I, Arnold JG. CMhyd user manual documentation for preparing simulated climate change data for hydrologic impact studies; 2016. https://riverbankcomputing.com/software/pyqt/intro
52. Rautela KS, Kumar M, Sofi MS, Kuniyal JC, Bhat SU. Modelling of streamflow and water balance in the Kuttiyadi River Basin using SWAT and remote sensing/GIS tools. Int J Environ Res. 2022;16(4):1–14. https://doi.org/10.1007/S41742-022-00416-7/TABLES/6.
53. Sahu RT, Turkane SD, Rathnayake U. Streamflow projections under climate change framework for the Mahanadi River catchment, India. J Water Clim Change. 2025;16(2):675–94. https://doi.org/10.2166/WCC.2025.693.
54. Schaefli B. Projecting hydropower production under future climates: a guide for decision-makers and modelers to interpret and design climate change impact assessments. In: Wiley interdisciplinary reviews: water, vol 2, Issue 4. Wiley; 2015, pp. 271–289. https://doi.org/10.1002/WAT2.1083.
55. Serur AB, Adi KA. Multi-site calibration of hydrological model and the response of water balance components to land use land cover change in a rift valley Lake Basin in Ethiopia. Sci Afr. 2022;15: e01093. https://doi.org/10.1016/J.SCIAF.2022.E01093.
56. Shahid M, Cong Z, Zhang D. Understanding the impacts of climate change and human activities on streamflow: a case study of the Soan River basin, Pakistan. Theor Appl Clim. 2018;134(1–2):205–19. https://doi.org/10.1007/S00704-017-2269-4/FIGURES/9.
57. Shaikh MM, Lodha P, Lalwani P, Mehta D. Climatic projections of Western India using global and regional climate models. Water Pract Technol. 2022. https://doi.org/10.2166/wpt.2022.090.

58. Shanmugam M, Lim S, Hosan ML, Shrestha S, Babel MS, Virdis SGP. Lapse rate-adjusted bias correction for CMIP6 GCM precipitation data: an application to the Monsoon Asia Region. Environ Monit Assess. 2024. https://doi.org/10.1007/s10661-023-12187-5.
59. Sharma N, Mishra BK, Baral S. Climate change impacts on Seti Gandaki River flow from hydropower perspectives. Nepal Sustain Water Resour Manag. 2024;10(1):1–18. https://doi.org/10.1007/S40899-023-01017-8/FIGURES/17.
60. Shrestha A, Shrestha S, Tingsanchali T, Budhathoki A, Ninsawat S. Adapting hydropower production to climate change: a case study of Kulekhani Hydropower Project in Nepal. J Clean Prod. 2021. https://doi.org/10.1016/j.jclepro.2020.123483.
61. Shrestha A, Shrestha S, Tingsanchali T, Budhathoki A, Ninsawat S. Adapting hydropower production to climate change: a case study of Kulekhani Hydropower Project in Nepal. J Clean Prod. 2021;279: 123483. https://doi.org/10.1016/J.JCLEPRO.2020.123483.
62. Shrestha S, Bajracharya AR, Babel MS. Assessment of risks due to climate change for the Upper Tamakoshi Hydropower Project in Nepal. Clim Risk Manag. 2016;14:27–41. https://doi.org/10.1016/j.crm.2016.08.002.
63. Shrestha S, Nepal S. Water balance assessment under different glacier coverage scenarios in the Hunza Basin. Water. 2019;11(6):1124. https://doi.org/10.3390/W11061124.
64. Singh D, Zhu Y, Liu S, Srivastava PK, Dharpure JK, Chatterjee D, Sahu R, Gagnon AS. Exploring the links between variations in snow cover area and climatic variables in a Himalayan catchment using earth observations and CMIP6 climate change scenarios. J Hydrol. 2022. https://doi.org/10.1016/j.jhydrol.2022.127648.
65. Singh L, Saravanan S. Simulation of monthly streamflow using the SWAT model of the Ib River watershed, India. HydroResearch. 2020;3:95–105. https://doi.org/10.1016/J.HYDRES.2020.09.001.
66. Su B, Huang J, Mondal SK, Zhai J, Wang Y, Wen S, Gao M, Lv Y, Jiang S, Jiang T, Li A. Insight from CMIP6 SSP-RCP scenarios for future drought characteristics in China. Atmos Res. 2021. https://doi.org/10.1016/j.atmosres.2020.105375.
67. Subedi SR, Manoj L, Dhungana S, Chalise B, Shishir B, Chaulagain U, Rakesh K. Assessing the impact of climate change on streamflow in the Tamor River Basin, Nepal: an analysis using SWAT and CMIP6 scenarios. Discov Civ Eng. 2024;1(1):1–20. https://doi.org/10.1007/S44290-024-00143-2.
68. Teutschbein C, Seibert J. Bias correction of regional climate model simulations for hydrological climate-change impact studies: review and evaluation of different methods. J Hydrol. 2012;456–457:12–29. https://doi.org/10.1016/j.jhydrol.2012.05.052.
69. Thapa BR, Ishidaira H, Pandey VP, Shakya NM. A multi-model approach for analyzing water balance dynamics in Kathmandu Valley. Nepal J Hydrol Region Stud. 2017;9:149–62. https://doi.org/10.1016/J.EJRH.2016.12.080.
70. Timilsina A, Talchabhadel R, Pandey VP. Rising temperature trends across the narayani river basin in Central Nepal projected by CMIP6 models. n.d. https://esgf-node.llnl.gov/search/cmip6/.
71. Van Vliet MTH, Wiberg D, Leduc S, Riahi K. Power-generation system vulnerability and adaptation to changes in climate and water resources. Nat Clim Change. 2016;6(4):375–80. https://doi.org/10.1038/nclimate2903.
72. Vigerstol KL, Aukema JE. A comparison of tools for modeling freshwater ecosystem services. J Environ Manag. 2011;92(10):2403–9. https://doi.org/10.1016/j.jenvman.2011.06.040.
73. Yadav VK, Nema MK, Khare D. Evaluation of SWAT model for simulating the water balance components for the Dudh Koshi River Basin in Nepal. 2022. pp.63–77. https://doi.org/10.1007/978-3-031-13467-8_5
74. Yang S, Tan ML, Song Q, He J, Yao N, Li X, Yang X. Coupling SWAT and Bi-LSTM for improving daily-scale hydro-climatic simulation and climate change impact assessment in a tropical river basin. J Environ Manag. 2023;330: 117244. https://doi.org/10.1016/J.JENVMAN.2023.117244.
75. Zhao F, Zhang L, Xu Z, Scott DF. Evaluation of methods for estimating the effects of vegetation change and climate variability on streamflow. Water Resour Res. 2010;46(3):3505. https://doi.org/10.1029/2009WR007702.
76. Zhao Y, Xu K, Dong N, Wang H. Projection of climate change impacts on hydropower in the source region of the Yangtze River based on CMIP6. J Hydrol. 2022. https://doi.org/10.1016/j.jhydrol.2022.127453.

water

MDPI

Article

Extreme Precipitation Dynamics and El Niño–Southern Oscillation Influences in Kathmandu Valley, Nepal

Deepak Chaulagain [1,2], Ram Lakhan Ray [3], Abdulfati Olatunji Yakub [1,2], Noel Ngando Same [1,2], Jaebum Park [1,2], Anthony Fon Tangoh [1,2], Jong Wook Roh [4], Dongjun Suh [1], Jeong-Ok Lim [2] and Jeung-Soo Huh [1,2,*]

[1] Department of Convergence & Fusion System Engineering, Graduate School, Kyungpook National University, Sangju 37224, Republic of Korea; chaulagaindeepu11@gmail.com (D.C.); yakubabdulfatail@gmail.com (A.O.Y.); samenoel1@gmail.com (N.N.S.); woqja133@naver.com (J.P.); fontangoh@gmail.com (A.F.T.); dongjunsuh@knu.ac.kr (D.S.)
[2] Institute for Global Climate Change & Energy, Kyungpook National University, Daegu 41566, Republic of Korea; jolim@knu.ac.kr
[3] Cooperative Agricultural Research Center, College of Agriculture, Food, and Natural Resources, Prairie View A & M University, Prairie View, TX 77446, USA; raray@pvamu.edu
[4] Department of Nano & Advanced Materials Science and Engineering, Kyungpook National University, Sangju 37224, Republic of Korea; jw.roh@knu.ac.kr
* Correspondence: jshuh@knu.ac.kr

Abstract: Understanding historical climatic extremes and variability is crucial for effective climate change adaptation, particularly for urban flood management in developing countries. This study investigates historical precipitation trends in the Kathmandu Valley, Nepal, focusing on precipitation frequency, intensity, and the influence of the El Niño–Southern Oscillation (ENSO), using extreme precipitation indices and the precipitation concentration index (PCI). The results reveal sharply fluctuating short-term precipitation from 1980 to 2022, with the exception of an increasing trend during spring (1.17 mm/year) and a decreasing trend in November and December. Trends in extreme precipitation indices are mixed: RX7day shows an increasing trend of 0.1 mm/year, with decadal analysis (1980–2001 and 2002–2022) indicating similar upward patterns. In contrast, RX1day, RX3day, RX5day, and R95pTOT exhibit inconsistent trends, while R99pTOT demonstrates a decreasing trend over the full period (1980–2022). Although the number of days with precipitation $\geq$ 35 mm has declined, the increasing trend in 7-day maximum precipitation, coupled with no significant change in total annual precipitation and highly variable short-term rainfall, points to a rising risk of unexpected extreme precipitation events. Precipitation patterns in the Kathmandu Valley remain highly irregular across seasons, except during summer. ENSO exhibits a negative correlation with annual precipitation, extreme precipitation indices, and the PCI but shows a positive correlation with the annual and summer PCI as well as 1-day maximum precipitation, emphasizing its significant influence on precipitation variability. These findings highlight the urgent need for targeted climate adaptation strategies and provide valuable insights for hydrologists, meteorologists, policymakers, and urban planners to enhance climate resilience and improve flood management in the Kathmandu Valley.

Keywords: climate change; extreme events; flood disaster; Kathmandu; precipitation indices; precipitation concentration index; Nepal

Academic Editor: Majid Mirzaei

Received: 30 March 2025
Revised: 30 April 2025
Accepted: 5 May 2025
Published: 6 May 2025

Citation: Chaulagain, D.; Ray, R.L.; Yakub, A.O.; Same, N.N.; Park, J.; Tangoh, A.F.; Roh, J.W.; Suh, D.; Lim, J.-O.; Huh, J.-S. Extreme Precipitation Dynamics and El Niño–Southern Oscillation Influences in Kathmandu Valley, Nepal. *Water* **2025**, *17*, 1397. https://doi.org/10.3390/w17091397

1. Introduction

Climate change is reshaping precipitation patterns at local, regional, and global scales, with significant consequences for hydrological cycles and extreme weather events [1].

The rapid rise in global average temperatures has increased atmospheric water vapor concentrations, thereby intensifying extreme precipitation events [2]. As a key component of the Earth's hydrological cycle, precipitation is experiencing dynamic transformations under the influence of global warming, resulting in notable changes in its frequency, intensity, and spatial distribution [3]. The acceleration of climate change further amplifies hydrometeorological disasters such as floods, droughts, and landslides [4]. South Asia, in particular, is among the world's most disaster-prone regions, witnessing an overall rise in extreme precipitation with spatially heterogeneous patterns [5]. Nepal is especially vulnerable, ranking fourth globally as the most climate hazard-prone country [6].

Numerous studies have explored precipitation patterns using both observed and projected datasets and applied various analytical approaches globally. Sun et al. (2021) [7] investigated extreme precipitation trends at global, continental, and regional scales using the one-day maximum (RX1day) and five-day maximum (RX5day) precipitation indices. Their results show that nearly two-thirds of global observation stations exhibit significant upward trends in extreme precipitation, particularly across Asia, Europe, and North America, with pronounced increases in regions such as central and eastern North America, northern Central America, northern Europe, the Russian Far East, eastern Central Asia, and East Asia. Similarly, Donat (2016) [8] examined total and extreme precipitation variations in wet and dry regions using both observational data and global climate model outputs. The study found that precipitation has historically increased in wet regions and is likely to continue rising, whereas dry regions may experience a sharp increase in extreme precipitation events by the late 21st century. Additionally, Papalexiou and Montanari (2019) [9] analyzed global precipitation trends from 1964 to 2013 and concluded that both the intensity and frequency of precipitation increased significantly over this period.

While global studies highlight broad trends, local investigations reveal more heterogeneous patterns. Safdar et al. (2023) [10] analyzed precipitation trends in Pakistan during the winter and pre-monsoon seasons from 2008 to 2018, reporting a decline in winter precipitation and a reduction in rainy days for both seasons. Similarly, Aditya et al. (2021) [11] employed the Mann–Kendall test and Sen's slope estimator to examine rainfall variability in West Kalimantan, Indonesia. Their findings indicate a declining annual precipitation trend in the Mempawah region, while the Kubu Raya region exhibited an increasing annual precipitation trend between 2000 and 2019. The study further identified a significant precipitation decrease of -33.2 mm/year in Sungai Kunyit, suggesting a potentially drier future for the area. A comparable downward trend was observed in India's Thoubal River watershed, where precipitation declined by 10.3 mm/year, accompanied by considerable variability [12]. Another study on India's precipitation patterns, with ref. [13] analyzing data from 2001 to 2018, reported decreasing precipitation in the Indo-Gangetic Plain and in Northeast India due to a weakening of the southwesterly moisture flow, while northwestern India experienced an increasing trend. In southern India, precipitation declined because of a northward shift in sinking air masses over the equatorial region. In Bangladesh, Jihan et al. (2025) [14] projected an overall increase in precipitation by 480.38 mm, with the most pronounced rise occurring during storm-prone months.

Situated along the southern slopes of the central Himalayas, Nepal is highly vulnerable to extreme precipitation events because of its complex topography and dynamic atmospheric interactions. The country's summer monsoon primarily originates from the Bay of Bengal, supplemented by mid-latitude cyclonic systems that produce exceptionally heavy rainfall when interacting with monsoonal flows. Additionally, moisture-laden systems originating from the Arabian Sea and the Bay of Bengal further contribute to extreme precipitation, increasing the risk of both pluvial and fluvial flooding [15]. Several studies have reported a rise in intense daily precipitation trends across Nepal, significantly contributing

to flash floods in various regions [16–18]. For instance, Chhetri et al. (2020) [19] investigated flooding in the Banke and Bardiya districts, attributing extreme flood events to overnight heavy rainfall in central–western Nepal.

Nepal's climate is influenced by both the summer monsoon and westerly circulation systems. The summer monsoon is driven by southeasterly winds that transport moisture from the Bay of Bengal, whereas moisture-laden winds from the Mediterranean Sea govern the westerly circulation. In addition to these large-scale systems, Nepal's complex topography is critical in shaping local weather conditions, resulting in substantial spatial variability in precipitation over short distances [20]. Shrestha et al. (2019) [21] analyzed precipitation trends in the Koshi and Kaligandaki river basins from 1981 to 2015 and found that precipitation rapidly decreased with elevation in the Kaligandaki basin, whereas the Koshi basin displayed the opposite trend. Orographic effects and rain-shadow phenomena further contribute to distinct spatial and temporal variations in precipitation patterns across the country [22,23].

Luo et al. (2024) [24] analyzed extreme precipitation trends in Nepal using 11 precipitation indices developed by the World Meteorological Organization's Expert Team on Climate Change Detection and Indices (ETCCDI) for the period 1971–2015 based on APHRODITE data. Their findings indicate an overall decline in extreme precipitation trends, although the number of maximum consecutive wet days increased at varying rates across western and eastern Nepal. This study also highlights the significant influence of the South Asian monsoon on Nepal's precipitation indices. Similarly, Lamichhane et al. (2024) [4] employed the PCI to investigate precipitation patterns across Nepal from 1990 to 2020, with particular attention to the role of El Niño–Southern Oscillation (ENSO) on PCI variability. Their results revealed that monthly precipitation in Nepal exhibits moderate to strong irregularity, with lower elevation regions experiencing greater variability than mountainous areas. Furthermore, annual precipitation trends show an increasing rate of 0.53 mm per decade, while ENSO-driven variability is notably and inversely correlated with the Niño 3.4 index across most regions of Nepal.

The Kathmandu Valley, situated in the central Himalayas, is characterized by bowl-shaped topography and a single drainage outlet at Chovar. Rapid urban expansion has intensified the impacts of extreme precipitation, resulting in frequent urban flooding [25]. For instance, on 6 September 2021, *The Kathmandu Post* reported that 121.5 mm of rainfall caused severe inundation in multiple areas, including Balkhu, Kuleshwor, Narephant, Balaju, and Mulpani, as well as along major roadways. These extreme precipitation events often lead to traffic disruptions, casualties, disturbances for pedestrians and school children, and broader socioeconomic consequences. The severity of such impacts in the Kathmandu Valley is amplified due to the high population exposure.

Although several hydrometeorological studies have been conducted in the Kathmandu Valley, most have concentrated on flood mapping rather than long-term precipitation trends [26–32]. While Prajapati et al. (2021) [33] analyzed precipitation days from 1971 to 2015, their focus was primarily on spatial rainfall distribution and interstation comparisons. Consequently, a significant research gap remains regarding the historical trends in extreme precipitation intensity, frequency, and variability, as well as the influence of ENSO on extreme precipitation events and the PCI in the Kathmandu Valley.

This study addresses these gaps by analyzing extreme precipitation patterns in the Kathmandu Valley, focusing on frequency, intensity, seasonal and annual variability, and the influence of ENSO. The Mann–Kendall test and Sen's slope estimator are employed to assess precipitation trends from 1980 to 2022 using extreme precipitation indices recommended by the World Meteorological Organization (WMO) and the PCI. Additionally, this study investigates the effects of ENSO using the Niño 3.4 index. The findings

offer valuable insights for hydrologists, urban planners, and policymakers seeking to improve flood forecasting and disaster preparedness by better understanding historical precipitation extremes.

2. Materials and Methods

2.1. Study Area

The study area, illustrated in Figure 1, is located in the central Himalayan region of Nepal and encompasses the capital city, Kathmandu, along with the districts of Bhaktapur, Kathmandu, and Lalitpur. Several major rivers, including the Bagmati, Bishnumati, Manohara, Hanumante, and Dhobikhola, traverse through the Kathmandu Valley. Geographically, it lies between 27°32′13″–27°49′10″ N latitude and 85°11′31″–85°31′38″ E longitude [34]. The Kathmandu Valley covers an area of approximately 664 km^2. The Kathmandu Valley ranges in elevation from 1350 m above sea level (masl) in the lowlands to nearly 2800 masl in the surrounding hills. The valley is home to roughly 24% of Nepal's urban population which is estimated to be 3.3 million and projected to reach 3.8 million by 2031 [30], making it particularly vulnerable to climate-induced hazards, including extreme precipitation events [35]. The region experiences four distinct seasons—summer, autumn, spring, and winter—and falls within a subtropical to temperate climate zone. The average annual precipitation is approximately 1778 mm, most of which occurs between June and September. The temperature in the valley varies throughout the year, with recorded highs reaching 23.8 °C and lows dropping to 11.4 °C [36].

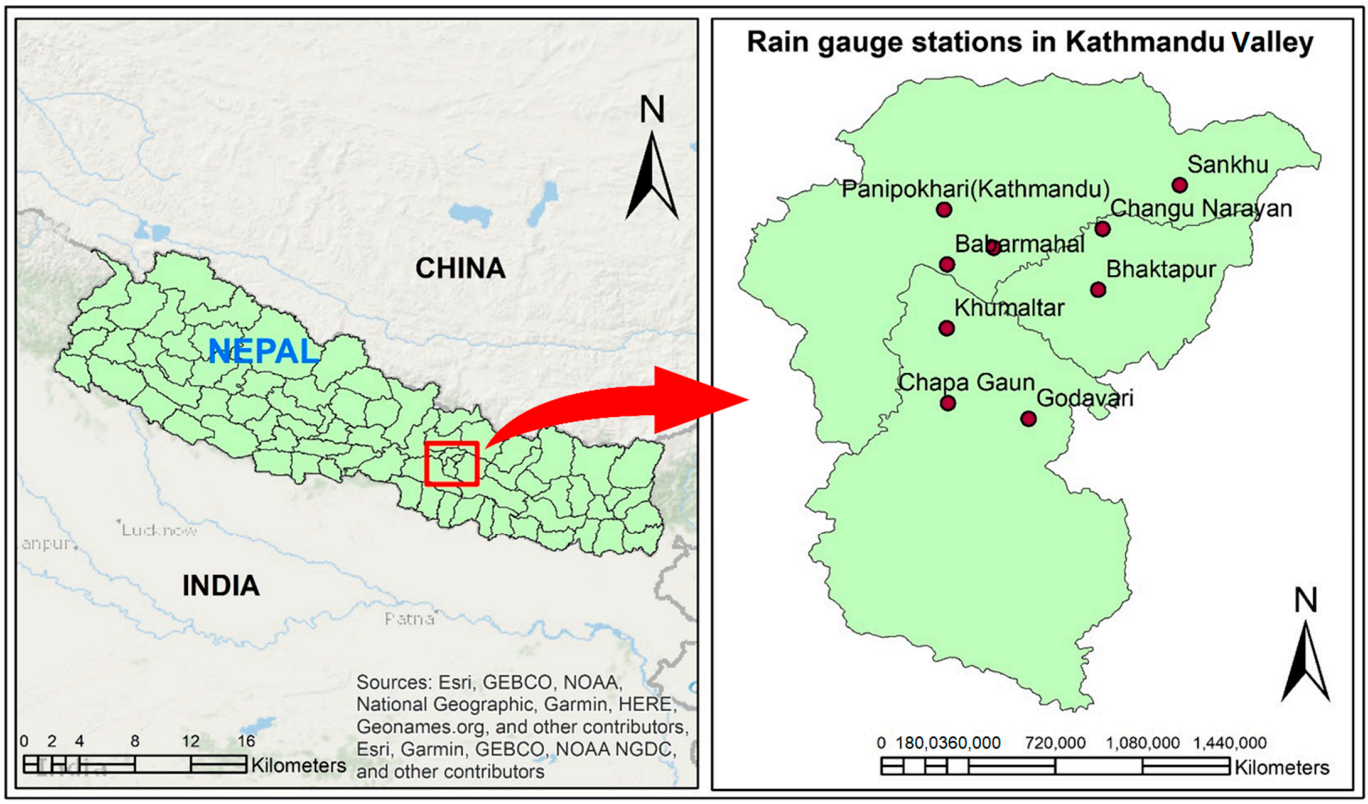

Figure 1. Study area with rain gauge stations.

2.2. Data Preparation

2.2.1. Observed Station Data

This study used daily observed rainfall data from nine rain gauge stations in the Kathmandu Valley covering the period from 1980 to 2022. The data were obtained from

Nepal's Department of Hydrology and Meteorology (DHM) [37]. Missing values in daily precipitation data, which accounted for less than 5% of the dataset, were filled in using data from nearby stations for the corresponding periods.

Given the spatial variability of precipitation across the Kathmandu Valley, it is essential to estimate the average precipitation in a manner that accounts for the unequal distribution of stations and the differing areas each station represents. Therefore, the average precipitation across the valley was estimated using the Thiessen polygon method. This approach delineates the area influenced by each station and assigns station-specific weights based on their respective catchment areas, ensuring that the computed average precipitation accurately reflects the spatial distribution of rainfall. The Thiessen polygon weights for each station are illustrated in Figure 2. The average daily precipitation of the Kathmandu Valley was calculated using the following equation [38]:

$$P = P_1W_1 + P_2W_2 + P_3W_3 + \ldots + P_nW_n \quad (1)$$

where P_1, P_2, P_3,. . ., and P_n represent the daily precipitation values at the respective stations, and W_1, W_2, W_3,. . ., and W_n are the corresponding Thiessen polygon weights. The Thiessen polygon weights *(W)* were determined as follows:

$$W_1 = \frac{A_1}{A_1 + A_2 + A_3 \ldots A_n}, \; W_2 = \frac{A_2}{A_1 + A_2 + A_3 \ldots A_n}, \; \ldots \; W_n = \frac{A_n}{A_1 + A_2 + A_3 \ldots A_n} \quad (2)$$

where A_1, A_2, A_3, . . ., and A_n denote the areas of the Thiessen polygons corresponding to each station.

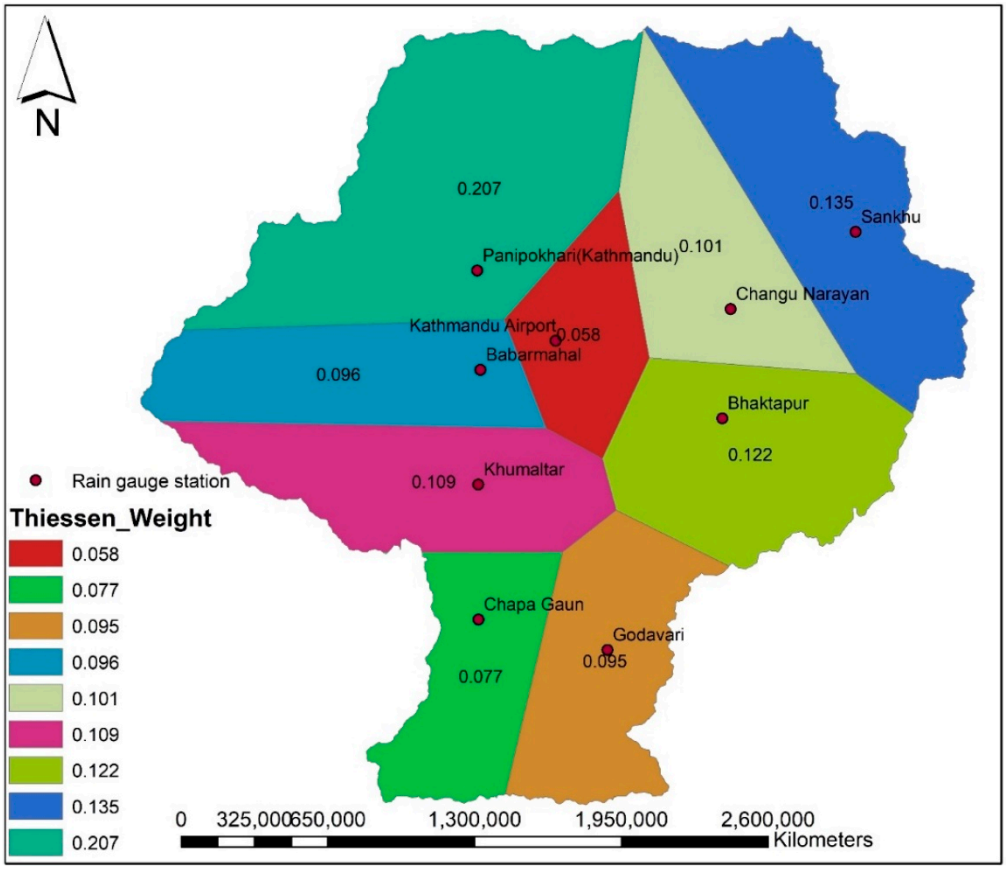

Figure 2. Thiessen polygon of the Kathmandu Valley.

2.2.2. ENSO Index

This study investigates the influence of tropical SST variations on precipitation patterns, PCI, and extreme precipitation indices. Specifically, SST anomalies in the Niño 3.4 region (5° N–5° S, 120° W–170° W) were used for analysis [4]. The SST anomalies were obtained from the Niño 3.4 index based on data from the Extended Reconstructed Sea Surface Temperature version 5 (ERSST V5) provided by the National Weather Service Climate Prediction Center, a division of NOAA accessed on 1 January 2025 (https://www.cpc.ncep.noaa.gov/data/indices/) [39]. The Niño 3.4 index, which has been widely used in previous studies [4,40–43], is available at a monthly resolution. This study assessed the relationship between ENSO and extreme precipitation and the PCI on annual and seasonal timescales from 1980 to 2022.

2.3. Data Analysis

2.3.1. Average Precipitation

This study analyzed the mean monthly precipitation in the Kathmandu Valley from 1980 to 2022. The precipitation dataset was initially processed using the Thiessen polygon method to account for spatial variability and was further analyzed to calculate the average precipitation for each month across the study period. The temporal distribution of precipitation was then visualized using a histogram to illustrate the monthly variations throughout the year.

2.3.2. Precipitation Trend Analysis (Mann–Kendall Test)

The Mann–Kendall statistical test, first introduced by Mann (1945) [44], is a widely used non-parametric method for detecting trends in time series data, particularly in the fields of hydrology and climatology [12]. One of the key advantages of this test is that it does not require the data to follow any specific distribution. It assumes that the time series is independently and identically distributed and is unaffected by serial correlation over time [24]. The null hypothesis (H_0) of the Mann–Kendall test posits that there is no trend in the dataset, meaning that the observations are randomly ordered. In contrast, the alternative hypothesis (H_1) indicates a trend within the time series [45].

In this study, the Mann–Kendall test statistic (S) was computed on an annual, seasonal, and monthly basis using the following equation:

$$S = \sum_{i=1}^{n-1} \sum_{j=i+1}^{n} sgn(x_j - x_i) \quad (3)$$

where n is the number of observations, and x_i and x_j are the data values at time indices i and j, respectively. The sign function $sng(x_j - x_i)$ is defined as follows:

$$sng(x_j - x_i) = \begin{cases} +1 \; if \; (x_j - x_i) > 0 \\ 0 \; if \; (x_j - x_i) = 0 \\ -1 \; if \; (x_j - x_i) < 0 \end{cases} \quad (4)$$

For datasets where n > 10, the test statistics S is approximately normally distributed with a mean of zero [12,24]. The variance of S is calculated as follows:

$$Var(S) = \frac{n(n-1)(2n+5) - \sum_{i=1}^{m} t(t-1)(2t+5)}{18} \quad (5)$$

where m is the number of tied groups, and t represents the number of tied values in each group.

For n > 10, the standardized normal variable Z is computed as follows:

$$Z = \begin{cases} \frac{S-1}{\sqrt{Var(S)}} \; if \; S > 0 \\ 0 \; if \; S = 0 \\ \frac{S+1}{\sqrt{Var(S)}} \; if \; S < 0 \end{cases} \quad (6)$$

A positive Z-value indicates an upward trend in the time series, whereas a negative Z-value signifies a downward trend. The statistical significance of the identified trend is evaluated against a predefined significance level.

2.3.3. Trend Magnitude Estimation (Sen's Slope)

Sen's slope (β) estimator is a non-parametric method used to quantify the magnitude of trends in time series data. It is widely employed in hydrology and climatology because of its robustness against outliers and applicability to data that do not follow a normal distribution [12]. This method calculates the slope between all possible pairs of data points and uses the median of these slopes to provide a reliable estimate of the overall trend magnitude. In this study, Sen's slope (β) was calculated on an annual, seasonal, and monthly basis using the following equation:

$$\beta = median \frac{x_i - x_j}{i - j} \quad (7)$$

where x_i and x_j are the data values at time steps t_i and t_j, respectively. A positive value of β indicates an upward trend, whereas a negative value signifies a downward trend in the dataset.

2.3.4. Extreme Precipitation Indices

Precipitation indices, summarized in Table 1 and recommended by the WMO, were used to evaluate precipitation characteristics in the Kathmandu Valley. These indices capture both the intensity and frequency of extreme precipitation events [24,46,47] and are widely used in hydrological and climatological studies because of their robustness in representing temporal and spatial variations in precipitation patterns.

This study categorizes precipitation indices into two main types: intensity-based and frequency-based. Intensity-based indices measure the magnitude of precipitation events and include the maximum 1-day (RX1day), 3-day (RX3day), 5-day (RX5day), and 7-day (RX7day) precipitation amounts. Threshold-based indices, such as very wet days (R95pTOT) and extremely wet days (R99pTOT), represent the total precipitation on days exceeding the 95th and 99th percentile thresholds, respectively. The Simple Daily Intensity Index (SDII) was also used to estimate the average precipitation on wet days.

Frequency-based indices assess the occurrence of extreme precipitation events, including the number of heavy precipitation days as follows: R10 mm, R20 mm, R35 mm, corresponding to days with precipitation exceeding 10 mm, 20 mm, and 35 mm, respectively. The longest consecutive dry days (CDDs, defined as precipitation <1 mm) and consecutive wet days (CWDs, defined as precipitation >1 mm) were also analyzed to evaluate extended dry and wet periods.

All indices were derived from daily precipitation records from 1980 to 2022 to identify trends in extreme precipitation events within the study area. To better understand temporal changes, trends were analyzed for the entire study period (1980–2022) and separately for two decades (1980–2001 and 2002–2022) using the Pettitt test, providing a clearer view of recent climate trends.

Table 1. Extreme precipitation indices.

Precipitation Indices	Abbreviation	Unit	Description
Maximum 1-day precipitation amount	RX1day	mm	Intensity of precipitation
Maximum 3-day precipitation amount	RX3day	mm	Intensity of precipitation
Maximum 5-day precipitation amount	RX5day	mm	Intensity of precipitation
Maximum 7-day precipitation amount	RX7day	mm	Intensity of precipitation
Total precipitation on days exceeding the 95th percentile (very wet days)	R95pTOT	mm	Intensity of precipitation
Total precipitation on days exceeding the 99th percentile (extremely wet days)	R99pTOT	mm	Intensity of precipitation
Count of days with precipitation $\geq$ 10 mm (heavy precipitation days)	R10 mm	days	Frequency of precipitation
Count of days with precipitation $\geq$ 20 mm (very heavy precipitation days)	R20 mm	days	Frequency of precipitation
Count of days with precipitation $\geq$ 35 mm (extreme precipitation days)	R35 mm	days	Frequency of precipitation
Maximum number of consecutive dry days (precipitation < 1 mm)	CDDs	days	Frequency of precipitation
Maximum number of consecutive wet days (precipitation > 1 mm)	CWDs	days	Frequency of precipitation
Simple Daily Intensity Index (SDII)—average precipitation on wet days	SDII	mm/day	Intensity of precipitation

2.3.5. Precipitation Concentration Index (PCI)

The PCI, introduced by Oliver (1980) [48], is widely used to assess the temporal distribution of precipitation across the 12 months of the year. It serves as a vital tool for evaluating the uniformity of irregularity of precipitation on both seasonal and annual scales, ranging from evenly distributed precipitation to highly irregular precipitation patterns [49], according to Table 2 thresholds. Variability in precipitation concentration significantly influences hydrological hazards such as floods, droughts, landslides, and soil erosion, as it reflects imbalances in precipitation distribution throughout the year [50]. In recent years, the PCI has gained increasing recognition in hydrological research for its ability to characterize precipitation variability [51,52]. In this study, the PCI was determined on both an annual and seasonal basis for 1980–2022 [4]. Daily average precipitation, estimated using the Thiessen polygon method, was aggregated into monthly totals for the Kathmandu Valley. The monthly precipitation values were then used to calculate the PCI using the following equations [4]:

$$PCI\ (yearly) = \frac{\sum_{i=1}^{12} P_i^2}{\left(\sum_{i=1}^{12} P_i\right)^2} \times 100 \quad (8)$$

$$PCI\ (Season) = \frac{\sum_{i=1}^{n} P_i^2}{(\sum_{i=1}^{n} P_i)^2}\ (\frac{n}{12} \times 100) \quad (9)$$

where P_i represents the monthly precipitation for each month within the season, i represents the specific month, and n denotes the number of months within the season under consideration. The PCI values were converted to percentages by multiplying the results by 100 in both equations.

Table 2. Precipitation concentration threshold index.

PCI Threshold	Description
<10	Uniform
11–15	Moderate
16–20	Irregular
>20	Strongly irregular

3. Results

3.1. Monthly Average Precipitation

Figure 3 presents the monthly average precipitation in the Kathmandu Valley from 1980 to 2022, revealing a clear seasonal pattern. The highest rainfall is recorded in July (425 mm), followed by August (375 mm), while June and September receive between 220 mm and 245 mm. In contrast, the driest months are January, February, March, November, and December, with precipitation levels below 50 mm. April, May, and October receive moderate rainfall ranging from 50 mm to 135 mm. The data show that approximately 80% of the total annual precipitation occurs during the monsoon months of June, July, August, and September, with the remaining 20% distributed across the other eight months. This highlights the region's pronounced dependence on seasonal rainfall.

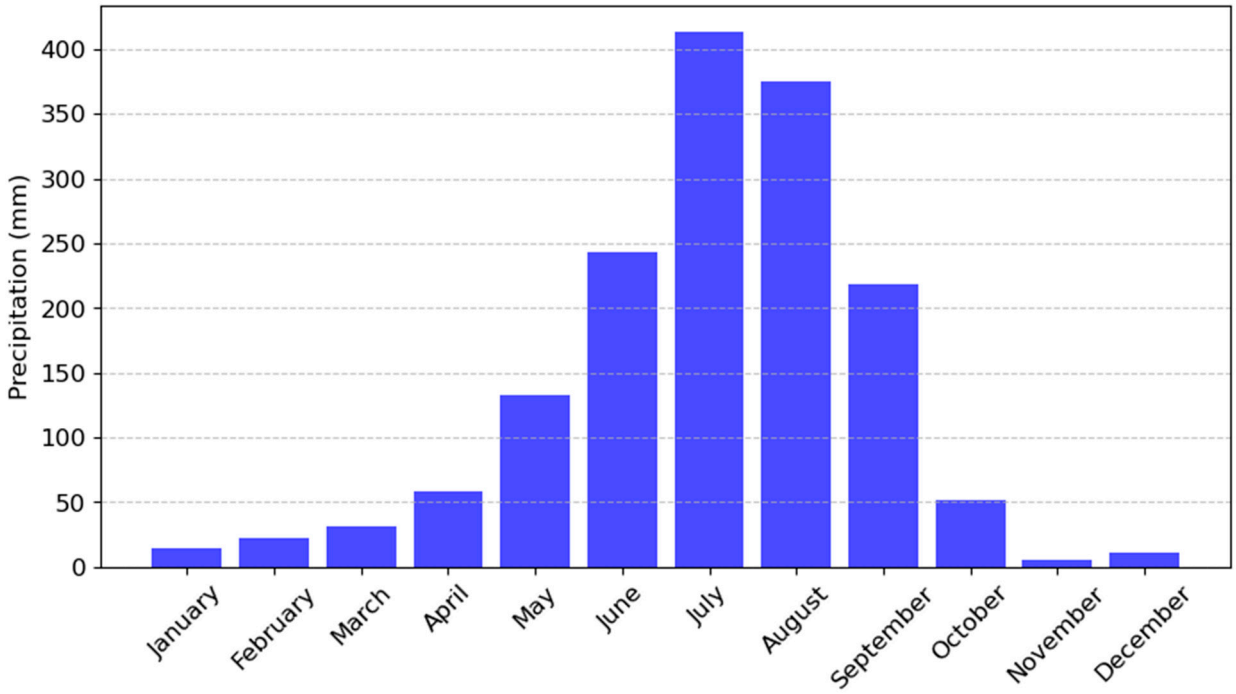

Figure 3. Monthly average precipitation in Kathmandu Valley from 1980 to 2022.

3.2. Precipitation Trends and Variability

Table 3 presents the results of the Mann–Kendall trend analysis for precipitation at monthly, seasonal, and annual scales, focusing on statistically significant trends. The seasonal classifications used in this study are winter (December–February), spring (March–May), summer (Monsoon) (June–August), and autumn (September–November). Among all the periods analyzed, only November, December, and the spring season exhibit statistically significant precipitation trends at the 0.05 significance level ($p < 0.05$). Specifically, November shows a declining trend of −0.035 mm/year ($p = 0.03$), December demonstrates a declining trend of −0.031 mm/year ($p = 0.02$), and spring shows an increasing trend of 1.17 mm/yr ($p = 0.04$). These significant downward trends suggest

an increase in aridity during the late autumn and early winter months, which may have implications for water availability in the dry season, whereas the spring season shows more water availability. For the remaining months and seasons and the annual scale, although positive or negative slopes were observed, the associated *p*-values exceed 0.05, indicating no statistically significant trends. In other time intervals, the precipitation is highly fluctuating.

Table 3. Results of the Mann–Kendall test for precipitation trends in the time series (1980–2022).

Period	Min (mm)	Max (mm)	Mean (mm)	SD (mm)	CV (%)	Mann–Kendall Z-Value	Mann–Kendall *p*-Value	Sen's Slope (mm/year)	Trend
January	0	70.2	14.4	17.6	121.8	−0.18	0.86	−0.006	NS
February	0	83.7	22.4	21.0	93.8	0.54	0.59	0.106	NS
March	0.2	98.6	31.0	24.0	77.4	0.12	0.91	0.024	NS
April	2.2	136.4	58.2	34.0	58.4	0.95	0.13	0.361	NS
May	44.2	251.2	132.6	50.3	37.9	0.37	0.17	0.211	NS
June	90.4	559.6	242.7	97.5	40.2	−0.32	0.75	−0.419	NS
July	247.2	621.6	413.2	95.2	23.0	0.14	0.89	0.226	NS
August	260.1	567.1	375.3	67.2	17.9	−1.37	0.17	−0.866	NS
September	103.4	430.4	218.4	74.8	34.3	−0.03	0.97	−0.016	NS
October	1.3	201.6	51.9	50.8	98.0	0.18	0.86	0.042	NS
November	0	64.2	5.6	11.3	202.5	−2.24	0.03	−0.035	↓
December	0	78.6	11.4	19.3	168.4	−2.39	0.02	−0.031	↓
Winter	0.2	143.1	48.3	32.7	67.7	−0.16	0.88	−0.088	NS
Summer	703.3	1386.9	1031.2	166.0	16.1	−0.83	0.41	−1.661	NS
Spring	104.5	368.7	221.8	67.9	30.6	1.37	0.04	1.174	↑
Autumn	119.2	567.8	275.8	92.9	33.7	−0.12	0.91	−0.125	NS
Annual	1155.7	2061.6	1577.1	224.7	14.2	−0.45	0.65	−0.806	NS

NS = not significant; ↑ = increasing trend; ↓ = decreasing trend.

Figure 4 illustrates the annual and seasonal precipitation variations in the Kathmandu Valley from 1980 to 2022, showing substantial fluctuations over time. The highest annual precipitation was recorded in 2002 (2061.6 mm), while the lowest occurred in 2009 (1155.7 mm). As summarized in Table 3, the mean annual precipitation is 1577.1 mm with a coefficient of variation (CV) of 14.2%, indicating relatively low variability. The standard deviation is 224.7 mm from the mean. Among the seasons, the summer (monsoon) season exhibits the greatest variability in precipitation, with values ranging from 703 mm to 1386.8 mm. Peak summer rainfall occurred in 2002, followed by 1995 (1325 mm) and 2003 (1300 mm). The average precipitation during this season is 1031 mm, with a standard deviation of 166 mm and a CV of 16.1%. The autumn season is the second-largest contributor to annual precipitation, with values ranging between 199.2 mm and 567.8 mm, an average of 275.8 mm, and a standard deviation of 92.9 mm. The highest autumn precipitation occurred in 1985, followed by 2007. Spring precipitation shows an increasing trend, peaking at 368.7 mm in 2002, followed by 350 mm in 2011. The minimum recorded value is 104.5 mm, with an average of 221.8 mm and a standard deviation of 67.9 mm. Winter contributes the least to annual precipitation, with near-zero precipitation in several years. The highest winter precipitation was recorded in 1997 (143.1 mm), highlighting its minimal contribution to the region's overall water availability.

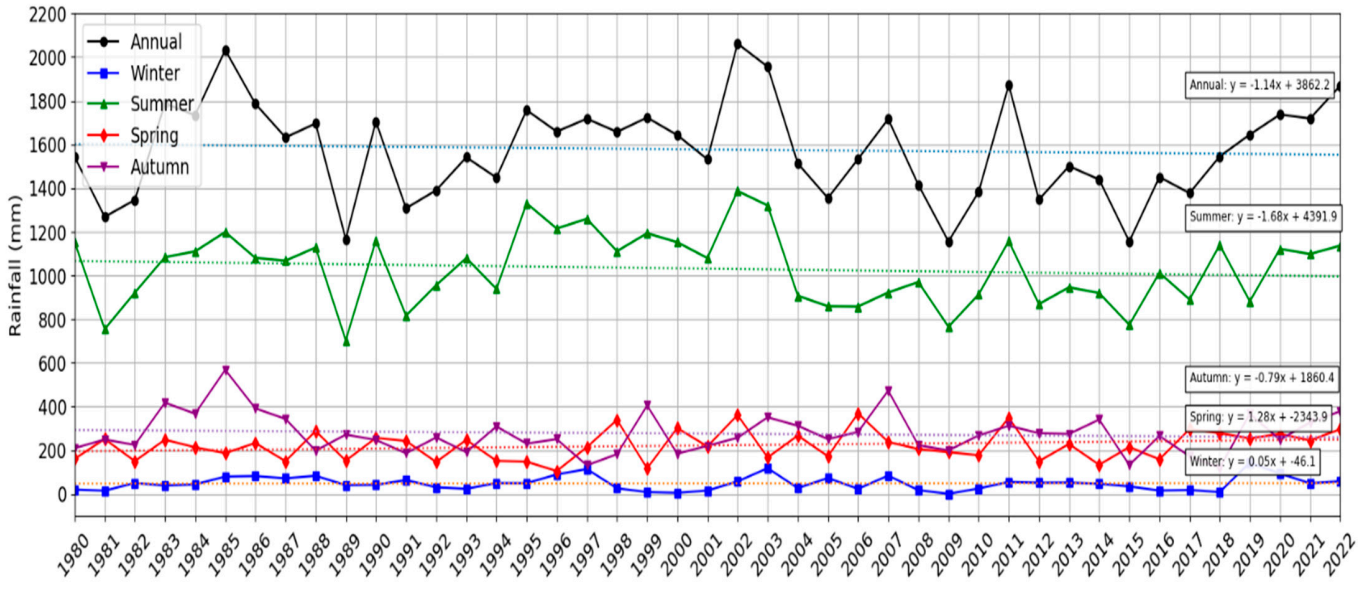

Figure 4. Seasonal and annual precipitation trends in the Kathmandu Valley from 1980 to 2022 with dotted trend line slopes: blue (annual, −1.14), green (summer, −1.68), purple (autumn, −0.79), red (spring, 1.28), and yellow (winter, 0.05) mm/year.

3.3. Temporal Patterns of Extreme Precipitation Indices

Extreme precipitation indices are categorized into various groups, each capturing different characteristics of extreme precipitation events. High-intensity indices include maximum precipitation over specific durations: one day (RX1day), three days (RX3day), five days (RX5day), and seven days (RX7day). Percentile-based indices capture extreme precipitation events based on statistical thresholds, including R95pTOT (precipitation exceeding the 95th percentile) and R99pTOT (precipitation exceeding the 99th percentile). Frequency-based indices measure the number of days with heavy rainfall, including R10mm (days with precipitation $\geq$ 10 mm), R20mm (days with precipitation $\geq$ 20 mm), and R35mm (days with precipitation $\geq$ 35 mm). Dry and wet spell indices quantify the duration of extreme conditions: consecutive dry days (CDDs) reflect extended dry periods (precipitation < 1 mm), while consecutive wet days (CWDs) indicate sustained wet conditions (precipitation > 1 mm). Finally, the Simple Daily Intensity Index (SDII) represents the average precipitation on wet days, thereby providing insights into the overall intensity of precipitation events throughout the year.

3.3.1. High-Intensity Precipitation Indices

Maximum 1-Day (RX1day), 3-Day (RX3day), 5-Day (RX5day), and 7-Day (RX7day) Precipitation

Figure 5 illustrates the temporal patterns of maximum precipitation over different durations—RX1day, RX3day, RX5day, and RX7day—from 1980 to 2022. Each subplot presents observed data along with trend lines for the entire study period (1980–2022) and two sub-periods (1980–2002 and 2003–2022), allowing for a comparative analysis of decadal changes. Over the full period, RX1day, RX3day, and RX5day exhibit no significant increasing or decreasing trend (Table 4), while RX7day shows a slightly increasing trend of 0.1 mm/year. A similar type of fluctuation is seen in the decadal analysis for RX1day, RX3day, and RX5day, but an increasing trend of precipitation in RX7day is significant in both decadal time intervals (Table 5). In 2002, the maximum precipitation values ranged from 178 mm to 346 mm across all indices. RX1day precipitation increased sharply between 1982 and 1987 but declined significantly during 1988–1989. A similar pattern is evident for RX3day, which experienced a slight decline in 1985. RX5day and RX7day increased

between 1982 and 1986, followed by a sharp decline from 1987 to 1999. From 1989 to 2001, all indices experienced considerable interannual fluctuations, peaking in 2002.

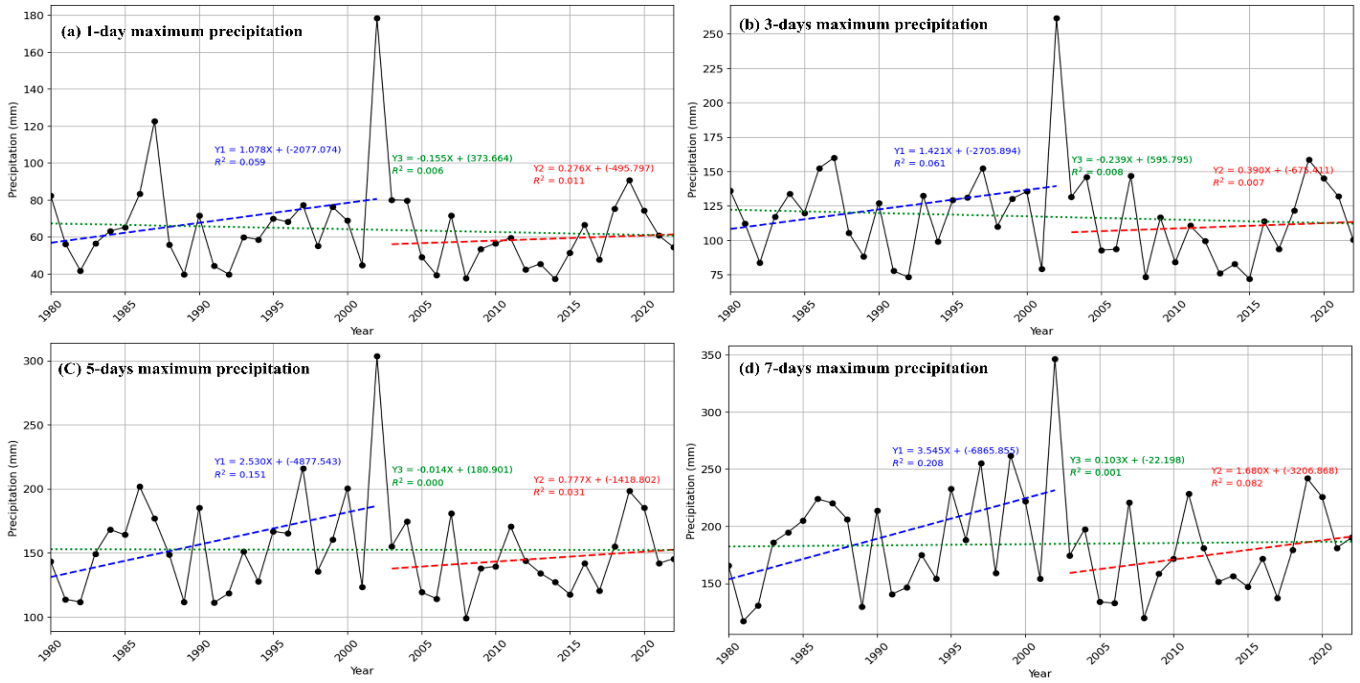

Figure 5. Time series of maximum-intensity precipitation.

Table 4. Results of the Mann–Kendall statistical test for extreme precipitation in the time series (1980–2022).

Precipitation Indices	Mean (mm)	SD (mm)	CV (%)	Mann–Kendall Z-Value	Mann–Kendall *p*-Value	Sen's Slope (mm/year)
RX1day	61.27	17.31	27.92	−0.06	0.60	−0.17
RX3day	113.56	26.16	22.76	−0.08	0.47	−0.26
RX5day	148.73	29.01	19.27	0.01	0.96	−0.04
RX7day	180.45	38.32	20.98	0.05	0.03 *	0.08
R95pTOT	586.83	173.51	29.21	−0.08	0.44	−2.00
R99pTOT	182.63	118.09	63.89	−0.16	0.03 *	−1.96
R10mm	54.74	9.00	16.25	0.03	0.75	−0.03
R20mm	20.45	4.82	23.28	−0.01	0.95	−0.01
R35mm	5.17	2.62	50.14	−0.18	0.05 *	−0.05
CDDs	73.81	24.92	33.36	0.24	0.02 *	0.69
CWDs	41.31	16.10	38.51	0.01	0.90	0.09
PRCPTOT	1550.62	215.38	13.72	−0.05	0.67	−1.12
SDII	10.19	1.08	10.51	−0.17	0.11	−0.02
PCI—autumn	17.72	3.64	20.32	0.04	0.68	0.02
PCI—spring	12.66	3.51	27.38	0.02	0.86	0.01
PCI—summer	9.07	0.66	7.24	−0.01	0.92	0.00
PCI—winter	16.15	5.11	31.28	0.23	0.03 *	0.14
PCI—annual	18.98	1.53	7.95	−0.07	0.50	−0.02

Note: * = statistically significant at 5% significance level.

Table 5. Results of the Mann–Kendall statistical test for extreme precipitation in the time series (1980–2002 and 2003 to 2022).

	1980–2002						2003–2022					
Precipitation Indices	**Mean (mm)**	**SD (mm)**	**CV (%)**	**Mann–Kendall Z-Value**	**Mann–Kendall *p*-Value**	**Sen's Slope (mm/year)**	**Mean (mm)**	**SD (mm)**	**CV (%)**	**Mann–Kendall Z-Value**	**Mann–Kendall *p*-Value**	**Sen's Slope (mm/year)**
RX1day	64.56	18.66	28.20	0.09	0.61	0.31	57.99	15.62	26.28	0.12	0.46	0.49
RX3day	119.21	24.54	20.09	0.08	0.65	0.62	107.91	27.09	24.50	0.13	0.42	0.80
RX5day	153.53	31.63	20.10	0.20	0.22	1.56	143.93	26.01	17.64	0.17	0.29	0.91
RX7day	186.92	41.97	21.91	0.33	0.04 *	3.48	173.97	34.07	19.11	0.24	0.05 *	1.76
R95pTOT	625.16	189.36	29.56	0.14	0.03 *	5.07	548.49	150.91	26.85	0.10	0.57	4.45
R99pTOT	213.62	113.67	51.93	0.08	0.65	2.21	151.64	116.84	75.19	0.04	0.79	−2.5
R10mm	56.10	8.97	15.60	0.20	0.20	0.50	53.38	9.05	16.54	0.18	0.26	0.40
R20mm	21.14	5.34	24.65	0.17	0.29	0.25	19.76	4.25	21.00	0.16	0.33	0.17
R35mm	6.00	2.63	42.72	0.04	0.81	0.00	4.33	2.39	53.92	0.09	0.58	0.00
CDDs	67.52	23.20	33.54	0.27	0.09 **	1.43	80.10	25.53	31.11	0.22	0.04 *	1.00
CWDs	39.90	16.18	39.56	−0.14	0.38	−0.30	42.71	16.30	37.24	−0.02	0.90	0.00
PRCPTOT	1581.39	210.72	13.00	0.07	0.70	2.43	1519.86	220.69	14.17	0.12	0.46	6.17
SDII	10.56	1.20	11.11	0.21	0.20	0.07	9.81	0.82	8.18	−0.08	0.65	−0.02

Note: * = statistically significant at 5% significance level; ** = statistically significant at 10% significance level.

Total Precipitation in R95pTOT and R99pTOT

Figure 6 presents the temporal variation in the total precipitation associated with extreme rainfall days, with subplot (a) representing days exceeding the 95th percentile (R95pTOT) and subplot (b) those exceeding the 99th percentile (R99pTOT), covering the period from 1980 to 2022. Trend lines are included for the entire study period as well as for two decadal intervals to assess long-term and short-term patterns. Over the full study period, both indices exhibit highly fluctuating precipitation, with a decreasing trend of R99pTOT at 1.9 mm/year being significant (Table 4). However, the decadal analysis reveals a more nuanced picture. From 1980 to 2002, R95pTOT shows a trend of precipitation increasing by 5.24 mm/year (Table 5), while for 2003–2022 both indices show highly fluctuating precipitation over the study period. For R95pTOT, the total precipitation increased sharply from 334 mm in 1981 to a peak of 1080 mm in 1985, followed by a rapid decrease to 293 mm in 1989 and 299.9 mm in 1991. The index then fluctuated, reaching a secondary peak of 1017 mm in 2002. After 2002, R95pTOT remained relatively stable, with a slight initial decline until 2005, followed by intermittent fluctuations with 705 mm recorded in 2022. In the case of R99pTOT, precipitation initially declined for three consecutive years before rising from 41.7 mm in 1982 to 357 mm in 1985. Between 1985 and 2001, the values fluctuated significantly, ranging from 40 mm to 382 mm and peaking at 544 mm in 2002. A continuous decline was observed for the next four years, reaching 39 mm in 2006. From 2006 to 2022, the index exhibited extreme variability, fluctuating between 0 mm and 309 mm.

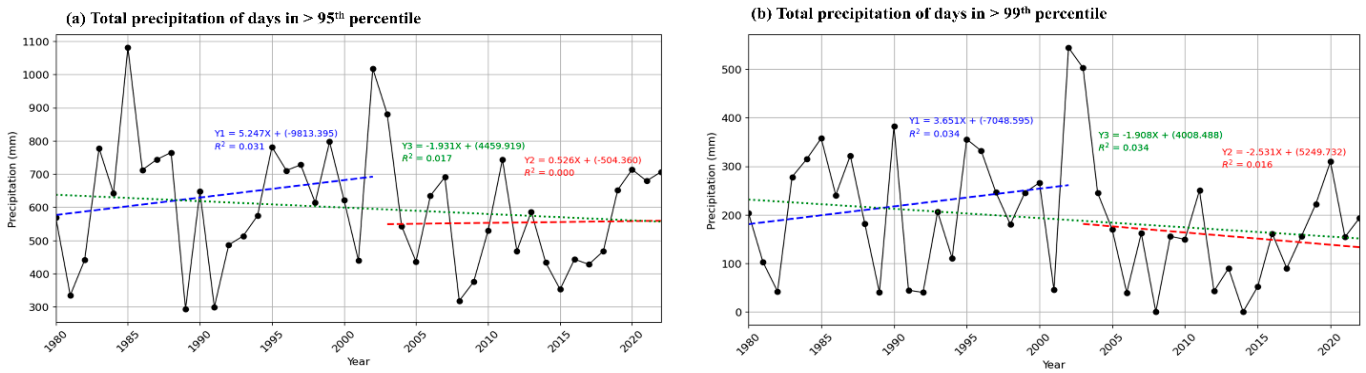

Figure 6. Time series of 95th and 99th percentile precipitation.

3.3.2. Precipitation Days at Different Thresholds

This study evaluates precipitation days based on three intensity thresholds: ≥10 mm (heavy precipitation days), ≥20 mm (very heavy precipitation days), and ≥35 mm (extreme precipitation days), as illustrated in Figure 7. Over the entire study period (1980–2022), the number of precipitation days shows a decreasing trend (−0.05 days/year) for extreme precipitation with precipitation ≥ 35 mm (Table 4), whereas for heavy and very heavy precipitation, an increasing or decreasing trend is not significant. Precipitation days ≥ 10 mm exhibit high interannual variability, increasing steadily through the early 1980s and peaking around 2002, followed by fluctuating patterns in subsequent years. Similarly, precipitation days ≥ 20 mm show pronounced fluctuations, with peaks in 1958 and in 2002, followed by a period of relative stabilization. In contrast, precipitation days ≥ 35 mm remain relatively low throughout the study period in both decadal analyses.

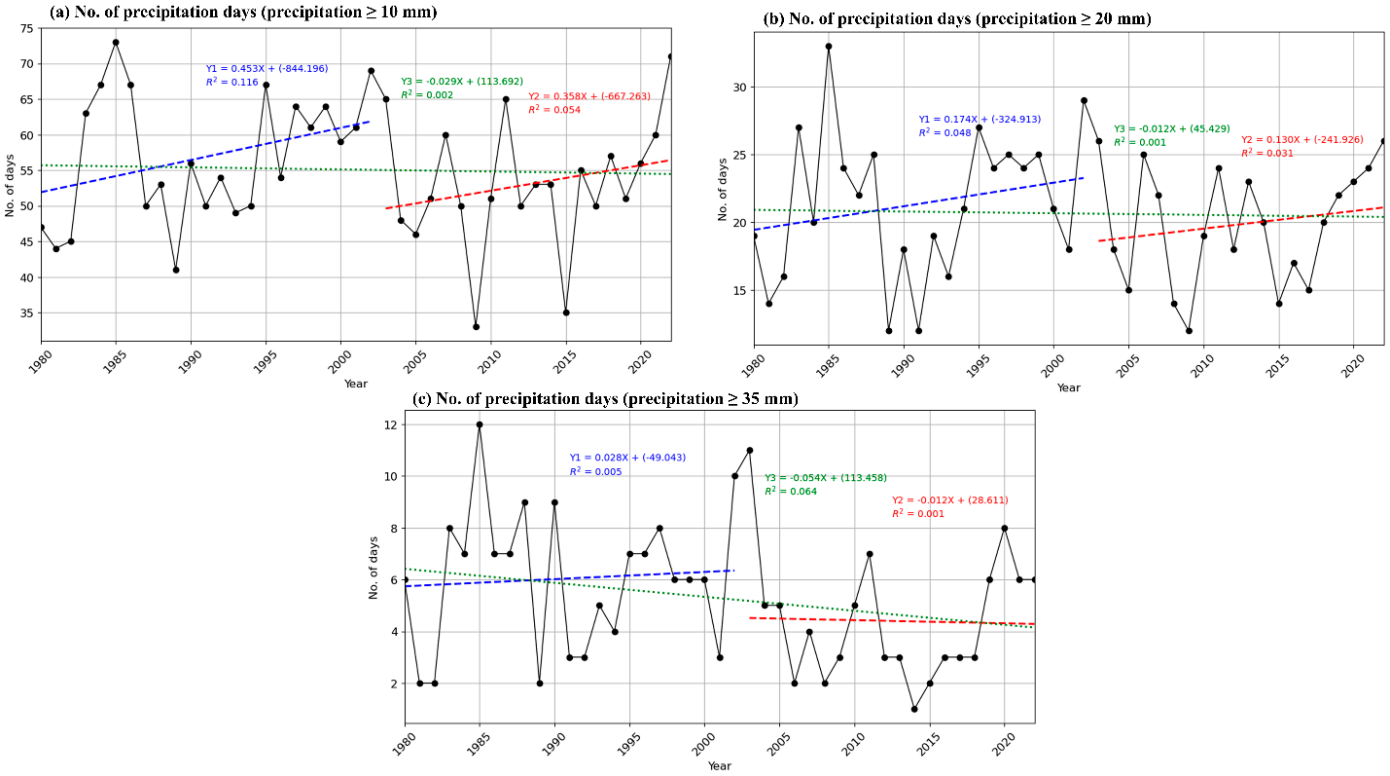

Figure 7. Precipitation days under different precipitation thresholds.

3.3.3. Annual Maximum Consecutive Wet and Dry Days

Figure 8 shows the trends in CWDs and CDDs. As shown in Figure 8a, CWDs display an overall fluctuation with no significant increasing trend. In contrast, Figure 8b shows a more pronounced increasing trend in CDDs at 0.69 days/year, indicating a notable rise in the duration of dry spells over the study period (Table 4). Decadal analysis reveals further details: between 1980 and 2002, consecutive wet days' increased trend is not significant, while consecutive dry days rose more sharply at 1.27 days/year with a 9% significant level with a continue rising trend at 0.708 days/year for 2003–2022 (Table 5) with a 4% significant level. Interannual variability is notable for both indices, with peaks in CWDs observed in the late 1990s and early 2000s, followed by fluctuations in subsequent years. Conversely, CDDs show a more consistent and pronounced upward trend, with peak values occurring more frequently after 2000, indicating an overall increase in prolonged dry periods across the Kathmandu Valley.

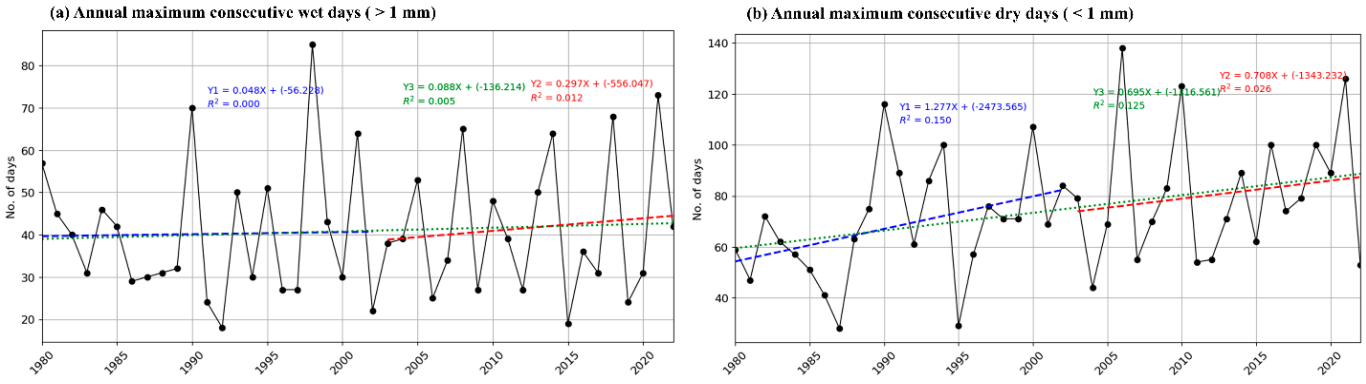

Figure 8. Annual consecutive wet and day days [(**a**) wet days (**b**) dry days].

3.3.4. Average Precipitation on Wet Days

Figure 9 illustrates the temporal variation in the average precipitation on wet days, showing an overall fluctuation over the study period (1980–2022). The decadal analysis also reveals no significant increasing or decreasing trend. Initially, the average precipitation increased from 8.5 mm in 1981 to a peak of 12.9 mm before declining to 8.4 mm in 1989. Following this decline, values fluctuated annually, reaching a maximum of 13 mm in 2002. Thereafter, a continuous decline was observed over the next three years, followed by a period of relative stability. From 2005 to 2022, the average precipitation on wet days remained within the range of 8.5–11.1 mm, with noticeable interannual variability throughout the period.

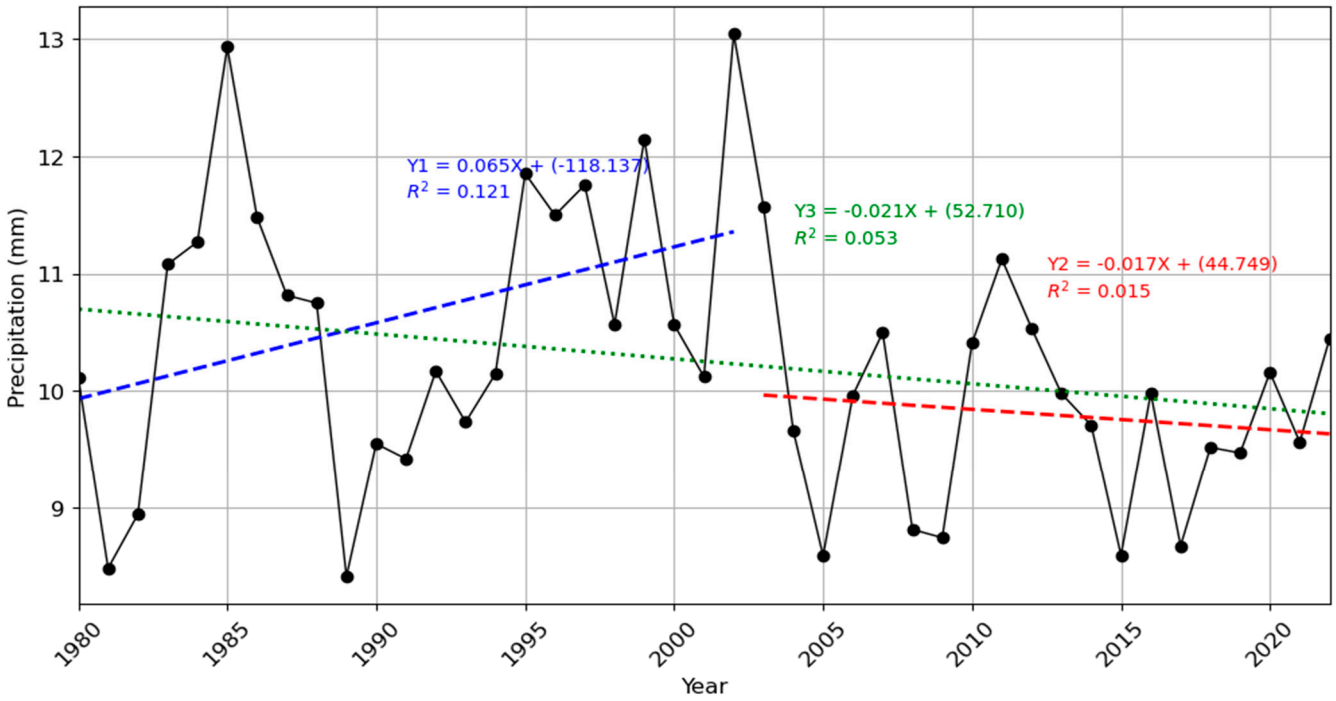

Figure 9. Wet-day average precipitation from 1980 to 2022.

3.4. Precipitation Concentration Index

Figure 10 presents the PCI for the Kathmandu Valley from 1980 to 2022, analyzed on both seasonal and annual scales.

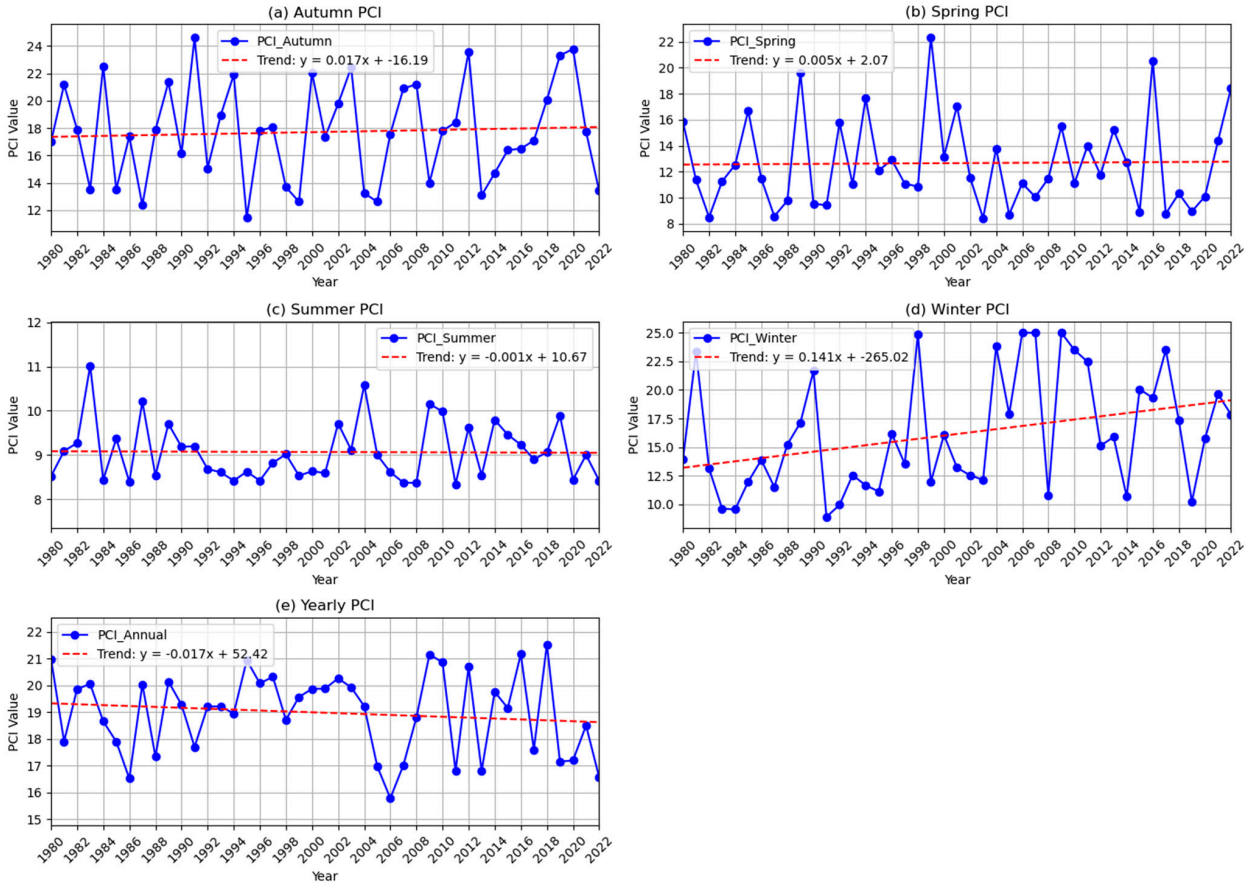

Figure 10. Time series of annual and seasonal precipitation concentration index.

The results show an increasing trend in the PCI during winter at a rate of 1.4 per decade with a 5% significant level (Table 4), whereas for autumn, spring, summer, and annual, there is no significant increasing or decreasing trend that exists. The average PCI values for the annual, autumn, and winter seasons are 18.98, 17.7, and 16.1, respectively, indicating irregular precipitation during these periods. In contrast, the average PCI values for summer and spring are 9 and 12.7, respectively, suggesting uniform and moderately concentrated precipitation during these seasons. In autumn, 17 years fall under the "irregular rainfall" category, while 13 years are classified as "strongly irregular." During spring, most years (22) exhibit moderate rainfall concentrations, with 10 years exhibiting uniform distribution, 9 years classified as irregular, and 2 years classified as very irregular. For winter, 17 years fall into the moderate category, whereas 11 years are strongly irregular, including 3 years in which the PCI exceeded 25—indicating that most precipitation during those years occurred within approximately one-third of the season. Although spring generally maintains a more uniform rainfall distribution over time, the annual PCI analysis reveals that only 6 years experienced strongly irregular precipitation, whereas the remaining years indicate irregular rainfall distribution across the Kathmandu Valley.

3.5. Mann–Kendall Trend Analysis of Extreme Precipitation for 1980–2022 with Decadal Segmentation (1980–2002 and 2003–2022)

Table 4 presents the results of the Mann–Kendall trend analysis for extreme precipitation indices and the PCI. The analysis reveals that the trends for RX7day, R99pTOT, R35mm, and CDDs are statistically significant at the 5% significance level ($p < 0.05$), indicating notable changes in these extreme precipitation characteristics over time. Additionally, the PCI for winter exhibits a significant increasing trend, suggesting a shift toward more uneven precipitation distribution during this season. In contrast, the trends for the remaining

precipitation indices and seasonal/annual PCI are not statistically significant ($p > 0.05$), implying that no consistent long-term trends were detected for these variables during the study period. Similarly, Table 5 depicts the results of the Mann–Kendall statistical test for extreme precipitation indices over the periods 1980–2002 and 2003–2022. The analysis reveals a significant increasing trend in RX7day precipitation, with Sen's slope values of 3.48 for 1980–2002 and 1.76 for 2003–2022, both significant at the 5% level. Additionally, R95pTOT shows a significant upward trend during 1980–2002, with a Sen's slope of 5.07 at the 5% significance level. The results also indicate a significant increase in consecutive dry days (CDDs) for 2003–2022, with a Sen's slope of 1.00 at the 5% level, while a similar increasing trend in CDDs is observed for 1980–2002 with a Sen's slope of 1.43, significant at the 10% level. For the remaining precipitation indices, although some trends are either increasing or decreasing, these are not statistically significant at the 10% level.

3.6. Influence of ENSO on Precipitation

The Niño 3.4 index exhibits both positive and negative correlations with precipitation indices in the Kathmandu Valley, Nepal. A negative correlation indicates that regional precipitation tends to be lower than average during warm anomaly phases in the eastern tropical Pacific (El Niño events). Figure 11 presents the correlation coefficients between various precipitation indices, the PCI, and the Niño 3.4 index, along with their corresponding levels of statistical significance. Total annual precipitation shows a negative correlation of −0.25 with the Niño 3.4 index, which is significant at the 0.1 level. Similarly, the R10mm index demonstrates a stronger negative correlation of −0.35, significant at the 0.05 level, while the R20mm index shows a negative correlation of −0.21, significant at the 0.1 level. The CWDs are also negatively correlated with Niño 3.4 (−0.32), with significance at the 0.05 level. For seasonal variability, the spring PCI exhibits a significant negative correlation of −0.35 with Niño 3.4 at the 0.05 level. In contrast, the annual PCI shows a positive correlation of 0.25, which is significant at the 0.1 level. Additionally, RX1day exhibits a positive correlation of 0.24, which is significant at the 0.1 level.

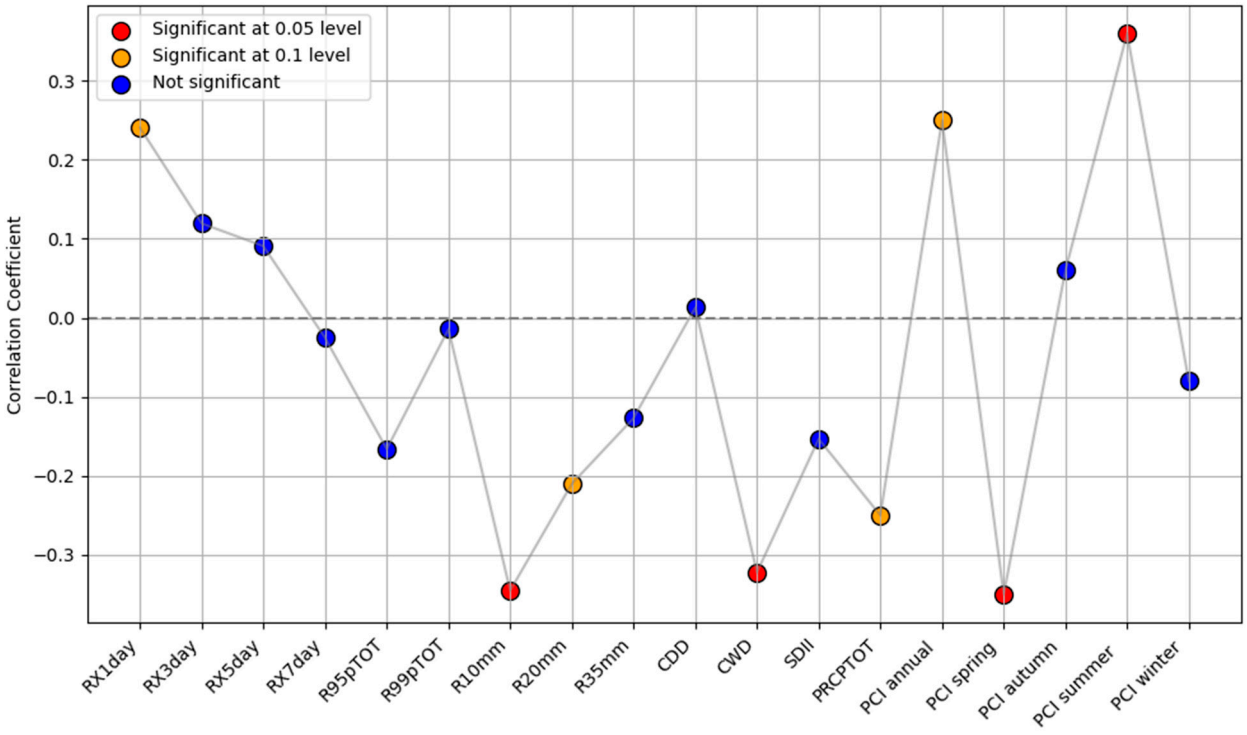

Figure 11. Correlation between the Nino 3.4 index and precipitation indices.

4. Discussion

Rapid urbanization and reduced infiltration areas in the Kathmandu Valley have heightened the impact of even minor precipitation events, resulting in frequent waterlogging and flooding. These occurrences routinely disrupt traffic, affect pedestrians, and cause property damage and loss of life. This study investigated extreme precipitation in terms of intensity, frequency, and variability using a suite of precipitation indices recommended by the WMO and supported by previous research [53–60]. The Mann–Kendall statistical test and Sen's slope estimator were applied to the precipitation data from 1980 to 2022 to assess trends.

Monthly precipitation analysis reveals that most of the annual rainfall is concentrated between June and September, with July (425 mm) and August (375 mm) having the highest totals. This pronounced seasonality is largely driven by the Indian summer monsoon, which transports moisture-laden southeasterly winds from the Bay of Bengal [61]. Long-term precipitation trends indicate a slight decline in winter, summer, autumn, and annual precipitation totals, while spring precipitation exhibits an increasing trend of 1.17 mm/year. Notably, July shows a marginal upward trend of 0.2 mm/year, reinforcing its role as the wettest month and a key contributor to flood risk in the Kathmandu Valley. During the wettest months (July and August), minimum precipitation levels range from 247 mm to 260 mm, while the maximum values range from 567 mm to 621 mm. This wide range significantly increases the potential for flooding. These findings are consistent with those of Prajapati and Talchabhadel et al. (2021) and Dhital and Kayastha (2013) [33,62], who identified July and August as the peak flood months. Similarly, Pradhan-Salike and Raj Pokharel (2017) [63] attributed pluvial flooding in the valley to intense, short-duration rainfall events.

Extreme precipitation analysis from 1980 to 2022 reveals an overall increasing trend in RX7day by 0.1 mm/year. However, the decadal analysis (1980–2001 and 2002–2022) indicates sharp fluctuations in extreme precipitation across the RX1day, RX3days, and RX5days indices with an increasing trend for RX7days precipitation being significant. Similar patterns of fluctuations of precipitation are observed for the percentile-based indices R95pTOT and R99pTOT for decadal analysis, whereas a decreasing trend of R99pTOT is significantly observed for 1980 to 2022. These findings suggest that short-duration precipitation demonstrates inconsistency and long-term precipitation shows a slightly increasing trend, which are both partially contradictory to the findings of Luo et al. (2024) [24], who reported a long-term decline in extreme precipitation with highly fluctuation events over Nepal due to the weakening of the South Asian Monsoon circulation, followed by a post-2003 shift toward increasing extreme precipitation, particularly in western Nepal. This trend aligns with broader regional patterns, including a threefold increase in widespread extreme rainfall events over central India between 1950 and 2015, contributing to more frequent flash floods and significant socioeconomic losses [64]. In 2002, Nepal faced an anomalous monsoon with extreme rainfall in the east and center and drought in the west. On 23 July 2002, Kathmandu recorded its highest 24 h rainfall in 14 years (177.0 mm), with nearby areas like Khokana (300.1 mm) and Thankot (249.2 mm) also experiencing record rain. This caused severe flooding and disruptions in the Kathmandu Valley [65].

In the Kathmandu Valley, the number of precipitation days at all thresholds ($\geq$35 mm) declined between 1980 and 2022. Despite this decline, the RX7day index exhibited an increasing trend, suggesting more intense rainfall events over fewer days—intensifying flood risk. Although consecutive wet days (CDDs) showed a slight increase, the average precipitation on wet days declined, indicating a shift toward more extreme precipitation events without a corresponding increase in total rainfall volume. These trends are further supported by Luo et al. (2024) [24], who observed a decrease in

moderate rainfall days (R10 mm, R20 mm) and increased extreme precipitation variability. The severe flooding events of September 2024, which brought 239.7 mm of rainfall in just 24 h and resulted in over 200 fatalities and widespread displacement [66], underscore the urgent need for adaptive infrastructure and enhanced disaster preparedness strategies in the Kathmandu Valley.

The PCI analysis reveals an annual PCI value of 18.9, indicating an overall irregular precipitation distribution. This finding aligns with the results of Lamichhane et al. (2024) [4], who reported PCI values across Nepal ranging from 14.06 (moderate) to 25.34 (strongly irregular), with increasing precipitation irregularity particularly evident in lowland regions. While their national analysis identified an increasing PCI trend of 0.53 per decade, the Kathmandu Valley exhibited an increasing trend of the PCI by 1.4 per decade in the winter season. A similar type of increasing PCI value has been observed in China [67] and India [68], where precipitation irregularity has been attributed to climate variability and shifts in monsoon dynamics. Similarly, Rahman and Islam (2019) [69] reported PCI values ranging from 0.57 to 0.632 in Bangladesh, indicating slightly higher precipitation variability than in Nepal.

The influence of ENSO on precipitation patterns across the Asia–Pacific region, including Nepal, is well established [2,70–73]. Several studies [4,74,75] confirm that during El Niño events, the westward shift of the Pacific warm pool toward the central and eastern Pacific results in the weakening of the Walker circulation and trade winds, along with reduced oceanic upwelling. These processes amplify positive SST anomalies in the eastern Pacific, disrupt global precipitation patterns, and weaken the summer monsoon. Concurrently, the western Pacific cools due to diminished convection, while the Indian Ocean warms as a delayed response through atmospheric teleconnections—independent of the Indian Ocean Dipole (IOD) [40]. In this study, annual precipitation, extreme precipitation indices, and overall precipitation variability in the Kathmandu Valley were negatively correlated with the Niño 3.4 index, consistent with the findings of Lamichhane et al. (2024) [4,24] and Luo et al. (2024) [4,24]. However, positive correlations were observed for the annual PCI (0.25), the summer PCI (0.36), and 1-day maximum precipitation (RX1day, 0.24), suggesting that ENSO influences not only the total precipitation amounts but also the temporal concentration and the occurrence of high-intensity, short-duration events.

5. Conclusions

This study investigates precipitation patterns in the Kathmandu Valley using observed data from 1980 to 2022, with a focus on trends in precipitation intensity, frequency, and concentration at both annual and seasonal scales. By applying the PCI and a set of extreme precipitation indices, this study also assesses the influence of the El Niño–Southern Oscillation (ENSO) on extreme precipitation events in the region.

The results indicate a slight overall increase in long-term precipitation across the Kathmandu Valley with inconsistent short-term precipitation. The spring precipitation exhibits an increasing trend of 1.17 mm per year, with November and December exhibiting an upward trend. The remaining months and seasons show high-fluctuation short-term precipitation contributing to heightened flood risks. The analysis of extreme precipitation indices reveals sharp inconsistency in RX1day, RX3day, and RX5day from 1980 to 2022, while RX7day exhibits a slight increase of 0.1 mm/year. Similarly, decadal analysis reveals a fluctuation trend across all extreme precipitation indices, including R95pTOT, which emphasizes the growing risk of pluvial and fluvial flooding in the valley. The annual precipitation patterns in the Kathmandu Valley are highly irregular, particularly during autumn and winter, whereas summer precipitation remains relatively evenly distributed. ENSO analysis indicates a negative correlation with annual precipitation, extreme precipitation

indices, and overall precipitation variability, while showing a positive correlation with the annual and summer PCI and 1-day maximum precipitation (RX1day). ENSO analysis indicates a negative correlation with annual precipitation, extreme precipitation indices, and overall precipitation variability, while showing a positive correlation with the annual and summer PCI and 1-day maximum precipitation (RX1day). Although some of these correlations are statistically significant, they align with established climatic mechanisms. Previous studies demonstrate that El Niño events typically weaken monsoon circulation and reduce moisture transport across Nepal, leading to below-normal rainfall [4,24]. In contrast, La Niña phases enhance moisture influx, often resulting in above-normal rainfall. These mechanisms support the observed variability in precipitation patterns in the Kathmandu Valley, though the influence of ENSO is controlled by local topography and regional atmospheric conditions.

Although this study is limited to a single geographic region with a restricted number of observation stations, its findings are applicable to other areas with similar topographic and climatic conditions throughout the Himalayan region. Future research should incorporate additional climatic variables—such as temperature, humidity, and wind speed—alongside global climate model (GCM) data to improve projections of future precipitation trends and their hydrological implications.

Author Contributions: D.C.: methodology, software, conceptualization, data curation, formal analysis, investigation, writing the original draft. R.L.R.: conceptualization, review and editing. A.O.Y.: writing. N.N.S.: editing. J.P.: analysis. A.F.T.: data collection. J.W.R.: software. D.S.: software. J.-O.L.: review. J.-S.H.: supervision, funding acquisition. All authors have read and agreed to the published version of the manuscript.

Funding: This work was supported by the National Research Foundation of Korea (NRF) grant funded by the Korea government (MSIT) (No. RS-2021-NR060108) and supported by the Korea Institute of Energy Technology Evaluation and Planning (KETEP) and the Ministry of Trade, Industry & Energy (MOTIE) of the Republic of Korea (No. RS-2022-KP002719).

Data Availability Statement: The original contributions presented in this study are included in the article. Further inquiries can be directed to the corresponding author.

Conflicts of Interest: The authors declare that they have no known competing financial interests or personal relationships that could have appeared to influence the work reported in this paper.

References

1. Summary for Policymakers. In *Climate Change 2022—Impacts, Adaptation and Vulnerability*; Cambridge University Press: Cambridge, UK, 2023; pp. 3–34. [CrossRef]
2. An, D.; Eggeling, J.; Zhang, L.; He, H.; Sapkota, A.; Wang, Y.-C.; Gao, C. Extreme precipitation patterns in the Asia–Pacific region and its correlation with El Niño-Southern Oscillation (ENSO). *Sci. Rep.* **2023**, *13*, 11068. [CrossRef] [PubMed]
3. Sun, G.; Tiwari, K.R.; Hao, L.; Amatya, D.; Liu, N.; Song, C. Climate change and forest hydrology in future forests. In *Future Forests: Mitigation and Adaptation to Climate Change*; Elsevier: Amsterdam, The Netherlands, 2024; pp. 95–124. [CrossRef]
4. Lamichhane, D.; Bao, Q.; Dhital, Y.P.; Devkota, R.; Bhattarai, U.; Nepal, B.; Pokharel, A.K.; Dawadi, B. Precipitation Concentration Variability and Its Association with Geographical Factors and ENSO Over Nepal from 1990 to 2020. *Earth Syst. Environ.* **2024**, *8*, 1–17. [CrossRef]
5. Karki, R.; Hasson, S.U.; Schickhoff, U.; Scholten, T.; Böhner, J. Rising Precipitation Extremes across Nepal. *Climate* **2017**, *5*, 4. [CrossRef]
6. Pandey, V.P.; Shrestha, D.; Adhikari, M. Characterizing natural drivers of water-induced disasters in a rain-fed watershed: Hydro-climatic extremes in the Extended East Rapti Watershed. *J. Hydrol.* **2021**, *598*, 126383. [CrossRef]
7. Sun, Q.; Zhang, X.; Zwiers, F.; Westra, S.; Alexander, L.V. A Global, Continental, and Regional Analysis of Changes in Extreme Precipitation. *J. Clim.* **2021**, *34*, 243–258. [CrossRef]
8. Donat, M.G.; Lowry, A.L.; Alexander, L.V.; O'Gorman, P.A.; Maher, N. Addendum: More extreme precipitation in the world's dry and wet regions. *Nat. Clim. Change* **2016**, *6*, 508–513. [CrossRef]

9. Papalexiou, S.M.; Montanari, A. Global and Regional Increase of Precipitation Extremes Under Global Warming. *Water Resour. Res.* **2019**, *55*, 4901–4914. [CrossRef]
10. Safdar, F.; Mahmood, F.; Khan, M.Z.A.; Arshad, M. Observed and predicted precipitation variability across Pakistan with special focus on winter and pre-monsoon precipitation. *Environ. Sci. Pollut. Res.* **2023**, *30*, 4510–4530. [CrossRef] [PubMed]
11. Aditya, F.; Gusmayanti, E.; Sudrajat, J. Rainfall trend analysis using Mann-Kendall and Sen's slope estimator test in West Kalimantan. *IOP Conf. Ser. Earth Environ. Sci.* **2021**, *893*, 012006. [CrossRef]
12. Rahaman, M.H.; Saha, T.K.; Masroor, M.; Roshani; Sajjad, H. Trend analysis and forecasting of meteorological variables in the lower Thoubal river watershed, India using non-parametrical approach and machine learning models. *Model Earth Syst. Environ.* **2024**, *10*, 551–577. [CrossRef]
13. Maharana, P.; Agnihotri, R.; Dimri, A.P. Changing Indian monsoon rainfall patterns under the recent warming period 2001–2018. *Clim. Dyn.* **2021**, *57*, 2581–2593. [CrossRef]
14. Jihan, M.A.T.; Popy, S.; Kayes, S.; Rasul, G.; Maowa, A.S.; Rahman, M. Climate change scenario in Bangladesh: Historical data analysis and future projection based on CMIP6 model. *Sci. Rep.* **2025**, *15*, 7856. [CrossRef] [PubMed]
15. Subba, S.; Ma, Y.-M.; Ma, W.-Q.; Han, C.-B. Extreme precipitation detection ability of four high-resolution precipitation product datasets in hilly area: A case study in Nepal. *Adv. Clim. Change Res.* **2024**, *15*, 390–405. [CrossRef]
16. Bell, R.; Fort, M.; Götz, J.; Bernsteiner, H.; Andermann, C.; Etzlstorfer, J.; Posch, E.; Gurung, N.; Gurung, S. Major geomorphic events and natural hazards during monsoonal precipitation 2018 in the Kali Gandaki Valley. *Geomorphology* **2021**, *372*, 107451. [CrossRef]
17. Fernando, N.S.; Shrestha, S.; Saurav, K.; Mohanasundaram, S. Investigating major causes of extreme floods using global datasets: A case of Nepal. *Prog. Disaster Sci.* **2022**, *13*, 100212. [CrossRef]
18. Khatri, S.K.; Hamal, R.; Poudel, K.R.; Poudel, K.P.; Paudel, N. Rainfall patterns and hazard susceptibility analysis of Pokhara City, Nepal: Implication of climate change. *Theor. Appl. Climatol.* **2025**, *156*, 146. [CrossRef]
19. Chhetri, T.B.; Dhital, Y.P.; Tandong, Y.; Devkota, L.P.; Dawadi, B. Observations of heavy rainfall and extreme flood events over Banke-Bardiya districts of Nepal in 2016–2017. *Prog. Disaster Sci.* **2020**, *6*, 100074. [CrossRef]
20. Adhikari, N.; Gao, J.; Yao, T.; Yang, Y.; Dai, D. The main controls of the precipitation stable isotopes at Kathmandu. *Tellus B Chem. Phys. Meteorol.* **2020**, *72*, 1721967. [CrossRef]
21. Shrestha, S.; Yao, T.; Kattel, D.B.; Devkota, L.P. Precipitation characteristics of two complex mountain river basins on the southern slopes of the central Himalayas. *Theor. Appl. Clim.* **2019**, *138*, 1159–1178. [CrossRef]
22. Karki, R.; Talchabhadel, R.; Aalto, J.; Baidya, S.K. New climatic classification of Nepal. *Theor. Appl. Clim.* **2015**, *125*, 799–808. [CrossRef]
23. Shrestha, S.; Yao, T.; Adhikari, T.R. Analysis of rainfall trends of two complex mountain river basins on the southern slopes of the Central Himalayas. *Atmos. Res.* **2019**, *215*, 99–115. [CrossRef]
24. Luo, Y.; Wang, L.; Hu, C.; Hao, L.; Sun, G. Changing Extreme Precipitation Patterns in Nepal Over 1971–2015. *Earth Space Sci.* **2024**, *11*, e2024EA003563. [CrossRef]
25. Shrestha, M.; Acharya, S.C. Assessment of historical and future land-use–land-cover changes and their impact on valuation of ecosystem services in Kathmandu Valley. *Land Degrad. Dev.* **2020**, *32*, 3731–3742. [CrossRef]
26. Chaudhary, U.; Shah, M.A.R.; Shakya, B.M.; Aryal, A. Flood Susceptibility and Risk Mapping of Kathmandu Valley Watershed. *Sustainability* **2024**, *16*, 7101. [CrossRef]
27. Danegulu, A.; Karki, S.; Bhattarai, P.K.; Pandey, V.P. Characterizing urban flooding in the Kathmandu Valley, Nepal: The influence of urbanization and river encroachment. *Nat. Hazards* **2024**, *120*, 10923–10947. [CrossRef]
28. Magar, B.G.; Poudel, J.M.; Paudel, B.; Pokharel, B. Climate change in outskirts of Kathmandu Valley: Local perception and narratives. *Nat. Hazards* **2024**, *120*, 8103–8120. [CrossRef]
29. Kc, S.; Shrestha, S.; Ninsawat, S.; Chonwattana, S. Predicting flood events in Kathmandu Metropolitan City under climate change and urbanisation. *J. Environ. Manag.* **2021**, *281*, 111894. [CrossRef]
30. Mesta, C.; Cremen, G.; Galasso, C. Urban growth modelling and social vulnerability assessment for a hazardous Kathmandu Valley. *Sci. Rep.* **2022**, *12*, 6152. [CrossRef]
31. Prajapati, R.; Upadhyay, S.; Talchabhadel, R.; Thapa, B.R.; Ertis, B.; Silwal, P.; Davids, J.C. Investigating the nexus of groundwater levels, rainfall and land-use in the Kathmandu Valley, Nepal. *Groundw. Sustain. Dev.* **2021**, *14*, 100584. [CrossRef]
32. Shrestha, D.; Basnyat, D.B.; Gyawali, J.; Creed, M.J.; Sinclair, H.D.; Golding, B.; Muthusamy, M.; Shrestha, S.; Watson, C.S.; Subedi, D.L.; et al. Rainfall extremes under future climate change with implications for urban flood risk in Kathmandu. *Int. J. Disaster Risk Reduct.* **2023**, *97*, 103997. [CrossRef]
33. Prajapati, R.; Talchabhadel, R.; Silwal, P.; Upadhyay, S.; Ertis, B.; Thapa, B.R.; Davids, J.C. Less rain and rainy days—Lessons from 45 years of rainfall data (1971–2015) in the Kathmandu Valley, Nepal. *Theor. Appl. Climatol.* **2021**, *145*, 1369–1383. [CrossRef]
34. Shrestha, S.; Semkuyu, D.J.; Pandey, V.P. Assessment of groundwater vulnerability and risk to pollution in Kathmandu Valley. *Sci. Total. Environ.* **2016**, *556*, 23–35. [CrossRef]

35. Bharti, P.; Biswas, A. Predicting Urban Growth of Kathmandu Valley Using Artificial Intelligence. *J. Geovisualization Spat. Anal.* **2024**, *8*, 40. [CrossRef]
36. Shrestha, S.; Neupane, S.; Mohanasundaram, S.; Pandey, V.P. Mapping groundwater resiliency under climate change scenarios: A case study of Kathmandu Valley. *Environ. Res.* **2020**, *183*, 109149. [CrossRef]
37. DHM. Available online: https://www.dhm.gov.np/ (accessed on 4 March 2025).
38. Ridwan, W.M.; Sapitang, M.; Aziz, A.; Kushiar, K.F.; Ahmed, A.N.; El-Shafie, A. Rainfall forecasting model using machine learning methods: Case study Terengganu. *Ain Shams Eng. J.* **2021**, *12*, 1651–1663. [CrossRef]
39. Climate Prediction Center—Monitoring & Data: Current Monthly Atmospheric and Sea Surface Temperatures Index Values. Available online: https://www.cpc.ncep.noaa.gov/data/indices/ (accessed on 4 March 2025).
40. Ehsan, M.A.; Tippett, M.K.; Robertson, A.W.; Singh, B.; Rahman, M.A. The ENSO Fingerprint on Bangladesh Summer Monsoon Rainfall. *Earth Syst. Environ.* **2023**, *7*, 617–627. [CrossRef]
41. Lenssen, N.J.L.; Goddard, L.; Mason, S. Seasonal Forecast Skill of ENSO Teleconnection Maps. *Weather. Forecast.* **2020**, *35*, 2387–2406. [CrossRef]
42. Sahoo, M.; Yadav, R.K. Teleconnection of Atlantic Nino with summer monsoon rainfall over northeast India. *Glob. Planet. Change* **2021**, *203*, 103550. [CrossRef]
43. Yang, Y.-M.; Park, J.-H.; An, S.-I.; Wang, B.; Luo, X. Mean sea surface temperature changes influence ENSO-related precipitation changes in the mid-latitudes. *Nat. Commun.* **2021**, *12*, 1495. [CrossRef]
44. Mann, H.B. Nonparametric Tests Against Trend. 1945. Available online: https://www.jstor.org/stable/1907187 (accessed on 1 January 2025).
45. Ahmed, I.A.; Shahfahad; Dutta, D.K.; Baig, M.R.I.; Roy, S.S.; Rahman, A. Implications of changes in temperature and precipitation on the discharge of Brahmaputra River in the urban watershed of Guwahati. *Environ. Monit. Assess.* **2021**, *193*, 518. [CrossRef]
46. Obuobie, E.; Osei, M.A.; Addi, M.; Agyekum, J.; Akurugu, B.A.; Bazaanah, P.; Gaisie-Essilfie, F.A.; Appiah, G. Analysis of spatio-temporal trends in climate extremes in the Lower Volta Basin. *Theor. Appl. Clim.* **2025**, *156*, 120. [CrossRef]
47. Zhang, X.; Alexander, L.; Hegerl, G.C.; Jones, P.; Tank, A.K.; Peterson, T.C.; Trewin, B.; Zwiers, F.W. Indices for monitoring changes in extremes based on daily temperature and precipitation data. *Wires Clim. Change* **2011**, *2*, 851–870. [CrossRef]
48. Oliver, J.E. Monthly Precipitation Distribution: A Comparative Index. *Prof. Geogr.* **1980**, *32*, 300–309. [CrossRef]
49. Bandar, Q.K.A.; Muslih, K.D. Spatial assessment of precipitation concentration and seasonality in Iraq. *Theor. Appl. Clim.* **2025**, *156*, 134. [CrossRef]
50. Du, J.; Yu, X.; Zhou, L.; Li, X.; Ao, T. Less concentrated precipitation and more extreme events over the Three River Headwaters region of the Tibetan Plateau in a warming climate. *Atmospheric Res.* **2024**, *303*, 107311. [CrossRef]
51. Bhattacharyya, S.; Sreekesh, S. Assessments of multiple gridded-rainfall datasets for characterizing the precipitation concentration index and its trends in India. *Int. J. Clim.* **2021**, *42*, 3147–3172. [CrossRef]
52. Tolika, K. On the analysis of the temporal precipitation distribution over Greece using the Precipitation Concentration Index (PCI): Annual, seasonal, monthly analysis and association with the atmospheric circulation. *Theor. Appl. Climatol.* **2019**, *137*, 2303–2319. [CrossRef]
53. Amiri, M.A.; Gocić, M. Analyzing the applicability of some precipitation concentration indices over Serbia. *Theor. Appl. Clim.* **2021**, *146*, 645–656. [CrossRef]
54. Balling, R.C.; Kiany, M.S.K.; Roy, S.S.; Khoshhal, J. Trends in Extreme Precipitation Indices in Iran: 1951–2007. *Adv. Meteorol.* **2016**, *2016*, 2456809. [CrossRef]
55. De Lima, M.I.P.; Santo, F.E.; Ramos, A.M.; Trigo, R.M. Trends and correlations in annual extreme precipitation indices for mainland Portugal, 1941–2007. *Theor. Appl. Climatol.* **2015**, *119*, 55–75. [CrossRef]
56. Gocic, M.; Shamshirband, S.; Razak, Z.; Petković, D.; Ch, S.; Trajkovic, S. Long-Term Precipitation Analysis and Estimation of Precipitation Concentration Index Using Three Support Vector Machine Methods. *Adv. Meteorol.* **2016**, *2016*, 7912357. [CrossRef]
57. Michiels, P.; Gabriels, D.; Hartmann, R. Using the seasonal and temporal Precipitation concentration index for characterizing the monthly rainfall distribution in Spain. *CATENA* **1992**, *19*, 43–58. [CrossRef]
58. Petković, D.; Gocic, M.; Trajkovic, S.; Milovančević, M.; Šević, D. Precipitation concentration index management by adaptive neuro-fuzzy methodology. *Clim. Change* **2017**, *141*, 655–669. [CrossRef]
59. Ryan, C.; Curley, M.; Walsh, S.; Murphy, C. Long-term trends in extreme precipitation indices in Ireland. *Int. J. Clim.* **2021**, *42*, 4040–4061. [CrossRef]
60. Sarr, M.A.; Zoromé, M.; Seidou, O.; Bryant, C.R.; Gachon, P. Recent trends in selected extreme precipitation indices in Senegal—A changepoint approach. *J. Hydrol.* **2013**, *505*, 326–334. [CrossRef]
61. Chhetri, R.; Pandey, V.P.; Talchabhadel, R.; Thapa, B.R. How do CMIP6 models project changes in precipitation extremes over seasons and locations across the mid hills of Nepal? *Theor. Appl. Clim.* **2021**, *145*, 1127–1144. [CrossRef]
62. Dhital, Y.; Kayastha, R. causes and impacts of flooding in the Bagmati River Basin. *J. Flood Risk Manag.* **2013**, *6*, 253–260. [CrossRef]

63. Pradhan-Salike, I.; Pokharel, J.R. Impact of Urbanization and Climate Change on Urban Flooding: A case of the Kathmandu Valley. *J. Nat. Resour. Dev.* **2017**, *7*, 56–66. [CrossRef]
64. Roxy, M.K.; Ghosh, S.; Pathak, A.; Athulya, R.; Mujumdar, M.; Murtugudde, R.; Terray, P.; Rajeevan, M. A threefold rise in widespread extreme rain events over central India. *Nat. Commun.* **2017**, *8*, 708. [CrossRef]
65. Society of Hydrologists and Meteorologists-Nepal. SOHAM_Newsletter_Vol-1_-No-1_October-Novermber-2002. Available online: https://soham.org.np/newsletter/soham-nepal-newsletter-8/ (accessed on 1 January 2025).
66. Durbar, S. A Preliminary Loss and Damage Assessment of Flood and Landslide National Disaster Risk Reduction and Management Authority Preliminary Loss and Damage Assessment of Flood and Landslide September 2024 Published by Government of Nepal Ministry of Home Affairs National Disaster Risk Reduction and Management Authority. 2024. Available online: www.bipad.gov.np (accessed on 12 March 2025).
67. Guo, E.; Wang, Y.; Jirigala, B.; Jin, E. Spatiotemporal variations of precipitation concentration and their potential links to drought in mainland China. *J. Clean. Prod.* **2020**, *267*, 122004. [CrossRef]
68. Nandargi, S.S.; Aman, K. Precipitation concentration changes over India during 1951 to 2015. *Sci. Res. Essays* **2018**, *13*, 14–26. [CrossRef]
69. Rahman, S.; Islam, A.R.M.T. Are precipitation concentration and intensity changing in Bangladesh overtimes? Analysis of the possible causes of changes in precipitation systems. *Sci. Total. Environ.* **2019**, *690*, 370–387. [CrossRef] [PubMed]
70. Rashid, I.U.; Abid, M.A.; Almazroui, M.; Kucharski, F.; Hanif, M.; Ali, S.; Ismail, M. Early summer surface air temperature variability over Pakistan and the role of El Niño–Southern Oscillation teleconnections. *Int. J. Clim.* **2022**, *42*, 5768–5784. [CrossRef]
71. Shrestha, A.; Kostaschuk, R. El Niño/Southern Oscillation (ENSO)-related variablity in mean-monthly streamflow in Nepal. *J. Hydrol.* **2005**, *308*, 33–49. [CrossRef]
72. Kadel, I.; Yamazaki, T.; Iwasaki, T.; Abdillah, M.R. Projection of future monsoon precipitation over the central Himalayas by CMIP5 models under warming scenarios. *Clim. Res.* **2018**, *75*, 1–21. [CrossRef]
73. Xu, Z.X.; Takeuchi, K.; Ishidaira, H. Correlation between El Niño-Southern Oscillation (ENSO) and precipitation in South-east Asia and the Pacific region. *Hydrol. Process.* **2003**, *18*, 107–123. [CrossRef]
74. Izumo, T.; Lengaigne, M.; Vialard, J.; Luo, J.-J.; Yamagata, T.; Madec, G. Influence of Indian Ocean Dipole and Pacific recharge on following year's El Niño: Interdecadal robustness. *Clim. Dyn.* **2013**, *42*, 291–310. [CrossRef]
75. Leupold, M.; Pfeiffer, M.; Watanabe, T.K.; Reuning, L.; Garbe-Schönberg, D.; Shen, C.-C.; Brummer, G.-J.A. El Niño-Southern Oscillation and internal sea surface temperature variability in the tropical Indian Ocean since 1675. *Clim. Past* **2021**, *17*, 151–170. [CrossRef]

water

MDPI

Article

Extreme Precipitation Dynamics and El Niño–Southern Oscillation Influences in Kathmandu Valley, Nepal

Deepak Chaulagain [1,2], Ram Lakhan Ray [3], Abdulfati Olatunji Yakub [1,2], Noel Ngando Same [1,2], Jaebum Park [1,2], Anthony Fon Tangoh [1,2], Jong Wook Roh [4], Dongjun Suh [1], Jeong-Ok Lim [2] and Jeung-Soo Huh [1,2,*]

[1] Department of Convergence & Fusion System Engineering, Graduate School, Kyungpook National University, Sangju 37224, Republic of Korea; chaulagaindeepu11@gmail.com (D.C.); yakubabdulfatail@gmail.com (A.O.Y.); samenoel1@gmail.com (N.N.S.); woqja133@naver.com (J.P.); fontangoh@gmail.com (A.F.T.); dongjunsuh@knu.ac.kr (D.S.)
[2] Institute for Global Climate Change & Energy, Kyungpook National University, Daegu 41566, Republic of Korea; jolim@knu.ac.kr
[3] Cooperative Agricultural Research Center, College of Agriculture, Food, and Natural Resources, Prairie View A & M University, Prairie View, TX 77446, USA; raray@pvamu.edu
[4] Department of Nano & Advanced Materials Science and Engineering, Kyungpook National University, Sangju 37224, Republic of Korea; jw.roh@knu.ac.kr
* Correspondence: jshuh@knu.ac.kr

Abstract: Understanding historical climatic extremes and variability is crucial for effective climate change adaptation, particularly for urban flood management in developing countries. This study investigates historical precipitation trends in the Kathmandu Valley, Nepal, focusing on precipitation frequency, intensity, and the influence of the El Niño–Southern Oscillation (ENSO), using extreme precipitation indices and the precipitation concentration index (PCI). The results reveal sharply fluctuating short-term precipitation from 1980 to 2022, with the exception of an increasing trend during spring (1.17 mm/year) and a decreasing trend in November and December. Trends in extreme precipitation indices are mixed: RX7day shows an increasing trend of 0.1 mm/year, with decadal analysis (1980–2001 and 2002–2022) indicating similar upward patterns. In contrast, RX1day, RX3day, RX5day, and R95pTOT exhibit inconsistent trends, while R99pTOT demonstrates a decreasing trend over the full period (1980–2022). Although the number of days with precipitation $\geq$ 35 mm has declined, the increasing trend in 7-day maximum precipitation, coupled with no significant change in total annual precipitation and highly variable short-term rainfall, points to a rising risk of unexpected extreme precipitation events. Precipitation patterns in the Kathmandu Valley remain highly irregular across seasons, except during summer. ENSO exhibits a negative correlation with annual precipitation, extreme precipitation indices, and the PCI but shows a positive correlation with the annual and summer PCI as well as 1-day maximum precipitation, emphasizing its significant influence on precipitation variability. These findings highlight the urgent need for targeted climate adaptation strategies and provide valuable insights for hydrologists, meteorologists, policymakers, and urban planners to enhance climate resilience and improve flood management in the Kathmandu Valley.

Keywords: climate change; extreme events; flood disaster; Kathmandu; precipitation indices; precipitation concentration index; Nepal

Academic Editor: Majid Mirzaei

Received: 30 March 2025
Revised: 30 April 2025
Accepted: 5 May 2025
Published: 6 May 2025

Citation: Chaulagain, D.; Ray, R.L.; Yakub, A.O.; Same, N.N.; Park, J.; Tangoh, A.F.; Roh, J.W.; Suh, D.; Lim, J.-O.; Huh, J.-S. Extreme Precipitation Dynamics and El Niño–Southern Oscillation Influences in Kathmandu Valley, Nepal. *Water* **2025**, *17*, 1397. https://doi.org/10.3390/w17091397

1. Introduction

Climate change is reshaping precipitation patterns at local, regional, and global scales, with significant consequences for hydrological cycles and extreme weather events [1].

The rapid rise in global average temperatures has increased atmospheric water vapor concentrations, thereby intensifying extreme precipitation events [2]. As a key component of the Earth's hydrological cycle, precipitation is experiencing dynamic transformations under the influence of global warming, resulting in notable changes in its frequency, intensity, and spatial distribution [3]. The acceleration of climate change further amplifies hydrometeorological disasters such as floods, droughts, and landslides [4]. South Asia, in particular, is among the world's most disaster-prone regions, witnessing an overall rise in extreme precipitation with spatially heterogeneous patterns [5]. Nepal is especially vulnerable, ranking fourth globally as the most climate hazard-prone country [6].

Numerous studies have explored precipitation patterns using both observed and projected datasets and applied various analytical approaches globally. Sun et al. (2021) [7] investigated extreme precipitation trends at global, continental, and regional scales using the one-day maximum (RX1day) and five-day maximum (RX5day) precipitation indices. Their results show that nearly two-thirds of global observation stations exhibit significant upward trends in extreme precipitation, particularly across Asia, Europe, and North America, with pronounced increases in regions such as central and eastern North America, northern Central America, northern Europe, the Russian Far East, eastern Central Asia, and East Asia. Similarly, Donat (2016) [8] examined total and extreme precipitation variations in wet and dry regions using both observational data and global climate model outputs. The study found that precipitation has historically increased in wet regions and is likely to continue rising, whereas dry regions may experience a sharp increase in extreme precipitation events by the late 21st century. Additionally, Papalexiou and Montanari (2019) [9] analyzed global precipitation trends from 1964 to 2013 and concluded that both the intensity and frequency of precipitation increased significantly over this period.

While global studies highlight broad trends, local investigations reveal more heterogeneous patterns. Safdar et al. (2023) [10] analyzed precipitation trends in Pakistan during the winter and pre-monsoon seasons from 2008 to 2018, reporting a decline in winter precipitation and a reduction in rainy days for both seasons. Similarly, Aditya et al. (2021) [11] employed the Mann–Kendall test and Sen's slope estimator to examine rainfall variability in West Kalimantan, Indonesia. Their findings indicate a declining annual precipitation trend in the Mempawah region, while the Kubu Raya region exhibited an increasing annual precipitation trend between 2000 and 2019. The study further identified a significant precipitation decrease of -33.2 mm/year in Sungai Kunyit, suggesting a potentially drier future for the area. A comparable downward trend was observed in India's Thoubal River watershed, where precipitation declined by 10.3 mm/year, accompanied by considerable variability [12]. Another study on India's precipitation patterns, with ref. [13] analyzing data from 2001 to 2018, reported decreasing precipitation in the Indo-Gangetic Plain and in Northeast India due to a weakening of the southwesterly moisture flow, while northwestern India experienced an increasing trend. In southern India, precipitation declined because of a northward shift in sinking air masses over the equatorial region. In Bangladesh, Jihan et al. (2025) [14] projected an overall increase in precipitation by 480.38 mm, with the most pronounced rise occurring during storm-prone months.

Situated along the southern slopes of the central Himalayas, Nepal is highly vulnerable to extreme precipitation events because of its complex topography and dynamic atmospheric interactions. The country's summer monsoon primarily originates from the Bay of Bengal, supplemented by mid-latitude cyclonic systems that produce exceptionally heavy rainfall when interacting with monsoonal flows. Additionally, moisture-laden systems originating from the Arabian Sea and the Bay of Bengal further contribute to extreme precipitation, increasing the risk of both pluvial and fluvial flooding [15]. Several studies have reported a rise in intense daily precipitation trends across Nepal, significantly contributing

to flash floods in various regions [16–18]. For instance, Chhetri et al. (2020) [19] investigated flooding in the Banke and Bardiya districts, attributing extreme flood events to overnight heavy rainfall in central–western Nepal.

Nepal's climate is influenced by both the summer monsoon and westerly circulation systems. The summer monsoon is driven by southeasterly winds that transport moisture from the Bay of Bengal, whereas moisture-laden winds from the Mediterranean Sea govern the westerly circulation. In addition to these large-scale systems, Nepal's complex topography is critical in shaping local weather conditions, resulting in substantial spatial variability in precipitation over short distances [20]. Shrestha et al. (2019) [21] analyzed precipitation trends in the Koshi and Kaligandaki river basins from 1981 to 2015 and found that precipitation rapidly decreased with elevation in the Kaligandaki basin, whereas the Koshi basin displayed the opposite trend. Orographic effects and rain-shadow phenomena further contribute to distinct spatial and temporal variations in precipitation patterns across the country [22,23].

Luo et al. (2024) [24] analyzed extreme precipitation trends in Nepal using 11 precipitation indices developed by the World Meteorological Organization's Expert Team on Climate Change Detection and Indices (ETCCDI) for the period 1971–2015 based on APHRODITE data. Their findings indicate an overall decline in extreme precipitation trends, although the number of maximum consecutive wet days increased at varying rates across western and eastern Nepal. This study also highlights the significant influence of the South Asian monsoon on Nepal's precipitation indices. Similarly, Lamichhane et al. (2024) [4] employed the PCI to investigate precipitation patterns across Nepal from 1990 to 2020, with particular attention to the role of El Niño–Southern Oscillation (ENSO) on PCI variability. Their results revealed that monthly precipitation in Nepal exhibits moderate to strong irregularity, with lower elevation regions experiencing greater variability than mountainous areas. Furthermore, annual precipitation trends show an increasing rate of 0.53 mm per decade, while ENSO-driven variability is notably and inversely correlated with the Niño 3.4 index across most regions of Nepal.

The Kathmandu Valley, situated in the central Himalayas, is characterized by bowl-shaped topography and a single drainage outlet at Chovar. Rapid urban expansion has intensified the impacts of extreme precipitation, resulting in frequent urban flooding [25]. For instance, on 6 September 2021, *The Kathmandu Post* reported that 121.5 mm of rainfall caused severe inundation in multiple areas, including Balkhu, Kuleshwor, Narephant, Balaju, and Mulpani, as well as along major roadways. These extreme precipitation events often lead to traffic disruptions, casualties, disturbances for pedestrians and school children, and broader socioeconomic consequences. The severity of such impacts in the Kathmandu Valley is amplified due to the high population exposure.

Although several hydrometeorological studies have been conducted in the Kathmandu Valley, most have concentrated on flood mapping rather than long-term precipitation trends [26–32]. While Prajapati et al. (2021) [33] analyzed precipitation days from 1971 to 2015, their focus was primarily on spatial rainfall distribution and interstation comparisons. Consequently, a significant research gap remains regarding the historical trends in extreme precipitation intensity, frequency, and variability, as well as the influence of ENSO on extreme precipitation events and the PCI in the Kathmandu Valley.

This study addresses these gaps by analyzing extreme precipitation patterns in the Kathmandu Valley, focusing on frequency, intensity, seasonal and annual variability, and the influence of ENSO. The Mann–Kendall test and Sen's slope estimator are employed to assess precipitation trends from 1980 to 2022 using extreme precipitation indices recommended by the World Meteorological Organization (WMO) and the PCI. Additionally, this study investigates the effects of ENSO using the Niño 3.4 index. The findings

offer valuable insights for hydrologists, urban planners, and policymakers seeking to improve flood forecasting and disaster preparedness by better understanding historical precipitation extremes.

2. Materials and Methods

2.1. Study Area

The study area, illustrated in Figure 1, is located in the central Himalayan region of Nepal and encompasses the capital city, Kathmandu, along with the districts of Bhaktapur, Kathmandu, and Lalitpur. Several major rivers, including the Bagmati, Bishnumati, Manohara, Hanumante, and Dhobikhola, traverse through the Kathmandu Valley. Geographically, it lies between 27°32′13″–27°49′10″ N latitude and 85°11′31″–85°31′38″ E longitude [34]. The Kathmandu Valley covers an area of approximately 664 km^2. The Kathmandu Valley ranges in elevation from 1350 m above sea level (masl) in the lowlands to nearly 2800 masl in the surrounding hills. The valley is home to roughly 24% of Nepal's urban population which is estimated to be 3.3 million and projected to reach 3.8 million by 2031 [30], making it particularly vulnerable to climate-induced hazards, including extreme precipitation events [35]. The region experiences four distinct seasons—summer, autumn, spring, and winter—and falls within a subtropical to temperate climate zone. The average annual precipitation is approximately 1778 mm, most of which occurs between June and September. The temperature in the valley varies throughout the year, with recorded highs reaching 23.8 °C and lows dropping to 11.4 °C [36].

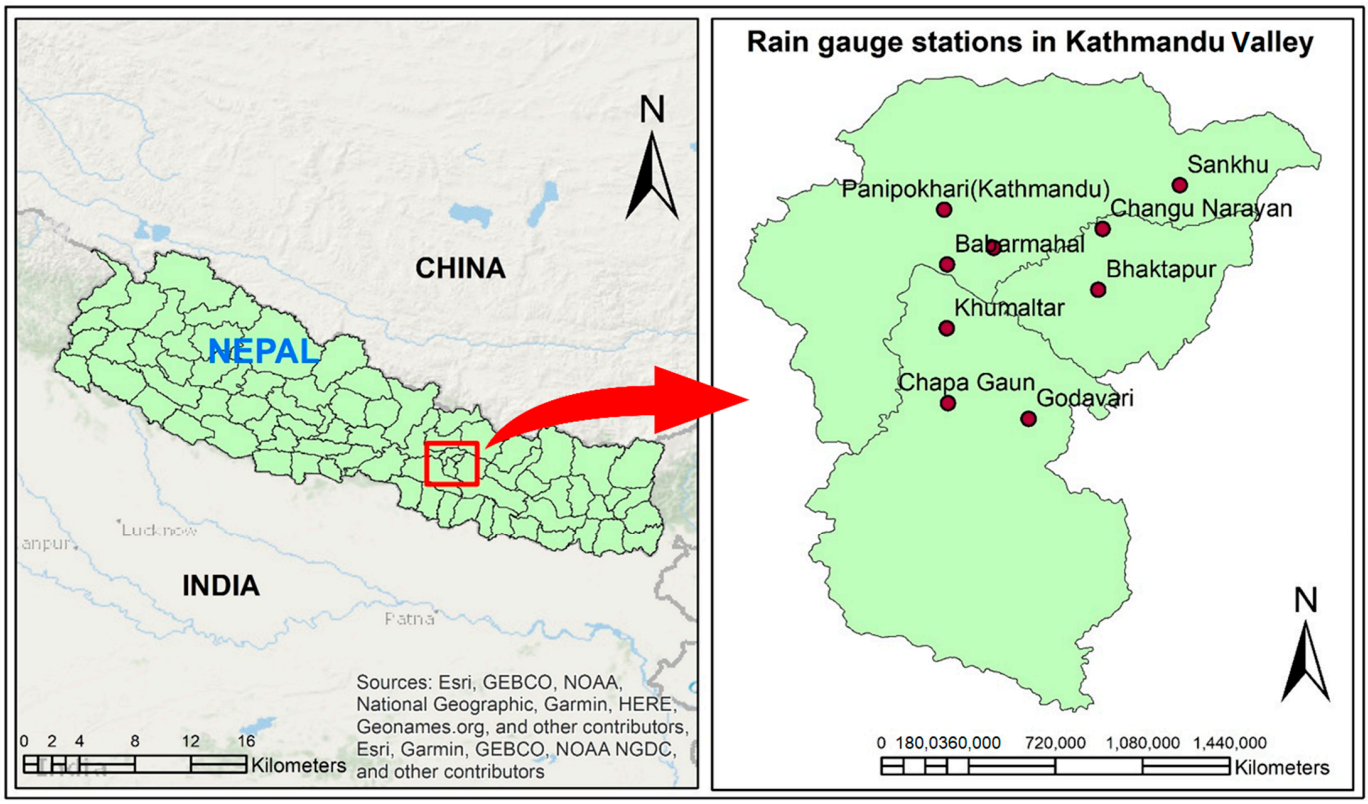

Figure 1. Study area with rain gauge stations.

2.2. Data Preparation

2.2.1. Observed Station Data

This study used daily observed rainfall data from nine rain gauge stations in the Kathmandu Valley covering the period from 1980 to 2022. The data were obtained from

Nepal's Department of Hydrology and Meteorology (DHM) [37]. Missing values in daily precipitation data, which accounted for less than 5% of the dataset, were filled in using data from nearby stations for the corresponding periods.

Given the spatial variability of precipitation across the Kathmandu Valley, it is essential to estimate the average precipitation in a manner that accounts for the unequal distribution of stations and the differing areas each station represents. Therefore, the average precipitation across the valley was estimated using the Thiessen polygon method. This approach delineates the area influenced by each station and assigns station-specific weights based on their respective catchment areas, ensuring that the computed average precipitation accurately reflects the spatial distribution of rainfall. The Thiessen polygon weights for each station are illustrated in Figure 2. The average daily precipitation of the Kathmandu Valley was calculated using the following equation [38]:

$$P = P_1W_1 + P_2W_2 + P_3W_3 + \ldots + P_nW_n \quad (1)$$

where P_1, P_2, P_3,. . ., and P_n represent the daily precipitation values at the respective stations, and W_1, W_2, W_3,. . ., and W_n are the corresponding Thiessen polygon weights. The Thiessen polygon weights *(W)* were determined as follows:

$$W_1 = \frac{A_1}{A_1 + A_2 + A_3 \ldots A_n}, \; W_2 = \frac{A_2}{A_1 + A_2 + A_3 \ldots A_n}, \; \ldots \; W_n = \frac{A_n}{A_1 + A_2 + A_3 \ldots A_n} \quad (2)$$

where A_1, A_2, A_3, . . ., and A_n denote the areas of the Thiessen polygons corresponding to each station.

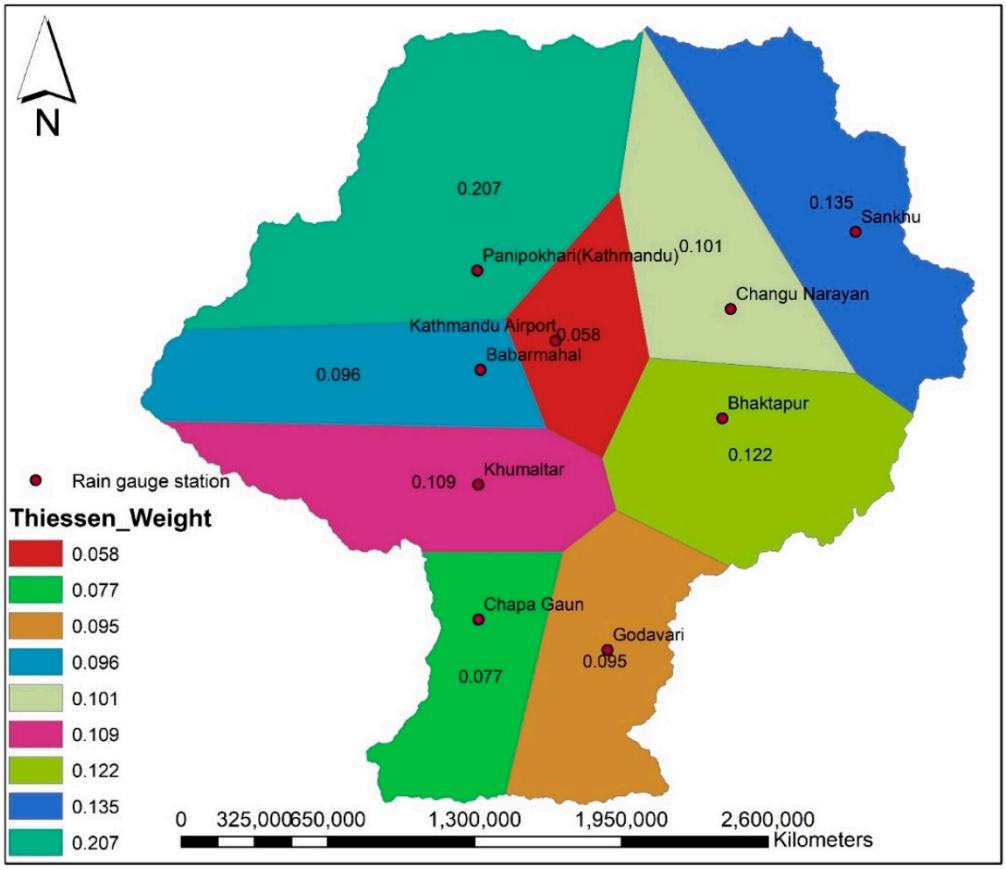

Figure 2. Thiessen polygon of the Kathmandu Valley.

2.2.2. ENSO Index

This study investigates the influence of tropical SST variations on precipitation patterns, PCI, and extreme precipitation indices. Specifically, SST anomalies in the Niño 3.4 region (5° N–5° S, 120° W–170° W) were used for analysis [4]. The SST anomalies were obtained from the Niño 3.4 index based on data from the Extended Reconstructed Sea Surface Temperature version 5 (ERSST V5) provided by the National Weather Service Climate Prediction Center, a division of NOAA accessed on 1 January 2025 (https://www.cpc.ncep.noaa.gov/data/indices/) [39]. The Niño 3.4 index, which has been widely used in previous studies [4,40–43], is available at a monthly resolution. This study assessed the relationship between ENSO and extreme precipitation and the PCI on annual and seasonal timescales from 1980 to 2022.

2.3. Data Analysis

2.3.1. Average Precipitation

This study analyzed the mean monthly precipitation in the Kathmandu Valley from 1980 to 2022. The precipitation dataset was initially processed using the Thiessen polygon method to account for spatial variability and was further analyzed to calculate the average precipitation for each month across the study period. The temporal distribution of precipitation was then visualized using a histogram to illustrate the monthly variations throughout the year.

2.3.2. Precipitation Trend Analysis (Mann–Kendall Test)

The Mann–Kendall statistical test, first introduced by Mann (1945) [44], is a widely used non-parametric method for detecting trends in time series data, particularly in the fields of hydrology and climatology [12]. One of the key advantages of this test is that it does not require the data to follow any specific distribution. It assumes that the time series is independently and identically distributed and is unaffected by serial correlation over time [24]. The null hypothesis (H_0) of the Mann–Kendall test posits that there is no trend in the dataset, meaning that the observations are randomly ordered. In contrast, the alternative hypothesis (H_1) indicates a trend within the time series [45].

In this study, the Mann–Kendall test statistic (S) was computed on an annual, seasonal, and monthly basis using the following equation:

$$S = \sum_{i=1}^{n-1} \sum_{j=i+1}^{n} sgn(x_j - x_i) \quad (3)$$

where n is the number of observations, and x_i and x_j are the data values at time indices i and j, respectively. The sign function $sng(x_j - x_i)$ is defined as follows:

$$sng(x_j - x_i) = \begin{cases} +1 \; if \; (x_j - x_i) > 0 \\ 0 \; if \; (x_j - x_i) = 0 \\ -1 \; if \; (x_j - x_i) < 0 \end{cases} \quad (4)$$

For datasets where n > 10, the test statistics S is approximately normally distributed with a mean of zero [12,24]. The variance of S is calculated as follows:

$$Var(S) = \frac{n(n-1)(2n+5) - \sum_{i=1}^{m} t(t-1)(2t+5)}{18} \quad (5)$$

where m is the number of tied groups, and t represents the number of tied values in each group.

For n > 10, the standardized normal variable Z is computed as follows:

$$Z = \begin{cases} \frac{S-1}{\sqrt{Var(S)}} \; if \; S > 0 \\ 0 \; if \; S = 0 \\ \frac{S+1}{\sqrt{Var(S)}} \; if \; S < 0 \end{cases} \quad (6)$$

A positive Z-value indicates an upward trend in the time series, whereas a negative Z-value signifies a downward trend. The statistical significance of the identified trend is evaluated against a predefined significance level.

2.3.3. Trend Magnitude Estimation (Sen's Slope)

Sen's slope (β) estimator is a non-parametric method used to quantify the magnitude of trends in time series data. It is widely employed in hydrology and climatology because of its robustness against outliers and applicability to data that do not follow a normal distribution [12]. This method calculates the slope between all possible pairs of data points and uses the median of these slopes to provide a reliable estimate of the overall trend magnitude. In this study, Sen's slope (β) was calculated on an annual, seasonal, and monthly basis using the following equation:

$$\beta = median \frac{x_i - x_j}{i - j} \quad (7)$$

where x_i and x_j are the data values at time steps t_i and t_j, respectively. A positive value of β indicates an upward trend, whereas a negative value signifies a downward trend in the dataset.

2.3.4. Extreme Precipitation Indices

Precipitation indices, summarized in Table 1 and recommended by the WMO, were used to evaluate precipitation characteristics in the Kathmandu Valley. These indices capture both the intensity and frequency of extreme precipitation events [24,46,47] and are widely used in hydrological and climatological studies because of their robustness in representing temporal and spatial variations in precipitation patterns.

This study categorizes precipitation indices into two main types: intensity-based and frequency-based. Intensity-based indices measure the magnitude of precipitation events and include the maximum 1-day (RX1day), 3-day (RX3day), 5-day (RX5day), and 7-day (RX7day) precipitation amounts. Threshold-based indices, such as very wet days (R95pTOT) and extremely wet days (R99pTOT), represent the total precipitation on days exceeding the 95th and 99th percentile thresholds, respectively. The Simple Daily Intensity Index (SDII) was also used to estimate the average precipitation on wet days.

Frequency-based indices assess the occurrence of extreme precipitation events, including the number of heavy precipitation days as follows: R10 mm, R20 mm, R35 mm, corresponding to days with precipitation exceeding 10 mm, 20 mm, and 35 mm, respectively. The longest consecutive dry days (CDDs, defined as precipitation <1 mm) and consecutive wet days (CWDs, defined as precipitation >1 mm) were also analyzed to evaluate extended dry and wet periods.

All indices were derived from daily precipitation records from 1980 to 2022 to identify trends in extreme precipitation events within the study area. To better understand temporal changes, trends were analyzed for the entire study period (1980–2022) and separately for two decades (1980–2001 and 2002–2022) using the Pettitt test, providing a clearer view of recent climate trends.

Table 1. Extreme precipitation indices.

Precipitation Indices	Abbreviation	Unit	Description
Maximum 1-day precipitation amount	RX1day	mm	Intensity of precipitation
Maximum 3-day precipitation amount	RX3day	mm	Intensity of precipitation
Maximum 5-day precipitation amount	RX5day	mm	Intensity of precipitation
Maximum 7-day precipitation amount	RX7day	mm	Intensity of precipitation
Total precipitation on days exceeding the 95th percentile (very wet days)	R95pTOT	mm	Intensity of precipitation
Total precipitation on days exceeding the 99th percentile (extremely wet days)	R99pTOT	mm	Intensity of precipitation
Count of days with precipitation $\geq$ 10 mm (heavy precipitation days)	R10 mm	days	Frequency of precipitation
Count of days with precipitation $\geq$ 20 mm (very heavy precipitation days)	R20 mm	days	Frequency of precipitation
Count of days with precipitation $\geq$ 35 mm (extreme precipitation days)	R35 mm	days	Frequency of precipitation
Maximum number of consecutive dry days (precipitation < 1 mm)	CDDs	days	Frequency of precipitation
Maximum number of consecutive wet days (precipitation > 1 mm)	CWDs	days	Frequency of precipitation
Simple Daily Intensity Index (SDII)—average precipitation on wet days	SDII	mm/day	Intensity of precipitation

2.3.5. Precipitation Concentration Index (PCI)

The PCI, introduced by Oliver (1980) [48], is widely used to assess the temporal distribution of precipitation across the 12 months of the year. It serves as a vital tool for evaluating the uniformity of irregularity of precipitation on both seasonal and annual scales, ranging from evenly distributed precipitation to highly irregular precipitation patterns [49], according to Table 2 thresholds. Variability in precipitation concentration significantly influences hydrological hazards such as floods, droughts, landslides, and soil erosion, as it reflects imbalances in precipitation distribution throughout the year [50]. In recent years, the PCI has gained increasing recognition in hydrological research for its ability to characterize precipitation variability [51,52]. In this study, the PCI was determined on both an annual and seasonal basis for 1980–2022 [4]. Daily average precipitation, estimated using the Thiessen polygon method, was aggregated into monthly totals for the Kathmandu Valley. The monthly precipitation values were then used to calculate the PCI using the following equations [4]:

$$PCI\ (yearly) = \frac{\sum_{i=1}^{12} P_i^2}{\left(\sum_{i=1}^{12} P_i\right)^2} \times 100 \quad (8)$$

$$PCI\ (Season) = \frac{\sum_{i=1}^{n} P_i^2}{(\sum_{i=1}^{n} P_i)^2}\ (\frac{n}{12} \times 100) \quad (9)$$

where P_i represents the monthly precipitation for each month within the season, i represents the specific month, and n denotes the number of months within the season under consideration. The PCI values were converted to percentages by multiplying the results by 100 in both equations.

Table 2. Precipitation concentration threshold index.

PCI Threshold	Description
<10	Uniform
11–15	Moderate
16–20	Irregular
>20	Strongly irregular

3. Results

3.1. Monthly Average Precipitation

Figure 3 presents the monthly average precipitation in the Kathmandu Valley from 1980 to 2022, revealing a clear seasonal pattern. The highest rainfall is recorded in July (425 mm), followed by August (375 mm), while June and September receive between 220 mm and 245 mm. In contrast, the driest months are January, February, March, November, and December, with precipitation levels below 50 mm. April, May, and October receive moderate rainfall ranging from 50 mm to 135 mm. The data show that approximately 80% of the total annual precipitation occurs during the monsoon months of June, July, August, and September, with the remaining 20% distributed across the other eight months. This highlights the region's pronounced dependence on seasonal rainfall.

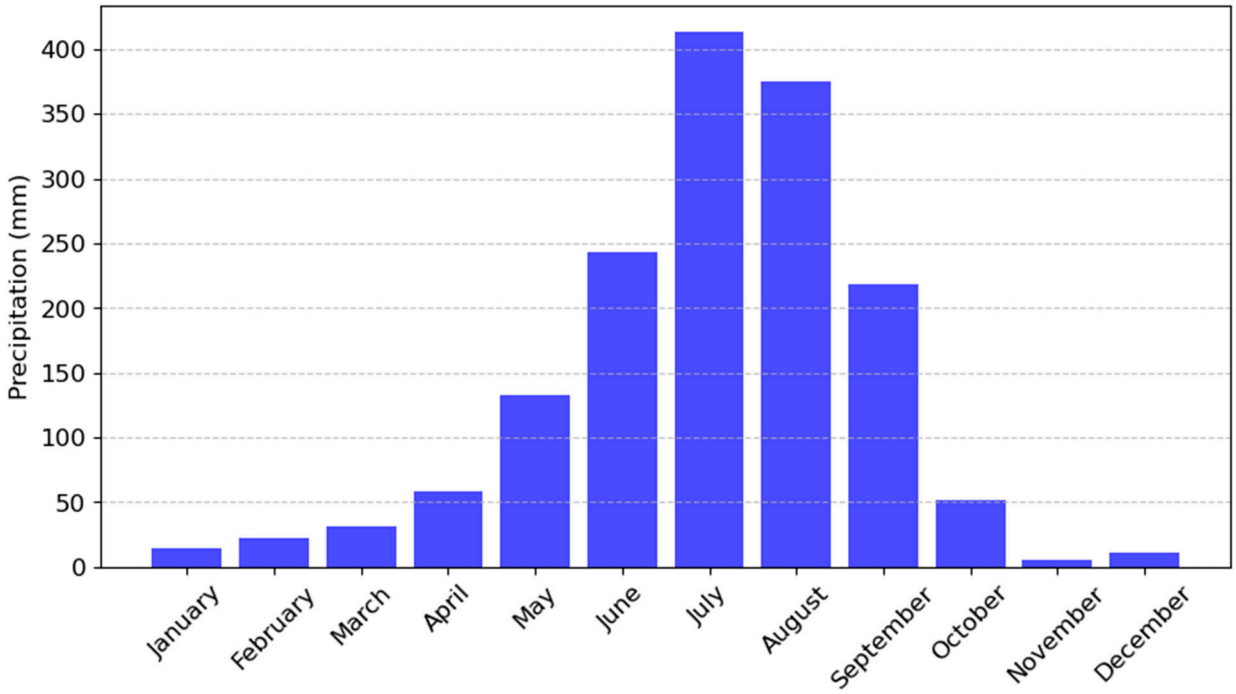

Figure 3. Monthly average precipitation in Kathmandu Valley from 1980 to 2022.

3.2. Precipitation Trends and Variability

Table 3 presents the results of the Mann–Kendall trend analysis for precipitation at monthly, seasonal, and annual scales, focusing on statistically significant trends. The seasonal classifications used in this study are winter (December–February), spring (March–May), summer (Monsoon) (June–August), and autumn (September–November). Among all the periods analyzed, only November, December, and the spring season exhibit statistically significant precipitation trends at the 0.05 significance level ($p < 0.05$). Specifically, November shows a declining trend of −0.035 mm/year ($p = 0.03$), December demonstrates a declining trend of −0.031 mm/year ($p = 0.02$), and spring shows an increasing trend of 1.17 mm/yr ($p = 0.04$). These significant downward trends suggest

an increase in aridity during the late autumn and early winter months, which may have implications for water availability in the dry season, whereas the spring season shows more water availability. For the remaining months and seasons and the annual scale, although positive or negative slopes were observed, the associated *p*-values exceed 0.05, indicating no statistically significant trends. In other time intervals, the precipitation is highly fluctuating.

Table 3. Results of the Mann–Kendall test for precipitation trends in the time series (1980–2022).

Period	Min (mm)	Max (mm)	Mean (mm)	SD (mm)	CV (%)	Mann–Kendall Z-Value	Mann–Kendall *p*-Value	Sen's Slope (mm/year)	Trend
January	0	70.2	14.4	17.6	121.8	−0.18	0.86	−0.006	NS
February	0	83.7	22.4	21.0	93.8	0.54	0.59	0.106	NS
March	0.2	98.6	31.0	24.0	77.4	0.12	0.91	0.024	NS
April	2.2	136.4	58.2	34.0	58.4	0.95	0.13	0.361	NS
May	44.2	251.2	132.6	50.3	37.9	0.37	0.17	0.211	NS
June	90.4	559.6	242.7	97.5	40.2	−0.32	0.75	−0.419	NS
July	247.2	621.6	413.2	95.2	23.0	0.14	0.89	0.226	NS
August	260.1	567.1	375.3	67.2	17.9	−1.37	0.17	−0.866	NS
September	103.4	430.4	218.4	74.8	34.3	−0.03	0.97	−0.016	NS
October	1.3	201.6	51.9	50.8	98.0	0.18	0.86	0.042	NS
November	0	64.2	5.6	11.3	202.5	−2.24	0.03	−0.035	↓
December	0	78.6	11.4	19.3	168.4	−2.39	0.02	−0.031	↓
Winter	0.2	143.1	48.3	32.7	67.7	−0.16	0.88	−0.088	NS
Summer	703.3	1386.9	1031.2	166.0	16.1	−0.83	0.41	−1.661	NS
Spring	104.5	368.7	221.8	67.9	30.6	1.37	0.04	1.174	↑
Autumn	119.2	567.8	275.8	92.9	33.7	−0.12	0.91	−0.125	NS
Annual	1155.7	2061.6	1577.1	224.7	14.2	−0.45	0.65	−0.806	NS

NS = not significant; ↑ = increasing trend; ↓ = decreasing trend.

Figure 4 illustrates the annual and seasonal precipitation variations in the Kathmandu Valley from 1980 to 2022, showing substantial fluctuations over time. The highest annual precipitation was recorded in 2002 (2061.6 mm), while the lowest occurred in 2009 (1155.7 mm). As summarized in Table 3, the mean annual precipitation is 1577.1 mm with a coefficient of variation (CV) of 14.2%, indicating relatively low variability. The standard deviation is 224.7 mm from the mean. Among the seasons, the summer (monsoon) season exhibits the greatest variability in precipitation, with values ranging from 703 mm to 1386.8 mm. Peak summer rainfall occurred in 2002, followed by 1995 (1325 mm) and 2003 (1300 mm). The average precipitation during this season is 1031 mm, with a standard deviation of 166 mm and a CV of 16.1%. The autumn season is the second-largest contributor to annual precipitation, with values ranging between 199.2 mm and 567.8 mm, an average of 275.8 mm, and a standard deviation of 92.9 mm. The highest autumn precipitation occurred in 1985, followed by 2007. Spring precipitation shows an increasing trend, peaking at 368.7 mm in 2002, followed by 350 mm in 2011. The minimum recorded value is 104.5 mm, with an average of 221.8 mm and a standard deviation of 67.9 mm. Winter contributes the least to annual precipitation, with near-zero precipitation in several years. The highest winter precipitation was recorded in 1997 (143.1 mm), highlighting its minimal contribution to the region's overall water availability.

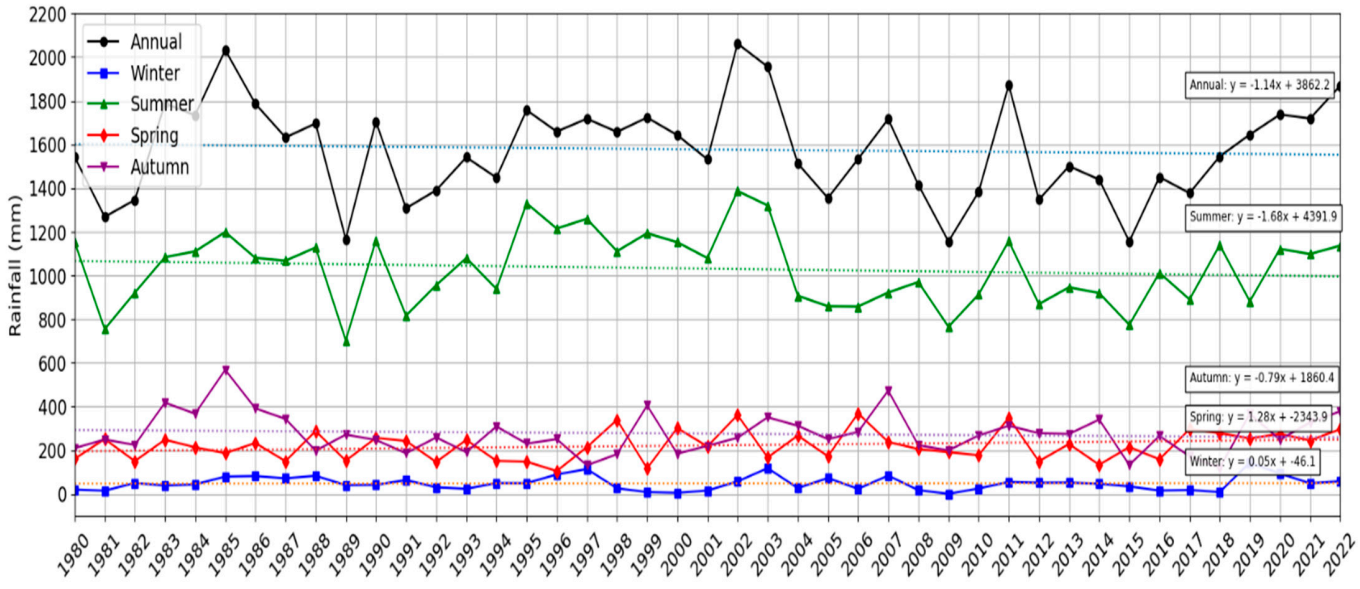

Figure 4. Seasonal and annual precipitation trends in the Kathmandu Valley from 1980 to 2022 with dotted trend line slopes: blue (annual, −1.14), green (summer, −1.68), purple (autumn, −0.79), red (spring, 1.28), and yellow (winter, 0.05) mm/year.

3.3. Temporal Patterns of Extreme Precipitation Indices

Extreme precipitation indices are categorized into various groups, each capturing different characteristics of extreme precipitation events. High-intensity indices include maximum precipitation over specific durations: one day (RX1day), three days (RX3day), five days (RX5day), and seven days (RX7day). Percentile-based indices capture extreme precipitation events based on statistical thresholds, including R95pTOT (precipitation exceeding the 95th percentile) and R99pTOT (precipitation exceeding the 99th percentile). Frequency-based indices measure the number of days with heavy rainfall, including R10mm (days with precipitation $\geq$ 10 mm), R20mm (days with precipitation $\geq$ 20 mm), and R35mm (days with precipitation $\geq$ 35 mm). Dry and wet spell indices quantify the duration of extreme conditions: consecutive dry days (CDDs) reflect extended dry periods (precipitation < 1 mm), while consecutive wet days (CWDs) indicate sustained wet conditions (precipitation > 1 mm). Finally, the Simple Daily Intensity Index (SDII) represents the average precipitation on wet days, thereby providing insights into the overall intensity of precipitation events throughout the year.

3.3.1. High-Intensity Precipitation Indices

Maximum 1-Day (RX1day), 3-Day (RX3day), 5-Day (RX5day), and 7-Day (RX7day) Precipitation

Figure 5 illustrates the temporal patterns of maximum precipitation over different durations—RX1day, RX3day, RX5day, and RX7day—from 1980 to 2022. Each subplot presents observed data along with trend lines for the entire study period (1980–2022) and two sub-periods (1980–2002 and 2003–2022), allowing for a comparative analysis of decadal changes. Over the full period, RX1day, RX3day, and RX5day exhibit no significant increasing or decreasing trend (Table 4), while RX7day shows a slightly increasing trend of 0.1 mm/year. A similar type of fluctuation is seen in the decadal analysis for RX1day, RX3day, and RX5day, but an increasing trend of precipitation in RX7day is significant in both decadal time intervals (Table 5). In 2002, the maximum precipitation values ranged from 178 mm to 346 mm across all indices. RX1day precipitation increased sharply between 1982 and 1987 but declined significantly during 1988–1989. A similar pattern is evident for RX3day, which experienced a slight decline in 1985. RX5day and RX7day increased

between 1982 and 1986, followed by a sharp decline from 1987 to 1999. From 1989 to 2001, all indices experienced considerable interannual fluctuations, peaking in 2002.

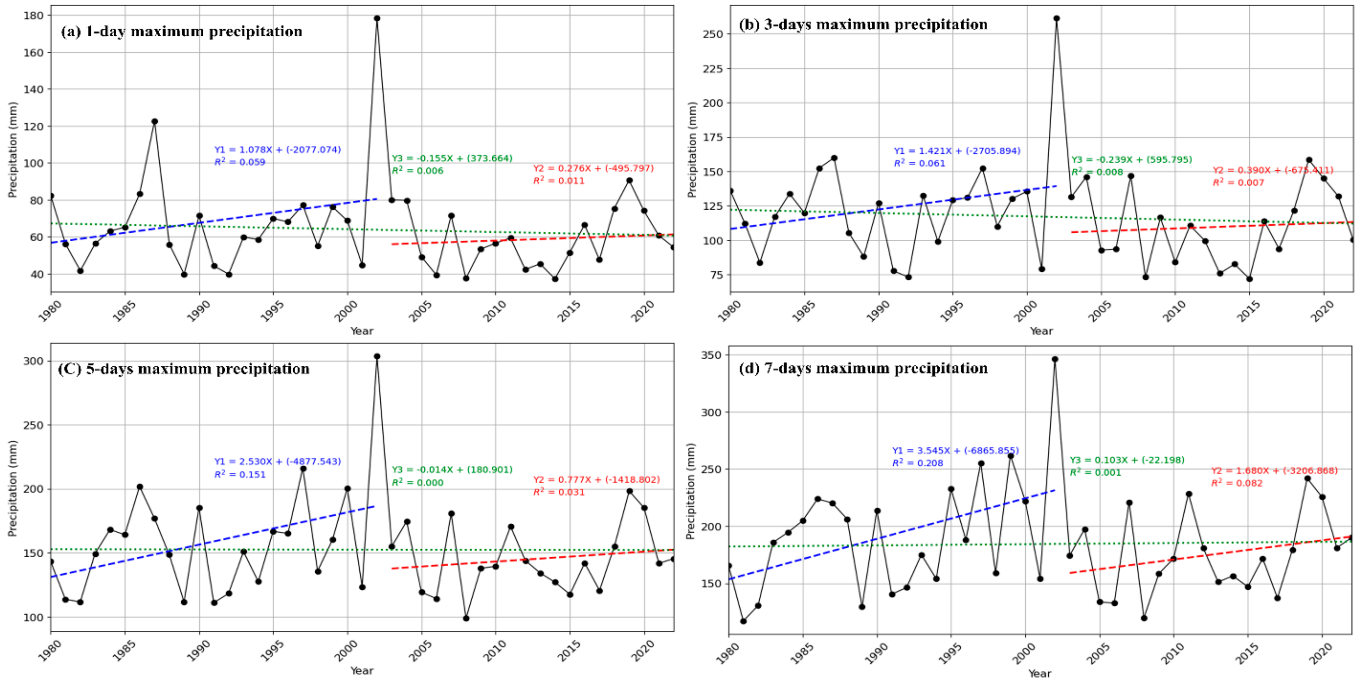

Figure 5. Time series of maximum-intensity precipitation.

Table 4. Results of the Mann–Kendall statistical test for extreme precipitation in the time series (1980–2022).

Precipitation Indices	Mean (mm)	SD (mm)	CV (%)	Mann–Kendall Z-Value	Mann–Kendall *p*-Value	Sen's Slope (mm/year)
RX1day	61.27	17.31	27.92	−0.06	0.60	−0.17
RX3day	113.56	26.16	22.76	−0.08	0.47	−0.26
RX5day	148.73	29.01	19.27	0.01	0.96	−0.04
RX7day	180.45	38.32	20.98	0.05	0.03 *	0.08
R95pTOT	586.83	173.51	29.21	−0.08	0.44	−2.00
R99pTOT	182.63	118.09	63.89	−0.16	0.03 *	−1.96
R10mm	54.74	9.00	16.25	0.03	0.75	−0.03
R20mm	20.45	4.82	23.28	−0.01	0.95	−0.01
R35mm	5.17	2.62	50.14	−0.18	0.05 *	−0.05
CDDs	73.81	24.92	33.36	0.24	0.02 *	0.69
CWDs	41.31	16.10	38.51	0.01	0.90	0.09
PRCPTOT	1550.62	215.38	13.72	−0.05	0.67	−1.12
SDII	10.19	1.08	10.51	−0.17	0.11	−0.02
PCI—autumn	17.72	3.64	20.32	0.04	0.68	0.02
PCI—spring	12.66	3.51	27.38	0.02	0.86	0.01
PCI—summer	9.07	0.66	7.24	−0.01	0.92	0.00
PCI—winter	16.15	5.11	31.28	0.23	0.03 *	0.14
PCI—annual	18.98	1.53	7.95	−0.07	0.50	−0.02

Note: * = statistically significant at 5% significance level.

Table 5. Results of the Mann–Kendall statistical test for extreme precipitation in the time series (1980–2002 and 2003 to 2022).

	1980–2002						2003–2022					
Precipitation Indices	**Mean (mm)**	**SD (mm)**	**CV (%)**	**Mann–Kendall Z-Value**	**Mann–Kendall *p*-Value**	**Sen's Slope (mm/year)**	**Mean (mm)**	**SD (mm)**	**CV (%)**	**Mann–Kendall Z-Value**	**Mann–Kendall *p*-Value**	**Sen's Slope (mm/year)**
RX1day	64.56	18.66	28.20	0.09	0.61	0.31	57.99	15.62	26.28	0.12	0.46	0.49
RX3day	119.21	24.54	20.09	0.08	0.65	0.62	107.91	27.09	24.50	0.13	0.42	0.80
RX5day	153.53	31.63	20.10	0.20	0.22	1.56	143.93	26.01	17.64	0.17	0.29	0.91
RX7day	186.92	41.97	21.91	0.33	0.04 *	3.48	173.97	34.07	19.11	0.24	0.05 *	1.76
R95pTOT	625.16	189.36	29.56	0.14	0.03 *	5.07	548.49	150.91	26.85	0.10	0.57	4.45
R99pTOT	213.62	113.67	51.93	0.08	0.65	2.21	151.64	116.84	75.19	0.04	0.79	−2.5
R10mm	56.10	8.97	15.60	0.20	0.20	0.50	53.38	9.05	16.54	0.18	0.26	0.40
R20mm	21.14	5.34	24.65	0.17	0.29	0.25	19.76	4.25	21.00	0.16	0.33	0.17
R35mm	6.00	2.63	42.72	0.04	0.81	0.00	4.33	2.39	53.92	0.09	0.58	0.00
CDDs	67.52	23.20	33.54	0.27	0.09 **	1.43	80.10	25.53	31.11	0.22	0.04 *	1.00
CWDs	39.90	16.18	39.56	−0.14	0.38	−0.30	42.71	16.30	37.24	−0.02	0.90	0.00
PRCPTOT	1581.39	210.72	13.00	0.07	0.70	2.43	1519.86	220.69	14.17	0.12	0.46	6.17
SDII	10.56	1.20	11.11	0.21	0.20	0.07	9.81	0.82	8.18	−0.08	0.65	−0.02

Note: * = statistically significant at 5% significance level; ** = statistically significant at 10% significance level.

Total Precipitation in R95pTOT and R99pTOT

Figure 6 presents the temporal variation in the total precipitation associated with extreme rainfall days, with subplot (a) representing days exceeding the 95th percentile (R95pTOT) and subplot (b) those exceeding the 99th percentile (R99pTOT), covering the period from 1980 to 2022. Trend lines are included for the entire study period as well as for two decadal intervals to assess long-term and short-term patterns. Over the full study period, both indices exhibit highly fluctuating precipitation, with a decreasing trend of R99pTOT at 1.9 mm/year being significant (Table 4). However, the decadal analysis reveals a more nuanced picture. From 1980 to 2002, R95pTOT shows a trend of precipitation increasing by 5.24 mm/year (Table 5), while for 2003–2022 both indices show highly fluctuating precipitation over the study period. For R95pTOT, the total precipitation increased sharply from 334 mm in 1981 to a peak of 1080 mm in 1985, followed by a rapid decrease to 293 mm in 1989 and 299.9 mm in 1991. The index then fluctuated, reaching a secondary peak of 1017 mm in 2002. After 2002, R95pTOT remained relatively stable, with a slight initial decline until 2005, followed by intermittent fluctuations with 705 mm recorded in 2022. In the case of R99pTOT, precipitation initially declined for three consecutive years before rising from 41.7 mm in 1982 to 357 mm in 1985. Between 1985 and 2001, the values fluctuated significantly, ranging from 40 mm to 382 mm and peaking at 544 mm in 2002. A continuous decline was observed for the next four years, reaching 39 mm in 2006. From 2006 to 2022, the index exhibited extreme variability, fluctuating between 0 mm and 309 mm.

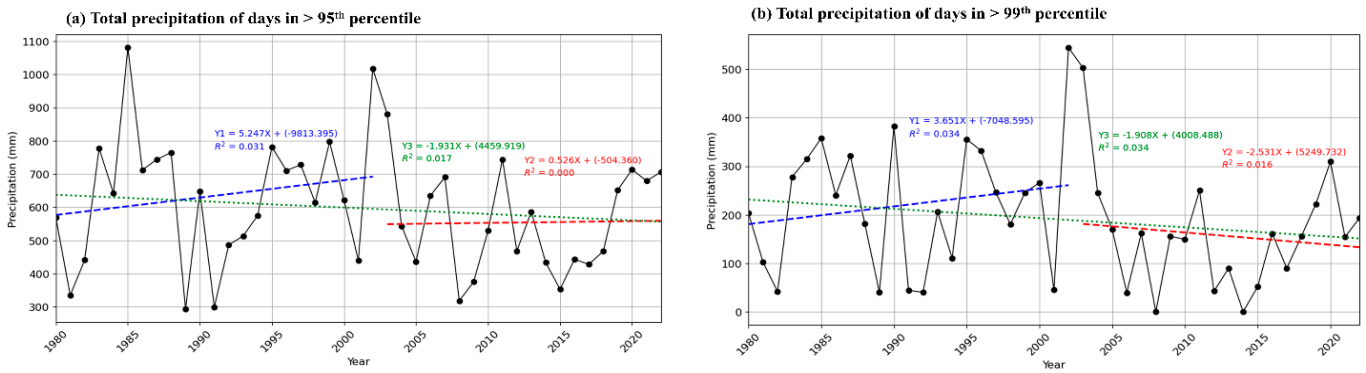

Figure 6. Time series of 95th and 99th percentile precipitation.

3.3.2. Precipitation Days at Different Thresholds

This study evaluates precipitation days based on three intensity thresholds: ≥10 mm (heavy precipitation days), ≥20 mm (very heavy precipitation days), and ≥35 mm (extreme precipitation days), as illustrated in Figure 7. Over the entire study period (1980–2022), the number of precipitation days shows a decreasing trend (−0.05 days/year) for extreme precipitation with precipitation ≥ 35 mm (Table 4), whereas for heavy and very heavy precipitation, an increasing or decreasing trend is not significant. Precipitation days ≥ 10 mm exhibit high interannual variability, increasing steadily through the early 1980s and peaking around 2002, followed by fluctuating patterns in subsequent years. Similarly, precipitation days ≥ 20 mm show pronounced fluctuations, with peaks in 1958 and in 2002, followed by a period of relative stabilization. In contrast, precipitation days ≥ 35 mm remain relatively low throughout the study period in both decadal analyses.

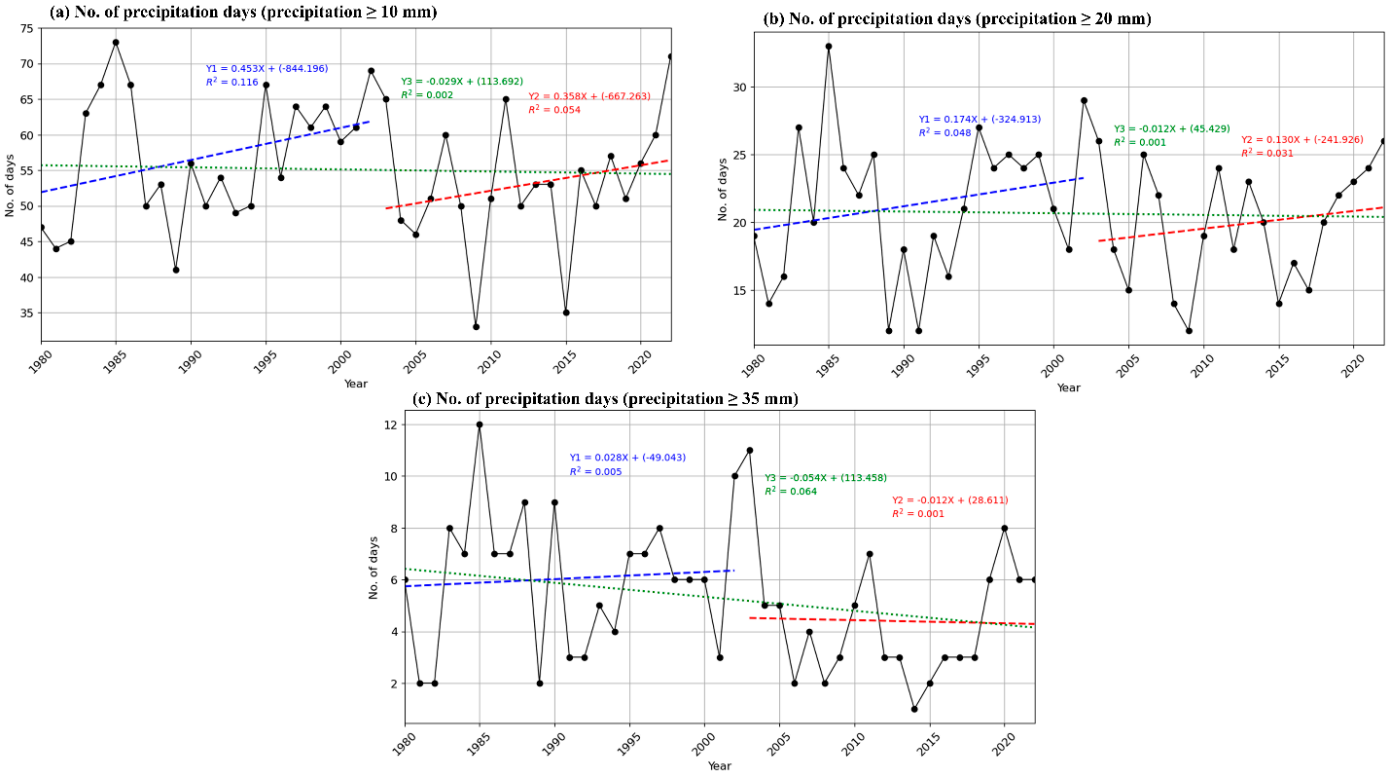

Figure 7. Precipitation days under different precipitation thresholds.

3.3.3. Annual Maximum Consecutive Wet and Dry Days

Figure 8 shows the trends in CWDs and CDDs. As shown in Figure 8a, CWDs display an overall fluctuation with no significant increasing trend. In contrast, Figure 8b shows a more pronounced increasing trend in CDDs at 0.69 days/year, indicating a notable rise in the duration of dry spells over the study period (Table 4). Decadal analysis reveals further details: between 1980 and 2002, consecutive wet days' increased trend is not significant, while consecutive dry days rose more sharply at 1.27 days/year with a 9% significant level with a continue rising trend at 0.708 days/year for 2003–2022 (Table 5) with a 4% significant level. Interannual variability is notable for both indices, with peaks in CWDs observed in the late 1990s and early 2000s, followed by fluctuations in subsequent years. Conversely, CDDs show a more consistent and pronounced upward trend, with peak values occurring more frequently after 2000, indicating an overall increase in prolonged dry periods across the Kathmandu Valley.

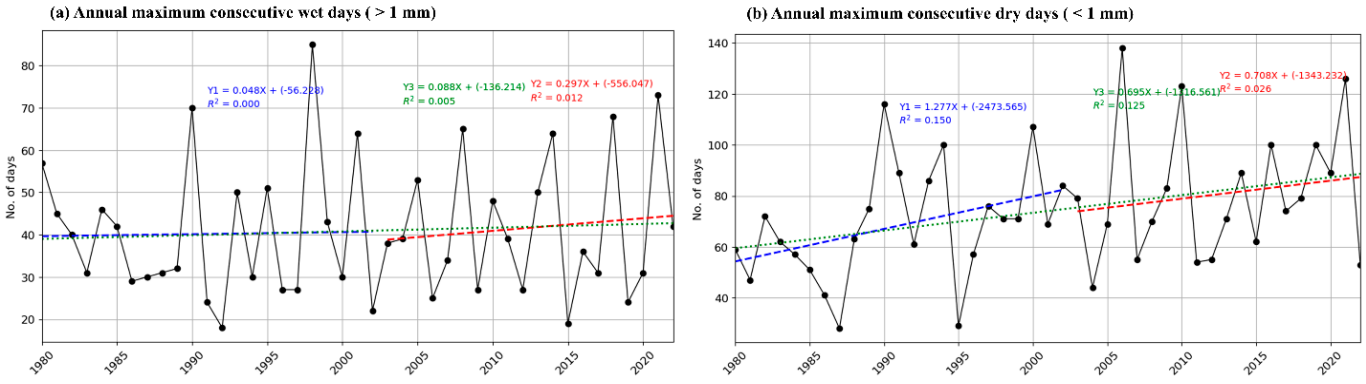

Figure 8. Annual consecutive wet and day days [(**a**) wet days (**b**) dry days].

3.3.4. Average Precipitation on Wet Days

Figure 9 illustrates the temporal variation in the average precipitation on wet days, showing an overall fluctuation over the study period (1980–2022). The decadal analysis also reveals no significant increasing or decreasing trend. Initially, the average precipitation increased from 8.5 mm in 1981 to a peak of 12.9 mm before declining to 8.4 mm in 1989. Following this decline, values fluctuated annually, reaching a maximum of 13 mm in 2002. Thereafter, a continuous decline was observed over the next three years, followed by a period of relative stability. From 2005 to 2022, the average precipitation on wet days remained within the range of 8.5–11.1 mm, with noticeable interannual variability throughout the period.

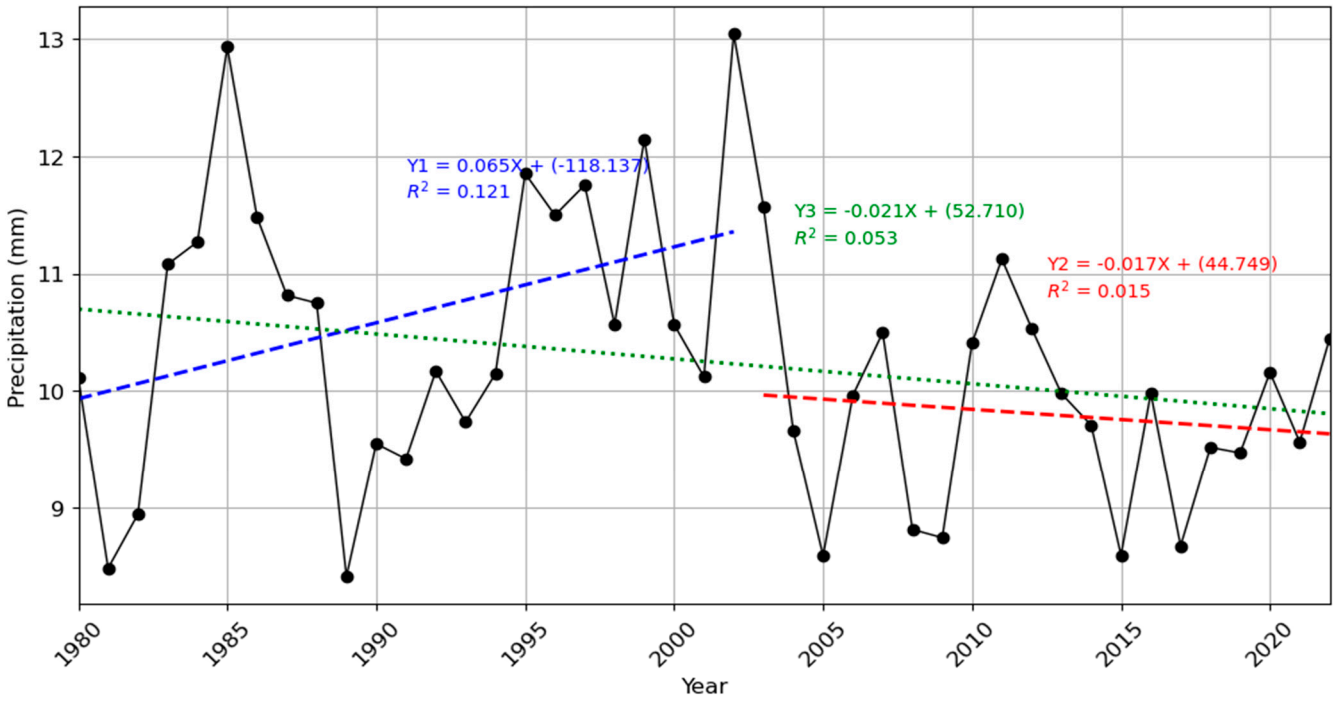

Figure 9. Wet-day average precipitation from 1980 to 2022.

3.4. Precipitation Concentration Index

Figure 10 presents the PCI for the Kathmandu Valley from 1980 to 2022, analyzed on both seasonal and annual scales.

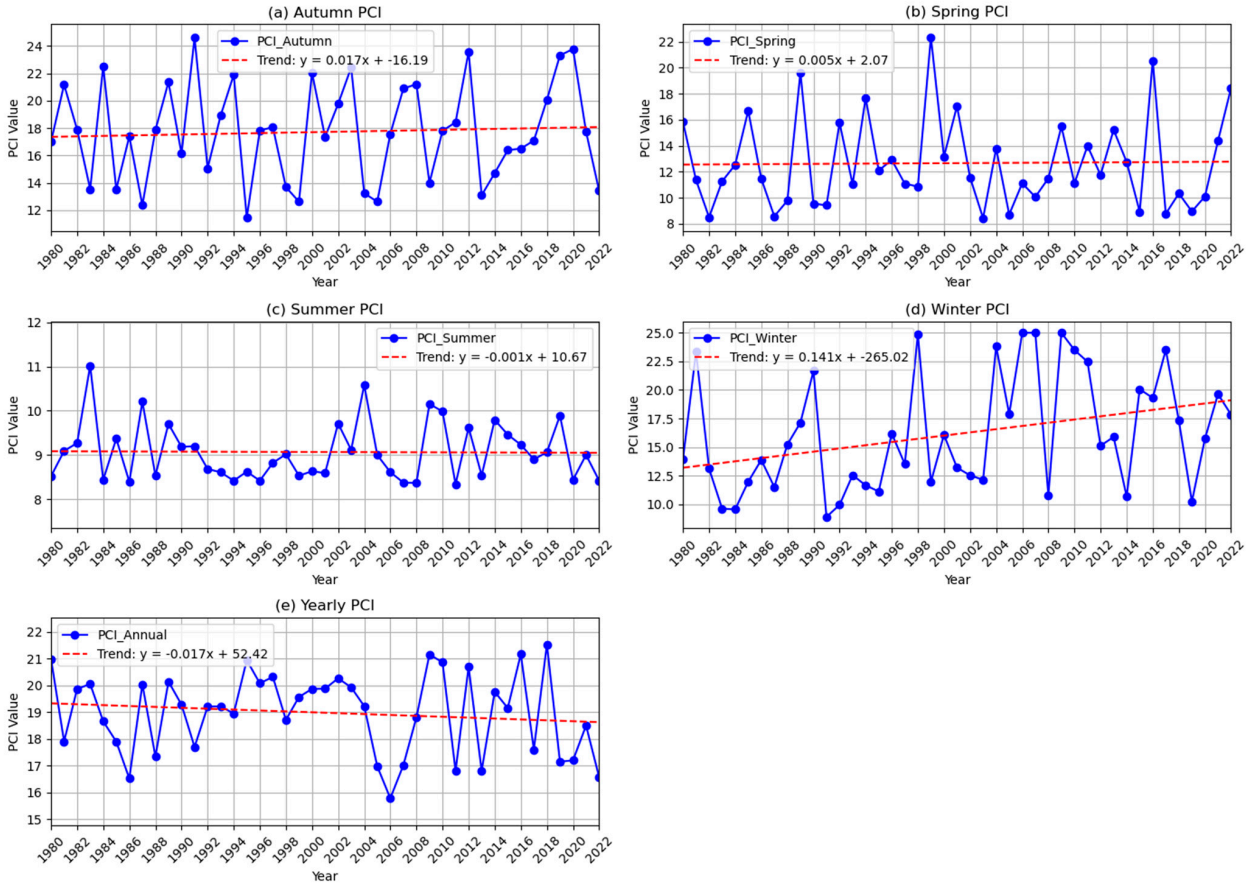

Figure 10. Time series of annual and seasonal precipitation concentration index.

The results show an increasing trend in the PCI during winter at a rate of 1.4 per decade with a 5% significant level (Table 4), whereas for autumn, spring, summer, and annual, there is no significant increasing or decreasing trend that exists. The average PCI values for the annual, autumn, and winter seasons are 18.98, 17.7, and 16.1, respectively, indicating irregular precipitation during these periods. In contrast, the average PCI values for summer and spring are 9 and 12.7, respectively, suggesting uniform and moderately concentrated precipitation during these seasons. In autumn, 17 years fall under the "irregular rainfall" category, while 13 years are classified as "strongly irregular." During spring, most years (22) exhibit moderate rainfall concentrations, with 10 years exhibiting uniform distribution, 9 years classified as irregular, and 2 years classified as very irregular. For winter, 17 years fall into the moderate category, whereas 11 years are strongly irregular, including 3 years in which the PCI exceeded 25—indicating that most precipitation during those years occurred within approximately one-third of the season. Although spring generally maintains a more uniform rainfall distribution over time, the annual PCI analysis reveals that only 6 years experienced strongly irregular precipitation, whereas the remaining years indicate irregular rainfall distribution across the Kathmandu Valley.

3.5. Mann–Kendall Trend Analysis of Extreme Precipitation for 1980–2022 with Decadal Segmentation (1980–2002 and 2003–2022)

Table 4 presents the results of the Mann–Kendall trend analysis for extreme precipitation indices and the PCI. The analysis reveals that the trends for RX7day, R99pTOT, R35mm, and CDDs are statistically significant at the 5% significance level ($p < 0.05$), indicating notable changes in these extreme precipitation characteristics over time. Additionally, the PCI for winter exhibits a significant increasing trend, suggesting a shift toward more uneven precipitation distribution during this season. In contrast, the trends for the remaining

precipitation indices and seasonal/annual PCI are not statistically significant ($p > 0.05$), implying that no consistent long-term trends were detected for these variables during the study period. Similarly, Table 5 depicts the results of the Mann–Kendall statistical test for extreme precipitation indices over the periods 1980–2002 and 2003–2022. The analysis reveals a significant increasing trend in RX7day precipitation, with Sen's slope values of 3.48 for 1980–2002 and 1.76 for 2003–2022, both significant at the 5% level. Additionally, R95pTOT shows a significant upward trend during 1980–2002, with a Sen's slope of 5.07 at the 5% significance level. The results also indicate a significant increase in consecutive dry days (CDDs) for 2003–2022, with a Sen's slope of 1.00 at the 5% level, while a similar increasing trend in CDDs is observed for 1980–2002 with a Sen's slope of 1.43, significant at the 10% level. For the remaining precipitation indices, although some trends are either increasing or decreasing, these are not statistically significant at the 10% level.

3.6. Influence of ENSO on Precipitation

The Niño 3.4 index exhibits both positive and negative correlations with precipitation indices in the Kathmandu Valley, Nepal. A negative correlation indicates that regional precipitation tends to be lower than average during warm anomaly phases in the eastern tropical Pacific (El Niño events). Figure 11 presents the correlation coefficients between various precipitation indices, the PCI, and the Niño 3.4 index, along with their corresponding levels of statistical significance. Total annual precipitation shows a negative correlation of −0.25 with the Niño 3.4 index, which is significant at the 0.1 level. Similarly, the R10mm index demonstrates a stronger negative correlation of −0.35, significant at the 0.05 level, while the R20mm index shows a negative correlation of −0.21, significant at the 0.1 level. The CWDs are also negatively correlated with Niño 3.4 (−0.32), with significance at the 0.05 level. For seasonal variability, the spring PCI exhibits a significant negative correlation of −0.35 with Niño 3.4 at the 0.05 level. In contrast, the annual PCI shows a positive correlation of 0.25, which is significant at the 0.1 level. Additionally, RX1day exhibits a positive correlation of 0.24, which is significant at the 0.1 level.

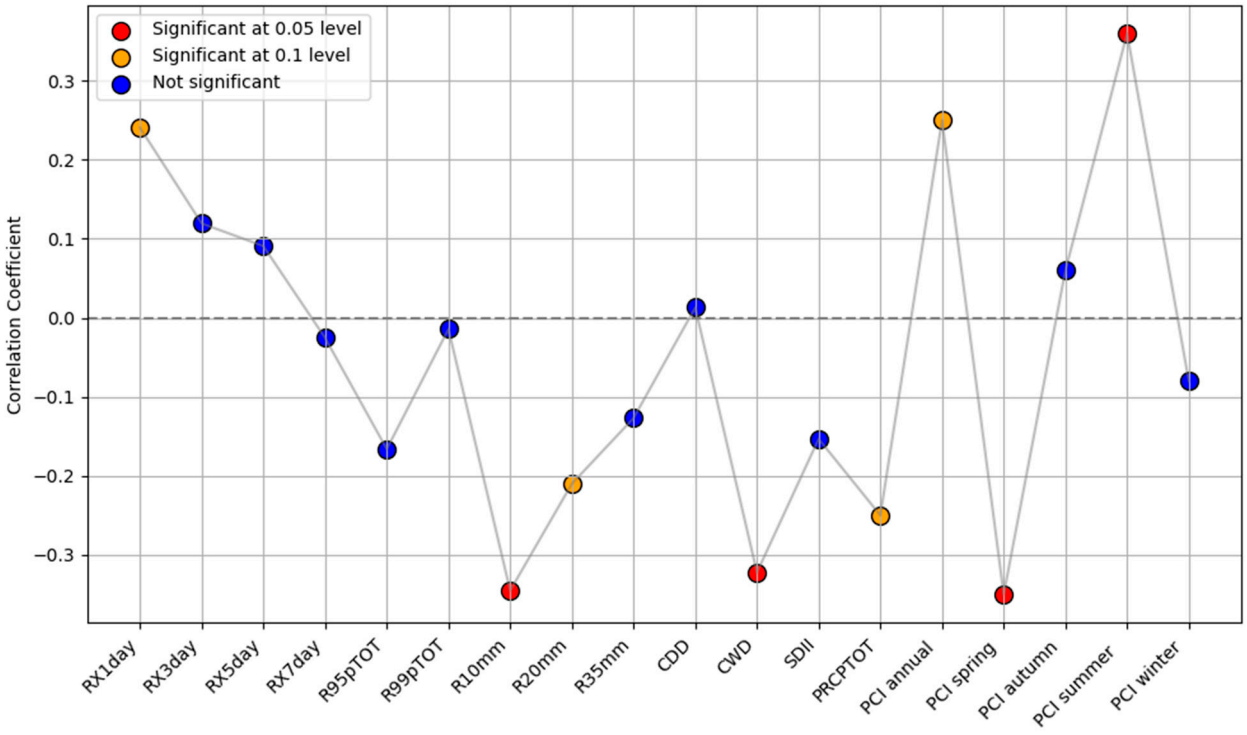

Figure 11. Correlation between the Nino 3.4 index and precipitation indices.

4. Discussion

Rapid urbanization and reduced infiltration areas in the Kathmandu Valley have heightened the impact of even minor precipitation events, resulting in frequent waterlogging and flooding. These occurrences routinely disrupt traffic, affect pedestrians, and cause property damage and loss of life. This study investigated extreme precipitation in terms of intensity, frequency, and variability using a suite of precipitation indices recommended by the WMO and supported by previous research [53–60]. The Mann–Kendall statistical test and Sen's slope estimator were applied to the precipitation data from 1980 to 2022 to assess trends.

Monthly precipitation analysis reveals that most of the annual rainfall is concentrated between June and September, with July (425 mm) and August (375 mm) having the highest totals. This pronounced seasonality is largely driven by the Indian summer monsoon, which transports moisture-laden southeasterly winds from the Bay of Bengal [61]. Long-term precipitation trends indicate a slight decline in winter, summer, autumn, and annual precipitation totals, while spring precipitation exhibits an increasing trend of 1.17 mm/year. Notably, July shows a marginal upward trend of 0.2 mm/year, reinforcing its role as the wettest month and a key contributor to flood risk in the Kathmandu Valley. During the wettest months (July and August), minimum precipitation levels range from 247 mm to 260 mm, while the maximum values range from 567 mm to 621 mm. This wide range significantly increases the potential for flooding. These findings are consistent with those of Prajapati and Talchabhadel et al. (2021) and Dhital and Kayastha (2013) [33,62], who identified July and August as the peak flood months. Similarly, Pradhan-Salike and Raj Pokharel (2017) [63] attributed pluvial flooding in the valley to intense, short-duration rainfall events.

Extreme precipitation analysis from 1980 to 2022 reveals an overall increasing trend in RX7day by 0.1 mm/year. However, the decadal analysis (1980–2001 and 2002–2022) indicates sharp fluctuations in extreme precipitation across the RX1day, RX3days, and RX5days indices with an increasing trend for RX7days precipitation being significant. Similar patterns of fluctuations of precipitation are observed for the percentile-based indices R95pTOT and R99pTOT for decadal analysis, whereas a decreasing trend of R99pTOT is significantly observed for 1980 to 2022. These findings suggest that short-duration precipitation demonstrates inconsistency and long-term precipitation shows a slightly increasing trend, which are both partially contradictory to the findings of Luo et al. (2024) [24], who reported a long-term decline in extreme precipitation with highly fluctuation events over Nepal due to the weakening of the South Asian Monsoon circulation, followed by a post-2003 shift toward increasing extreme precipitation, particularly in western Nepal. This trend aligns with broader regional patterns, including a threefold increase in widespread extreme rainfall events over central India between 1950 and 2015, contributing to more frequent flash floods and significant socioeconomic losses [64]. In 2002, Nepal faced an anomalous monsoon with extreme rainfall in the east and center and drought in the west. On 23 July 2002, Kathmandu recorded its highest 24 h rainfall in 14 years (177.0 mm), with nearby areas like Khokana (300.1 mm) and Thankot (249.2 mm) also experiencing record rain. This caused severe flooding and disruptions in the Kathmandu Valley [65].

In the Kathmandu Valley, the number of precipitation days at all thresholds ($\geq$35 mm) declined between 1980 and 2022. Despite this decline, the RX7day index exhibited an increasing trend, suggesting more intense rainfall events over fewer days—intensifying flood risk. Although consecutive wet days (CDDs) showed a slight increase, the average precipitation on wet days declined, indicating a shift toward more extreme precipitation events without a corresponding increase in total rainfall volume. These trends are further supported by Luo et al. (2024) [24], who observed a decrease in

moderate rainfall days (R10 mm, R20 mm) and increased extreme precipitation variability. The severe flooding events of September 2024, which brought 239.7 mm of rainfall in just 24 h and resulted in over 200 fatalities and widespread displacement [66], underscore the urgent need for adaptive infrastructure and enhanced disaster preparedness strategies in the Kathmandu Valley.

The PCI analysis reveals an annual PCI value of 18.9, indicating an overall irregular precipitation distribution. This finding aligns with the results of Lamichhane et al. (2024) [4], who reported PCI values across Nepal ranging from 14.06 (moderate) to 25.34 (strongly irregular), with increasing precipitation irregularity particularly evident in lowland regions. While their national analysis identified an increasing PCI trend of 0.53 per decade, the Kathmandu Valley exhibited an increasing trend of the PCI by 1.4 per decade in the winter season. A similar type of increasing PCI value has been observed in China [67] and India [68], where precipitation irregularity has been attributed to climate variability and shifts in monsoon dynamics. Similarly, Rahman and Islam (2019) [69] reported PCI values ranging from 0.57 to 0.632 in Bangladesh, indicating slightly higher precipitation variability than in Nepal.

The influence of ENSO on precipitation patterns across the Asia–Pacific region, including Nepal, is well established [2,70–73]. Several studies [4,74,75] confirm that during El Niño events, the westward shift of the Pacific warm pool toward the central and eastern Pacific results in the weakening of the Walker circulation and trade winds, along with reduced oceanic upwelling. These processes amplify positive SST anomalies in the eastern Pacific, disrupt global precipitation patterns, and weaken the summer monsoon. Concurrently, the western Pacific cools due to diminished convection, while the Indian Ocean warms as a delayed response through atmospheric teleconnections—independent of the Indian Ocean Dipole (IOD) [40]. In this study, annual precipitation, extreme precipitation indices, and overall precipitation variability in the Kathmandu Valley were negatively correlated with the Niño 3.4 index, consistent with the findings of Lamichhane et al. (2024) [4,24] and Luo et al. (2024) [4,24]. However, positive correlations were observed for the annual PCI (0.25), the summer PCI (0.36), and 1-day maximum precipitation (RX1day, 0.24), suggesting that ENSO influences not only the total precipitation amounts but also the temporal concentration and the occurrence of high-intensity, short-duration events.

5. Conclusions

This study investigates precipitation patterns in the Kathmandu Valley using observed data from 1980 to 2022, with a focus on trends in precipitation intensity, frequency, and concentration at both annual and seasonal scales. By applying the PCI and a set of extreme precipitation indices, this study also assesses the influence of the El Niño–Southern Oscillation (ENSO) on extreme precipitation events in the region.

The results indicate a slight overall increase in long-term precipitation across the Kathmandu Valley with inconsistent short-term precipitation. The spring precipitation exhibits an increasing trend of 1.17 mm per year, with November and December exhibiting an upward trend. The remaining months and seasons show high-fluctuation short-term precipitation contributing to heightened flood risks. The analysis of extreme precipitation indices reveals sharp inconsistency in RX1day, RX3day, and RX5day from 1980 to 2022, while RX7day exhibits a slight increase of 0.1 mm/year. Similarly, decadal analysis reveals a fluctuation trend across all extreme precipitation indices, including R95pTOT, which emphasizes the growing risk of pluvial and fluvial flooding in the valley. The annual precipitation patterns in the Kathmandu Valley are highly irregular, particularly during autumn and winter, whereas summer precipitation remains relatively evenly distributed. ENSO analysis indicates a negative correlation with annual precipitation, extreme precipitation

indices, and overall precipitation variability, while showing a positive correlation with the annual and summer PCI and 1-day maximum precipitation (RX1day). ENSO analysis indicates a negative correlation with annual precipitation, extreme precipitation indices, and overall precipitation variability, while showing a positive correlation with the annual and summer PCI and 1-day maximum precipitation (RX1day). Although some of these correlations are statistically significant, they align with established climatic mechanisms. Previous studies demonstrate that El Niño events typically weaken monsoon circulation and reduce moisture transport across Nepal, leading to below-normal rainfall [4,24]. In contrast, La Niña phases enhance moisture influx, often resulting in above-normal rainfall. These mechanisms support the observed variability in precipitation patterns in the Kathmandu Valley, though the influence of ENSO is controlled by local topography and regional atmospheric conditions.

Although this study is limited to a single geographic region with a restricted number of observation stations, its findings are applicable to other areas with similar topographic and climatic conditions throughout the Himalayan region. Future research should incorporate additional climatic variables—such as temperature, humidity, and wind speed—alongside global climate model (GCM) data to improve projections of future precipitation trends and their hydrological implications.

Author Contributions: D.C.: methodology, software, conceptualization, data curation, formal analysis, investigation, writing the original draft. R.L.R.: conceptualization, review and editing. A.O.Y.: writing. N.N.S.: editing. J.P.: analysis. A.F.T.: data collection. J.W.R.: software. D.S.: software. J.-O.L.: review. J.-S.H.: supervision, funding acquisition. All authors have read and agreed to the published version of the manuscript.

Funding: This work was supported by the National Research Foundation of Korea (NRF) grant funded by the Korea government (MSIT) (No. RS-2021-NR060108) and supported by the Korea Institute of Energy Technology Evaluation and Planning (KETEP) and the Ministry of Trade, Industry & Energy (MOTIE) of the Republic of Korea (No. RS-2022-KP002719).

Data Availability Statement: The original contributions presented in this study are included in the article. Further inquiries can be directed to the corresponding author.

Conflicts of Interest: The authors declare that they have no known competing financial interests or personal relationships that could have appeared to influence the work reported in this paper.

References

1. Summary for Policymakers. In *Climate Change 2022—Impacts, Adaptation and Vulnerability*; Cambridge University Press: Cambridge, UK, 2023; pp. 3–34. [CrossRef]
2. An, D.; Eggeling, J.; Zhang, L.; He, H.; Sapkota, A.; Wang, Y.-C.; Gao, C. Extreme precipitation patterns in the Asia–Pacific region and its correlation with El Niño-Southern Oscillation (ENSO). *Sci. Rep.* **2023**, *13*, 11068. [CrossRef] [PubMed]
3. Sun, G.; Tiwari, K.R.; Hao, L.; Amatya, D.; Liu, N.; Song, C. Climate change and forest hydrology in future forests. In *Future Forests: Mitigation and Adaptation to Climate Change*; Elsevier: Amsterdam, The Netherlands, 2024; pp. 95–124. [CrossRef]
4. Lamichhane, D.; Bao, Q.; Dhital, Y.P.; Devkota, R.; Bhattarai, U.; Nepal, B.; Pokharel, A.K.; Dawadi, B. Precipitation Concentration Variability and Its Association with Geographical Factors and ENSO Over Nepal from 1990 to 2020. *Earth Syst. Environ.* **2024**, *8*, 1–17. [CrossRef]
5. Karki, R.; Hasson, S.U.; Schickhoff, U.; Scholten, T.; Böhner, J. Rising Precipitation Extremes across Nepal. *Climate* **2017**, *5*, 4. [CrossRef]
6. Pandey, V.P.; Shrestha, D.; Adhikari, M. Characterizing natural drivers of water-induced disasters in a rain-fed watershed: Hydro-climatic extremes in the Extended East Rapti Watershed. *J. Hydrol.* **2021**, *598*, 126383. [CrossRef]
7. Sun, Q.; Zhang, X.; Zwiers, F.; Westra, S.; Alexander, L.V. A Global, Continental, and Regional Analysis of Changes in Extreme Precipitation. *J. Clim.* **2021**, *34*, 243–258. [CrossRef]
8. Donat, M.G.; Lowry, A.L.; Alexander, L.V.; O'Gorman, P.A.; Maher, N. Addendum: More extreme precipitation in the world's dry and wet regions. *Nat. Clim. Change* **2016**, *6*, 508–513. [CrossRef]

9. Papalexiou, S.M.; Montanari, A. Global and Regional Increase of Precipitation Extremes Under Global Warming. *Water Resour. Res.* **2019**, *55*, 4901–4914. [CrossRef]
10. Safdar, F.; Mahmood, F.; Khan, M.Z.A.; Arshad, M. Observed and predicted precipitation variability across Pakistan with special focus on winter and pre-monsoon precipitation. *Environ. Sci. Pollut. Res.* **2023**, *30*, 4510–4530. [CrossRef] [PubMed]
11. Aditya, F.; Gusmayanti, E.; Sudrajat, J. Rainfall trend analysis using Mann-Kendall and Sen's slope estimator test in West Kalimantan. *IOP Conf. Ser. Earth Environ. Sci.* **2021**, *893*, 012006. [CrossRef]
12. Rahaman, M.H.; Saha, T.K.; Masroor, M.; Roshani; Sajjad, H. Trend analysis and forecasting of meteorological variables in the lower Thoubal river watershed, India using non-parametrical approach and machine learning models. *Model Earth Syst. Environ.* **2024**, *10*, 551–577. [CrossRef]
13. Maharana, P.; Agnihotri, R.; Dimri, A.P. Changing Indian monsoon rainfall patterns under the recent warming period 2001–2018. *Clim. Dyn.* **2021**, *57*, 2581–2593. [CrossRef]
14. Jihan, M.A.T.; Popy, S.; Kayes, S.; Rasul, G.; Maowa, A.S.; Rahman, M. Climate change scenario in Bangladesh: Historical data analysis and future projection based on CMIP6 model. *Sci. Rep.* **2025**, *15*, 7856. [CrossRef] [PubMed]
15. Subba, S.; Ma, Y.-M.; Ma, W.-Q.; Han, C.-B. Extreme precipitation detection ability of four high-resolution precipitation product datasets in hilly area: A case study in Nepal. *Adv. Clim. Change Res.* **2024**, *15*, 390–405. [CrossRef]
16. Bell, R.; Fort, M.; Götz, J.; Bernsteiner, H.; Andermann, C.; Etzlstorfer, J.; Posch, E.; Gurung, N.; Gurung, S. Major geomorphic events and natural hazards during monsoonal precipitation 2018 in the Kali Gandaki Valley. *Geomorphology* **2021**, *372*, 107451. [CrossRef]
17. Fernando, N.S.; Shrestha, S.; Saurav, K.; Mohanasundaram, S. Investigating major causes of extreme floods using global datasets: A case of Nepal. *Prog. Disaster Sci.* **2022**, *13*, 100212. [CrossRef]
18. Khatri, S.K.; Hamal, R.; Poudel, K.R.; Poudel, K.P.; Paudel, N. Rainfall patterns and hazard susceptibility analysis of Pokhara City, Nepal: Implication of climate change. *Theor. Appl. Climatol.* **2025**, *156*, 146. [CrossRef]
19. Chhetri, T.B.; Dhital, Y.P.; Tandong, Y.; Devkota, L.P.; Dawadi, B. Observations of heavy rainfall and extreme flood events over Banke-Bardiya districts of Nepal in 2016–2017. *Prog. Disaster Sci.* **2020**, *6*, 100074. [CrossRef]
20. Adhikari, N.; Gao, J.; Yao, T.; Yang, Y.; Dai, D. The main controls of the precipitation stable isotopes at Kathmandu. *Tellus B Chem. Phys. Meteorol.* **2020**, *72*, 1721967. [CrossRef]
21. Shrestha, S.; Yao, T.; Kattel, D.B.; Devkota, L.P. Precipitation characteristics of two complex mountain river basins on the southern slopes of the central Himalayas. *Theor. Appl. Clim.* **2019**, *138*, 1159–1178. [CrossRef]
22. Karki, R.; Talchabhadel, R.; Aalto, J.; Baidya, S.K. New climatic classification of Nepal. *Theor. Appl. Clim.* **2015**, *125*, 799–808. [CrossRef]
23. Shrestha, S.; Yao, T.; Adhikari, T.R. Analysis of rainfall trends of two complex mountain river basins on the southern slopes of the Central Himalayas. *Atmos. Res.* **2019**, *215*, 99–115. [CrossRef]
24. Luo, Y.; Wang, L.; Hu, C.; Hao, L.; Sun, G. Changing Extreme Precipitation Patterns in Nepal Over 1971–2015. *Earth Space Sci.* **2024**, *11*, e2024EA003563. [CrossRef]
25. Shrestha, M.; Acharya, S.C. Assessment of historical and future land-use–land-cover changes and their impact on valuation of ecosystem services in Kathmandu Valley. *Land Degrad. Dev.* **2020**, *32*, 3731–3742. [CrossRef]
26. Chaudhary, U.; Shah, M.A.R.; Shakya, B.M.; Aryal, A. Flood Susceptibility and Risk Mapping of Kathmandu Valley Watershed. *Sustainability* **2024**, *16*, 7101. [CrossRef]
27. Danegulu, A.; Karki, S.; Bhattarai, P.K.; Pandey, V.P. Characterizing urban flooding in the Kathmandu Valley, Nepal: The influence of urbanization and river encroachment. *Nat. Hazards* **2024**, *120*, 10923–10947. [CrossRef]
28. Magar, B.G.; Poudel, J.M.; Paudel, B.; Pokharel, B. Climate change in outskirts of Kathmandu Valley: Local perception and narratives. *Nat. Hazards* **2024**, *120*, 8103–8120. [CrossRef]
29. Kc, S.; Shrestha, S.; Ninsawat, S.; Chonwattana, S. Predicting flood events in Kathmandu Metropolitan City under climate change and urbanisation. *J. Environ. Manag.* **2021**, *281*, 111894. [CrossRef]
30. Mesta, C.; Cremen, G.; Galasso, C. Urban growth modelling and social vulnerability assessment for a hazardous Kathmandu Valley. *Sci. Rep.* **2022**, *12*, 6152. [CrossRef]
31. Prajapati, R.; Upadhyay, S.; Talchabhadel, R.; Thapa, B.R.; Ertis, B.; Silwal, P.; Davids, J.C. Investigating the nexus of groundwater levels, rainfall and land-use in the Kathmandu Valley, Nepal. *Groundw. Sustain. Dev.* **2021**, *14*, 100584. [CrossRef]
32. Shrestha, D.; Basnyat, D.B.; Gyawali, J.; Creed, M.J.; Sinclair, H.D.; Golding, B.; Muthusamy, M.; Shrestha, S.; Watson, C.S.; Subedi, D.L.; et al. Rainfall extremes under future climate change with implications for urban flood risk in Kathmandu. *Int. J. Disaster Risk Reduct.* **2023**, *97*, 103997. [CrossRef]
33. Prajapati, R.; Talchabhadel, R.; Silwal, P.; Upadhyay, S.; Ertis, B.; Thapa, B.R.; Davids, J.C. Less rain and rainy days—Lessons from 45 years of rainfall data (1971–2015) in the Kathmandu Valley, Nepal. *Theor. Appl. Climatol.* **2021**, *145*, 1369–1383. [CrossRef]
34. Shrestha, S.; Semkuyu, D.J.; Pandey, V.P. Assessment of groundwater vulnerability and risk to pollution in Kathmandu Valley. *Sci. Total. Environ.* **2016**, *556*, 23–35. [CrossRef]

35. Bharti, P.; Biswas, A. Predicting Urban Growth of Kathmandu Valley Using Artificial Intelligence. *J. Geovisualization Spat. Anal.* **2024**, *8*, 40. [CrossRef]
36. Shrestha, S.; Neupane, S.; Mohanasundaram, S.; Pandey, V.P. Mapping groundwater resiliency under climate change scenarios: A case study of Kathmandu Valley. *Environ. Res.* **2020**, *183*, 109149. [CrossRef]
37. DHM. Available online: https://www.dhm.gov.np/ (accessed on 4 March 2025).
38. Ridwan, W.M.; Sapitang, M.; Aziz, A.; Kushiar, K.F.; Ahmed, A.N.; El-Shafie, A. Rainfall forecasting model using machine learning methods: Case study Terengganu. *Ain Shams Eng. J.* **2021**, *12*, 1651–1663. [CrossRef]
39. Climate Prediction Center—Monitoring & Data: Current Monthly Atmospheric and Sea Surface Temperatures Index Values. Available online: https://www.cpc.ncep.noaa.gov/data/indices/ (accessed on 4 March 2025).
40. Ehsan, M.A.; Tippett, M.K.; Robertson, A.W.; Singh, B.; Rahman, M.A. The ENSO Fingerprint on Bangladesh Summer Monsoon Rainfall. *Earth Syst. Environ.* **2023**, *7*, 617–627. [CrossRef]
41. Lenssen, N.J.L.; Goddard, L.; Mason, S. Seasonal Forecast Skill of ENSO Teleconnection Maps. *Weather. Forecast.* **2020**, *35*, 2387–2406. [CrossRef]
42. Sahoo, M.; Yadav, R.K. Teleconnection of Atlantic Nino with summer monsoon rainfall over northeast India. *Glob. Planet. Change* **2021**, *203*, 103550. [CrossRef]
43. Yang, Y.-M.; Park, J.-H.; An, S.-I.; Wang, B.; Luo, X. Mean sea surface temperature changes influence ENSO-related precipitation changes in the mid-latitudes. *Nat. Commun.* **2021**, *12*, 1495. [CrossRef]
44. Mann, H.B. Nonparametric Tests Against Trend. 1945. Available online: https://www.jstor.org/stable/1907187 (accessed on 1 January 2025).
45. Ahmed, I.A.; Shahfahad; Dutta, D.K.; Baig, M.R.I.; Roy, S.S.; Rahman, A. Implications of changes in temperature and precipitation on the discharge of Brahmaputra River in the urban watershed of Guwahati. *Environ. Monit. Assess.* **2021**, *193*, 518. [CrossRef]
46. Obuobie, E.; Osei, M.A.; Addi, M.; Agyekum, J.; Akurugu, B.A.; Bazaanah, P.; Gaisie-Essilfie, F.A.; Appiah, G. Analysis of spatio-temporal trends in climate extremes in the Lower Volta Basin. *Theor. Appl. Clim.* **2025**, *156*, 120. [CrossRef]
47. Zhang, X.; Alexander, L.; Hegerl, G.C.; Jones, P.; Tank, A.K.; Peterson, T.C.; Trewin, B.; Zwiers, F.W. Indices for monitoring changes in extremes based on daily temperature and precipitation data. *Wires Clim. Change* **2011**, *2*, 851–870. [CrossRef]
48. Oliver, J.E. Monthly Precipitation Distribution: A Comparative Index. *Prof. Geogr.* **1980**, *32*, 300–309. [CrossRef]
49. Bandar, Q.K.A.; Muslih, K.D. Spatial assessment of precipitation concentration and seasonality in Iraq. *Theor. Appl. Clim.* **2025**, *156*, 134. [CrossRef]
50. Du, J.; Yu, X.; Zhou, L.; Li, X.; Ao, T. Less concentrated precipitation and more extreme events over the Three River Headwaters region of the Tibetan Plateau in a warming climate. *Atmospheric Res.* **2024**, *303*, 107311. [CrossRef]
51. Bhattacharyya, S.; Sreekesh, S. Assessments of multiple gridded-rainfall datasets for characterizing the precipitation concentration index and its trends in India. *Int. J. Clim.* **2021**, *42*, 3147–3172. [CrossRef]
52. Tolika, K. On the analysis of the temporal precipitation distribution over Greece using the Precipitation Concentration Index (PCI): Annual, seasonal, monthly analysis and association with the atmospheric circulation. *Theor. Appl. Climatol.* **2019**, *137*, 2303–2319. [CrossRef]
53. Amiri, M.A.; Gocić, M. Analyzing the applicability of some precipitation concentration indices over Serbia. *Theor. Appl. Clim.* **2021**, *146*, 645–656. [CrossRef]
54. Balling, R.C.; Kiany, M.S.K.; Roy, S.S.; Khoshhal, J. Trends in Extreme Precipitation Indices in Iran: 1951–2007. *Adv. Meteorol.* **2016**, *2016*, 2456809. [CrossRef]
55. De Lima, M.I.P.; Santo, F.E.; Ramos, A.M.; Trigo, R.M. Trends and correlations in annual extreme precipitation indices for mainland Portugal, 1941–2007. *Theor. Appl. Climatol.* **2015**, *119*, 55–75. [CrossRef]
56. Gocic, M.; Shamshirband, S.; Razak, Z.; Petković, D.; Ch, S.; Trajkovic, S. Long-Term Precipitation Analysis and Estimation of Precipitation Concentration Index Using Three Support Vector Machine Methods. *Adv. Meteorol.* **2016**, *2016*, 7912357. [CrossRef]
57. Michiels, P.; Gabriels, D.; Hartmann, R. Using the seasonal and temporal Precipitation concentration index for characterizing the monthly rainfall distribution in Spain. *CATENA* **1992**, *19*, 43–58. [CrossRef]
58. Petković, D.; Gocic, M.; Trajkovic, S.; Milovančević, M.; Šević, D. Precipitation concentration index management by adaptive neuro-fuzzy methodology. *Clim. Change* **2017**, *141*, 655–669. [CrossRef]
59. Ryan, C.; Curley, M.; Walsh, S.; Murphy, C. Long-term trends in extreme precipitation indices in Ireland. *Int. J. Clim.* **2021**, *42*, 4040–4061. [CrossRef]
60. Sarr, M.A.; Zoromé, M.; Seidou, O.; Bryant, C.R.; Gachon, P. Recent trends in selected extreme precipitation indices in Senegal—A changepoint approach. *J. Hydrol.* **2013**, *505*, 326–334. [CrossRef]
61. Chhetri, R.; Pandey, V.P.; Talchabhadel, R.; Thapa, B.R. How do CMIP6 models project changes in precipitation extremes over seasons and locations across the mid hills of Nepal? *Theor. Appl. Clim.* **2021**, *145*, 1127–1144. [CrossRef]
62. Dhital, Y.; Kayastha, R. causes and impacts of flooding in the Bagmati River Basin. *J. Flood Risk Manag.* **2013**, *6*, 253–260. [CrossRef]

63. Pradhan-Salike, I.; Pokharel, J.R. Impact of Urbanization and Climate Change on Urban Flooding: A case of the Kathmandu Valley. *J. Nat. Resour. Dev.* **2017**, *7*, 56–66. [CrossRef]
64. Roxy, M.K.; Ghosh, S.; Pathak, A.; Athulya, R.; Mujumdar, M.; Murtugudde, R.; Terray, P.; Rajeevan, M. A threefold rise in widespread extreme rain events over central India. *Nat. Commun.* **2017**, *8*, 708. [CrossRef]
65. Society of Hydrologists and Meteorologists-Nepal. SOHAM_Newsletter_Vol-1_-No-1_October-Novermber-2002. Available online: https://soham.org.np/newsletter/soham-nepal-newsletter-8/ (accessed on 1 January 2025).
66. Durbar, S. A Preliminary Loss and Damage Assessment of Flood and Landslide National Disaster Risk Reduction and Management Authority Preliminary Loss and Damage Assessment of Flood and Landslide September 2024 Published by Government of Nepal Ministry of Home Affairs National Disaster Risk Reduction and Management Authority. 2024. Available online: www.bipad.gov.np (accessed on 12 March 2025).
67. Guo, E.; Wang, Y.; Jirigala, B.; Jin, E. Spatiotemporal variations of precipitation concentration and their potential links to drought in mainland China. *J. Clean. Prod.* **2020**, *267*, 122004. [CrossRef]
68. Nandargi, S.S.; Aman, K. Precipitation concentration changes over India during 1951 to 2015. *Sci. Res. Essays* **2018**, *13*, 14–26. [CrossRef]
69. Rahman, S.; Islam, A.R.M.T. Are precipitation concentration and intensity changing in Bangladesh overtimes? Analysis of the possible causes of changes in precipitation systems. *Sci. Total. Environ.* **2019**, *690*, 370–387. [CrossRef] [PubMed]
70. Rashid, I.U.; Abid, M.A.; Almazroui, M.; Kucharski, F.; Hanif, M.; Ali, S.; Ismail, M. Early summer surface air temperature variability over Pakistan and the role of El Niño–Southern Oscillation teleconnections. *Int. J. Clim.* **2022**, *42*, 5768–5784. [CrossRef]
71. Shrestha, A.; Kostaschuk, R. El Niño/Southern Oscillation (ENSO)-related variablity in mean-monthly streamflow in Nepal. *J. Hydrol.* **2005**, *308*, 33–49. [CrossRef]
72. Kadel, I.; Yamazaki, T.; Iwasaki, T.; Abdillah, M.R. Projection of future monsoon precipitation over the central Himalayas by CMIP5 models under warming scenarios. *Clim. Res.* **2018**, *75*, 1–21. [CrossRef]
73. Xu, Z.X.; Takeuchi, K.; Ishidaira, H. Correlation between El Niño-Southern Oscillation (ENSO) and precipitation in South-east Asia and the Pacific region. *Hydrol. Process.* **2003**, *18*, 107–123. [CrossRef]
74. Izumo, T.; Lengaigne, M.; Vialard, J.; Luo, J.-J.; Yamagata, T.; Madec, G. Influence of Indian Ocean Dipole and Pacific recharge on following year's El Niño: Interdecadal robustness. *Clim. Dyn.* **2013**, *42*, 291–310. [CrossRef]
75. Leupold, M.; Pfeiffer, M.; Watanabe, T.K.; Reuning, L.; Garbe-Schönberg, D.; Shen, C.-C.; Brummer, G.-J.A. El Niño-Southern Oscillation and internal sea surface temperature variability in the tropical Indian Ocean since 1675. *Clim. Past* **2021**, *17*, 151–170. [CrossRef]

frontiers | Frontiers in Environmental Science

TYPE Policy and Practice Reviews
PUBLISHED 19 January 2023
DOI 10.3389/fenvs.2023.1089391

OPEN ACCESS

EDITED BY
Maria Alzira Pimenta Dinis,
Fernando Pessoa University, Portugal

REVIEWED BY
Diogo Guedes Vidal,
University of Coimbra, Portugal
Hamisai Hamandawana,
National Research Council (CNR), Italy

*CORRESPONDENCE
Jeung-Soo Huh,
jshuh@knu.ac.kr
Benyoh Emmanuel Kigha Nsafon,
luxnsafon@yahoo.ca

SPECIALTY SECTION
This article was submitted to Environmental Economics and Management, a section of the journal Frontiers in Environmental Science

RECEIVED 04 November 2022
ACCEPTED 09 January 2023
PUBLISHED 19 January 2023

CITATION
Nsafon BEK, Same NN, Yakub AO, Chaulagain D, Kumar NM and Huh J-S (2023), The justice and policy implications of clean energy transition in Africa. *Front. Environ. Sci.* 11:1089391. doi: 10.3389/fenvs.2023.1089391

The justice and policy implications of clean energy transition in Africa

Benyoh Emmanuel Kigha Nsafon[1,2]*, Noel Ngando Same[1,3], Abdulfatai Olatunji Yakub[1,3], Deepak Chaulagain[1,3], Nallapaneni Manoj Kumar[4,5] and Jeung-Soo Huh[1,2,3]*

[1]Institute for Global Climate Change and Energy, Kyungpook National University, Daegu, South Korea, [2]Department of Energy Convergence and Climate Change, Graduate School, Kyungpook National University, Daegu, South Korea, [3]Department of Convergence and Fusion System Engineering, Graduate School, Kyungpook National University, Daegu, South Korea, [4]School of Energy and Environment, City University of Hong Kong, Kowloon, Hong Kong SAR, China, [5]Center for Circular Supplies, HICCER—Hariterde International Council of Circular Economy Research, Palakkad, Kerala, India

Despite the low local energy access rates, Africa is considered a key player in the global energy transition due to its large supply of fossil fuels and a large reserve of critical minerals essential for manufacturing renewable energy components in the energy sector and storage devices in the transportation and electronics sectors. But building a sustainable society at all levels across nations would only come when there exists a just and inclusive energy transition based on the idea of "leave no one behind". While many African countries have embarked on ambitious and transformative transition strategies, and many energy projects classified as "clean" have economic, environmental, and social implications that jeopardize the wellbeing of those already vulnerable to the impacts of climate change. This paper explores the policy implications of the just transition to ensure that efforts to steer Africa towards a lower carbon future are supported by fair, equity, and justice considerations. Our analyses provide valuable evidence for considering a just transition in Africa that will not exacerbate the current socio-economic challenges the region is facing but will support sustained poverty reduction and the achievement of faster economic growth. Our findings show that the African continent's multiple challenges of energy security, economic growth, and affordable access must feature in its clean energy transition. We draw conclusions that an incremental transition emphasizing low-carbon development is the most feasible and pragmatic approach to transform the region's economy and address climate change challenges.

KEYWORDS

clean energy, just transition, energy justice, policy implications, economic development

1 Introduction

The Global North, notably the European Union (EU), has been at the forefront of developing technologies and implementing policies to generate energy from renewable sources and mitigate climate change (Okpanachi et al., 102934), even though this transition has been progressing at varying rates among EU member states (Müller et al., 2021). But when we see the Global South, the actions on clean energy transitions vary highly from country to country, especially in Asia and Africa. Looking at Africa, although there is less information on "clean" energy transitions as well as actions than there is in the EU, the interest in this subject is developing both in academic and policy circles (Castán Broto et al., 2018), (International Renewable Energy Agency, 2019a). Initiatives for renewable energy policy have gotten a boost from pressure to promote technological innovation, competitiveness, and economic growth in

Africa concerns over greenhouse gas emissions, idealistic expectations of a post-fossil fuel future, and growing economic unpredictability in a post-COVID era. Similar to the EU, growth in Africa has been uneven, with different nations taking different political pathways and certain regions of the continent receiving less research attention than others. Although Africa's share of global investments in renewable energy development and installed capacity remains relatively small, the continent's recent robust economic growth and rapid population growth will require more energy resources to drive future development. In contrast to a projected 10% growth in worldwide energy consumption, it is predicted that by 2040, energy demand in Africa might be almost 30% more than it is today (Johnston, 2020).

During the COVID-19 pandemic lockdowns, energy demand in most African countries declined because of significantly reduced commercial and industrial electricity use (Johnston, 2020). However, while the economic impact of the pandemic was severe, the experience offers an opportunity for countries in Africa to make transformational changes and structural adjustments in how energy is generated and stored. The exacerbating impacts of climate change across the continent emphasize the need to transition from a fossil fuel-based, regional economy to one powered by clean energy. Africa is extremely vulnerable to the impacts of climate change because of its low adaptive capacity. Moreover, the continent is highly dependent on shrinking natural resources. Therefore, investing in clean energy will help African economies address the immediate consequences and long-term socio-economic impacts of the COVID-19 pandemic and the ongoing climate crisis.

Despite a historical and present contribution to carbon emissions below 3%, the continent's commitment to cutting emissions is admirable. However, Africa still confronts a unique challenge in gaining access to modern energy to meet its development objectives, including enhancing climate resilience (Renewable Energy Agency et al., 2021). Despite the fact that Africa is highly endowed with energy resources to supply both present and future demand, approximately 600 million people live without access to power on the continent. While several nations, notably Burundi and Chad, still only have access rates of 10% or less, South Africa and the nations that makeup Northern Africa have almost universal access to electricity (African Development Bank, 2022), (Carley and Konisky, 2020). This unequivocally underscores the need to focus on and customize initiatives to raise access rates in Africa. Additionally, the availability of power should not be seen as a stand-alone, binary signal because a poor, constrained, or expensive electrical supply may restrict its value. In order to meet its climate pledges, Africa must significantly increase its contemporary power generation and consumption in light of the continent's population, urbanization, and economic growth patterns.

Socio-cultural specificity that may undermine efforts regarding energy transition in Africa is the lack of awareness and understanding about the benefits of renewable energy sources. This is because many Africans still use traditional energy sources like wood, charcoal, and kerosene since they are both affordable and easily available (Simelane and Abdel-Rahman, 1243). As a result, people might not be willing to pay more for renewable energy options that are better for the environment. Furthermore, the lack of political will and leadership to promote and invest in renewable energy is another culturally distinctive aspect of this society. Meeting the short-term energy demands of their populations, many African governments care less about long-term sustainability (Simelane and Abdel-Rahman, 1243). Without strong leadership, getting financial and political backing for renewable energy initiatives can be challenging. Additionally, some African cultures may prioritize traditional energy production and consumption forms, such as using wood as a primary cooking fuel (Simelane and Abdel-Rahman, 1243). These cultural practices may be difficult to change, especially if they are deeply ingrained in the community.

Transforming Africa's energy sector will require technological advancements to reconcile economic growth with the conservation of natural resources. However, technical progress alone will not be sufficient to transition away from a conventional energy system; a strong political will, strategic planning, and a comprehensive policy fully utilizing renewable energy are also needed. Although the specific paths to a clean energy transition may differ, depending on the particular requirements of various nations and regions, all paths must be equitable and inclusive to help achieve the United Nations Sustainable Development Goals (SDGs) (S&P Global), (Hafner and Tagliapietra, 2020). A just and inclusive energy transition based on the idea of "leave no one behind" would improve individuals' wellbeing and health, boost resilience, and inspire innovation to achieve a sustainable society at all levels while spurring massive investment (Ceres Roadmap, 2030). This argument is based on the premise that proactively identifying and confronting obstacles can result in far better outcomes than those that can be resulted from doing nothing or waiting too long to act. Changing behaviors and a fair and just energy transition will require a negotiated vision and process centered on discussion and backed by a set of guiding principles (Eskom, 2022). The main objective of this work is to inform policymakers on the impacts of strategic decision-making in clean energy development. In this work, we analyze the just and policy implications of the clean energy transition in Africa, emphasizing the challenges hindering this transition, policy recommendations, and finally, the linkage between SDG and energy transition in Africa. Our analysis provides valuable evidence for considering a variety of policy interventions for a just energy transition in Africa.

2 Just and policy implications of clean energy transition

The transition to clean energy in Africa has important justice and policy implications that should be carefully considered to ensure that this transition's benefits and burdens are distributed fairly. Environmental justice is a key aspect of this transition, as it involves ensuring that all people, regardless of their socioeconomic status, race, or ethnicity, have the right to live in a healthy and safe environment (U.S. Environmental Protection Agency, 2021). Africa requires a just and equitable energy transition that enhances inclusion and synergies while reducing inequality and empowering people through modern energy access. A cost-effective, dependable, and sustainable energy system is crucial not only for lifting millions of Africans out of poverty; the transition must create new opportunities and strengthen the rights of the poor but also for enhancing climate resilience, enhancing climate preparedness, and minimizing climate vulnerability (African Development Bank, 2022), (García-García et al., 2020). The equity ramifications and difficulties brought on by energy poverty, low consumption, and the unmet energy demand for economic growth and transformation in Africa must be carefully considered for a just energy transition. In the context of the transition to clean energy in Africa, this means ensuring that marginalized

groups and vulnerable individuals are not disproportionately impacted by the transition and that their needs and perspectives are taken into account in the planning and implementation of clean energy projects.

There are a number of marginalized groups and vulnerable individuals in Africa who may be disproportionately impacted by the transition to clean energy. These groups include but are not limited to, indigenous communities, rural communities, and low-income households (United nations development). These groups may be particularly vulnerable to the impacts of climate change, as they often rely on natural resources for their livelihoods and may have limited capacity to adapt to changing conditions (World Bank Group, 2021). Additionally, these groups may face barriers to accessing clean energy technologies and may be less able to afford the upfront costs of transitioning to clean energy. As more countries in Africa formulate and implement clean energy policies, failing to integrate justice into the process often leads to inequalities, uneven cost-sharing, and negative impacts associated with clean energy projects (Carley and Konisky, 2020). Recent debates have focused on the adverse impact of the energy transition on individuals, communities, and countries across Africa. The impacts often take the form of an excessive burden or a lack of access to possibilities for the energy transition in terms of affordability and access and inequalities that arise despite the benefits of clean energy projects. This section provides a comprehensive overview of the status of the clean energy transition in Africa, indicating the challenges which hinder a just energy transition and, in addition, a plea for striking a balance between Africa's energy needs and international climate obligations and gives practical strategy and policy suggestions.

2.1 Russia–Ukraine war and energy security: A lesson for Africa

What is seen as just in one situation might be considered unfair in another? According to Hirsch et al. (Hirsch et al., 2017), it is more challenging to implement a just transition in countries that have weak social support systems and heavy reliance on fossil fuel production than it is in countries that have robust social support systems and diverse industrial bases (Zinecker et al., 2018). African clean energy transition should not only entail replacing fossil fuels with renewables but also developing new, efficient, and flexible power systems fed by renewable energy sources and decentralized (including off-grid) facilities to minimize conditions wherein high demand must be satisfied by fossil fuels. While Africa's energy investment needs are significant, the additional demands connected with a shift to low-carbon energy may be viewed as realistic and pragmatic. The Russia–Ukraine conflict has caused energy prices to skyrocket in the European Union (EU), which is heavily reliant on Russian oil, gas, and coal (Besson, 2022). Despite decarbonization regulations, fossil fuels still account for a significant portion of the EU's energy mix. Leaders in the clean energy transition now face a dilemma; for example, Germany relies on Russia for roughly half of its natural gas and coal and more than one-third of its oil. Germany's near-term action is to increase the use of coal-fired power plants. This shows that in Africa, which faces problems of economic development and growth, energy security and affordable access must feature in its clean energy transition. The most feasible and pragmatic solution for Africa will be an incremental transition emphasizing low-carbon development rather than net-zero pathways.

2.2 Oil and gas *versus* economic development

Africa's energy transition must be predicated on leveraging the enormous prospects for energy access, employment, and industrialization based on the continent's tremendous renewable energy resources (Songwe et al., 2022). With appropriate technological and financial assistance, Africa can revolutionize its economies and become a global leader in inclusive green energy growth using its abundant energy resources. Figure 1 compares Africa with the rest of the world in terms of fossil fuel consumption and the GDP of the world. This shows that higher fossil fuel use is associated with a higher GDP, implying that countries require greater energy use to industrialize. Hence, for a country to attain a certain level of industrial growth, some amount of dependence on oil and gas is currently required. However, the societal and economic damages caused by climate change mean that dependence on greenhouse gas-emitting energy sources must be strongly discouraged globally. North America and Europe, having attained the highest level of industrialization, must work to significantly reduce their dependence on fossil fuels. The clean energy revolution cannot be restricted to small, incremental changes; to create a livable future, these efforts must be transformational, involving a system redesign based on the swift upscaling and use of all available clean and carbon-reducing technologies (United Nation Organization, 2021).

For continents with lower rates of economic development, less energy security, less affordable access, and poorer environmental sustainability, a different approach is needed. For Africa, a step-by-step transition must involve adjustments to an energy system that will not disrupt how established social, political, and economic systems coexist.

2.3 Evidence-based decision-making

While many African countries have embarked on ambitious and transformative transition strategies targeting underserved communities, many energy projects classified as "clean" have economic, environmental, and social implications that jeopardize the wellbeing of groups most vulnerable to the impacts of climate change.

2.3.1 Gender-inclusive policies

Gender inequality in many communities in Africa limits opportunities for women to participate in policy- and decision-making, affecting clean energy development. The 2019 Africa Gender Index Report (Gender, 2020) says that senior decision-makers in African firms are primarily male, with an Africa Gender Index score of just 22.9 percent. Women are underrepresented in parliament (25.3 percent). Very few managers, professionals, and technicians in Africa are women (41.4 percent) (Gender, 2020). A just transition should address the inequalities between men and women, as well as indigenous and minority groups, in decision-making processes. Marginalized or minority groups should be included in different stages of clean energy transition projects by including them in decision-making bodies.

2.3.2 Human rights in the mining industry

Critical materials used in manufacturing batteries and solar energy technology, such as cobalt and copper, are mined in Africa.

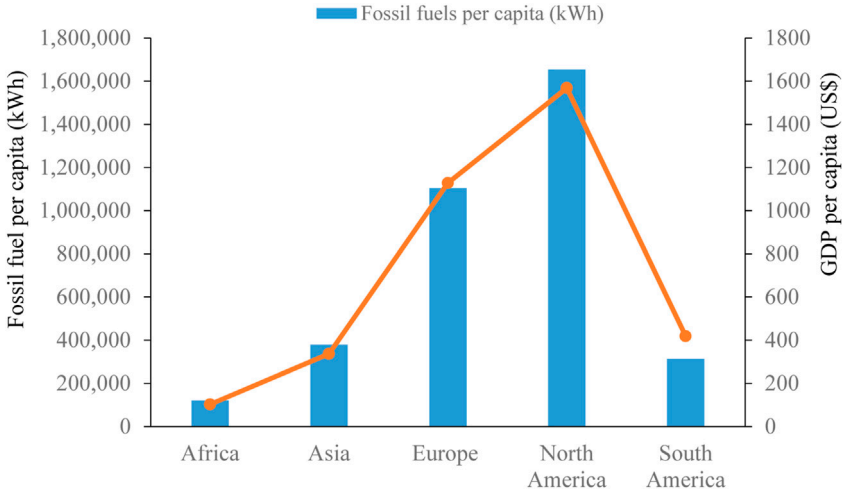

FIGURE 1
Fossil fuels *per capita* against GDP of the world (World Bank, 2022a), (Our World in Data, 2020).

More than 70 percent of the world's cobalt is produced in the Democratic Republic of the Congo (DRC), and 15–30 percent of Congolese cobalt is produced by artisanal and small-scale mining operations (Baumann-Pauly, 2022). A 2016 report from Amnesty International (Amnesty International, 2016) states that thousands of children mine cobalt in the DRC under hazardous conditions, and the DRC government and mining companies fail to protect mine workers from human rights abuses. A just energy transition requires a sustainable supply of critical materials produced in such a way that it respects the fundamental rights of miners and other workers.

2.3.3 Women, farmland, and energy transition

Women laborers are of vital importance to rural economies in Africa, providing 60–80 percent of the labor that supports African agriculture (Palacios-Lopez et al., 2017), (The World Bank, 2022). African women are known to live in poverty. According to (UN Women Data Hub, 2022), roughly 63 percent of the world's extremely poor women live in sub-Saharan Africa. While rural women play a critical role in Africa's economy, there have been multiple claims of women losing agricultural land to energy projects. For example, in Tanzania, there are claims that farmland was taken from a farmer in the coastal region to be used for a biofuel project (Makoye, 2013). If not managed well, these actions may increase the risk of food insecurity on the continent. Therefore, a just transition to clean energy must recognize the critical role rural women play and minimize their risk of losing access to agricultural land.

2.4 Strategies and policy Approaches for inclusive benefits

The transition to clean energy has the potential to bring numerous benefits to Africa, including improved access to electricity, increased economic opportunities, and reduced greenhouse gas emissions (International Renewable Energy Agency, 2019a). However, it is important to ensure that these benefits are distributed fairly, and that marginalized groups and vulnerable individuals are not left behind. In order to achieve this, a just and inclusive policy approach is needed. There are several key strategies that can be pursued to transition to clean energy in Africa.

- One of these is increasing the deployment of renewable energy technologies, such as solar panels and wind turbines, which can provide a source of electricity to communities that are not connected to the grid (International Renewable Energy Agency, 2019b). Renewable energy technologies can also create jobs and economic opportunities, particularly in rural areas, which can help to improve the livelihoods of marginalized communities.
- Promoting energy efficiency: Energy efficiency measures can help to reduce the overall demand for energy, which can in turn, reduce the need for fossil fuel generation. This can be achieved through a variety of means, such as implementing building codes and standards that require the use of energy-efficient appliances and equipment, providing incentives for the use of energy-efficient technologies, and promoting the adoption of energy-efficient behaviors.
- In addition to these strategies, it is also important to promote the use of clean cooking solutions in Africa. Traditional cooking methods, such as open fires and inefficient stoves, are a major source of air pollution and greenhouse gas emissions on the continent. Promoting the use of clean cooking solutions, such as improved stoves and clean fuels, can help to reduce these emissions and improve public health.
- Finally, it is important to support capacity building and technology transfer in Africa in order to fully transition to clean energy. Many countries on the continent lack the technical expertise and infrastructure needed to embrace clean energy technologies fully. Supporting capacity building and technology transfer can help build the necessary skills and infrastructure needed to support the clean energy sector's growth.

In order to effectively transition to clean energy and ensure that the benefits are distributed fairly, it is essential to adopt a just and

inclusive policy approach. This may involve implementing policies that support the deployment of clean energy technologies, such as feed-in tariffs or renewable energy targets, and implementing policies that support the needs of marginalized groups and vulnerable individuals, such as targeted support for low-income households to access clean energy technologies or training programs to help indigenous communities develop the skills needed to participate in the clean energy sector. By pursuing these strategies and adopting a just and inclusive policy approach, Africa can transition to clean energy and reap its numerous benefits.

3 Synergies between clean energy and sustainable development goals

The United Nations 2030 Agenda for Sustainable Development, also known as the Sustainable Development Goals (SDGs), is a global framework for achieving a better and more sustainable future for all. It aims to end poverty, protect the planet, and ensure peace and prosperity for all people, particularly those in developing countries (International Institute for Applied Systems Analysis, 2018). While the SDGs have the potential to address some of Africa's needs, they also have some limitations and challenges when it comes to fulfilling Africa's needs. One of the main criticisms of the SDGs is that they have an ethnocentric approach, projected by western countries, and do not adequately consider the specific needs and context of different regions and cultures (Cheever and Dernbach, 2015), (Matikainen, 2019). The goals and targets are often based on the values and priorities of the global north, rather than the realities and priorities of the global south. This can lead to a one-size-fits-all approach that does not adequately address the complex and diverse challenges facing Africa.

For example, the goal of universal access to electricity and modern energy sources is important for Africa, where many people still live without access to electricity. However, the goal does not adequately consider the specific energy needs and contexts of different countries in Africa (Matikainen, 2019). It does not consider the fact that some countries may have abundant renewable energy resources, such as solar or wind power, while others may rely more on fossil fuels or other non-renewable sources. The goal also does not consider the fact that some countries may have more developed infrastructure and capacity to implement renewable energy projects, while others may lack the necessary resources and capacity. Another example is the goal of achieving gender equality and empowering all women and girls. While this goal is important for Africa, where women and girls face numerous barriers to equality and empowerment, it does not adequately consider the specific cultural and social context of different countries in Africa (Security and Human Rights, 2017). It does not consider the fact that some cultures may have more traditional gender roles and expectations, which can be a barrier to women's empowerment. It also does not consider the fact that some countries may have more developed infrastructure and capacity to implement gender equality initiatives, while others may lack the necessary resources and capacity.

Despite these limitations, the SDGs can still be a useful framework for addressing Africa's needs, if they are implemented in a way that is sensitive to the specific context and needs of different countries in Africa. For example, the SDGs can be used as a roadmap for prioritizing and investing in key areas such as education, health, agriculture, and infrastructure (International Renewable Energy Agency, 2019a). These sectors are critical for Africa's development and have the potential to make a significant impact on people's lives and wellbeing. One way to ensure that the SDGs are more effective in addressing Africa's needs is to involve African stakeholders in the implementation process (International Renewable Energy Agency, 2019a), (International Institute for Applied Systems Analysis, 2018). This includes local communities, civil society organizations, governments, and the private sector. By involving these stakeholders in the planning and implementation of the SDGs, it is more likely that the goals and targets will be relevant and achievable in the African context. Another way to make the SDGs more effective in addressing Africa's needs is to ensure that they are aligned with other regional and national development frameworks and initiatives. For example, the African Union's Agenda 2063 (African Union Commission, 2022), which is a vision for Africa's development over the next 50 years, can be used to complement and support the implementation of the SDGs in Africa. By aligning the SDGs with Agenda 2063 and other regional and national development frameworks, it is more likely that the goals and targets will be relevant and achievable in the African context. We discuss eight of them in the context of a just transition to clean energy in Africa.

3.1 SDG #1: End poverty in all its forms everywhere

Increased power generation capacity can help eliminate poverty through many channels, and it is important to distinguish its macro- and micro-impacts (Lockwood and Pueyo, 20132013). Increased electric power capacity can indirectly reduce poverty at a macro level by promoting economic growth, as shown in Figure 2. The energy industry boosts economic growth in two ways. First, energy is a vital economic sector that provides jobs and creates value by producing, transmitting, and distributing energy across an economy (Alam et al., 2018). Second, the energy industry's effects spread throughout the economy. Energy is a necessary component in producing almost all goods and services in an economy and supports economic activity in all sectors. Electricity alone cannot provide all the conditions needed for economic growth; however, it is vital to meeting households' basic demands and supporting economic activity (Oda and Tsujita, 2011). Several factors, such as employment and productivity, health, and education, can explain the relationship between access to electricity and poverty alleviation. The most recent research on energy and poverty emphasizes the connection between the two (Khandker et al., 2012). Poverty limits access to power and energy consumption, restricting opportunities for education and economic growth; for example, often-prohibitive connection fees can prevent homes from connecting to the electricity grid (Golumbeanu and Barnes, 2013).

Of the approximately 39 percent of Cameroon's population living below the poverty line of $1.90 per day (Food and Agriculture Organization, 2019), most do not have access to clean, affordable energy; thus, people are forced to spend many hours covering big distances to gather firewood for cooking. Although access to electricity has gradually increased over the years, in 2016 only 60 percent of Cameroon's population had access to electricity, comprising only 21.3 percent in rural areas when compared with 92.0 percent in urban areas (The World Bank, 2020a). Reliability issues in

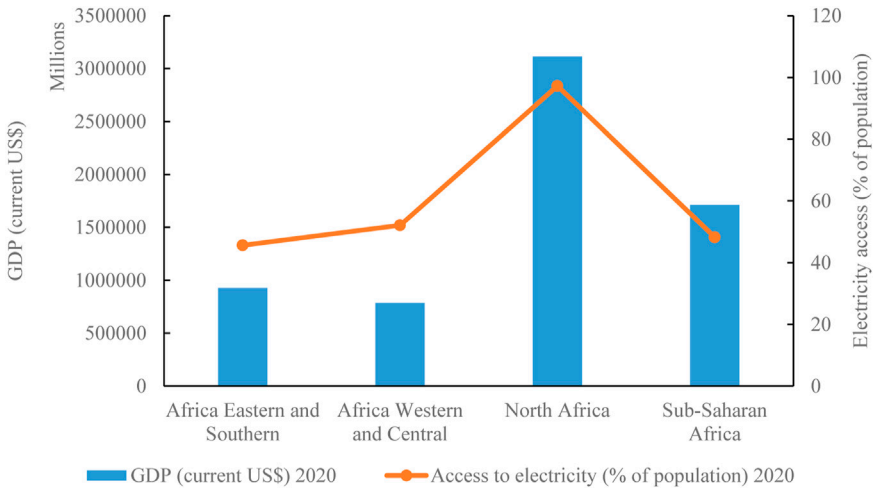

FIGURE 2
Access to Energy and GDP, Africa's context (The World Bank, 2021a), (The World Bank, 2021b).

Cameroon's electricity sector are severe. Thus, businesses and homes are without electricity for several hours each day and occasionally for several days. Access to electricity is essential for basic services, such as hospitals and schools, and the growth of small businesses at the household level (Alam et al., 2018).

Improving Cameroon's energy infrastructure will require proportionate expenditures as energy demand rises. Investments in the energy sector will increasingly need to focus on renewable energy so that the country can avoid being locked into unsustainable energy systems in the face of climate change and realize the potential benefits clean energy offers. According to Qudrat-Ullah et al. (Qudrat-Ullah and Nevo, 2021), a 1 percent increase in renewable energy consumption is predicted to result in short-term growth of 0.7 percent and strong long-term growth of 1.9 percent in Africa (Qudrat-Ullah and Nevo, 2021). Cameroon has abundant renewable energy resources, and deploying renewable energy systems through microgrids could significantly increase household incomes *via* job creation. According to (Wei et al., 2010), expanding a renewable energy infrastructure can create many jobs, including construction, installation, and operations, and supports other economic activities that produce job opportunities. For example, during the construction phase of the Memve'ele and Nachtigal hydropower plants, 10,000 and 1,500 jobs were created, respectively (Nachtigal Hydro Power Company, 2017), (Wikipedia, 2022). This increased the wealth of households in those communities. In addition, people may increase their working hours, diversify their sources of income, and even switch to jobs that are more productive. This is because of the increased amount of time they can spend with the lights on. Furthermore (Dinkelman, 2011), discovered many benefits of electricity availability on women's employment, likely because of a reduction in time spent performing housekeeping chores, freeing women to pursue paying jobs. Energy is a crucial input in producing goods and services across the agricultural, industrial, and service sectors. It is needed to improve irrigation systems and mechanize farms, which increases agricultural output, which, in turn, provides more income and food security for millions of households and increases agricultural exports, thereby reducing poverty. Growth in these industries requires a greater supply of energy, which can be achieved through the deployment of renewable technologies.

3.2 SDG #2: End hunger, achieve food security and improved nutrition, and promote sustainable agriculture

Climate change and expanding populations may significantly affect agricultural output and the agriculture sector's environmental impact, particularly concerning irrigated agriculture, which produces nearly 40 percent of the world's food on just 18 percent of its cropland. Because of changes in rainfall patterns, hydrological regimes, and weather patterns, as well as an increased reliance on land and water resources, rain-fed food production systems will also experience significant strain, further degrading available resources and reducing productivity. According to (Schwerhoff and Sy, 2017), food production is most vulnerable in Africa. One reason is that much of Africa's crop production depends on rain, and changes in climate and precipitation have a direct impact on crop output. Long-lasting droughts and intense rainstorms can drastically alter water supplies and exacerbate risks already present in agriculture. Crop production relies on energy inputs to provide even the most basic food output. Depending on a country's degree of development, on-farm food production consumes two to five percent of commercial energy (Khan and Hanjra, 2009). Similarly, a good deal of energy is used to transport raw materials to processing facilities where they are frozen, canned, dried, ground, baked, and undergo other processes. The dependence of the world's food systems on energy is further highlighted by the food processing and agricultural support businesses probably already requiring more energy than farming itself.

According to (Food and Agriculture Organization, 2013), total food losses in sub-Saharan Africa are estimated at $4 billion annually, an amount that could feed 48 million people. Hunger is predicted to increase due to adverse effects of climate change, such as drought, high temperatures, and increased pest attacks, on crops. This is likely to reduce agricultural productivity, increase food prices, and severely

increase famine among vulnerable groups, especially in rural areas. According to Morel et al. (Morel, Mungai), the agriculture sector employs approximately 28 percent of Gambia's working population, and approximately 80 percent of the country's rural households are, in one way or another, employed in the agricultural sector. Unfortunately, Gambia's agriculture is threatened by climate change, the agriculture sector has been underperforming compared to the rest of the economy, and its contribution to the country's GDP has been decreasing. Specifically, the agricultural sector's share of GDP decreased from 29% in 2010% to 16.9% in 2017. This will, in turn, increase the country's undernourished population.

Increased usage of renewable energy technology and customized energy systems reduces the percentage of the population that is undernourished by improving agricultural production, helping to ensure food security and end hunger (The World Bank, 2020b). Most farmers in sub-Saharan Africa still water their gardens and farms using labor-intensive bucket-lifting techniques, which is particularly hard for women, who do most of the labor (Morel, Mungai). Solar-powered irrigation systems and water pumps would help farmers maintain and increase their yields in areas affected by drought. Some irrigation and water pumping technologies have significant potential to ensure food supplies throughout the year and generate additional household income (Karekezi et al., 2005). An increase in household income helps ensure regular access to food. In addition, solar-powered meteorological stations could be built in rural areas to provide data that can guide farmers on planting and irrigation dates.

Customized energy systems can also help combat hunger by reducing post-harvest losses, Gambia wastes a lot of food due to a lack of transport and storage facilities. According to (Jallow et al., 2020), more than 45 percent of composted waste in Gambia comes from food waste. Losses of cereals due to poor handling are high and are likely greater for perishable products. The impact of high post-harvest losses on the poor is twofold. First, it implies that available food is less nutritious than the perishables that are wasted, leaving the poor undernourished. Second, post-harvest losses equate to lost potential income. Therefore, developing solar-powered grain silos and ovens to store excess food produced during farming seasons could reduce food waste and increase food security. Furthermore, the need for energy to process food would add value and thus increase household incomes.

3.3 U.N. SDG #3: Ensure healthy lives and promote wellbeing for all

Living without stable energy reduces options for education and employment, compromising health and overall wellbeing. The lack of energy impacts the ability of healthcare facilities to serve patients, affecting lighting, heating, ventilation, and cooling systems, blood banking, storage of vaccines and other medications, and information and communication technology (ICT) services, limiting the availability of life-saving care. Businesses cannot operate, transportation networks cannot run, and homes and workplaces cannot be heated and cooled to comfortable temperatures without reliable electricity. Around 2.4 billion people, the majority of whom reside in low- and middle-income countries, still cook over open fires and inefficient stoves that burn solid fuels (including wood, crop wastes, charcoal, coal, and dung) and kerosene (World Health Organization, 1748). These inefficient cooking methods contribute significantly to indoor air pollution, including tiny soot particles that can get deep into the lungs. Indoor smoke in poorly ventilated homes can produce levels of fine particles that can be 100 times greater than what is considered safe. Women and young children spend the most time close to a domestic stove or fireplace and are therefore at the greatest risk for exposure. Each year, respiratory illnesses, such as pneumonia, linked to exposure to indoor and outdoor air pollution kill almost 600,000 children under the age of five (World Health Organization, 2016). Most of these households' energy services are purchased and utilized by women and girls, who suffer the brunt of the health hazards and other costs associated with the usage of unclean and inefficient home energy systems.

Nigeria's industrial sector is still growing, and ambient air pollution has not yet reached harmful levels; however, household air pollution (HAP) is the highest contributor to ambient air pollution. According to Ifegbesan et al. (Ifegbesan et al., 2016), nearly 81 percent of homes in rural regions rely on solid fuel—primarily firewood—kerosene, and liquefied petroleum gas (LPG) for cooking. Biomass fuel (BMF) used for cooking and space heating is one of Nigeria's biggest sources of ambient air pollution and has contributed to an estimated 114,100 early deaths in the country [1]. Several studies (Ifegbesan et al., 2016) show that people who use biomass fuels are more likely to develop respiratory morbidity and chronic obstructive pulmonary disorders.

Providing access to high-quality healthcare and fulfilling the SDGs requires consistent access to reliable electricity. In most African countries, more than half of all healthcare institutions lack access to reliable electricity or do not have any electricity at all. Reliable energy is essential for healthcare institutions to operate at night, pump water, store vaccines and other medicines, and manage hazardous waste. The health of hundreds of millions of people, particularly women and children who frequently suffer from inadequate primary healthcare, is at risk due to the lack of sufficient and dependable power. More than 289,000 women worldwide die each year due to difficulties associated with pregnancy and childbirth; many of these deaths could be avoided with improved lighting and other electricity-dependent medical services (Porcaro, 2019). Therefore, access to dependable electricity can greatly impact people's health and wellbeing, especially in terms of reproductive and children's health. Increasing access to reliable electric power through renewable energy technologies could increase access to safe drinking water, provide clean power for heating and cooking that would reduce indoor pollution, and provide a variety of communication tools (such as radio, television, and the Internet) that can significantly impact efforts to provide healthcare and combat diseases. Without a reliable source of light and power, doctors are unable to perform medical procedures or assess patients at night. Access to reliable power would improve the ability to provide labor and delivery services—thereby reducing deaths associated with childbirth—make vaccines more widely available through refrigeration; and support critical medical equipment in health clinics.

1 "2019_nigeria". State of Global air 2019. Health Effects Institute.

3.4 SDG #4: Ensure inclusive and equitable quality education and promote lifelong learning for all

Energy poverty is a challenge faced by both students and teachers across sub-Saharan Africa, at home and in school. According to (United Nations Educational Scientific and Cultural Organization, 2022), more than 25 percent of schools in rural areas have access to electricity in India, while approximately 90 percent of pupils in sub-Saharan Africa attend educational institutions that lack electricity. Approximately 190 million students in Cameroon, Nigeria, Liberia, South Sudan, Central African Republic, Chad, Sierra Leone, and Malawi (Lindeman, 2022) combined attend schools that do not have electricity. The inability to access reliable electricity severely limits teachers' and students' ability to access and use instructional supplies and classroom materials, directly contributing to significant barriers that prevent people from achieving escape velocity from the clutches of poverty.

Access to electricity supports education by improving household incomes, which directly affects a family's ability to afford tuition. In 2010, 11.4 million pupils repeated a primary grade in sub-Saharan Africa, representing more than one-third of the global total (United Nations Educational Scientific and Cultural Organization, 2022). In Rwanda, for example, a lack of reliable electricity has been a major barrier to education. Many schools in rural areas do not have access to electricity, which limits the ability of teachers to use instructional materials and technology. This has led to lower enrollment and retention rates, as students may be unable to afford tuition or may be discouraged from attending school due to a lack of resources. In addition, the lack of electricity can make it difficult for schools to offer vocational training and other specialized classes that require lab equipment or other resources. The government of Rwanda has enforced regulatory and legal reforms to attract private investors and operators into isolated or standalone grid facilities like isolated grids operated by Virunga SARL, which was founded by the Virunga National park's Virunga Foundation, and received donor funding to build and operate mini-grids Mutwanga powered by two HPPs of 0.38 and 1.35 MW respectively, and a 13.1 MW HPP at Matebe serving 5,520 customers (World Bank Group, 2022). This has greatly increased access to electricity in various regions and has also encouraged school enrollment for youngsters as ICT and other lab equipment are being introduced in education. The benefits of increasing access to electricity in schools also include the ability to use a variety of ICT technologies, such as computers and the Internet, which are critical to fully participating in modern society. It also provides better staff retention and teacher training and generally increases school performance as students are more motivated to learn, which reduces truancy and absenteeism.

3.5 SDG #6: Access to clean water and sustainable sanitation practices

Access to clean water and sustainable sanitation practices is a critical development challenge in many African countries, as a lack of access to these basic services can have serious consequences for public health, economic development, and food security. Coupled with the impact of climate change, this means that roughly 771 million people in the world lack access to clean water (Project World Impact, 2022). Particularly in sub-Saharan Africa, access to clean water requires financing, transportation, and even physical labor. The inability to efficiently meet the growing water demand can lead to food insecurity (Mehta et al., 2015). Mitigating the global challenge of providing access to clean water requires a sustainable energy approach, particularly in rural areas of the country where most households lack access to clean water. According to (Food and Agriculture Organization, 2017), agricultural production will increase by 60 percent, causing the demand for water for irrigation to increase to about 11 percent. In this context, it is important to consider the role of renewable energy technologies and sustainable sanitation practices in addressing these challenges and in improving access to clean water and sanitation for all. One example of a country in Africa that is addressing the challenge of water access and management through the use of renewable energy technologies is Senegal. According to the African Ministers' Council on Water (AMCOW), approximately 84% of the Senegalese population has access to improved drinking water sources, but access is still limited in some rural areas (Weltbank, 2011). To address this challenge, the Senegalese government has implemented a number of initiatives to increase access to clean water, including the deployment of solar-powered water pumping systems in rural areas (International Renewable Energy Agency, 2019b). These systems can help to increase the availability of water for agricultural and domestic use and can help to reduce the reliance on fossil fuels, which can be expensive and environmentally damaging.

Another example can be seen in Tanzania, where the Tanzanian government has implemented water conservation and management strategies to conserve and manage water resources more effectively, including through the use of rainwater harvesting and efficient irrigation systems (Bank, 2017). These systems can help to increase the availability of water for agricultural and domestic use and can help to reduce the reliance on fossil fuels, which can be expensive and environmentally damaging. Addressing the challenge of providing access to clean water and sustainable sanitation practices in Africa requires a holistic and integrated approach that considers the role of clean energy, sustainable sanitation practices, and community engagement and education. By addressing these issues together, it is possible to improve water quality and availability and reduce food insecurity and other development challenges.

3.6 SDG #8: Promote inclusive and sustainable economic growth, employment, and decent work for all

Energy is an indispensable force driving all economic activity (Alam, 2006). Reliable energy could increase production capacity globally, fostering greater economic growth. Although there is no one way "when energy is scarce, it imposes a strong constraint on the growth of the economy, but when energy is abundant, its effect on economic growth is much reduced" (Stern, 2011). The lack of reliable electricity makes it impossible for many industries to reach production capacity. Almost 80 percent of industrial enterprises in Cameroon face output losses ranging from 16 to 50 percent due to power outages. It was reported in (Tei Mensah, 2016) that a 1-percent increase in power outage reduces production in Cameroon by 0.6–1.1 percent. According to the country's national electricity demand forecast (MINEE, 2030), electricity consumption in Cameroon will double by 2030, and the Ministry of Economy, Planning, and Regional

Development reports that power outages would reduce Cameroon's GDP by 5 percent. Therefore, responding to the urgent need for energy is a sustainable way to stimulate economic growth through industrial production. Since energy is needed across all sectors of an economy to support growth, its productive use is a critical facilitator of income-generating activities. While access to electricity is not the only factor affecting economic growth, studies suggest that power usage and GDP tend to be related, as shown in Figure 2, and access to electricity is expected to be a major facilitator of economic growth.

Similarly, in Burundi, access to electricity has also been a major challenge for economic development. According to International Renewable Energy Agency (IRENA) ("ENERGY PROFILEa), only about 11.7% of the population had access to electricity in 2020. This has had a significant impact on the country's economic growth, as many businesses and industries are unable to operate at full capacity due to the lack of reliable power. The government of Burundi has made efforts to increase access to electricity through initiatives such as the Decentralized Rural Electrification Strategy (2015–2017) (The World Bank, 2019), which aims to optimize the social effect of distributed renewable energy while addressing issues at the individual, institutional, and policy levels. One major goal is to facilitate the transfer of knowledge, expertise, and techniques from academic and research institutions to businesses and community organizations, allowing their members to better serve the needs of rural youth and families. The energy value chain is a significant source of job opportunities. A just energy transition would use people with various skill sets, degrees of expertise, and backgrounds. Africa's economic development rate in 2013 was insufficient to guarantee sufficient job opportunities for its fast-growing population (International Labour Organization, 2013). However, the International Renewable Energy Agency (IRENA) shows that the renewable energy sector might provide up to 30 million jobs by 2030 (up from 11 million in 2018) and up to 42 million jobs by 2050.

3.7 SDG #9: Build resilient infrastructure, promote inclusive and sustainable industrialization, and foster innovation

Over the past 2 decades, electricity has been crucial to industrial expansion, gaining priority for economic development among academic researchers and decision-makers (Abbasi et al., 2022). To prosper economically, a country needs a strong industrial base, and countries with a strong industrial sector have experienced relatively high economic growth in the past. Encouraging sustainable and effective use of natural assets can be greatly aided by creating new, greener facilities, retrofitting or reconfiguring existing infrastructure systems, and making good use of smart technologies.

Effective, sustainable industrial and innovation strategies must be accompanied by reliable energy policies and planning (United Nations Industrial Development Organization, 1984). Indeed, a country's industrialization is determined by its rational and efficient use of energy (Armel et al., 2015). In 2010, 43.5 percent of the electricity produced in Cameroon was consumed in the industrial sector when compared with 23 percent and 19 percent in the residential and public sectors, respectively (Modeste et al., 2015). This indicates that energy is a key input to industrialization. Furthermore, energy is needed to foster innovation as testing and scaling new technology requires energy. A system to regulate energy use is needed in order to allow technology start-ups to test concepts, models, and theories that help promote innovation. Energy's key role in industrialization is the basis for the highest projection of energy consumption in Africa, as shown in Figure 3.

An example of the importance of energy access in fostering industrialization in Africa can be seen in Ethiopia, which has made significant progress in expanding its electricity generation capacity in recent years. In 2015, the country launched its Growth and Transformation Plan (GTP), which included a goal of increasing electricity generation capacity from 2.8 to 4.9 GW by 2020 ("ENERGY PROFILEb). To achieve this goal, the government implemented a number of initiatives, including the construction of large hydroelectric dams, the expansion of solar and wind power generation, and the development of geothermal energy sources. The results of these efforts have been impressive. By 2019, Ethiopia had exceeded its GTP target, reaching a generation capacity of over 4.6 GW ("ENERGY PROFILEb). This expansion of electricity access has had a significant impact on the country's industrial sector, with a number of new factories and industrial parks being established in areas that previously had limited or no access to electricity. One such example is the Hawassa Industrial Park, which was established in 2016 with the support of the Ethiopian government and international investors (World Bank, 2022b). Located in the southern region of the country, the park has attracted a number of major international companies, including H&M, PVH, and the Chinese textile firm Zhongtai. These companies have been attracted to the park due to its low-cost labor, favorable investment climate, and access to reliable electricity. As a result, the park has become a major contributor to Ethiopia's economic growth and development, generating over $500 million in exports in its first 3 years of operation. Similarly, in Ghana, access to electricity has been a key factor in the country's industrialization efforts. The government has implemented a number of initiatives to increase access to electricity, including the construction 17 MW solar farm. Because of this initiative, more Ghanaians now have access to power, which has spawned the establishment of Meridian Industrial Park, which is home to around 68 businesses and directly supports the employment of 7,000 people in Ghana (BFT Online, 2021).

In conclusion, the relationship between energy access and industrialization in Africa is clear. Access to reliable, renewable energy is an important factor in enabling industrialization and fostering innovation in African countries. Through the implementation of initiatives to increase access to electricity and the promotion of renewable energy sources, African countries can create the conditions necessary for economic growth and prosperity. Countries that have made significant progress in expanding their electricity generation capacity often experience significant economic growth and development. Furthermore, access to reliable, renewable electricity helps to build a healthier, better-educated population that can support various industries and innovate. By promoting access to education and better healthcare, countries can build a more resilient infrastructure that is better equipped to support industrialization and innovation. Overall, it is important for African countries to prioritize the expansion of their energy generation capacity and the promotion of renewable energy sources in order to create the conditions necessary for economic growth and prosperity.

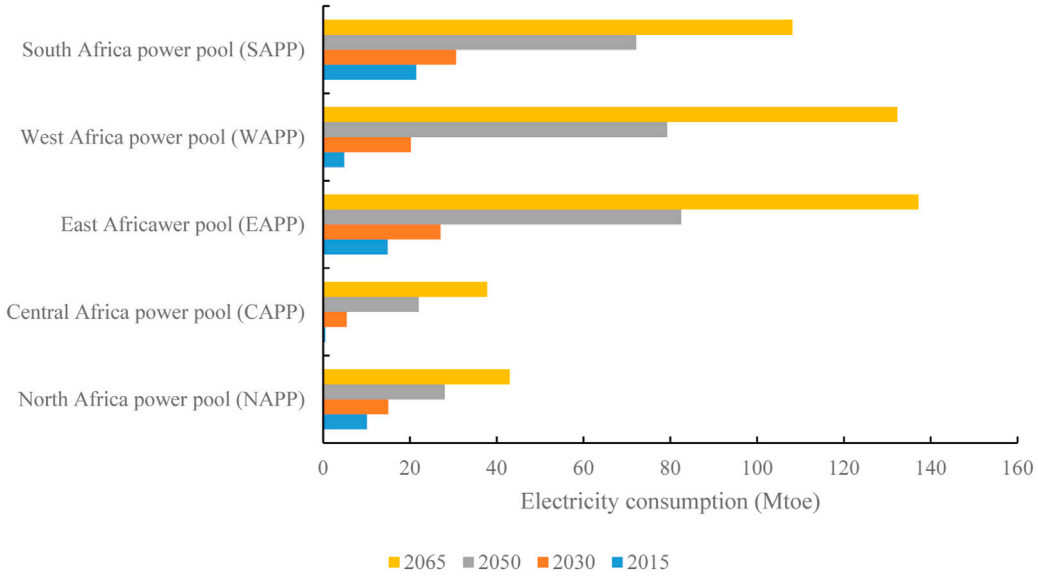

FIGURE 3
Projection of energy consumption in Africa—highest scenario (Pappis et al., 2019).

3.8 SDG #13: Take urgent action to combat climate change and its impacts

Rapid temperature increases in Europe, the United States, and other regions of the world are evidence that the consequences of climate change are being felt all across the globe. As a result, reducing emissions of greenhouse gases has become an urgent global concern. In order to reduce emissions, electrification is recommended by IRENA (Simelane and Abdel-Rahman, 1243); however, this strategy cannot stand alone and must be linked with renewable energy production. It is critical for African nations to translate RE policy into implementation change in light of the fact that many industrialized nations have set objectives for the total integration of renewable energy systems into their respective grid networks. Reducing greenhouse gas emissions is essential to decreasing the rate of global warming, which makes combating climate change and its effects an important worldwide concern. Many developed countries have set targets for fully incorporating renewable energy systems into their grid networks; for Africa to make a meaningful contribution to international efforts to mitigate climate change, it must do the same. Morocco is an example of an African country that is working to cut emissions and expand its usage of renewable energy. Morocco plans to generate 52% of its power from renewable sources by 2030 (Simelane and Abdel-Rahman, 1243), as stated by the International Renewable Energy Agency (IRENA). The government of Morocco has undertaken a variety of programs to this end, such as the construction of large-scale solar and wind projects and the installation of decentralized renewable energy systems in rural communities (Simelane and Abdel-Rahman, 1243). In addition to lowering its carbon footprint, Morocco is strengthening its energy independence and decreasing its dependence on fossil fuels by boosting the use of renewable energy sources.

Similarly, Nigeria relies on fossil fuels for its electricity needs. To a large extent, Nigeria did not begin tapping its renewable resource potentials until quite recently. As a result, Nigeria would have a more difficult time meeting its 2020 and 2030 renewable energy targets than will several other ECOWAS Member States. One-sixth of Nigeria's electricity supply is expected to come from renewables by 2030, under the country's National Renewable Energy and Energy Efficiency Policy 2015 (ICREEE, 2015). Although there has been a rise in the use of renewable energy in recent years, significant increases in deployment over the next decade will be necessary to reach the target. The Energy Commission of Nigeria (ECN) released a draft analysis and modeling in 2012 demonstrating how to achieve the 16% renewables aim by 2030 as part of the Nigerian Renewable Energy Roadmap (ICREEE, 2015). Insight into the document's meaning is provided by these findings. Small hydropower (7.07%), solar (5.90%), biomass (2.78%), and wind (0.25%) all make up less than 5% of total electricity consumption. Hence it is possible to meet the goal of delivering 16% renewable energy by 2030 with domestic activity. These percentages are not a limit on Nigeria's ambition but rather a depiction of how the country may achieve its 16% renewable energy goal. Changes in the energy industry and advances in technology mean that the relative importance of different industries may shift over time. Nigeria is committed to meeting its renewable energy goals, and the federal government is putting in place the framework and launching the necessary programs to make that happen.

Another example is Egypt as it plans to use renewable energy sources more extensively and lessen its dependency on fossil fuels. Hydropower accounted for 2.8 GW of the country's built renewable energy capacity in 2020, while solar and wind energy each accounted for around 0.9 GW (Renewable Energy Agency, 2018). The ISES to 2035 reports that Egypt's government has set lofty goals to expand the share of renewable energy in the country's electrical mix, with the objective of 20% by 2022% and 42% by 2035 (Renewable Energy Agency, 2018). The Egyptian government has established a feed-in tariff program, established a national renewable energy fund, and developed large-scale renewable energy projects like solar and wind farms in order to meet these objectives.

4 Conclusion

This study highlighted the importance of a just and inclusive transition in the move towards clean energy in Africa. Achieving a just energy transition in Africa requires a comprehensive policy framework that ensures that the most vulnerable and marginalized groups are not left behind. This includes considering the needs and perspectives of countries that currently rely heavily on fossil fuels, as a complete transformation from fossil-based energy production and consumption systems to renewable energy sources could create economic hardship. To overcome the multiple challenges faced by Africa and create economic, environmental, and social benefits for marginalized groups and vulnerable individuals, it is essential that the global and local challenges of energy security, economic growth, and affordable access are considered in the clean energy transition. This includes addressing the issue of climate change and formulating and implementing inclusive policies that do not jeopardize the wellbeing of groups most vulnerable to its impacts.

To ensure that efforts to transition to clean energy are effective and sustainable, it is important for policymakers to base their decisions on evidence and the experiences of individuals and communities. This requires a thorough understanding of the socio-economic conditions of the African continent and the specific needs and challenges faced by different countries and regions. In order to effectively address the global issue of climate change and the local environmental problems faced by Africa, a planned energy transition strategy must take into account the current socio-economic conditions of the continent and the specific needs and perspectives of countries that depend mainly on fossil fuels. This will ensure that the transition to clean energy is equitable and inclusive, and that it benefits all members of society. In summary, it is clear that the transition to clean energy in Africa requires a comprehensive and inclusive approach that considers the needs and perspectives of all stakeholders, including marginalized groups and vulnerable individuals. By ensuring that this transition is just and equitable, it is possible to create economic, environmental, and social benefits for all members of society.

Author contributions

Conceptualization was by BK and data collection was done by NS, AY, DC, and NK. Writing of original draft was done by all the authors. Supervision and review was done by J-SH. All the authors have read the final version of the manuscript submitted to the journal.

Funding

This work was supported by the National Research Foundation of Korea (NRF), a grant funded by the Korean government Ministry of Science and ICT (MSIT) (No. NRF-2021R1A5A8033165); the Korea Institute of Energy Technology Evaluation and Planning (KETEP) and the Ministry of Trade, Industry & Energy (MOTIE) of the Republic of Korea (No. 20224000000150).

Conflict of interest

The authors declare that the research was conducted in the absence of any commercial or financial relationships that could be construed as a potential conflict of interest.

Publisher's note

All claims expressed in this article are solely those of the authors and do not necessarily represent those of their affiliated organizations, or those of the publisher, the editors and the reviewers. Any product that may be evaluated in this article, or claim that may be made by its manufacturer, is not guaranteed or endorsed by the publisher.

References

Abbasi, K. R., Hussain, K., Radulescu, M., and Ozturk, I. (2022). Asymmetric impact of renewable and non-renewable energy on the industrial sector in Pakistan: Fresh evidence from Bayesian and non-linear ARDL. *Renew. Energy* 187, 944–957. doi:10.1016/J.RENENE.2022.02.012

African Development Bank Climate resilience and a just energy TRANSITION in AFRICA. https://www.afdb.org/sites/default/files/2022/05/25/aeo22_chapter2_eng.pdf.

African Union Commission. Second continental report ON the implementation of agenda 2063, Accessed: Dec. 22, 2022. [Online]. Available: https://au.int/en/documents/20220210/second-continental-report-implementation-agenda-2063#:~:text=Second%20Continental%20Report%20on%20The%20Implementation%20of%20Agenda%202063,-Share%3A&text=Agenda%202063%20is%20Africa's%20development,five%20ten%2Dyear%20implementation%20plans.

Alam, M. S. (2006). Economic growth with energy. *Munich Personal. RePEc Arch. (MPRA)* 1260, 1–25., no.

Alam, M. S., Miah, M. D., Hammoudeh, S., and Tiwari, A. K. (2018). The nexus between access to electricity and labour productivity in developing countries. *Energy Policy* 122, 715–726. doi:10.1016/J.ENPOL.2018.08.009

Amnesty International (2016). Democratic Republic of Congo: 'This is what we die for': Human rights abuses in the Democratic Republic of the Congo power the global trade in cobalt, https://www.amnesty.org/en/documents/afr62/3183/2016/en/ (accessed Aug 17, 2022).

Armel, T. K. F., Vidal, A. K. C., and René, T. (2015). Energy analysis and Exergy Utilization in the residential sector of Cameroon. *Energy Power Eng.* 7 (3), 93–104. doi:10.4236/epe.2015.73009

Bank, W. (2017). Reaching for the SDGs, https://elibrary.worldbank.org/doi/abs/10.1596/28435. doi:10.1596/28435

Baumann-Pauly, D., Why cobalt mining in the DRC needs urgent attention, *Counc. Foreign Relat.*, 29, (accessed Aug. 26, 2022).

Besson, V., The Ukraine/Russia conflict: An accelerator to the energy crisis, 2022, https://home.kpmg/fr/fr/blogs/home/posts/2022/03/how-the-russia-ukraine-crisis-impacts-energy-industry.html (accessed Aug. 17, 2022).

Bft Online, Meridian industrial park: Ghana South Africa business Chamber visits park, 2021, https://thebftonline.com/2021/09/17/ghana-south-africa-business-chamber-visits-meridian-industrial-park/ (accessed Dec. 23, 2022).

Carley, S., and Konisky, D. M. (2020). The justice and equity implications of the clean energy transition. *Nat. Energy* 5 (8), 8569–8577. doi:10.1038/s41560-020-0641-6

Castán Broto, V., Baptista, I., Kirshner, J., Smith, S., and Neves Alves, S. (2018). Energy justice and sustainability transitions in Mozambique. *Appl. Energy* 228, 645–655. doi:10.1016/J.APENERGY.2018.06.057

Ceres Roadmap, A just and inclusive transition | Ceres roadmap, 2030." https://roadmap2030.ceres.org/ai-expectation/just-and-inclusive-transition (accessed Aug. 10, 2022).

Cheever, F., and Dernbach, J. C. (2015). Sustainable development and its Discontents. *Transnatl. Environ. Law* 4 (2).

Dinkelman, T. (2011). The effects of rural electrification on employment: New evidence from South Africa. *Am. Econ. Rev.* 101 (7), 3078–3108, Dec. doi:10.1257/AER.101.7.3078

"Energy PROFILEa". *IRENA energy profile for Burundi*. International Renewable Energy Agency (IRENA).

"Energy PROFILEb". *IRENA energy profile for Ethiopia*. International Renewable Energy Agency (IRENA).

Eskom, A just energy transition for South Africa", Accessed: Aug. 10, 2022. [Online]. Available: https://www.eskom.co.za/about-eskom/just-energy-transition-jet/#:~:text=Eskom's%20Just%20Energy%20Transition%20(JET,an%20increase%20in%20sustainable%20jobs.

Food and Agriculture Organization (2019). Cameroon - Response overview - October 2019. https://reliefweb.int/report/cameroon/cameroon-response-overview-october-2019.

Food and Agriculture Organization (2013). Food balance Sheet data. http://faostat.fao.org/site/354/default.aspx (accessed Mar. 12, 2020).

Food and Agriculture Organization, Water for sustainable food and agriculture A report produced for the G20 Presidency of Germany. 2017, [Online]. Available: https://www.fao.org/3/i7959e/i7959e.pdf.

García-García, P., Carpintero, Ó., and Buendía, L. (2020). Just energy transitions to low carbon economies: A review of the concept and its effects on labour and income. *Energy Res. Soc. Sci.* 70 (Dec), 101664. doi:10.1016/j.erss.2020.101664

Gender, A. (2020). Africa gender INDEX report. https://www.afdb.org/en/documents/africa-gender-index-report-2019-analytical-report.

Golumbeanu, R., and Barnes, D. (2013). Connection Charges and electricity access in sub-Saharan africa. https://elibrary.worldbank.org/doi/abs/10.1596/1813-9450-6511.

Hafner, M., and Tagliapietra, S. (2020). *The global energy transition: A review of the existing literature*. Berlin, Germany: Springer, 1–24. doi:10.1007/978-3-030-39066-2_1

Hirsch, T., Matthess, M., and Fünfgelt, J. (2017). Guiding principles and Lessons Learnt for a just energy transition in the Global South. Geneva, Switzerland. https://library.fes.de/pdf-files/iez/13955.pdf.

Icreee, Nigeria NATIONAL renewable energy ACTION plans. 2015, (NREAP)-1.docx." https://view.officeapps.live.com/op/view.aspx?src=https%3A%2F%2Frise.esmap.org%2Fdata%2Ffiles%2Flibrary%2Fnigeria%2FRenewable%2520Energy%2FSupporting%2520Documentation%2FNigeria_NATIONAL%2520RENEWABLE%2520ENERGY%2520ACTION%2520PLANS%2520(NREAP)-1.docx&wdOrigin=BROWSELINK (accessed Dec. 23, 2022).

Ifegbesan, A. P., Rampedi, I. T., and Annegarn, H. J. (2016). Nigerian households' cooking energy use, determinants of choice, and some implications for human health and environmental sustainability. *Habitat Int.* 55, 17–24. doi:10.1016/J.HABITATINT.2016.02.001

International Institute for Applied Systems Analysis (2018). Transformations to achieve the sustainable development goals report prepared by the world in 2050 initiative. https://previous.iiasa.ac.at/web/home/research/twi/TWI2050_Report_web-small-071018.pdf. doi:10.22022/TNT/07-2018.15347

International Labour Organization, *Recovering from a second jobs dip Global Employment Trends 2013 Recovering from a second jobs dip*, INTERNATIONAL LABOUR OFFICE GENEVA Contents Contents," 2013, Genève, Switzerland, Accessed: Aug. 10, 2022. [Online]. Available: www.ilo.org/publns

International Renewable Energy Agency (2019). Off-grid renewable energy solutions to expand electricity access: An opportunity not to be missed. https://www.irena.org/publications/2019/Jan/Off-grid-renewable-energy-solutions-to-expand-electricity-to-access-An-opportunity-not-to-be-missed.

International Renewable Energy Agency (2019). Scaling up renewable energy deployment in Africa. https://www.irena.org/-/media/Files/IRENA/Agency/Publication/2020/Feb/IRENA_Africa_Impact_Report_2020.pdf?la=en&hash=B1AD828DFD77D6430B93185EC90A0D1B72D452CC.

Jallow, A. A. K., Karcher, S., Atwa, A., Soezer, A., Sanyang, F., and Jallow, B. (2020). Circular GHG mitigation opportunities the Gambia. www.shiftingparadigms.nl/projects.

Johnston, A., (2020). The impacts of the Covid-19 crisis on global energy demand and CO2 emissions. https://www.iea.org/reports/global-energy-review-2020 (accessed Jul 28, 2022).

Karekezi, S., Kimani, J., Wambille, A., Balla, P., Magessa, F., Kithyoma, W., et al. (2005). The potential contribution of non-electrical renewable Energy technologies (RETs) to poverty reduction in East Africa. https://citeseerx.ist.psu.edu/document?repid=rep1&type=pdf&doi=207a61e22961c8a1a415c50f23e60b4e11dd6c9e.

Khan, S., and Hanjra, M. A. (2009). Footprints of water and energy inputs in food production – global perspectives. *Food Policy* 34 (2), 130–140. doi:10.1016/J.FOODPOL.2008.09.001

Khandker, S. R., Samad, H. A., Ali, R., and Barnes, D. F. (2012). Who benefits most from rural electrification? Evidence in India. https://www.iaee.org/ej/ejexec/EJ%2035-2_04%20S.R.%20Khandker%20ExecSummary%2012-060%20Templated.pdf.

Lindeman, T., Without electricity, 1.3 billion are living in the dark - Washington Post. 2022, https://www.washingtonpost.com/graphics/world/world-without-power/ (accessed Sep. 06, 2022).

Lockwood, M., and Pueyo, A. (2013). The evidence of benefits for poor people of electricity Provision: Scoping Note and review Protocol. https://opendocs.ids.ac.uk/opendocs/handle/20.500.12413/2894.

Makoye, K., Tanzania farmers accuse biofuel investors of land grab. 2013, https://landmatrix.org/media/uploads/trustorgitem20130718134927-q50zx.pdf (accessed Aug. 26, 2022).

Matikainen, O. A. (2019). Sustaining the one-Dimensional: An Ideology Critique of Agenda 2030 and the SDGs. https://www.diva-portal.org/smash/record.jsf?dswid=30&pid=diva2%3A1326645.

Mehta, L., Cordeiro-Netto, O., Oweis, T., Ringler, C., Schreiner, B., and Varghese, S., Water for food security and nutrition A report by the high level panel of Experts on food security and nutrition," 2015, Accessed: Aug. 10, 2022. [Online]. Available: https://www.fao.org/fileadmin/user_upload/hlpe/hlpe_documents/PT_Water/Docs/HLPE_Water_Project-Team_24_February-2014.pdf.

Minee, "Assistance au Ministère de l ' Energie et de l ' Eau dans l ' élaboration du Plan de Développement à long terme du Secteur de l ' Électricité Horizon 2030 (*PDSE 2030*)," vol. 2, no. *Pdse* 2030, 2006.

Modeste, K. N., Mempouo, B., René, T., Costa, Á. M., Orosa, J. A., Raminosoa, C. R. R., et al. (2015). Resource potential and energy efficiency in the buildings of Cameroon: A review. *Renew. Sustain. Energy Rev.* 50, 835–846. doi:10.1016/j.rser.2015.05.052

Morel, G., and Mungai, R. *The Gambia: A look at agriculture*. Washington, DC, USA: World Bank.

Müller, F., Neumann, M., Elsner, C., and Claar, S. (2021). Assessing African energy transitions: Renewable energy policies, energy justice, and SDG 7. *Assess. Afr. energy transitions Renew. energy policies, energy justice, SDG 7, " Polit. Gov.* 9 (1), 119–130. doi:10.17645/PAG.V9I1.3615

Nachtigal Hydro Power Company (2017). Nachtigal Hydro power plant. https://www.nsenergybusiness.com/projects/nachtigal-hydro-power-plant/.

Oda, H., and Tsujita, Y. (2011). The determinants of rural electrification: The case of Bihar, India. *Energy Policy* 39 (6), 3086–3095. doi:10.1016/J.ENPOL.2011.02.014

Okpanachi, E., Ambe-Uva, T., and Fassih, A. (2022). Energy regime reconfiguration and just transitions in the Global South: Lessons for West Africa from Morocco's comparative experience. *Futures* 139, 102934. doi:10.1016/J.FUTURES.2022.102934

Our World in Data, Per capita fossil energy consumption vs. GDP per capita, 2020." https://ourworldindata.org/grapher/per-capita-fossil-energy-vs-gdp (accessed Aug. 22, 2022).

Palacios-Lopez, A., Christiaensen, L., and Kilic, T. (2017). How much of the labor in African agriculture is provided by women? *Food Policy* 67, 52–63. doi:10.1016/j.foodpol.2016.09.017

Pappis, I., Howells, M., Sridharan, V., Usher, W., Shivakumar, A., and Gardumi, F. (2019). Energy projections for African countries. https://www.researchgate.net/profile/Ioannis-Pappis/publication/337154878_Energy_projections_for_African_countries/links/5dc847e3a6fdcc57503dd5c1/Energy-projections-for-African-countries.pdf.

Porcaro, J., Energy and health: Making the connection. 2019, https://www.seforall.org/news/energy-and-health-making-the-connection (accessed Aug10, 2022).

Project World Impact, Water Scarcity | Nonprofits that help water Scarcity | PWI. https://projectworldimpact.com/cause/Water-Scarcity (accessed Aug. 10, 2022).

Qudrat-Ullah, H., and Nevo, C. M. (2021). The impact of renewable energy consumption and environmental sustainability on economic growth in Africa. *Energy Rep.* 7, 3877–3886, Nov. doi:10.1016/J.EGYR.2021.05.083

Renewable Energy Agency, I., Development Bank, K., and Gesellschaft für Internationale Zusammenarbeit, D., The renewable energy transition in africa powering access, resilience and prosperity, https://www.irena.org/-/media/Files/IRENA/Agency/Publication/2021/March/Renewable_Energy_Transition_Africa_2021.pdf, On behalf of the".

Renewable Energy Agency, I. (2018). Renewable energy outlook: Egypt (executive summary). https://www.irena.org/-/media/Files/IRENA/Agency/Publication/2018/Oct/IRENA_Outlook_Egypt_2018_En.pdf.

Security and Human Rights (2017). Feminist Critiques of the sustainable development goals analysis and Bibliography 2017. https://genderandsecurity.org/sites/default/files/Feminist_Critiques_of_the_SDGs_-_Analysis_and_Bibliography_-_CGSHR.pdf.

S&P Global *S&P global*. https://www.spglobal.com/en/research-insights/articles/what-is-energy-transition.What is energy transition?

Schwerhoff, G., and Sy, M. (Aug. 2017). Financing renewable energy in Africa – key challenge of the sustainable development goals. *Renew. Sustain. Energy Rev.* 75, 393–401. doi:10.1016/J.RSER.2016.11.004

Simelane, T., and Abdel-Rahman, M. The renewable energy transition in africa. https://policycommons.net/artifacts/1243341/energy-transition-in-africa/1796410/.

Songwe, V., Ogunbiyi, D., and Abou-Zeid, A., Africa's energy transition calls for pragmatic measures to keep the continent competitive | United Nations Economic Commission for Africa." https://www.uneca.org/stories/africa%E2%80%99s-energy-transition-calls-for-pragmatic-measures-to-keep-the-continent-competitive (accessed Aug. 26, 2022).

Stern, D. I. (2011). The role of energy in economic growth. *Ann. N. Y. Acad. Sci.* 1219 (1), 26–51. doi:10.1111/j.1749-6632.2010.05921.x

Tei Mensah, J. (2016). Bring Back Our light: Power outages and industrial performance in sub-Saharan africa. Accessed: Sep. 07, 2022. [Online]. Available: https://ideas.repec.org/p/fae/wpaper/2016.20.html.

The World Bank (2021). Access to electricity (% of population) | Data. https://data.worldbank.org/indicator/EG.ELC.ACCS.ZS.

The World Bank (2020). Access to electricity (% of population)-Cameroon. https://data.worldbank.org/indicator/EG.ELC.ACCS.ZS?locations=CM.

The World Bank (2021). GDP (current US$) | Data. https://data.worldbank.org/indicator/NY.GDP.MKTP.CD.

The World Bank (2019), Population density (people per sq. km of land area). Accessed: Dec. 23, 2022. [Online]. Available: https://data.worldbank.org/indicator/EN.POP.DNST.

The World Bank (2020). Prevalence of undernourishment (% of population) - Gambia, the | Data. https://data.worldbank.org/indicator/SN.ITK.DEFC.ZS?locations=GM.

The World Bank, Women, agriculture and work in africa. https://www.worldbank.org/en/programs/africa-myths-and-facts/publication/women-agriculture-and-work-in-africa (accessed Aug. 26, 2022).

Un Women Data Hub, Poverty deepens for women and girls, according to latest projections, ." https://data.unwomen.org/features/poverty-deepens-women-and-girls-according-latest-projections, 2022, (accessed Aug. 26, 2022).

United Nation Organization (2021). Theme report on energy transition towards the achievement of sdg 7 and net-zero emissions. https://www.un.org/sites/un2.un.org/files/2021-twg_2-062321.pdf.

United Nations Development, United NATIONS development PROGRAMME, https://www.undp.org/, 2 Did you know?"

United Nations Educational Scientific and Cultural Organization (2022). According to United Nation 42% of African school children will drop out before the end of primary education. https://www.developafrica.org/providing-comprehensive-educational-support-africa#:~:text=According%20to%20the%20United%20Nations,activities%20with%20their%20potential%20wasted. (accessed Mar. 13, 2020).

United Nations Industrial Development Organization (1984). Energy and industrialization. *OPEC Rev.* 8 (4), 409–433. doi:10.1111/j.1468-0076.1984.tb00287.x

U.S. Environmental Protection Agency (2021). Climate Adaptation action plan. https://www.epa.gov/climate-adaptation/climate-adaptation-plans.

Wikipedia, Memve'ele hydropower station in Cameroon, 2022, https://en.wikipedia.org/wiki/Memve%27ele_Hydroelectric_Power_Station#:~:text=Memve'ele%20Hydroelectric%20Power%20Station%20is%20a%20211%20megawatt%20hydroelectric,80%20megawatts%20in%20April%202019 (accessed Jul. 07, 2022).

Wei, M., Patadia, S., and Kammen, D. M. (2010). Putting renewables and energy efficiency to work: How many jobs can the clean energy industry generate in the US? *Energy Policy* 38 (2), 919–931. doi:10.1016/j.enpol.2009.10.044

Weltbank, *Water supply and sanitation in Senegal turning finance into services for 2015 and beyond*," 2011, weltbank, Washington, DC, USA.

World Bank, GDP per capita (current US$) | Data." https://data.worldbank.org/indicator/NY.GDP.PCAP.CD (accessed Aug. 22, 2022).

World Bank Group, Increasing access to electricity in the Democratic Republic of Congo: Opportunities and challenges, Accessed: Dec. 22, 2022. [Online]. Available: https://openknowledge.worldbank.org/handle/10986/33593.

World Bank Group, Vanuatu climate risk country PROFILE," 2021, Accessed: Dec. 22, 2022. [Online]. Available: https://climateknowledgeportal.worldbank.org/sites/default/files/country-profiles/15825-WB_Vanuatu%20Country%20Profile-WEB.pdf.

World Bank, Hawassa industrial park community impact evaluation Ethiopia context", Accessed: Dec. 23, 2022. [Online]. Available: https://thedocs.worldbank.org/en/doc/434121573654466886-0050022019/original/15073PolicyBriefEthiopiaHawassa.pdf.

World Health Organization Accelerating SDG 7 achievement policy BRIEF 10 health and energy LINKAGES-MAXIMIZING health benefits from the sustainable energy TRANSITION. https://sustainabledevelopment.un.org/content/documents/17486PB10.pdf.

World Health Organization (2016). Burning opportunity: Clean household energy for health, sustainable development, and wellbeing of women and children. https://apps.who.int/iris/bitstream/handle/10665/204717/9789241565233_eng.pdf.

Zinecker, A., Gass, P., Gerasimchuk, I., Jain, P., Moerenhout, T., Oharenko, Y., et al. (2018). Real people, real change strategies for just energy transitions. https://policycommons.net/artifacts/614301/real-people-real-change/1594547/.

sustainability

MDPI

Article

Comprehensive Analysis of Land Use Change and Carbon Sequestration in Nepal from 2000 to 2050 Using Markov Chain and InVEST Models

Deepak Chaulagain [1,2], Ram Lakhan Ray [3], Abdulfatai Olatunji Yakub [1,2], Noel Ngando Same [1,2], Jaebum Park [1,2], Dongjun Suh [1], Jeong-Ok Lim [1,2] and Jeung-Soo Huh [1,2,*]

[1] Department of Convergence & Fusion System Engineering, Graduate School, Kyungpook National University, Sangju 37224, Republic of Korea; chaulagaindeepu11@gmail.com (D.C.); yakubabdulfatai1@gmail.com (A.O.Y.); samenoel1@gmail.com (N.N.S.); woqja133@naver.com (J.P.); dongjunsuh@knu.ac.kr (D.S.); jolim@knu.ac.kr (J.-O.L.)
[2] Institute for Global Climate Change & Energy, Kyungpook National University, Daegu 41566, Republic of Korea
[3] Cooperative Agricultural Research Centre, College of Agriculture, Food, and Natural Resources, Prairie View A & M University, Prairie View, TX 77446, USA; raray@pvamu.edu
* Correspondence: jshuh@knu.ac.kr

Abstract: The escalating pace of migration and urbanization in Nepal has triggered profound alterations in land use practices. This event has resulted in a considerable diminution of ecological diversity and a substantial decline in the potential for carbon sequestration and other ecosystem services, thereby impeding climate change mitigation efforts. To address this, a comprehensive assessment of land use change and carbon storage was conducted from 2000 to 2019 and forecasted to 2050 in Nepal. Employing the Markov chain and InVEST models, this study evaluated the loss and gain of carbon, elucidating its economic value and spatial distribution. The findings revealed that carbon storage in 2000 and 2019 were 1.237 and 1.271 billion tons, respectively, with a projected increase to 1.347 million tons by 2050. Carbon sequestration between 2000 and 2019 amounted to 34.141 million tons, which is anticipated to surge to 76.07 million tons from 2019 to 2050, translating to economic valuations of 110.909 and 378.645 million USD, respectively. Forests emerged as pivotal in carbon storage, exhibiting higher carbon pooling than other land use types, expanding from 37% to 42% of the total land area from 2000 to the predicted year 2050. Notably, carbon distribution was concentrated in parts of the terai and mountain regions, alongside significant portions of the hilly terrain. The findings from this study offer valuable insights for governing Nepal and REDD+ in developing and implementing forest management policies. The results emphasize the importance of providing incentives to local communities judiciously to promote effective conservation measures.

Keywords: carbon distribution; ecological diversity; ecosystem services; forest; local communities; mitigation

Citation: Chaulagain, D.; Ray, R.L.; Yakub, A.O.; Same, N.N.; Park, J.; Suh, D.; Lim, J.-O.; Huh, J.-S. Comprehensive Analysis of Land Use Change and Carbon Sequestration in Nepal from 2000 to 2050 Using Markov Chain and InVEST Models. *Sustainability* **2024**, *16*, 7377. https://doi.org/10.3390/su16177377

Academic Editor: Anna De Marco

Received: 21 July 2024
Revised: 8 August 2024
Accepted: 25 August 2024
Published: 27 August 2024

1. Introduction

Carbon storage is about where and how carbon is retained in various reservoirs for long time periods, which can occur naturally or through human intervention, while carbon sequestration focuses on the process of actively capturing atmospheric CO_2 and storing it in these reservoirs [1]. Forest ecosystems, such as tropical, temperate, and boreal forests, are essential to the global carbon cycle. Collectively, they contain about 85% of the world's terrestrial aboveground biomass (AGB) [2]. These forests, rich in biodiversity, are substantial carbon reservoirs, contributing to approximately 40% of the global aboveground carbon pool. Research has indicated that tropical forests alone store between 250 and 300 gigatons of vegetation carbon, with a significant portion, approximately 200 gigatons, present in AGB [3,4]. Understanding the dynamics of biomass, which encompasses all organic matter

above ground, is crucial for gauging how these ecosystems mitigate atmospheric carbon dioxide [5]. Effective management of these forests enhances their ability to absorb CO_2, incorporating it into the biomass and subsequently enriching the soil. In this context, the carbon cycle involves several key storage pools, including soil organic carbon (SOC), deadwood carbon, AGB, and belowground biomass (BGB), each of which plays a significant role in carbon sequestration and the overall health of the ecosystem [6–8]. Carbon released from these pools is reabsorbed by vegetation, highlighting the importance of efficient carbon management [9,10].

Initiatives such as the Green India Mission and REDD have been implemented globally to reduce CO_2 emissions. The Clean Development Mechanism under the UNFCCC promotes carbon sequestration through afforestation and reforestation. Meanwhile, REDD+ focuses on reducing emissions from deforestation and enhancing forest carbon stocks, demonstrating the critical role of forestry in mitigating climate change [11].

Recent studies have highlighted the viability of afforestation as a climate policy, indicating it as a highly effective alternative to combating the consequences of deforestation. Afforestation not only addresses the root cause but also offers a sustainable solution for carbon management [12,13]. The carbon cycle, which involves various storage pools, such as vegetation and firewood plantations, plays a critical role in this context. This cycle, detailed by researchers such as in [14,15] involves the release and reabsorption of carbon, which is influenced by land use changes. Hernández-Guzmán et al. in 2019 [15] analyzed land use and land cover (LULC) changes in a hydrologic basin in Mexico and their effects on carbon storage. We projected LULC changes up to 2050 and used the InVEST model for carbon storage estimation by employing unsupervised classification of Landsat images and cellular automata Markov (CA-Markov) chain modeling. They found significant landscape modifications, particularly an increase in exposed soils and a decrease in evergreen and tropical dry forests, leading to a reduction in carbon stock from 362.9 Tg C in 1986 to an expected 317.9 Tg C in 2050 [15]. Chen et al. [3] studied the dynamics of ecosystem services (ESs) in response to urbanization in China's Yangtze River Economic Belt. They used the future land use simulation (FLUS) model to simulate short-, medium-, and long-term land use changes and assessed six ESs under different land use scenarios. The study found intensive urban sprawl and a decrease in cropland, leading to declining trends in all ESs except a few under one scenario. This study highlights the impact of urbanization on ESs, including carbon storage, which is expected to decline by 1.95–6.781% [3]. These studies collectively showed the importance of strategic land management and afforestation in enhancing carbon sequestration and mitigating climate change.

In addition, Zhao et al. [16] evaluated the impact of ecological engineering on carbon storage in the semiarid northwestern region of China. They simulated land use/cover changes following ecological engineering programs and assessed their impact on carbon storage by linking the CA-Markov and InVEST models. The results indicated an increase in carbon storage by 10.27 Tg from 2015 to 2029, with a relative error of 0.22% in the linked model, indicating its high applicability in such assessments [16,17]. Focusing on the semiarid region of Sergipe, Brazil, the study highlights that deforestation and land degradation significantly reduced carbon stock, while restoration efforts can provide substantial carbon sequestration benefits. This research investigates the economic and environmental importance of preserving and restoring natural ecosystems [17]. Zhang et al. [18] investigated the effects of rapid urbanization in Shanghai, China, revealing a substantial decline in carbon stock due to the conversion of forested and agricultural lands into urban areas. The study outlines the critical role of urban green spaces and adaptative management in encountering the negative impacts of urban expansion on carbon emission. The investigation into wetland changes in China's coastal urban agglomerations demonstrates the fluctuating carbon storage trends and the effectiveness of ecological protection in enhancing carbon sequestration [19]. Hoque et al. analyzed forest plantations in coastal Bangladesh, revealing significant increases in regional carbon storage due to the expansion of mangrove areas under different land management strategies. The study also

highlighted the trade-offs between carbon storage and food supply, emphasizing the need for balanced land use policies to address both climate adaptation and food security [20]. These studies employed the CLUE-S, CA-Markov, and InVEST models and collectively highlighted the critical need for sustainable land use planning and the adoption of multi-faceted strategies to improve carbon sequestration and achieve environmental goals using the CLUE-S, CA-Markov, and InVEST models.

A study in the Sariska Tiger Reserve highlights the necessity of integrating ecological and economic valuation in land management, with improved conservation scenarios significantly reducing carbon loss [21]. In addition, Saha et al. evaluated the biophysical and economic values of ESs in the Sundarbans Biosphere Region, India. They used Net Primary Productivity models, InVEST, and CA-Markov to assess the impact of climate change and land use dynamics from 1982 to 2045. The study observed significant variations in ES values, with the highest values in habitat service, nutrient cycling, and gas regulation. The study found that regulating services were most affected by land use and climate change [22]. Verma et al. assessed carbon sequestration mapping and its economic quantification in the Askot Wildlife Sanctuary, Western Himalayas. They employed a novel approach combining machine learning and spatial–temporal techniques for LULC simulation with the InVEST model. The study revealed significant economic losses owing to rapid forest cover decline, highlighting the importance of conservation strategies for forested landscapes [23].

Various methodologies exist to enhance the accuracy of carbon storage assessments, encompassing techniques such as biomass assessment, stock volume analysis, chamber measurements, and sampling methodologies. However, these methods face significant challenges in portraying carbon storage dynamics across large spatial areas over prolonged periods [24]. This study introduces a unique approach by combining the InVEST model with CA-Markov, offering an innovative technology for spatial representation, dynamic analysis, and quantitative evaluation of ESs [24]. Recent studies have witnessed the integration of various LULC simulation models, such as the multilayer perceptron (MLP) neural network-Markov chain [25], SD-CLUE-S [26], Logistic-CA-MC [27], FLUS [28], and the PLUS model [29], with the InVEST model. These integrated models are reliable techniques for assessing the impact of climate and LULC changes on ecosystem carbon storage. The InVEST model's carbon module primarily relies on land use data from key sources, making it well suited for large landscapes and extended time series. The precision of the InVEST model outcomes depends on the accuracy of the LULC maps used in the base and predicted years. CA-Markov in Terrset demonstrates a higher accuracy and is user-friendly in presenting LULC maps for current and projected years compared with other LULC simulation models.

Land use changes, along with forest and soil degradation, contribute to increased greenhouse gas emissions. Nepal, with its highly fragile ecosystem, faces significant challenges related to forest and soil degradation and carbon sequestration [30]. This issue warrants deep analysis due to its severity. Over the past few decades, both anthropogenic and natural impacts have continually altered land use and land cover in Nepal [31]. Agriculture is the primary economic activity, and rural populations heavily depend on forest resources for fuelwood and timber. The mountainous and hilly regions are particularly sensitive to land use and land cover changes, even with minimal human interference [31]. Since the 1970s, land use change trends in Nepal have accelerated due to population growth, leading to the conversion of significant forest areas into agricultural land and built-up area [32]. Recent studies indicate that forests accounted for 44.47% of total land area in 2018. Agricultural land expanded rapidly from 1910 to 2010 but has slightly declined since 2010 due to rapid urban expansion [33].

The application of the InVEST model integrated with CA-Markov in Nepal is limited. Rimal et al. [34] applied the InVEST model within a confined geographical area, specifically the Koshi River basin, incorporating a support vector machine approach. Similarly, Bastola et al. [35] employed the InVEST model in the Bagmati River basin for water yield analysis. However, these studies are unable to present a comprehensive overview of imminent land

use change and carbon storage across the entire country, encompassing future predictions and economic valuation of sequestered carbon. To address this gap, the current study provides a holistic perspective by presenting total carbon storage and sequestration from 2000 to 2050, including economic values and the spatial distribution of carbon storage throughout the nation using the InVEST model coupled with CA-Markov of TerrSet for the prediction of land use change. This research segments the study area into three regions with alike features for higher accuracy and refines the results through averaging the carbon densities of similar studies of comparable regions. This technique both reinforces the findings and highlights the advanced methodology employed in this study. With Nepal setting ambitious net-zero emission targets for 2050, this research emerges as an informative tool for the government, assisting in the development of policies for effective land use management and the strategic allocation of incentives to local communities for sustainable forest management.

Furthermore, the comprehensive analysis of carbon sequestration, economic analysis, and presenting models of this study are beneficial for global policymakers in the realm of carbon trading. This study employs specific carbon and discount rates that are particularly relevant for countries with economies characteristics similar to Nepal, enabling them to assess their carbon outputs and thus facilitating their entry into international carbon markets. It proposes a plan for sustainable land management and climate change strategies that aim to strike a balance between environment protection and economic growth. This approach influences global environmental management policies and supports equitable economic development through engagement in international carbon markets.

2. Materials and Methods

The evaluation of carbon sequestration in Nepal encompassed the prediction of land use using CA-Markov of Terrset IDRISI, the tabulation of the carbon density of each land use type, and the measurement of carbon loss and sequestration through the application of the InVEST model. The research framework of this study is shown in Figure 1.

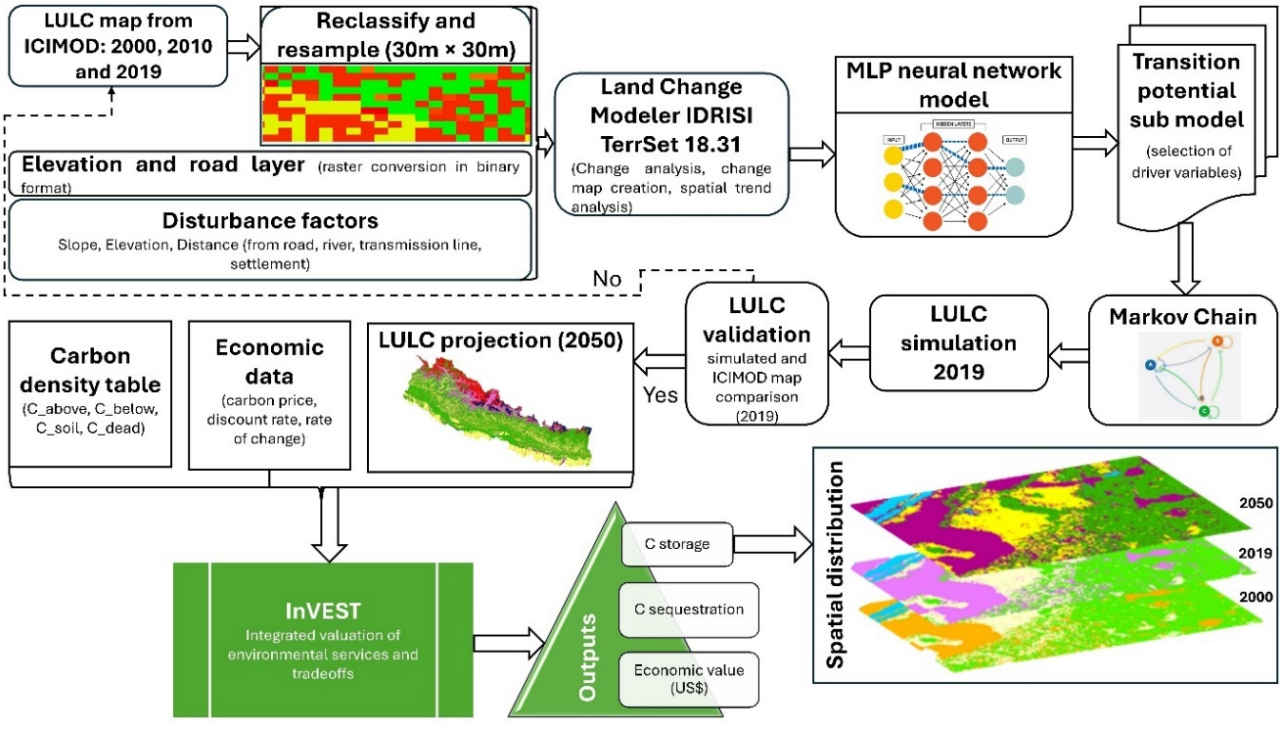

Figure 1. A conceptual framework showing the steps involved in this study.

2.1. Model Description

2.1.1. InVEST Model

Materials developed collaboratively by Stanford University, the University of Minnesota, the Nature Conservancy, and the Worldwide Fund for Nature (WWF), the InVEST model encompasses four modules for assessing terrestrial ESs. These modules focus on soil conservation, water retention, carbon storage, and biodiversity assessment, providing a comprehensive measurement of regional Ess [24]. Specifically, the carbon storage model within InVEST combines four distinct pools: aboveground biomass carbon, belowground biomass carbon, dead organic carbon, and SOC, each assigned to various LULC categories [36]. The formula for calculating the total carbon storage in Nepal is articulated as follows [8,24]:

$$C_{total} = C_{above} + C_{below} + C_{soil} + C_{dead}, \quad (1)$$

where C_{total} is the total carbon storage, C_{above} is the aboveground carbon storage, C_{below} is the underground carbon storage, C_{soil} is the soil carbon storage, and C_{dead} is the dead organic matter carbon storage.

Based on the carbon pooling and land use data, the carbon storage of each land use type in Nepal is calculated as follows [24]:

$$C_{totali} = (C_{abovei} + C_{belowi} + C_{soili} + C_{deadi}) \times A_i, \quad (2)$$

where i is the average carbon density of each land use and A_i is the area of this land use.

2.1.2. CA-Markov Model

The CA-Markov chain model was used to forecast land use changes over different periods. This model stands out as a reliable method because of its efficient algorithm, which is particularly adept at eliminating any ambiguities in land use transfer [37]. This model comprises four integral components: cells and cell states, neighborhood, and conversion rules. The cell, which is the smallest computational unit, is instrumental in the model, with the cell state representing the category assigned to each cell. The neighborhood aspect pertains to the conversion state of the current cell, whereas the conversion denotes the specific rule in which the cell transforms. The general CA model formula is as follows [36]:

$$S_{(t+1)} = f\left(S_{(t)}, N\right), \quad (3)$$

where S is a finite and discrete state set of cells; N is the neighborhood of the cell; t and $t + 1$ represent two different moments; and f is the state transition rule.

Markov models perform matrix analysis within random time series through mathematical modeling, projecting the likelihood based on the existing state and evolving trends in LULC. The formulation of the Markov model can be articulated by the following formula [36]:

$$A_n = A_{n-1} \times P_{ij}, \quad (4)$$

where A_n and A_{n-1} are the spatial distribution states of land use at two moments, and P_{ij} is the state transition probability matrix, which is calculated as follows [38]:

$$P = P_{ij} = \begin{pmatrix} P_{11} & P_{12} & P_{1n} \\ P_{21} & P_{22} & P_{2n} \\ P_{n1} & P_{n2} & P_{nn} \end{pmatrix}, \sum_{i=1}^{n} P_{ij} = 1. \quad (5)$$

In the given formula, P represents the matrix of Markov transitions, where i and j denote the categories of LULC for the initial and successive timeframes, respectively. The variable "n" represents the number of LULC classes, and P_{ij} signifies the probability or likelihood of a specific type of land transitioning from one LULC category to another.

2.2. Study Area

Nepal is rich in a remarkable diversity of ecosystems, spanning from low-lying flatlands at 59 m above sea level (masl) to towering mountains reaching 8849 masl with geographical coordinates ranging from 26°20′53″ to 30°26′51″ N in latitude and from 80°03′30″ to 88°12′05″ E in longitude [39]. The predominant hilly and mountainous regions of Nepal play crucial roles as carbon sinks. Notably, community forests, extending from lowlands to high mountains, are exemplary models for carbon sequestration in South Asia. The study area was classified into three distinct parts [40]: terai (flat land), hill, and mountain, reflecting the highly heterogeneous environment and the significant variation in carbon density, particularly in forested areas across these regions. The major land use types in Nepal include forest, cropland, grassland, snow/glacier, wooded land (shrubland), barren land (sand, gravel, and rock), lakes and rivers, and built-up areas [31]. Among these land use types, forest covers approximately 39.1%, followed by cultivated lands at 29.83%, and grassland at 7.90%. The remaining land is covered by wooded land (shrub land), lakes, rivers, snow/glaciers, and built-up areas [41]. The common soils in the Tarai and Middle Mountain physiographic regions are Entisols, Inceptisols, Alfisols, and Mollisols. In contrast, the Siwaliks and High Mountain regions are predominantly covered with Entisols and Inceptisols. The High Himalayan region is characterized by the prevalence of Inceptisols and Spodosols, alongside rock outcrops [42]. The total population of Nepal is 29,164,578 [43]. A visual representation of the study area is shown in Figure 2.

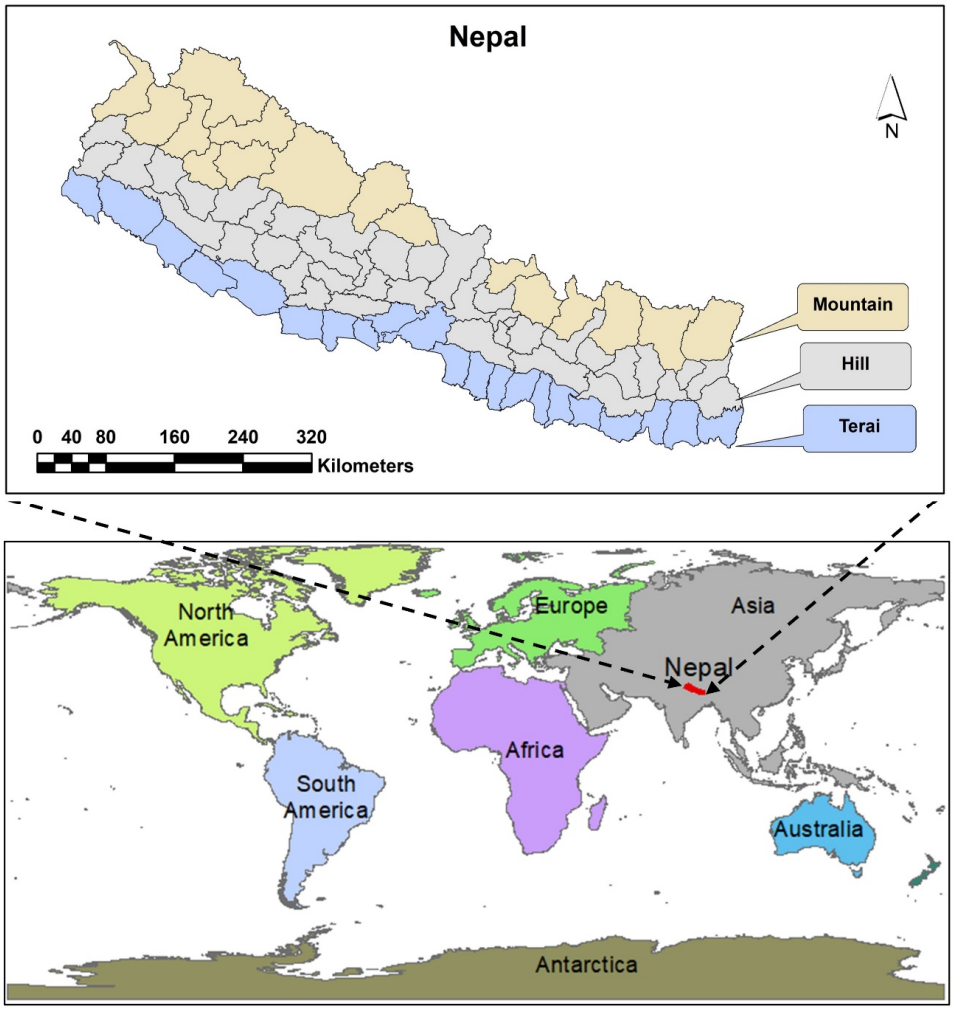

Figure 2. Geographical distribution of the study area.

2.3. LULC Map Preparation

This study employed the LULC map of Nepal created by ICIMOD, featuring a grid size of 30 m × 30 m. The ICIMOD map originally included 11 land use classes. In our research, we reclassified the map, merging snow and glaciers into a single category called snow/glacier and combining riverbed, bare soil, and bare rock into the category of bare land. The final map used in this study comprises the following land use types: wooded land (shrub land), waterbody, agricultural land, built-up area, forest, snow/glacier, grassland, and bare land.

The ICIMOD map is noted for its high accuracy, which is attributed to the use of a regional land cover monitoring system. This approach addresses challenges such as limited data accessibility, lack of transparency in data collection methodologies, and inconsistencies in land cover classification. The ICIMOD map stands out for its yearly generation of high-resolution land cover data for the Hindu Kush Himalaya region. Moreover, it employs a cloud-based machine learning system to generate the land cover map, validating its accuracy through extensive field monitoring [44].

2.4. LULC Map Prediction for 2050 Using CA-Markov in TerreSet

The prediction of future land use dynamics in Nepal was performed using the CA-Markov environmental simulation model, available in the Terrset 2020 version 19.0.8. This model's prediction process involved three fundamental steps: (1) change analysis and land use transition, (2) transition potentials, and (3) change demand modeling using the Markov chain.

Change analysis and land use transition were conducted using the Land Change Modeler within Terrset, using LULC maps, elevation maps, and road layers from 2000 to 2010 in the study area. The inputs were prepared in ArcGIS 10.5 and converted into the IDRISI format. A threshold of 5000 ha was set to ignore transitions below this value, resulting in a transition map illustrating 42 transitions from one land class to another between 2000 and 2010.

The study area, encompassing flat land, hills, and mountain regions, experienced LULC changes influenced by driver variables, such as slope, elevation, distance from the river [45], distance from the road [46], distance from settlement [47], and distance from transmission lines [48]. Cramer's V values were calculated for all variables, and those with low values were also included. The MLP neural network was employed for the transition sub-model, as it is an artificial neural network capable of handling nonlinear relationships without user intervention.

The final step in land use prediction involved the use of a Markov chain for change demand modeling. All sub-models, including the MLP neural network, were integrated to produce a single map for the predicted year. Initially, LULC maps for the years 2000 and 2010, prepared by ICIMOD, were employed to simulate the LULC map for 2019. This simulation was then compared with the ICIMOD-prepared map for 2019, which is known for its high accuracy, attained through comprehensive field survey validation. Once a high accuracy was achieved between the predicted and observed maps, the model was extended to predict the LULC map for 2050. The Markov chain method applied in this study relies on the conditional probability of past and present transitions, employing a soft prediction modeling approach with a logical "OR" aggregation type.

2.5. Assessment and Prediction of Carbon Sequestration Using the InVEST Model

In the assessment of carbon sequestration using the InVEST model, land use maps of Nepal were categorized into three regions—terai, hill, and mountain—using ArcGIS. The carbon pooling table for each land use type in these regions was constructed based on the IPCC guidelines [49] and relevant literature [21,34,35]. Table 1 presents carbon pools in AGB, BGB, SOC, and dead wood carbon across different classes of the LULC map.

Table 1. Carbon pool estimated (Mg/ha) for the InVEST model.

LULC Code	LULC_Name	C_Above	C_Below	C_Soil	C_Dead
1	Waterbody	0	0	0	0.01
2	Snow	0	0	0.01	0
3	Forest (Terai)	77.88	26.12	33.66	6.95
	Forest (Hill)	66.42	21.14	59.01	2.97
	Forest (Mountain)	114.27	38.09	114.03	2.97
4	Baresoil	3.6	4	10	0
5	Built-up	5	1	5	0
6	Agriculture	3.95	2	6.6	1
7	Grassland	0	0	84.9	0
8	Wooded land	13.3	5.15	27.24	2.54

The carbon trade agreement between the government of Nepal and the World Bank, which valued carbon at USD $5 per ton, was integrated into the study to incorporate economic considerations. The economic analysis employed a market discount rate of 3%, and the annual rate of change in the carbon price was assumed to be zero, drawing from the information obtained from [21].

This study spanned two-time intervals: 2000–2019 and 2019–2050. For the initial period (2000–2019), the LULC map for the base year 2000 was used, with the predicted year being 2019. Similarly, for the subsequent interval (2019–2050), the initial year was 2019, and the predicted year was set to 2050. After inputting all necessary information into the InVEST model, the simulation was executed, generating an output map that was then imported into ArcGIS to extract the required information. The model presents the carbon storage data for the years 2000, 2019, and 2050, utilizing information from the land use map and carbon pool table. Net carbon sequestration for the periods 2000–2019 and 2019–2050 was determined by calculating the difference in carbon storage between 2000 and 2019, and between 2019 and 2050, respectively, using the InVEST model.

2.6. Spatial Distribution and Cluster Characteristics of Carbon Storage

In ArcGIS, the carbon storage maps for Nepal's terai, hill, and mountain regions were merged to create a comprehensive raster map covering the entire country. This map delineates carbon storage for the years 2000, 2019, and 2050, employing a grid size of 30 m × 30 m. The map was subjected to natural breaks (Jenks) classification to enhance interpretability, resulting in six distinct classes. These classes are defined as follows: "no carbon" for areas with 0 tons, "very low" for those within the 0–1.16 tons range, "low" for 1.16–3.95 tons, "moderate" for 3.95–8 tons, "high" for 8–12.9 tons, and "very high" for 12.9–24 tons. This classification schema offers a detailed depiction of carbon storage dynamics across Nepal, facilitating a nuanced analysis of carbon distribution patterns for the specified years.

This study employed Global Moran's *I* to characterize the spatial differentiation of carbon storage in the study area, using the following formula [24]:

$$I = \frac{n\sum_{i=1}^{n}\sum_{j=1}^{n} w_{ij}\,(x_i - \overline{x})(x_j - \overline{x})}{\sum_{i=1}^{n}\sum_{j=1}^{n} \omega_{ij}\sum_{i=1}^{n}(x_i - \overline{x})^2}, \quad (6)$$

where w_{ij} is the spatial weight, x is the attribute mean, x_i and x_j are the attribute values of elements i and j, respectively, and n is the number of cells. The correlation is considered significant when $|z| > 1.96$ corresponds to a 95% confidence level in hypothesis testing using the standard normal distribution. This statistical approach provides insights into the spatial patterns and characteristics of carbon storage, helping to discern significant correlations within the study area.

3. Results

3.1. LULC Mapping and Prediction

In Figure 3, the distribution of land classes is presented for the years 2000, 2019, and the projected year 2050. In 2000, forest land covered the largest area at 55,702.51 km^2 (37.54%), followed by agriculture land at 39,618.94 km^2 (26.7%) and grassland at 19,889.78 km^2 (13.4%). In 2019, the trend continued with forest covering 58,306.22 km^2 (39.3%), agriculture land covering 36,440.35 km^2 (24.56%), and grassland covering 18,979.76 km^2 (12.79%). Projected for 2050, forest land is expected to cover the largest portion at 62,062.05 km^2 (41.83%), followed by agriculture land at 38,371.04 km^2 (25.86%) and bare land at 18,898.57 km^2 (12.74%). Waterbodies consistently occupy the smallest area, less than 1%, whereas wooded land slightly decreases from 2.19% to 2.02%, as shown in Table 2. Similarly, the dynamics of land use changes during the 2000–2019 interval and the projected 2019–2050 interval are presented in Table 2. In the past time interval, the snow/glacier land use type experienced a 2.25% increase, followed by a 5.12% decrease in the projected time interval, showcasing a consistent trend. The built-up area demonstrated minimal change over both intervals. Conversely, bare land and agricultural land witnessed a decrease of 1.58% and 2.15% in the past, only to increase by 4.44% and 1.3%, respectively, in the projected period. Notably, the forest area exhibited growth in both time intervals, with a 1.75% increase in the past and a more substantial 2.53% increase in the projected period. These observations provide insights into the dynamic nature of land use changes, reflecting historical trends and anticipated shifts in the landscape over specified timeframes.

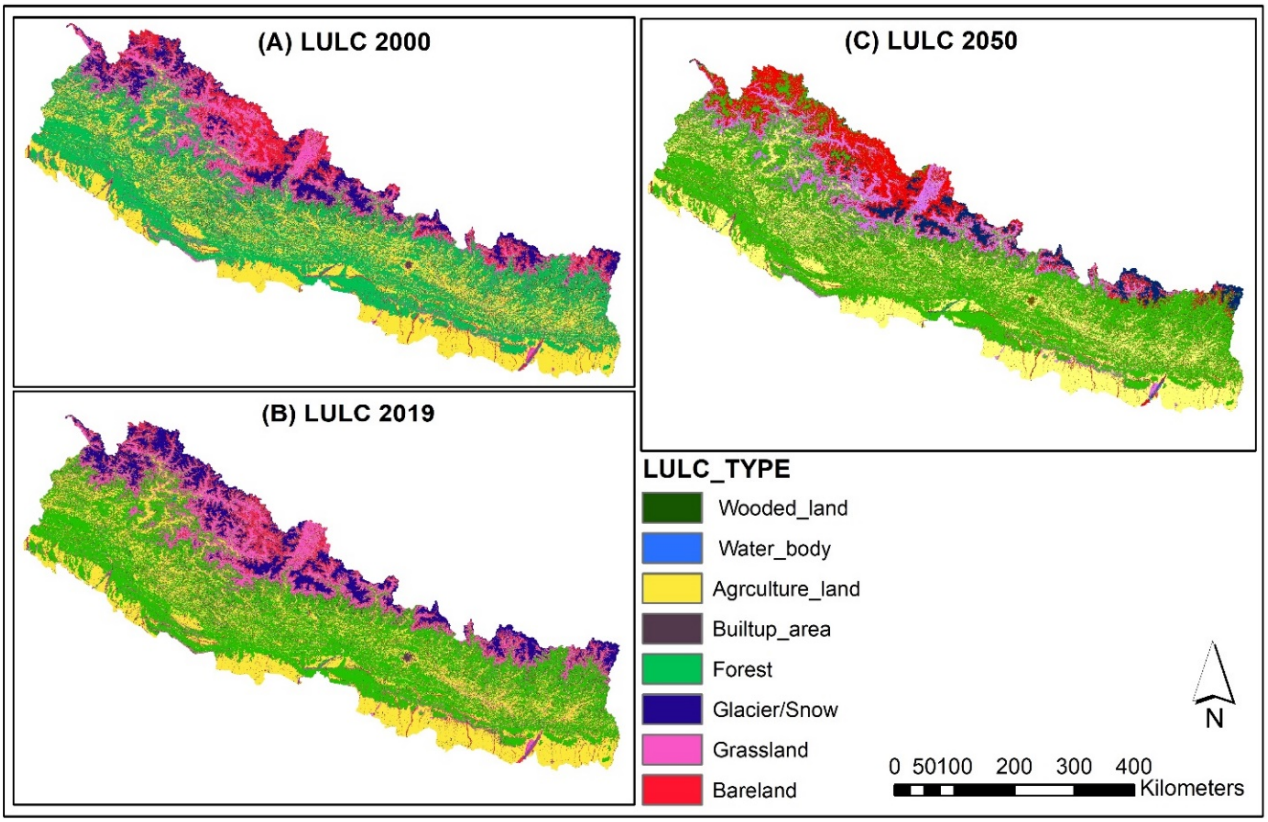

Figure 3. Historical and future projection maps of land use and land cover changes over time.

Table 2. Area-wise distribution of land use and land cover change over time intervals.

LULC Type	Year 2000		Year 2019		Year 2050		Change (%)	
	Area (km^2)	Area (%)	Area (km^2)	Area (%)	Area (km^2)	Area (%)	2000–2019	2019–2050
Waterbody	505.34	0.34	541.36	0.36	477.65	0.32	0.02	−0.04
Snow/Glacier	9793.64	6.6	13,134.41	8.85	5437.79	3.66	2.25	−5.19
Forest	55,702.51	37.54	58,306.22	39.3	62,062.05	41.83	1.76	2.53
Bare land	14,643.18	9.87	12,304.31	8.29	18,898.57	12.74	−1.58	4.45
Built-up area	4974.9	3.35	5471.52	3.69	5079.38	3.42	0.34	−0.27
Agriculture land	39,618.94	26.7	36,440.35	24.56	38,371.04	25.86	−2.14	1.3
Grass land	19,889.78	13.4	18,979.76	12.79	15,055.89	10.15	−0.61	−2.64
Wooded land	3251.26	2.19	3201.64	2.16	2997.2	2.02	−0.03	−0.14

3.2. Accuracy Assessment for Model Validation

The accuracy assessment involved a comparison between the predicted land use map and the LULC map prepared by ICIMOD, which is widely acknowledged for its high accuracy. Using the base year's LULC map of 2000 and the present year's map of 2010, the LULC map for 2019 was predicted through the integration of the MLP-Markov chain analysis (MLP-MCA) method. This projected map was then compared with the ICIMOD's validated map for 2019 for model validation, resulting in an overall average accuracy of 90.4%. The accuracy of the model for individual land use types was 98.7% for forest areas, 94.7% for agricultural land, 99.4% for grassland, and 71.3% for the snow/glacier land use type, as illustrated in Figure 4.

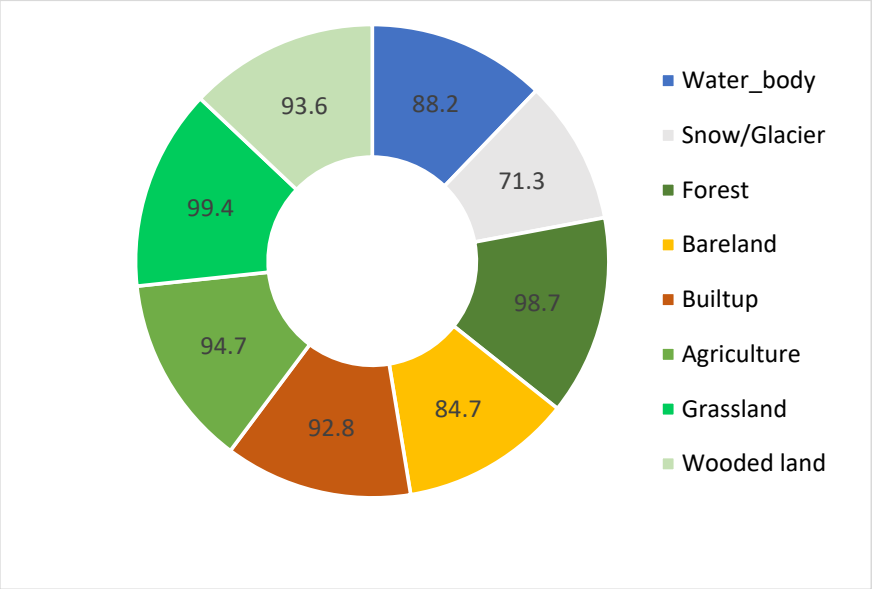

Figure 4. Accuracy of predicted model for individual land use types.

3.3. Carbon Storage and Sequestration in Nepal

Table 3 offers a comprehensive overview of carbon storage and sequestration in Nepal's diverse landscapes across different land use types for three distinct years. Figure 5 visually depicts the rate of change in carbon storage over specified time intervals. In 2000, the total carbon storage stood at 1.237 billion tons, increasing to 1.271 billion tons in 2019 with a projected rise to 1.347 billion tons in 2050. Forests play a crucial role, contributing significantly with carbon storage of 927 million tons in the initial year, 985 million tons in 2019, and an expected 1047 million tons in 2050. Grasslands follow suit, with approximately 149 million tons in 2000, 120 million tons in 2019, and an estimated 115 million tons in 2050. Agriculture land stored 69.4 million tons in 2000, 67.07 million tons in 2019, and an

anticipated 73.05 million tons in 2050. Notably, carbon storage in forests increased by 6.3% from 2000 to 2019, whereas grasslands experienced a 19.9% decrease, and agricultural land witnessed a substantial 3.4% decrease in carbon storage during the same period. Looking ahead to the 2019–2050 period, forest and bare land storage are anticipated to grow by 6.2% and 50%, respectively. Waterbodies and snow/glacier land types exhibit low carbon storage, each holding less than 7.6 million tons of carbon. Waterbodies display a 5.7% increase from 2000 to 2019 but a 51% decrease for 2019 to 2050, whereas snow/glacier storage increases by 26.9% and decrease by 21.9% in the respective periods. Bare land and built-up areas had storage of 48.4 and 16.2 million tons, respectively, in 2000, and projected increases by 50% and decrease by 10.1% in 2019–2050, expected to reach 60 and 26.1 million tons, respectively.

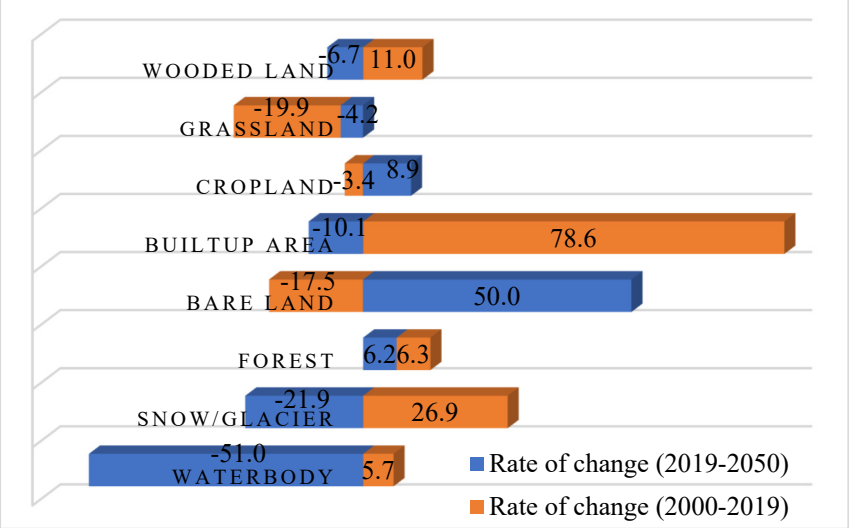

Figure 5. Proportion of change in carbon storage over different periods.

Between 2000 and 2019, total carbon sequestration was 34.141, which will be increased to 76 million tons in the projected 2019–2050 period, a remarkable increase. Bare land and cropland initially experienced decreases but are anticipated to rebound in 2019–2050. The carbon sequestration in both time intervals is positive at 58.2 million and 61.4 million tons in forest, which is major source of atmospheric carbon sequestration.

Table 3. Total carbon storage and sequestration in Nepal at different time intervals.

LULC Type	Carbon Storage_2050 (Tons)	Carbon Storage_2019 (Tons)	Carbon Storage_2000 (Tons)	Carbon Sequestration (2019–2050) (Tons)	Carbon Sequestration (2000–2019) (Tons)
Waterbody	338,242.8	690,891	653,862.6	−352,648.2	37,028.4
Snow/glacier	6,000,000	7,685,170.9	6,055,617.5	−1,685,170.9	1,629,553.4
Forest	1,047,090,863	985,614,088	927,336,647.4	61,476,774.5	58,277,440.6
Bare land	60,000,000	40,000,000	48,489,857.6	20,000,000	−8,489,857.6
Built-up area	26,112,506.3	29,049,802.2	16,266,090.9	−2,937,295.9	12,783,711.3
Cropland	73,052,858.3	67,079,110	69,452,611.8	5,973,748.3	−2,373,501.8
Grassland	115,000,000	120,000,000	149,822,066.6	−50,000,00	−29,822,066.6
Wooded land	19,710,590	21,115,590	19,016,129.4	−1,405,000	2,099,460.6
Total	**1,347,305,060**	**1,271,234,652**	**1,237,092,884**	**76,070,407.8**	**34,141,768.3**

3.4. Economic Loss and Gain from Carbon Sequestration

Figure 6 outlines the economic valuation of overall carbon sequestration in Nepal for two distinct periods, calculated by summing the loss and gain of carbon in three regions:

Terai, Hill, and Mountain. The total price of sequestered carbon in the 2000–2019 interval was 110.9 million US dollars, projected to increase more than threefold to 378.64 million US dollars in the 2019–2050 interval.

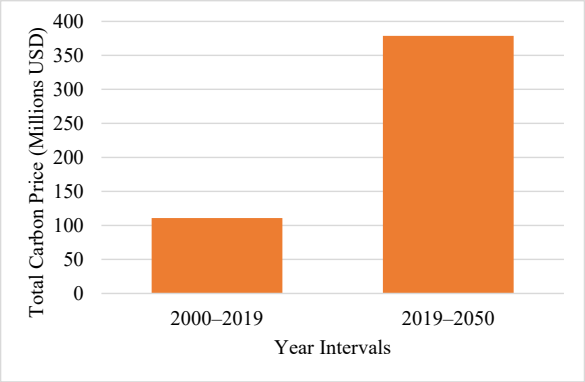

Figure 6. Economic valuation of sequestrated carbon over different periods.

3.5. Spatial Distribution of Carbon Storage in Different Years

A 30 m × 30 m grid was employed to create a carbon storage map in Nepal, ranging from 0 to 24 tons per grid cell. Carbon storage was categorized into classes ranging from "no carbon" to "very high carbon" using natural breaks (Jenk) classification in ArcGIS. Specifically, the classification scheme was as follows: 0 tons as no carbon, 0–1.16 tons as very low, 1.16–3.95 tons as low, 3.95–8 tons as moderate, 8–12.9 tons as high, and 12.9–24 tons as very high. Over the years 2000 to 2050, areas with very high carbon storage were prominent in the Chure range, hills, and mountains (excluding snow and glaciers). Land use changes were evident, with regions initially high in carbon storage shifting to moderate and low in 2019, projected to return to high in 2050. Notably, areas with very low carbon storage were predominantly found in agricultural lands in the terai and hilly regions, as shown in Figure 7.

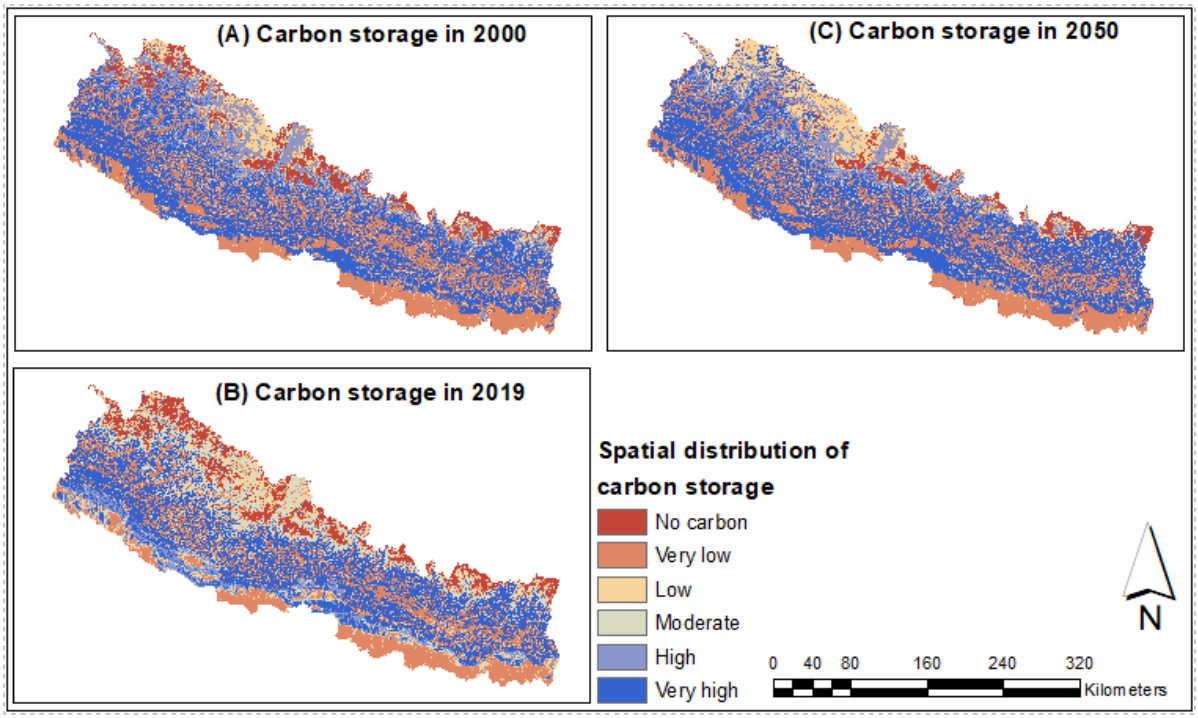

Figure 7. Spatial distribution of carbon storage in different years.

3.6. Spatial Cluster Characteristics of Carbon Storage

The carbon storage maps of 2000, 2019, and 2050 were gridded with a grid size of 30 m × 30 m, and the Moran's I index at the grid scale was calculated (Table 4). The Moran's value was greater than 0.4, $p < 0.001$ in all three years, indicating a significant spatial positive correlation and spatial cluster effect in the distribution of carbon storage in the study area. The significantly high Z-score of Z > 332, along with the low p value for study years, strongly supports the rejection of the null hypothesis of spatial randomness for carbon storage. In essence, the carbon storage map exhibits a robust and meaningful spatial structure, with carbon storage values displaying a notable tendency to spatially coalesce rather than being randomly dispersed across the landscape.

Table 4. Global Moran's I of carbon storage in different years.

Year	Moran's I	Z	*p*
2000	0.4444	336.19	0.00
2019	0.454	343.46	0.00
2050	0.4392	332.24	0.00

4. Discussions

Compared to prior research, our study observes a prevalent use of the CA-Markov chain for land use change prediction, coupled with InVEST models for carbon sequestration, as it consistently yields highly accurate results [16,20,23,50,51]. However, alternative studies [18,22] have employed CLUE-S and MOLUSCE for land use prediction. Notably, driver variables play a crucial role in predicting land use. For instance, ref. [21] incorporated elevation, slope, distance from roads, and distance from urban areas, whereas [17] considered factors such as distance from roads, water bodies, city headquarters, and conservation unit distances. In our study, we incorporated distance from roads, rivers, settlements, slope, elevation, and transmission lines, a factor particularly pertinent to Nepal. During disturbance factor selection, some studies [21] excluded factors with Cramer's V values below 0.15. We included disturbance factors with values higher and lower than 0.15 owing to our larger study area, aligning with the approach of others [23,52].

Investigating carbon sequestration within diverse land use types in the natural landscape represents a pivotal approach to conserving and managing natural resources, given its inherent role as a natural regulatory process [16,21]. The assessment of sequestered carbon, coupled with future projections, serves as a tangible indicator of national commitment to mitigating atmospheric carbon emissions. Studying the total carbon stock and projecting its future levels is crucial for the effective management of landscape based ESs and the development of strategies to achieve the government of Nepal's target of zero emissions by 2050. Additionally, spatial distribution and economic analyses play a crucial role in facilitating carbon trading and generating revenue, particularly for communities situated in areas with elevated carbon concentrations. Realizing the importance of sequestered carbon assessment and its trade potential, we utilized the InVEST model to predict carbon storage and sequestration across three distinct scenarios: 2000, 2019, and the projected LULC for 2050. Our findings highlight the significance of forested areas in Nepal as primary contributors to carbon storage and sequestration across all three periods, potentially aiding in global warming aligning with national commitment for emission reduction. Our projections suggest an upward trend in carbon sequestration compared to previous intervals, with economic gains anticipated to exceed threefold.

The terrestrial ecosystem's carbon cycle is directly or indirectly impacted by land use practices, given that it serves as a significant source and sink of carbon [53]. Accurate LULC mapping is a crucial input for measuring carbon sequestration using the InVEST model [15]. In this study, the predicted land use accuracy exceeded 90%, which was attributed to the use of a base year LULC map prepared by ICIMOD.

In our study, the observed increase in forest, bare land, and agriculture is attributed to anticipated land use transitions from snow/glaciers and grassland in the future. Despite forest land covering less than half of the total land, it consistently contributes to over three-quarters of the total carbon storage owing to its high atmospheric carbon sequestration capacity. Forests serve as effective carbon sinks through above- and below-ground biomass, as well as soil carbon, including decomposed organic matter.

The projected results of the study indicate that water bodies, snow/glaciers, built-up areas, wooded land (shrub land), and grasslands will decrease their carbon sequestration and carbon storage, whereas forests, croplands, and bare lands will potentially increase their carbon sequestration and carbon storage. This trend is positively correlated with changes in land use type over the projected timeframe [54]. The study [31] explains that in past decades in Nepal, grasslands have decreased due to harsh climatic conditions, poor management, and overgrazing. Several studies report that snow, glaciers, and water resources in the mountainous regions of Nepal are directly affected by climatic conditions and are highly sensitive to increases in global temperatures, which will likely accelerate the decline of these land types in the future [55,56]. There is a higher probability of converting shrubs into forests or agricultural land and built-up areas into bare lands due to high migration of people from rural to core city areas. The increase in forest land use in Nepal, both in the past and projected for the future, is attributed to the strict implementation of forest management policies during construction and development activities, as well as reduced intervention by local communities in the forests [57]. Studies in specific areas of Pakistan, Brazil, and China indicate that carbon storage will increase in forest and agricultural lands due to high carbon density and efforts to preserve natural resources [16,58,59] Conversely, the study in Iran presents that carbon loss occurs due to the shift from natural land cover to anthropogenic land cover and vice versa [60].

The distribution patterns of carbon storage, both historical and predicted, demonstrate significant clustering, with notably high carbon storage in specific parts of the terai and mountain regions, and most hilly regions, including the Chure. This concentration is attributed to extensive forest coverage, and our assumption regarding input values for carbon pooling remains consistent across all forest categories. This assumption aligns similarly with other land use types in the study area.

The findings of our study reveal exceptionally high carbon storage in forest landscapes, which is attributed to substantial carbon pooling values and extensive coverage. From 2000 to 2050, the total carbon storage in Nepal is projected from 1.237 to 1.347 billion tons, with forests making a significant contribution. Our study estimated the aggregate carbon storage in forest and wooded land in 2000 at 946.35 million tons, aligning closely with the 961 million tons calculated by [10]. Moreover, our study calculated the economic value of sequestered carbon using a carbon rate of US $5 per ton of CO_2 equivalent, following the agreement between the Nepal government and the World Bank for carbon trade [61]. We adopted a discount rate of 3% and an annual rate of change of price of zero, consistent with the approach taken by [21].

Numerous studies have underscored a significant transformation in land use across Nepal over the past two to three decades, driven by factors such as a high rate of migration, rural road construction, and escalating population density [62]. Although existing research in Nepal predominantly concentrates on carbon sequestration within forests in the current timeframe [10,30,63], a limited number of studies have delved into soil carbon measurement within specific geographic areas [64]. Notably, a research gap exists in presenting a comprehensive assessment of total carbon storage and sequestration across various land uses in Nepal, along with a lack of future predictions. In addition, essential information concerning the monetary value associated with carbon loss and sequestration, including the spatial distribution of carbon storage in Nepal's landscape, remains absent. This research aims to address such gaps in studies conducted in Nepal.

Managing carbon in the landscape involves essential details, such as the spatial distribution of carbon, annual carbon sequestration/loss, and the impact of land use

changes on carbon sequestration [21]. This study provides necessary information for carbon management in Nepal's landscape, offering insights into the status of carbon distribution and the consequences of land use changes on carbon sequestration. Aligning with Nepal's commitment on emission reduction, this research aids in planning sustainable measures to mitigate human-induced development activities that lead to forest degradation. Additionally, this study encourages the adoption of sustainable alternative energy sources in local communities, thereby reducing reliance on fuelwood. In addition, quantifying ecosystem services in monetary terms and assessing their concentration in the landscape are important tools for the government and stakeholders engaged in carbon financing. This approach facilitates the provision of fair incentives to local communities, raising awareness among the populace about the importance of protecting forests and promoting plantation initiatives.

5. Conclusions

This study investigates the carbon storage dynamics in Nepal's landscape from 2000 to 2050 using the InVEST model. Despite its limitations, such as an oversimplified carbon cycle representation and the assumption of constant carbon pools, the model provided valuable insights into carbon storage trends across diverse land use types. This study utilized carbon pool data from similar studies and categorized the analysis into three distinct regions—Terai, Hill, and Mountain (Supplementary Materials)—each with unique features and varying carbon densities in forests and soil, thereby allowing for a more nuanced and accurate analysis of carbon storage across diverse landscapes of Nepal. Key findings reveal that by 2050, forests will cover 41.83% of Nepal's land, making them the primary contributor to carbon storage, followed by grasslands. The total carbon storage is projected to range from 1.237 to 1.347 billion tons, with annual sequestration ranging from 34.14 to 76 million tons. Significant carbon concentrations were identified in the Terai, hilly regions, and mountains. The economic valuation of carbon storage showed an increase from 110.909 million USD in 2000 to a projected 3.4-fold increase by 2050.

For future studies, it is recommended to expand the research including comparative analyses with similar ecosystems in other regions or countries. This will address the limitations of the InVEST model, validate the methodology, and enhance understanding of global carbon dynamics. Such expansion will increase the applicability of our findings, aiding policymakers and scientists in implementing effective strategies for sustainable land use and climate change mitigation.

Policy Recommendations

Based on the findings, the study proposes the following policy implications for governing bodies of Nepal to develop effective environmental, energy and forest management policies to achieve zero emission determination.

- Community-Based Conservation Incentives: In Nepal, forest management has evolved from primarily government-based practices to community-driven approaches since the implementation of the "*Panchayat Forest*" system in 1978 and the 1988 forest sector master plan. Recognized as a role model in Asia, this shift signifies the importance of local community involvement in forest conservation and carbon restoration. This study suggests the need for the Nepalese government to implement targeted incentive programs for local communities, which could include financial rewards for forest conservation, community development funds tied to conservation results, and initiatives focused on capacity building of local communities;
- Policy Framework for Sustainable Land Use: The study recommends the development of a comprehensive policy framework encompassing this finding to promote sustainable land use for both ecological sustainability and economic development;
- Carbon Credit Mechanisms: This study recommends the establishment of national carbon credit mechanisms encompassing all land use types strengthening to $REDD^{+}$ based on these findings on carbon sequestration. The mechanism would facilitate

Nepal's participation in international carbon markets, offering economic incentives for the preservation and improvement of carbon stocks;

- ❖ Public-Private Partnerships for Conservation: The study recommends the promotion of public-private partnerships that focus on conservation and sustainable land use (converting bare land into agroforestry). This approach can leverage private sector resources and expertise, augmenting governmental efforts in environmental stewardship;
- ❖ Expand Biogas Infrastructure: Promote the installation of biogas plants in rural communities, providing an eco-friendly alternative to traditional biomass fuels. This will reduce dependence on firewood and mitigate deforestation;
- ❖ Subsidies for Hydroelectricity Use in Rural Communities: Offer subsidies and declare free electricity of certain units to encourage the use of hydroelectricity for cooking and other household purposes in rural areas. This will decrease the frequency of forest visits for fuelwood, thus preserving forest resources;
- ❖ Implement Emission Charges: Impose emission charges on vehicles and industries that use petroleum products to incentivize the shift towards cleaner energy sources;
- ❖ Addressing GHG Emissions from Waste: In Nepal, greenhouse gas emissions from open dumping of waste pose a significant problem. Converting municipal waste to energy is an effective solution to reduce these emissions and manage waste sustainably.

The policy suggestions of this study, given their scalability and adaptability, could be effectively applied in other regions with similar ecological and socio-economic challenges. The study encourages governments in these areas to tailor and adopt these recommendations according to their unique circumstances.

Supplementary Materials: The following supporting information can be downloaded at: https://www.mdpi.com/article/10.3390/su16177377/s1, Carbon Pools in Terai, Hill, and Mountain.

Author Contributions: Methodology, software, conceptualization, data curation, formal analysis, investigation, writing—original draft, D.C.; conceptualization, editing, revision, R.L.R.; editing, A.O.Y. and J.P.; data analysis, N.N.S.; software, D.S. and J.-O.L.; investigation, supervision, funding acquisition, J.-S.H. All authors have read and agreed to the published version of the manuscript.

Funding: This work was supported by the National Research Foundation of Korea (NRF) grant funded by the Korea government (MIST) [grant number NRF-2021R1A5A8033165]; the Korea Institute of Energy Technology Evaluation and Planning (KETEP); and the Ministry of Trade, Industry & Energy (MOTIE) of the Republic of Korea [grant number 20224000000150].

Institutional Review Board Statement: Not applicable.

Informed Consent Statement: Not applicable.

Data Availability Statement: The original contributions presented in the study are included in the article/supplementary material, further inquiries can be directed to the corresponding author.

Conflicts of Interest: The authors declare that they have no known competing financial interests or personal relationships that could have appeared to influence the work reported in this paper.

References

1. What Is Carbon Capture and Storage? | CCS Explained | National Grid Group. Available online: https://www.nationalgrid.com/stories/energy-explained/what-is-ccs-how-does-it-work (accessed on 5 August 2024).
2. Fryer, J.; Williams, I.D. Regional carbon stock assessment and the potential effects of land cover change. *Sci. Total Environ.* **2021**, *775*, 145815. [CrossRef]
3. Chen, D.; Jiang, P.; Li, M. Assessing potential ecosystem service dynamics driven by urbanization in the Yangtze River Economic Belt, China. *J. Environ. Manag.* **2021**, *292*, 112734. [CrossRef] [PubMed]
4. Fan, L.; Cai, T.; Wen, Q.; Han, J.; Wang, S.; Wang, J.; Yin, C. Scenario simulation of land use change and carbon storage response in Henan Province, China: 1990–2050. *Ecol. Indic.* **2023**, *154*, 110660. [CrossRef]
5. Guo, Y.; Ren, Z.; Wang, C.; Zhang, P.; Ma, Z.; Hong, S.; Hong, W.; He, X. Spatiotemporal patterns of urban forest carbon sequestration capacity: Implications for urban CO_2 emission mitigation during China's rapid urbanization. *Sci. Total. Environ.* **2024**, *912*, 168781. [CrossRef] [PubMed]

6. Abdo, Z.A.; Satyaprakash. Modeling urban dynamics and carbon sequestration in Addis Ababa, Ethiopia, using satellite images. *Arab. J. Geosci.* **2021**, *14*, 445. [CrossRef]
7. Huang, J.; Chen, Q.; Wang, Q.; Gao, J.; Yin, Y.; Guo, H. Future carbon storages of ecosystem based on land use change and carbon sequestration practices in a large economic belt. *Environ. Sci. Pollut. Res.* **2023**, *30*, 90924–90935. [CrossRef] [PubMed]
8. Alaoui, H.I.; Chemchaoui, A.; El Asri, B.; Ghazi, S.; Brhadda, N.; Ziri, R. Modeling predictive changes of carbon storage using invest model in the Beht watershed (Morocco). *Model. Earth Syst. Environ.* **2023**, *9*, 4313–4322. [CrossRef]
9. Khanal, Y.; Sharma, R.; Upadhyaya, C. Soil and vegetation carbon pools in two community forests of Palpa district, Nepal. *Banko Janakari* **1970**, *20*, 34–40. [CrossRef]
10. Nath Oli, B.; Shrestha, K. Carbon Status in Forests of Nepal: An Overview. *J. For. Livelihood* **2009**, *8*, 62–66.
11. Sannigrahi, S.; Zhang, Q.; Joshi, P.; Sutton, P.C.; Keesstra, S.; Roy, P.; Pilla, F.; Basu, B.; Wang, Y.; Jha, S.; et al. Examining effects of climate change and land use dynamic on biophysical and economic values of ecosystem services of a natural reserve region. *J. Clean. Prod.* **2020**, *257*, 120424. [CrossRef]
12. Adams, A.B.; Pontius, J.; Galford, G.L.; Merrill, S.C.; Gudex-Cross, D. Modeling carbon storage across a heterogeneous mixed temperate forest: The influence of forest type specificity on regional-scale carbon storage estimates. *Landsc. Ecol.* **2018**, *33*, 641–658. [CrossRef]
13. Pechanec, V.; Purkyt, J.; Benc, A.; Nwaogu, C.; Štěrbová, L.; Cudlín, P. Modelling of the carbon sequestration and its prediction under climate change. *Ecol. Inform.* **2018**, *47*, 50–54. [CrossRef]
14. Chhabra, A.; Palria, S.; Dadhwal, V. Growing stock-based forest biomass estimate for India. *Biomass-Bioenergy* **2002**, *22*, 187–194. [CrossRef]
15. Hernández-Guzmán, R.; Ruiz-Luna, A.; González, C. Assessing and modeling the impact of land use and changes in land cover related to carbon storage in a western basin in Mexico. *Remote Sens. Appl. Soc. Environ.* **2019**, *13*, 318–327. [CrossRef]
16. Zhao, M.; He, Z.; Du, J.; Chen, L.; Lin, P.; Fang, S. Assessing the effects of ecological engineering on carbon storage by linking the CA-Markov and InVEST models. *Ecol. Indic.* **2019**, *98*, 29–38. [CrossRef]
17. Fernandes, M.M.; Fernandes, M.R.d.M.; Garcia, J.R.; Matricardi, E.A.T.; de Almeida, A.Q.; Pinto, A.S.; Menezes, R.S.C.; Silva, A.d.J.; Lima, A.H.d.S. Assessment of land use and land cover changes and valuation of carbon stocks in the Sergipe semiarid region, Brazil: 1992–2030. *Land Use Policy* **2020**, *99*, 104795. [CrossRef]
18. Zhang, F.; Xu, N.; Wang, C.; Wu, F.; Chu, X. Effects of land use and land cover change on carbon sequestration and adaptive management in Shanghai, China. *Phys. Chem. Earth* **2020**, *120*, 102948. [CrossRef]
19. Zhang, Z.; Jiang, W.; Peng, K.; Wu, Z.; Ling, Z.; Li, Z. Assessment of the impact of wetland changes on carbon storage in coastal urban agglomerations from 1990 to 2035 in support of SDG15.1. *Sci. Total Environ.* **2023**, *877*, 162824. [CrossRef] [PubMed]
20. Hoque, M.Z.; Cui, S.; Islam, I.; Xu, L.; Ding, S. Dynamics of plantation forest development and ecosystem carbon storage change in coastal Bangladesh. *Ecol. Indic.* **2021**, *130*, 107954. [CrossRef]
21. Babbar, D.; Areendran, G.; Sahana, M.; Sarma, K.; Raj, K.; Sivadas, A. Assessment and prediction of carbon sequestration using Markov chain and InVEST model in Sariska Tiger Reserve, India. *J. Clean. Prod.* **2021**, *278*, 123333. [CrossRef]
22. Saha, S.; Bera, B.; Shit, P.K.; Bhattacharjee, S.; Sengupta, N. Estimation of carbon budget through carbon emission-sequestration and valuation of ecosystem services in the extended part of Chota Nagpur Plateau (India). *J. Clean. Prod.* **2022**, *380*, 135054. [CrossRef]
23. Verma, P.; Siddiqui, A.R.; Mourya, N.K.; Devi, A.R. Forest carbon sequestration mapping and economic quantification infusing MLPnn-Markov chain and InVEST carbon model in Askot Wildlife Sanctuary, Western Himalaya. *Ecol. Inform.* **2024**, *79*, 102428. [CrossRef]
24. Xiang, M.; Wang, C.; Tan, Y.; Yang, J.; Duan, L.; Fang, Y.; Li, W.; Shu, Y.; Liu, M. Spatio-temporal evolution and driving factors of carbon storage in the Western Sichuan Plateau. *Sci. Rep.* **2022**, *12*, 8114. [CrossRef] [PubMed]
25. Nasiri, V.; Darvishsefat, A.A.; Rafiee, R.; Shirvany, A.; Hemat, M.A. Land use change modeling through an integrated Multi-Layer Perceptron Neural Network and Markov Chain analysis (case study: Arasbaran region, Iran). *J. For. Res.* **2019**, *30*, 943–957. [CrossRef]
26. Liang, Y.; Liu, L.; Huang, J. Integrating the SD-CLUE-S and InVEST models into assessment of oasis carbon storage in northwestern China. *PLoS ONE* **2017**, *12*, e0172494. [CrossRef]
27. Guan, D.; Zhao, Z.; Tan, J. Dynamic simulation of land use change based on logistic-CA-Markov and WLC-CA-Markov models: A case study in three gorges reservoir area of Chongqing, China. *Environ. Sci. Pollut. Res.* **2019**, *26*, 20669–20688. [CrossRef]
28. Liang, X.; Liu, X.; Li, X.; Chen, Y.; Tian, H.; Yao, Y. Delineating multi-scenario urban growth boundaries with a CA-based FLUS model and morphological method. *Landsc. Urban Plan.* **2018**, *177*, 47–63. [CrossRef]
29. Tao, Y.; Tian, L.; Wang, C.; Dai, W. Dynamic simulation of land use and land cover and its effect on carbon storage in the Nanjing metropolitan circle under different development scenarios. *Front. Ecol. Evol.* **2023**, *11*, 1102015. [CrossRef]
30. Upadhyay, T.; Sankhayan, P.L.; Solberg, B. A review of carbon sequestration dynamics in the Himalayan region as a function of land-use change and forest/soil degradation with special reference to Nepal. *Agric. Ecosyst. Environ.* **2005**, *105*, 449–465. [CrossRef]
31. Paudel, B.; Zhang, Y.L.; Li, S.C.; Liu, L.S.; Wu, X.; Khanal, N.R. Review of studies on land use and land cover change in Nepal. *J. Mt. Sci.* **2016**, *13*, 643–660. [CrossRef]

32. Collins, R.; Jenkins, A. The impact of agricultural land use on stream chemistry in the Middle Hills of the Himalayas, Nepal. *J. Hydrol.* **1996**, *185*, 71–86. [CrossRef]
33. Paudel, B.; Adhikari, B.R. Land Use and Land Cover. In *The Soils of Nepal*; Springer: Cham, Switzerland, 2021; pp. 41–51. [CrossRef]
34. Rimal, B.; Sharma, R.; Kunwar, R.; Keshtkar, H.; Stork, N.E.; Rijal, S.; Rahman, S.A.; Baral, H. Effects of land use and land cover change on ecosystem services in the Koshi River Basin, Eastern Nepal. *Ecosyst. Serv.* **2019**, *38*, 100963. [CrossRef]
35. Bastola, S.; Lee, S.; Shin, Y.; Jung, Y. An assessment of environmental impacts on the ecosystem services: Study on the Bagmati Basin of Nepal. *Sustainability* **2020**, *12*, 8186. [CrossRef]
36. Zhu, G.; Qiu, D.; Zhang, Z.; Sang, L.; Liu, Y.; Wang, L.; Zhao, K.; Ma, H.; Xu, Y.; Wan, Q. Land-use changes lead to a decrease in carbon storage in arid region, China. *Ecol. Indic.* **2021**, *127*, 107770. [CrossRef]
37. Rahnama, M.R. Forecasting land-use changes in Mashhad Metropolitan area using Cellular Automata and Markov chain model for 2016–2030. *Sustain. Cities Soc.* **2021**, *64*, 102548. [CrossRef]
38. Atef, I.; Ahmed, W.; Abdel-Maguid, R.H. Future land use land cover changes in El-Fayoum governorate: A simulation study using satellite data and CA-Markov model. *Stoch. Environ. Res. Risk Assess.* **2023**, *38*, 651–664. [CrossRef]
39. Khanal, S.; Nolan, R.H.; Medlyn, B.E.; Boer, M.M. Mapping soil organic carbon stocks in Nepal's forests. *Sci. Rep.* **2023**, *13*, 8090. [CrossRef]
40. Map of Nepal | Everything about Nepal Map with 25 HD Images. Available online: https://www.imnepal.com/map-nepal/ (accessed on 17 January 2024).
41. Baniya, B.; Tang, Q.; Pokhrel, Y.; Xu, X. Vegetation dynamics and ecosystem service values changes at national and provincial scales in Nepal from 2000 to 2017. *Env. Dev.* **2019**, *32*, 100464. [CrossRef]
42. Vaidya, S.N.; Sherchan, D.P.; Tiwari, K.R.; Subedi, S.; Karki, K.B.; Panday, D.; Ojha, R.B. Soil Types, Soil Classification, and Mapping. In *The Soils of Nepal*; Springer: Cham, Switzerland, 2021; pp. 63–90. [CrossRef]
43. National Population and Housing Census 2021 Results. Available online: https://censusnepal.cbs.gov.np/results (accessed on 5 August 2024).
44. Mapping Land Cover—ICIMOD. Available online: https://www.icimod.org/success-stories/chapter-2/mapping-land-cover/ (accessed on 11 January 2024).
45. EarthExplorer. Available online: https://earthexplorer.usgs.gov (accessed on 7 July 2017).
46. ICIMOD | RDS. Available online: https://rds.icimod.org/DatasetMasters/Download/3620 (accessed on 7 July 2024).
47. Settlements in Nepal—Humanitarian Data Exchange. Available online: https://data.humdata.org/dataset/settlements-in-nepal? (accessed on 7 July 2024).
48. Nepal—Electricity Transmission Network—Dataset—ENERGYDATA.INFO. Available online: https://energydata.info/dataset/nepal-electricity-transmission-network-2013 (accessed on 7 July 2024).
49. Eggleston, H.S.; Intergovernmental Panel on Climate Change. National Greenhouse Gas Inventories Programme, and Chikyū Kankyō Senryaku Kenkyū Kikan, 2006 IPCC Guidelines for National Greenhouse Gas Inventories. Available online: https://www.osti.gov/etdeweb/biblio/20880391 (accessed on 20 July 2024).
50. Sahle, M.; Saito, O.; Fürst, C.; Demissew, S.; Yeshitela, K. Future land use management effects on ecosystem services under different scenarios in the Wabe River catchment of Gurage Mountain chain landscape, Ethiopia. *Sustain. Sci.* **2019**, *14*, 175–190. [CrossRef]
51. Yang, Y.; Lu, Z.; Yang, M.; Yan, Y.; Wei, Y. Impact of land use changes on uncertainty in ecosystem services under different future scenarios: A case study of Zhang-Cheng area, China. *J. Clean. Prod.* **2024**, *434*, 139881. [CrossRef]
52. Rajbanshi, J.; Das, S. Changes in carbon stocks and its economic valuation under a changing land use pattern—A multitemporal study in Konar catchment, India. *Land Degrad. Dev.* **2021**, *32*, 3573–3587. [CrossRef]
53. Wang, Y.; Liang, D.; Wang, J.; Zhang, Y.; Chen, F.; Ma, X. An analysis of regional carbon stock response under land use structure change and multi-scenario prediction, a case study of Hefei, China. *Ecol. Indic.* **2023**, *151*, 110293. [CrossRef]
54. Rijal, S.; Rimal, B.; Acharya, R.P.; Stork, N.E. Land use/land cover change and ecosystem services in the Bagmati River Basin, Nepal. *Environ. Monit. Assess.* **2021**, *193*, 651. [CrossRef] [PubMed]
55. Khadka, D.; Babel, M.S.; Shrestha, S.; Tripathi, N.K. Climate change impact on glacier and snow melt and runoff in Tamakoshi basin in the Hindu Kush Himalayan (HKH) region. *J. Hydrol.* **2014**, *511*, 49–60. [CrossRef]
56. Molden, D.J.; Shrestha, A.B.; Immerzeel, W.W.; Maharjan, A.; Rasul, G.; Wester, P.; Wagle, N.; Pradhananga, S.; Nepal, S. The Great Glacier and Snow-Dependent Rivers of Asia and Climate Change: Heading for Troubled Waters. In *Water Security Under Climate Change*; Springer: Singapore, 2022; pp. 223–250. [CrossRef]
57. Chhetri, R.; Yokying, P.; Smith, A.; Hoek, J.V.D.; Hurni, K.; Saksena, S.; Fox, J. Forest, agriculture, and migration: Contemplating the future of forestry and agriculture in the middle-hills of Nepal. *J. Peasant. Stud.* **2023**, *50*, 411–433. [CrossRef]
58. Bacani, V.M.; da Silva, B.H.M.; Sato, A.A.d.S.A.; Sampaio, B.D.S.; da Cunha, E.R.; Vick, E.P.; de Oliveira, V.F.R.; Decco, H.F. Carbon storage and sequestration in a eucalyptus productive zone in the Brazilian Cerrado, using the Ca-Markov/Random Forest and InVEST models. *J. Clean. Prod.* **2024**, *444*, 141291. [CrossRef]
59. Zafar, Z.; Zubair, M.; Zha, Y.; Mehmood, M.S.; Rehman, A.; Fahd, S.; Nadeem, A.A. Predictive modeling of regional carbon storage dynamics in response to land use/land cover changes: An InVEST-based analysis. *Ecol. Inform.* **2024**, *82*, 102701. [CrossRef]

60. Kohestani, N.; Kohestani, N.; Rastgar, S.; Rastgar, S.; Heydari, G.; Heydari, G.; Jouibary, S.S.; Jouibary, S.S.; Amirnejad, H.; Amirnejad, H. Spatiotemporal modeling of the value of carbon sequestration under changing land use/land cover using InVEST model: A case study of Nour-rud Watershed, Northern Iran. *Environ. Dev. Sustain.* **2023**, *26*, 14477–14505. [CrossRef]
61. Aryal, K.; Ojha, B.R.; Maraseni, T. Perceived importance and economic valuation of ecosystem services in Ghodaghodi wetland of Nepal. *Land Use Policy* **2021**, *106*, 105450. [CrossRef]
62. Ishtiaque, A.; Shrestha, M.; Chhetri, N. Rapid urban growth in the Kathmandu Valley, Nepal: Monitoring land use land cover DYNAMICS of a Himalayan City with landsat imageries. *Environments* **2017**, *4*, 72. [CrossRef]
63. Gurung, M.B.; Bigsby, H.; Cullen, R.; Manandhar, U. Estimation of carbon stock under different management regimes of tropical forest in the Terai Arc Landscape, Nepal. *For. Ecol. Manag.* **2015**, *356*, 144–152. [CrossRef]
64. Bishwakarma, B.; Dahal, N.; Allen, R.; Rajbhandari, N.; Dhital, B.; Gurung, D.; Bajracharya, R.; Baillie, I. Effects of improved management and quality of farmyard manure on soil organic carbon contents in small-holder farming systems of the Middle Hills of Nepal. *Clim. Dev.* **2015**, *7*, 426–436. [CrossRef]

Publications of Session 2025 - 2026

Jalal-Abad International University

SURVIVAL VS. RECURRENCE OF SUPRATENTORIAL MENINGIOMA AFTER SURGICAL RESECTION: PROGNOSTIC IMPACT OF SIMPSON GRADE IN ADULTS AGED

Dipak Chaulagain[1],[2]
[1]Uzhhorod National University, Uzhhorod, Ukraine
[2]Jalal-Abad International University, Jalal-Abad, Kyrgyzstan

Abstract

Background: Supratentorial meningiomas, accounting for a significant proportion of intracranial tumors in adults, are primarily managed through surgical resection. The Simpson grading system, a historical standard, classifies the extent of resection and its impact on recurrence and survival. This PRISMA-2020 compliant systematic literature review (SLR) investigates the prognostic role of Simpson grade on recurrence, overall survival (OS), progression-free survival (PFS), and quality of life (QOL) in adults aged 18–60, while comparing it with other factors such as tumor size, WHO grade, Ki-67 index, peritumoral edema, tumor location, and adjuvant radiotherapy (RT).

Methods: PubMed, Google Scholar, and Cochrane databases were searched for studies published between 2019 and 2024. Inclusion criteria encompassed cohort studies of adults aged 18–60 with supratentorial meningioma treated by surgical resection, reporting outcomes of recurrence, OS, PFS, or QOL. Exclusions included case reports, series with fewer than 10 patients, pediatric (<18), elderly-only (>60), or infratentorial/skull base-only cohorts. Data on study characteristics, prognostic factors, and outcomes were extracted. Narrative synthesis was performed due to heterogeneity; meta-analysis was not feasible.

Results: From 120 identified records, 5 studies (n=1,250 patients) were included. Simpson grades I/II were associated with lower recurrence rates (hazard ratio [HR] 2.0–2.5) and improved PFS (median 86–92 vs. 60–70 months for grades III–V). WHO grades II/III and Ki-67 >5% were stronger predictors of recurrence in multivariate analyses. Limited QOL data indicated improved seizure control with complete resection. Adjuvant RT enhanced PFS in incomplete resections. OS differences were minimal in low-grade tumors.

Conclusion: Simpson grade remains a significant prognostic factor for recurrence and PFS, but its impact is modulated by tumor biology. This SLR provides evidence-based insights, contrasting narrative reviews by focusing on recent, population-specific data. Future studies should integrate molecular markers and standardized QOL metrics for enhanced prognostication.

Keywords: Supratentorial meningioma, Simpson grade, recurrence, surgical resection, prognostic factors

ВЫЖИВАЕМОСТЬ И РЕЦИДИВ СУПРАТЕНТОРИАЛЬНОЙ МЕНИНГИОМЫ ПОСЛЕ ХИРУРГИЧЕСКОЙ РЕЗЕКЦИИ: ПРОГНОСТИЧЕСКОЕ ЗНАЧЕНИЕ СТЕПЕНИ ЗЛОКАЧЕСТВЕННОСТИ ПО СИМПСОНУ У ВЗРОСЛЫХ

Дипак Чаулагаин[1],[2]
[1]Ужгородский национальный университет, Ужгород, Украина
[2]Джалал-Абадский международный университет, Джалал-Абад, Кыргызстан

Аннотация

Введение: Супратенториальные менингиомы, составляющие значительную долю внутричерепных опухолей у взрослых, лечатся преимущественно хирургическим путем. Система оценки по Симпсону, являющаяся историческим стандартом, классифицирует степень резекции и ее влияние на рецидив и выживаемость. В этом систематическом обзоре литературы (SLR), соответствующем требованиям PRISMA-2020, изучается прогностическая роль степени злокачественности по Симпсону в отношении рецидива, общей выживаемости (ОВ), выживаемости без прогрессирования (ВБП) и качества жизни (КЖ) у взрослых в возрасте 18–60 лет в сравнении с другими факторами, такими как размер опухоли, степень злокачественности по ВОЗ, индекс Ki-67, перитуморальный отек, локализация опухоли и адъювантная лучевая терапия (ЛТ).

Методы: Был проведен поиск исследований, опубликованных в период с 2019 по 2024 год, в базах данных PubMed, Google Scholar и Cochrane. Критерии включения включали когортные исследования взрослых в возрасте 18–60 лет с супратенториальной менингиомой, прошедших хирургическую резекцию, с указанием результатов рецидива, ОВ, ВБП или КЖ. Исключения включали описания случаев, серии с менее чем 10 пациентами, педиатрические (<18), только пожилые (>60) или только инфратенториальные/основание черепа когорты. Были извлечены данные о характеристиках исследований, прогностических факторах и исходах. Был выполнен нарративный синтез в связи с гетерогенностью; метаанализ был невозможен.

Результаты: Из 120 идентифицированных записей было включено 5 исследований (n=1250 пациентов). Степени I/II по Симпсону были связаны с более низкой частотой рецидивов (коэффициент риска [HR] 2,0–2,5) и улучшением ВБП (медиана 86–92 против 60–70 месяцев для степеней III–V). Степени II/III по ВОЗ и Ki-67 >5% были более сильными предикторами рецидива в многофакторном анализе. Ограниченные данные о качестве жизни указали на улучшение контроля над приступами при полной резекции. Адъювантная лучевая терапия улучшала ВБП при неполных резекциях. Различия в общей выживаемости были минимальными при опухолях низкой степени злокачественности.

Заключение: Степень злокачественности по Симпсону остается значимым прогностическим фактором рецидива и выживаемости без прогрессирования заболевания, но ее влияние регулируется биологией опухоли. В данном обзоре представлены основанные на фактических данных выводы, контрастирующие с обзорами, основанные на актуальных данных, характерных для данной популяции. В будущих исследованиях следует интегрировать молекулярные маркеры и стандартизированные показатели качества жизни для повышения прогностической эффективности.

Ключевые слова: супратенториальная менингиома, степень злокачественности по Симпсону, рецидив, хирургическая резекция, прогностические факторы.

Introduction:
Meningiomas are the most prevalent primary intracranial neoplasms, constituting 36–38% of all brain tumors in adults [1]. Supratentorial meningiomas, encompassing convexity, falcine, parasagittal, and sphenoid wing subtypes, account for approximately 70–80% of all meningiomas [2]. In adults aged 18–60, these tumors frequently present with symptoms such as headaches, seizures, motor deficits, or cognitive impairments, significantly impacting productivity, social functioning, and quality of life [3]. Surgical resection remains the cornerstone of treatment, aiming to achieve maximal tumor removal while minimizing neurological morbidity and recurrence risk [4].

Introduced in 1957, the Simpson grading system classifies the extent of resection based on macroscopic completeness: grade I involves complete tumor excision with removal of involved dura and bone; grade II includes dural coagulation without excision; grade III is gross total resection (GTR) without dural handling; grade IV is subtotal resection (STR); and grade V is biopsy only [4]. Historically, lower Simpson grades have been associated with reduced recurrence rates, with seminal studies reporting 9% recurrence for grade I, 19% for grade II, and 29% for grade III at 5 years [4]. However, advancements in neuroimaging (e.g., high-resolution MRI), microsurgical techniques, and adjuvant therapies have prompted re-evaluation of its prognostic utility, particularly for supratentorial meningiomas where anatomical accessibility often permits more complete resections compared to skull base tumors [5].

In younger adults (18–60), who typically exhibit fewer comorbidities and better surgical tolerance, achieving lower Simpson grades may yield significant benefits in recurrence prevention and functional preservation. However, other prognostic factors, including tumor size (>6 cm, associated with technical challenges), WHO grade (updated in 2016 and 2021 to incorporate molecular markers like TERT promoter mutations for grade III), Ki-67 proliferation index (>5%, indicating aggressive behavior), peritumoral edema (linked to seizures and neurological deficits), tumor location (convexity vs. eloquent areas), and adjuvant RT (recommended for incomplete resections or higher-grade tumors), may interact with or supersede the impact of resection extent [3, 6, 7]. For example, WHO grade II/III meningiomas exhibit recurrence rates of 30–50% even after GTR, compared to 10–20% for grade I [8].

Quality of life, often underexplored in survival-focused studies, is a critical consideration in this age group, where long-term functionality is paramount. Proxy measures such as seizure freedom, Karnofsky Performance Status (KPS), or patient-reported outcomes (e.g., SF-36) reflect postoperative functional status [9]. Recent evidence suggests that incomplete resections may lead to persistent symptoms, such as seizures or cognitive deficits, adversely affecting QOL [10].

This SLR has three objectives: (1) to evaluate the predictive role of Simpson grade (I–V) on recurrence, OS, PFS, and QOL in adults aged 18–60 with supratentorial meningioma; (2) to compare its prognostic strength with other factors like tumor size, WHO grade, and adjuvant RT; and (3) to contrast findings with existing systematic or narrative reviews. By focusing on studies from 2019–2024, this review incorporates recent advancements, including the WHO 2021 classification and modern surgical techniques, addressing gaps in age- and location-specific analyses.

Methods:

This SLR adhered to the PRISMA-2020 guidelines to ensure methodological rigor and transparency [11]. No protocol was pre-registered, but methods were predefined to maintain consistency.

Eligibility Criteria:

Population: Adults aged 18–60 with primary supratentorial meningioma (convexity, falcine, parasagittal, sphenoid wing, etc.); mixed-age cohorts with subgroup analyses for 18–60 were included.

Intervention: Surgical resection classified by Simpson grade, with or without adjuvant RT.

Comparators: Other prognostic factors, including tumor size, WHO grade (2016/2021), Ki-67 index, peritumoral edema, tumor location, and adjuvant RT.

Outcomes: Primary: tumor recurrence; Secondary: OS, PFS, QOL (e.g., SF-36, KPS, seizure freedom).

Study Types: Retrospective or prospective cohort studies with n⩾10; case reports, series with <10 patients, reviews, and animal studies were excluded.

Time Frame: Published January 1, 2019–December 31, 2024.

Language: English only.

Information Sources and Search Strategy: Databases searched included PubMed, Google Scholar, and Cochrane Library. The search string was: ("supratentorial meningioma" AND "Simpson grade" AND ("recurrence" OR "survival" OR "quality of life") AND "surgical resection") with date filters (2019–2024). Hand-searching of reference lists from included studies and relevant reviews supplemented the electronic search. No gray literature was included to maintain focus on peer-reviewed publications.

Selection Process: Two reviewers independently screened titles and abstracts using Rayyan software, a web-based platform for systematic review management. Disagreements were resolved through discussion and consensus. Full-text articles were retrieved and assessed for eligibility based on predefined criteria.

Data Collection and Items: Data were extracted using a standardized form capturing: study design, sample size, patient demographics (age range/mean, sex distribution), tumor characteristics (location, WHO grade, size, Ki-67 index), Simpson grades achieved, outcomes (recurrence rates, hazard ratios [HRs] for PFS/OS, QOL metrics), and risk of bias. The Newcastle-Ottawa Scale (NOS) was used to assess cohort study quality, focusing on selection, comparability, and outcome assessment.

Synthesis Methods: Due to clinical and methodological heterogeneity (e.g., varying follow-up durations, inconsistent outcome definitions), narrative synthesis was employed. Subgroup analyses by WHO grade and tumor location were conducted where data permitted. Meta-analysis was considered but deemed unfeasible due to insufficient comparable quantitative data (e.g., inconsistent HRs across studies for forest plots). Risk of bias assessments were integrated into the synthesis to contextualize findings.

Results:

Study Selection: The study selection process is summarized in the PRISMA-2020 flow diagram (Figure 1). A total of 120 records were identified: PubMed (n=50), Google Scholar (n=60),

and Cochrane Library (n=10). After removing 35 duplicates, 85 records were screened, and 40 were excluded due to irrelevance (e.g., non-meningioma focus, pre-2019 publication). Forty-five full-text articles were assessed for eligibility, with 30 excluded: 10 case reports, 10 infratentorial/skull base-only studies, 10 pediatric (<18) or elderly-only (>60) cohorts, and 10 for other reasons (e.g., non-English, non-cohort designs). Five studies were included, comprising 1,250 patients.

Prisma Protocol (2020) – Flow Diagram

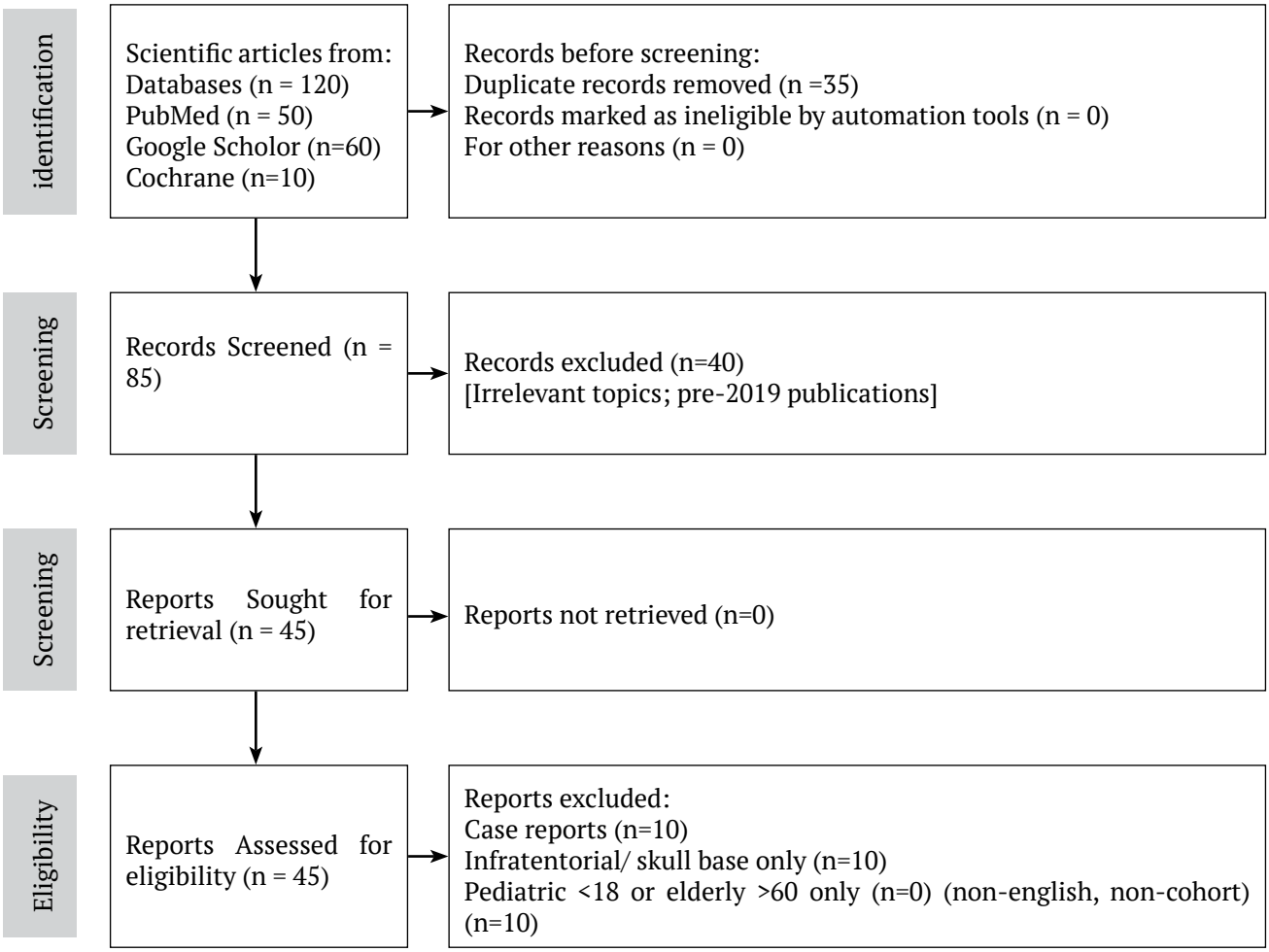

Note: Total included studies from all sources : n=5, Manual screening n=10; no automation tools used.
Adapted to PRISMA 2020 formate (Page Mj et al., BMJ 2021;372:n71, CC bY 4.0)

• *Figure1: PRISMA 2020 flow diagram illustrating the study selection process [11]*

Source: Adapted from Page et al. (2021), licensed under CC BY 4.0 (https://creativecommons.org/licenses/by/4.0/).

Study Characteristics: All included studies were retrospective cohorts, with NOS scores of 7–8, indicating good quality. The total sample size was 1,250 patients, with mean ages ranging from 45–55 years, either fully within or including subgroups of the 18–60 age range. All studies focused on supratentorial meningiomas.

• *Table 1: Characteristics of Included Studies*

Study	*Year*	*N*	*Population*	*Design*	*Outcomes Reported*
Schneider et al. [9]	2019	343	Adults (mean 57, subgroup 18–60) with supratentorial meningioma	Retrospective cohort	Seizure freedom (QOL proxy), recurrence
Nowak-Choi et al. [12]	2021	440	Adults 18–60 with WHO grade I meningioma (supratentorial subset)	Retrospective	Recurrence, OS
Gadot et al. [13]	2021	112	Adults (mean 52) with supratentorial meningioma	Retrospective	Seizure outcome, PFS
Spille et al. [14]	2022	250	Adults 18–60 with WHO grade I meningioma (supratentorial)	Retrospective	Recurrence, PFS
Driver et al. [15]	2024	105	Adults (mean 48, supratentorial subgroup)	Retrospective/ prospective mixed	PFS, OS, RT response

Prognostic Factors and Outcomes:

Data extraction revealed consistent associations between Simpson grade and outcomes, modulated by other prognostic factors.

• *Table 2: Prognostic Factors and Outcomes*

Factor	*Studies Reporting*	*Impact on Recurrence/PFS*	*Impact on OS*	*Impact on QOL*
Simpson Grade (I/II vs. III–V)	All 5 [9, 12–15]	Lower grades: 10–20% vs. 30–50% recurrence (HR 2.0–2.5, p<0.05); PFS 86–92 vs. 60–70 months	Minimal difference in WHO I (p>0.05); shorter in higher grades with STR (HR 1.5, p=0.04)	Improved seizure control (OR 2.2, p=0.003) [9, 13]; better KPS (p=0.02) [15]
WHO Grade (I vs. II/III)	4 [12–15]	Higher grade: HR 3–6 (p<0.01); PFS 48 vs. 84 months	Shorter in grade III (60 vs. 120 months, p=0.02)	Worse functional status (p<0.05) [15]
Ki-67 (>5%)	3 [13–15]	HR 2–4 (p<0.01); reduced PFS (p=0.008)	Shorter (HR 2.1, p=0.008)	Neurological deficits [14]
Tumor Size (>6 cm)	2 [12, 14]	OR 1.8 (p=0.04); no PFS impact in multivariate	No impact (p>0.05)	Not reported
Peritumoral Edema	1 [9]	HR 1.6 (p=0.02)	Not reported	Reduced QOL (p=0.01)
Location (Convexity vs. Other)	3 [9, 13, 14]	Convexity: PFS 90 vs. 70 months (p=0.03)	No impact	Fewer deficits (p=0.04)
Adjuvant RT	2 [12, 15]	HR 0.5 (p=0.047); PFS +24 months	No benefit in WHO I (p>0.05)	Potential RT morbidity

Synthesis of Results: Narrative synthesis indicated that Simpson grades I/II consistently reduced recurrence rates (10–20% vs. 30–50% at 5 years) and improved PFS (median 86–92 months) compared to grades III–V across all studies [9, 12–15]. In WHO grade I tumors, PFS exceeded 80 months with GTR, particularly in convexity locations [12, 14]. However, in multivariate models, WHO grade II/III and Ki-67 >5% were stronger predictors of recurrence (HR 3–6 vs. 2.0–2.5 for Simpson grade) [14, 15]. OS differences were minimal in low-grade tumors but significant in grade III with incomplete resection [15].

QOL data were limited to proxy measures like seizure freedom and KPS. Complete resection (grade I) achieved 70–80% seizure control, enhancing QOL [9, 13]. Adjuvant RT improved PFS in STR cases by approximately 24 months but was not routinely recommended for grade I tumors [12, 15]. Convexity tumors facilitated GTR, leading to better PFS and QOL outcomes compared to falcine or parasagittal tumors [9, 13, 14]. Heterogeneity in follow-up periods (24–60 months) and outcome definitions precluded meta-analysis. Risk of bias was low, with minimal selection bias in retrospective designs.

Discussion:

This PRISMA-2020 compliant SLR reaffirms the prognostic significance of the Simpson grading system in predicting recurrence and PFS following surgical resection of supratentorial meningiomas in adults aged 18–60. Simpson grades I/II were consistently associated with lower recurrence rates (10–20% vs. 30–50% at 5 years) and prolonged PFS (86–92 vs. 60–70 months) across all included studies [9, 12–15]. These findings align with historical data from Simpson's seminal work [4], but they provide a modern perspective by incorporating WHO 2021 classification updates and contemporary surgical advancements [6]. However, the impact of resection extent is increasingly contextualized by tumor biology, with WHO grade and Ki-67 index emerging as stronger predictors in multivariate analyses [14, 15]. This suggests a paradigm shift towards integrated prognostic models combining surgical and molecular factors.

Comparison Across Included Studies:

Schneider et al. [9] highlighted the role of complete resection in improving seizure outcomes, a critical QOL metric, with grade I resections achieving 80% seizure freedom compared to 50% for grade III. This was corroborated by Gadot et al. [13], who reported an odds ratio (OR) of 2.2 (p=0.003) for seizure control with GTR, but noted that peritumoral edema independently worsened QOL, suggesting that resection alone may not address all morbidity sources. For instance, edema-related seizures persisted in 20% of patients despite GTR, indicating the need for adjunctive therapies like antiepileptic drugs [9]. In contrast, Nowak-Choi et al. [12] and Spille et al. [14] focused on recurrence, finding that Simpson grade's prognostic effect was attenuated in WHO grade II tumors, where Ki-67 >5% increased the HR for recurrence to 3–4, compared to 2 for incomplete resection. This suggests that biological aggressiveness may override surgical extent in higher-grade tumors.

Driver et al. [15] provided molecular insights, demonstrating that adjuvant RT extended PFS in grade III tumors with STR, improving median PFS from 48 to 72 months. This aligns with EANO guidelines recommending RT for incomplete resections of atypical or anaplastic meningiomas [3]. However, the lack of OS benefit in low-grade tumors with RT highlights the need for selective application to avoid unnecessary morbidity [12]. Subgroup analyses by tumor location further revealed that convexity meningiomas achieved GTR more frequently,

leading to better PFS (90 vs. 70 months) and fewer neurological deficits compared to falcine or parasagittal tumors, where vascular or eloquent cortex involvement limited resection extent [9, 13, 14].

Comparison with Narrative and Comprehensive Reviews:

Narrative reviews, such as Nanda et al. [5], have questioned the universal applicability of the Simpson grading system, particularly for skull base meningiomas where anatomical constraints often prevent GTR. In contrast, this SLR's focus on supratentorial meningiomas reaffirms the system's relevance, as these tumors are more amenable to complete resection [9, 13, 14]. For example, convexity tumors achieved grade I/II in 70–80% of cases, correlating with lower recurrence rates [14]. Comprehensive reviews, such as Rogers et al. [8], report broader recurrence rates of 20–30% across all meningioma types and age groups, whereas this SLR's age-specific analysis shows lower rates (10–20% for GTR) in adults 18–60, likely due to better surgical tolerance and fewer comorbidities in this population.

The inclusion of WHO 2021 classification updates in this review, particularly the integration of molecular markers like TERT promoter mutations for grade III meningiomas, distinguishes it from earlier reviews [6]. Narrative reviews often emphasize surgical technique over biology, but this SLR highlights the superior prognostic power of WHO grade and Ki-67, aligning with recent studies advocating molecular stratification [15]. For instance, Spille et al. [14] found that NF2 mutations doubled recurrence risk independently of Simpson grade, suggesting that genetic profiling could guide surgical planning.

Prognostic Factors in Context:

Tumor size (>6 cm) was associated with increased recurrence risk in two studies [12, 14], likely due to technical challenges in achieving GTR, echoing findings from a 2024 study on high-risk meningiomas [6]. Larger tumors often involve critical structures, increasing the likelihood of STR and subsequent recurrence (OR 1.8, p=0.04) [12]. Tumor location further modulated outcomes: convexity meningiomas benefited from easier GTR, resulting in better PFS and QOL [9, 13, 14], while falcine or parasagittal tumors faced higher recurrence due to vascular encasement or proximity to eloquent cortex [3]. Adjuvant RT significantly reduced recurrence in STR cases (HR 0.5, p=0.047) [12, 15], supporting its role in grade II/III tumors but questioning its necessity in low-grade tumors, where narrative reviews often advocate broader application [8].

Ki-67 >5% and WHO grade II/III were consistently stronger predictors of recurrence than Simpson grade in multivariate models [14, 15]. For example, Ki-67 >5% increased recurrence risk by up to fourfold, compared to twofold for Simpson grade III/IV [14]. This aligns with emerging evidence on molecular markers, such as NF2 alterations, which worsen prognosis in supratentorial meningiomas [14]. Peritumoral edema, reported in one study [9], was associated with higher seizure recurrence and reduced QOL, underscoring the need for comprehensive postoperative management beyond resection.

Quality of Life Considerations:

QOL data were sparse, primarily limited to proxy measures like seizure freedom and KPS. Grade I resections achieved 70–80% seizure control, significantly improving QOL [9, 13], while incomplete resections were associated with persistent seizures and lower KPS scores [15]. Peritumoral edema further exacerbated QOL deficits, with 20–30% of patients experiencing ongoing neurological symptoms [9]. This contrasts with broader meningioma QOL reviews,

which highlight cognitive impairments and reduced health-related QOL (HRQOL) due to treatment-related morbidity [10, 16]. The lack of standardized QOL tools, such as the EORTC QLQ-BN20 or SF-36, in the included studies represents a significant gap, particularly for younger adults where long-term functionality is critical.

Clinical Implications:
The findings advocate for maximizing GTR in supratentorial meningiomas, particularly for convexity tumors, to minimize recurrence and optimize QOL. However, in WHO grade II/III tumors or those with high Ki-67, adjuvant RT or emerging targeted therapies (e.g., mTOR inhibitors) may be necessary to address biological aggressiveness [15]. Molecular profiling, including NF2 and TERT mutations, could guide personalized treatment plans, as suggested by recent studies [6, 14]. For example, patients with NF2-mutated tumors may benefit from early RT or clinical trials targeting specific pathways. Online predictive tools integrating Simpson grade, WHO grade, and molecular markers could enhance surgical decision-making, as proposed by Driver et al. [15].

Strengths and Limitations:
Strengths: This SLR's PRISMA-2020 compliance ensures methodological rigor, and its focus on recent (2019–2024) and population-specific (18–60, supratentorial) data addresses gaps in prior reviews. The inclusion of WHO 2021 classification updates and modern surgical contexts enhances relevance.

Limitations: Only five studies precisely matched the age and location criteria, limiting generalizability. Heterogeneity in follow-up durations (24–60 months) and outcome definitions precluded meta-analysis, potentially reducing statistical power. Publication bias favoring positive surgical outcomes may exist, as negative results are less likely to be reported. The reliance on retrospective data and proxy QOL measures (e.g., seizure freedom) limits the depth of functional outcome analysis.

Future Directions: Future research should prioritize prospective, multicenter studies with standardized QOL assessments (e.g., EORTC QLQ-BN20, SF-36) to capture patient-reported outcomes comprehensively. Long-term follow-up (>5 years) is needed to assess OS impacts, particularly in WHO grade I tumors where recurrence may manifest later. Molecular profiling, including NF2, TERT, and other genetic markers, should be integrated into prognostic models to refine risk stratification [14, 15]. Additionally, machine learning-based tools combining clinical, surgical, and molecular data could predict recurrence risk with higher accuracy, facilitating personalized treatment plans. Finally, studies exploring the cost-effectiveness of adjuvant therapies and their impact on QOL in younger adults are warranted to inform healthcare policy.

In summary, while Simpson grade remains a key prognostic factor, its impact is context-dependent, modulated by tumor biology and location. Multimodal approaches integrating surgical, molecular, and adjuvant strategies are essential for optimizing outcomes in supratentorial meningioma management.

Conclusion:
This SLR confirms the prognostic importance of Simpson grade in reducing recurrence and enhancing PFS in supratentorial meningioma resection among adults aged 18–60. However, WHO grade and Ki-67 index exert stronger influences, particularly in higher-grade tumors, underscoring the need for integrated prognostic models. Adjuvant RT mitigates risks associated with incomplete resections, while QOL improvements are closely tied to complete resection and seizure control. Compared to narrative reviews, this evidence-based synthesis highlights the value of population-specific data and modern classifications. Future prospective studies with robust QOL metrics and molecular profiling are critical to refine treatment strategies and improve patient outcomes.

References

1. Ostrom, Q. T., Cioffi, G., Gittleman, H., Patil, N., Waite, K., Kruchko, C., & Barnholtz-Sloan, J. S. (2019). CBTRUS Statistical Report: Primary Brain and Other Central Nervous System Tumors Diagnosed in the United States in 2012–2016. Neuro-Oncology, 21(Supplement_5), v1–v100. https://doi.org/10.1093/neuonc/noz150
2. Buerki, R. A., Horbinski, C. M., Kruser, T., Horowitz, P. M., James, C. D., & Lukas, R. V. (2018). An overview of meningiomas. Future Oncology, 14(21), 2161–2177. https://doi.org/10.2217/fon-2018-0006
3. Goldbrunner, R., Stavrinou, P., Jenkinson, M. D., Sahm, F., Mawrin, C., Weber, D. C., … & Minniti, G. (2021). EANO guideline on the diagnosis and management of meningiomas. Neuro-Oncology, 23(11), 1821–1834. https://doi.org/10.1093/neuonc/noab150
4. Simpson, D. (1957). The recurrence of intracranial meningiomas after surgical treatment. Journal of Neurology, Neurosurgery, and Psychiatry, 20(1), 22–39. https://doi.org/10.1136/jnnp.20.1.22
5. Nanda, A., Bir, S. C., Maiti, T. K., Konar, S. K., Missios, S., & Guthikonda, B. (2017). Relevance of Simpson grading system and recurrence-free survival after surgery for World Health Organization Grade I meningioma. Journal of Neurosurgery, 126(1), 201–211. https://doi.org/10.3171/2016.1.JNS151842
6. Louis, D. N., Perry, A., Wesseling, P., Brat, D. J., Cree, I. A., Figarella-Branger, D., … & Ellison, D. W. (2021). The 2021 WHO Classification of Tumors of the Central Nervous System: A summary. Neuro-Oncology, 23(8), 1231–1251. https://doi.org/10.1093/neuonc/noab106
7. Rogers, L., Barani, I., Chamberlain, M., Kaley, T. J., McDermott, M., Raizer, J., … & Vogelbaum, M. A. (2015). Meningiomas: Knowledge base, treatment outcomes, and uncertainties. A RANO review. Journal of Neurosurgery, 122(1), 4–23. https://doi.org/10.3171/2014.7.JNS131644
8. Rogers, L., Zhang, P., Vogelbaum, M. A., Perry, A., Ashby, L. S., Modi, J. M., … & Mehta, M. P. (2018). Intermediate-risk meningioma: Initial outcomes from NRG Oncology RTOG 0539. Journal of Neurosurgery, 129(1), 35–47. https://doi.org/10.3171/2016.11.JNS161170
9. Schneider, M., Güresir, Á., Borger, V., Hamed, M., Rácz, A., Vatter, H., Güresir, E., & Schuss, P. (2019). Preoperative tumor-associated epilepsy in patients with supratentorial meningioma: Factors influencing seizure outcome after meningioma surgery. Journal of Neurosurgery, 132(6), 1835–1841. https://doi.org/10.3171/2019.7.JNS19433
10. Zamanipoor Najafabadi, A. H., van der Meer, P. B., Boele, F. W., Taphoorn, M. J. B., Klein, M., van Zandvoort, M. J. E., & Dirven, L. (2021). Determinants and predictors of health-related quality of life in meningioma patients: A systematic review. Neuro-Oncology Practice, 8(4), 389–400. https://doi.org/10.1093/nop/npab023
11. Page, M. J., McKenzie, J. E., Bossuyt, P. M., Boutron, I., Hoffmann, T. C., Mulrow, C. D., … & Moher, D. (2021). The PRISMA 2020 statement: An updated guideline for reporting systematic reviews. BMJ, 372, n71. https://doi.org/10.1136/bmj.n71
12. Nowak-Choi, K., Palmer, J. D., Casey, J., Chitale, A., Kalchman, I., Buss, E., Tzeng, S., Venur, V., & Patil, C. (2021). Resected WHO grade I meningioma and predictors of local control. Journal of Neuro-Oncology, 151(2), 307–313. https://doi.org/10.1007/s11060-020-03688-1
13. Gadot, R., Khan, A. B., Patel, R., Goethe, E., Shetty, A., Hadley, C. C., … & Patel, A. J. (2021). Predictors of postoperative seizure outcome in supratentorial meningioma. Journal of Neurosurgery, 137(2), 515–524. https://doi.org/10.3171/2021.9.JNS211738
14. Spille, D. C., Adeli, A., Sporns, P. B., Hess, K., Streckert, E. M. S., Brokinkel, C., … & Brokinkel, B. (2022). Predicting the risk of postoperative recurrence and high-grade histology in patients with intracranial

meningiomas using routine preoperative MRI. Acta Neurochirurgica, 164(8), 2189–2198. https://doi.org/10.1007/s00701-022-05240-8
15. Driver, J., Weber-Levine, C., Mirchia, K., Hayat, H., Fiester, P. J., Jones, J. L., ... & Tavanaiepour, D. (2024). Molecular classification to refine surgical and radiotherapeutic decision-making in meningioma. Nature Medicine, 30, 1947–1957. https://doi.org/10.1038/s41591-024-03167-4
16. Benz, L. S., Wrenger, M. R., Weinberg, J. S., Noll, K. R., & Wefel, J. S. (2023). Neurocognitive outcomes in patients with intracranial meningiomas. Current Oncology Reports, 25, 149–157. https://doi.org/10.1007/s11912-022-01346-4

Received / Получено 02.07.2025
Revised / Пересмотрено 22.07.2025
Accepted / Принято 20.08.2025

COMPARATIVE STUDY BETWEEN JALALABAD AND LAHORE ABOUT DENGUE FEVER AND LIFESTYLE OF PEOPLE AS A PREVENTIVE MEASURE FROM MOSQUITOES

Muhammad Abdullah Farooq Cheema[1], Hammad Jamshaid[1], Dipak Chaulagain[2,3]
[1]Student of Jalalabad State University Named After B.Osmonov, Jalal-Abad, Kyrgyzstan
[2]Uzhhorod National University, Uzhhorod, Ukraine
[3]Jalal-Abad International University, Jalal-Abad, Kyrgyzstan

Abstract:
Dengue fever, a mosquito-borne viral illness, continues to pose a significant threat to public health, particularly in densely populated tropical and subtropical regions. This comparative study explores the influence of lifestyle-related factors on dengue prevalence by analyzing two contrasting urban environments: Jalalabad, Kyrgyzstan (a region with no reported dengue cases) and Lahore, Pakistan (where dengue is endemic).

Using structured questionnaires, data were collected from 300 participants (150 from each city), focusing on awareness, preventive behaviors, sanitation practices, and environmental conditions. Despite limited awareness about dengue in Jalalabad, participants demonstrated healthier lifestyle habits and better environmental management. Conversely, although Lahore respondents showed higher awareness of the disease, their preventive practices and environmental hygiene were less consistent.

The findings underscore a strong relationship between personal and communal lifestyle factors; such as water storage, dietary habits, sanitation, and mosquito protection measures and the likelihood of dengue transmission. The study concludes that enhanced public health education, behavioral interventions, and infrastructure improvements are essential for effective dengue control, particularly in high-risk areas. Promoting healthier lifestyles may serve as a key strategy in reducing the burden of vector-borne diseases globally.

Keywords: Dengue Fever, Mosquitoes, Vector borne diseases, Endemic, Sanitation

СРАВНИТЕЛЬНОЕ ИССЛЕДОВАНИЕ ЛИХОРАДКИ ДЕНГЕ И ОБРАЗА ЖИЗНИ ЛЮДЕЙ В ДЖАЛАЛ-АБАДЕ И ЛАХОРЕ КАК МЕРЫ ПРОФИЛАКТИКИ УКУСОВ КОМАРОВ

Мухаммад Абдулла Фарук Чима[1], Хаммад Джамшаид[1], Дипак Чаулагаин[2,3]
[1]Студент Джалал-Абадского государственного университета имени Б. Осмонова
[2]Ужгородский национальный университет, Ужгород, Украина
[3]Джалал-Абадский международный университет, Джалал-Абад, Кыргызстан

Аннотация
Лихорадка денге, вирусное заболевание, переносимое комарами, продолжает представлять значительную угрозу для здоровья населения, особенно в густонаселенных тропических и субтропических регионах. Данное сравнительное исследование изучает влияние факторов образа жизни на распространенность лихорадки денге, анализируя два контрастных городских региона: Джалал-Абад, Кыргызстан (регион, где не зарегистрировано ни одного случая лихорадки денге) и Лахор, Пакистан (где лихорадка денге эндемична). С помощью структурированных анкет были собраны

данные у 300 участников (по 150 из каждого города), уделяя особое внимание осведомленности, профилактическим действиям, санитарным нормам и состоянию окружающей среды. Несмотря на ограниченную осведомленность о лихорадке денге в Джелалабаде, участники продемонстрировали более здоровый образ жизни и более эффективное управление окружающей средой. Напротив, хотя респонденты из Лахора продемонстрировали более высокую осведомленность об этом заболевании, их профилактические меры и гигиена окружающей среды были менее последовательны.

Результаты подчеркивают тесную взаимосвязь между личными и общественными факторами образа жизни, такими как запасы воды, пищевые привычки, санитария и меры защиты от комаров, и вероятностью передачи лихорадки денге. В исследовании сделан вывод о том, что повышение уровня информированности населения в области здравоохранения, поведенческие вмешательства и улучшение инфраструктуры имеют решающее значение для эффективной борьбы с лихорадкой денге, особенно в районах высокого риска. Пропаганда здорового образа жизни может служить ключевой стратегией снижения бремени трансмиссивных заболеваний во всем мире.

Ключевые слова: лихорадка денге, комары, трансмиссивные заболевания, эндемия, санитария

Introduction

Dengue fever is a mosquito-borne viral infection caused by four distinct serotypes of dengue virus, primarily transmitted by Aedes aegypti and Aedes albopictus mosquitoes [1]. Globally, dengue has become a major public health concern, with the World Health Organization (WHO) estimating that nearly half of the world's population is at risk [1]. It poses a major public health threat in tropical and subtropical regions, with an estimated 100–400 million infections annually [2]. The disease ranges from mild flu-like symptoms to severe forms like dengue hemorrhagic fever and dengue shock syndrome, which can lead to significant morbidity and mortality [1]. The global incidence of dengue has increased dramatically over the past two decades, fueled by climate change, rapid urbanization, poor sanitation, and global travel [2][3]. Despite efforts to develop vaccines, prevention still relies heavily on mosquito control and public awareness [1][3]. Notably, lifestyle factors such as hygiene practices, environmental cleanliness, and awareness levels play a critical role in dengue prevention [3] [4]. This study compares the prevalence of dengue and related lifestyle practices between two cities: Jalalabad, Kyrgyzstan (non-endemic), and Lahore, Pakistan (endemic).

Objectives

To study the impact of knowledge on prevention practice rating the sources of information about dengue fever and to access the level of public knowledge and prevention practice about dengue fever

To improve early diagnosis and case management. To defect epidemic early and to respond to potentially epidermias effectively. To strengthen monitoring and evaluation to ensure optimal programme implementation, Management and performances.

Rationale
It is alarming infection from last two years and death rate is increasing due to dengue virus in Pakistan.

Methodology
Study Design:

A comparative study is created to find the difference between the lifestyle and occurrence of dengue fever.

Study Area:

For our research, we choose Jalalabad, Kyrgyzstan and Lahore, Pakistan as research areas in which Jalalabad is taken as ideal or control group where occurrence of dengue is 0%

Study Duration:

We started our research from September 1, 2022 and finished on December 20, 2022.

Inclusion Criteria:

Study population includes workers of Jalalabad having education level of primary and secondary, and also workers of Lahore in Pakistan with same education level and age between 25-40 years old.

Exclusion Criteria:

We excluded the respondent that are not willing to participate in research, younger age, education level more than secondary and inconvenient for us to approach.

Study Sample:

Total Sample size is 300 in which 150 from Jalalabad, Kyrgyzstan and 150 from Lahore, Pakistan. We choose non-probability, conventional sampling model for research due to language barrier and difficulty to approach people.

Study tool:

For research, we made demographic profile and knowledge-based questionnaire, we made social demographic profile which based on the age, marital Status, gender

profession, education level and nationality. We made 12 knowledge-based questions in which asked about knowledge regarding degree and life style of people. We analysed the data on SPSS for authentic results and calculation.

Results
Total respondents are 300 and they are workers of hostel and hotel from which 150 from Jalalabad and 150 from Pakistan, in which, we made four age groups, 21-25, 26-30, 31- 35, 36-40 in which 250 are married and 50 are unmarried. In our total respondents 100 are males and 200 are females from which 210 have education level primary and 90 have secondary education level.

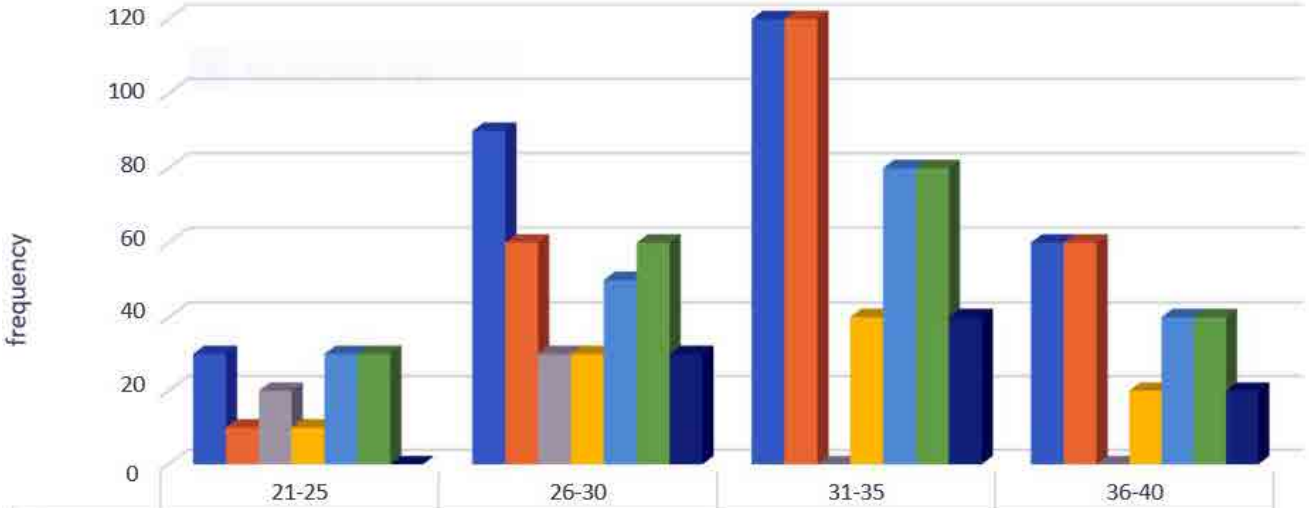

	21-25	26-30	31-35	36-40
People	30	90	120	60
Married	10	60	120	60
single	20	30	0	0
Male	10	30	40	20
Female	30	50	80	40
Primary	30	60	80	40
Secondary	0	30	40	20

There are 12 questions regarding dengue virus and life style against mosquitoes that we asked from locals of Jalalabad and Lahore and analysed their answers as data for our result.

- In Kyrgyzstan 0% people know about dengue virus and 100% didn't know about it.
- In Pakistan, 87% people know about dengue virus and 13% people didn't know about dengue virus.

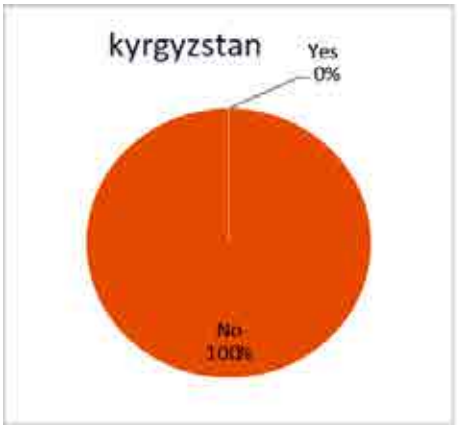

All Lahore respondents give right answer, mosquitoes and no one mark other answer like ant, rabbit, and dog. In Jalalabad, 27% marked Ants, 18% marked Dog, 18% marked Rabbit and 37% marked mosquitoes and these 37% marked right answer by chance because, they didn't know about dengue virus.

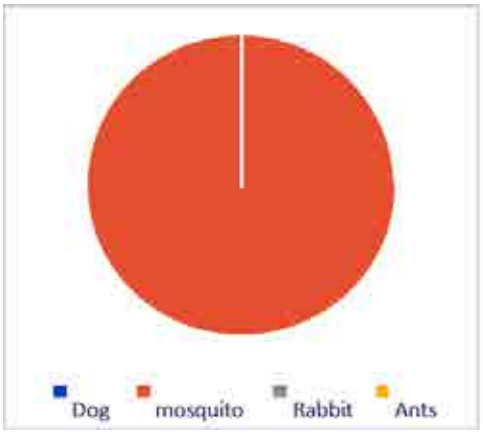

- 0% of Kyrgyzstan respondents is infected by dengue virus therefore 100% respondents marked the answer No .67% of Lahore respondents is infected in their life by dengue virus and 33% didn't infected by dengue virus

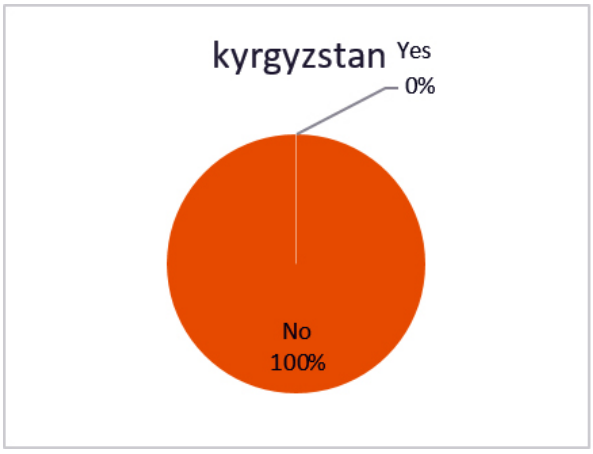

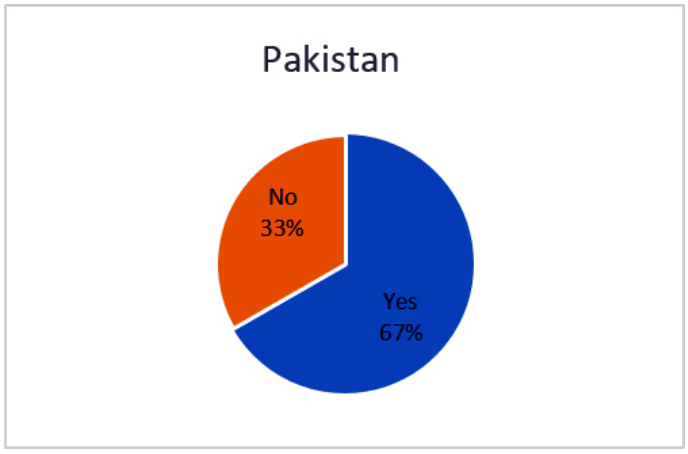

- Lahore respondents, 20% use net around Windows, 7% use mosquitoes spray and 73% people use anti- mosquitoes' oil as a preventive measure for mosquitoes.
- Jalalabad respondents, 20% use spray and 80% use net around Windows as preventive measures and no one use anti- mosquito's oil.

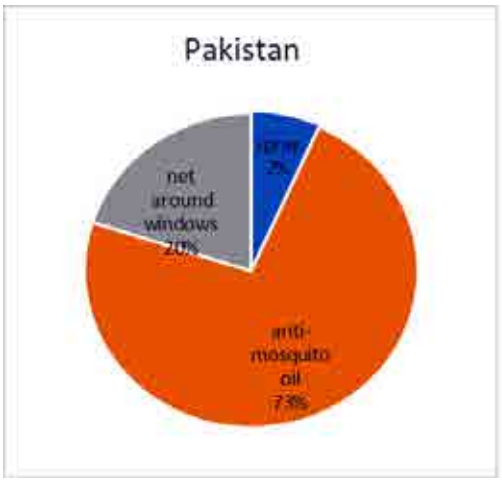

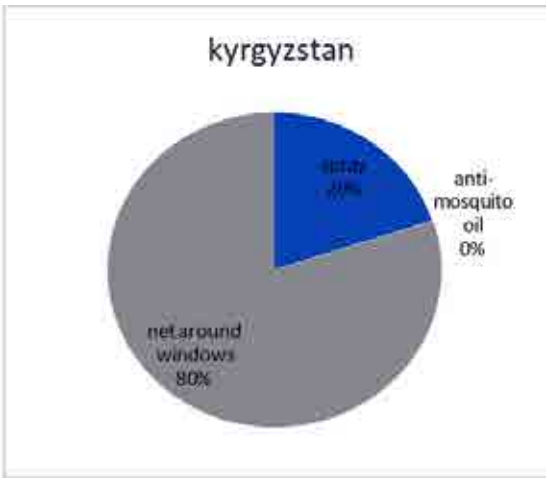

All respondents of Lahore marked answer Yes for storage of water in house and no one marked No.

90 respondents of Jalalabad store water at home, in which some may be or maybe not, and in which 60 didn't store water at home.

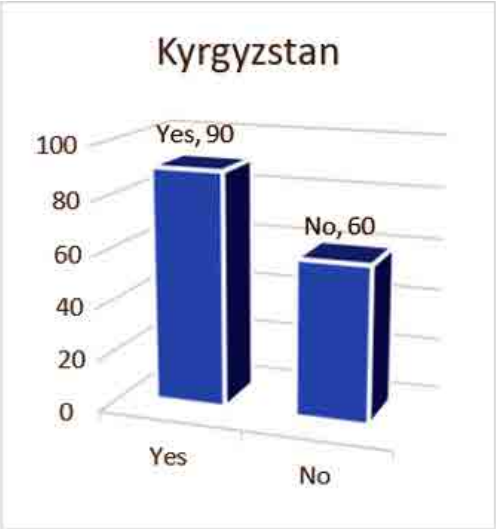

- 13% of Lahore respondents Don't like vegetables to eat, 27 % take less, 27% take normal and 33% take high proportion of vegetables in their diet. Atleast no one mark that they don't like, Jalalabad respondents 20% take less, 33% take ordinary and 47% take high proportion of vegetables in their diet.

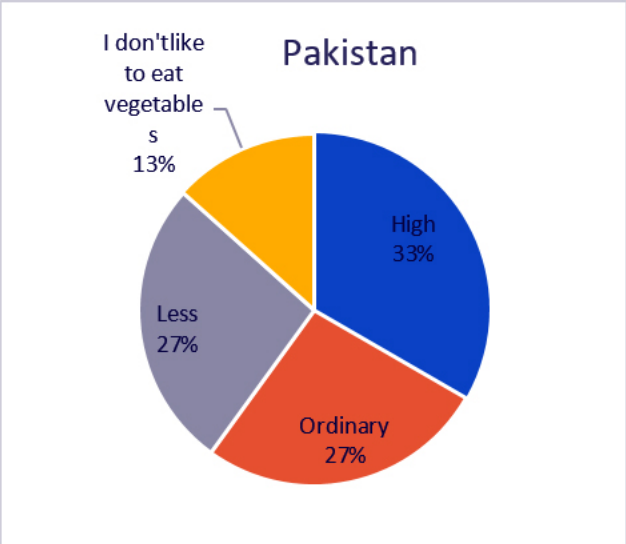

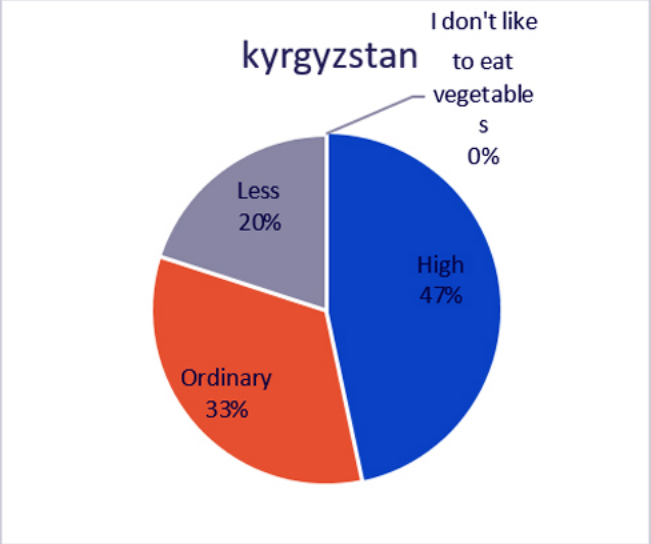

14 respondents from Lahore share their accessories with others but only 1 didn't share their soap, towel, comb etc with others. In Jalalabad 5 respondent share their accessories and 8 didn't share their accessories , that is good thing to stay safe.

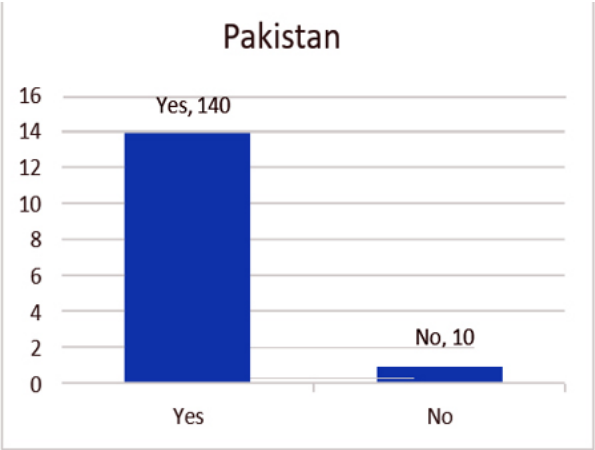

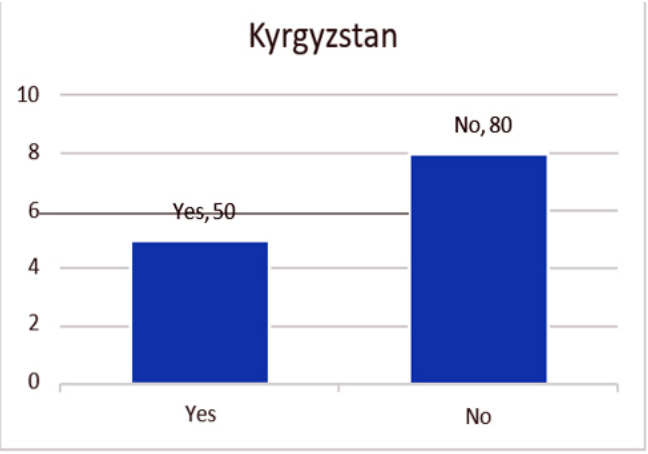

Both Lahore and Jalalabad respondents have not knowledge regarding this question, some give right answer by chance like 20% in Lahore and 7% in Jalalabad.

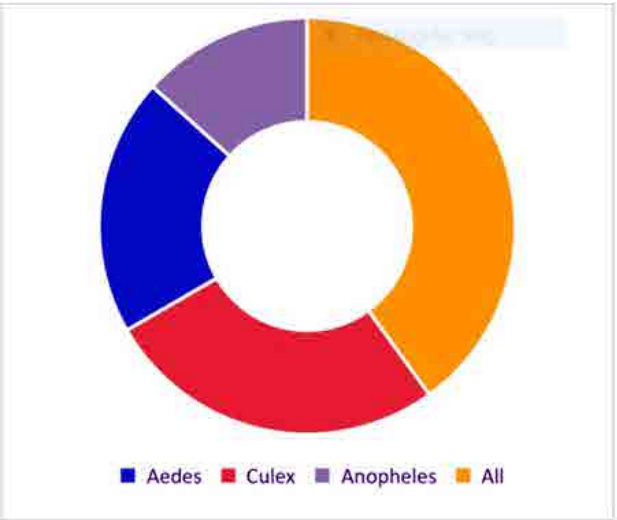

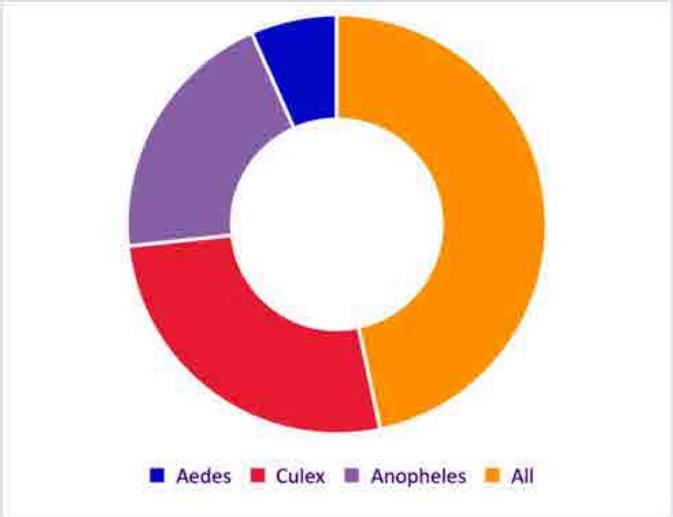

140 Lahore respondents marked yes, that, weather is suitable for mosquitoes' growth and only 10 marked No. Jalalabad respondents marked 60% No and 40% yes, because in whole year mostly there is winters but in month of August there is a lot of mosquitoes at garbage site.

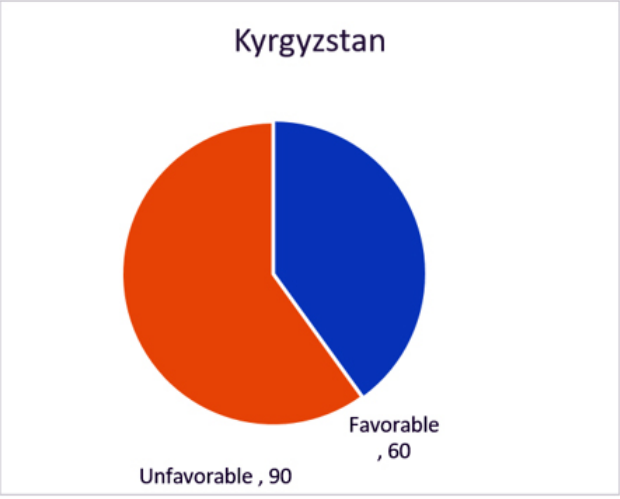

From Lahore respondents, 60 through garbage in front of their homes, 20 far away from home, 20 in local dump and 50 through by chance or randomly. In Jalalabad, No one through in front of their house and no one through randomly. 80 of them through the garbage far away from home and 70 in local dump.

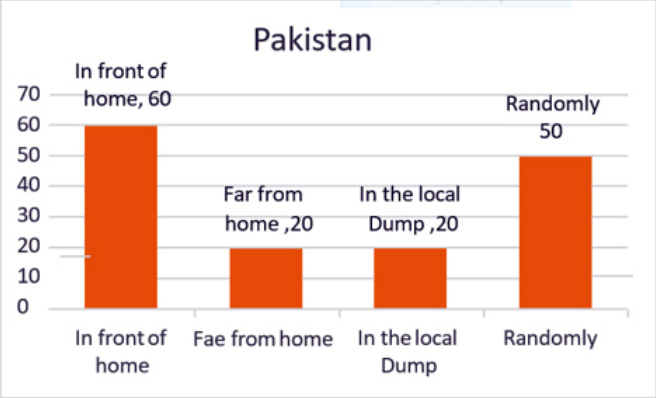

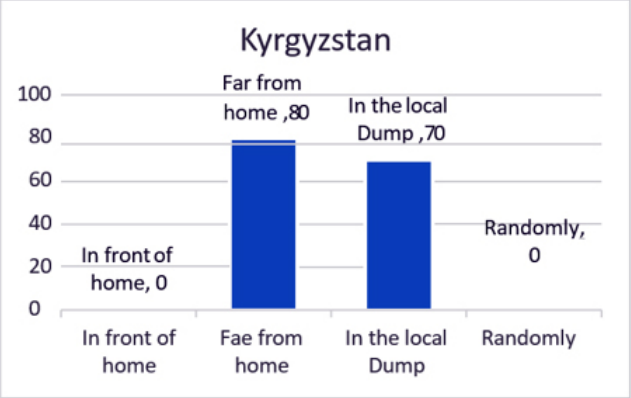

From Lahore respondents, 80% of people don't take calcium and vitamins tablet, and 20% take tablets. From Jalalabad, 53% of people don't take and 47% of people take calcium and vitamins tablets.

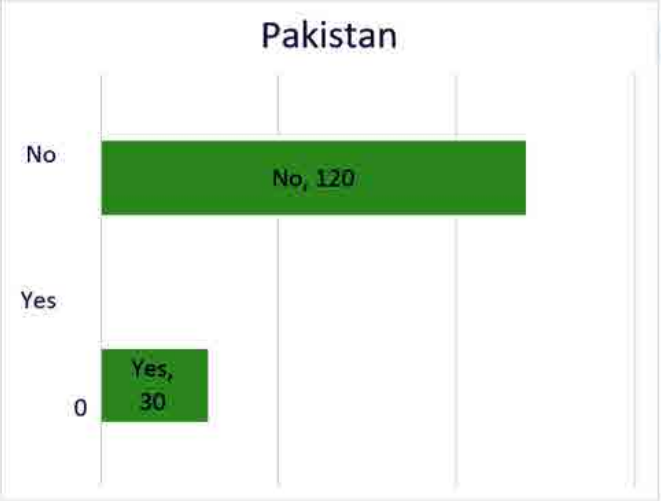

In Lahore 13 respondents are not statisfy from their sewerage system of country and 2 are satisfied. In Jalalabad respondents, all are statisfied from the sewerage system of their country.

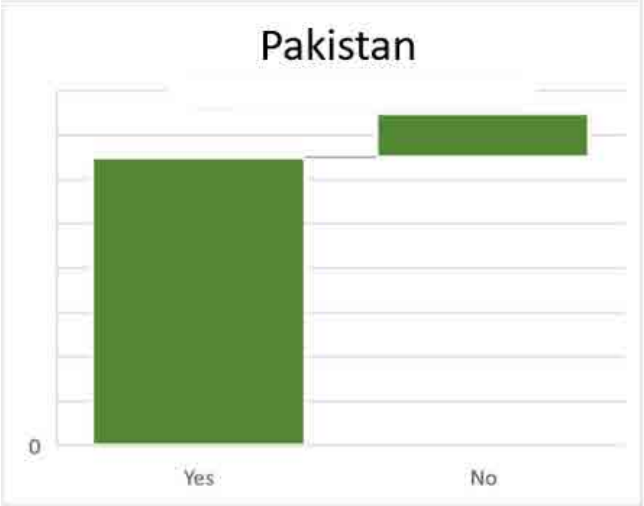

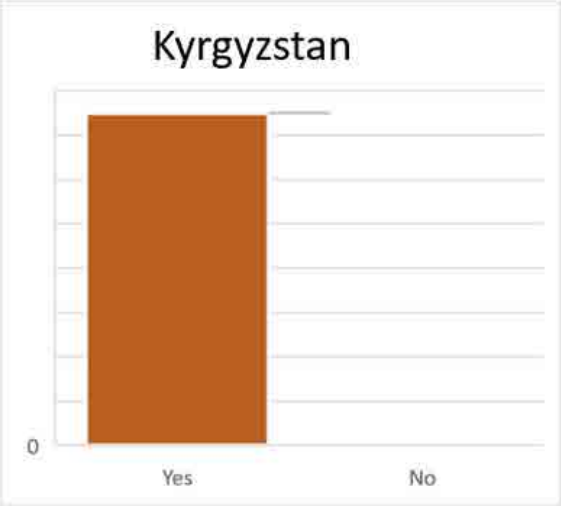

Discussion

This study aimed to compare the knowledge, awareness, and preventive practices regarding dengue fever between residents of Lahore, Pakistan, a high-risk dengue endemic region and Jalalabad, Kyrgyzstan; where no cases have been officially reported. The findings reveal significant lifestyle-related differences that influence the incidence and risk of dengue infection.

In Lahore, most respondents were aware of dengue fever and recognized its transmission through Aedes mosquitoes [1]. However, despite higher awareness, actual preventive practices were inconsistent. A large number of respondents shared personal accessories, stored stagnant water at home, and reported dissatisfaction with the sewerage system, conditions favourable for mosquito breeding and viral transmission [3]. These findings align with global observations that urban overcrowding, poor sanitation, and unplanned development are major contributors to dengue outbreaks in low- and middle-income countries [2].

In contrast, respondents from Jalalabad displayed minimal knowledge of dengue fever but practiced healthier environmental hygiene, such as avoiding water storage and using window nets [4]. These behaviours may be shaped more by cultural habits and environmental conditions (e.g., a colder climate less conducive to mosquito survival) than by active health education [5]. Importantly, despite the lack of awareness, the preventative lifestyle observed in Jalalabad indirectly aligns with WHO's recommendations for vector control—reducing breeding sites and limiting exposure to mosquitoes [1][6].

Our findings support the hypothesis that lifestyle factors, such as waste disposal, water storage habits, and the use of repellents, play a critical role in the prevention of dengue fever [3][4]. These lifestyle patterns may significantly mitigate the risk of infection, even in the absence of targeted health interventions. Conversely, higher awareness does not always translate into effective prevention if it is not accompanied by practical changes in daily behaviour [4][7].

Moreover, the study reaffirms that dengue prevention is multifactorial. While public knowledge is important, physical infrastructure (e.g., sanitation systems), government vector control programs, and personal hygiene practices collectively determine disease outcomes [1][3]. The disconnect observed between knowledge and practice in Lahore highlights the need for community-based intervention programs that not only educate but also facilitate the adoption of practical preventive measures [3].

Finally, climate change and increased urbanization continue to alter the epidemiology of dengue fever. With global warming expanding the geographical range of Aedes mosquitoes, regions like Jalalabad may become susceptible soon if environmental changes occur [2][8]. Therefore, proactive education and surveillance even in non-endemic regions are essential [2].

Conclusion

This comparative study between Lahore and Jalalabad highlights how lifestyle factors significantly influence the risk of dengue fever, regardless of awareness levels [3][4]. In Lahore, although most respondents were knowledgeable about dengue and its transmission [1], preventive practices were inconsistent and often inadequate [3]. Factors such as poor waste management, stagnant water storage, lack of personal hygiene, and unsatisfactory sewerage systems contributed to an environment conducive to mosquito breeding and disease transmission [3][4]. Conversely, in Jalalabad—despite limited awareness about dengue—residents demonstrated healthier lifestyle habits, such as reduced water storage, better waste

disposal, and use of protective measures like window nets [4]. These practices have likely contributed to the absence of dengue cases in the region [5]. This finding underscores that effective lifestyle behaviours can serve as a strong barrier against dengue, even in the absence of formal health education or endemic risk [4][6].

Overall, the research supports the notion that awareness must be paired with actionable behaviour change [4][7]. Preventive strategies must be practical, community-based, and culturally adapted [3][9]. Dengue prevention is not solely the responsibility of healthcare systems—it also depends on individual and collective commitment to sustainable practices that minimize mosquito breeding and exposure [1][6].

References

1. World Health Organization. Dengue and severe dengue. https://www.who.int/news-room/fact-sheets/detail/dengue
2. World Health Organization. Dengue - Global situation. https://www.who.int/emergencies/disease-outbreak-news/item/2024-DON518
3. BMC Public Health. Factors associated with the increase of dengue cases in Pakistan. https://bmcpublichealth.biomedcentral.com/articles/10.1186/s12889-020-09064-2
4. Frontiers in Public Health. Knowledge, attitude, and practice regarding dengue in Pakistan. https://www.frontiersin.org/journals/public-health/articles/10.3389/fpubh.2022.929814/full
5. Ebi KL, Nealon J. Dengue in a changing climate. Environ Res. 2016;151:1-14. https://www.ncbi.nlm.nih.gov/pmc/articles/PMC7118965/
6. World Health Organization. Dengue: Guidelines for diagnosis, treatment, prevention and control. 2009. https://www.who.int/publications/i/item/9789241547871
7. Simmons CP, Farrar JJ, Nguyen VV, Wills B. Dengue. N Engl J Med. 2007;366(15):1423-1432.
8. Cardona-Ospina JA, Arteaga-Livias K, Rodríguez-Morales AJ. Dengue and climate change: A systematic review. Curr Trop Med Rep. 2020;7:85-94. https://link.springer.com/article/10.1007/s40475-020-00208-4
9. Gubler DJ. Dengue, urbanization and globalization: The unholy trinity of the 21st century. Trop Med Health. 2010;39(4 Suppl):3-11. https://www.ncbi.nlm.nih.gov/pmc/articles/PMC3317603/
10. Balmaseda, A., Hammond, S. N., Pérez, L., Téllez, Y., Saborío, S. I., Mercado, J. C., ... & Harris, E. (2010). Trends in patterns of dengue transmission over 4 years in a pediatric cohort study in Nicaragua. The Journal of Infectious Diseases, 201(1), 5–14. https://doi.org/10.1086/648592
11. Cardona-Ospina, J. A., Villamil-Gómez, W. F., Pérez-Díaz, C. E., Bonilla-Aldana, D. K., & Mondragón-Cardona, A. 2021. Dengue situation in Pakistan. National Center of Vector Borne Diseases Control – Ministry of Health, Pakistan.
12. Deubel, V. (2001). The contribution of molecular techniques to the diagnosis of dengue infections. In D. J. Gubler & G. Kuno (Eds.), Dengue and Dengue Hemorrhagic Fever (pp. 335–365). Cambridge: CABI Publishing.
13. Guzman, M. G., Halstead, S. B., Artsob, H., Buchy, P., Farrar, J., Gubler, D. J., ... & Peeling, R. W. (2010). Dengue: A continuing global threat. Nature Reviews Microbiology, 8(12), S7–S16. https://doi.org/10.1038/nrmicro2460
14. Priyadarshini, S. (2008). Single test to detect all dengue serotypes. Nature India. https://doi.org/10.1038/nindia.2008.109
15. Saxena, P., Dash, P. K., Santhosh, S. R., Shrivastava, A., Parida, M. M., & Rao, P. V. (2008). Development and evaluation of one step single tube multiplex RT-PCR for rapid detection and typing of dengue viruses. Virology Journal, 5, 20. https://doi.org/10.1186/1743-422X-5-20
16. Simmons, C. P., Farrar, J. J., Nguyen, V. V., & Wills, B. (2006). Understanding pathogenesis, immune response and viral factors. In Report of the Scientific Working Group Meeting on Dengue, Geneva, 1–5 October 2006 (pp. 54–60). Geneva: World Health Organization.
17. Tanner, L., Schreiber, M. J., Low, J. G., Ong, A., Tolfvenstam, T., Lai, Y. L., ... & Hibberd, M. L. (2008). Decision tree algorithms predict the diagnosis and outcome of dengue fever in the early phase of illness. PLoS Neglected Tropical Diseases, 2(3), e196. https://doi.org/10.1371/journal.pntd.0000196

19. Vazquez-Prokopec, G. M., Stoddard, S. T., Paz-Soldan, V., Morrison, A. C., Elder, J. P., Kochel, T. J., & Scott, T. W. (2010). Quantifying the spatial dimension of dengue virus epidemic spread within a tropical urban environment. PLoS Neglected Tropical Diseases, 4(12), e920. https://doi.org/10.1371/journal.pntd.0000920
20. Vazquez-Prokopec, G. M., Chaves, L. F., Ritchie, S. A., Davis, J., & Kitron, U. (2010). Unforeseen costs of cutting mosquito surveillance budgets. PLoS Neglected Tropical Diseases, 4(10), e858. https://doi.org/10.1371/journal.pntd.0000858
21. Vorndam, V., & Kuno, G. (2001). Laboratory diagnosis of dengue virus infections. In D. J. Gubler & G. Kuno (Eds.), Dengue and Dengue Hemorrhagic Fever (pp. 313–333). Cambridge: CABI Publishing.
22. World Health Organization. (2009). Dengue: Guidelines for diagnosis, treatment, prevention and control. Geneva: WHO and the Special Programme for Research and Training in Tropical Diseases.
23. World Health Organization. (2022). Dengue and severe dengue. Retrieved from https://www.who.int/news-room/fact-sheets/detail/dengue-and-severe-dengue
24. World Life Expectancy. (2020). Kyrgyzstan dengue statistics. Retrieved from https://www.worldlifeexpectancy.com/kyrgyzstan-dengue-fever
25. World Health Organization. (2022). Dengue and severe dengue. https://www.who.int/news-room/fact-sheets/detail/dengue-and-severe-dengue
26. Guzman MG, Harris E. (2015). Dengue. The Lancet, 385(9966), 453–465. [https://doi.org/10.1016/S0140-6736(14)60572-9](https://doi.org/10.1016/S0140-6736%2814%2960572-9)
27. Gubler DJ. (2010). Dengue viruses: their evolution, history, and emergence as a global public health problem. Infectious Disease Clinics, 24(1), 1–13.
28. Simmons CP, Farrar JJ, Nguyen vV, Wills B. (2007). Dengue. New England Journal of Medicine, 366(15), 1423–1432.
29. Cardona-Ospina JA, Villamil-Gomez WE, et al. (2020). Dengue in the time of COVID-19: A double threat for public health. Journal of Clinical Virology, 127, 104398. https://doi.org/10.1016/j.jcv.2020.104398
30. World Health Organization. (2009). Dengue: Guidelines for Diagnosis, Treatment, Prevention and Control. Geneva: WHO Press.

Received / Получено 22.07.2025
Revised / Пересмотрено 28.07.2025
Accepted / Принято 02.08.2025

BULLOSIS DIABETICORUM COMPLICATED BY SECONDARY INFECTION AND NECROSIS IN A 29-YEAR-OLD MALE WITH NEWLY DIAGNOSED DIABETES MELLITUS: A CASE REPORT

Hammad Jamshaid[1], Dipak Chaulagain[2],[3]
[1]Medical Student, Jalalabad State University Named after B. Osmonov
[2]Uzhhorod National University, Uzhhorod, Ukraine
[3]Jalal-Abad International University, Jalal-Abad, Kyrgyzstan

Abstract
Bullosis diabeticorum (BD) is a rare cutaneous manifestation of diabetes mellitus characterized by spontaneous bullous eruptions, predominantly on the extremities. This report describes a 29-year-old male car driver from Dubai who presented with pruritus on the right foot, progressing to vesicles, papules, pustules, bullae, and eventual necrosis despite multiple interventions. The condition was complicated by secondary infection and swelling, with laboratory findings revealing mild leukocytosis, eosinophilia, and elevated HbA1c, confirming newly diagnosed diabetes mellitus. Multidisciplinary management involving antimicrobial therapy, antifungal agents, wound care, and lifestyle modifications led to clinical improvement and glycemic stabilization. This case underscores the potential for BD to progress to necrosis in poorly controlled diabetes and highlights the importance of early diagnosis and comprehensive management.

Keywords: Bullosis diabeticorum, diabetic foot, bullous lesions, necrosis, diabetes mellitus

ДИАБЕТИЧЕСКИЙ БУЛЛЕЗ, ОСЛОЖНЕННЫЙ ВТОРИЧНОЙ ИНФЕКЦИЕЙ И НЕКРОЗОМ, У 29-ЛЕТНЕГО МУЖЧИНЫ С ВПЕРВЫЕ ДИАГНОСТИРОВАННЫМ САХАРНЫМ ДИАБЕТОМ: КЛИНИЧЕСКИЙ СЛУЧАЙ

Хаммад Джамшаид[1], Дипак Чаулагайн[2],[3]
[1]Студент-медик Джалал-Абадского государственного университета им. Б. Осмонова
[2]Ужгородский национальный университет, Ужгород, Украина
[3]Джалал-Абадский международный университет, Джалал-Абад, Кыргызстан

Аннотация
Диабетический буллез (ДБ) — редкое кожное проявление сахарного диабета, характеризующееся спонтанными буллезными высыпаниями, преимущественно на конечностях. В данном сообщении описывается 29-летний водитель автомобиля из Дубая, у которого был зуд на правой стопе, прогрессирующий до образования везикул, папул, пустул, булл и, в конечном итоге, некроза, несмотря на многочисленные вмешательства. Состояние осложнилось вторичной инфекцией и отёком. Лабораторные данные выявили лёгкий лейкоцитоз, эозинофилию и повышенный уровень HbA1c, что подтвердило впервые выявленный сахарный диабет. Многопрофильное лечение, включающее антимикробную терапию, противогрибковые препараты, уход за раной и изменение образа жизни, привело к клиническому улучшению и стабилизации гликемии. Данный случай подчёркивает вероятность прогрессирования БД до некроза при плохо контролируемом диабете и подчеркивает важность ранней диагностики и комплексного лечения.

Ключевые слова: Bullosis diabeticorum, диабетическая стопа, буллезные поражения, некроз, сахарный диабет

Introduction

Bullosis diabeticorum (BD), or diabetic bullae, is an uncommon dermatologic complication of diabetes mellitus, manifesting as tense, fluid-filled blisters, primarily on the lower extremities [1, 2]. Although its etiology is poorly understood, associations with poor glycemic control, neuropathy, and microangiopathy have been proposed [3]. Typically self-limiting, BD can become complicated by secondary bacterial or fungal infections, leading to ulceration, necrosis, and significant morbidity [4]. Risk factors include longstanding diabetes, male gender, and peripheral neuropathy, with lesions often arising spontaneously or following minor trauma. Histologically, BD shows intraepidermal or subepidermal cleavage without significant inflammation, distinguishing it from autoimmune bullous disorders. This case report details a rare presentation of BD in a young male with newly diagnosed diabetes, complicated by secondary infection and necrosis, emphasizing the critical role of prompt diagnosis, glycemic optimization, and integrated care to prevent severe outcomes such as amputation.

Case Presentation

A 29-year-old male car driver from Dubai, with an 8-hour daily work schedule involving prolonged sitting and potential exposure to heat and friction, presented with a one-week history of pruritus on the dorsal right foot, rapidly progressing to vesicles and papules (Figure 1). Vital signs were unremarkable (blood pressure 120/80 mmHg, heart rate 78 bpm, temperature 36.8°C), and the patient reported no systemic symptoms such as fever, malaise, or weight loss. He had no prior history of diabetes, skin disorders, allergies, or immunosuppressive conditions, and denied recent trauma, insect bites, or exposure to irritants.

Initial management with topical aciclovir 5% cream (suspecting a viral etiology like herpes simplex) and oral ebastine (10 mg daily for antihistaminic relief) provided no improvement after 5 days. The lesions spread distally, forming intertarsal pustules (Figure 2), prompting hospital evaluation. Pustule drainage revealed seropurulent fluid, and sterile bandaging was applied. However, new lesions emerged on the plantar surface within a week, accompanied by diffuse erythema, edema, and warmth suggestive of cellulitis (Figures 3, 4). The patient reported increasing pain (VAS score 6/10) and difficulty bearing weight.

Oral ampicillin-cloxacillin (500 mg twice daily for 7 days) was initiated under medical supervision, but symptoms worsened with progressive swelling, erythema, and induration. Subsequent treatment included itraconazole (100 mg daily for 7 days, suspecting fungal superinfection), serratiopeptidase (10 mg thrice daily for anti-inflammatory and fibrinolytic effects), and fusidic acid cream applied topically twice daily (Table 5). Two tense, fluid-filled bullae (approximately 2-3 cm in diameter) developed on the lateral foot margin (Figure 7), requiring aseptic drainage and daily wound care with saline irrigation. Despite these interventions, the plantar surface became necrotic and eschar-formed within two days (Figure 6), followed by dorsal necrosis the next day. Sensory examination revealed intact pressure and fine touch sensation, with no evidence of peripheral neuropathy on monofilament testing.

Treatment was escalated to mupirocin 2% ointment (applied twice daily for broad-spectrum bacterial coverage), terbinafine (250 mg daily for antifungal therapy), levofloxacin (500 mg daily for gram-negative coverage), and metronidazole (500 mg thrice daily for anaerobic organisms). Initial healing was noted with reduced exudate and eschar sloughing over several

days, but three days later, multiple dorsal bullae recurred (Figure 8), necessitating repeated drainage and debridement. Clinical examination at this stage revealed hyperpigmented, necrotic skin on the toes and dorsum with bullous lesions, crusting, malodorous exudate, and surrounding maceration (Figures 1–10). No signs of deep tissue involvement, such as crepitus or probing to bone, were observed, and radiographs ruled out osteomyelitis.

Laboratory findings on admission included mild leukocytosis (WBC 11.0 × 10^3/μL, reference 4–10), neutrophilia (64.31%), eosinophilia (8.63%, reference 1–6), lymphopenia (19.11%, reference 20–40), and elevated red cell distribution width (RDW-CV 14.3%, reference 11.6–14.0), suggesting inflammatory response and possible nutritional deficiency. Repeat hematology confirmed persistent leukocytosis (WBC 10.60 × 10^3/μL) and neutrophilia (71%). Pus culture yielded no bacterial growth, possibly due to prior antibiotic use. Random blood glucose was within normal limits (116 mg/dL), but HbA1c was elevated at 6.00% (reference <5.7%), confirming pre-diabetes transitioning to overt diabetes (Tables 11–14).

A comprehensive wellness panel four weeks post-infection revealed borderline dyslipidemia (HDL cholesterol 39.50 mg/dL, reference 40–60, indicating increased cardiovascular risk; LDL cholesterol 132.00 mg/dL, reference <100 optimal, suggesting early atherogenesis), vitamin D deficiency (25-OH vitamin D 10.93 ng/mL, reference <20, potentially impairing immune function and wound healing), and mild iron deficiency (serum iron 63.00 μg/dL, reference 65–175, linked to chronic inflammation). Persistent leukocytosis (WBC 11.70 × 10^3/μL) and eosinophilia (9.10%, absolute 1.10 × 10^3/μL, reference 0.02–0.5) indicated ongoing subclinical inflammation, possibly exacerbated by medications or occupational exposures such as prolonged driving in a hot climate (Tables 15–17). Thyroid function, renal profile, and hormone assays were unremarkable.

Following diabetes diagnosis, lifestyle interventions were implemented, including a low-glycemic diet (emphasizing whole grains, vegetables, and lean proteins), moderate exercise (30 minutes of walking daily, adjusted for foot healing), vitamin D and iron supplementation, and metformin initiation (500 mg twice daily). These measures normalized glucose (average 110 mg/dL) and lipid profiles within two months, correlating with lesion improvement. Wound care continued with regular debridement, hydrocolloid dressings, and offloading using orthopedic footwear, leading to gradual epithelialization without scarring or amputation (Figure 18).

• *Figure 1: Initial dorsal foot with vesicles, papules and early bullae showing erythema and swelling*

• *Figure 2: Spreading of infection in toes*

• *Figure 3: Swelling and redness after cleaning the wound in second week of infection look like cellulitis*

• *Figure 4 : Extension of infection to planter surface*

• *Figure 6: Foot with crusting and healing lesions*

• *Figure 7: Comparing the healthy and infected foot after recurrence of bullae after 3 days of cleaning*

• *Figure 8 : progression of bullous formation after debridement*

• *Figure 9: Dorsal foot in later stage with residual necrosis and bullae After drainage*

• *Figure 10: Result after cleaning and bandages with saline solution, povidone-iodine , hydrogen peroxide and triple antibiotic ointment*

• *Table 5: Prescription started after two week of infection*

Medicine Name	*Strength*	*Dosage*	*Frequency*	*Duration*	*Qty*	*Remarks*
Itrazol 100Mg 4 Tab	100 Mg	1	Every 12 Hours	7D	14	Use 1 Capsules Every 12 Hours For A Duration Of 7 Days. After Food
Amoclan Forte 625Mg Tab 15S	125 Mg/ 500 Mg	1	Every 12 Hours	3D	6	Use 1 Tablets Every 12 Hours For A Duration Of 3 Days. After Food
Fucidin Cream 30Gm	2%	1	Every 12 Hours	7D	1	Use 1 Gm Every 12 Hours For A Duration Of 7 Days

• *Table 11: Hematology report leukocytosis & eosinophilia*

Test Name	*Result*	*Units*	*Ref. Range*	*Method*
WBC Count	11.03*	10^3/µL	4-10	El. Impedance
Neutrophils (%)	64.31 L	%	40-80	El. Impedance
Lymphocytes (%)	19.11 L	%	20-40	El. Impedance
Monocytes (%)	7.80	%	2-10	El. Impedance
Eosinophils (%)	8.63 H	%	1-6	El. Impedance
Basophils (%)	0.15	%	0-1	El. Impedance
RBC Count	5.38	10^6/µL	4.5-5.9	El. Impedance
HEMOGLOBIN (Hb)	16.31	g/dL	13-17	El. Impedance
HEMATOCRIT (HCT/PCV)	48.7	%	40-50	El. Impedance
MCV (Mean Cell Volume)	90.6	fL	78-100	Calculation
MCH (Mean Cell Hemoglobin)	29.9	pg	27-32	Calculation
MCHC (Mean Cell Hemoglobin Conc)	29.9	g/dL	31.5-34.5	Calculation
RDW CV	13.1	%	11.6-14.0	El. Impedance
RDW SD	45.5	fL	36.5-46.0	El. Impedance
Platelet Count	354.9	10^3/µL	150-400	El. Impedance

• *Table 12: Additional hematology confirming infection markers*

Test Name	*Result*	*Ref. Range*	*Units*	*Method*
RBC (CBC sample)	4.80	4.5-5.9	10^6/µL	Hydrodynamically focused DC
Haemoglobin	14.30	13.5-18	g/dL	RBC pulse height
Hematocrit	43.30	40-58	%	Cell count computation
MCV	90.3*	80-101	fL	Cell count computation
MCH	29.6	27-35	pg	Cell count computation
Red Cell Distribution Width	10.4 H	11-16	%	Cytometry Flow
Total WBC Count	10.4 H	3.4-10.4	10^3/µL	Cytometry Flow
Neutrophils (%)	71.60	40-75	%	Fluorescence Flow
Lymphocytes (%)	18.6 L	20-40	%	Fluorescence Flow
Eosinophils (%)	4.7	1-6	%	Cytometry Flow
Monocytes (%)	3.7	2-10	%	Cytometry Flow
Basophils (%)	0.3	0-2	%	Cytometry Flow
Absolute Neutrophil Count	7.53 H	2-7	10^3/µL	Cytometry Flow
Absolute Lymphocyte Count	1.76	1-3	10^3/µL	Fluorescence Flow
Absolute Eosinophil Count	0.50	0.02-0.5	10^3/µL	Cytometry Flow

• *Table 13: Report of specimen culture of pus*

Section	*Detail*	*Result*
Investigation	MICROBIOLOGY	-
Specimen	Pus	-
Culture	Pus	No Pathogen Grown after 36 hours of Aerobic Incubation
Note	-	*** Kindly correlate with Clinical History

• *Table 14: Biochemistry report with normal random blood*

Test Name	*Result*	*Biological Interval Reference*	*Units*	*Specimen*	*Test Method*
Random Blood Sugar	116	Diabetic: >200 mg/dL (ADA Guidelines)	mg/dL	Fluoride Plasma	Enzymatic Hexokinase

Notes: Factors such as type and time of food intake, infection, physical or psychological stress, exercise and drugs can influence the blood glucose level.

• *Table 15: Hematology report after 4 weeks of infection*

Test Name	*Value*	*Units*	*Bio. Ref. Range*	*Methodology*
*Total Leucocytes Count (Wbc)	11.70	$X10^3$/Ml	4.0-11.0	Coulter Principle
*Hemoglobin	16.20	G/Dl	13-17	Photometric Measurement
*Platelet Count	372.00	$X10^3$/Ml	150-410	Coulter Principle
*Total Rbc	5.38	$X10^6$/Ml	4.5-5.5	Coulter Principle
*Hematocrit (Pcv)	48.70	%	40-50	Calculated Rbc
Mean Corpuscular Volume (Mcv)	90.60	Fl	78-101	Derived Rbc Histogram
Mean Corpuscular Hemoglobin (Mch)	30.20	Pg	27-32	Calculated
Mean Corpuscular Hemoglobin Conc (Mchc)	33.40	G/Dl	31.5-34.5	Calculated
Red Cell Distribution Width - Rdw-Sd	43.80	Fl	37.1-48.3	Derived Rbc Histogram
Rdw-Cv Distribution Width	13.70	%	11.6-14	Derived Rbc Histogram
(Rdw-Cv) Neutrophils	58.10	%	40-80	Histogram/Impedance
*Lymphocyte Percentage	23.40	%	20-40	Optical/Impedance
*Monocytes	8.90	%	2-10	Optical/Impedance
*Eosinophils	9.10	%	1-6	Optical/Impedance
*Basophils	0.50	%	<1-2	Optical/Impedance
*Neutrophils - Absolute Count	6.80	$X10^3$/Ml	2.0-7.0	Calculated
*Lymphocytes - Absolute Count	2.70	$X10^3$/Ml	1.0-3.0	Calculated
Monocytes - Absolute Count	1.00	$X10^3$/Ml	0.2-1.0	Calculated
*Eosinophils - Absolute Count	1.10	$X10^3$/Ml	0.02-0.5	Calculated
*Basophils - Absolute Count	0.10	$X10^3$/Ml	0.02-0.1	Calculated
*Mean Platelet Volume (Mpv)	8.80	Fl	7.5-11.2	Derived Plt Histogram

• *Table 16: Lipid Profile, Liver function test after 4 weeks of infection*

Test Name	*Value*	*Units*	*Bio. Ref. Range*	*Methodology*
LIPID PROFILE				
*Total Cholesterol	186.00	mg/dL	Desirable <200 mg/dL, Borderline high 200-239 mg/dL, High ⩾240 mg/dL	Enzymatic Assay
*HDL Cholesterol - Direct	39.50	mg/dL	40-60 mg/dL, High >60 mg/dL	Elimination/ Catalase
*LDL Cholesterol - Direct	132.00	mg/dL	Optimal <100, Near optimal 100-129, Borderline high 130-159, High ⩾160-189, Very high ⩾190	Enzymatic/ Colorimetric Method
*Triglycerides	133.00	mg/dL	<150 Normal, 150-199 Borderline high, 200-499 High, ⩾500 Very high	Enzymatic Assay
VLDL Cholesterol	26.60	mg/dL	2-30	Calculated
Non-HDL Cholesterol	146.50	mg/dL	<160, 160-189	Calculated
TC/HDL Cholesterol Ratio	4.71	Ratio	3.5-5.0	Calculated
LIVER FUNCTION TEST				
LDL/HDL Ratio	3.34	Ratio	<3.5	Calculated
*Bilirubin Total Test	0.39	mg/dL	0.3-1.2	Vanadate Oxidation
*Bilirubin - Direct	0.14	mg/dL	⩽0.3	Vanadate Oxidation
Bilirubin (Indirect)	0.25	mg/dL	0-0.9	Calculated
*Aspartate Aminotransferase (SGOT)	22.00	U/L	<34	IFCC (without pyridoxal phosphate)
*Alanine Transaminase (SGPT)	37.00	U/L	10-49	IFCC (without pyridoxal phosphate)
*Alkaline Phosphatase	97.00	U/L	46-116	IFCC Standardization
*Gamma Glutamyl Transferase (GGT)	52.00	U/L	<73	Modified IFCC Method
*Protein - Total	7.48	g/dL	5.7-8.2	Biuret Method
*Albumin - Serum	4.47	g/dL	3.2-4.8	Dye Binding: Bromocresol Green
Serum Globulin	3.01	g/dL	2.2-4.0	Calculated
Serum ALB/Globulin Ratio	1.49	Ratio	>1	Calculated

• *Table 17: Renal function test, Diabetic Profile, Thyroid Function test, Hormone Assay, Vitamin and Iron Profile after 4 weeks of infection*

Test Name	*Value*	*Units*	*Bio. Ref. Range*	*Methodology*
Renal Function Test				
*Blood Urea Nitrogen (Bun)	11.57	Mg/Dl	9-23	Gldh Kinetic Assay
Bun/S.creatinine Ratio	14.65	Ratio	9:1-23:1	Modified Jaffe Kinetic Calculated
Est. Glomerular Filtration Rate (Egfr)	121.00	Ml/ Min/1.73M²	>90	Photometry
*Uric Acid	5.74	Mg/Dl	3.7-9.2	Uricase/Peroxidase
*Calcium	8.90	Mg/Dl	8.3-10.6	Enzymatic Colorimetric Method
Diabetic Profile				
*Hba1c	6.00	%	Normal <5.7, Pre Diabetes 5.7-6.4, Diabetes >6.5	H.p.l.c
Average Blood Glucose (Abg)	125.50	Mg/Dl	90-120	Calculated
Thyroid Function Test				
*Thyroid Stimulating Hormone (Tsh)	1.93	Miu/Ml	Adult 0.55-4.78, 1St Trimester 0.48-2.50, 2Nd 0.20-3.00, 3Rd 0.20-3.0, Newborn >20	Two Site Sandwich Immunoassay
*Free Thyroxine (Ft4)	1.40	Ng/Dl	0.89-1.76	Clia
*Free Triiodothyronine (Ft3)	3.21	Pg/Ml	2.3-4.2	Clia
Hormone Assay				
*Testosterone	479.70	Ng/Dl	260-1000	Clia
Vitamin				
*25-Oh Vitamin D (Total)	10.93	Ng/Ml	Deficiency <20 Ng/Ml, Insufficiency 20-30 Ng/Ml, Sufficiency 30-100 Ng/Ml	Clia
*Vitamin B-12	354.00	Pg/Ml	211-911	Clia
Iron Profile				
*Iron	63.00	Mg/Dl	65-175	Ferrozine Sequential Release & Uptake Of Iron
*Total Iron Binding Capacity (Tibc)	281.00	Mg/Dl	240-450	Immunoturbidimetry
% Transferrin Saturation	22.42	%	16-50%	Calculated

Discussion

• *Figure 18: Image after cleaning, drainage of reoccurred bullous and recovery phase*

This case presents a rare and severe manifestation of bullosis diabeticorum (BD) in a 29-year-old male with newly diagnosed diabetes mellitus, characterized by rapid progression from pruritus to bullae, secondary infection, and necrosis [5]. Unlike typical BD, which manifests as painless blisters in patients with longstanding diabetes, this case was exacerbated by occupational factors, including prolonged sitting and potential heat or friction exposure as a car driver, alongside undiagnosed hyperglycemia, which likely intensified microvascular and immune dysfunction [1]. The initial eosinophilia (8.63%) suggests a possible allergic or environmental trigger, such as footwear irritation or heat exposure in Dubai's climate, though parasitic infection was not confirmed via stool analysis or serology. Differential diagnoses included bullous impetigo, excluded by negative pus culture; necrotizing fasciitis, ruled out due to the absence of systemic toxicity or crepitus; pyoderma gangrenosum [6]; and drug-induced bullous pemphigoid [7]. The strong temporal association with new-onset diabetes and the response to broad-spectrum antimicrobials and glycemic control confirmed BD with superinfection. Necrosis, a rare complication of BD, highlights the risks of uncontrolled diabetes, where impaired immunity and tissue perfusion can lead to tissue death, consistent with prior reports requiring surgical intervention [8].

In 2009, Lopez et al. reported a 54-year-old male with type 2 diabetes and neuropathy who developed painless bullae on the lower legs and feet without clear triggers. Managed conservatively with aspiration and topical antiseptics, the lesions resolved within three weeks without infection or necrosis [10]. In contrast, our patient's case was complicated by rapid infectious progression and necrosis, likely due to undiagnosed diabetes and occupational stressors, highlighting the role of early glycemic control in preventing complications. In 2012, Bello et al. described two cases of BD triggered by long-distance bus journeys in patients with poorly controlled type 2 diabetes. The first, a 59-year-old male, developed bilateral foot bullae with secondary staphylococcal infection, resolving in four weeks with antibiotics and glycemic management. The second, a 47-year-old female, progressed to purulent discharge and dry gangrene, necessitating toe disarticulation [11]. Similar to our case, necrosis occurred, but our patient avoided amputation through aggressive antimicrobial therapy and timely diabetes diagnosis, suggesting that early intervention can mitigate severe outcomes.

In 2013, Zhang et al. documented a 56-year-old male with longstanding type 2 diabetes and neuropathy presenting with haemoserous plantar blisters. Conservative management with aspiration, antiseptic washes, and pressure offloading led to resolution in 3–6 weeks without complications [12]. Unlike our case, the absence of infection or necrosis may reflect established diabetes management and lack of weight-bearing trauma, underscoring the impact of undiagnosed diabetes in our patient's severe presentation. In 2014, Gupta et al. reported a 27-year-old male with uncontrolled type 1 diabetes developing painless elbow blisters following minor trauma (sleeping on a hard surface). Biopsy-confirmed BD resolved in four weeks with hydrotherapy and elbow protection, without infection or necrosis [13]. The milder course and upper extremity involvement contrast with our case's lower extremity

severity, likely exacerbated by weight-bearing stress and occupational factors. These comparisons demonstrate that BD's clinical course varies with glycemic control, anatomical site, and external triggers. Our patient's young age, undiagnosed diabetes, and occupational exposures (prolonged sitting, heat, and friction) likely amplified the risk of infection and necrosis, distinguishing this case from milder presentations [10,12,13]. The progression to necrosis aligns with the severe case reported by Bello et al. [11], though our patient's favorable outcome, avoiding amputation, underscores the efficacy of escalated antimicrobial therapy and early glycemic intervention. Initial treatment resistance necessitated broad-spectrum antimicrobials targeting polymicrobial infection, including anaerobes, reflecting the complexity of superinfected BD. Early HbA1c screening was pivotal, as glycemic optimization facilitated healing [3]. Addressing comorbidities, such as dyslipidemia, vitamin D deficiency, and iron insufficiency, through lifestyle modifications and supplementation further supported recovery and reduced recurrence risk. This case advocates for a multidisciplinary approach, integrating dermatology, endocrinology, infectious disease expertise, and podiatry, potentially incorporating advanced therapies like negative pressure wound therapy for refractory cases.

Conclusion

Bullosis diabeticorum can manifest aggressively in young patients with undiagnosed diabetes, progressing to necrosis when complicated by secondary infections. Early diagnosis, optimized glycemic control, and targeted antimicrobial therapy are critical to mitigating morbidity. This case underscores the importance of screening for diabetes in patients presenting with unexplained bullous foot lesions and highlights occupational factors as potential precipitants.

References

1. Larsen, K., Jensen, T., Karlsmark, T., & Holstein, P. E. (2008). Incidence of bullosis diabeticorum – A controversial cause of chronic ulcerations. International Wound Journal, 5(1), 66–69. https://doi.org/10.1111/j.1742-481X.2007.00379.x
2. Bullosis diabeticorum: A rare complication of diabetes mellitus. PMC. https://pmc.ncbi.nlm.nih.gov/articles/PMC7951251/
3. Derella, C. C., Tingen, R. M., Blanks, J. B., & others. (2020). Bullosis diabeticorum: Is there a correlation between hyperglycemia and symptomatology? Wounds. https://www.hmpgloballearningnetwork.com/site/wounds/article/bullosis-diabeticorum-there-correlation-between-hyperglycemia-and-symptomatology
4. Choi, S. W., Shin, J. Y., Lee, S. Y., Kim, J. E., & Chung, J. O. (2018). Bullosis diabeticorum: A diabetic bullosis, commonly unknown. Journal of Wound Management and Research, 14(2), 113–116. https://www.jwmr.org/m/journal/view.php?number=36
5. Barde, C., Shukla, A., Bharti, R., & Singhi, M. K. (2014). Diabetic bullae: A case series and a new model of surgical management. ResearchGate. https://www.researchgate.net/publication/263095426_Diabetic_bullae_A_case_series_and_a_new_model_of_surgical_management
6. Ma, L., Li, Z., Wang, S., & Liu, Y. (2025). Case report: Pyoderma gangrenosum misdiagnosed as diabetic foot. Frontiers in Endocrinology, 16, Article 1604157. https://doi.org/10.3389/fendo.2025.1604157
7. Geller, S., Gat, A., Zeidenweber, D., & Ergaz-Shaltiel, Z. (2021). Bullous pemphigoid in diabetic patients treated by gliptins: The other side of the coin. Journal of Translational Medicine, 19(1), 512. https://doi.org/10.1186/s12967scaras: 0px; font-size: 12px;">8. Armstrong, D. G., & Boulton, A. J. M. (2018). Diagnosis and management of diabetic foot. Diabetes Spectrum, 31(3), 252–258. https://doi.org/10.2337/db20182-1
9. Basu, S., & McBride, M. (2024). Bullosis Diabeticorum. In StatPearls [Internet]. Treasure Island, FL: StatPearls Publishing. https://www.ncbi.nlm.nih.gov/books/NBK539872/
10. Lopez, P. R., Leicht, S., Sigmon, J. R., & Stigall, L. (2009). Bullosis diabeticorum associated with a prediabetic state. Southern Medical Journal, 102(6), 643–644. https://pubmed.ncbi.nlm.nih.gov/19434040/
11. Bello, F., Samaila, M. O., Lawal, Y., & Nkoro, U. K. (2012). 2 Cases of Bullosis Diabeticorum following Long-Distance Journeys by Road: A Report of 2 Cases. Case Reports in Endocrinology, 2012, Article ID 367218. https://pmc.ncbi.nlm.nih.gov/articles/PMC3479936/

12. Zhang, A. J., Garret, M., & Miller, S. (2013). Bullosis diabeticorum: case report and review. The New Zealand Medical Journal, 126(1371), 91–94. https://nzmj.org.nz/journal/vol-126-no-1371/bullosis-diabeticorum-case-report-and-review
13. Gupta, V., Gulati, N., Bahl, J., Bajwa, J., & Dhawan, N. (2014). Bullosis Diabeticorum: Rare Presentation in a Common Disease. Case Reports in Endocrinology, 2014, Article ID 862912. https://www.researchgate.net/publication/269186492_Bullosis_Diabeticorum_Rare_Presentation_in_a_Common_Disease

Received / Получено 10.06.2025
Revised / Пересмотрено 06.07.2025
Accepted / Принято 14.08.2025

A HOSPITAL BASED STUDY: EPIDEMOLOGY AND PRESENTATION OF BENIGN PROSTATIC HYPERPLASIA

Astanov Shavkatbek Mominjanovich[1], Ravi Roshan Khadka[2], Meena Gyawali[2], Muhammed Yaseen Shikhavudeen[3], Adhwaith Athrapulikkal[3]
[1]Jalal-Abad International University, Jalal-Abad, Kyrgystan
[2]Asia International University, Bukhara Uzbekistan
[3]Jalal-Abad State University, Jalalabad, Kyrgystan

Abstract
Introduction: Benign prostatic hyperplasia, is one of the most prevalent disorders that affects male population in every part of the world. The incidence of BPH has increased over the past ten years due to an increase in modifiable risk factors, such as obesity and metabolic disease whereas aging is found to be the most common non modifiable risk factor for BPH.

Objective: The main objective of this study is to find the epidemiology and presentation of BPH cases with their treatment modilaty at hospital in Jalalabad.

Method and methodology: Its a retrospective study of 75 patients who were diagnosed with BPH and came for different types of intervention and treatment in City Hospital in the year 2022 at Jalalabad, Kyrgystan.

Results: The age distribution in this study shows the maximum respondents age group of 60-75 years with 66.6%. According to our study 61.33% of the respondents are having a BMI value more than 25. More than 70% respondents were following up case of BPH who were under medication. Most of respondents had multiple disease whereas most common associate disease are hypertension (22.6%) and diabetes mellitus (13.3%). On symptoms analysis, Frequency of micturation was most common presentation found (86.66 %). Among the respondent, 41.33% were suffering from moderate symptoms and 38.66% were suffering from severe symptoms. 56.66% of the respondents have prostate size between 40-90cc and most common complication associate was acute retention of urine (9.33%). Most of respondent (49.4%) were currently on medical management and 34.6% of respondents underwent surgical management. patient who patient who underwent surgery, 80.76 % underwent TURP followed by open prostatectomy.

Conclusion: The study shows that the increasing age is the risk factor for the prevalence of BPH. In the future, this condition will undoubtedly become even more common and a significant burden for all health care systems due to a shifting demographic profile and an aging population in practically every society. Exercise and nutrition recommendations are crucial strategies in addition to medication and surgery, as they empower patients to take charge of their own health.

Keywords: Benign Prostatic Hyperplasia (BPH), Epidemiology, Hospital

ИССЛЕДОВАНИЕ, ПРОВЕДЕННОЕ В УСЛОВИЯХ СТАЦИОНАРА: ЭПИДЕМОЛОГИЯ И ПРОЯВЛЕНИЯ ДОБРОКАЧЕСТВЕННОЙ ГИПЕРПЛАЗИИ ПРЕДСТАТЕЛЬНОЙ ЖЕЛЕЗЫ

Астанов Шавкатбек Моминджанович[1], Рави Рошан Хадка[2], Мина Гьявали[2], Мухаммед Ясин Шихавудин[3], Адвайт Атрапуликкал[3]
[1]Джалал-Абадский международный университет, Джалал-Абад, Кыргызстан
[2]Азиатский международный университет, Бухара, Узбекистан
[3]Джалал-Абадский государственный университет, Джалал-Абад, Кыргызстан

Аннотация

Введение: Доброкачественная гиперплазия предстательной железы (ДГПЖ) — одно из самых распространенных заболеваний, поражающих мужское население во всем мире. Заболеваемость ДГПЖ увеличилась за последние десять лет в связи с ростом модифицируемых факторов риска, таких как ожирение и метаболические заболевания, в то время как старение является наиболее распространенным немодифицируемым фактором риска ДГПЖ.

Цель: Основная цель данного исследования — изучить эпидемиологию и клиническую картину случаев доброкачественной гиперплазии предстательной железы (ДГПЖ) с учетом методов их лечения в больнице г. Джалал-Абад.

Методология: Проведено ретроспективное исследование 75 пациентов с диагнозом ДГПЖ, обратившихся в городскую больницу в 2022 году в г. Джалал-Абад, Кыргызстан, для проведения различных видов вмешательства и лечения.

Результаты: Возрастное распределение в данном исследовании показывает максимальную возрастную группу респондентов 60-75 лет — 66,6%. Согласно нашему исследованию, 61,33% респондентов имели ИМТ более 25. Более 70% респондентов находились под наблюдением в связи с ДГПЖ и принимали лекарственные препараты. У большинства респондентов имелось несколько заболеваний, наиболее распространенными из которых являются гипертония (22,6%) и сахарный диабет (13,3%). При анализе симптомов наиболее распространенным проявлением было учащенное мочеиспускание (86,66%). У 41,33% респондентов наблюдались умеренные симптомы, а у 38,66% – тяжелые. У 56,66% респондентов размер предстательной железы составлял 40–90 см3, а наиболее частым сопутствующим осложнением была острая задержка мочи (9,33%). Большинство респондентов (49,4%) в настоящее время находились на фармакотерапии, а 34,6% респондентов прошли хирургическое лечение. 80,76% пациентов, перенесших операцию, перенесли ТУРП, а затем открытую простатэктомию.

Заключение: Исследование показывает, что возраст является фактором риска развития ДГПЖ. В будущем это заболевание, несомненно, станет еще более распространенным и станет значительным бременем для всех систем здравоохранения в связи с изменением демографического профиля и старением населения практически в каждом обществе. Рекомендации по физическим упражнениям и питанию являются важнейшими стратегиями, помимо медикаментозной терапии и хирургического вмешательства, поскольку они позволяют пациентам самостоятельно заботиться о своем здоровье.

Ключевые слова: Доброкачественная гиперплазия предстательной железы (ДГПЖ), Эпидемиология, Больница

Introduction

Benign prostatic hyperplasia (BPH) is a nonmalignant growth or hyperplasia of the prostate tissue and is a very common cause of lower urinary tract symptoms (LUTS) in old-aged men. Disease prevalence is seen to be increasing with advancing age.Risk factors for the development of BPH include family history, diabetes, diet, genetic factors, obesity and metabolic syndrome. [1]

The symptoms of BPH include urinary frequency, urgency, lower urinary tract symptoms, incomplete bladder emptying, urinary retention, weak urinary stream, post-void dribbling and UTIs.Clinical examination includes Digital Rectal Exam (DRE) which allows for assessment of the size and condition of the prostate gland.[2] Tests commonly performed for patients with benign prostatic hyperplasia (BPH) include, Prostate-Specific Antigen (PSA) Test which measures the level of PSA, a protein produced by the prostate gland. Urinalysis for signs of infection.Uroflowmetry which is a non-invasive test measures the rate and amount of urine voided to assess urinary flow and potential obstruction, Ultrasound abdomen uses ultrasound waves for the imaging the prostate and surrounding tissues for the evaluation of size and structure of the gland.[3]

Medications commonly prescribed include alpha blockers such as tamsulosin, terazosin, and doxazosin, which relaxes the prostate and bladder neck muscles to improve urine flow. Additionally, 5 alpha reductase inhibitors are added for large (>40 gram) symptomatic prostrate, which reduces the size of prostate. Patients with surgical indication commonly undergoes transurethral resection of prostate. [4]

In 2019, the global incidence of benign prostatic hyperplasia was 94 million cases compared to 51.1 million in 2000. The age-standardized prevalence of benign prostatic hyperplasia was 2480 per 100,000 people. Although the global number of prevalent cases increased by 70.5% between 2000 and 2019, the global age-standardized prevalence remained stable.[5] In Eastern Europe, age-standardized prevalence was between 6480 and 987 per 100,000 in 2019, followed by North Africa and the Middle East.[6]

In a comprehensive survey for 2021-2022 with 3265 men of various ages in Kyrgyz Republic, showed the early incidence and prevalence of prostate diseases in Chui region (12%), Issyk-Kul region (36%), Talas region (32%), Osh region (13%) and Jalal- Abad regions (9%). Among the men who applied, 37.8% were urban residents and 62.2% were rural residents. In the survey, 28.4% of the men (in the group of middle and old age) were suffering from Benign prostate hyperplasia. [7]

Methods and methodology

This was a retrospective, descriptive study which was done for a year period of time in the year 2022 in the Urology department of City hospital in Jalalabad. After ethical clearance from committee board and hospital authorities, we have used standard questionnaire to collect the data for final conclusion. There were total 75 patients who were undertaken for this study. The data that are summarized in this study were collected from different sources like folders of investigations, patient's registers, hospital and surgical records from the hospital.

Results

• *Table 1. Distribution of respondents according to their respective age*

Responses	*Frequency*	*Percentage*
40-59	19	25.33
60-75	50	66.6
75 and above	6	8
Total		

Above Table shows that the distribution of respondents according to their age which shows the maximum age group belongs to 60-75 years with 66.6% and followed by age group 40-59 (25.33%) .

• *Table 2. Distribution of respondents according to their BMI*

Responses	*Frequency*	*Percentage*
24.9 or below	29	38.66
25.0 or above	46	61.33
Total	75	100

The distribution of respondents according to their Body Mass Index (BMI) which shows majority 61.33% of the respondents are having a BMI value 25.0 and above and remaining 38.66% of respondents were having the BMI value of 24.9 and below.

• *Table 3. Distribution of respondents according to their history and the time it was diagnosed*

Respondents	*Frequency*	*Percentage*
More than 1 years ago	36	48
Less than a year ago	17	22.66
New cases	22	29.33
Total	75	100.0

According to the previous history of diagnosis, above table shows 48% respondents were diagnosed for more than 1 year ago 29.33% respondents were newly diagnosed and remaining 22.6% respondents were diagnosed less than 1 year ago only.

• *Table 4. Distribution of respondents according to other health conditions they experience*

Responses	*Frequency*	*Percentage*
Diabetes Mellitus	10	13.33
Hypertension	17	22.66
Heart Diseases	8	10.66
Pulmonary Diseases	6	8
Multiple Diseases	28	37.33
No Diseases	6	8
Total	75	100

Above Table shows majority 37.33% of respondents had multiple disease where as 22.6% respondents had hypertension, 13.3% had diabetes mellitus and 10.6% had some heart diseases and remaining 8% had pulmonary diseases and remaining 8% had no any diseases along with their current problem.

• *Table 5. Distribution of respondents according to the presenting urinary symptoms associated with BPH*

Responses	*Frequency*	*Percentage*
Frequency of micturition during daytime		
No	10	13.33
yes	65	86.66
Frequency of micturition during night time (Nocturia)		
None	13	17.33
Once	24	32
2 or more	38	50.66
Urgency to Urinate		
No	14	18.66
yes	61	81.33
Intermettency		
No	17	22.66
yes	58	77.33
Weak urine stream		
No	12	16
yes	63	84
Sense of incomplete voiding of the bladder		
No	16	21.33
yes	59	78.66
Strain during urination		
No	14	18.66
Yes	61	81.33
Other symptoms		
Acute urinary retention	11	14.66
Hematuria	3	4
Severity of urinary symptoms (IPSS score)		
0-7 Mild	15	20
8-19 Moderate	31	41.33
20-35 Severe	29	38.66

The above table on symptoms assessment shows frequency of micturation was most common presentation found in 86.66 % of the respondents, followed by weak urinary stream (84%) and Nocturia (82.66%). Among the respondent, 38.66% were suffering from severe symptoms and 14.66% presented with acute retention of urine.

• *Table 6. Distribution of respondents according to the findings of relevant diagnostic test--done*

Responses	*Frequency*	*Percentage*
Size of Prostate (USG abdomen)		
Below 5*3*5 (40 cc)	29	38.66
Between 5*3*5-6*4*6 (40-90 cc)	41	54.67
Above 6*4*6 (>90 cc)	5	6.67
Other Findings (USG & Lab)		
Bladder Calculi	2	2.66
Hydronephrosis	3	4
UTI	7	9.33

Above Table on Laboratory and Diagnostic Tests shows that 54.67% of the respondents have prostate size between 40-90cc and 6.67% have huge prostate. 14.66 % respondent developed UTI while 4% have hydronephrosis and 2.66 % have associate bladder calculi.

• *Table7. Distribution of respondents according to current treatment status for BPH*

Responses	*Frequency*	*Percentage*
Obervation and follow up	12	16
Medical management	37	49.4
Surgical management	26	34.6
Total	75	100

Above Table shows 49.4% of respondents are currently on medical management as a treatment for BPH and 34.6% of respondents went through surgical management and remaining 16% respondents were under observationa and follow up for their condition.

• *Table 8. Distribution of respondents according to the surgery performed for BPH*

Response	*Frequency*	*Percentage*
TURP	21	80.76
Open surgery	5	19.23
Total	26	34.7
Additional intervention		
Urethral catherization	5	6.7
Suprapubic cystostomy	2	2.7
Total	7	

Above Table shows, out of 26 patient who underwent surgery, 80.76 % underwent TURP, while for rst of cases, open prostatectomy was done. Out of 9 cases of acute retention of urine; 5 patients were managed by urethral catheterization and 2 were managed by suprapubic cystostomy. After cathererization, 4 patients underwent surgical management and 3 were discharged with medical management and follow up plan.

Discussion

Benign prostatic hyperplasia (BPH) refers to the non-malignant growth or hyperplasia of prostate tissue and is common cause of lower urinary tract symptoms (LUTS) in older men. This study aims to investigate the epidemiology and presentation of Benign Prostate Hyperplasia (BPH) cases at the hospitals in Jalalabad, Kyrgyzstan. Disease prevalence has been shown to increase with advancing age. In our survey, more than 70% cases were diagnosed case of BPH under management where as in the survey conducted by Lim K.B, in his study it shows that on prostate disease awareness, 55.2% of respondents claimed they were unaware of the condition, 11.3% of respondents were unable to assess their own health, 52.2% of respondents said they did not trust doctors, however, 41% of respondents reported that the disease was detected for the first time. [8]

Most of the respondents belongs to age group 60-75 i.e., 66.6% and the respondents who were aged between 40-59years of age were 25.33%. A systematic analysis for the Global Burden of BPH showed men aged 65–74 years shared the greatest absolute burden of benign prostatic hyperplasia, accounting for 42% of the total prevalent cases. Our findings are consistent with global standard (9). A study done in mainland China, shows the prevalence of BPH was with increasing age after the age of 40 years. (10)

According to our data majority men with BPH i.e 61.33%, have BMI 25 or above and rest of patient have BMI less than 25. The growth of the prostate gland corresponds with body mass index (BMI) and waist circumference. According to the WHO classification BMI greater than 35kg/m2 have a 3.5 times higher risk of developing BPH (10). Study conducted by Betai K et al showed significant correlation of BMI with prostate volume. Patients with larger prostates (>75cc) had significantly higher BMI compared to patients with smaller prostate volume (<75cc) (11)

Fowke and colleagues showed that prostate volume was significantly positively associated with BMI, waist-hip ratio, waist circumference, percent body fat, total fat mass, and total lean mass [12]. Kim et al. demonstrated positive correlations between BMI and prostate volume and between BMI and International Prostate Symptom Score among Korean men [13].

In our study, majority 37.33% of respondents had multiple disease where as 22.6% respondents had hypertension, 13.3% had diabetes mellitus and 10.6% had some heart diseases and remaining 8% had pulmonary diseases. There have been multiple studies interested in demonstrating the link between metabolic syndrome and BPH, but findings have been inconsistent. Some studies have reported how diabetes and hyperlipidemia [14,15) were correlated with BPH, while other studies have failed to demonstrate an association [16]. On comparison with the study on Effect of Obesity and Hyperglycemia on BPH in Elderly Patients with Newly Diagnosed Type 2 Diabetes, the respondents with diabetes mellitus type1 where more prone to have BPH (17). Ageing population has higher incidence of cardiovascular disease and diabetis. BPH occurs at a high frequency in the aging man and is usually present with 1 or more comorbidities. Accordingly, the choice of BPH treatment should be guided by the presence of medical conditions such as diabetes, metabolic syndrome, CV disease and hypertension (18)

Symptoms assessment of BPH patient in our study shows, frequency of micturation was most common presentation found in 86.66 % of the respondents, followed by weak urinary stream (84%) and Nocturia (82.66%). Among the respondent, 41.33% were suffering from moderate symptoms & 38.66% were suffering from severe symptoms and 9.33% presented with acute retention of urine. Although BPH is not a life-threatening condition, the impact of BPH on

quality of life can be significant and should not be underestimated.Moderate-to-severe LUTS was seen in 41 % of the patients on community-based done in the United Kingdom (18,19) and Literature review showed frequency was the most common symptoms followed by weak urinary stream and dribbling of urine (20), these findings were consistent with our study.

Study shows that 56.66% of the respondents have prostate size between 40-90cc and 6.66% have huge prostate. In this study it shows that 14.66 % respondent developed acute retention of urine and 9.33% UTI, while 4% have hydronephrosis and 2.66 % have associate bladder calculi. The commonest range of prostate volume was 50–89 cc as shown in study done by obiesie et al.Review article by speakman MJ showed, the most common presenting complication of BPH that requires hospitalization is acute urinary retention, which greatly affects patients' quality of life and is an important health issue. Many of the other complications of BPH are in part due to complications of chronic urinary retention; these include recurrent urinary tract infections formation of bladder calculi, hematuria, and damage to bladder wall and kidneys. Finally, there is an important association between BPH/BOO and male erectile dysfunction. (21)

Our study showed, 49.4% of respondents are currently on medical management as a treatment for BPH and 34.6% of respondents went through surgical management and remaining 16% respondents were under observational and follow up for their condition. Out of 26 patient who underwent surgery, 80.76 % under went TURP, while for rest of cases, open prostatectomy was done. Out of 9 cases of acute retention of urine; 5 patients were managed by urethral catheterization and 2 were managed by suprapubic cystostomy. After cathererization, four patient underwent surgical management and 3 were discharged with medical management and follow up plan.

After lifestyle modifications, medication is generally first line in the treatment of symptomatic BPH. Two drug classes became accepted standard care are 5-alpha-reductase inhibitors and Alpha-blockers. Although monotherapy, with alpha blockers and 5 alpha reductase inhibitors, is beneficial, the combination of these drugs is highly effective (22). Surgical intervention are reserved to patient with complications and refractory to medical therapy. TURP has long been considered the historical gold standard for the surgical treatment of BPH and open techniques are reserved for large prostate (>90 cc) if Holmium laser enucleation of the prostate (HoLEP) are not available (23).

Conclusion

In this study it highlights that the increasing incident of Prostatic Hyperplasia is seen with majority of population with growing age. As we can see in many countries aging population are increasing in trends which means that the incidence of BPH might be increases in coming days. With increasing age from the study, it also highlights that the commodities such as diabetes, hypertension are might lead to more complication with BPH patients. From the study we can see that in treatment approaches huge number of populations they receive medical management while few they undergo surgical managements such as transurethral resection of the prostate (TURP). Overall, as a recommendation we would like to highlight on healthy dietary pattern, lifestyle modification early screening and diagnosis are essential for timely intervention and better management of BPH.

References

1. Dwitawira Wibowo N, Rizky Hidayat M. The Impact Of Benign Prostate Hyperplasia Treatment Modalities On The Incidence And Progression Of Urethral Stricture : A Comprehensive Systematic Review. Journal Of Advanced Research In Medical And Health Science (Issn 2208-2425) [Internet]. 2024 Apr 29 [Cited 2024 Dec 11];10(4):124–32.
2. Levi A Deters, MD; Chief Editor: Edward David Kim, MD, FACS [Updated: Mar 22, 2023], available from :https://emedicine.medscape.com/article/437359-overview#a5
3. National Cancer Institute. Prostate-Specific Antigen (PSA) Test. Cancer.gov. [Internet]. Available from: https://www.cancer.gov
4. Haile ES, Sotimehin AE, Gill BC. Medical management of benign prostatic hyperplasia. Cleveland Clinic journal of medicine. 2024 Mar 1;91(3):163–70.
5. Ye Z, Wang J, Xiao Y, Luo J, Xu L, Chen Z. Global burden of benign prostatic hyperplasia: results from the global burden of disease study 2019. BMC Urology. 2024 Sep 5;24(1).
6. GBD 2019 BPH collaborators, Omid Dadras. The global, regional, and national burden of benign prostatic hyperplasia in 204 countries and territories from 2000 to 2019: a systematic analysis for the Global Burden of Disease Study 2019
7. Kurmanbekov N.K., Keneev R.N., Satybaldyev E.E.,Stambekova K.N., Kylychbekov M.B. Analysis of the incidence of prostate diseases and their early detection based on the results of a scientific project for the study of the male population in the Kyrgyz Republic. Health care of Kyrgyzstan 2022, No. 3, pp. 140-147.
8. Lim K. B. (2017). Epidemiology of clinical benign prostatic hyperplasia. Asian journal of urology, 4(3), 148–151. https://doi.org/10.1016/j.ajur.2017.06.004
9. Awedew AF, Han H, Abbasi B, Abbasi-Kangevari M, Ahmed MB, Almidani O, et al. The global, regional, and national burden of benign prostatic hyperplasia in 204 countries and territories from 2000 to 2019: a systematic analysis for the Global Burden of Disease Study 2019. The Lancet Healthy Longevity [Internet]. 2022 Nov 1;3(11):e754–76.
10. Wang W, Guo Y, Zhang D, Tian Y, Zhang X. The prevalence of benign prostatic hyperplasia in mainland China: evidence from epidemiological surveys. Scientific Reports. 2015 Aug 26;5(1).
11. Batai K, Phung M, Bell R, Aye Aye Lwin, Hynes K, Price E, et al. Correlation between body mass index and prostate volume in benign prostatic hyperplasia patients undergoing holmium enucleation of the prostate surgery. BMC Urology. 2021 Jun 10;21(1).
12. Fowke JH, Koyama T, Fadare O, Clark PE. Does Inflammation Mediate the Obesity and BPH Relationship? An Epidemiologic Analysis of Body Composition and Inflammatory Markers in Blood, Urine, and Prostate Tissue, and the Relationship with Prostate Enlargement and Lower Urinary Tract Symptoms. Hurst R, editor. PLOS ONE. 2016 Jun 23;11(6):e0156918.
13. Kim JM, Song PH, Kim HT, Moon KH. Effect of Obesity on Prostate-Specific Antigen, Prostate Volume, and International Prostate Symptom Score in Patients with Benign Prostatic Hyperplasia. Korean Journal of Urology. 2011;52(6):401.
14. Nandy PR, Saha S. Association between components of metabolic syndrome and prostatic enlargement: An Indian perspective. Medical Journal Armed Forces India. 2016 Oct;72(4):350–5.
15. Shih HJ, Huang CJ, Lin JA, Kao MC, Fan YC, Tsai PS. Hyperlipidemia is associated with an increased risk of clinical benign prostatic hyperplasia. The Prostate. 2017 Nov 9;78(2):113–20.
16. Egan KB, Burnett AL, McVary KT, Ni X, Suh M, Wong DG, et al. The Co-occurring Syndrome—Coexisting Erectile Dysfunction and Benign Prostatic Hyperplasia and Their Clinical Correlates in Aging Men: Results From the National Health and Nutrition Examination Survey. Urology [Internet]. 2015 Jun 17 [cited 2025 Jan 28];86(3):570–80
17. Irene Pascual Mathey L (2022) Benign Prostatic Hyperplasia: Epidemiology, Pathophysiology, and Clinical Manifestations. Molecular Mechanisms in Cancer. IntechOpen. Available at: http://dx.doi.org/10.5772/intechopen.104823.
18. Mobley D, Feibus A, Baum N. Benign prostatic hyperplasia and urinary symptoms: Evaluation and treatment. Postgraduate Medicine. 2015 Mar 30;127(3):301–7.
19. Obiesie AE, A M E Nwofor, Oranusi CK, Mbonu OO. Correlation between Prostate Volume Measured by Ultrasound and Symptoms Severity Score in Patients with Benign Prostatic Hypertrophy in Southeastern Nigeria. Nigerian Journal of Clinical Practice [Internet]. 2022 Aug 1 [cited 2025 Jan 28];25(8):1279–86.
20. Speakman M, Cheng X. Management of the complications of BPH/BOO. Indian Journal of Urology. 2014;30(2):208.

21. Lokeshwar SD, Harper BT, Webb E, Jordan A, Dykes TA, Neal Jr DE, et al. Epidemiology and treatment modalities for the management of benign prostatic hyperplasia. Translational Andrology and Urology [Internet]. 2019 Oct;8(5):529–39
22. Bishr M, Boehm K, Trudeau V, Tian Z, Dell'Oglio P, Schiffmann J, et al. Medical management of benign prostatic hyperplasia: Results from a population-based study. Canadian Urological Association journal = Journal de l'Association des urologues du Canada [Internet]. 2016;10(1-2):55–9
23. Ng M, Leslie SW, Baradhi KM. Benign Prostatic Hyperplasia. [Updated 2024 Jan 11]. In: StatPearls [Internet]. Treasure Island (FL): StatPearls Publishing; 2024 Jan-. Available from: https://www.ncbi.nlm.nih.gov/books/NBK558920/

Received / Получено 25.06.2025
Revised / Пересмотрено 16.07.2025
Accepted / Принято 12.08.2025

EARLY CLINICAL EXPOSURE FOR FIRST-YEAR MEDICAL STUDENTS AT JALALABAD INTERNATIONAL UNIVERSITY

Kumar Deivanai[1], Astanov Shavkatbek Mominjanovich[2], Dipak Chaulagain[2,3], Farjana Afrin[2]
[1]Medical Student, Jalal-Abad International University, Jalal-Abad, Kyrgyzstan
[2]Jalal-Abad International University, Jalal-Abad, Kyrgyzstan
[3]Uzhhorod National University, Uzhhorod, Ukraine

Abstract
Aim and Background: Early Clinical Exposure (ECE) serves to bridge the divide between preclinical education and clinical practice from the outset of the MBBS program. It enables students to integrate foundational sciences with patient-centered care, fostering a cohesive medical education experience. This study evaluated the influence of ECE on the learning outcomes, motivation, and clinical comprehension of first-year MBBS students at Jalalabad International University (JAIU).

Objectives: To assess the effects of ECE on student motivation, interest in learning, and formation of professional identity. To examine how ECE contributes to the foundational development of medical knowledge among first-year students.

Materials and Methods: A cross-sectional, perception-based study was conducted among first-year MBBS students following over six months of ECE implementation. A pre-validated questionnaire comprising 6 demographic items and 9 closed-ended questions addressing all preclinical subjects was distributed via Google Forms. Data collection spanned two weeks, with responses analyzed using SPSS version 27. Descriptive statistics (frequencies, percentages, means) were employed, and statistical significance was set at $p < 0.05$.

Results: Of the respondents, 92% reported enhanced understanding of basic sciences through clinical contextualization, 89% indicated increased motivation, 85% noted improvements in communication skills, 80% affirmed heightened interest in medicine, 78% believed ECE reduced anxiety in later clinical settings, and 82% reported improved teamwork skills.

Conclusion: ECE during the first year of MBBS at JAIU emerges as an effective educational strategy, bolstering comprehension, motivation, confidence, and professional orientation among students.

Keywords: Early Clinical Exposure, MBBS, Preclinical Education, Student Motivation, Clinical Reasoning

РАННЕЕ КЛИНИЧЕСКОЕ ОБУЧЕНИЕ СТУДЕНТОВ-МЕДИКОВ ПЕРВОГО КУРСА ДЖАЛАЛ-АБАДСКОГО МЕЖДУНАРОДНОГО УНИВЕРСИТЕТА

Кумар Дейванай[1], Астанов Шавкатбек Моминджанович[2], Дипак Чаулагайн[2,3], Фарджана Африн[2]
[1]Студент-медик Джалал-Абадского международного университета, Джалал-Абад, Кыргызстан
[2] Джалал-Абадский международный университет, Джалал-Абад, Кыргызстан
[3] Ужгородский национальный университет, Ужгород, Украина

Аннотация
Цель и обоснование: Раннее клиническое обучение (РКО) служит для преодоления разрыва между доклиническим образованием и клинической практикой с самого начала программы MBBS. Оно позволяет студентам интегрировать фундаментальные

науки с пациентоориентированным подходом к оказанию медицинской помощи, способствуя формированию целостного медицинского образования. В данном исследовании оценивалось влияние РКО на результаты обучения, мотивацию и понимание клинической практики студентами первого курса MBBS Джалал-Абадского международного университета (JAIU). Цели: Оценить влияние доклинического образования (ДО) на мотивацию студентов, интерес к обучению и формирование профессиональной идентичности. Изучить, как доклиническое образование (ДО) способствует формированию основ медицинских знаний у студентов первого курса.

Материалы и методы: Было проведено поперечное исследование, основанное на восприятии, среди студентов первого курса программы MBBS после более чем шести месяцев внедрения доклинического образования (ДО). Предварительно валидированная анкета, включающая 6 демографических пунктов и 9 вопросов закрытого типа, охватывающая все доклинические исследования, была распространена через Google Формы. Сбор данных занял две недели, ответы анализировались с помощью SPSS версии 27. Использовалась описательная статистика (частоты, проценты, средние значения). Статистическая значимость была установлена на уровне $p < 0,05$. Результаты: 92% респондентов сообщили об улучшении понимания базовых наук благодаря клинической контекстуализации, 89% отметили повышение мотивации, 85% отметили улучшение коммуникативных навыков, 80% подтвердили повышенный интерес к медицине, 78% считают, что ECE снижает тревожность в дальнейшей клинической практике, а 82% сообщили об улучшении навыков командной работы.

Заключение: ECE в течение первого года обучения по программе MBBS в Университете Джайпура-Айленда (JAIU) представляет собой эффективную образовательную стратегию, способствующую пониманию материала, мотивации, уверенности в себе и профессиональной ориентации студентов.

Ключевые слова: Раннее клиническое знакомство, MBBS, доклиническое образование, мотивация студентов, клиническое мышление

Introduction

Clinical exposure is a cornerstone of health professions education, encompassing diverse learning environments such as ward-based teaching, technical skills acquisition, clinically contextualized academic pursuits, and outpatient interactions [1]. Early Clinical Exposure (ECE) is defined as authentic human engagement in social or clinical contexts that amplifies the comprehension of health, illness, disease, and the health professional's role during the preclinical undergraduate years [2]. By integrating ECE into the MBBS curriculum, students can link basic science disciplines—such as anatomy, physiology, and biochemistry—with their clinical applications, enriching traditional pedagogical approaches without diminishing their value [3].

Mandated by the National Medical Commission within the 2019 Competency-Based Medical Education framework, ECE addresses the disconnect between theoretical knowledge and practical application [3]. Studies from Indian institutions, including those in Bhopal, Faridabad, and Tamil Nadu, highlight ECE's efficacy in enhancing knowledge retention, clinical reasoning, and motivation, with Objective Structured Clinical Examination (OSCE)

performance improving significantly post-ECE and over 90% of participants endorsing its value [4]. Beyond cognitive gains, ECE fosters non-cognitive competencies like empathy, professional identity formation, and interdisciplinary collaboration—essential for compassionate clinical practice [4].

This study investigates the impact of ECE on the educational trajectory, clinical acumen, and motivational dynamics of first-year MBBS students at JAIU, emphasizing its role in scaffolding preclinical learning for subsequent clinical proficiency.

Aim

To investigate the impact of ECE on the learning experience, clinical reasoning, and motivation of first-year MBBS students through patient-oriented learning in the preclinical curriculum.

Objectives

To evaluate the influence of ECE on student motivation, learning engagement, and professional identity development.

To determine how ECE facilitates comprehension of clinical practices and strengthens the foundational medical knowledge base among first-year students.

Materials and Methods

This cross-sectional study employed a perception-based survey targeting first-year MBBS students at JAIU who had undergone ECE for over six months. A pre-validated questionnaire, developed for reliability and validity, included 6 demographic questions and 9 closed-ended items (using Likert-scale responses) covering all preclinical subjects (anatomy, physiology, biochemistry). The instrument was distributed via Google Forms through student email lists, social media, and institutional academic groups. Data were collected over a two-week period (May 27, 2025, to June 7, 2025), with weekly reminders to maximize response rates.

Responses were exported to SPSS version 27 for analysis. Descriptive statistics (means, frequencies, percentages) characterized demographics and perceptual responses, with inferential statistics assessing associations where applicable ($p < 0.05$ denoted significance). Ethical considerations included informed consent embedded in the survey and response anonymization.

The questionnaire items were:

1. Do you consider ECE important in first-year MBBS?
2. Did ECE enhance your classroom attention?
3. Did ECE facilitate better topic comprehension?
4. Does ECE promote lifelong learning when integrated with applied aspects?
5. Do you prefer ECE to traditional teaching methods?
6. Did ECE aid in recognizing attitudes, ethics, and professionalism in doctor-patient interactions?
7. Can early clinical exposure assist in selecting future specialties?
8. Does early clinical skills practice alleviate anxiety in subsequent postings or OSCEs?
9. Does ECE foster teamwork?

Results

The survey collected responses from 120 first-year MBBS students, achieving a response rate of 80%. Demographic analysis revealed a predominant age of 20 years (36%), followed by 21 years (23%) and 19 years (21%), with the range spanning 18 to 24 years, consistent with typical MBBS entry demographics (Figure 1). Gender distribution showed a slight male

predominance (55% male, 45% female), suggesting potential for subgroup analyses to explore gender-based perceptual differences (Figure 2).

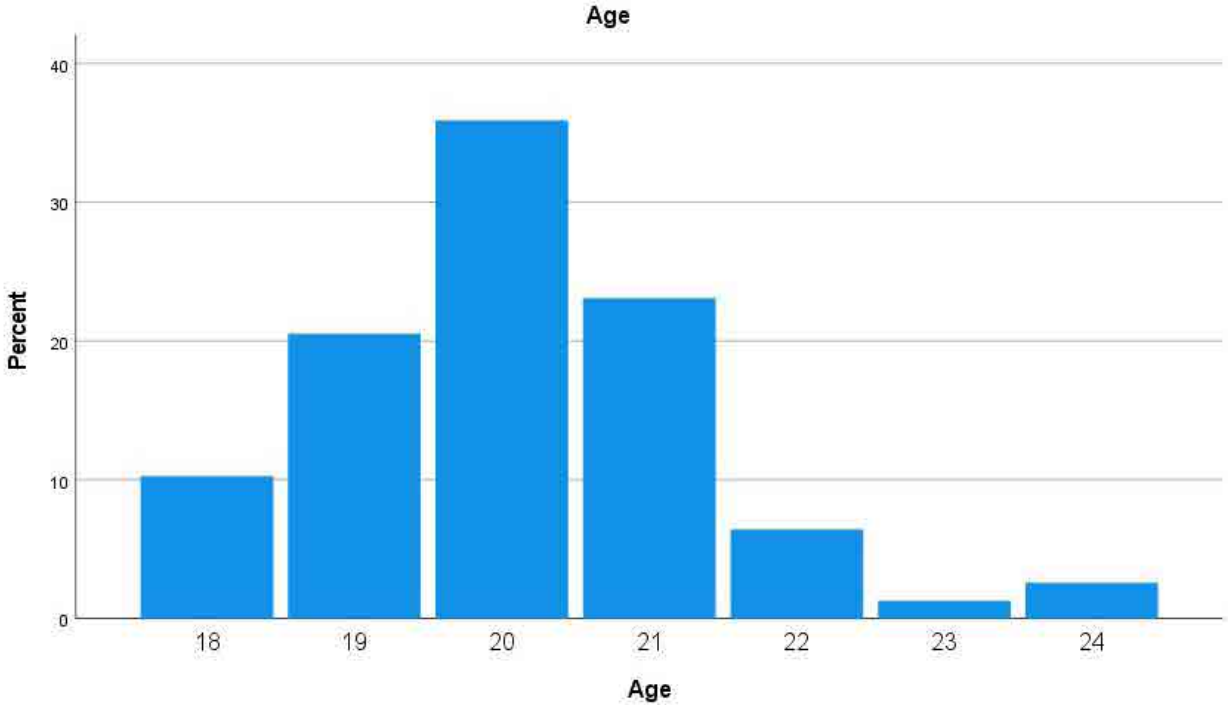

• *Figure1: Consistent with typical MBBS entry demographics*

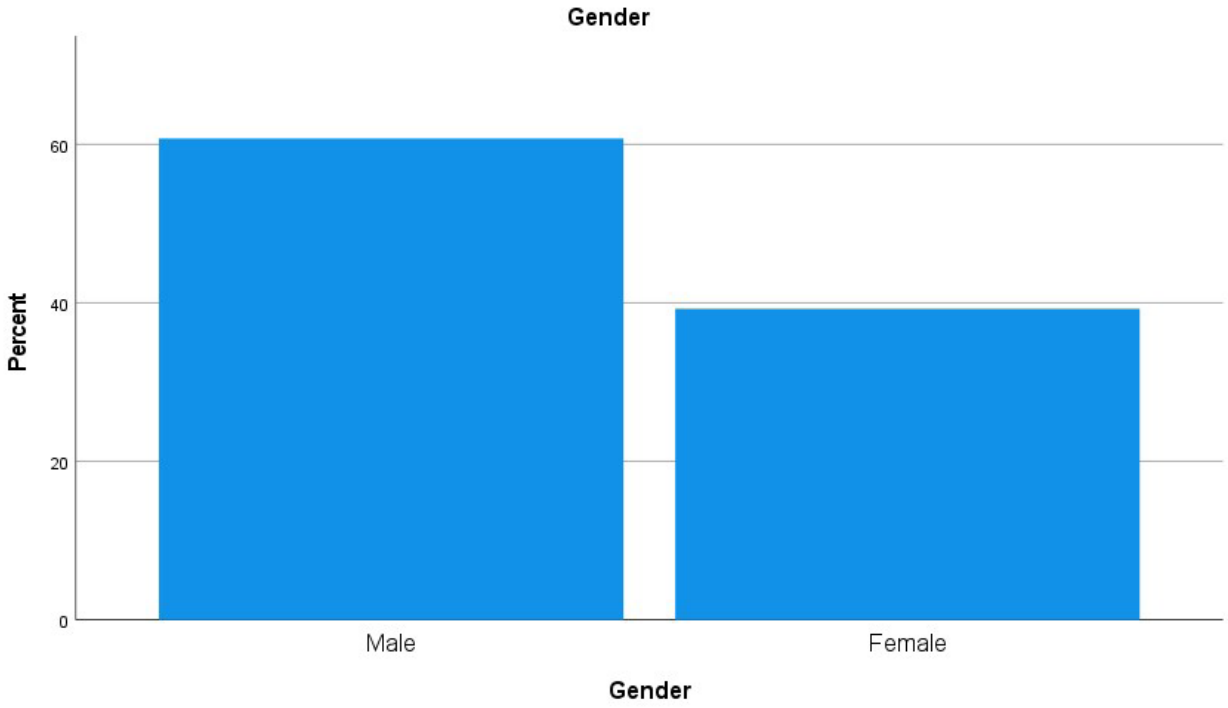

• *Figure2: Gender distribution showed a slight male predominance*

Perceptual feedback underscored ECE's transformative impact across multiple domains:

Comprehension of Basic Sciences: 92% of students reported improved understanding of basic sciences when contextualized with clinical relevance ($p < 0.001$), reflecting ECE's ability

to transform abstract concepts into practical applications, thereby enhancing knowledge retention and critical thinking.

Motivation: 89% expressed heightened motivation to engage with preclinical subjects after observing their clinical utility ($p < 0.001$), highlighting ECE's role in sustaining enthusiasm within a demanding curriculum.

Communication Skills: 85% noted improvements in communication skills due to early patient interactions ($p < 0.001$), likely fostering empathy and effective dialogue critical for patient-centered care.

Interest in Medicine and Role Clarity: 80% affirmed increased interest in medicine and a clearer understanding of physician responsibilities ($p < 0.001$), contributing to early professional identity formation.

Anxiety Reduction: 78% believed ECE reduced anxiety during later clinical postings or OSCEs ($p < 0.01$), suggesting early exposure builds confidence in high-stakes settings.

Teamwork: 82% reported enhanced teamwork skills ($p < 0.001$), attributed to collaborative clinical activities fostering interdisciplinary cooperation.

These findings indicate robust statistical significance and high agreement levels, reinforcing ECE's integrative value across cognitive and non-cognitive domains.

Figure 1. Age distribution of participants (bar chart: 19 years: 21%, 20 years: 36%, 21 years: 23%, others: 20%).

Figure 2. Gender distribution of participants (pie chart: Male: 55%, Female: 45%).

Discussion

The findings at JAIU demonstrate ECE's profound impact, with 92% of students reporting enhanced comprehension, 89% noting increased motivation, 85% observing improved communication skills, 80% affirming greater interest in medicine, 78% reporting reduced anxiety, and 82% acknowledging enhanced teamwork. These results align closely with prior studies, reinforcing ECE's efficacy while highlighting nuances in implementation and outcomes.

Das et al. (2017) studied 150 first-year MBBS students and found 92% reported ECE made basic sciences more engaging and clinically relevant, though 8% cited time constraints as a challenge [5]. Their objective pre- and post-test scores showed significant improvements ($p = 0.04$), complementing our perceptual data and suggesting that integrating objective assessments could strengthen future studies at JAIU [5]. Similarly, Patil et al. (2021) reported that 95% of 100 students found ECE improved concept understanding, 90% deemed it highly useful, and over 80% noted increased subject interest, with significant gains in learning strategies ($p < 0.05$) [6]. Their use of motivational videos and case-specific ward visits achieved 100% recognition of clinical relevance, suggesting potential enhancements for JAIU's broader preclinical approach [6].

In contrast, Sood et al. (2023) reported more modest outcomes among 88 students, with 68.2% agreeing ECE aided topic understanding and 51.1% noting communication improvements, possibly due to their focus on academic metrics over motivational aspects [7]. Rawekar et al. (2016) demonstrated significant score improvements ($p < 0.05$) in a smaller cohort of 40 students but lacked detailed perceptual data, limiting direct comparison to our attitudinal findings [8]. Govindarajan et al. (2018) emphasized ECE's motivational and skill-building benefits without specific percentages, reinforcing its general efficacy across diverse settings [9].

These comparisons highlight that while JAIU's results are consistent with high-performing ECE programs, variations in methodology (perceptual vs. objective) and implementation (broad vs. case-specific) influence outcomes. Resource constraints and scheduling, noted as limitations, align with challenges reported by Das et al. (2017) and Sood et al. (2023), underscoring the need for strategic planning to optimize ECE delivery [5, 7].

Conclusion

The ECE program at JAIU significantly enhances first-year MBBS education by fostering clinical reasoning, confidence, and hands-on proficiency. By immersing students in clinical settings early, ECE establishes a robust foundation for holistic medical training, warranting its continued integration.

Limitations

1. First-year students' limited foundational knowledge may hinder understanding of complex pathologies during ECE.
2. Computer-assisted modules and simulators entail high costs, infrastructural dependencies, and technical expertise requirements.
3. Resource limitations and scheduling conflicts may impede seamless ECE implementation.
4. Future efforts should focus on scalable solutions to address these challenges while maintaining ECE's quality and impact.

References

1. McLean, M. (2004). Sometimes we do get it right! Early clinical contact is a rewarding experience.Education for Health, 17(1), 42–52. https://doi.org/10.1080/13576280310001656178
2. Dornan, T., & Bundy, C. (2004). What can experience add to early medical education? Consensus survey. BMJ, 329(7470), 834. https://doi.org/10.1136/bmj.329.7470.834
3. Medical Council of India. (2019). Early clinical exposure for the undergraduate medical education training program. Medical Council of India.
4. Kharay, S. S., Vohra, H., Puri, S., & Bansal, P. (2023). Phase I medical students' perceptions of early clinical exposure in classroom and hospital setting: A qualitative and quantitative analysis. Future Health, 1(1), 1–7. https://doi.org/10.25259/FH_20230101_1
5. Das, P., Biswas, S., Singh, R., Mukherjee, S., Ghoshal, S., & Pramanik, D. (2017). Effectiveness of early clinical exposure in learning respiratory physiology among the newly entrant MBBS students. Journal of Advances in Medical Education & Professionalism, 5(1), 6–10.https://www.ncbi.nlm.nih.gov/pmc/articles/PMC5238496/
6. Patil, V. S., Patil, V. P., Kanabur, D. R., & Kangokar, P. R. (2021). Effectiveness of early clinical exposure as a motivational tool to improve students' learning in MBBS phase 1. Indian Journal of Medical Biochemistry, 25(2), 51–59. https://doi.org/10.5005/jp-journals-10054-0179
7. Sood, A. K., Singh, S., Gupta, U., Gupta, U., Sethi, P., & Puri, S. (2023). Impact of early clinical exposure on first-year medical undergraduates: Student's perspective. Journal of Medical Academics, 6(2), 56–61. https://doi.org/10.5005/jp-journals-11003-0131
8. Rawekar, A., Jagzape, A., Srivastava, T., & Gotarkar, S. (2016). Skill learning attitude and experiences of newly enrolled medical students: A Project of the Medical Education Unit of NKP Salve Institute of Medical Sciences, Nagpur. Journal of the Indian Academy of Medical Sciences,8(3),18–25.
9. Govindarajan, S., Vasanth, G., Kumar, P. A., Priyadarshini, C., Radhakrishnan, S. S., Kanagaraj, V., Balaji, N., Koteeswaran, V., & Arivazhagan, N. (2018). Impact of a comprehensive early clinical exposure program for preclinical year medical students. Health Professions Education, 4(2), 133–138. https://doi.org/10.1016/j.hpe.2017.12.002

Received / Получено 23.07.2025
Revised / Пересмотрено 28.07.2025
Accepted / Принято 02.08.2025

PREVALENCE AND FACTORS ASSOCIATED WITH THE UTILIZATION OF CONTRACEPTIVES AMONG WOMEN OF REPRODUCTIVE AGE IN JALALABAD, KYRGYZSTAN

Mohammad Irfan Alam[1], Farjana Afrin[2], Dipak Chaulagain[2,3]
[1]Medical Student, Jalal-Abad State University named after B. Osmonov, Jalal-Abad, Kyrgyzstan
[2]Jalal-Abad International University, Jalal-Abad, Kyrgyzstan
[3]Uzhhorod National University, Uzhhorod, Ukraine

Abstract
Globally, sexual and reproductive health remains a critical public health concern for women of reproductive age. The utilization of modern contraceptives is essential for managing fertility, reducing unintended pregnancies, abortions, and associated health complications. This study aimed to assess the prevalence and factors associated with contraceptive use among women aged 15–35 years in Jalalabad, Kyrgyzstan. A descriptive cross-sectional study was conducted using online Google Forms over three months (September to November 2024). A structured questionnaire was administered to 150 randomly selected women, and data were analyzed using SPSS version 22.0. Results revealed that 88.7% of respondents were married, 88.7% resided in rural areas, and 35.9% had more than two children, all of which were associated with higher contraceptive use. Conversely, women aged 15–25 years showed lower utilization. The majority of women demonstrated good knowledge of contraceptives, though some reported side effects such as vaginal discharge or irritation. These findings underscore the need to address socioeconomic, geographic, and cultural barriers to enhance contraceptive effectiveness and promote maternal and child health.

Keywords: Contraceptive utilization, reproductive health, socioeconomic factors, maternal health

РАСПРОСТРАНЕННОСТЬ И ФАКТОРЫ, СВЯЗАННЫЕ С ИСПОЛЬЗОВАНИЕМ КОНТРАЦЕПТИВОВ СРЕДИ ЖЕНЩИН РЕПРОДУКТИВНОГО ВОЗРАСТА В ДЖАЛАЛ-АБАДЕ, КЫРГЫЗСТАН

Мохаммад Ирфан Алам[1], Фарджана Африн[2], Дипак Чаулагайн[2,3]
[1]Студент-медик, Джалал-Абадский государственный университет им. Б. Осмонова, Джалал-Абад, Кыргызстан
[2]Джалал-Абадский международный университет, Джалал-Абад, Кыргызстан
[3]Ужгородский национальный университет, Ужгород, Украина

Аннотация
Во всем мире сексуальное и репродуктивное здоровье остается важнейшей проблемой общественного здравоохранения для женщин репродуктивного возраста. Использование современных контрацептивов имеет решающее значение для контроля фертильности, снижения числа нежелательных беременностей, абортов и связанных с ними осложнений. Целью данного исследования была оценка распространенности и факторов, связанных с использованием контрацептивов среди женщин в возрасте 15–35 лет в Джалал-Абаде, Кыргызстан. Описательное поперечное исследование проводилось с использованием онлайн-форм Google в течение трёх месяцев (с сентября по ноябрь 2024 года). Структурированный опрос был разослан 150 случайно выбранным женщинам, а данные были проанализированы с помощью SPSS версии

22.0. Результаты показали, что 88,7% респондентов состоят в браке, 88,7% проживают в сельской местности, а 35,9% имеют более двух детей. Все эти факторы связаны с более частым использованием контрацептивов. Напротив, женщины в возрасте 15–25 лет используют контрацептивы реже. Большинство женщин продемонстрировали хорошие знания о контрацептивах, хотя некоторые сообщали о побочных эффектах, таких как выделения из влагалища или раздражение. Эти результаты подчёркивают необходимость устранения социально-экономических, географических и культурных барьеров для повышения эффективности контрацептивов и укрепления здоровья матери и ребёнка.

Ключевые слова: Использование контрацептивов, репродуктивное здоровье, социально-экономические факторы, здоровье матери

Introduction

Rapid population growth poses a significant challenge in developing countries, threatening global health and sustainability [1]. Family planning services are not only critical for controlling population growth and improving maternal and child health but are also recognized as a fundamental human right [2]. Despite the availability of contraceptive methods, unintended pregnancies remain prevalent, with approximately 80 million women worldwide experiencing them annually, of which 45 million results in abortions [3]. These unintended pregnancies contribute to over half a million maternal deaths and 120 million disabilities each year [4].

The ability to adopt effective contraceptive methods is influenced by factors such as access to healthcare, community attitudes, cultural values, and personal beliefs [5]. Studies, particularly from the global north, highlight barriers such as limited understanding of reproductive cycles, overestimation of withdrawal method effectiveness, and cultural influences on contraceptive use [6]. For instance, research among Hispanic women in the United States revealed that economic constraints, healthcare access, and cultural values significantly impact contraceptive behaviors [6].

Modern contraceptive methods, including barrier methods (e.g., condoms, diaphragms), hormonal contraceptives (e.g., oral pills, injectables, implants), and intrauterine devices (IUDs), are designed to prevent pregnancy [7]. These methods offer non-contraceptive health benefits, such as reduced risks of endometrial and ovarian cancer, but also carry risks like increased cardiovascular disease with oral contraceptives or infection with IUDs in high-risk groups [4]. Globally, of the 1.9 billion women of reproductive age in 2021, 1.1 billion required family planning, with 874 million using modern contraceptives and 164 million facing an unmet need [3].

This study evaluates the prevalence and factors associated with modern contraceptive utilization among women of reproductive age in Jalalabad, Kyrgyzstan, using a national demographic and health survey framework. The findings aim to inform the design and implementation of interventions to enhance contraceptive use and reduce maternal and child morbidity and mortality.

Materials and Methods

A descriptive cross-sectional study was conducted from September to November 2024 in Jalalabad, Kyrgyzstan. Data were collected using a structured questionnaire administered via online Google Forms to 150 randomly selected women aged 15–35 years. The questionnaire captured socio-demographic characteristics, contraceptive knowledge, and utilization patterns. Data were analyzed using the Statistical Package for the Social Sciences (SPSS) version 22.0. Associations between dependent (contraceptive use) and independent variables (e.g., age, marital status, residence) were assessed using chi-square tests. Ethical approval was obtained, and informed consent was secured from all participants.

Results

Socio-Demographic Characteristics

Of the 150 respondents, 83.3% had completed university education, while 16.7% had only primary education. The majority (96.7%) were Muslim, with 3.3% identifying as Christian. Age distribution showed 42.0% (n=63) aged 30–35 years, 35.3% (n=53) aged 25–30 years, and 20.0% (n=30) aged 15–25 years. Regarding family income, 87.3% were from middle-income households, and 12.7% were from high-income households. Most respondents (88.7%) were married, while 11.3% were divorced. Employment status indicated 69.3% were employed, and 28.7% were housewives. Geographically, 88.7% resided in rural areas, and 11.3% lived in urban areas (Table.1).

• *Table 1: Factors associated with contraceptive utilization*

		No	***Yes***
Respondent's current age	15-20	4 (100)	00 (00)
	20-25	10 (33.33)	20 (66.66)
	25-30	30 (56.6)	23 (43.39)
	30-35	13 (20.63)	50 (70.36)
Religion	Muslim	66 (45.20)	80 (54.79)
	Hindu	1 (25)	3 (75)
Current marital status	Married	60 (45.11)	73 (54.88)
	Unmarried	9 (52.94)	8 (47.05)
knowledge of any contraceptive method	85 (56.66)	65 (43.34)	

Factors Associated with Contraceptive Utilization

Contraceptive use was higher among married women (88.7%), those living in rural areas (88.7%), and those with more than two children (35.9%). Conversely, women aged 15–25 years exhibited lower contraceptive use. The majority of respondents demonstrated good knowledge of contraceptives, though some reported side effects, including vaginal discharge and irritation.

Discussion

The findings from this study indicate that marital status, rural residence, and parity (having more than two children) are significant predictors of higher contraceptive utilization among women of reproductive age in Jalalabad, Kyrgyzstan. Conversely, younger women (aged 15–25 years) showed lower rates of contraceptive use. These results align with broader national and regional trends in Kyrgyzstan, where the modern contraceptive prevalence rate (mCPR) among married women is estimated at approximately 23-25% [8]. This relatively low mCPR reflects ongoing challenges in family planning, including an increasing unmet need for contraception, which rose from 19.9% in 2006 to 22.5% in 2018 [9].

Comparatively, our observation that having more than two children promotes contraceptive use is consistent with other studies in Kyrgyzstan. For instance, a study found that men with three living children had significantly higher odds of using modern contraceptives (adjusted odds ratio [aOR] 3.534, 95% CI 1.221–10.229), suggesting a similar pattern among couples aiming to limit family size after achieving desired parity [10]. This parity-related factor is also echoed in Ethiopian studies, where the number of living children was associated with modern contraceptive utilization [11].

The association with marital status in our study, where married women had higher utilization (88.7%), corresponds to the focus of national surveys on married women, as unmarried women often face cultural barriers to accessing reproductive health services [12]. Rural residence promoting use in our sample (88.7%) contrasts with some findings; previous research identified area of residence as a factor in unmet need, potentially indicating that rural women in Jalalabad may have better access to certain methods like IUDs, which are prominent in Kyrgyzstan but declining in use nationally [9].

Lower use among younger women aligns with global patterns in low- and middle-income countries, where adolescents and young adults often have limited knowledge, face stigma, or lack youth-friendly services [3]. This is particularly relevant in Kyrgyzstan, where the unmet need is influenced by women's age [9].

While the majority of women in our study had good knowledge of contraceptives, side effects such as vaginal discharge and irritation were reported, highlighting the need for improved counseling [7]. These side effects may contribute to discontinuation, as seen in declining trends of reversible methods like pills, injections, and IUDs nationally [9]. Overall, our results underscore the importance of addressing socioeconomic (e.g., income, employment), geographic (rural-urban disparities), and cultural barriers to improve contraceptive uptake. Interventions should include comprehensive sexual health education for youth, strengthened supply chains for contraceptives, and training for healthcare providers [5].

Conclusion

This study highlights the critical role of modern contraceptives in reproductive health among women in Jalalabad, Kyrgyzstan. Factors such as marital status, rural residence, and parity significantly influence utilization, while younger age is associated with lower use. Despite good knowledge levels, side effects remain a concern. Interventions targeting socioeconomic, geographic, and cultural barriers are essential to improve contraceptive access and effectiveness, ultimately reducing maternal and child morbidity and mortality.

References

1. Rastak, L. (2005). Correlation between socio-demographic characteristics and contraceptive methods. Sharecrop University of Medical Sciences Journal, 45-52.
2. Belfield, T. (2009). Principles of contraceptive care: Choice, acceptability and access. Best Practice & Research Clinical Obstetrics & Gynaecology, 23(2), 177-185.
3. United Nations Department of Economic and Social Affairs, Population Division. (2022). World family planning 2022: Meeting the changing needs for family planning: Contraceptive use by age and method.
4. National Research Council. (1989). Contraception and reproduction: Health consequences for women and children in the developing world. National Academies Press.
5. Singh, R., Frost, J., Jordan, B., & Wells, E. (2009). Beyond a prescription: Strategies for improving contraceptive care. Contraception, 79(1), 1-4.
6. Sangi-Haghpeykar, H., Ali, N., Posner, S., & Poindexter, A. N. (2006). Disparities in contraceptive knowledge, attitude and use between Hispanic and non-Hispanic whites. Contraception, 74(2), 125-132.
7. Almalik, M., & Mosleh, S. (2018). Are users of modern and traditional contraceptive methods in Jordan different? Eastern Mediterranean Health Journal, 24(2), 154-162.
8. Track20. (2023). Kyrgyz Republic 2023 summary brief and handout. Retrieved from https://track20.org/download/pdf/Country%20Indicators/2023/2023%20Combo%20Briefs/English/Kyrgyz%20Rep.%202023%20Summary%20Brief%20and%20Handout.pdf
9. Dolonbaeva, Z., et al. (2024). Unmet need for contraception among married women in the Kyrgyz Republic using the datasets from the 2006, 2014 and 2018 Multiple Indicator Cluster Survey: a cross-sectional study. BMC Public Health, 24(1), 977. https://doi.org/10.1186/s12889-024-18518-6
10. Bayramova, L., & Kulczycki, A. (2017). Prevalence and socio-economic factors determining use of modern contraception among married men in Kyrgyzstan: Evidence from a demographic and health survey. Public Health, 142, 56-63. https://doi.org/10.1016/j.puhe.2016.10.008
11. Beyene, K. M., Bekele, S. A., & Abu, M. K. (2023). Factors affecting utilization of modern contraceptive methods among women of reproductive age in Ethiopia. [Journal details from original].
12. Whitaker, A. K., Johnson, L. M., Harwood, B., Chiappetta, L., Creinin, M. D., & Gold, M. A. (2008). Adolescent and young adult women's knowledge of and attitudes toward the intrauterine device. Contraception, 78(3), 211-217.

Received / Получено 03.07.2025
Revised / Пересмотрено 23.07.2025
Accepted / Принято 28.07.2025

УДК 529. 128. 53

ВЛИЯНИЕ ГОРНОГО КЛИМАТА НА ТРАВМУ

Матсаков Каныбек Сулайманкулович[1]
[1]Жалал-Абадский международный университет, Жалал-Абад, Кыргызстан

Аннотация
Результаты экспериментального исследования свидетельствуют, что заживление раны мягких тканей и костной раны нижней челюсти у кроликов складываются из резорбции некротических масс мягких тканей и секвестров, пролиферации макрофагов и фибробластов, формирования грануляционной и соединительной ткани вначале рыхлой, а затем волокнистой а также новообразования хряща с последующей заменой его остеоидной и костной ткани.

Ключевые слова: соединительная ткань, макрофаг, резорбция, фибробласт, нижняя челюсть, кролик, секвестр, адаптация, кость.

THE INFLUENCE OF THE MOUNTAIN CLIMATE ON TRAUMA

Matsakov Kanibek Sulaymankulovich[1]
[1]Jalal-Abad International University, Jalal-Abad, Kyrgyzstan

Abstract
The results of the experimental study indicate that the healing of soft tissue wounds and bone wounds of the mandible in rabbits consist of resorption of necrotic masses of soft tissues and sequesters, proliferation of macrophages and fibroblasts, the formation of granulation and connective tissue initially loose and then fibrous, as well as the regeneration of cartilage with subsequent replacement of its osteoid and bone tissue.

Keywords: connective tissue, macrophage, resorption, fibroblast, mandible, rabbit, sequester, adaptation, bone.

Актуальность темы. Кыргызская Республика горная страна, занимает западную половину Кыргызской Ала-Тоо (горные массивы Тянь-Шаня в переводе с китайского языка означает Недостигаемые горы) и Алайской горной системы Памира (С перевода с тибетского означает Крыша мира). Ее рельефотличается редкими высотными контрастами (от 500м до 7495м над уровнем моря, большим разнообразием форм). Средней высоты находятся в пределах 2500-3000м, преобладают высоты до 3800-4200 м. Почти 90% территории Кыргызстана лежит выше 1500м над уровнем моря. Размеры Кыргызстана достигают 198,5 тыс. кв.м., здесь проживает более 7 млн населения (данные переписи за 2021г).

Проблемы высокогорья и адаптации к нему отражены в довольно значительном числе исследований. Работы в этом направлении не потеряли своей актуальности и сегодня

хотя вскрыты многие аспекты морфофункциональных изменений организма на высоте. Так, обнаружено, что биологическое значение имеет не только абсолютная высота над уровнем моря, но и целый комплекс других геоклиматических параметров региона. Кроме того, на высоте значительно изменяются функциональные характеристики всех органов и систем, характер которых во многом зависит от уровня адаптации. Оптимальным проявлением последней являются повышение резистентности организма и неблагоприятным факторам внешней среды, на примере: золоторудный комбинат Кумтор на высоте более 4000 метров.

Среди доступных нам источников литературы, посвященных различным вопросам заживления травм и их осложнений влияние высокогорья, на патологических процессов в зависимости от климата-географических условия, мы не нашли работ, связанных с интересующей нас проблемой. [1,2,3,4,5]

Вышеизложенное определило цель и задачи предпринятого исследования.

Цель исследования. Цель нашей работы состояло в том, чтобы путем комплексного клинического и морфологического анализа экспериментального материала выявить влияние условий высокогорья на заживление травм и их осложнения челюстно-лицевой области.

Задачи исследования. Изучить в хроническом опыте на кроликах с использованием рентгенологической и экспертной морфологической оценки клинические и морфологические проявления заживления перелома нижней челюсти после травмы в высокогорья.

Объем и методика хронического эксперимента на животных по исследованию на репаративные процессы при заживлении переломов нижней челюсти в условиях горного климата.

Экспериментальное исследование имела цель изучение течение заживления травматической раны нижней челюсти в условиях высокогорья. Эксперименты проведены на 24 половозрелых кроликах породы «Шишнила» весом 2,5-3,5 кг на 12 животных содержались в одинаковых условиях вивария ЦНИЛ Кыргызского государственного медицинского института на обычном рационе питания, 12 кролика переведены из г. Бишкек (760 м над уровнем моря) в высокогорную местность Ала-Арча (2500 м над уровнем моря) Кыргызского Ала-Тоо.

Методика эксперимента. Операция проведения под внутрибрюшинным наркозом 2,5% раствором тиопентала натрия (0,5 на кг веса животного), при соблюдении условий асептики и антисептики. После удаления волос по краю тела нижней челюсти справа производился послойный разрез кожи, фасции, мышц и надкостницы длинной 4см мягкие ткани отслаивались распатором, тело нижней челюсти справа пересекалось диском вертикально начиная с наружной поверхности. В краях костных отломков №2 шаровидным бором машины создавалось по два сквозных отверстия. Костные фрагменты нижней челюсти сопоставлялись в правильном анатомическом положении и сшивались хромированным кетгутом, проведенным через сквозные отверстия. Надкостница и мышцы послойно ушивались кетгутовыми, а кожа - шелковыми швами. Рана обрабатывалась раствором бриллиантовой зелени. После операции всем животным дважды внутримышечно введен бициллин-1 по 300 000 ЕД.У животных контрольных групп (№1 и №2) заживления раны, кожи, мягких тканей и костной ткани изучались при обычных условиях. Репаративные процессы изучались гистологически.

Для гистологического исследования иссекались фрагменты отломков нижней челюсти вместе с мягкими тканями на расстоянии 3-4см от раны. Раздельно врезались кусочки мягких тканей и кости: фрагменты кости врезались в поперечном направлении по отношению декальцировались в 5% растворе азотной кислоты. Материал обычным образом обезвоживался и уплотнялся, и заливался парафином. С каждого блока приготавливались короткие серии срезов толщиной -7 микрон. Срезы окрашивались гематоксилин-эозином, по Ван-Гизону, импрегировались серебром по Футу, в части случаев поставлена ШИК-реакция.

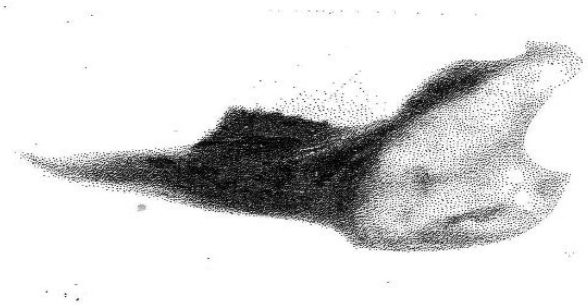

• *Рис. 1 Нижняя челюсть кролика до операции (макропрепарат).*

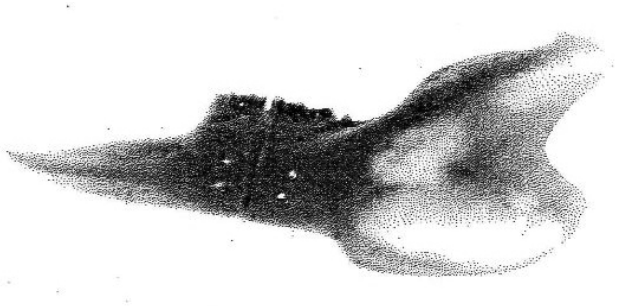

Рис 2. Нижняя челюсть кролика после операции остеосинтеза нижней челюсти (макропрепарат).

Динамика заживления перелома челюсти после травмыв условиях высокогорья.

3 сутки опыта. Клинически животные были малоактивными вплоть до выведения из опыта. Пищу воспринимали с трудом, как бы щадя прооперированную челюсть. Края кожной раны сопоставлены правильно, сухие с массивным послеоперационным отеком, швы удерживаются хорошо. На мацерированных препаратах выявлено, что у всех животных фрагменты нижней челюсти сопоставлены правильно, уровни кортикального вещества и нижнечелюстного канала совпадают. Щель перелома на всем протяжении выполнена тканевым детритом, состоявшим из некротических пасс и измененных фрагментов мягких тканей, опилок кости и корней зубов, а также свертков крови. Анализ микроскопических препаратов показал, что на 3 сутки опыта мягкие ткани краев раны на значительном протяжении некротизированы, некротические массы инфильтрованы большим количеством лейкоцитов. Полость костной раны выполнена некротическими массами и костными секвестрами (рис 3). В отличие от опытов, проведенных в низкогорье, инфильтрация лейкоцитами более массивна, имеются абсцессы, а образование грануляционной ткани менее выражено. Костные секвестры различной величины и формы, лишены остеоцитов, базофильны, линии склеивания не определяются. Костные каналы расширены, в некоторых из них содержится белковый детрит (рис 3).

Компактная пластинка в области краев раны лишена остеоцитов, базофильна, в просвете каналов содержится детрит (рис 3). Со стороны эндоста, периоста и костного мозга имеется разрастание островков грануляционной ткани; местами они определяются в просвете гаверсовых каналов. Пролиферация клеточных элементов выражена, чем в условиях низкогорья. Грануляционная ткань представлена капиллярами, тонкими коллагеновыми волоконцами и клеточными элементами. Среди них имеются

остеокласты, прилегающие к секвестрам (рис 5). На стенках отдельных гаверсовых каналов вдали от краев раны видна узкая прослойка остеоида (рис 4).

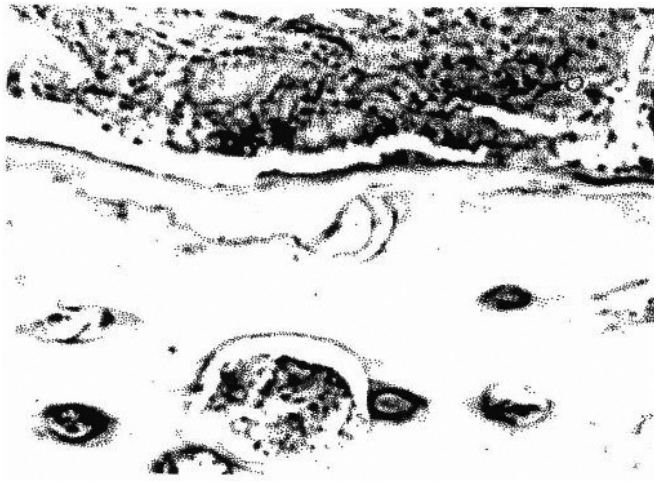

• Рис 3. Некротические массы и секвестр с детритом в костных каналах. Ув.х 63; Окр. Гематоксилин-эозином.

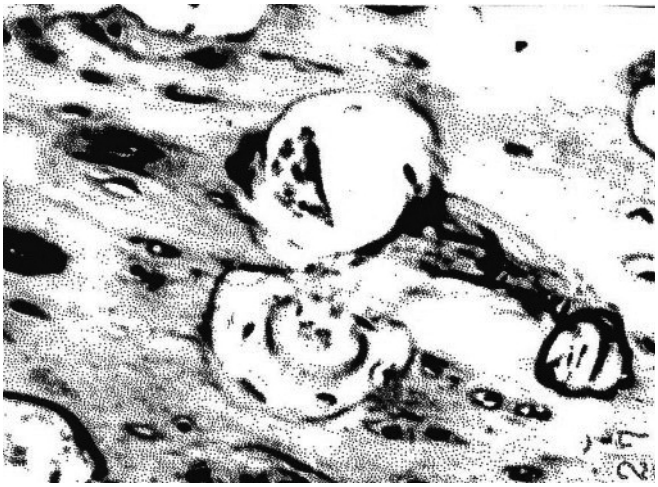

• Рис 4. Остеоид в стенках гаверсовых каналов. Ув. х 63; Окр. Гематоксилин-эозином.

6 сутки опыта. Животные были неактивными; первые 3-4 дня после операции они неохотно принимали пищу. Послеоперационный отек пальпировался вплоть до выведения животных из опыта. На мацерированных препаратах нижней челюсти кроликов между передними и задними фрагментами четко определяется щель перелома. Отломки костей не смещены, прочно фиксированы кетгутовыми швами. Поверхность опила по линии перелома гладкая.

• Рис 5. Грануляционная ткань с остеокластами по краю компактной костной пластинки. Увел. х 100; Окр. по Ван-Гизону.

• Рис 6. Хрящ поверх компактной костной пластинки края раны. Ув. х 63; Окр. гематоксилин-эозином.

Гистологически в мягких тканях выявляются крупные фокусы сухого некроза с ядерным детритом. Они более крупные, чем у животных, оперированных в условиях

низкогорья, а перифокальная инфильтрация лейкоцитами более массивна; кроме того, в мягкихтканях имеются абсцессы. Перифокально от зон некроза и абсцессов видно выраженное разрастание грануляционной ткани. Компактная костная пластинка краев раны некротизирована. Гаверсовы каналы ее резко расширены, просвет их выполнен детритом и лейкоцитами. В просвете отдельных гаверсовых каналов имеется грануляционная ткань с остеокластами (рис 7) со стороны периоста и эндоста вблизи краев операционной раны разрастание грануляционной ткани, рыхлой соединительной ткани и образование отростков хряща (рис 6).

В отличие от животных, оперированных в низкогорье, новообразованный хрящ выявляется только на отдельных участках полости раны. На остальном протяжении рана плотно выполнена грануляционной тканью, а местами и рыхлой соединительной тканью. В глубине грануляционной ткани имеются фокусы сухого некроза, инфильтрированные лейкоцитами и секвестры (рис 8). Гаверсовы каналы расширены, в прилегающей грануляционной ткани имеются остеокласты. Имеется также фокусное пазушное рассасывание. По краям костных пластинок губчатого вещества, прилегающим к ране. Скопление остеобластов и образование небольших островков хряща и узкой зона остеоида.

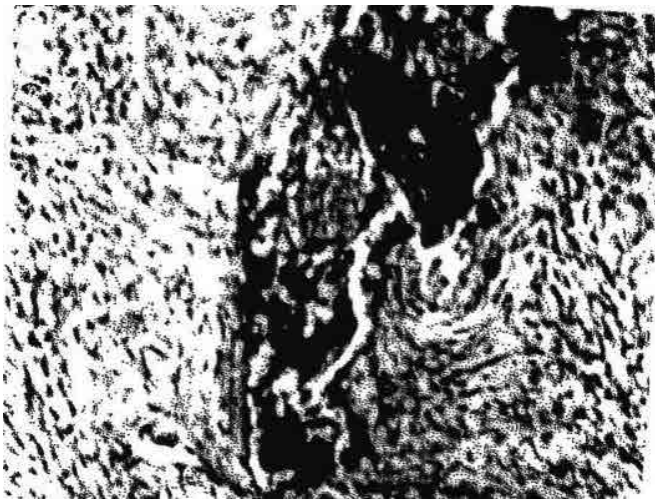

• *Рис 7. Волокнистая соединительная ткань вокруг некротических массы в костномозговом канале. Ув. х 63; Окр. гематоксилин-эозином.*

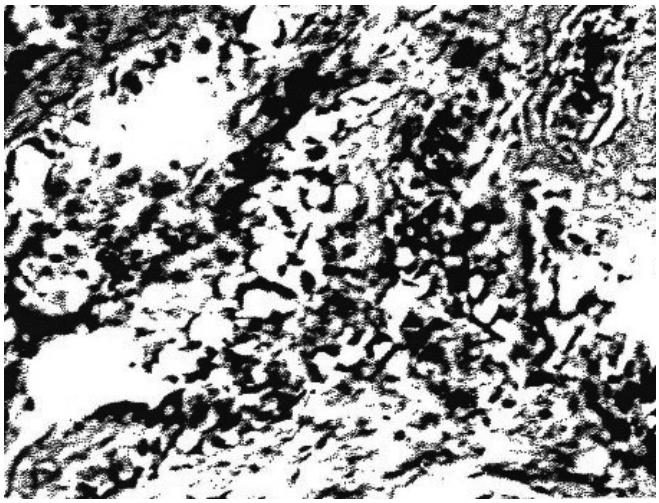

• *Рис 8. Хрящ и грануляционная ткань в костном мозгу. Ув. х 63; Окр. гематоксилин-эозином.*

21 сутки опыта.Клинически после первых 2-3 суток малой активности, к концу первой недели после операции все животные стали подвижными. Хотя пищу пережевывали медленно. Послеоперационный отек пальпировался в течении 9-10 суток. Раны мягких тканей у двух кроликов зажили вторичным натяжением, у одного кролика в подчелюстной области открылся свищ. К 21 суткам животные активны и хорошо пережёвывают пищу.

На мацерированных препаратах щель перелома нижней челюсти кроликов определяются. Фрагменты кости сопоставлены правильно, плотно удерживаются хромированным кетгутом. В щели перелома определяются небольшие регенераты. У

одного кролика определяется гнойный свищ, абсцессы и секвестры.Гистологически в мягких тканях грубый рубец, перифокально от которого выявляются абсцессы и фокусы некроза, более многочисленные и крупные, чем у животных в условиях низкогорья. Щель перелома челюсти выполнена грануляционной и волокнистойсоединительной тканью. В периосте и эндосте поверх раны и по ее краям располагается зона хрящевой ткани; хрящевые пластинки образуют балочные структуры, между ними располагается различной величины прослойки грануляционной ткани (рис 9).

Местами хрящевые балки заменены узкой зоной с остеоида. В глубине губчатого вещества имеются крупные абсцессы с костными секвестрами (рис 10) местами здесь же находятся немногочисленные балки хряща, небольшие участки остеоида. Вокруг мелких секвестров разрастание грануляционной ткани (рис 11). по сравнению с животным, оперированными в условиях низкогорья, репаративные процессы менее выражены.

• Рис 9. Хрящ со стороны периоста. Ув. х 100; Окр. гематоксилин-эозином.

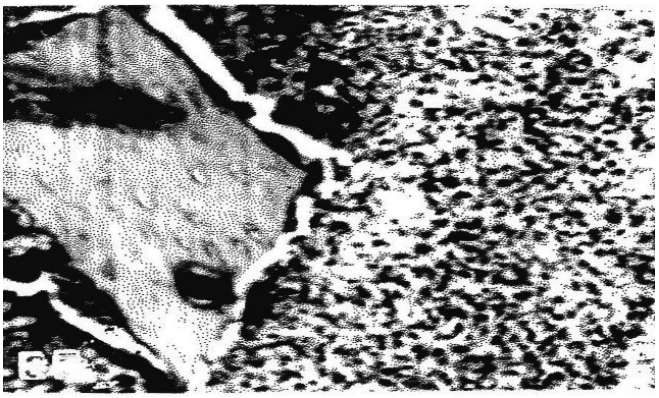

• Рис 10. Нагноение вокруг секвестра. Ув. х 100; Окр. гематоксилин-эозином.

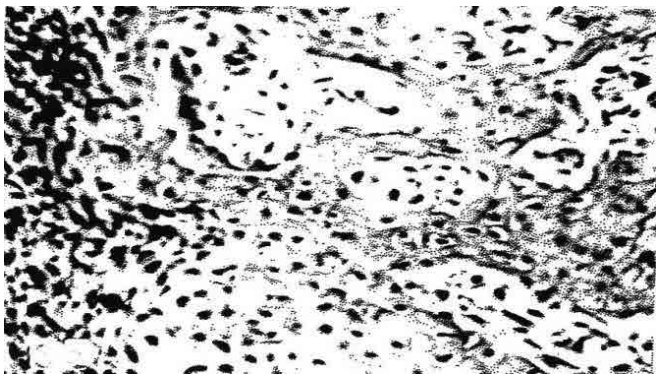

• Рис 11. Волокна соединительной ткани и хрящ со стороны периоста. Увел. х100; Окр. по Ван-Гизону.

• Рис 12. Островки хряща и костные балочки в мягких тканях поверх раны, утолщённый за счет разрастания соединительной ткани периост. Ув. х 100; Окр. гематоксилин-эозином.

30 сутки опыта. В первые сутки после операции животные были вялыми. Отек мягких тканей пальпировался на протяжении недели. Раны у всех кроликов зажили

вторичным натяжением, причем у двух на них на 30 сутки опыта в подчелюстной области образовались гнойные свищи. На 30 сутки опыта все животные ведут себя активно, охотно принимают пищу.На мацерированных препаратах нижней челюсти у одного кролика поверх раны и по ее краям определяются фокусы новообразованной соединительной ткани. Костные отломки челюсти подвижны (ложный сустав). У двух кроликов в мягких тканях имеются свищевые ходы с гнойным отделяемым, ведущие в костномозговой канал. Фрагменты отломков челюсти также подвижны. Щель перелома выполнена новообразованной соединительнойтканью, частью зияет. При рассечении челюсти выявляются секвестры.

Гистологически в мягких тканях вокруг грубых рубцов выявлены инкапсулированные фокусы некроза, абсцессы и свищи, в мышцах - очаговые круглоклеточные инфильтраты. Периост и эндоста утолщены за счет разрастания волокнистой соединительной ткани. Поверх раны в периосте и эндосте имеется прерывистая сеть анастомизирующих друг с другом костных и хрящевых оболочек (рис 12). Образование хрящевой и костной ткани менее выражено, чем в условиях низкогорья рана выполнена грубоволокнистой соединительной ткани. В глубине ее имеются инкапсулированные абсцессы с секвестры, частью сообщающиеся со свищом (рис 13).

Вокруг секвестров располагается грануляционная ткань с немногочисленными остеокластами. Однако резорбция секвестров незначительна. Со стороны эндоста и костного мозга располагаются немногочисленные хрящевые и костные балочки окруженные грануляционной тканью.

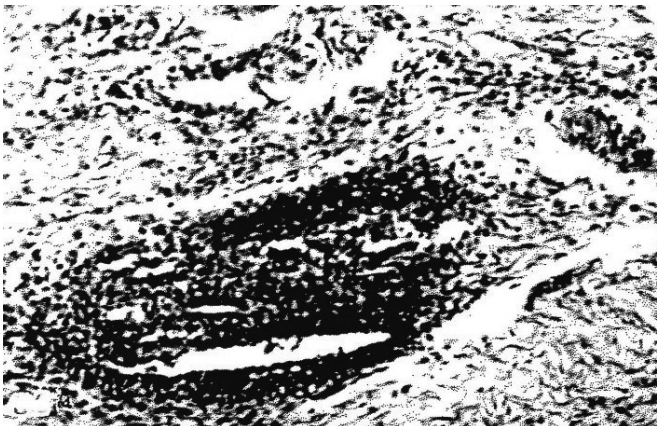

• *Рис. 13. Глубоковолнистая соединительная ткань с инкапсулированным абсцессом в глубине раны.Увел. х 100; Окр. по Ван-Гизону.*

Заключение

Результаты экспериментального исследования свидетельствуют, что заживление раны мягких тканей и костной раны нижней челюсти у кроликов складываются из резорбции некротических масс мягких тканей и секвестров, пролиферации макрофагов и фибробластов, формирования грануляционной и соединительной ткани вначале рыхлой, а затем волокнистой а также новообразования хряща с последующей заменой его остеоидной и костной ткани. Новообразование хрящевой и костной ткани идет со стороны эндоста, периоста и губчатого вещества.

Динамика репаративных процессов в условиях низкогорья и высокогорья однотипна. Однако выраженность структурных изменений неодинакова. В условиях высокогорья более резко выражена воспалительная реакция. Морфологически она проявляется

формированием абсцессов мягких тканей и пери фокальных абсцессов в глубине костной раны вокруг секвестров. У 6 животных из 12 подопытных прооперированных в высокогорье на различных сроках опыта (21-30) сутки выявлены свищи, а у 3 кроликов на 30 сутки опыта клинически диагностировали травматический остеомиелит нижней челюсти; у одного кролика в области костной травмы наблюдался ложный сустав.

В то же время из 12 кроликов, оперированных в условиях низкогорья, лишь у 3 животных раны зажили вторичным натяжением. Клиника травматического остеомиелита диагностирована только у одного кролика.

Формирование грануляционной хрящевой, а затем костной ткани в условиях высокогорья происходит в те же сроки опыта, что и в низкогорье. Однако выраженность репаративных процессов здесь существенно меньшая. Это проявляется фокусным образованием грануляционной ткани, хряща и очаговой замены его костной тканью. В результате полноценная первичная костная мозоль к 30 суткам опыта у животных в условиях высокогорья не образуется. Костная рана выполнена грубоволокнистой; соединительной тканью с отдельными хрящевыми и костными балками. У одного животного на 30 сутки образовался ложный сустав.

Литература

1. Агожанион Н.А., Миррахим М.М. Горы и резистентность организма. М: Наука, 1970-184 с
2. Алиев М.А. Адаптация и горному климату при ортериальной гипертонии. - Фрунзе. Илим. - 1978 - 202 с.
3. Бахитов Ф.Ю. Консолидация переломов в эндомической по зобу местности. - Автореф. дис… канд. мед. наук. - Фрунзе, 1971.-20с
4. Датхаев Ю.И. Сравнительные данные о заживлении переломов в условиях высокогорья и долины. (Эксперементальные исследования). Авто реф. дис… канд. мед. наук. - Столинобад 1955.- 16 с.
5. Лямсев В.Т., Матсаков К.С.
6. Морфлогия зажилвния травматической раны челюсти в условиях низко-и высокогорья // проблемы морфлогий. 5-Конференция Республик Средней Азии и Казахстана, г. Чолпон-Ата, 1991.

Received / Получено 12.05.2025
Revised / Пересмотрено 09.06.2025
Accepted / Принято 04.07.2025

ОСАДКИ И СКЛОНОВЫЕ ПРОЦЕССЫ: ГЕОЭКОЛОГИЧЕСКИЙ АНАЛИЗ УЧАСТКА «ЧЫЙЫРЧЫК» (ЮЖНЫЙ КЫРГЫЗСТАН)

Мирзалиев Мурадил[1], Канетова Динара Эменовна[1], Мадалиева Зинагул Жуманалиевна[1], Асилова Зульфия Атамырзаевна[1]
[1]Жалал-Абадский научный центр ЮО НАН КР, Жалал-Абад, Кыргызстан

Аннотация
Целью исследования является установление взаимосвязи между атмосферными осадками, скоростью смещений и объёмом смещающихся масс на горных склонах Южного Кыргызстана. Объектом анализа выбран склон в районе месторождения «Чыйырчык», характеризующийся высокой трещиноватостью, переменной влажностью и присутствием рыхлых грунтов. Для оценки геоэкологических условий использован комплекс инженерно-геологических методов: геодезическая съёмка, бурение, вертикальное электрическое зондирование (ВЭЗ), лабораторные исследования физико-механических свойств грунтов и климатические наблюдения на метеостанции «Гулча». Среднегодовое количество осадков составляет 520 мм, при этом в весенне-летний период фиксируются кратковременные ливни до 76 мм/сутки, оказывающие влияние на поровое давление и фильтрационные процессы. Выявлено, что критические условия формируются в весенне-летний период при сочетании обводнения глинистых пород и трещиноватости карбонатного основания. Интерпретация данных ВЭЗ и буровых скважин подтверждает наличие зон пониженной устойчивости на глубинах 6–12 м. Разработка верхнего горизонта карьера может снизить геодинамическое напряжение и минимизировать риск склоновых деформаций. Результаты подчёркивают необходимость учёта климатических и гидрогеологических факторов при инженерной оценке склонов и проектировании защитных мероприятий.

Ключевые слова: оползень, атмосферные осадки, скорость смещений, объем смещающихся масс, инженерно-геологические изыскания

SEDIMENT AND SLOP PROCESSES: GEOECOLOGICAL ANALYSIS OF THE CHYYIRCHYK SITE (SOUTHERN KYRGYZSTAN)

Mirzaliev Muradil[1], Kanetova Dinara Emenovna[1], Madalieva Zinagul Zhumanalievna[1], Asilova Zulfiya Atamyrzaevna[1]
[1]Jalal-Abad Scientific Center of the South Ossetia National Academy of Sciences of the Kyrgyz Republic, Jalal-Abad, Kyrgyzstan

Abstract
The aim of this study is to identify the relationship between precipitation, displacement velocity, and the volume of moving masses on mountain slopes in southern Kyrgyzstan. The research focuses on a slope near the "Chyyrchyk" deposit, characterized by high jointing, variable moisture conditions, and the presence of loose soils. A set of engineering and geological methods was used to assess geoenvironmental conditions, including geodetic surveying, drilling, vertical electrical sounding (VES), laboratory testing of physical and mechanical soil properties, and meteorological observations from the "Gulcha" weather station. The average annual precipitation is 520 mm, with peak rainfall events up to 76 mm/day occurring in the

spring–summer period, contributing to pore pressure development and filtration processes. Critical conditions are observed during this period due to the combination of saturated clay layers and jointed carbonate bedrock. Interpretation of VES profiles and borehole data confirms the presence of low-stability zones at depths of 6–12 meters. The development of the upper quarry horizon is expected to reduce geodynamic stress and mitigate landslide risks. The results emphasize the importance of considering climatic and hydrogeological factors in slope stability assessment and the design of protective measures.

Keywords: landslide, precipitation, displacement velocity, mass movement volume, engineering geological survey

Введение

Современные климатические изменения и усиление антропогенного воздействия на природную среду приводят к увеличению частоты и интенсивности экзогенных геодинамических процессов, включая оползни, обвалы и склоновые деформации. Особенно уязвимыми к подобным явлениям являются горные регионы, такие как южные районы Кыргызстана, где сочетание сложного рельефа, трещиноватых пород и обильных атмосферных осадков создает предпосылки к нарушению устойчивости склонов [1,2].

Одним из ключевых факторов, провоцирующих смещения горных масс, являются атмосферные осадки. Их интенсивность, продолжительность и сезонность оказывают прямое влияние на фильтрационные потоки, повышение порового давления и снижение прочностных характеристик грунтов [3,4]. В мировой практике отмечается устойчивая тенденция к росту локальных оползней, вызванных кратковременными, но мощными ливневыми осадками, особенно на фоне нарушенной геомеханической структуры склонов в результате хозяйственной деятельности [5].

Актуальность исследования заключается в необходимости детального изучения взаимосвязи между параметрами склоновых деформаций (скоростью, объёмом) и осадками в условиях реальных геоэкологических объектов. В качестве объекта исследования выбран склон в районе Чыйырчыкского месторождения известняка-ракушечника (Ошская область, Кыргызстан), где наблюдаются признаки нестабильности геологического массива [6].

Цель работы — установить количественные и качественные зависимости между параметрами осадков и характеристиками смещений, выявить геофизические признаки нестабильности, а также определить возможные меры по снижению геоэкологического риска при освоении территории.

Материалы и методы

Исследования проводились на участке «Чыйырчык» (Ошская область, Кыргызстан), расположенном на высотах 2450–2550 м н.у.м. в пределах юго-западного склона Ферганского хребта. Объект характеризуется чередованием закарстованных известняков и суглинков с признаками потенциальной оползневой активности [1,2].

1. Геодезическая и топографическая съёмка

Выполнена GPS-съёмка 18 точек (скважины, ВЭЗ, канавы) с привязкой в системе WGS-84. Построен топографический план масштаба 1:2000 с горизонталями через 1 м, на основе которого составлена инженерная схема склонов [1].

2. Буровые и шурфовые работы

Пройдено 5 скважин общей глубиной 76 м. В скважине №2 зафиксирована типичная для участка последовательность:

– 0–0,6 м — суглинок,
– 0,6–4,5 м — влажный суглинок,
– 4,5–9,8 м — трещиноватый известняк,
– 9,8–19 м — глинистый алевролит [2].

Также выполнено описание керна и определение уровня подземных вод.

3. Электроразведка (ВЭЗ)

Проведено 9 точек вертикального электрического зондирования по методике Шлюмберже. Питающая линия — до 90 м, глубина исследования — до 22 м. Методика обработки — графоаналитическая, по шкале Пылаева. Полученные данные позволили выделить чередующиеся слои:

– поверхностные суглинки с низким УЭС (70–80 Ом·м),
– водонасыщенные глины с УЭС 500–550 Ом·м,
– плотные известняки (УЭС 350–400 Ом·м), что соответствует результатам бурения и указывает на потенциальную плоскость скольжения в зоне 6–12 м (см. табл. 1, рис. 8).

Расположение точек бурения, зондирования, канав и обнажений представлено на рис. 1.

• *Рисунок 1. Размещение точек инженерных изысканий на участке «Чыйырчык» (координаты в системе WGS-84).*

• Таблица 1. Результаты ВЭЗ на участке «Чыйырчык»

Точка ВЭЗ	Глубина, м	УЭС, Ом·м	Интерпретация
ВЭЗ-1	0–1.2 / 1.2–7.0 / 7.0–20.0	70 / 550 / 400	Суглинок / Глина / Известняк
ВЭЗ-2	0–1.5 / 1.5–6.5 / 6.5–18.0	60 / 520 / 380	Суглинок/Глинистый суглинок/Трещиноватый известняк
ВЭЗ-3	0–2.0 / 2.0–8.0 / 8.0–22.0	75 / 500 / 420	Суглинок/Глина/Плотный известняк

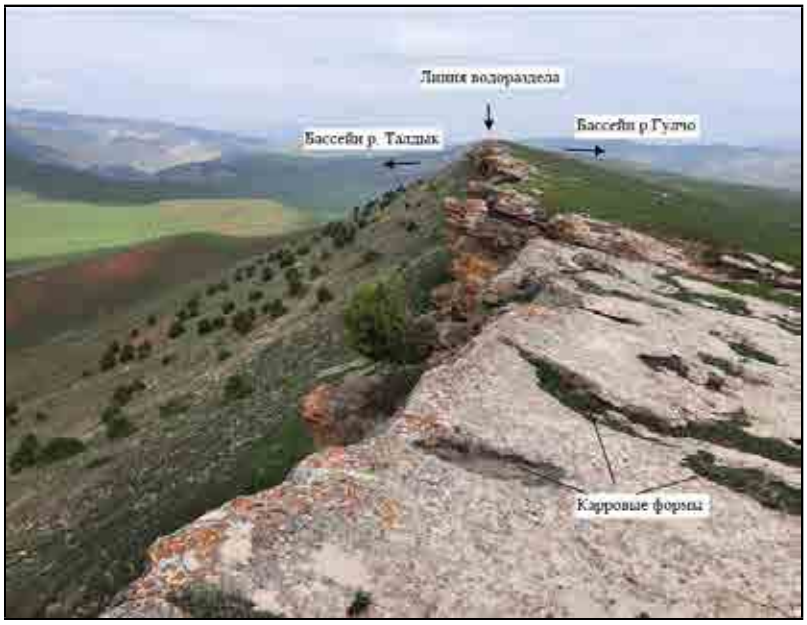

• Рисунок 2. Бронирующая поверхность пласта известняка с уклоном 8–10°, восточная экспозиция.

• Рисунок 3. Канава у подножья обрывистого склона с проявлениями карровых форм; граница водоразделов бассейнов рек Талдык и Гулча.

• Рисунок 4. Обрывистый склон на восточной границе участка, в нижней части — глыбы известняка, отделившиеся от материнской толщи.

• Рисунок 5. Проведение буровых работ вблизи карстованного разрыва.

• Рисунок 6. Обнажённый фрагмент бронирующей поверхности известняков в зоне тектонического контакта.

• *Рисунок 7. Образцы пород, отобранные из скважины №2 (керн: глина, известняк, алевролит).*

Интерпретация результатов

ВЭЗ-3: Интервалы глубин:

0,0–1,2 м — суглинок, УЭС 70 Ом·м
1,2–7,0 м — влажная глина, УЭС 550 Ом·м
7,0–20,0 м — известняк, УЭС 300–400 Ом·м

Такая структура указывает на высокую водонасыщенность средних горизонтов, а также наличие водоупоров в зоне глин, что увеличивает риск подпорного насыщения и активации скольжения.

ВЭЗ-6:

– Мощность глинистых горизонтов до 16,2 м;
– УЭС от 25 до 45 Ом·м, коррозионная активность высокая — признаки закарстованности и обводнённости в основании склона.

Интерпретационные выводы

– Верхние слои (0–3 м) характеризуются низким сопротивлением (30–70 Ом·м), что соответствует рыхлым, суглинистым или влажным отложениям.
– Средние горизонты (3–15 м) чаще всего представлены глинами с УЭС 500–550 Ом·м — водоудерживающие и слабоуплотнённые.
– Глубинные уровни (15–35 м) отражают плотные, устойчивые породы — известняки, с УЭС >400 Ом·м.

Такие данные указывают на потенциальное наличие скользящей плоскости на глубине 6–12 м, что совпадает с инженерно-геологическими наблюдениями в шурфах и скважинах.

Геоэкологическое значение. Зоны пониженного сопротивления, выявленные на профильных линиях ВЭЗ, совпадают с местами отрыва глыб и суффозионных процессов. Это подтверждает необходимость интеграции ВЭЗ в регулярную систему мониторинга оползневой опасности и планирования разработки верхнего пласта.

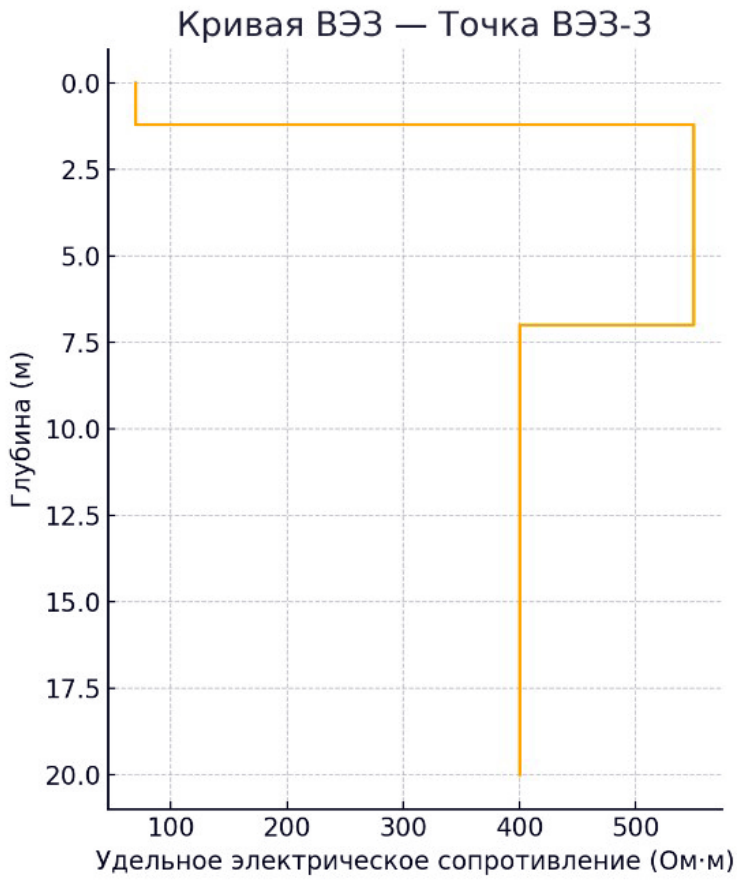

• *Рисунок 8. Интерпретированная кривая удельного сопротивления для точки ВЭЗ-3 (метод Шлюмберже).*

4. Проходка канав и описание обнажений

Описано более 6 литологических разрезов. В обнажении №2 зафиксированы трещиноватые известняки толщиной до 12 м, с признаками карра и выветривания. Обнаружены глыбы до 2–3 м, свидетельствующие о поверхностных смещениях [1].

В рамках инженерно-геологических работ на участке «Чыйырчык» произведено описание трёх естественных обнажений и двух разведочных канав. Цель — уточнение литологического строения верхней части разреза, анализ трещиноватости, признаков выветривания и склоновых деформаций.

Особенности: трещины до 5 см, заполнены глиной; наблюдаются выщелачивания на поверхности известняка.

Геоморфологическая роль: представляет зону водораздела и частичной эрозии поверхности коренных пород.

Геомеханическая интерпретация. Фиксация карровых форм (борозды, углубления), высокой трещиноватости и поверхностных обрушений в известняках подтверждает физико-геологические процессы выщелачивания и фрагментации массивов, предрасполагающие к отрыву глыб и деформациям склонов. Эти процессы, как отмечают исследователи, усиливаются при сезонном увлажнении и чередовании промерзания/оттаивания.

5. Лабораторные исследования

Проведены испытания 14 проб.

– Влажность: 10,9–22,9%
– Плотность: 1,83–1,95 г/см³
– Сцепление: 0,35–0,43 кг/см²
– Угол внутреннего трения: 31–40° Методика испытаний — по ГОСТ 12248-2010 и ГОСТ 5180-2015 [1,4].

6. Климатические данные.

Климат района участка «Чыйырчык» относится к горно-континентальному с резкой сезонностью температур и увлажнения. По данным метеостанции «Гулча» (абсолютная отметка 1542 м, многолетние наблюдения с 1937 г.), среднегодовая температура составляет +7,3°C, абсолютный минимум достигает –32°C, максимум — +37°C.

Гидрометеорологические показатели:

Показатель	*Значение*
Среднегодовая сумма осадков	520 мм
Суточный максимум	76 мм (конвективные дожди)
Наиболее влажный период	Апрель – май
Средняя температура июля	+19,2 °C
Суммарная влажность воздуха летом	до 82 % в обеденное время
Испаряемость летом	высока, но переменчива

Сезонность оползнеобразования

Исследования подтверждают, что наибольшая активность оползневых процессов на горных склонах приходится на весенний и ранне-летний периоды. Это связано с:

– накоплением влаги в виде снега в зимний период;
– быстрым насыщением выветрелых пород талой и дождевой водой весной;
– развитием порового давления в зонах глин и суглинков;
– высокой интенсивностью кратковременных осадков в мае-июне.

Данные многолетнего мониторинга склонов на сопредельных участках показывают прямую зависимость между осадками выше 120–140 % нормы и массовой активизацией старых и новых оползней.

Наибольшая интенсивность осадков фиксируется в апреле–мае, что совпадает с пиком порового давления в обводнённых зонах суглинков и глин. Этот период климатически соответствует наиболее опасному для склоновой устойчивости (см. рис. 9)

Анализ метеоданных позволяет утверждать, что регион характеризуется благоприятными условиями для сезонной активации склоновых деформаций, особенно в переходный весенне-летний период. Интенсивные осадки даже при несущественной превышении нормы могут привести к нарушению устойчивости склонов с развитой трещиноватостью и водоупорами.

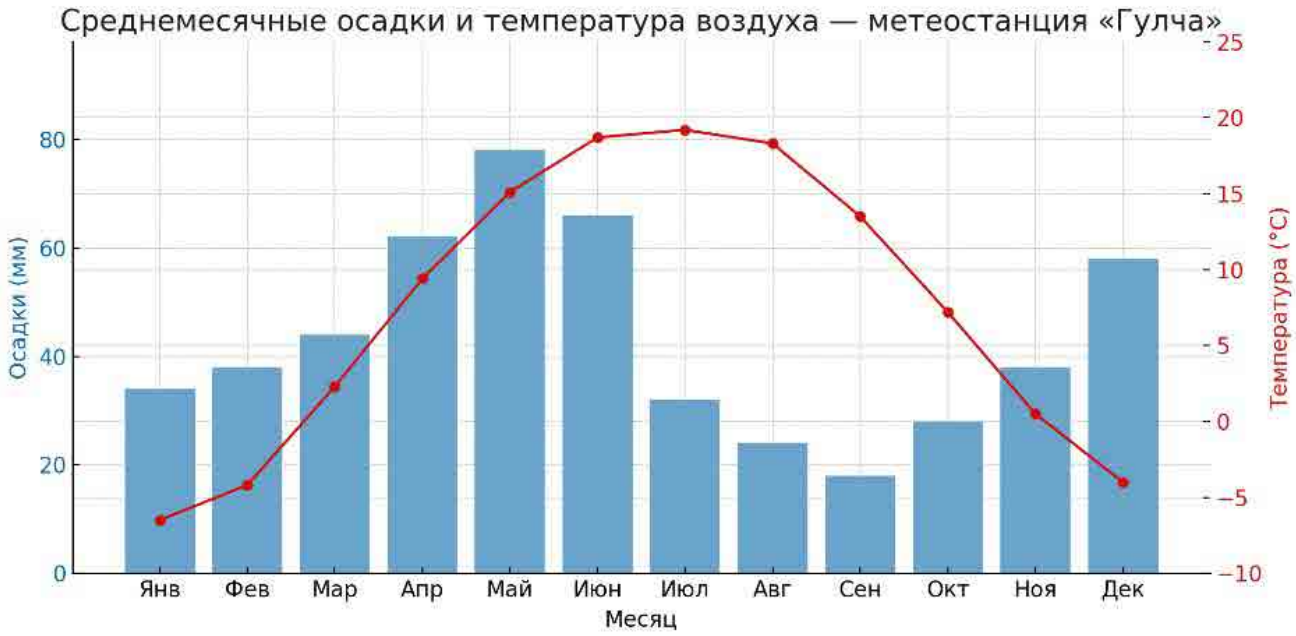

• *Рисунок 9. Среднемесячные значения осадков и температуры воздуха по метеостанции «Гулча» (среднемноголетние данные).*

7. Химический анализ подземных вод

Для оценки агрессивности подземных вод по отношению к известняковым породам и определения их влияния на устойчивость массива был проведён отбор и анализ проб из двух скважин и родника. Отбор осуществлялся по методике ГОСТ 2761-84 с консервацией и транспортировкой проб в лабораторию.

Гидрохимические параметры:

Показатель	*Значения*	*Характеристика*
pH	6,9 – 7,9	Слабощелочная реакция среды
Минерализация	0,7 – 0,9 г/л	Пресные воды
Жёсткость	Средняя (временами повышенная)	Кальциево-магниевый тип
Ионный состав	Гидрокарбонатно-сульфатный	Доминирование HCO_3^- и SO_4^{2-}
Агрессивность к $CaCO_3$	Умеренная–высокая	Потенциальное выщелачивание известняков

Интерпретация

Преобладание гидрокарбонатов и сульфатов, совместно с нейтральной и слабощелочной реакцией, указывает на водно-углекислотную агрессию по отношению к известнякам. Это может вызывать:

– частичное растворение карбонатного цемента;
– развитие карровых форм;
– ослабление трещиноватых зон.

Выводы подтверждаются также наблюдением поверхностных карров в обнажении №2 и результатами геофизических измерений зон пониженного сопротивления, совпадающих с предполагаемыми путями фильтрации.

Влияние на оползнеопасность

Как установлено в методологических работах (Фоменко И.К., 2013; Харр М., Цытович Н.А.), присутствие вод с растворяющей активностью в трещиноватых и пористых известняках способно резко снижать прочность пород, увеличивать поровое давление и провоцировать развитие фильтрационных деформаций — суффозии, кольматации, фильтрационного выпора.

Результаты

В результате комплексных инженерно-геологических и гидроклиматических исследований на участке «Чыйырчык» получены следующие ключевые данные, позволяющие оценить оползневую опасность и устойчивость склонов.

1. Геолого-литологическое строение

Анализ разрезов бурения и обнажений (см. рис. 3–4) показал, что геологическое строение представлено трёхзвенной последовательностью:

• верхние рыхлые суглинки (0–4 м);
• влажные пластичные глины и глинистые суглинки (до 10–14 м);
• трещиноватые известняки-ракушечники, часто закарстованные (12–30 м).

Обнаружены глыбы, вероятно, оторвавшиеся в результате поверхностного скольжения по границе глина–известняк.

2. Геофизические признаки неустойчивости

Вертикальное электрическое зондирование (ВЭЗ) выявило:

• зоны пониженного сопротивления (70–80 Ом·м) в верхних горизонтах;
• высокие значения УЭС (500–550 Ом·м) в глинистых слоях;
• стабильные значения (400 Ом·м) в известняках (табл. 1, рис. 8).

Интерпретация указывает на наличие возможной плоскости скольжения в интервале глубин 6–12 м.

3. Свойства грунтов

Лабораторные исследования (табл. 2) показали:

• влажность: 10,9–22,9 %;
• сцепление: 0,35–0,43 кг/см²;
• угол внутреннего трения: 31–40°.

Это соответствует средней степени устойчивости при условии сухого состояния и снижению устойчивости при водонасыщении.

4. Влияние осадков

По данным метеостанции «Гулча» (рис. 9), интенсивные осадки (до 76 мм/сутки) и их весенне-летняя концентрация формируют поровое давление в водоудерживающих горизонтах. Период апреля–мая является критическим по риску активизации оползней.

5. Влияние подземных вод

Химический анализ подземных вод показал:

• pH: 6,9–7,9;
• минерализация: 0,7–0,9 г/л;
• средняя жёсткость;
• агрессивность к карбонатным породам — умеренная до высокой.

Фиксируются признаки карстования и растворения цементирующего вещества в известняках (рис. 2, 6).

6. Интегральная оценка

На основе полученных данных выделены три зоны различной устойчивости:

1. Верхняя часть склона — условно стабильная.
2. Средний склон (5–15 м глубины) — потенциально активная зона скольжения.
3. Нижняя часть — зона аккумуляции глыб и продуктов разрушения.

Разгрузка массива (путём разработки карьера) потенциально снижает риск накопления напряжений и активизации смещений.

Обсуждение

Результаты полевых, лабораторных и аналитических исследований позволяют утверждать, что участок «Чыйырчык» обладает всеми признаками склоновой нестабильности, характерными для высокогорных территорий Центральной Азии.

1. Сравнение с аналогичными регионами

Проведённый анализ выявил сходство с условиями, описанными в исследованиях на склонах Кавказа и Памира, где также отмечены:

– контактные плоскости между глинистыми и карбонатными породами;
– сезонная фильтрация вод по трещинам;
– карровые формы как маркеры выщелачивания и суффозии [1,2]. В частности, в работах Гакаева (2024) и Фоменко (2013) подтверждается, что глинистые горизонты с влажностью свыше 18–20 % при наличии подстилающего известняка являются типовой схемой для формирования скольжения глубиной 6–12 м [1,3].

2. Механизмы деформации

Накопление влаги в суглинках и глинах в весенний период вызывает:

– увеличение порового давления;
– снижение эффективных напряжений;
– потерю сцепления в пределах водоудерживающего горизонта;
– фильтрационное давление на контактной границе с известняками.

Дополнительно, наблюдаемая трещиноватость способствует ускоренной инфильтрации, а карстово-глыбовая структура нарушает сплошность массива.

3. Условия активизации

Критическим фактором является сочетание следующих условий:

– кратковременные осадки более 50 мм/сутки (рис. 9);
– влажность глинистых горизонтов >20 % (табл. 2);
– закарстованный характер известняка (рис. 2, 4, 6);
– наличие водоупора в зоне ВЭЗ 6–12 м (рис. 8).

Таким образом, участок попадает в зону локальной оползневой предрасположенности.

4. Практические рекомендации

– В целях освоения участка карьера рекомендуется:
– проводить сезонный мониторинг влажности, УПВ и осадков;
– соблюдать последовательность вскрытия массива сверху вниз;
– минимизировать сейсмические и гидродинамические воздействия в весенне-летний период;
– организовать дренажные мероприятия (горизонтальные скважины или гравитационные коллекторы).
– В случае продолжения работ следует рассмотреть интеграцию постоянного ВЭЗ-мониторинга или GNSS-наблюдения за деформациями [4].

Заключение

Проведённое инженерно-геологическое и геоэкологическое исследование участка «Чыйырчык» позволило выявить комплексную взаимосвязь между параметрами атмосферных осадков, геологическим строением и устойчивостью склонов.

Установлено, что:

– геолого-литологическая структура включает рыхлые суглинки, водоудерживающие глины и трещиноватые карстовые известняки;
– по результатам ВЭЗ и бурения в интервале 6–12 м формируется потенциальная плоскость скольжения;
– весенне-летний максимум осадков (до 76 мм/сутки) вызывает резкое увеличение влажности глин и порового давления;
– химический состав подземных вод указывает на агрессивность по отношению к известняку, что подтверждает выщелачивание и потерю прочности.

Наиболее уязвимой к деформациям является средняя часть склона, где формируется скользящий контакт и фиксируются следы прошлых смещений (глыбы, карры, борозды).

Практическая значимость результатов заключается в обосновании необходимости:

– сезонного мониторинга влажности и деформаций;
– ограничения работ в периоды весеннего увлажнения;
– использования дренажных и разгрузочных мер при разработке массива.

Полученные данные могут быть применены для прогноза оползневой активности в аналогичных геоморфологических условиях Центральной Азии, а также при проектировании горнотехнических мероприятий с учётом климатических сценариев.

Список использованных литератур

1. Гакаев Р.А. Геоэкологическая оценка оползневых процессов горных территорий Чеченской Республики: дис. … канд. геогр. наук. — Грозный, 2024.
2. Фоменко И.К. Методология оценки и прогноза оползневой опасности. — М.: МГРИ–РГГРУ, 2013. — 294 с.
3. Чалкова Ю.С., Черепанов Б.М. Оползневые процессы, их прогнозирование и борьба с ними // Ползуновский вестник. — 2007. — № 1–2. — С. 80–83.
4. КыргызГИИЗ. Технический отчёт по результатам инженерных изысканий участка «Чыйырчык». Ошский филиал. — Ош, 2023.
5. Малдыбаев У.А. Исследование факторов активизации оползневых процессов в природных условиях Кыргызстана: дис. … магистр. — Томск: ТПУ, 2017.

6. ГОСТ 2761-84. Источники централизованного хозяйственно-питьевого водоснабжения. Гигиенические требования.
7. СНиП КР 23-02-00. Климатология. Нормы и правила проектирования. — Бишкек: Госстрой КР, 2005.
8. РСН 64-87. Инженерные изыскания. Требования к производству геофизических работ. Электроразведка.
9. TPU387731.pdf. Результаты многолетнего анализа сезонной устойчивости склонов Кыргызстана. — Томск: ТПУ, 2020.
10. Методология оценки оползневой опасности. — PDF. — 2020.
11. Zhang K., Liu C., Wang Y. A review of landslide monitoring and early warning systems // Geomatics, Natural Hazards and Risk. — 2019. — Vol. 10(1). — P. 1683–1712.
12. Crosta G.B., Frattini P. Rainfall-induced landslides: mechanisms, prediction and warning // Landslides. — 2008. — Vol. 5(1). — P. 61–78.
13. Zuska A.V. Kinematic model of landslide slopes. — Dnipro: NGU, 2014. — 140 p.
14. Fell R., Corominas J. et al. Guidelines for landslide susceptibility, hazard and risk zoning // Engineering Geology. — 2008. — Vol. 102. — P. 85–98.
15. Aleotti P., Chowdhury R. Landslide hazard assessment: summary review and new perspectives // Bulletin of Engineering Geology and the Environment. — 1999. — Vol. 58. — P. 21–44.

Received / Получено 12.07.2025
Revised / Пересмотрено 20.07.2025
Accepted / Принято 12.08.2025

Research

conducted by Jalal-Abad International University


EURASIAN JOURNAL OF SCIENTIFIC AND
MULTIDISCIPLINARY RESEARCH
CLINIC BASE


CLINIC BASE


МИНИСТЕРСТВО НАУКИ, ВЫСШЕГО ОБРАЗОВАНИЯ И ИННОВАЦИЙ
MINISTRY OF SCIENCE, HIGHER EDUCATION AND INNOVATION
CLINIC BASE
Dr. Deepak Chaulagain
Associate Professor (MD,MS,FMAL,PhD)
Deputy- Editor in Chief, EJSMR


EURASIAN JOURNAL
EURASIAN JOURNAL OF SCIENTIFIC AND MULTIDISCIPLINARY RESEARCH
CERTIFICATE


EURASIAN JOURNAL OF SCIENTIFIC AND MULTIDISCIPLINARY RESEARCH
CERTIFICATE
OF PARTICIPATION
Katanze Tushar Nakul


EURASIAN JOURNAL OF SCIENTIFIC AND MULTIDISCIPLINARY RESEARCH
CERTIFICATE
OF PARTICIPATION
Divanai Kumar

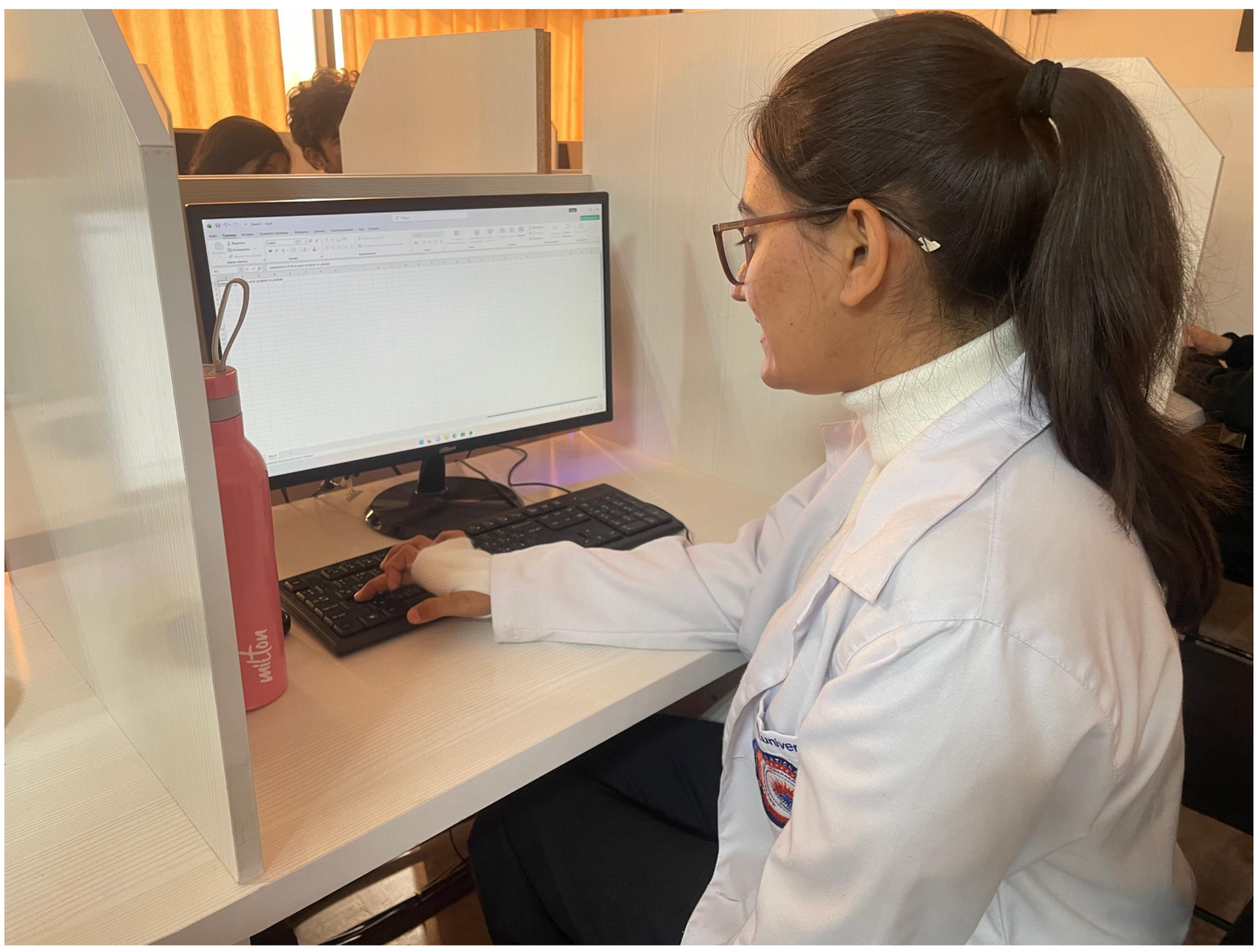


MEDICINE
SURGERY
SURGERY
PEDIATRICS
OPTHALMOLOGY
BIOCHEMISTRY
ENT
LIBRARY RULES!
Students should not brake locks, open the shelf and take books without permission!
Students should take books from the Librarian!


Jalal-Abad International University

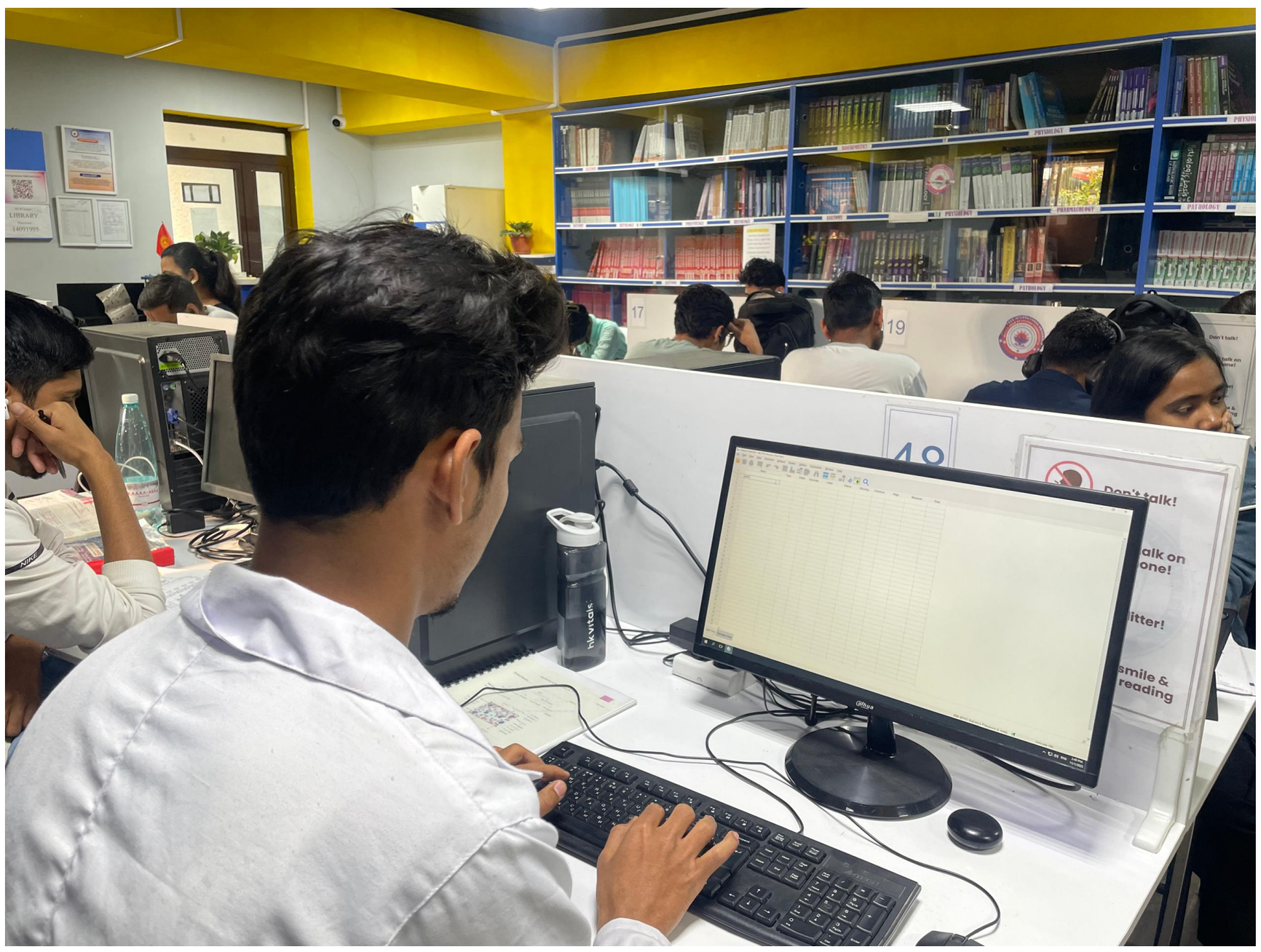
LIBRARY
PHYSIOLOGY
PHARMACOLOGY
PATHOLOGY
Don't talk!
smile &
reading

1st EJSMR International Conference

Held by Jalal-Abad International University


EURASIAN INTERNATION
MULTIDISCIPLINARY CONFE


JALAL-ABAD INTERNATIONAL
MULTIDISCIPLINARY CONFERENCE


JALAL-ABAD INTERNATIONAL UNIVERSITY
ЖАЛАЛ-АБАДСКИЙ МЕЖДУНАРОДНЫЙ УНИВЕРСИТЕТИ
ЖАЛАЛ-АБАД ЭЛ АРАЛЫК УНИВЕРСИТЕТИ